Development of Eco-compatible Catalysts and Reagents for Important Organic Reactions

Thesis Submitted for the Degree of

Doctor of Philosophy (Science)

of

Jadavpur University

2021

By

ASIT KUMAR DAS

Department of Chemistry
Jadavpur University
Kolkata-700 032
India

যাদবপুর বিশ্ববিদ্যালয়
কলকাতা-৭০০ ০৩২, ভারত

JADAVPUR UNIVERSITY
KOLKATA-700 032, INDIA

FACULTY OF SCIENCE DEPARTMENT OF CHEMISTRY ORGANIC CHEMISTRY SECTION

Dr. Sanjay Bhar
Professor

CERTIFICATE FROM THE SUPERVISOR

This is to certify that the thesis entitled **"Development of Eco-compatible Catalysts and Reagents for Important Organic Reactions"** submitted by Sri **Asit Kumar Das,** who got his name registered on ***03-11-2015*** for the award of ***Ph.D. (Science) degree of Jadavpur University***, is absolutely based upon his own work under my supervision and that neither this thesis nor any part of it has been submitted for either any degree / diploma or any other academic award anywhere before.

Sanjay Bhar
06/09/2021

(Signature of the Supervisor
with date and official seal)

DR. SANJAY BHAR
PROFESSOR
Department of Chemistry
Organic Chemistry Section
Jadavpur University
Kolkata - 700 032

E-mail: sanjay.bhar@jadavpuruniversity.in


Dedicated to.....
Maa & Baba

ACKNOWLEDGEMENTS

At the outset, I would like to convey my cordial gratitude and profound reverence to my Supervisor, Professor Sanjay Bhar, Department of Chemistry, Organic Chemistry Section, Jadavpur University, Kolkata 700032, for his affectionate guidance, insightful comments, precious advice, persistent help, enthusiastic encouragement, constructive criticism as well as endless support throughout the tenure my research programme. It was a great pleasure for me to carry out my research work under his supervision which stimulates my original thinking and initiative. He not only gave me all the necessary requirements to pursue my doctoral program but also gave me every freedom to choose and realize the objectives of my research. Moreover, his timely suggestions with kindness, prompt inspiration, scholarly advice, meticulous scrutiny, scientific approach, enthusiasm, and dynamism have enabled me to accomplish this task. He did not only unravel the secrets of Synthetic Organic Chemistry in me but also his professionalism, organizational skills and above all his constant support throughout my research have encouraged me to perform any job with supreme devotion and utmost honesty.

I would also like to express my sincere gratitude to Professor Brindaban Chandra Ranu, Department of Chemistry, Indian Association for the Cultivation of Science (IACS), Professor Chandan Kumar Jana, Department of Chemistry, Indian Institute of Technology Guwahati, and Professor Parthasarathi Bera, NAL, Bengaluru for their valuable suggestions in different occasions.

I express my deep regards to Professor Swapan Kumar Bhattacharya, Head, Department of Chemistry, Jadavpur University and all other respected teachers of Jadavpur University for their assistance and intellectual support during my research journey.

I am grateful to Professor Arup Gayen, Department of Chemistry, Jadavpur University for his invaluable cooperation and intimate support during my research journey.

I thank profusely the authority of Jadavpur University for providing me infrastructural and instrumental facilities for my research investigations. Financial support which I have enjoyed from the University Grants Commission, New Delhi, Government of India and RUSA-2-Programme and UGC-CAS-II programme in Chemistry at Jadavpur University is gratefully acknowledged.

My special thanks to Mr. Raju Biswas of Jadavpur University and Mr. Nirmalya Dutta of IACS for their helpful cooperation in several matters of my research.

I am extremely thankful to my lab seniors and lab mates, Dr. Subrata Kumar Chaudhuri, Dr. Manabendra Saha, Dr. Sanchita Roy, Dr. Amit Pramanik, Dr. Sagar Khan, Dr. Rimi Roy, Dr. Avishek Ghatak, and Mrs. Sneha Nandy for their whole-hearted co-operation throughout the entire tenure of my research work inside and outside the laboratory as well as during the preparation of my thesis.

Special word of gratefulness to Mr. Milan Maji, Dr. Aniruddha Das, Mr. Souvik Mandal, Mr. Rohan Dey, Mr. Dibyajyoti Panja, Mr. Koushik Mondal for their helpful cooperation and intimate support in several matters of my research.

My sincere thanks to Dr. Safalla Kr Ghosh, Dr. Bisweswar Banerjee, Dr. Sanjay Nath, Dr. Shrabani Barman, Dr. Umasankar Roy, Dr. Jaharlal Pratihar, Dr. Tapan Kr Pradhan, Dr. Bikramaditya Mondal, Dr. Dasarath Mal, Dr. Sandip Saha, Dr. Soumyadipta Rakshit, Mr. Debopam Sinha, Mr. Saikat Gayen, Miss. Pameli Ghosh, Mr. Pranesh Das, Mr. Satyajit Maity, Mr. Satya Narayan Sahoo, Mr. Subrata Mondal, Mr. Soumitra Manna, Mr. Apurba Giri and Mr. Sudarsan Taral for their inspiration and help at many steps.

I am always indebted to My Father, Mr. Abhiram Das and My Mother, Mrs. Saraswati Das for their unwavering support and encouragement throughout my journey. These persons would try to bring me back on my mettle when I felt terrible.

My deepest appreciation belongs to my other family members, Mr. Asim Das (Elder Brother), Mrs. Sampa Das (Sister-in-law), Mr. Angshuman Das (Nephew), Mr. Joydev Maity (Brother-in-law), Mrs. Sampa Maity (Elder Sister), and Mrs. Puja Das (Wife) for always believing in me and encouraging me to follow my dreams. My research work would have been impossible without the immense patience and dedication of all the family members.

Asit Kumar Das 06/09/2019

(ASIT KUMAR DAS)

Department of Chemistry
Organic Chemistry Section
Jadavpur University
Kolkata-700032

PREFACE

Investigations embodied in this dissertation entitled **"Development of Eco-compatible Catalysts and Reagents for Important Organic Reactions"**, submitted for the degree of Ph. D. (Science) of Jadavpur University, were initiated in November 2015 under the supervision of Professor Sanjay Bhar, Department of Chemistry, Organic Chemistry Section, Jadavpur University, Kolkata-700032.

The objective of the present study delineated in the aforesaid thesis was to develop eco-compatible catalysts and reagents for synthetically important organic transformations having greater merit and wider applicability compared to the conventional ones in terms of operational simplicity, improved selectivity and excellent yield, redundant side reactions as well as utilization of inexpensive reagents and catalysts having low toxicity in order to proceed for a 'sustainable future'. The entire investigations in this thesis have been divided into four Chapters. **Chapter-I** deals with the catalytic efficiency of β-cyclodextrin hydrate towards the eco-compatible synthesis of bis-(indolyl)methanes in an aqueous medium by the chemoselective reaction of indoles with differently substituted aryl and alkyl aldehydes under mild reaction conditions. Furthermore, the catalytic attributes of β-cyclodextrin hydrate were demonstrated through molecular docking and DFT studies. **Chapter-II** demonstrates an economically efficient and operationally simple ligand-free protocol for the chemoselective oxidation of benzylic alcohols to carbonyl compounds using alumina-supported mesoporous nickel nanoparticles as a stable recyclable heterogeneous catalyst along with potassium tert-butoxide as a base in the presence of aerial oxygen as an eco-friendly oxidant without affecting aliphatic alcoholic moieties. Investigations described in **Chapter-III** initiate with an eco-friendly synthesis of natural resource mediated magnetite (Fe_3O_4) nanoparticle and its catalytic application has been extended towards an eco-friendly chemoselective reduction of nitroarenes under an ambient atmosphere in an aqueous medium in the presence of hydrazine hydrate as the hydrogen source with the tolerance of various sensitive moieties. The direct oxidative transformation of aldehydes to nitriles using commercially available non-toxic copper acetate as an inexpensive catalyst and ammonium acetate as the source of nitrogen in the presence of aerial oxygen as an eco-friendly oxidant under ligand-free condition includes in **Chapter-IV**.

Abbreviations and Symbols

Ac	acetyl
Bn	benzyl
bp	boiling point
BET	Brunauer-Emmett-Teller
CD	cyclodextrin
CDH	cyclodextrin hydrate
CDC	cross dehydrogenative coupling
DA	Diels-Alder
DCM	dichloromethane
DDQ	2, 3-dichloro-5, 6-dicyano-*p*-benzoquinone
DFT	density-functional theory
DMF	*N*, *N*-dimethylformamide
DMSO	dimethyl sulfoxide
DLS	dynamic light scattering
EA	ethyl acetate
EAA	ethyl acetoacetate
EDG	electron donating group
Equiv	equivalent
EWG	electron withdrawing group
Et	ethyl
EAA	Ethyl acetoacetate
EDTA	Ethylenediaminetetraacetic acid
EDX	Energy dispersive x-ray analysis
GC	Gas Chromatograph
h / hrs	hours
HMDS	hexamethyldisilazane
HRMS	high resolution mass spectrum
HRTEM	high-resolution transmission electron microscopy
IR	infrared

J	coupling constant
Me	methyl
min	minutes
mL	mililitre
mp	melting point
MCR	multi component reaction
MW	microwave
NFSI	N-fluorobenzenesulfonimide
NHC	N-heterocyclic carbine
NMR	nuclear magnetic resonance
PEG	polyethylene glycol
Ph	phenyl
PMHS	polymethylhydrosiloxane
ppm	parts per million
rt	room temperature
SEM	scanning electron microscopy
SET	single electron transfer
TBAI	tetrabutylammonium iodide
TBDMS	tert-butyldimethylsilyl
TBHP	tert-butyl hydroperoxide
TEM	transmission electron microscopy
TEMPO	2,2,6,6-tetramethylpiperidinyloxy
THF	tetrahydrofuran
TLC	thin layer chromatography
TMS	tetramethylsilane
TMSCl	trimethylsilyl chloride
TMSCN	trimethylsilyl cyanide
$TMSN_3$	azidotrimethylsilane
Ts	tosyl
UV	ultraviolet
XPS	X-ray photoelectron spectroscopy

XRD	X-ray diffraction
σ	substituent constant
ρ	reaction constant
δ	chemical shift
ν	frequency

CONTENTS

CHAPTER I

Catalytic Efficiency of β-cyclodextrin Hydrate-Chemoselective Reaction of Indoles with Aldehydes in Aqueous Medium

I. Catalytic Efficiency of β-cyclodextrin Hydrate-Chemoselective Reaction of Indoles with Aldehydes in Aqueous Medium

I.1. Introduction

Alkylation of indoles is one of the most powerful, straightforward, and convenient methods for fundamental carbon-carbon (C-C) bond formation reaction and has been proven to be the construction of important classes of building blocks.[1] Indole derivatives constitute an important structural scaffold due to their widespread occurrence in biologically active natural products.[2] Among them, bis-(indolyl)methanes (BIMs) analogues are present in a wide range of biologically and pharmacologically active compounds,[3] such as antibiotics, anticancer, antitumor, antifungal, antibacterial, and HIV-1 integrase inhibitor. In addition, structurally diverse bis-indole moieties are very attractive compounds for chemosensing.[4] Owing to their relevant biological and pharmacological properties, the development of efficient synthetic protocols for the construction of bis-indolylmethane framework has received immense attention at all times. A brief account surveying the recent developments for the synthesis of bis-indolylmethanes is being described in the following review.

I.2. Construction of Bis-indolylmethanes Framework: A Review

Late transition metal complex catalyzed Friedel-Crafts alkylation reaction of indoles with aldehydes was developed by Mohapatra *et al.*[5a] where $PdCl_2(MeCN)_2$ catalyst activated the carbonyl group and promoted the synthesis of bis-indolylmethanes at room temperature in dichloroethane solvent with the survival of various functional groups (Scheme 1). Notably, electron-withdrawing substituents provided the desired products in good yields within a shorter reaction time, whereas electron-rich arenes took a longer reaction time for full conversion, and yields of desired products were moderate. Besides, this catalytic system was also effective for the reaction indoles with enones.

Scheme 1 Palladium-catalyzed synthesis of bis-indolylmethane derivatives

An efficient oxidative approach was introduced[5b] for the synthesis of bis(indolyl)methanes by the reaction of indoles with benzylamines in the presence of $Fe(OTf)_2$ as a catalyst and molecular oxygen as an eco-friendly oxidant in chlorobenzene solvent at 110°C (Scheme 2). Aromatic, aliphatic as well as heterocyclic amines were well tolerated under this protocol and produced the corresponding functionalized bis(indolyl)methanes with moderate to excellent yields. Moreover, this protocol promised versatility, cost-effectiveness, efficiency and allows for gram-scale production.

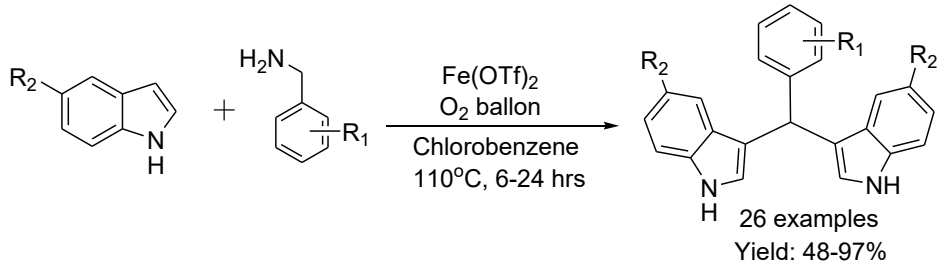

Scheme 2 Iron-catalyzed oxidative coupling of benzylamines and indoles

Lenardao and co-workers[5c] have reported ammonium niobium oxalate ($NH_4[NbO(C_2O_4)_2(H_2O)_x].nH_2O$) catalyzed synthesis of bis-indolylmethanes by the electrophilic substitution of indoles with carbonyl compounds using water or glycerol as the reaction medium under conventional heating in water (at 50°C) or under sonication in glycerol (at 110°C) (Scheme 3). Here, glycerol solvent under ultrasonic irradiation accelerates the reaction from several hours to few minutes. In addition, simplicity of the procedure, short reaction time, easy product separation, and reusability of the catalyst were the attractive features of this protocol.

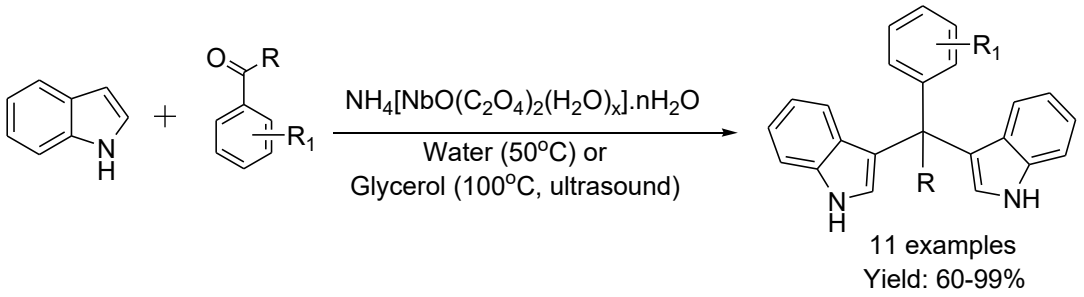

Scheme 3 Ammonium niobium oxalate catalyzed synthesis of bis(indolyl)methanes

An efficient enzymatic bio-catalytic route for the Friedel-Crafts alkylation reaction of indoles with aromatic aldehydes was described in an aqueous medium by Le and co-workers.[5d] Several enzymes were tested to perform this reaction, but α-Chymotrypsin was found to be the efficient biocatalyst and a series of bis-indolylmethanes were obtained in moderate to excellent yields (from 65% to 97%) under green reaction conditions (Scheme 4).

Notably, electron-withdrawing arenes render a positive effect on the yield of the desired products, whereas electron-donating substituents decrease the yield of the reaction.

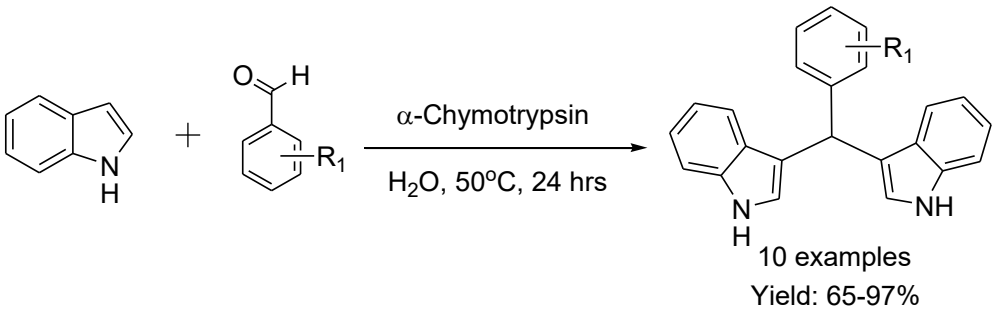

Scheme 4 Synthesis of bis-indolylmethanes catalyzed by *α*-chymotrypsin

$BF_3.OEt_2$ catalyzed synthesis of bis-indolylmethanes by the electrophilic substitution reaction of indoles bearing various electron-donating and electron-withdrawing substituents with differently substituted aromatic, hetero-aromatic and aliphatic aldehydes was disclosed by A. Swetha *et al.*[5e] in dichloromethane solvent at room temperature (Scheme 5). This procedure tolerates a broad range of functional groups and gave the desired products in good to excellent yields (from 71% to 95%).

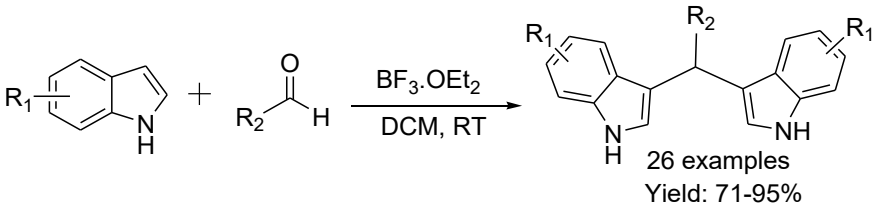

Scheme 5 Reaction of indoles with aldehydes in the presence of $BF_3.OEt_2$

The organometallic Lewis acid-mediated Friedel-Crafts reaction of indoles with *N*-sulfonyl aldimines was achieved by Wang *et al.*[6a] using titanocene dichloride (Cp_2TiCl_2) as an organometallic Lewis acid precursor and acetonitrile (CH_3CN) as the solvent at 25°C (Scheme 6). Several phenol derivatives were screened as an efficient ligand to establish the efficiency of the catalyst and it was observed that *o*-aminophenol enhanced the reactivity of titanocene catalyst and promoted the synthesis of bis-indolylmethanes with good to excellent yields with the tolerance of various functional groups.

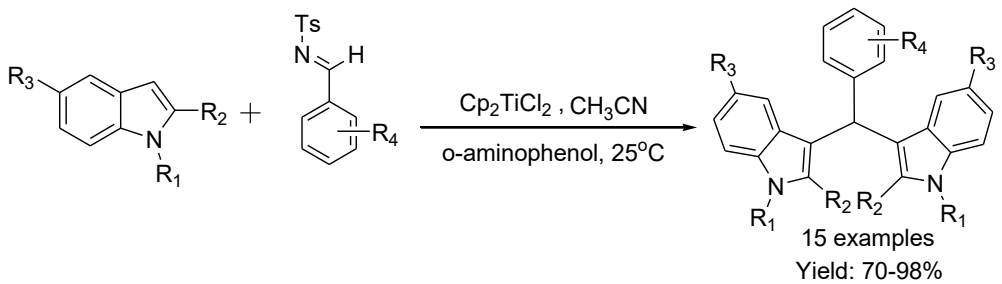

Scheme 6 Reaction of indoles with *N*-sulfonyl aldimines catalyzed by Cp_2TiCl_2

Cu(I)Br nanocatalyst supported on graphene oxide (GO-CuBr) was developed by Srivastava *et al.*[6b] and proven as an effective heterogeneous catalyst for the electrophilic activation of aldehydes to the synthesis of bis-indole derivatives under the solvent-free condition at 50°C (Scheme 7). Both electron-releasing, as well as electron-withdrawing substituents at the various positions of benzaldehydes, were found to exhibit a similar reactivity towards indole and produced the desired products with good to excellent yields. Moreover, the synthesized compounds have been screened for in-vitro anti-HIV-1 activity and a molecular modeling study was used to understand its binding mechanism to the active enzyme site.

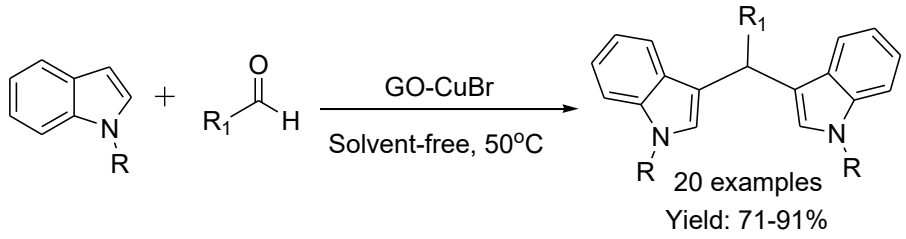

Scheme 7 Synthesis of bis-indolylmethanes using GO-CuBr nanocatalyst

Non-metal@MOF composite catalytic host-guest system was introduced by Zhu *et al.*[6c] for the Friedel-Crafts alkylation of indoles with substituted aromatic and aliphatic acetals using I_2@Cu_4I_4-MOF as heterogeneous catalyst under solvent-free conditions at room temperature (Scheme 8). The tandem acetal deprotonation to aldehydes followed by nucleophilic addition of indoles is the major advantage of this protocol and the desired alkylated products were obtained with good yield.

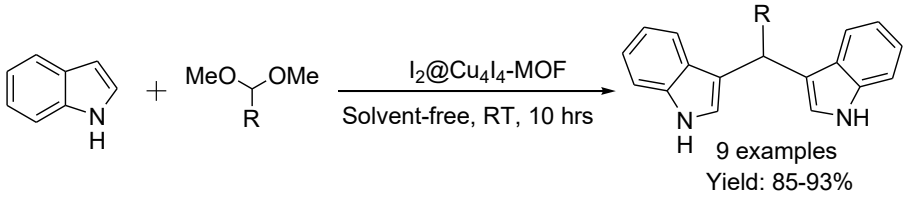

Scheme 8 Reaction of indoles with acetals for the synthesis of bis-indolylmethanes

An eco-compatible protocol for the synthesis of bis-indole derivatives via the Friedel-Crafts alkylation of indoles with aldehydes was developed by J. Tong *et al.*[6d] (Scheme 9). The reaction was found to be highly efficient, affording good to high yields of the desired alkylated products with a wide variety of substituents. The notable advantages of this protocol were simple reaction procedure, short reaction time, easy product separation, recovery, and reusability of acidic ionic liquid [DABCO-H][HSO_4].

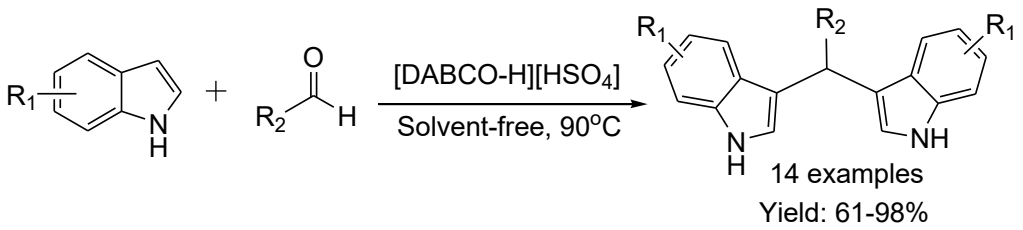

Scheme 9 Synthesis of bis-indole derivatives catalyzed by [DABCO-H][HSO_4]

Isoskeletal tetranuclear 3d/4f coordination clusters[6e] was used as an efficient catalyst for the Friedel Crafts alkylation reaction of indoles with aldehydes under ethanol-water reaction medium at room temperature (Scheme 10). A variety of aldehydes were successfully reacted and obtained the bis-indolylmethanes with good to excellent yield by using this protocol. The reaction was only limited to aromatic aldehydes. But, ketones (aromatic as well as aliphatic) did not produce any products even at longer reaction time and higher temperature.

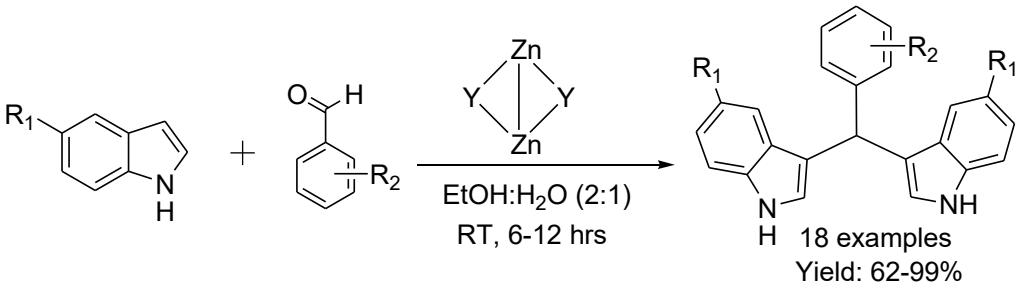

Scheme 10 Tetranuclear coordination clusters catalyzed synthesis of bis-indolylmethanes

An ultrasonic-assisted electrophilic substitution reaction of indoles with aldehydes was established by Gao *et al.*[7a] for the preparation of bis(indolyl)methanes under mild reaction conditions using ethyl lactate-water (EL: H_2O) mixture as the reaction medium (Scheme 11). Some other solvents (EtOAc, CH_3CN, PEG 400, DCM, DMF, dioxane) were also examined under ultrasound condition, but ethyl lactate/water (3:2) was found to be the most efficient reaction medium. In this process, several aromatic, hetero-aromatic and aliphatic aldehydes underwent electrophilic substitution reaction to afford the corresponding products with good yields. In addition, isatin derivatives were also equally efficient under this protocol.

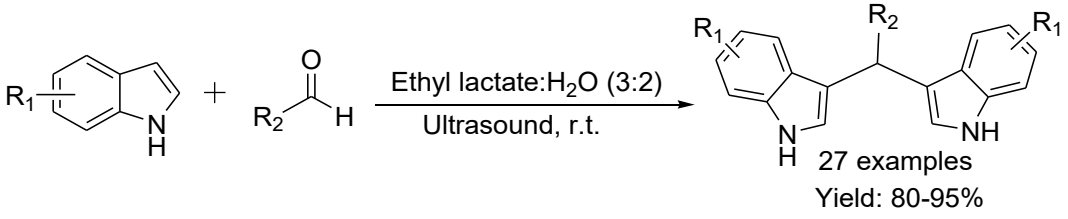

Scheme 11 Ultrasound-assisted synthesis of bis(indolyl)methanes in EL/H_2O medium

Sulfonylbis(1,4-phenylene)bissulfamic acid (SPSA) catalyzed electrophilic substitution of indole derivatives with differently substituted aromatic aldehydes was disclosed by Zeydi *et al.*[7b] under the solvent-free condition at 110°C (Scheme 12). Both electron-donating and electron-withdrawing substituents produce bis-indole derivatives with good to excellent yields. This protocol offers several advantages such as shorter reaction times, high yields of the desired products, simple work-up procedure, solvent-free conditions, and recyclability of the catalyst without much loss of its catalytic activity.

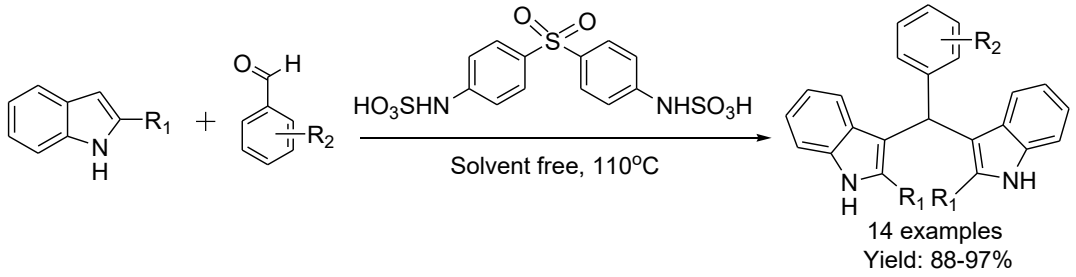

Scheme 12 SPSA catalyzed synthesis of bis-indole derivatives under solvent-free condition

Photoredox catalyzed radical reaction of indoles with ethers followed by Friedel-Crafts alkylation of another indole substrate for the synthesis of bis-indolylmethanes was reported by Loh and co-workers[7c] using $Ru(bpy)_3(PF_6)_2$ as photocatalyst and 2-methoxybenzenediazonium tetrafluoroborate as a single-electron-transfer reagent in dicholoethane solvent under Ar atmosphere (Scheme 13). Both electron-donating and electron-withdrawing groups containing substrates worked well and produced the corresponding bis-indole derivatives with moderate to good yield.

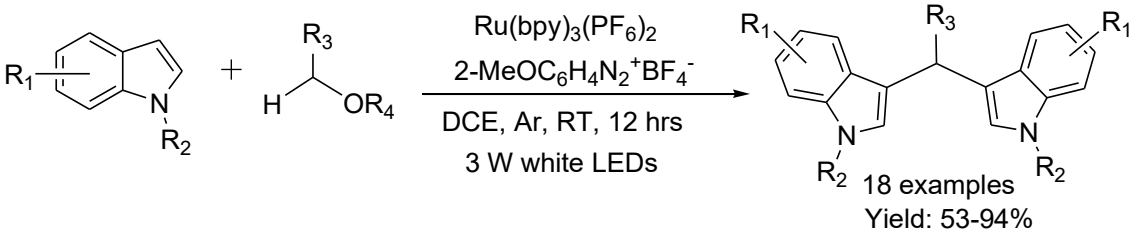

Scheme 13 Photoredox catalyzed radical reaction of indoles with ethers

Reduced graphene oxide (RGO) supported MoS_2 nanocomposite[7d] was found to be an effective heterogeneous catalyst for the synthesis of functionalized bis-indoles by the electrophilic substitution of indoles with carbonyl compounds under aqueous condition (Scheme 14). Several electron-donating, as well as electron-withdrawing substituents attached at the various position of a benzene ring, were well tolerated and produce the corresponding bis-indolylmethanes with good to excellent yield.

Scheme 14 Synthesis of bis-indolylmethanes using MoS_2@RGO nanocatalyst

Aza-crown ether ionic liquids supported on magnetic Fe_3O_4@SiO_2 core-shell particles were synthesized by Jing and co-workers[7e] and employed as an efficient heterogeneous acidic catalyst for the Friedel-Crafts alkylation of indoles with carbonyl compounds under convenient reaction conditions (Scheme 15). Aromatic as well as aliphatic aldehydes and ketones responded under this protocol and the desired alkylated products were obtained with good yields. In addition, this magnetic catalyst was readily recovered by an external magnet and reused five times without significant loss of its catalytic activity.

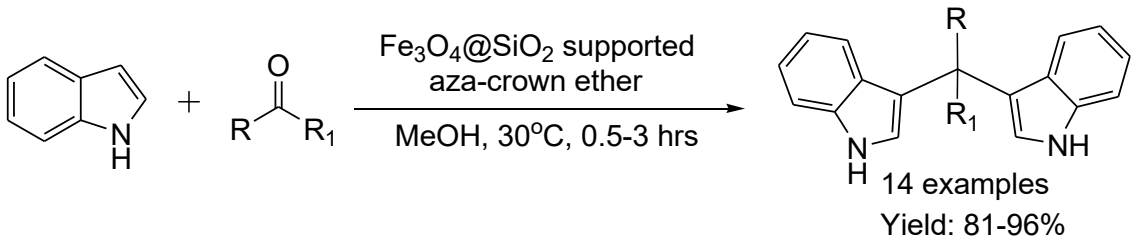

Scheme 15 Friedel-Crafts alkylation reaction of indoles with carbonyl compounds

Sami and co-workers[7f] reported a convenient approach for the three-component alkylation reaction of indoles with aromatic aldehydes using heteropoly-11-tungsto-1-vanadophosphoric acid supported on natural clay (HPVAC-20) as the recyclable catalyst under solvent-free condition (Scheme 16). The reaction was found to be versatile, affording good yields with a wide variety of substituents consisting of both electron-donating and electron-withdrawing functional groups at 70°C. The notable advantages of this protocol were lower reaction times, high yields of the products, simple work-up procedure, solvent-free conditions, and reusability of the catalyst.

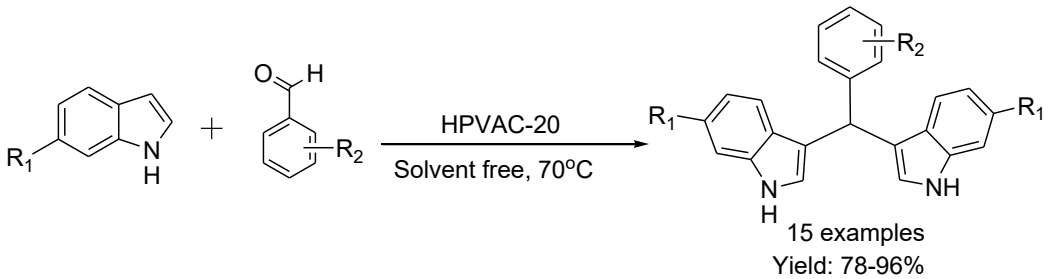

Scheme 16 HPVAC-20 catalyzed synthesis of bis-indole derivatives

The organocatalyzed Lewis acid-mediated synthesis of bis-indole derivatives was achieved by Boekell *et al.*[7g] using triarylmethyl cation as the tunable organocatalyst and dichloromethane as the solvent at 35°C (Scheme 17). Triarylmethyl cation tuning allows for the use of less reactive electrophiles by increasing the reactivity of the catalyst. In addition, this organocatalyst tuning for the less electrophilic substrate gave the desired products in good yields with a broad range of functional groups and substitution patterns. They also observed that sterically hindered aldehydes and ketones were found to be very slow to react and bis-indolylmethanes bearing cyclohexanone derivative was obtained in only 61% yield after 4 days.

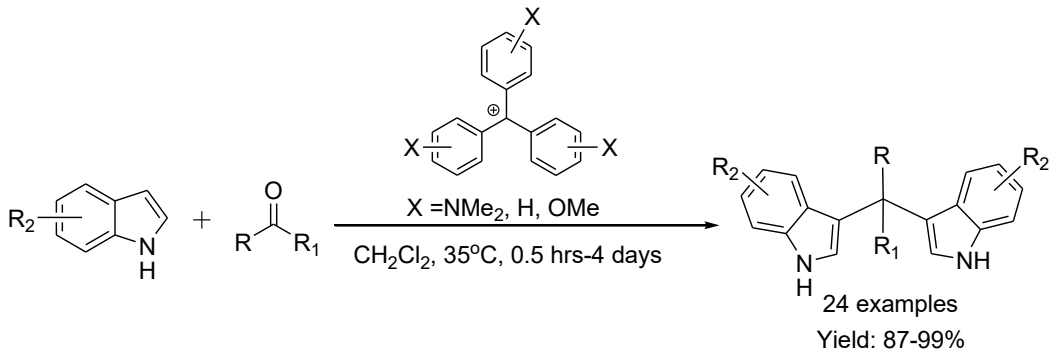

Scheme 17 Organocatalyzed Lewis acid-mediated synthesis of bis-indolylmethanes

Utilization of flow methodology for the synthesis of structurally diverse bis-indolylmethanes was described by Ley and co-workers[7h] using $Sc(OTf)_3$ as the Lewis acid catalyst and tetrahydrofuran as the solvent in both plug and continuous flow modes (Scheme 18). Excellent yields were achieved for a variety of substrates with a broad range of functional group tolerance. The reaction was highly regioselective for C-3 functionalization of indoles with aldehydes, occurring short reaction times allowing for the rapid formation of the desired products with a straightforward workup procedure.

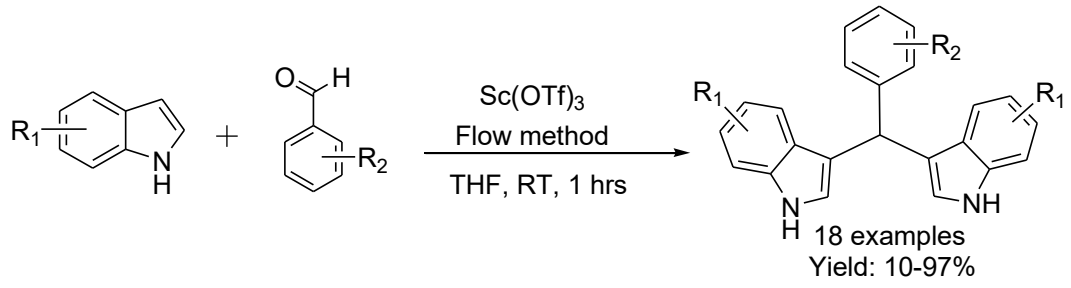

Scheme 18 $Sc(OTf)_3$ catalyzed synthesis of bis-indolylmethanes using flow method

ZnO nanoparticles uniformly distributed on the surface of reduced graphene oxide (RGO)[8a] were utilized as an efficient and heterogeneous catalyst for the electrophilic substitution of indoles with differently substituted aromatic aldehydes under ambient reaction

conditions (Scheme 19). Both aromatic, as well as aliphatic aldehydes, were found to be equally compatible under this protocol and the corresponding bis-indolylmethanes were obtained with moderate to good yields. In addition, the reactions were carried out in a green reaction medium with ethanol and water as the solvent and the absence of by-products formed in the reaction makes the strategy green and sustainable. Furthermore, the nanohybrid catalyst was recovered several times without any significant loss in catalytic activity.

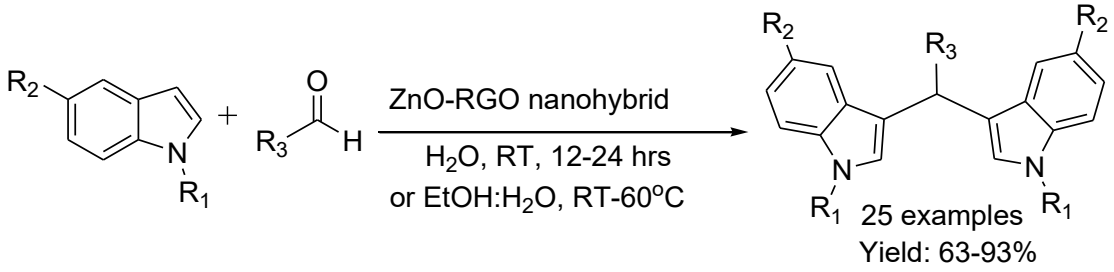

Scheme 19 Synthesis of bis-indolylmethanes using ZnO@RGO nanocatalyst

The electrochemical approach for the synthesis of bis-indolylmethanes from a broad range of indoles and ethers was described by Du *et al.*[8b] (Scheme 20). The reactions were carried out at a constant current in an undivided cell equipped with a Pt foil cathode and a Pt wire anode under ambient conditions in the presence of 10 mol% $LaCl_3$ and 0.2 M $LiClO_4$ in THF/CH_3CN (2:1) as the solvent mixture. Besides, no chemical oxidants as well as expensive reagents were required. The reaction shows a wide range of substrate scope and good functional group compatibility.

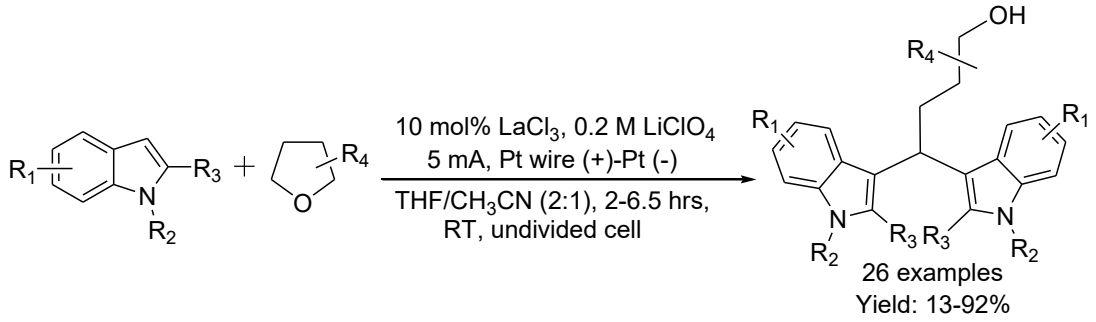

Scheme 20 Synthesis of bis-indolylmethanes through an electrochemical approach

Hyper-cross-linked polyaromatic spheres decorated with bromomethyl groups[8c] have been found as an efficient and recyclable heterogeneous catalyst for the electrophilic substitution reaction of indoles with aldehydes under the solvent-free condition at 60°C (Scheme 21). No remarkable reactivity differences were observed by the presence of electron-releasing as well as electron-withdrawing substituents in the aromatic ring. The notable features of this protocol were the easy way of catalyst synthesis, high yields of

product, environmental benignity, lower reaction time, wide substrate scope, and recyclability of the catalyst.

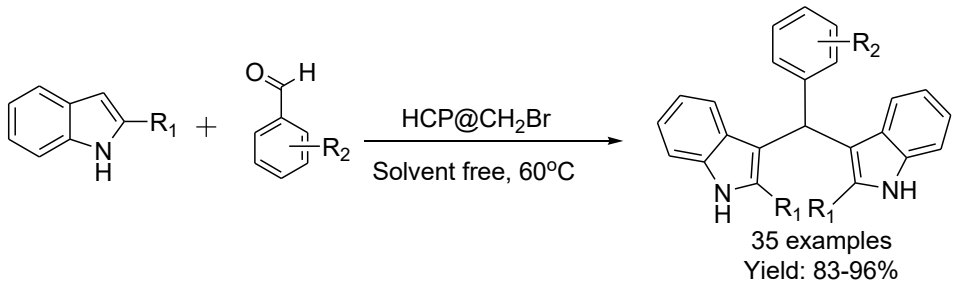

Scheme 21 HCP@CH_2Br catalyzed synthesis of bis-indolylmethanes

The Lewis acid-promoted alkylation strategy has been developed by He and co-workers.[8d] Here $B(C_6F_5)_3$ acts as Lewis acid catalyst and triethylsilane (Et_3SiH) as reductant was used for the direct functionalization of indoles at room temperature under neat condition (Scheme 22). This Friedel-Crafts alkylation reaction of indole with carboxylic acids proceeds with a broad range of substrate and good functional group tolerance. Moreover, this metal-free protocol allows selective reduction of carboxylic acids to aldehydes followed by nucleophilic attack of substituted indole at the C3 position with aldehydes to produce the corresponding product with up to 98% yield of the desired product.

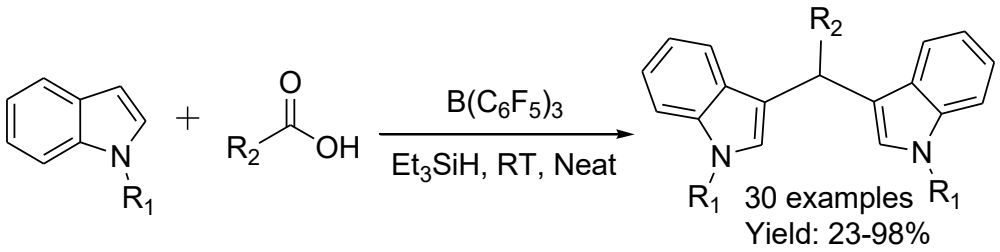

Scheme 22 Reductive coupling of indoles with carboxylic acids catalyzed by $B(C_6F_5)_3$

Tetracationic acidic organic salts (TCAOS) based on DABCO containing both hydrogen sulfate and sulfonic acidic group in the structure has been found as the green catalyst for the synthesis of bis-indolylmethanes in an aqueous medium under the ambient condition at 40°C (Scheme 23).[8e] Various aromatic aldehydes bearing both electron-donating as well as electron-withdrawing substituents on the phenyl ring are suitable substrates in this protocol with the formation of products in good to excellent yields. Due to the strong acidic character, this protocol was also applied for the synthesis of xanthenes, benzoxanthenes in water with excellent turnover frequency.

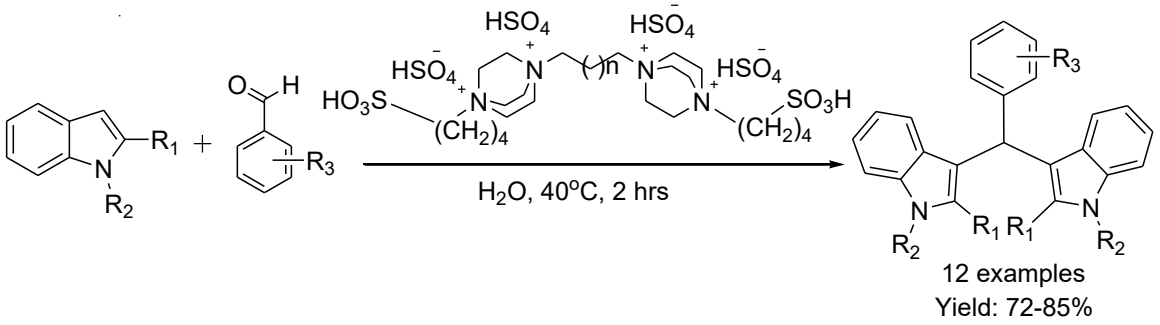

Scheme 23 TCAOS mediated synthesis of bis(indolyl)methanes

Palladium-catalyzed reductive carbonylation of aryl iodides followed by nucleophilic addition of indoles for the synthesis of bis(indolyl)methanes has been established by Qi *et al.*[8f] Here benzene-1,3,5-triyl triformate (TFBen) was used as the solid CO source and a series of aryl iodides were transformed to the corresponding aryl aldehydes in the presence of $PdCl_2(PPh_3)_2$ as the catalyst and Et_3N as the base in DMSO solvent (Scheme 24). Indoles were reacted with the in-situ generated aryl aldehydes to form the bis(indolyl)methane derivatives in moderate to excellent yields. In addition to the broad substrate scope of aryl iodides, both N-substituted and NH-free indoles were equally compatible under this protocol without any problem.

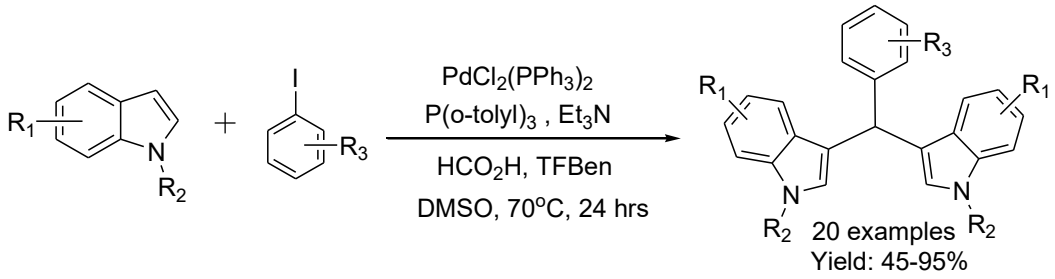

Scheme 24 Palladium-catalyzed carbonylative synthesis of bis(indolyl)methanes

Zhang *et al.*[8g] described visible-light-induced aerobic double Friedel-Craft alkylation reaction between glycine derivatives and indoles by merging photocatalysis with acid catalysis. Here, rhodamine 6G (Rh-6G) and citric acid were used as the photocatalyst and acid catalyst respectively in dichloroethane solvent under the irradiation of a 5W blue LED bulb (Scheme 25). The reaction exhibits good tolerance of functional groups and the corresponding bis(indolyl)methanes were obtained with moderate to good yields. Furthermore, the applicability of this protocol was fully demonstrated through the total syntheses of the alkaloid natural products streptindole and arsindoline B.

Scheme 25 Visible-light induced Rh catalyzed reaction of indoles with glycine esters

Sulfonic acid-substituted imidazolium-based ionic liquid functionalized magnetic silica NPs and immobilization of Ni NPs (Ni@SIL-MN) onto these NPs were synthesized and employed as an efficient catalyst for the aerobic oxidation of primary benzylic alcohols followed by nucleophilic addition of indole in aqueous medium at 80°C (Scheme 26).[8h] A wide range of bis-indole derivatives were obtained with good to excellent yield using this protocol. The catalyst was recovered using an external magnet and reused several times without much obvious less of its activity. Besides, the catalytic system was designed for the tandem oxidative synthesis of alkylacrylonitriles in an aqueous medium.

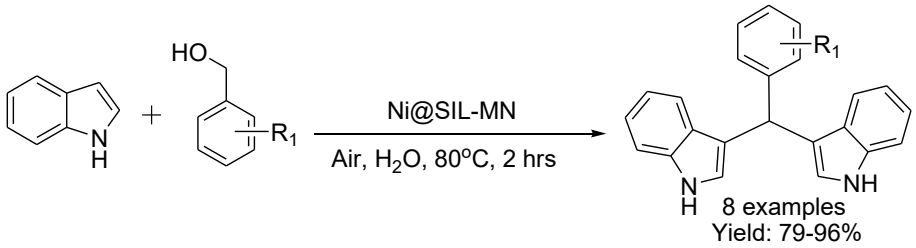

Scheme 26 Ni@SIL-MN catalysed reaction of indoles with benzyl alcohols

$PdCl_2$ catalyzed synthesis of bis-indole derivatives from the reaction of substituted indoles with a variety of aldehydes have reported by Guo and his group in toluene solvent under argon (Ar) atmosphere (Scheme 27).[9a] Indoles bearing electron-donating and electron-withdrawing groups preferably at 5 or 6 positions reacted smoothly and transformed into the desired bis(indolyl)alkanes in moderate to high yields, but 5-F and 5-NO_2 substituted indoles failed under this protocol. Several kinds of aldehydes were also efficiently performed and provided the desired products with good yields. They have also developed a CuBr catalyzed C-3 dicarbonyl indoles from the reaction of indoles with aldehydes using pyridine as the base in dioxane solvent under oxygen pressure.

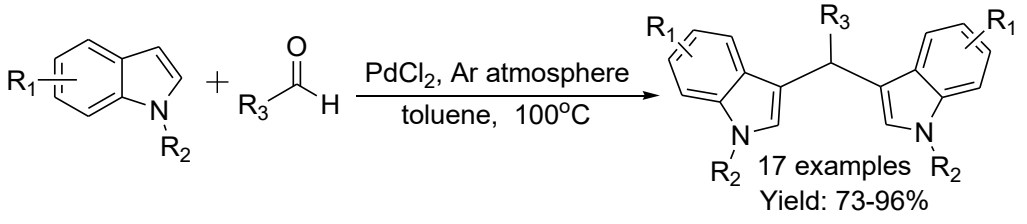

Scheme 27 $PdCl_2$-Catalyzed synthesis of bis(indolyl)methanes under Ar atmosphere

Direct cross-dehydrogenative coupling of indoles with methanol without the addition of any external additives has been developed by Qiang *et al.*[9b] using Ir/Mg_4AlO as the heterogeneous catalyst at 150°C under nitrogen atmosphere (Scheme 28). A variety of substituted indoles bearing reducible functional groups were selectively converted to their corresponding bis-indolylmethanes in moderate to good yields by using methanol as bridging methylene (−CH_2−) donor. The operational simplicity, sustainability, chemoselectivity, and reusability of the catalyst made this approach a highly step-economical tool to construct C−C bond directly from methanol in the synthesis of 3,3-CH_2-linked bis-indole derivatives.

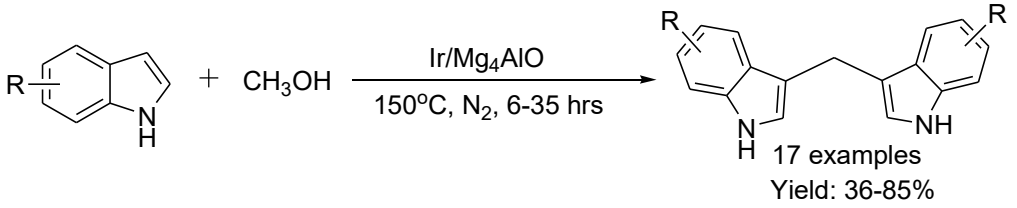

Scheme 28 Cross-dehydrogenative coupling of indoles and methanol catalyzed by Ir/Mg_4AlO

Aminocatalytic nucleophilic addition of indoles to aryl aldehydes was reported by Basumatary *et al.* for the synthesis of bis-indole derivatives via aminocatalytic addition substitution reaction (Scheme 29).[9c] Here, L-prolinamide was used as the amino-catalyst and ethanol as the eco-friendly solvent under refluxing conditions. The substituent effect of electron-donating and electron-withdrawing groups on the phenyl ring was nominal and produced the corresponding desired products in good to excellent yield. DFT studies were carried out and confirmed the addition-substitution pathway in the formation of bis(indolyl)methanes through the reaction of indole and aldehydes.

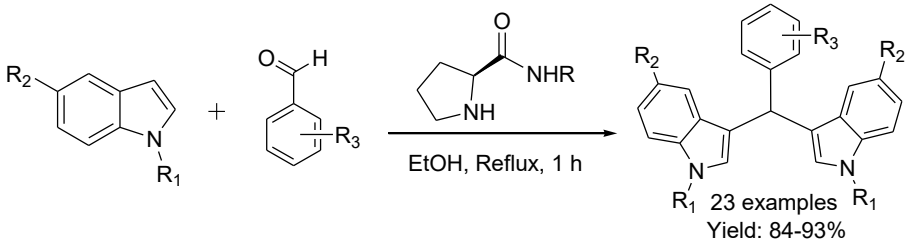

Scheme 29 Aminocatalytic nucleophilic addition of indoles to aryl aldehydes

Regioselective synthesis of symmetrical and unsymmetrical bis(heteroaryl)methane (BHM)-containing amino acids by the reaction of cyclic enecarbamate with heteroaromatics has been developed by Haq and co-workers[9d] in the presence of $AlCl_3$ as the Lewis acid catalyst and dichloromethane as the solvent at 25-60°C (Scheme 30). The methodology worked well with substituted indoles as well as with other heteroaromatics like furan and pyrrole. Also, the desired BIM-amino acids produce a new series of homologated tryptophan

analogs. Moreover, the desired products were also achieved in moderate to good yields by using this protocol.

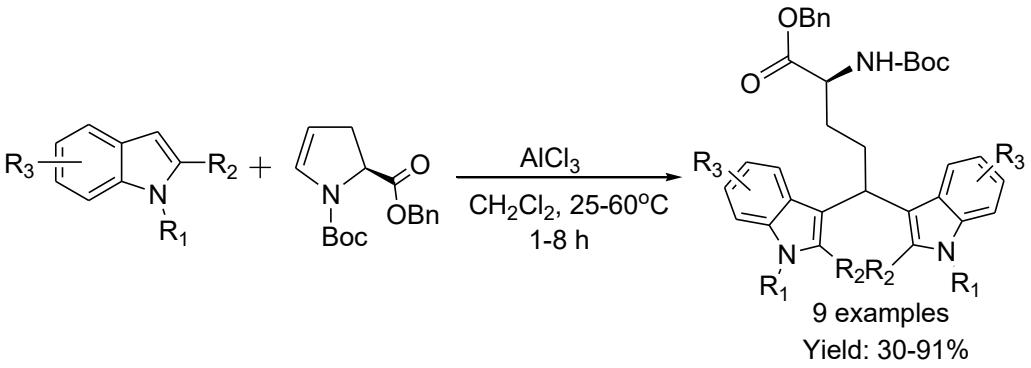

Scheme 30 $AlCl_3$ catalyzed regioselective synthesis of bis-indole derivatives

Meglumine (amino sugar sequestered from sorbitol-possessing with chemical notation $C_7H_{17}NO_5$) -catalyzed electrophilic substitution of indoles with carbonyl compounds has been developed by Nemallapudi *et al.*[9e] (Scheme 31) at ambient temperature under aqueous conditions. Clean reaction, easily available reactant, eco-friendly reaction conditions, simple workup procedure, and easy product isolation/purification are the notable advantages of this green methodology. Moreover, the synthesized bis-indolylmethane derivatives were tested for antimicrobial activity, and the results indicated that the compound having nitro substituent on the aromatic ring, exhibited an excellent potent inhibitory activity against *Pseudomonas aeruginosa* and *Penicillium chrysogenum*.

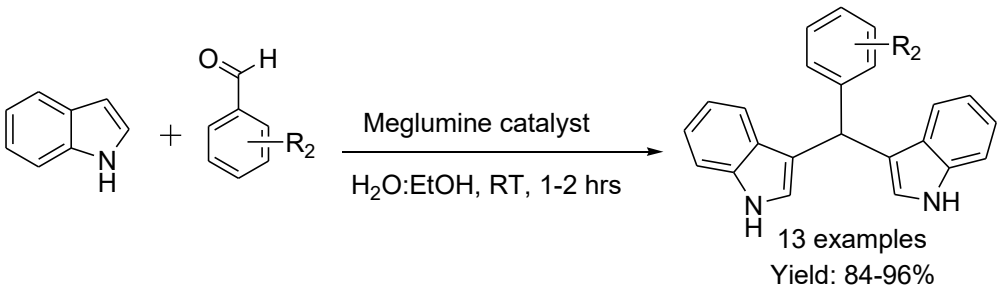

Scheme 31 Electrophilic substitution of indoles with aldehydes catalyzed by Meglumine

Transition Metal-free alkylation strategy for the synthesis of 3,3'-bisindolylmethane derivatives with excellent regioselectivity has been developed using graphene oxide[9f] as an efficient Lewis acid catalyst in acetonitrile solvent at 25°C (Scheme 32). Dichotomous catalytic behavior of the graphene oxide catalyst in the C-C bond oxidative coupling and in C-O bond cleavage has been observed. Moderate to excellent yields of the desired products were obtained with a broad indole substrate scope and excellent regioselectivities under mild reaction conditions.

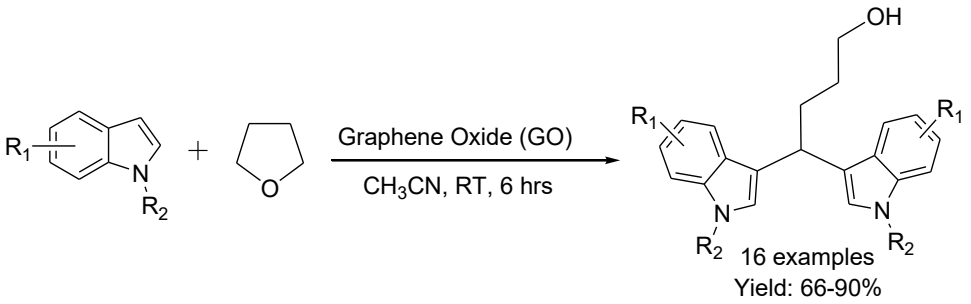

Scheme 32 Graphene oxide catalyzed reaction of indoles with ethers

An in situ developed Lewis acid-surfactant-SiO_2-combined (LASSC) nano catalytic system[9g] has been proven as a highly efficient and promoting medium for the electrophilic activation of aldehydes under microwave and grinding condition (Scheme 33). Apart from LASSC acting as a Lewis acid, it also demonstrates the surfactant activity to form stable colloidal dispersion systems with the organic molecules. The nucleophilic addition of indoles to the activated aldehydes produces a high yield of bis(indolyl)methanes. The notable advantages of using this nanocatalyst include avoiding the generation of wastewater containing sodium dodecyl sulfate, the use of expensive as well as toxic reagents, and excellent reusability of the nanocatalyst.

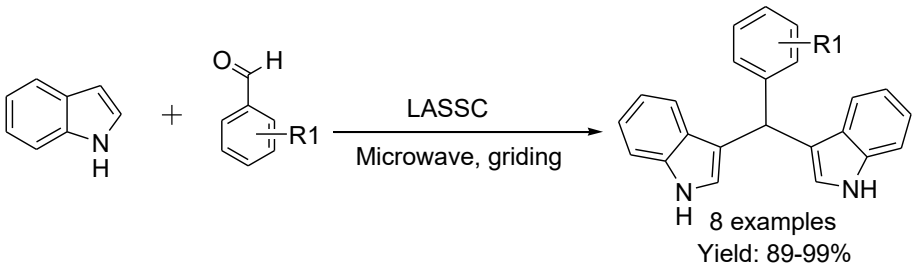

Scheme 33 LASSC catalyzed synthesis of bis-indoles under microwave condition

Asymmetric Friedel-Crafts ring-opening reaction of 3-indolylsulfamidates with indoles has been established toward the synthesis of biologically important enantioenriched bisindolylarylmethane derivatives containing the phenylsulfamate group using chiral BINOL-derived phosphoric acid as the Brønsted acidic catalyst and toluene as the solvent at room temperature (Scheme 34).[9h] A diverse range of sulfamate derivatives was achieved in good yields (up to 89%) and with moderate to high enantioselectivities (up to 94:6 er).

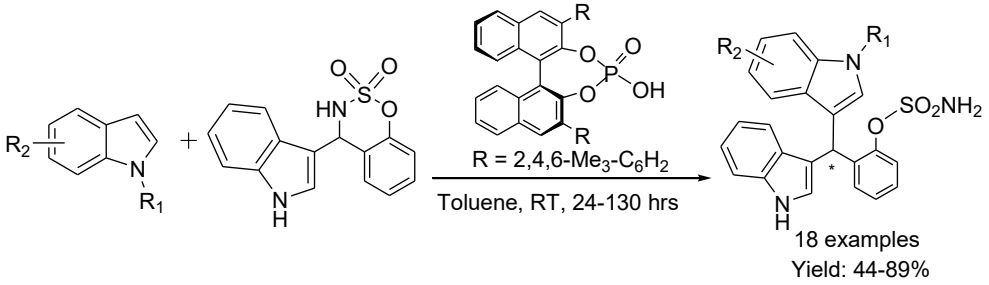

Scheme 34 Synthesis of enantioenriched bisindolylmethanes using an asymmetric catalyst

Unsymmetrical bisindolylmethanes has been synthesized by Petrini and co-workers[10a] through the Friedel-Crafts reaction of sulfonyl indoles with an excess of indoles in the presence of excess methylmagnesium bromide in THF solvent at 20°C (Scheme 35). Initially, indolylmagnesium bromides were formed by the reaction of MeMgBr with indoles at low temperature which on subsequent reaction with sulfonyl indoles to afford the corresponding unsymmetrical bisindolylmethane in moderate to good yields.

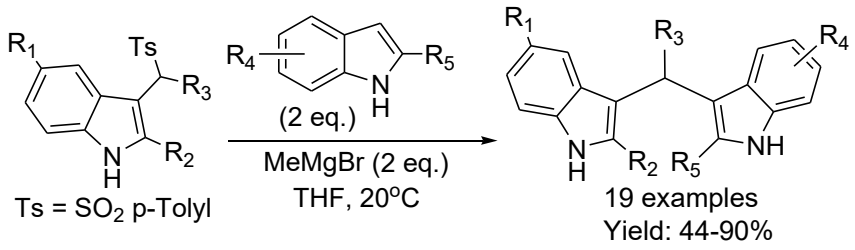

Scheme 35 MeMgBr catalyzed synthesis of unsymmetrical bisindolylmethanes

Acridine-derived air-stable Ru pincer complex catalyzed selective synthesis of bis-indolylmethanes has been developed by Biswas *et al.*[10b] in the presence of KOH at 135°C under Argon atmosphere in toluene solvent (Scheme 36). The in-situ generated aldehydes through the dehydrogenation of alcohols by Ru pincer complex reacted with differently substituted indoles to produce the desired products in moderate to good yield. Moreover, this protocol was also effective for the direct C-3 alkylation of indoles with various aliphatic primary and secondary alcohols including cyclic alcohols as well as benzylic alcohols under ace pressure tube conditions.

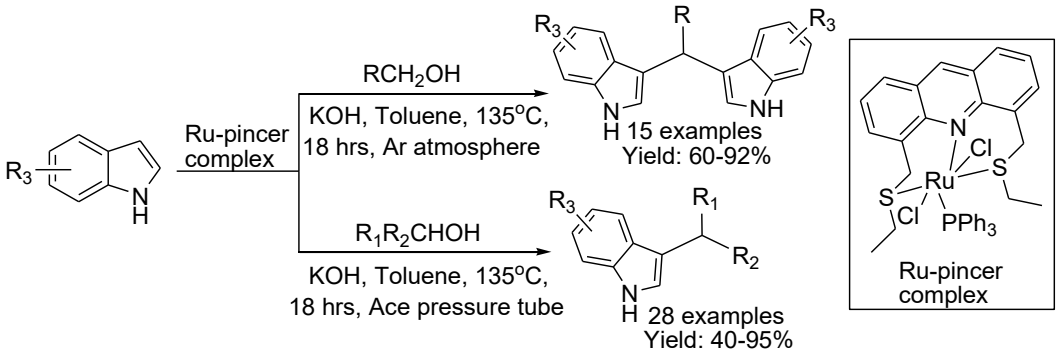

Scheme 36 Ru pincer complex catalyzed selective synthesis of bis-indolylmethanes

Enzyme catalyzed eco-friendly and highly efficient methodology for the synthesis of bis(indolyl)methanes by the reaction of indoles with aldehydes in an aqueous medium within 36-72 hours has been developed by Fu *et al.*[10c] under mild reaction conditions (Scheme 37). Several enzymes were screened to get the best result, but Lipase from *Thermomyces lanuginosus* immobilized on particle silica gel (TLIM) was found to be the effective catalyst.

Various functional groups tolerance, excellent yields, procedural simplicity, and recyclability, as well as reusability of the catalyst, were the attractive features of this method.

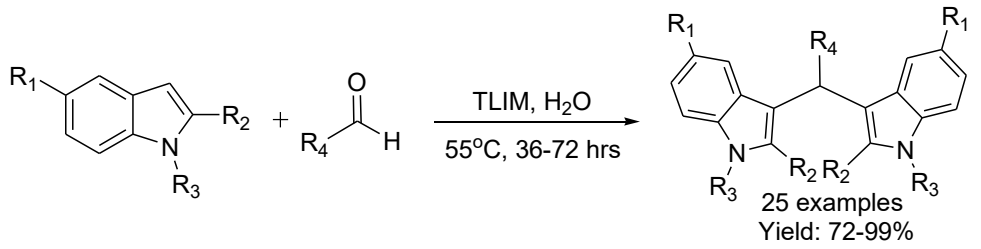

Scheme 37 TLIM catalyzed synthesis of bis-indolylmethanes in an aqueous medium

Thus the aforesaid comprehensive account provides a glimpse of different synthetic protocols for the construction of substituted bis(indolyl)methanes with a plethora of starting materials, catalysts, reagents as well as solvents and prompted to explore the urgency, essentiality, and timeliness of the recent developments going to be presented in the next section.

I.3. Present Investigation

I.3.1. Background of the Present Investigation

Bis-(indolyl)methanes (BIMs) represents one of the most abundant and important heterocycles in nature exhibiting wide-ranging biological activity. Due to their remarkable applicability in biological and medicinal sciences, the development of atom-economical and eco-friendly protocols for the synthesis of bis-(indolyl)methanes have continued to be of immense interest. Many of the previously reported protocols suffer from disadvantages such as high reaction temperature,[5b,6d,7b,9a,9b,9h,10b] harsh reaction condition,[7c,9a,9b,10b] prolonged reaction time,[5a,5d,6c,6e,7c,7d,7g,8a,8f,8g,10c] use of expensive catalysts,[5a,6a,7h,8d,8f,9a,9b,10b,10c] multistep synthesis of catalyst,[6b-6e,7d,7e,8c,8e,8h,10b] limitation in gram scale production,[5c,5d,6e,7e,9a,9c] recovery problem of the catalyst,[5a,5b,5e,6a,7c,9a,9c,10b] lack of chemoselectivity,[5c,7a,7d,7e,7g] disposal of waste,[5a,5b,5e,6a,7c,8d,8f,8g,9a,9c,10b] and use of organic solvents[5a,5b,5e,6a,7c,7g,7h,8b,8f,8g,9a,9d,9f,10a] having less scope to recover and recycle. Therefore, development of a new cost-effective and operationally simple method for the construction of BIM-framework through chemoselective transformation under mild and eco-compatible condition using easily accessible and recyclable catalyst is always of great demand and highly relevant from academic as well as applied perspectives.

The development of efficient and sustainable protocols for important organic transformations by identifying alternative reaction conditions and avoiding the use of toxic

organic solvents as reaction medium constitutes an essential target[11] of the scientific community all over the globe. In recent times, organic synthesis in aqueous conditions using nonhazardous and inexpensive catalysts has drawn tremendous interest[12] because water is considerably most abundant, safe, non-toxic, environmentally acceptable, and economically affordable reaction medium compared to other organic solvents. Macrocyclic oligosaccharides are commonly known as supramolecular catalysts possessing hydrophobic cavities which embrace the starting molecules selectively through inclusion complexes electronically as well as entropically and thus efficiently catalyze the organic reactions under milder reaction conditions compared to homogeneous counterparts, often with improved unique selectivity.[13] Cyclodextrins (CDs) and crown ethers, apart from being widely used for pharmaceutical purposes,[14a] agriculture,[14b] and molecular recognition,[14c] often demonstrate the attributes of biomimetic catalysts towards various novel organic transformations due to their unique reactivity, better biocompatibility, and economic viability. The catalytic applications[15] of CDs for the synthesis of biologically important heterocycles like thiazoles, quinazolines, quinoxalines, tryptanthrin, oxindoles, and azepins have been reported. But surprisingly the catalytic attributes of β-cyclodextrin hydrate, which behaves differently from β-cyclodextrin, have not been explored much after the maiden report from our group.[16] Inspired by the aforesaid literature precedence we initiated a detailed and systematic investigation on the catalytic efficiency of β-cyclodextrin hydrate towards the eco-friendly synthesis of bis-(indolyl)methanes through the chemoselective reaction of indoles with aldehydes in an aqueous medium where the assistive role of water molecules present inside the cavity of the β-CD hydrate was established.

I.3.2. Results and Discussion:

At the outset, the reaction between 2-methylindole **1a** (1 mmol) with 4-methoxybenzaldehyde **2a** (0.5 mmol) at 60°C in the presence of different catalysts with the variation of reaction time and catalyst loading was studied (Table 1) to obtain the product **3a**.

Table 1 Optimization of reaction conditions[a]

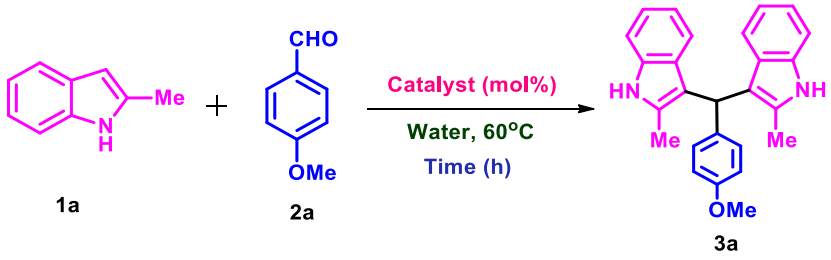

Entry	Catalyst	Mole (%)	Time (h)	Yield of 3a (%)[b]
1	- -	- -	10	- -
2	β-CD	2	3	52
3	β-CD	6	6	61
4	β-CD	8	6	68
5	β-CD hydrate	2[c]	6	80
6	**β-CD hydrate**	**4[c]**	**3**	**92**
7	β-CD hydrate	6[c]	5	92
8	β-CD hydrate	8[c]	3	93
9	α- CD	10	10	25
10	γ-CD	10	10	20
11	18-crown-6	6	8	Trace
12	Starch	6	8	--

[a]Reaction conditions: **1a** (1.0 mmol), **2a** (0.5 mmol), catalyst (as indicated), water (3mL) at 60°C. [b]Isolated yield. [c]Based on the molecular formula $C_{42}H_{70}O_{35}\cdot 11H_2O$[17]

As shown in Table 1, the reaction did not occur at all in the absence of any catalyst (Entry 1), the unreacted substrates were isolated intact. The reaction was less responsive in the presence of α-CD (Entry 9), γ-CD (Entry 10), and 18-crown-6 (Entry 11). With β-CD, **3a** was obtained with moderate yield (entries 2-4). Surprisingly, when β-CD hydrate was used as a catalyst in a lesser amount (2 mol %) the yield of the product was significantly increased to 80% (entry 5) but no reaction took place in the absence of β-CD hydrate even at the higher temperature (80°C). Therefore, the necessity, efficacy, and applicability of β-CD hydrate for this organic transformation were firmly established. Looking for an improvement in yield, the amount of catalyst was increased. The best result was obtained using 4 mol % of β-CD hydrate where the yield was increased to 92% in lesser time (entry 6). Excess catalyst beyond this proportion (4 mol %) did not afford better substrate conversion and increment of the yield (entries 7, 8). Hence the optimized condition for further studies has been chosen according to entry 6. Using starch as the catalyst in place of β-cyclodextrin hydrate, the reaction did not occur at all and the unreacted substrates were isolated intact (entry 12). The greater catalytic efficacy of β-CD hydrate in the present metal-free reaction in an aqueous medium (entries 5-8) compared to β-CD (entries 2-4) is at par with our previous experience.[16]

To further establish the efficacy of β-CD hydrate, we next carried out a comparative study between β-CD and β-CD hydrate using **1a** (1 mmol) and **2a** (0.5 mmol) in presence of H_2O and D_2O at 60°C (Table 2).

Table 2 Comparative study between β-CD and β-CD hydrate[a]

Entry	Catalyst	Solvent (3 mL)	Mole (%)	Time (h)	Conversion(%)[b]
1	β-CD	H_2O	4	3	67
2	β-CD	D_2O	4	3	28
3	β-CD hydrate	H_2O	4	3	100
4	β-CD hydrate	D_2O	4	3	62

[a]Reaction conditions: **1a** (1.0 mmol), **2a** (0.5 mmol), temperature 60°C. [b]Measured by ^{1}H NMR.

It was observed that the reactions were faster in the presence of β-CD hydrate in H_2O as well as in D_2O compared to β-CD. Furthermore, the progress of the reaction was monitored at different time intervals using β-CD and β-CD hydrate separately as catalysts under the optimized reaction condition using H_2O as well as D_2O as the reaction medium (Figure 1). It was evident from Figure 1 that the reactions in H_2O were faster than in D_2O and better conversion was achieved in the former case. Hence, the isotope effect rendered by the reaction medium has been observed. The extent of conversion using β-CD as a catalyst in H_2O was moderate. Hence the essentiality of water molecules inside the cavity of the β-CD hydrate was conclusively proved.

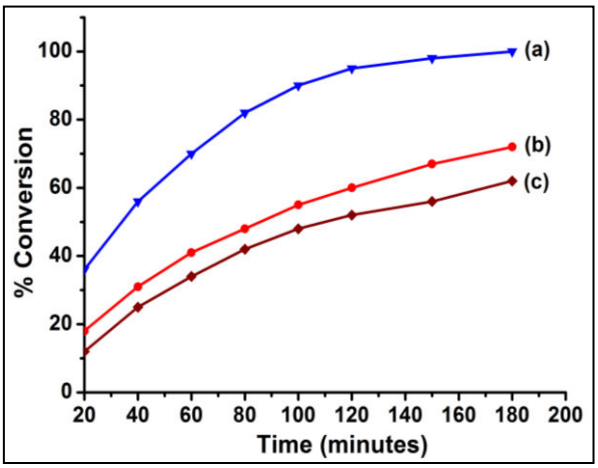

Figure 1 Plot of the percentage conversion of **3a** with time using **1a** (1.0 mmol), **2a** (0.5 mmol) and catalyst (4 mol %) at 60^{0}C in solvent (3 mL); (a) β-CD hydrate in H_2O; (b) β-CD in H_2O; (c) β-CD hydrate in D_2O.

β- CD hydrate bears negligible toxicity as evident from its MSDS.[18] This is sparingly soluble in water under ambient conditions but becomes completely miscible in the aqueous reaction medium at the reaction temperature (60°C). Thus it offers the advantages of homogeneous catalysts during the reaction as well as the benefits of heterogeneous catalysts during isolation of the products and separation of the catalyst. After the completion of the reaction, the reaction mixture was cooled in ice-water and the crude product was dissolved in ethyl acetate. The precipitated catalyst was separated by filtration, washed with ethyl acetate, dried, and reused directly in a fresh reaction with a little variation of yield (Figure 2).

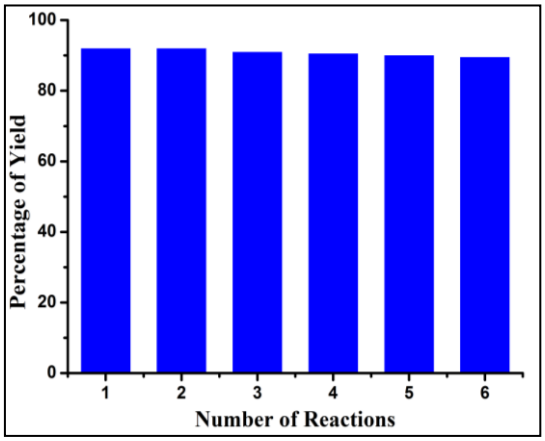

Figure 2 Recycling of β-CD hydrate using **1a** (1.0 mmol), **2a** (0.5 mmol), and β–CD hydrate (4 mol %) as the catalyst at 60°C for 3 hours in water (3 mL); % of yield was the yield of isolated product **3a**.

The present metal-free reactions took place in an aqueous condition and did not require an inert environment and any organic co-solvent as the reaction medium. It utilizes ethyl acetate as an eco-friendly solvent for the isolation of the product. Moreover, the reactions are highly atom-efficient and generate water as the sole and innocuous side-product. Therefore, this novel β-CD hydrate catalyzed metal-free reaction in an aqueous medium seems to be eco-compatible in terms of the reaction medium, operational simplicity, and recyclability of catalysts and solvents of insignificant toxicity. The green metrics calculated for the optimized reaction (between **1a** and **2a**) showed a high atom economy and small E-factor (Table 3). So this metal-free catalytic protocol in an aqueous medium is proved to be highly sustainable from the standpoints of efficacy, less toxicity, economical viability, recyclability of the catalyst as well as minimized waste formation.

Table 3 Green Metrics Calculation for "β-cyclodextin hydrate" Catalyzed Synthesis of bis-(indol-3-yl)methanes (**3a**)

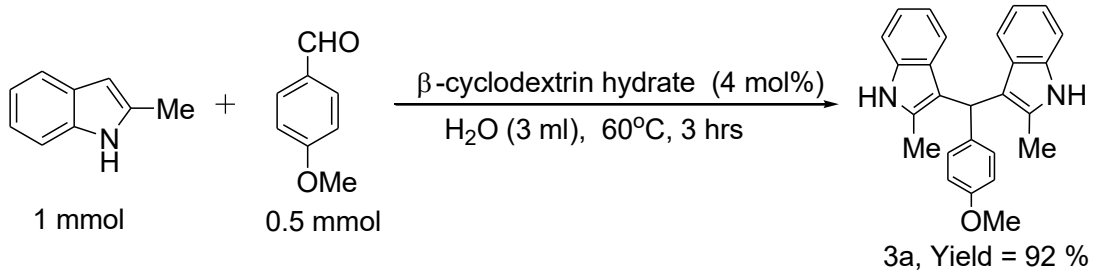

1 mmol 0.5 mmol 3a, Yield = 92 %

Entry	Input	Amount	Output	Amount
1	2-methylindole (**1a**)	131 mg	**3a**	175 mg
2	4-methoxybenzaldehyde (**2a**)	68 mg	β-CD hydrate	27 mg
3	β-CD hydrate	27 mg	Water	3000 mg
4	Water	3000 mg		
	Total	3226 mg	Total	3202 mg

E- Factor = (3226-3202)/175 = 0.14

Mass Intensity = (3226+27)/175 = 18.6

Atom Economy = 380/ (262+136) × 100 = 95.5%

Atom Efficiency = 100 % × 0.92% = 92%

The molecular docking study (Figure 3) revealed that the presence of water molecules inside the cavity of β-CD hydrate (β-CDH) might facilitate the inclusion of the benzaldehyde more effectively through hydrogen bonding than simple β-CD due to different interaction of benzaldehyde with β-CDH and β-CD with a preferred orientation of the ligands inside the cavity. The docked pose of benzaldehyde was more included within the cavity of β-CDH than β-CD. The –CHO group of benzaldehyde formed one hydrogen bond (1.78 Å) with the water molecules present within the cavity of β-CDH (Figure 3b) whereas the same formed two hydrogen bonds (2.17 Å and 2.86 Å) with the -CH_2OH group of β-CD located near the wider side (secondary hydroxy rim) (Figure 3a). However, the binding modes of 2-methylindole with β-CD and β-CDH seem to be nearly similar (Figures 3c and 3d). The hydrogen bonding interaction of benzaldehyde with the water molecules inside the β-CDH cavity (which are also believed to possess more protic behavior due to flip-flop movement) might increase the electrophilicity of the formyl carbon; therefore the nucleophilic attack of 2-methylindole on benzaldehyde seems to be facilitated. The docked pose of corresponding bis-

(indolyl)methane was more excluded through one hydrogen bonding interaction (2.86 Å) in the β-CDH whereas it was slightly included inside the cavity of β-CD (Figures 3e and 3f).

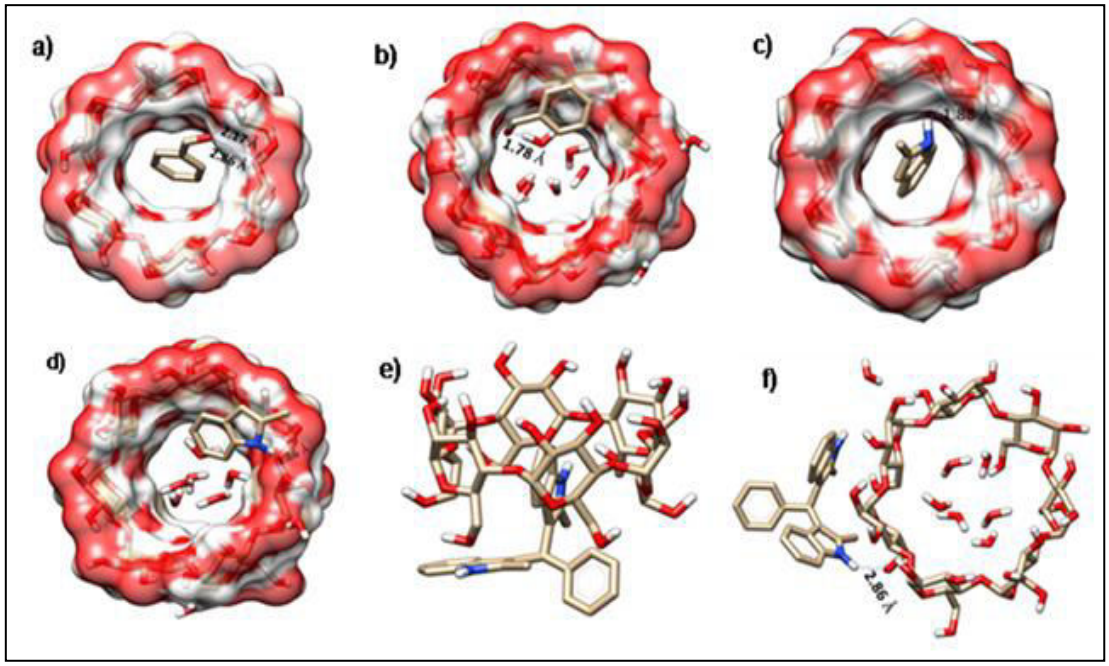

Figure 3 Docking poses showing the interaction sites of a) benzaldehyde with β-CD, b) benzaldehyde with β-CD hydrate, c) 2-methylindole with β-CD, d) 2-methylindole with β-CD hydrate, e) bis-(indolyl)methane with β-CD, f) bis-(indolyl)methane with β-CD hydrate.

We tried to get a deeper insight into the beneficiary effect of water molecules present inside the cavity of β-CD hydrate towards this aqueous reaction using density functional theory (DFT). The structures of 2-methylindole, as well as benzaldehyde with hydrogen bonded water at a distance of 1.78 Å (Figure 3b) and without hydrogen bonding (Figure 3a), were optimized (Figure 4). The result shows that the hydrogen bonding between the carbonyl oxygen and water increases the positive Mulliken charge on the carbonyl carbon (Figure 4a, ii). Thus, due to hydrogen bonding with the water molecule inside the cavity of β-CD hydrate, the electrophilicity of carbonyl carbon of benzaldehyde is increased accompanied by the greater stabilization of its HOMO and LUMO (Figure 4b). Under the hydrogen-bonded condition, HOMO and LUMO of benzaldehyde are stabilized by 0.24 eV and 0.29 eV respectively (Figure 4b). Therefore, the nucleophilic attack by 2-methylindole through its high energy HOMO to the low energy LUMO of hydrogen-bonded benzaldehyde is more facilitated with respect to benzaldehyde devoid of hydrogen bonding (Figure 4b**,** shown with the dotted line). Calculations also indicate that the orbital coefficients of frontier molecular orbitals are enhanced due to hydrogen bonding on the carbonyl carbon atom of (ii) over (i)

and its LUMO of the same symmetry with the HOMO of C_2-C_3 bond in 2-methylindole (Figure 4b). These observed results provide a supportive rationale towards the better catalytic attributes of β-CD hydrate compared to β-CD for the present reaction.

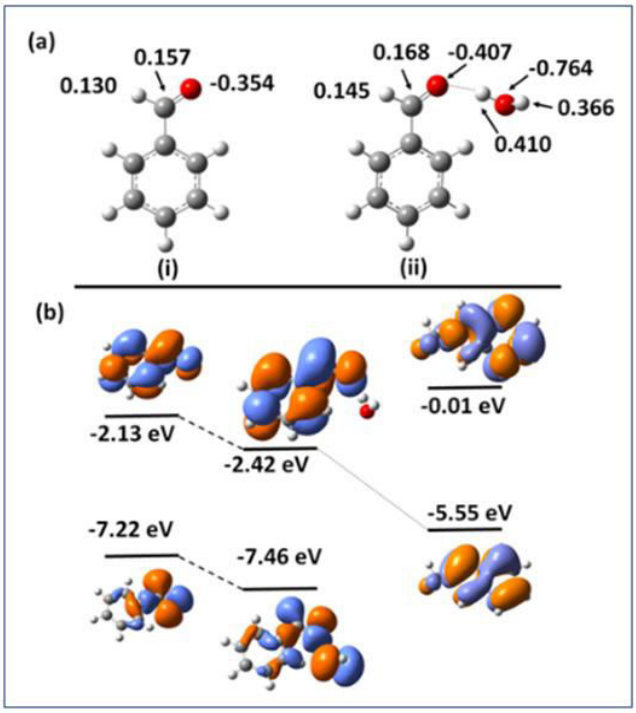

Figure 4 (a) Optimized structures of benzaldehyde with and without hydrogen-bonded water and (b) The frontier orbital energy level of HOMO and LUMO of 2-methylindole and benzaldehyde with as well as without hydrogen-bonded water.

To explore the scope and limitations of this meal-free eco-friendly protocol, indoles **1** were reacted with structurally varied aldehydes **2** in an aqueous medium in the presence of β-CD hydrate as a catalyst (Table 4). As evident from Table 4, 2-methylindole (**1a**) reacted efficiently with the benzaldehyde as well as other aryl aldehydes bearing electron-donating substituents (**2a**-**2e**) and electron-withdrawing substituents (**2f**-**2i**) to give the corresponding bis-indolylmethanes with excellent yield (**3a-3i**). The reaction between **1a** and less electrophilic aromatic aldehyde (**2e**) under the optimized condition is known as the Ehrlich test.[19] Similarly, unsubstituted indole (**1b**) was found equally efficient to participate in the same protocol to yield the corresponding products (**3n**-**3s**). Phenolic-OH groups remained unaffected during this reaction and the reaction was very facile even with the –OH group at the *ortho*-position (**3p**-**3r**). Acid-sensitive heteroaryl moieties also survived during this reaction which paved the way towards the efficient construction of important molecular skeletons densely loaded with heterocycles (**3j**, **3k,** and **3t**) in good yields.

Table 4 β-CD hydrate catalyzed reactions of indoles with aldehydes

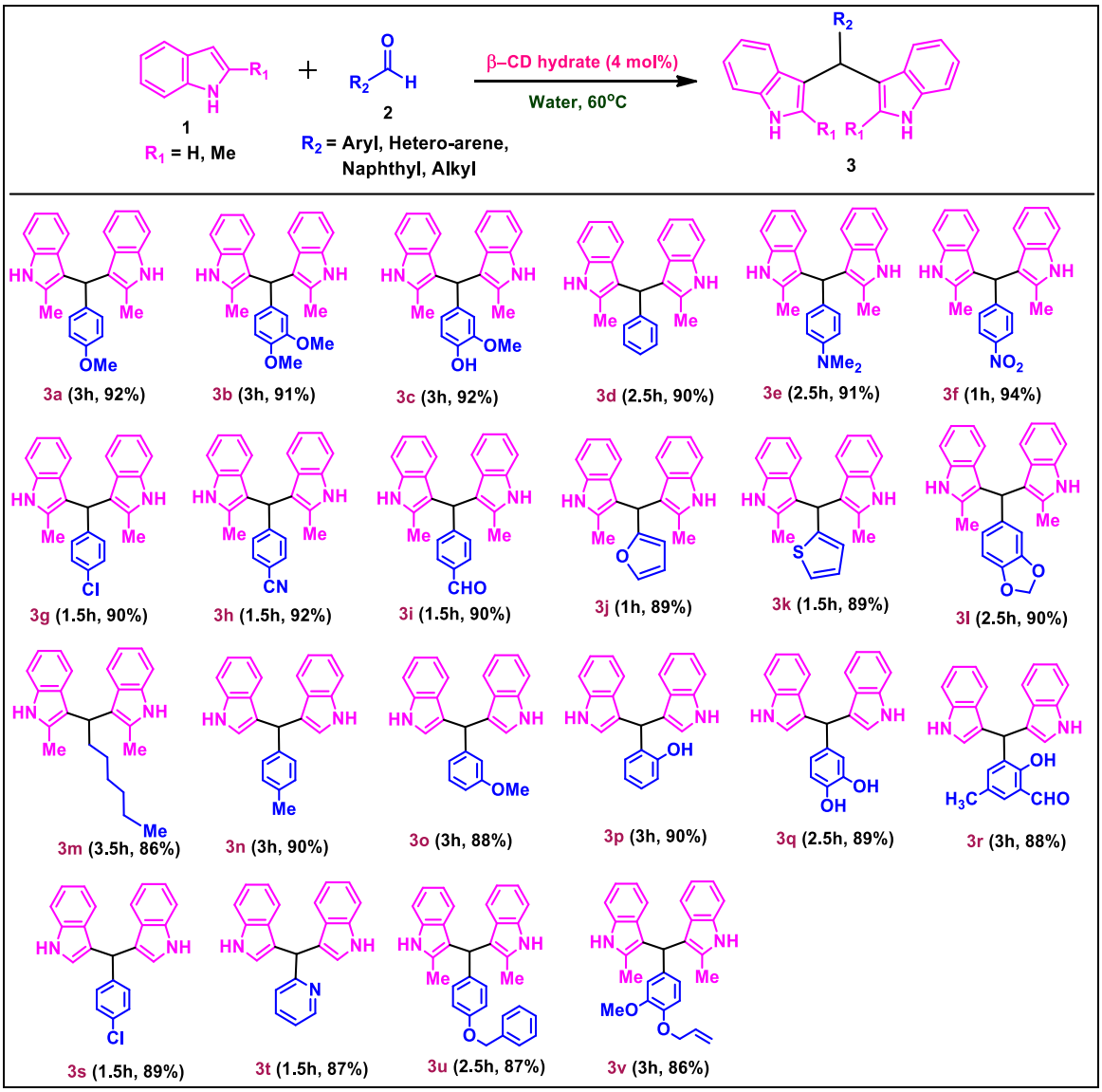

Reaction conditions: **1** (1.0 mmol), **2** (0.5 mmol), β CD hydrate (4 mol%), water (3 mL) at 60°C for indicated time.

Hydrolyzable group like methylenedioxy also remained unaffected in the aqueous reaction medium to produce **3l** in good yield. It is extremely important to note the remarkable survival of another acid-sensitive hydrolyzable functional group -CN in this aqueous protocol, where the corresponding product **3h** was obtained with 92% yield. The survival of -CN was confirmed by the signal at δ119.4 (specific for -CN) in the ^{13}C-NMR spectrum of **3h**. With terephthaldehyde (**2i**), the bis-(indolyl)methane (**3i**) was obtained in high yield (90%) where one –CHO

participated in the reaction and the other –CHO remained unaffected in spite of using a higher concentration of **1a**. A sharp singlet at δ9.96 in ^{1}H NMR spectrum, as well as a signal at δ197.0 in ^{13}C NMR spectrum, confirmed the presence of one formyl group in **3i**. Such regioselectivity was also observed in **3r.** This is an extremely important attribute of the present protocol in contrast to many reported methods where no such regioselectivity was observed.[5d,5e,7e,7f,7h,8e] Aliphatic aldehyde (**2m**) also reacted quite efficiently in the present protocol with **1a** to produce **3m** in 86% yield. Highly vulnerable groups like O-benzyl and O-allyl were also tolerated under the optimized reaction condition to furnish the products **3u** and **3v** in 87% and 86% yields respectively. The bis-(indolyl)methane (**3q**), obtained in 89% yield through the reaction between 3,4-dihydroxybenzaldehyde and **1b**, has been reported to exhibit excellent biological activity such as HIV-1 integrase inhibition.[5e]

Interestingly, aryl alkyl ketone, diaryl ketone, and dialkyl ketone (acetophenone, benzophenone, and 2-butanone respectively), as well as ester (methyl benzoate), did not react with indole under this β-CD hydrate catalyzed aqueous protocol where the substrates were recovered unaffected (List 1).

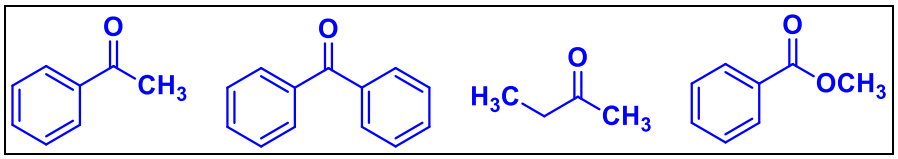

List 1 List of unreacted carbonyl compounds under the β-CD hydrate catalyzed protocol.

Encouraged by the above observations, we ventured to investigate the chemoselectivity of our newly developed aqueous protocol. Intermolecular competition reaction was carried out with a mixture of 2-methylindole (**1a**), benzaldehyde (**2d**), and acetophenone (**2w**) under the optimized reaction condition which produced **3d** (derived from benzaldehyde) exclusively, and acetophenone (**2w**) was recovered unaffected (Scheme 1).

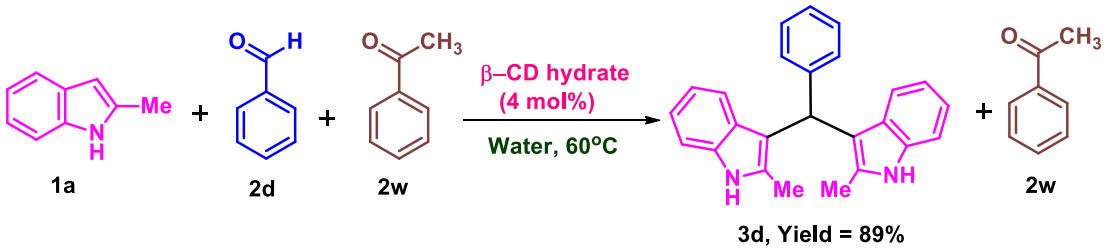

Scheme 1 Intermolecular competition experiment to demonstrate chemoselectivity.

The aforesaid protocol was further applied to the intramolecular competition experiment with 4-acetylbenzaldehyde (**2x**) where only the formyl group reacted selectively with **1a** leading to the product **4** exclusively with 90% yield leaving the keto-methyl moiety intact (Scheme 2). This is a vital and additional attribute of the said protocol in contrast to many of the earlier reports[5c,7a,7d,7e,7g] where no such chemoselectivity was observed. Survival of ketomethyl moiety in **4** was confirmed by a singlet at δ = 2.58 ppm (in the ^{1}H NMR spectrum) as well as a signal at δ = 198.3 ppm (in the ^{13}C NMR spectrum).

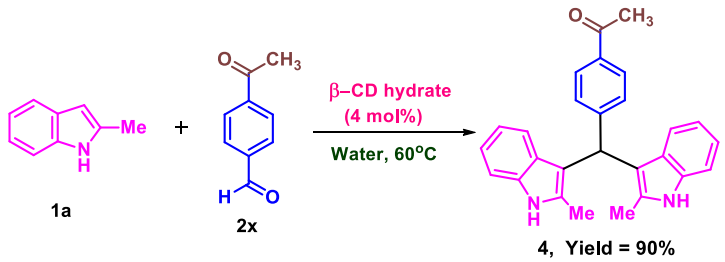

Scheme 2 Intramolecular competition experiment to demonstrate chemoselectivity.

A plausible mechanism for this β-CD hydrate catalyzed aqueous reaction is depicted in Scheme 3. Based on the aforesaid investigations (Figures 3b and 4a, ii), it is presumed that nucleophilic attack from higher energy HOMO of 2-methylindole to lower energy LUMO of benzaldehyde (due to its hydrogen bonding with the water molecules inside the cavity of β-CD hydrate) is enhanced and the intermediate (A) was rapidly formed in the first step. Subsequent dehydration of the intermediate (A) forms the corresponding 3-arylidene-3*H*-indole (B), which on the further nucleophilic attack by another 2-methylindole affords the product.

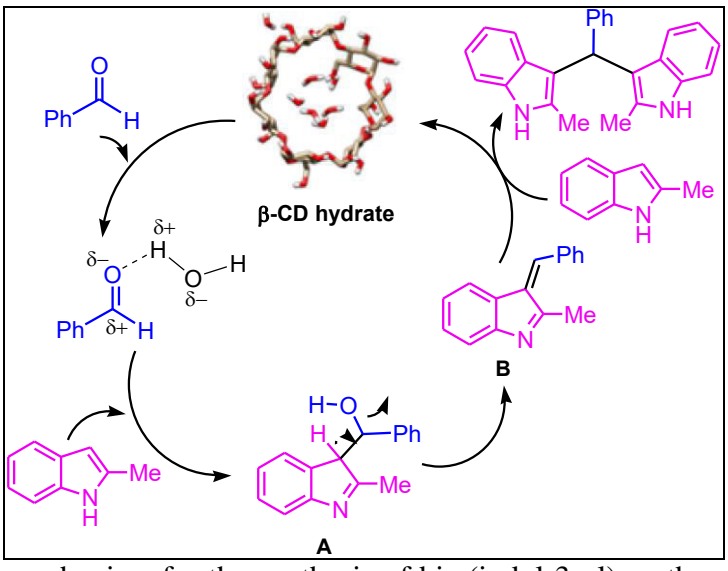

Scheme 3 Plausible mechanism for the synthesis of bis-(indol-3-yl)-methane catalyzed by β-CD hydrate.

To demonstrate the practical utility and scalability of our newly developed protocol, a gram scale reaction between **1a** and **2a** was carried out (Scheme 4). The reaction mixture was extracted with EtOAc and the crude product **3a** was further purified by filtration chromatography on a short column of silica gel using ethyl acetate-hexane as eluent.

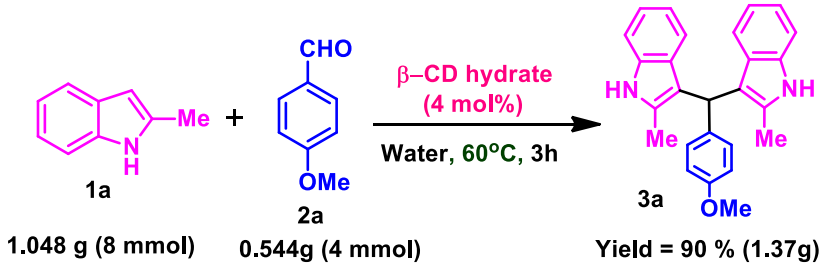

Scheme 4 Gram-scale applicability of β-CD hydrate catalyzed protocol.

The comparison of our present metal-free protocol with some of the earlier reports is summarized in Table 5.

Table 5 Comparison of the catalytic efficiency of various catalyst reported in the literature for the synthesis of 3,3'-(*p*-tolylmethylene)bis(1H-indole)

Entry	Catalyst	Solvent	Time (h), Temp(^{o}C)	Yield (%)	Ref.
1	--	Ethyl lactate: H_2O	0.5h, U.S., RT	91	7a
2	[DABCO-H][HSO_4]	--	2h, 90^{o}C	79	6d
3	α-chymotrypsin	H_2O	24h, 70^{o}C	90	5d
4	Lipase enzyme	H_2O	36h, 55^{o}C	95	10c
5	ZnO-RGO	EtOH:H_2O	12h, RT	86	8a
6	TPPMS/CBr_4	CH_3CN	4h, RT	72	20
7	β-CD hydrate	H_2O	3h, 60^{o}C	89	This work

Some of the studies listed in Table 5 (entries 1-6) involved the use of costly catalyst, multistep synthesis of catalyst, long reaction time, lack of chemoselectivity, and the tedious product isolation procedure for the synthesis of BIMs. The present β-cyclodextrin hydrate-catalyzed metal-free protocol in an aqueous medium mostly does away with these shortcomings (entry 7). Therefore, the present protocol seems to have enough potential to be a better, economically viable, eco-compatible, and sustainable alternative with greater merits and wider

applicability compared to many of the earlier methods reported for the construction of bis-(indolyl)methane framework.

I.4. Conclusion

In conclusion, the catalytic efficiency of β-cyclodextrin hydrate has been investigated towards the eco-friendly synthesis of bis-(indol-3-yl)-methanes through the reaction of indoles with aryl, heteroaryl as well as alkyl aldehydes under mild reaction condition. This newly developed atom-economical protocol shows good chemoselectivity which has been substantiated through intermolecular as well as intramolecular competition experiments. The practical synthetic utility was also demonstrated by gram scale applicability. The salient features of the present method are procedural simplicity, excellent chemoselectivity, tolerance of various sensitive moieties during the reaction, wide substrate scope as well as eco-compatibility in terms of using water as the most innocuous reaction medium, the ready accessibility and recyclability of the catalyst of lower toxicity compared to most of the existing ones, minimization of waste formation owing to high atom economy and small E-factor as well as generation of water as the sole and innocuous by-product.

I.5. Experimental

General Methods:

All organic solvents used for the synthesis were purchased from SRL, India, and were distilled before use. All reactants were purchased from SRL, AVRA Chemicals, Alfa-aesar, Spectrochem, and Sigma Aldrich and used as received without further purification. β-Cyclodextrin hydrate was purchased from Sigma Aldrich. ^{1}H and ^{13}C NMR spectra were obtained on a Bruker spectrometer (300 MHz and 400 MHz) in $CDCl_3$ and DMSO-d_6 solutions with TMS as an internal reference. Mass spectra were recorded on HRMS (Qtof micro YA263). Melting points were determined in open capillary on electrical bath which is uncorrected. Column chromatography was performed on silica gel (60-120 mesh) from SRL, India. Thin layer chromatographic separations were performed on pre-coated silica gel plates using silica gel G for TLC (E. Merck). The molecular docking studies were carried out by using the Auto Dock 4.2.0 software package. The DFT calculations were carried out by using GAUSSIAN 09 program package. All the calculations were done using Becke three parameters hybrid exchange and the

Lee-Yang-Parr correlation functional (B3LYP). 6-31G basis set was used to optimize the geometry of benzaldehyde.

General experimental procedure for the β-CD hydrate catalyzed reactions of indoles with aldehydes:

To a suspension of indole **1** (1.0 mmol), and aldehyde **2** (0.5 mmol) in water (3 mL), the β-CD hydrate (4 mol %) was added and the mixture was stirred at 60^{o}C and the progress of the reaction was monitored with TLC. After completion of the reaction, the reaction mixture was cooled to 5^{o}C, ethyl acetate (15 mL) was added to the reaction mixture and the catalyst was separated by filtration for reuse. The residual catalyst was repeatedly washed with ethyl acetate (3×5 mL). The combined organic layer was separated and dried with anhydrous sodium sulfate. The solvent was removed under reduced pressure to furnish the crude product **3**, which was further purified by column chromatography on a short column of silica gel using 5-15% ethyl acetate-hexane as eluent.

Procedure for the gram-scale synthesis of bis-(indol-3-yl)-methane (3a):

To a suspension of indole **1a** (8.0 mmol, 1.048 g), and aldehyde **2a** (4.0 mmol, 0.544 g) in water (24 mL), the β-CD hydrate (0.213 g, 4.0 mol %) was added and the mixture was stirred at 60^{o}C and the progress of the reaction was monitored with TLC. After the reaction was complete, ethyl acetate (120 mL) was added after cooling the reaction mixture to 5^{o}C. The catalyst was separated by filtration. The residual catalyst was repeatedly washed with ethyl acetate (3×40 mL). The combined organic layer was separated. After drying with anhydrous sodium sulfate, the solvent was removed under reduced pressure to furnish the crude product **3a**, which was further purified by column chromatography on a short column of silica gel using ethyl acetate-hexane as eluent. (Yield: 90%, 1.37 g).

Spectral and analytical data of the compounds:

3, 3'-((4-methoxyphenyl)methylene)bis(2-methyl-*1H*-indole)(3a)[8c]: Yield: 92%; Red solid; Mp 191-193 ^{0}C (Lit.[21e] 193–194 ^{0}C); ^{1}H NMR ($CDCl_3$, 300 MHz); δ (ppm): 7.70 (2H, br. s); 7.24-7.16 (4H, m); 7.06-6.98 (4H, m); 6.88-6.78 (4H, m); 5.94 (1H, s); 3.79 (3H, s); 2.04 (6H, s). ^{13}C NMR ($CDCl_3$, 75 MHz); δ (ppm): 157.8, 135.8, 135.0, 131.7, 129.9, 128.9, 120.5, 119.3, 119.0, 113.7, 113.4, 109.9, 55.2, 38.4, 12.4.

3, 3'-((3, 4-dimethoxyphenyl)methylene)bis(2-methyl-*1H*-indole) (3b)[21a]: Yield: 91%; Red solid; Mp 251-253 ^{0}C; ^{1}H NMR ($CDCl_3$, 300 MHz); δ (ppm): 7.73 (2H, br. s); 7.22 (1H, s); 7.05-7.00 (5H, m); 6.90-6.83 (3H, m); 6.73 (2H, s); 5.94 (1H, s); 3.85 (3H, s); 3.69 (3H, s); 2.06 (6H, s). ^{13}C NMR ($CDCl_3$, 75 MHz); δ (ppm): 148.7, 147.3, 136.3, 135.0, 131.7, 128.9, 120.8, 120.5, 119.3, 119.0, 113.5; 112.7, 110.7, 109.9, 55.8, 36.8, 12.4.

4-(bis(2-methyl-*1H*-indol-3-yl)methyl)-2-methoxyphenol (3c)[21a]: Yield: 92%; Dark red solid; Mp 227-230 ^{0}C (Lit.[21e] 227-229 ^{0}C); ^{1}H NMR ($CDCl_3$, 300 MHz); δ (ppm): 7.72 (2H, br. s); 7.26-7.22 (3H, m); 7.03 (4H, t, *J* = 7.5 Hz); 6.88-6.83 (3H, m); 6.79 (1H, s); 5.93 (1H, s); 5.50 (1H, s); 3.69 (3H, s); 2.06 (6H, s). ^{13}C NMR ($CDCl_3$, 75 MHz); δ (ppm): 146.4, 143.8, 135.6, 135.0, 131.6, 128.9, 121.6, 120.6, 119.3, 119.0, 113.8, 113.6, 111.9, 109.8, 55.9, 38.9, 12.4.

3, 3'-(phenylmethylene)bis(2-methyl-1H-indole) (3d)[8c]: Yield: 90%; Red solid; Mp 181-183 ^{0}C; ^{1}H NMR ($CDCl_3$, 300 MHz); δ (ppm): 7.73 (2H, br. s); 7.63 (2H, d, *J* = 9.0 Hz); 7.18-7.29 (4H, m); 6.96-7.08 (5H, m); 6.82-6.87 (2H, m); 6.00 (1H, s); 2.06 (6H, s). ^{13}C NMR ($CDCl_3$, 75 MHz); δ (ppm): 143.7, 135.0, 131.8, 129.1, 129.0, 128.1, 125.9, 120.6, 119.3, 119.1, 113.4, 109.9, 39.3, 12.4.

4-(bis(2-methyl-*1H*-indol-3-yl)methyl)-N,N-dimethylaniline (3e)[21a]: Yield: 91%; Dark red solid; Mp 213-216 ^{0}C; ^{1}H NMR ($CDCl_3$, 300 MHz); δ (ppm): 7.69 (2H, br. s); 7.23 (3H, t, *J* = 6.0 Hz); 7.12 (2H, d, *J* = 9.0 Hz); 7.04-6.99 (4H, m); 6.85 (2H, t, *J* = 7.5 Hz); 6.65 (2H, d, *J* = 9.0 Hz); 5.92 (1H, s); 2.90 (6H, s); 2.06 (6H, s). ^{13}C NMR ($CDCl_3$, 75 MHz); δ (ppm): 149.0, 135.0, 131.9, 131.6, 129.5, 129.1, 120.4, 119.4, 118.9, 114.1, 112.7, 109.8, 53.4, 40.9, 12.4.

3, 3'-((4-nitrophenyl)methylene)bis(2-methyl-*1H*-indole) (3f)[8c]: Yield: 94%; Dark red solid; Mp 241-243 ^{0}C (Lit.[8c] 240-242 ^{0}C); ^{1}H NMR ($CDCl_3$, 300 MHz); δ (ppm): 10.3 (2H, s); 8.57 (2H, d, *J* = 9.0 Hz); 7.93 (2H, d, *J* = 9.0 Hz); 7.78 (2H, d, *J* = 9.0 Hz); 7.48 (2H, t, *J* = 7.5 Hz); 7.39 (2H, d, *J* = 6.0 Hz); 7.29 (2H, d, *J* = 6 Hz); 6.54 (1H, s); 2.62 (6H, s). ^{13}C NMR ($CDCl_3$, 75 MHz); δ (ppm): 152.7, 145.9, 135.2, 132.6, 129.7, 128.2, 123.0, 120.1, 118.5, 111.0, 110.4, 39.8, 12.2.

3, 3'-((4-chlorophenyl)methylene)bis(2-methyl-*1H*-indole) (3g)[21b]: Yield: 90%; Red solid; Mp 200-203 ^{0}C (Lit.[21e] 202-204 ^{0}C); ^{1}H NMR ($CDCl_3$, 300 MHz); δ (ppm): 10.3 (2H, s); 7.30 (6H, t, *J* = 9.0 Hz); 7.04-6.97 (4H, m); 6.83 (2H, d, *J* = 9.0 Hz); 5.99 (1H, s); 2.17 (6H, s). ^{13}C NMR

($CDCl_3$, 75 MHz); δ (ppm): 143.7, 135.5, 132.6, 131.6, 130.9, 130.7, 129.5, 129.1, 128.5, 128.3, 120.1, 118.7, 118.5, 112.1, 110.9, 39.3, 12.3.

4-(bis(2-methyl-*1H*-indol-3-yl)methyl)benzonitrile (3h)[21b]: Yield: 92%; Dark red solid; Mp 224-227 ^{0}C; ^{1}H NMR ($CDCl_3$, 300 MHz); δ (ppm): 7.82 (2H, br. s); 7.53 (2H, d, *J* = 9.0 Hz); 7.37 (2H, d, *J* = 9.0 Hz); 7.27 (2H, d, *J* = 6.0 Hz); 7.06 (2H, t, *J* = 7.5 Hz); 6.89 (4H, t, *J* = 7.5 Hz); 6.01 (1H, s); 2.07 (6H, s). ^{13}C NMR ($CDCl_3$, 75 MHz); δ (ppm): 149.8, 135.0, 132.9, 132.0, 129.8, 128.5, 120.9, 119.4, 119.3, 119.0, 111.9, 110.2, 109.7, 39.5, 12.4.

4-(bis(2-methyl-*1H*-indol-3-yl)methyl)benzaldehyde (3i)[21c]: Yield: 90%; Red semisolid; ^{1}H NMR ($CDCl_3$, 300 MHz); δ (ppm): 10.1 (2H, br. s); 9.96 (1H, s); 7.74 (2H, d, *J* = 6.0 Hz); 7.43 (2H, d, *J* = 6.0 Hz); 7.26 (2H, d, *J* = 9.0 Hz); 6.97-6.87 (4H, m); 6.74 (2H, t, *J* = 7.5 Hz); 6.01 (1H, s); 2.10 (6H, s). ^{13}C NMR ($CDCl_3$, 75 MHz); δ (ppm): 197.0, 157.0, 140.1, 139.1, 137.4, 134.5, 134.3, 133.2, 124.8, 123.5, 123.2, 116.3, 115.3, 44.7, 17.1.

3, 3'-(furan-2-ylmethylene)bis(2-methyl-*1H*-indole) (3j)[21c]: Yield: 89%; Red solid; Mp 217-219 ^{0}C; ^{1}H NMR ($CDCl_3$, 300 MHz); δ (ppm): 10.1 (2H, br. s); 7.86 (1H, s), 7.70 (2H, d, *J* = 9.0 Hz); 7.51-7.41 (5H, m); 7.29 (2H, d, *J* = 9.0 Hz); 6.76 (1H, s); 6.33 (2H, s), 2.63 (6H, s). ^{13}C NMR ($CDCl_3$, 75 MHz); δ (ppm): 162.1, 145.5, 140.0, 136.8, 133.0, 124.7, 123.2, 123.2, 115.8, 115.2, 115.1, 112.0, 38.0, 16.6.

3, 3'-(thiophen-2-ylmethylene)bis(2-methyl-*1H*-indole) (3k)[21c]: Yield: 89%; White solid; Mp 224-227 ^{0}C; ^{1}H NMR ($CDCl_3$, 300 MHz); δ (ppm): 7.74 (2H, s); 7.22-6.29 (11H, m); 6.17 (1H, s); 2.13 (6H, s). ^{13}C NMR ($CDCl_3$, 75 MHz); δ (ppm): 148.9, 135.3, 128.6, 126.6, 125.7, 124.6, 123.8, 120.8, 119.7, 118.5, 113.8, 110.1, 34.9, 12.5.

3, 3'-(benzo[d][1,3]dioxol-5-ylmethylene)bis(2-methyl-*1H*-indole) (3l)[5c]: Yield: 90%; Dark red solid; Mp 94-97 ^{0}C; ^{1}H NMR ($CDCl_3$, 400 MHz); δ (ppm): 7.70 (2H, br. s); 7.23 (2H, t, *J* = 8.0 Hz); 7.02 (4H, t, *J* = 8.0 Hz); 6.86 (2H, t, *J* = 8.0 Hz); 6.75-6.67 (3H, m); 5.90 (3H, s); 2.04 (6H, s). ^{13}C NMR ($CDCl_3$, 75 MHz); δ (ppm): 147.5, 145.6, 137.8, 135.0, 131.7, 128.9, 121.9, 120.6, 119.7, 119.3, 119.1, 113.4, 109.6, 107.8, 100.7, 38.9, 12.4.

3, 3'-(heptane-1,1-diyl)bis(2-methyl-*1H*-indole) (3m)[21b]: Yield: 86%; Green oil; ^{1}H NMR ($CDCl_3$, 300 MHz); δ (ppm): 7.65 (2H, d, *J* = 9.0 Hz); 7.54 (2H, br. s); 7.18 (2H, d, *J* = 6.0 Hz); 7.08-6.97 (4H, m); 4.41 (1H, t); 2.28 (6H, s), 1.37-1.26 (9H, m), 0.90-0.84 (4H, m) . ^{13}C NMR

($CDCl_3$, 75 MHz); δ (ppm): 134.6, 130.3, 127.5, 118.9, 118.3, 117.4, 113.7, 109.6, 39.3, 38.8, 34.1, 31.1, 28.8, 28.5, 21.9, 13.4, 11.9.

3, 3'-(p-tolylmethylene)bis(*1H*-indole) (3n)[8c]: Yield: 90%; Red solid; Mp 101-103^{0}C (Lit.[5c] 102-105 ^{0}C); ^{1}H NMR ($CDCl_3$, 300 MHz); δ (ppm): 7.87 (2H, br. s); 7.43-7.03 (12H, m); 6.60 (2H, s); 5.87 (1H, s); 2.35 (3H, s). ^{13}C NMR ($CDCl_3$, 75 MHz); δ (ppm): 141.0, 136.7, 135.5, 128.9, 128.6, 127.1, 123.6, 121.9, 120.0, 119.8, 119.2, 111.1, 39.8, 21.1.

3, 3'-((3-methoxyphenyl)methylene)bis(*1H*-indole) (3o)[5e]: Yield: 88%; Dark Red solid; Mp 180-183 ^{0}C (Lit.[5e] 182-184 ^{0}C); ^{1}H NMR ($CDCl_3$, 300 MHz); δ (ppm): 7.91 (2H, br. s); 7.41-7.33 (4H, m); 7.22-7.14 (4H, m); 7.02-6.92 (4H, m); 6.67 (2H, s); 5.86 (1H, s); 3.73 (3H, s). ^{13}C NMR ($CDCl_3$, 75 MHz); δ (ppm): 159.5, 145.7, 136.7, 129.1, 127.1, 123.5, 121.9, 121.3, 119.9, 119.5, 119.2, 114.7, 111.2, 111.0, 55.1, 40.2.

2-(di(*1H*-indol-3-yl)methyl)phenol (3p)[5e]: Yield: 90%; Dark red solid; Mp 187-189 ^{0}C (Lit.[5e] 186-188 ^{0}C); ^{1}H NMR ($CDCl_3$, 300 MHz); δ (ppm): 7.96 (2H, br. s); 7.41-7.34 (4H, m); 7.20 (4H, t, *J* = 6.0 Hz); 7.03 (2H, t, *J* = 7.5 Hz); 6.87 (2H, t, *J* = 7.5 Hz); 6.74 (2H, s); 6.00 (1H, s); 5.43 (1H, s). ^{13}C NMR ($CDCl_3$, 75 MHz); δ (ppm): 154.5, 136.9, 129.9, 129.0, 128.0, 126.8, 123.6, 122.3, 120.8, 119.9, 119.6, 117.2, 116.6, 111.2, 35.9.

4-(di(*1H*-indol-3-yl)methyl)benzene-1,2-diol (3q)[21f]: Yield: 89%; Dark red solid; Mp 232-235 ^{0}C; ^{1}H NMR ($CDCl_3$, 300 MHz); δ (ppm): 8.03 (2H, br. s); 7.70 (2H, d, *J* = 9.0 Hz); 7.60 (1H, s); 7.39 (3H, t, *J* = 7.5 Hz); 7.25-7.16 (5H, m); 6.46 (2H, s), 5.74 (1H, s), 5.30 (2H, s). ^{13}C NMR ($CDCl_3$, 75 MHz); δ (ppm): 143.0, 141.8, 137.2, 136.6, 135.8, 127.8, 124.2, 123.6, 121.9, 120.7, 119.9, 119.6, 115.8, 111.2, 102.5, 39.4.

3-(di(*1H*-indol-3-yl)methyl)-2-hydroxy-5-methylbenzaldehyde (3r): Yield: 88%; Red solid; Mp 172-174 ^{0}C; ^{1}H NMR (DMSO-d_6, 300 MHz); δ (ppm): 11.15 (1H, s); 10.83 (2H, br. s); 9.95 (1H, s); 7.27-7.37 (6H, m); 7.03 (2H, t, *J* = 9 Hz); 6.82-6.89 (4H, m); 6.26 (1H, s); 2.28 (3H, s). ^{13}C NMR (DMSO-d_6, 75 MHz); δ (ppm): 197.8, 156.2, 137.7, 137.1, 133.3, 131.8, 128.6, 127.1, 124.2, 121.4, 121.0, 119.2, 118.7, 117.5, 112.0, 32.0, 20.5; HRMS (ESI-TOF, m/z) calculated for $C_{25}H_{20}N_2O_2$ [M + H^+] 381.1605, found 381.2796.

3, 3'-((4-chlorophenyl)methylene)bis(*1H*-indole) (3s)[5c]: Yield: 89%; Red solid; Mp 72-75 ^{0}C (Lit.[5c] 74–75 ^{0}C); ^{1}H NMR ($CDCl_3$, 300 MHz); δ (ppm): 7.74 (2H, br. s); 7.42-7.04 (12H, m);

6.55 (2H, s), 5.88 (1H, s). ^{13}C NMR ($CDCl_3$, 75 MHz); δ (ppm): 142.6, 136.7, 131.8, 130.1, 128.4, 126.9, 123.7, 122.1, 119.8, 119.4, 119.1, 111.2, 39.6.

3, 3'-(pyridin-2-ylmethylene)bis(*1H*-indole) (3t)[21d]: Yield: 87%; Dark red solid; Mp 135-137 ^{0}C; ^{1}H NMR ($CDCl_3$, 300 MHz); δ (ppm): 8.54 (1H, d, *J* = 7.5 Hz); 8.16 (2H, br. s); 7.62 (1H, t, *J* = 7.5 Hz); 7.36 (5H, t, *J* = 9.0 Hz); 7.15 (4H, t, *J* = 7.5 Hz); 7.00 (2H, t, *J* = 9.0 Hz); 6.78 (2H, s), 6.09 (1H, s). ^{13}C NMR ($CDCl_3$, 75 MHz); δ (ppm): 163.4, 149.3, 136.6, 136.5, 127.0, 123.4, 122.9, 121.9, 121.3, 119.8, 119.2, 118.2, 111.0, 43.1.

3, 3'-((4-(benzyloxy)phenyl)methylene)bis(2-methyl-*1H*-indole) (3u)[21e]: Yield: 87%; Red solid; Mp 206-208 ^{0}C (Lit.[21e] 205-207 ^{0}C); ^{1}H NMR ($CDCl_3$, 300 MHz); δ (ppm): 7.63 (2H, br. s), 7.46-7.37 (5H, m), 7.20 (4H, t, *J* = 7.6 Hz); 7.07-7.01 (4H, m); 6.90-6.86 (4H, m); 5.96 (1H, s), 5.05 (2H, s), 2.02 (6H, s). ^{13}C NMR ($CDCl_3$, 75 MHz); δ (ppm): 157.1, 137.2, 136.2, 135.0, 131.7, 129.9, 128.9, 128.5, 127.8, 127.5, 120.5, 119.4, 119.0, 114.5, 113.6, 109.9, 70.1, 38.4, 12.3.

3, 3'-((4-(allyloxy)-3-methoxyphenyl)methylene)bis(2-methyl-*1H*-indole) (3v): Yield: 86%; Dark red semisolid; ^{1}H NMR ($CDCl_3$, 400 MHz); δ (ppm): 7.71 (2H, br. s), 7.20 (2H, d, *J* = 8.4 Hz); 7.05-7.02 (4H, m); 6.92 (1H, s); 6.89-6.85 (2H, m); 6.74 (2H, t, *J* = 8.0 Hz); 6.08 (1H, m); 5.94 (1H, s); 5.39 (1H, dd, J_1 = 16.0 Hz, J_2 = 1.2 Hz); 5.26 (1H, dd, J_1 = 10.2 Hz, J_2 = 1.2 Hz); 4.58 (2H, d, *J* = 5.2 Hz); 3.67 (3H, s); 2.01 (6H, s). ^{13}C NMR ($CDCl_3$, 100 MHz); δ (ppm): 149.5, 146.4, 137.6, 137.0, 135.2, 133.7, 131.8, 129.0, 125.4, 121.3, 120.6, 119.8, 119.5, 119.1, 117.8, 113.7, 113.4, 110.5, 70.1, 56.0, 38.9, 12.4. HRMS (ESI-TOF, m/z) calculated for $C_{29}H_{28}N_2O_2$ [M^+] 436.2151, found 436.2689.

1-(4-(bis(2-methyl-1H-indol-3-yl)methyl)phenyl)ethanone (4): Yield: 90%; Red solid; Mp 171-173 ^{0}C; ^{1}H NMR ($CDCl_3$, 300 MHz); δ (ppm): 7.85 (2H, d, *J* = 6.0 Hz); 7.79 (2H, br s); 7.36 (2H, d, *J* = 9.0 Hz); 7.25 (2H, d, *J* = 9.0 Hz); 7.02-7.08 (2H, m); 6.96 (2H, d, *J* = 6.0 Hz); 6.83-6.89 (2H, m); 6.03 (1H, s); 2.58 (3H, s); 2.05 (6H, s). ^{13}C NMR ($CDCl_3$, 75 MHz); δ (ppm): 198.3, 150.0, 135.2, 135.1, 132.1, 129.4, 128.8, 128.5, 120.9, 119.4, 119.3, 112.6, 110.2, 39.5, 29.8, 12.5. HRMS (ESI-TOF, m/z) calculated for $C_{27}H_{24}N_2O$ [M^+ + Na^+] 415.1786, found 415.3459.

^{1}H NMR and ^{13}C NMR Spectra of Some Representative Compounds

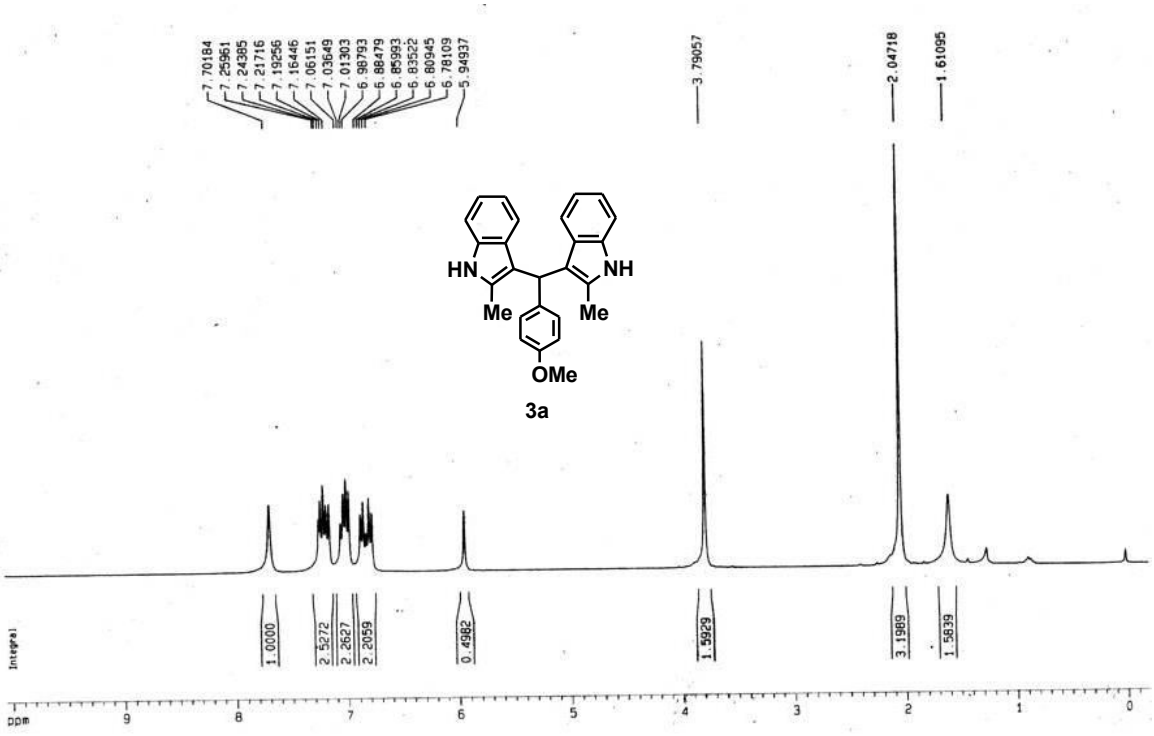

Figure 1: ^{1}H NMR of 3,3'-((4-methoxyphenyl)methylene)bis(2-methyl-*1H*-indole)(3a).

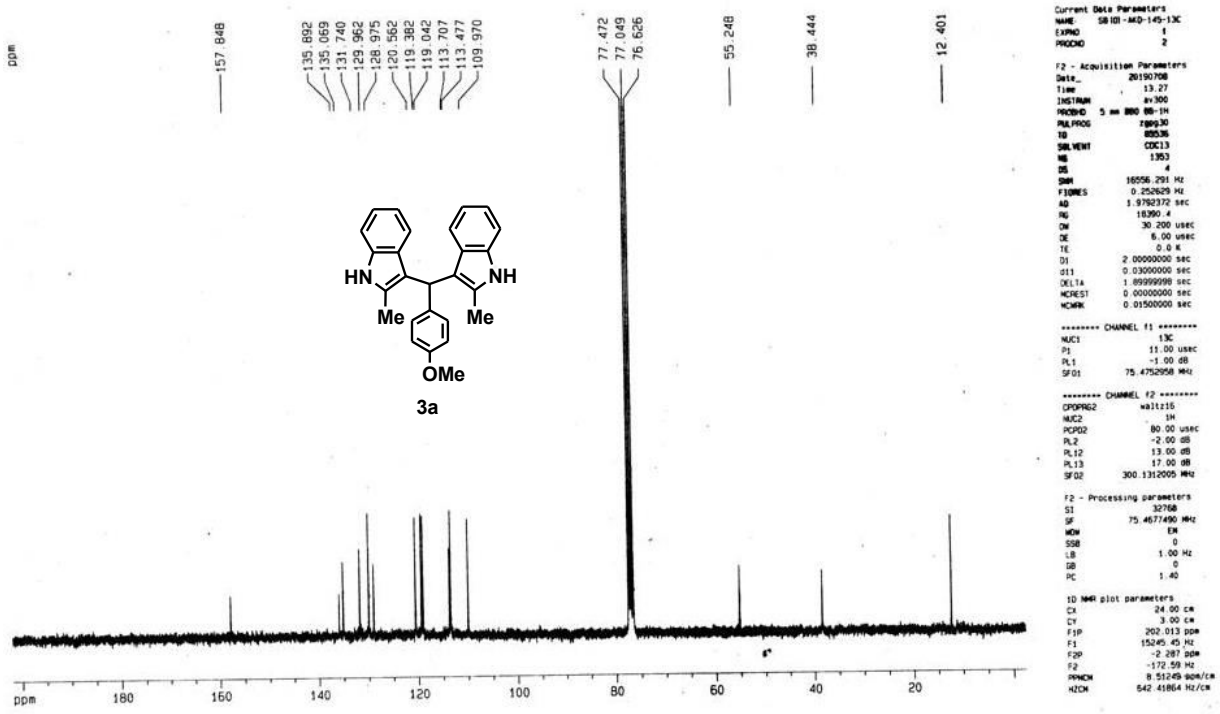

Figure 2: ^{13}C NMR of 3,3'-((4-methoxyphenyl)methylene)bis(2-methyl-*1H*-indole)(3a).

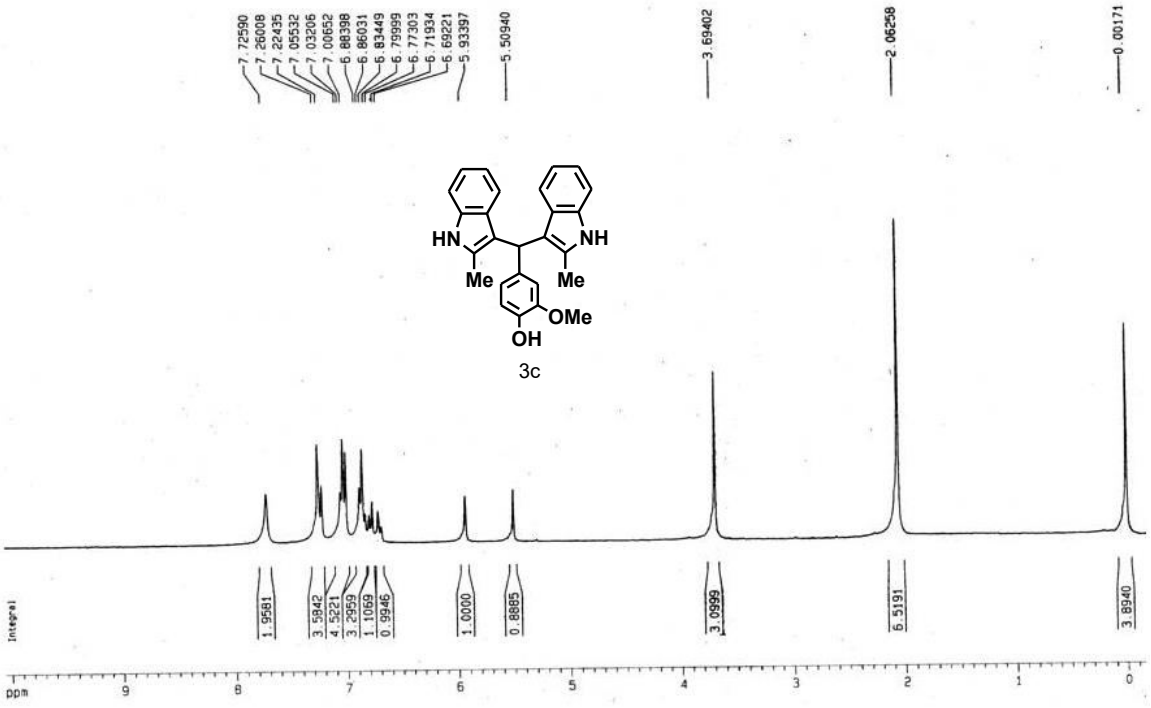

Figure 3: [1]H NMR of 4-(bis(2-methyl-*1H*-indol-3-yl)methyl)-2-methoxyphenol (3c).

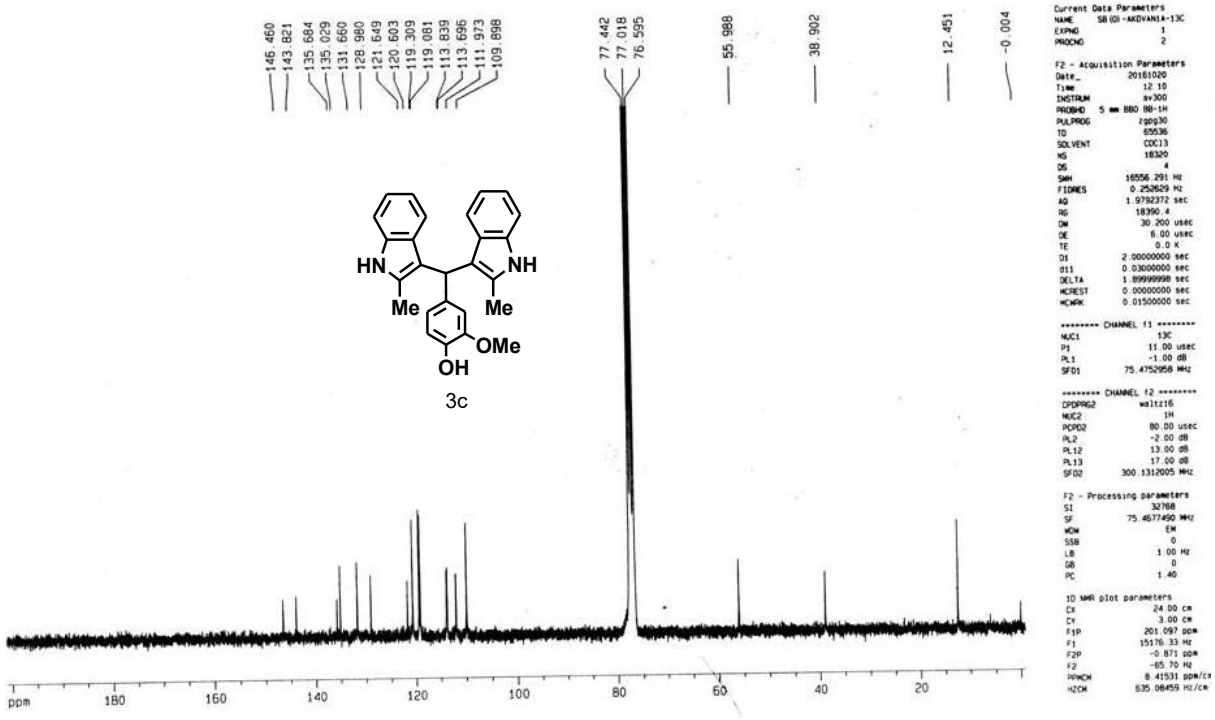

Figure 4: [13]C NMR of 4-(bis(2-methyl-*1H*-indol-3-yl)methyl)-2-methoxyphenol (3c).

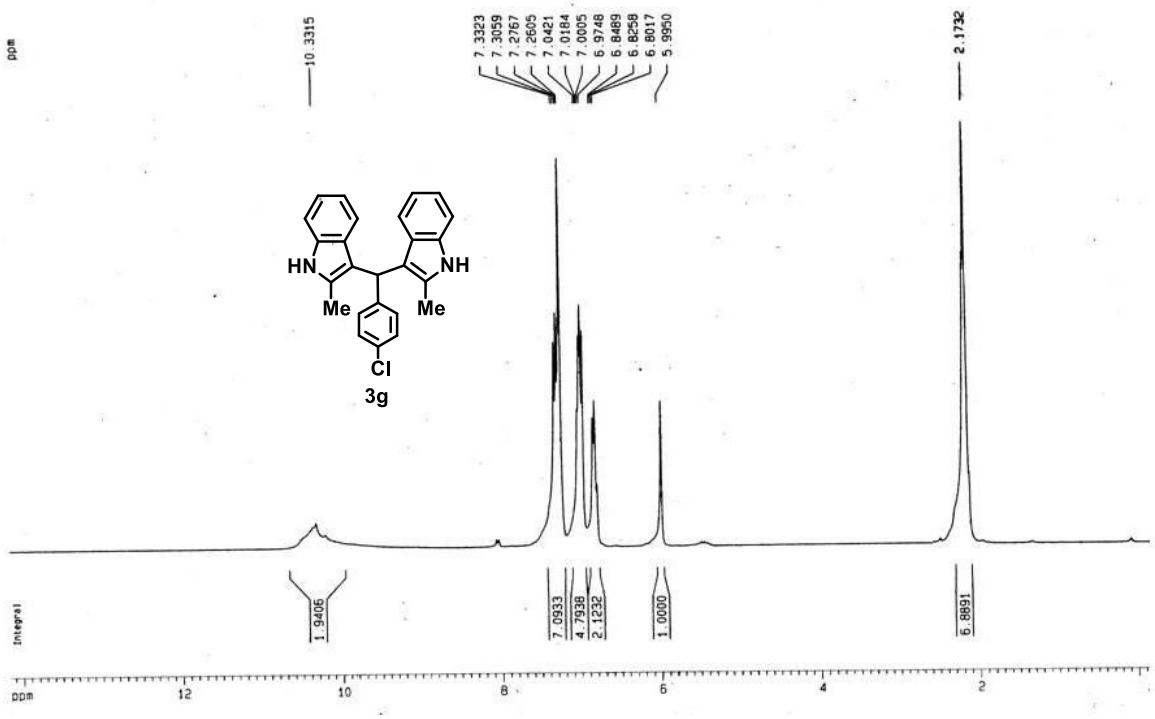

Figure 5: ^{1}H NMR of 3, 3'-((4-chlorophenyl)methylene)bis(2-methyl-*1H*-indole) (3g).

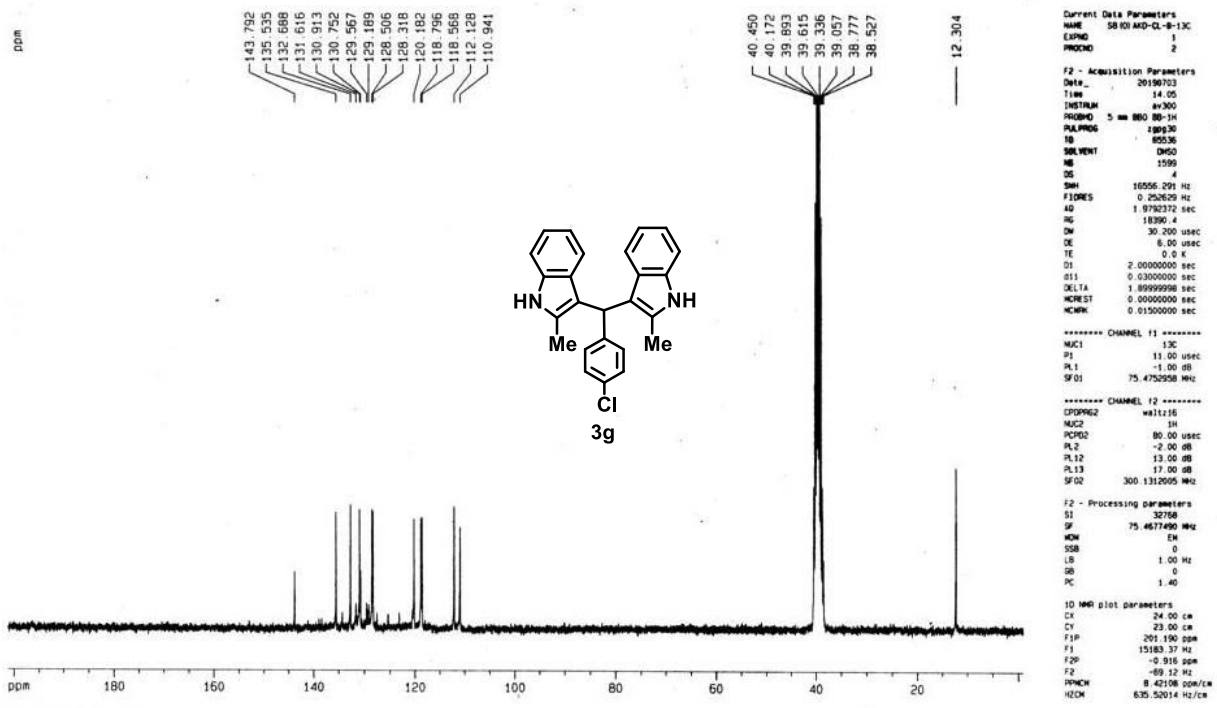

Figure 6: ^{13}C NMR of 3, 3'-((4-chlorophenyl)methylene)bis(2-methyl-*1H*-indole) (3g).

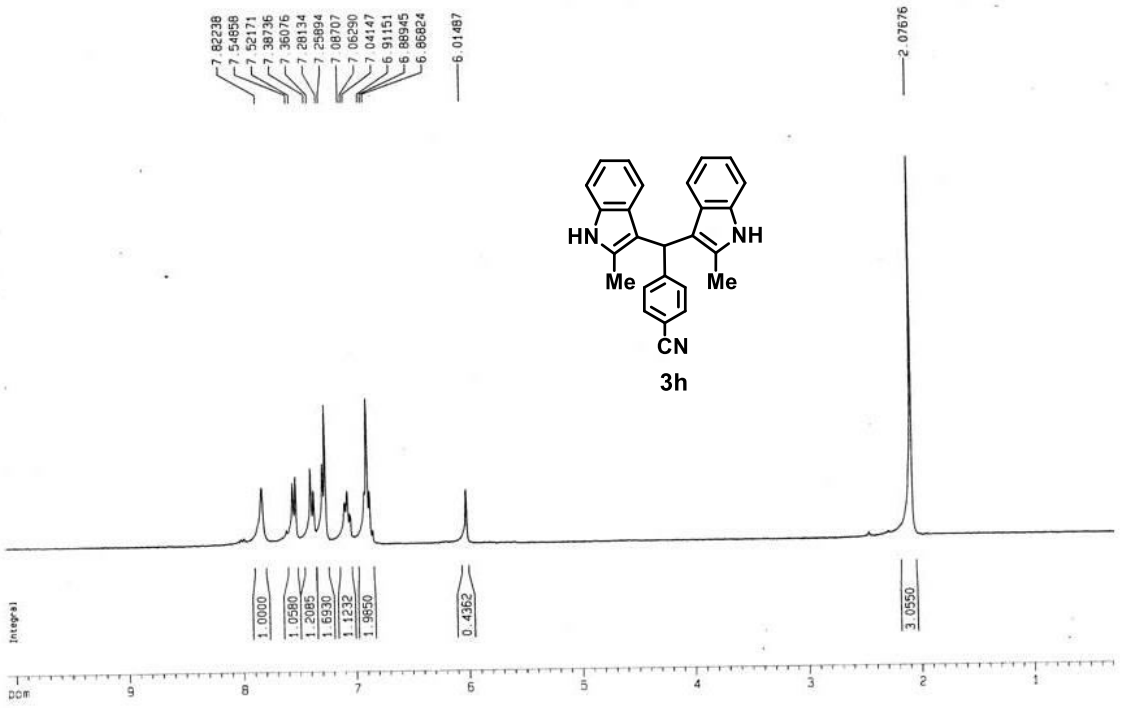

Figure 7: [1]H NMR of 4-(bis(2-methyl-*1H*-indol-3-yl)methyl)benzonitrile (3h).

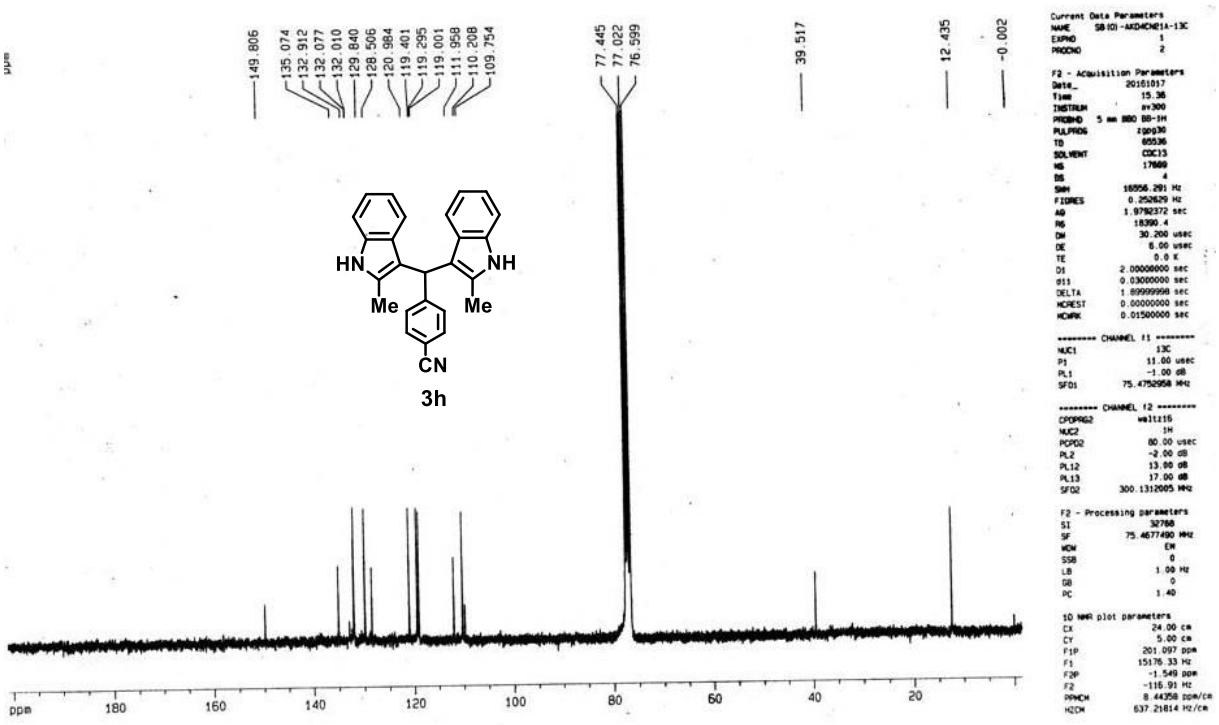

Figure 8: [13]C NMR of 4-(bis(2-methyl-*1H*-indol-3-yl)methyl)benzonitrile (3h).

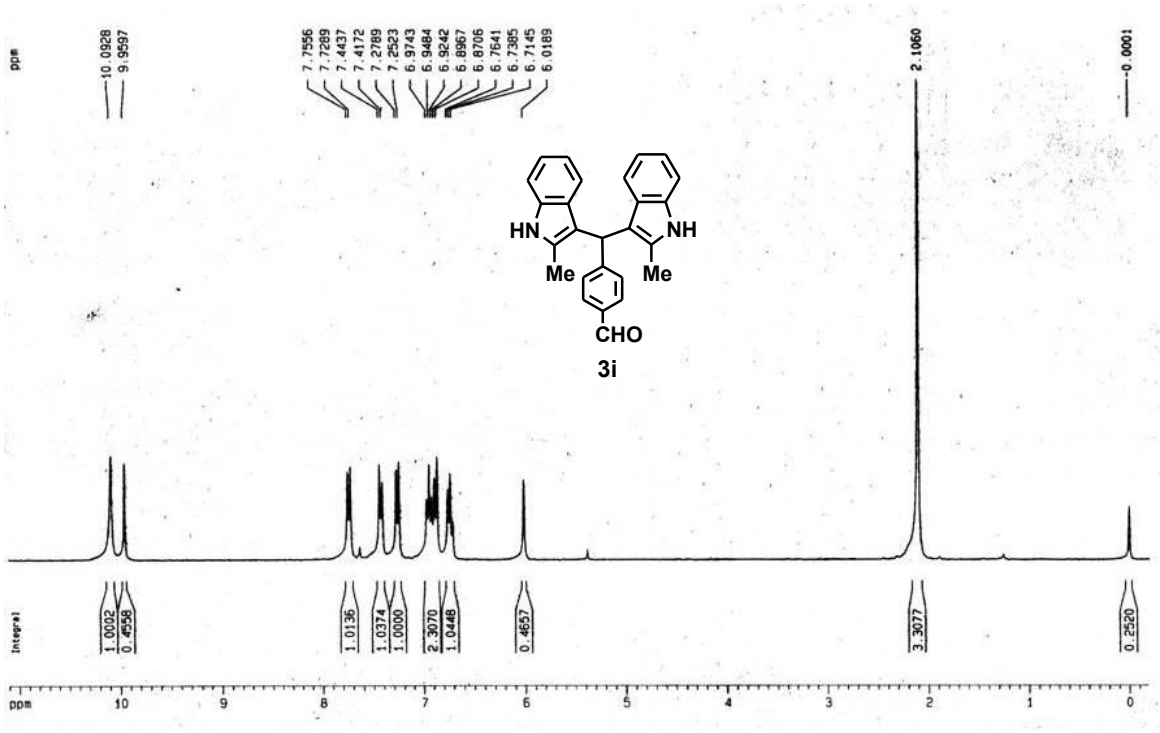

Figure 9: [1]H NMR of 4-(bis(2-methyl-*1H*-indol-3-yl)methyl)benzaldehyde (3i).

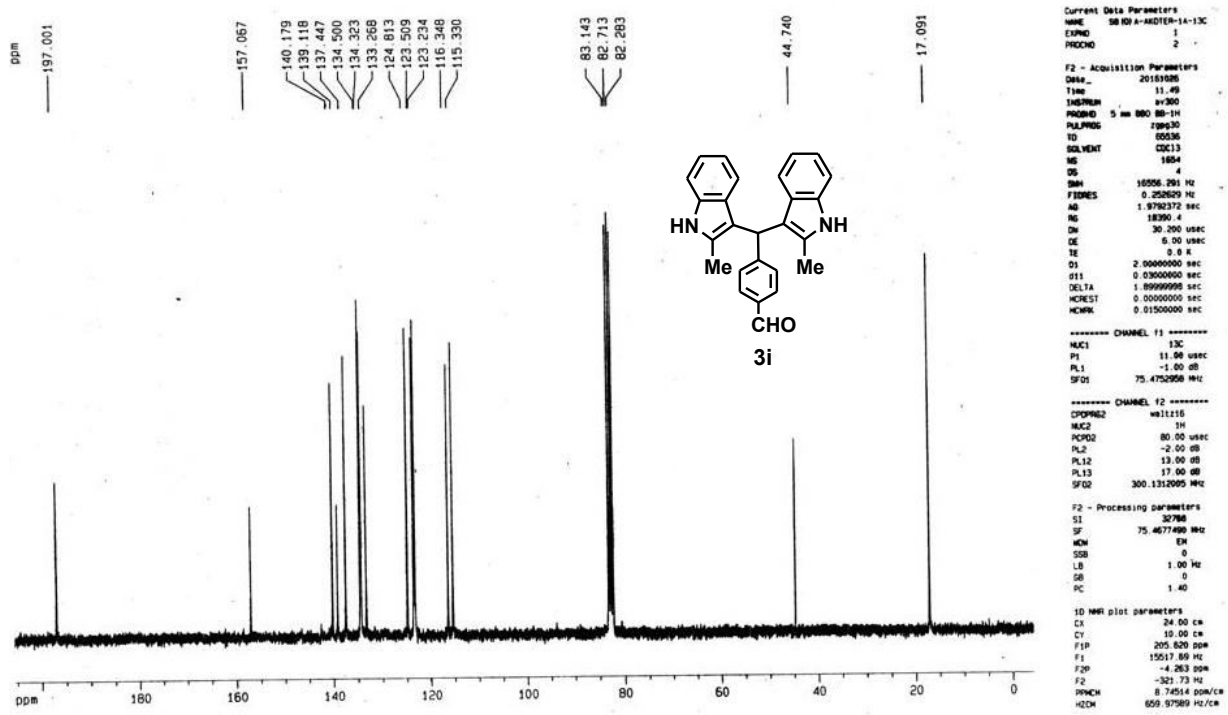

Figure 10: [13]C NMR of 4-(bis(2-methyl-*1H*-indol-3-yl)methyl)benzaldehyde (3i).

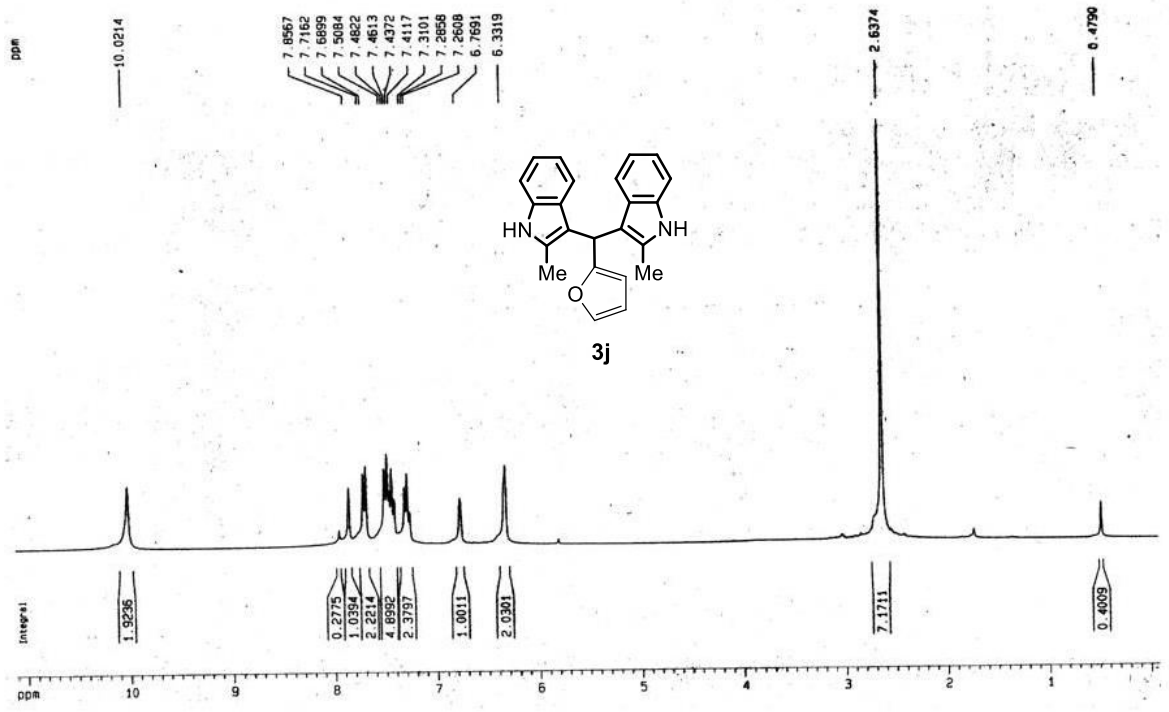

Figure 11: [1]H NMR of 3, 3'-(furan-2-ylmethylene)bis(2-methyl-*1H*-indole) (3j).

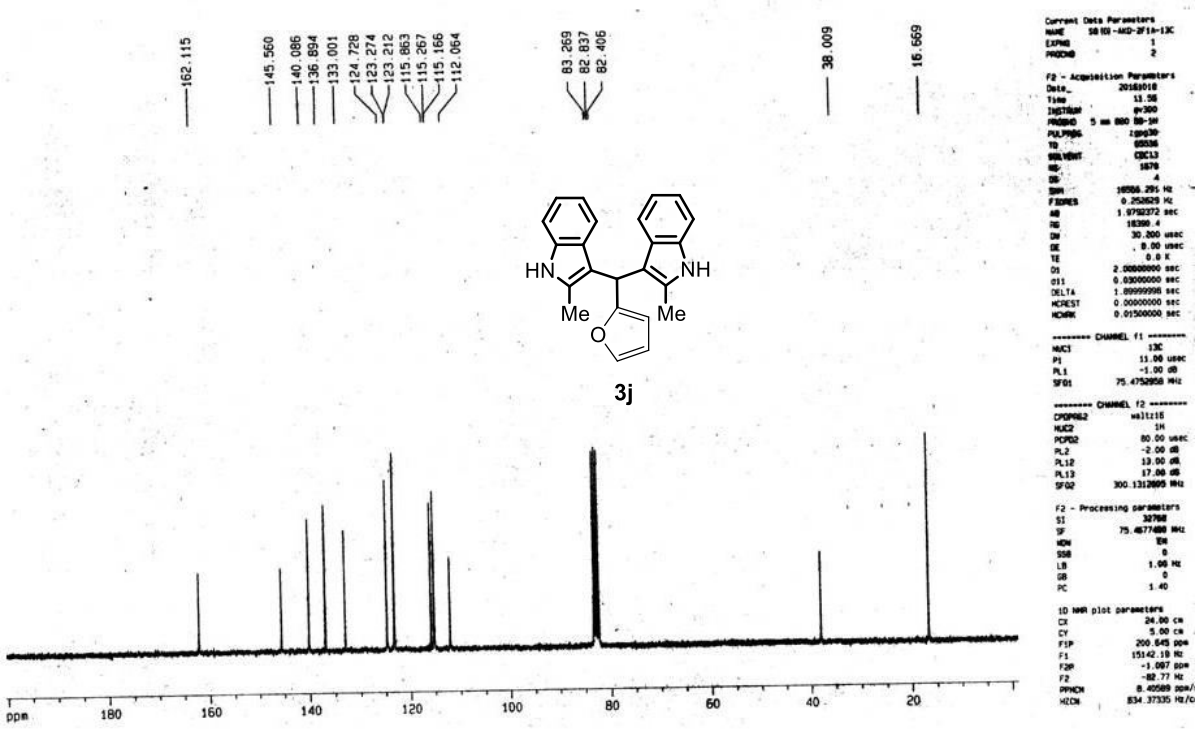

Figure 12: [13]C NMR of 3, 3'-(furan-2-ylmethylene)bis(2-methyl-*1H*-indole) (3j).

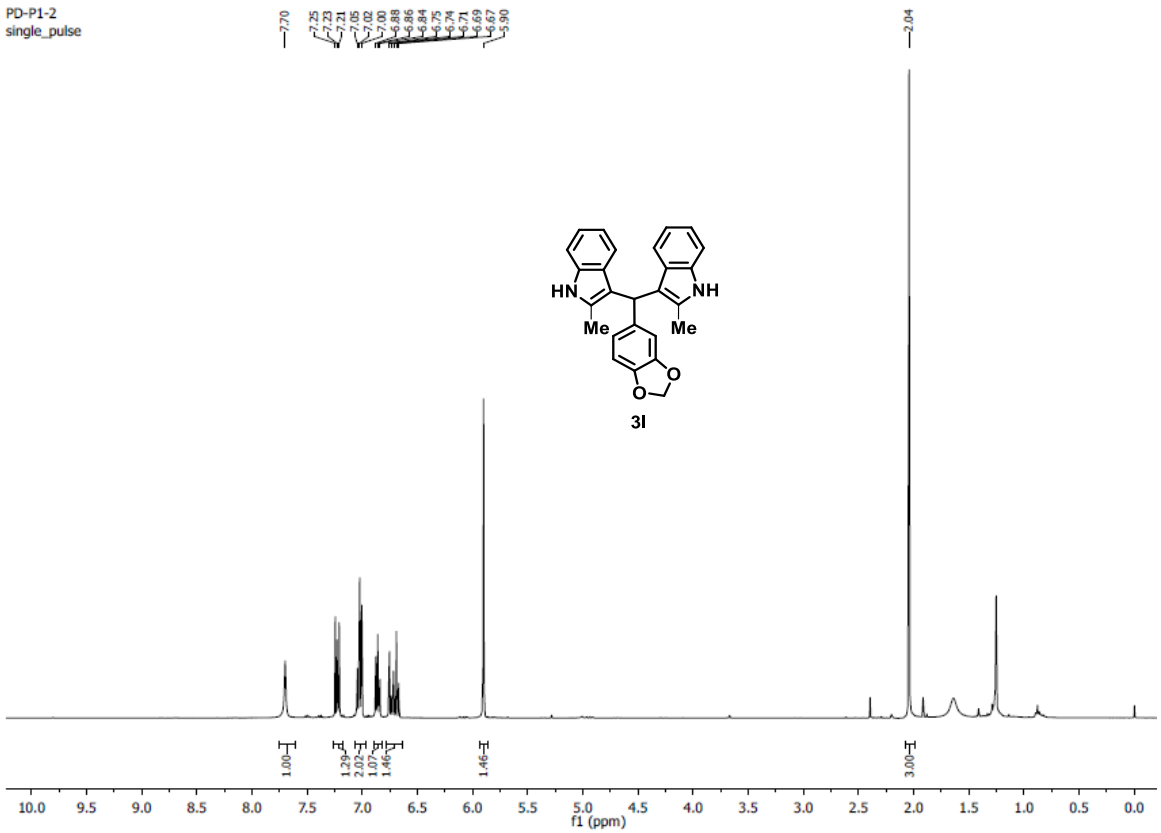

Figure 13: ^{1}H NMR of 3,3'-(benzo[d][1,3]dioxol-5-ylmethylene)bis(2-methyl-*1H*-indole) (3l).

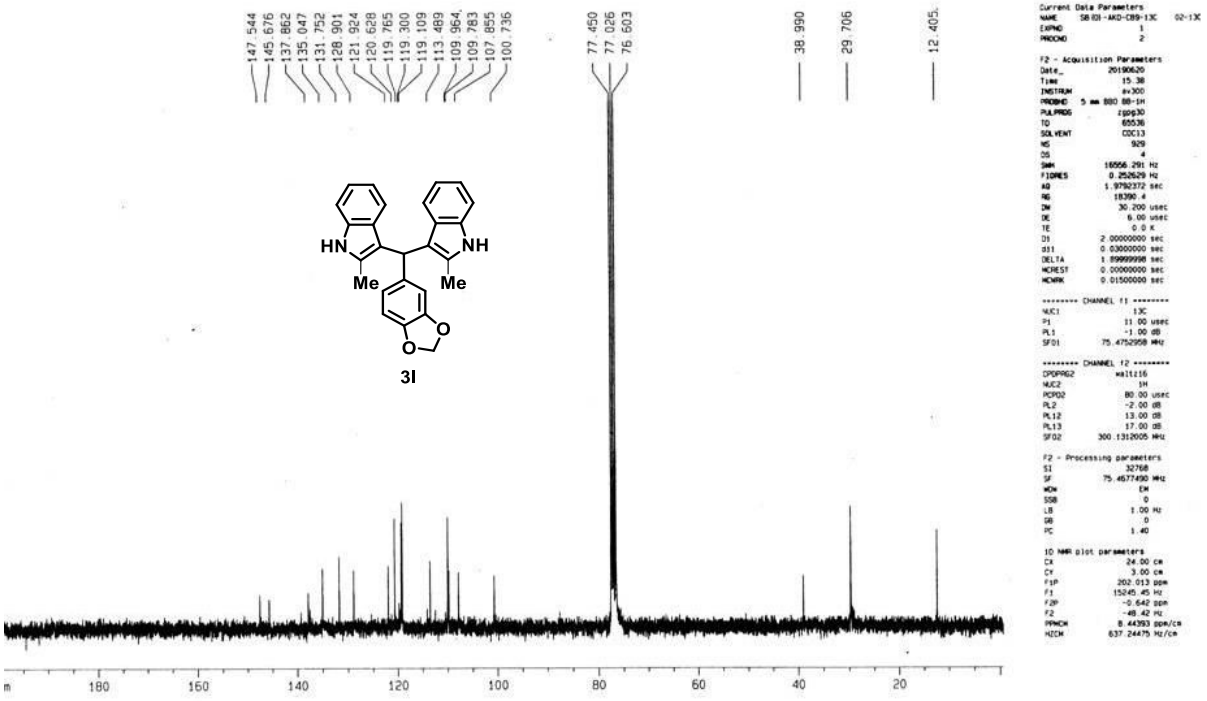

Figure 14: ^{13}C NMR of 3,3'-(benzo[d][1,3]dioxol-5-ylmethylene)bis(2-methyl-*1H*-indole) (3l).

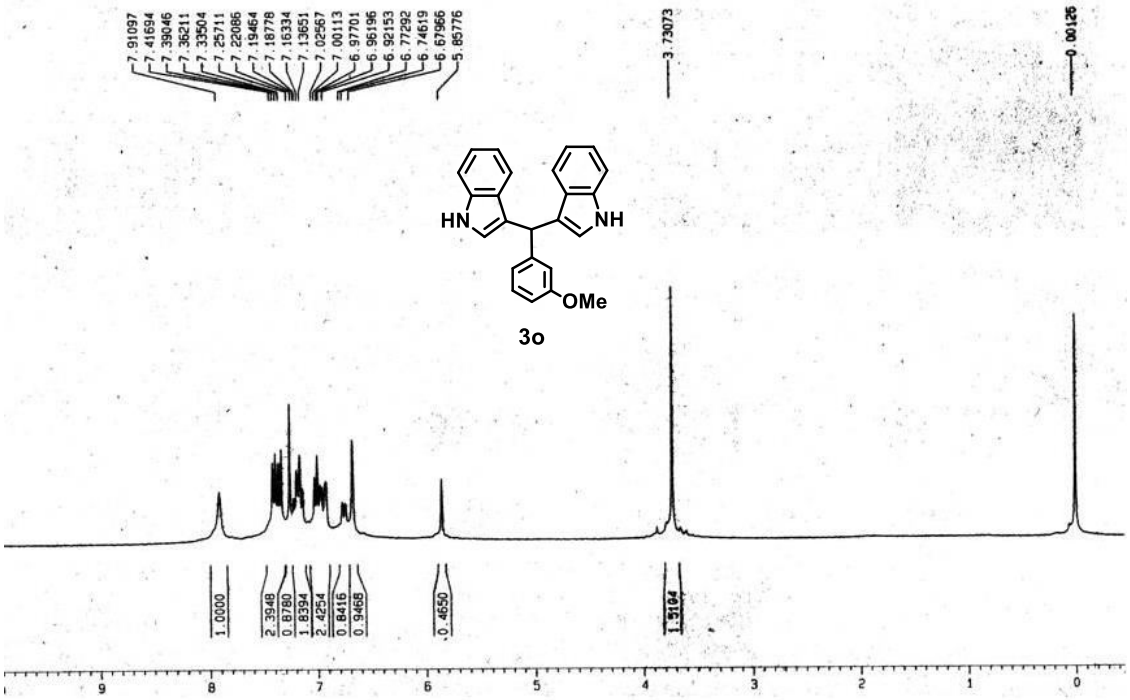

Figure 15: ^{1}H NMR of 3, 3'-((3-methoxyphenyl)methylene)bis(*1H*-indole) (3o).

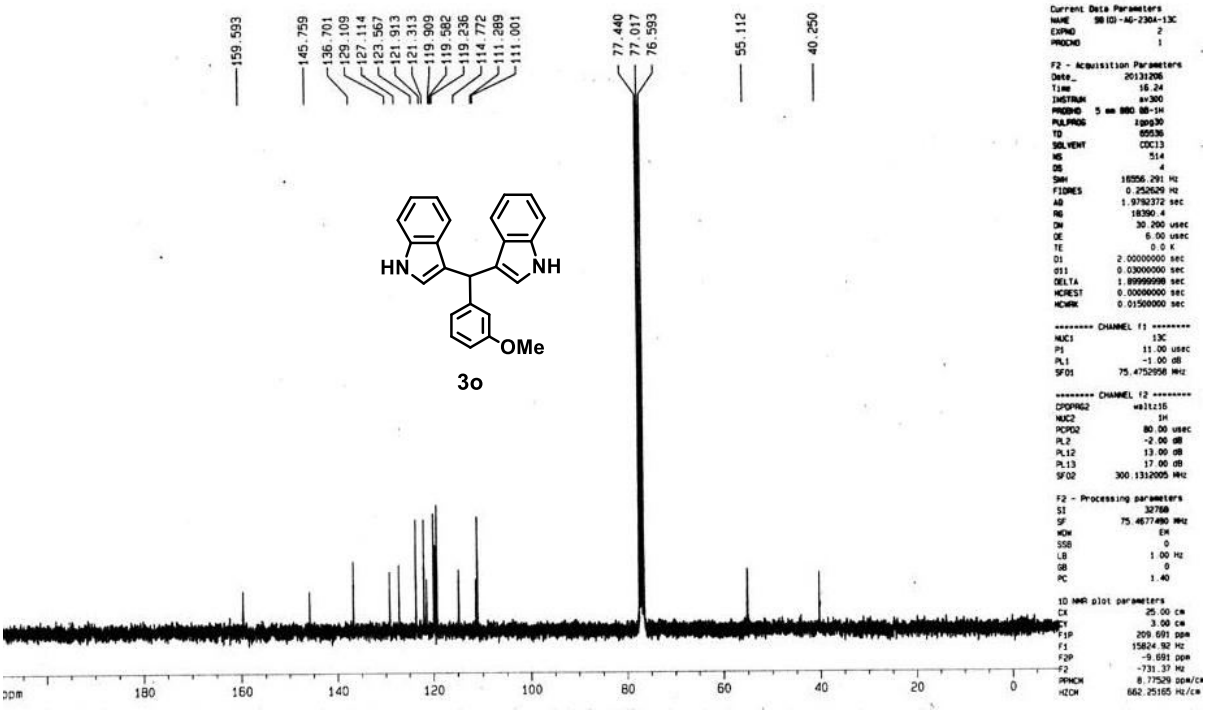

Figure 16: ^{13}C NMR of 3, 3'-((3-methoxyphenyl)methylene)bis(*1H*-indole) (3o).

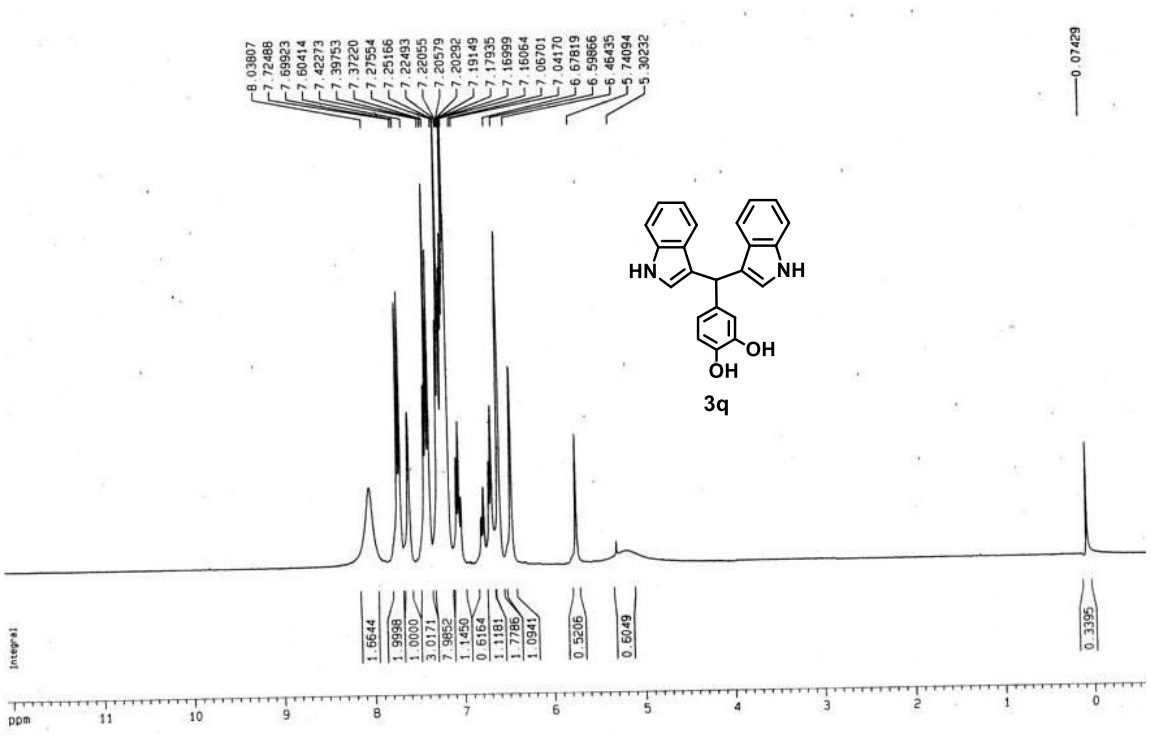

Figure 17: [1]H NMR of 4-(di(*1H*-indol-3-yl)methyl)benzene-1,2-diol (3q).

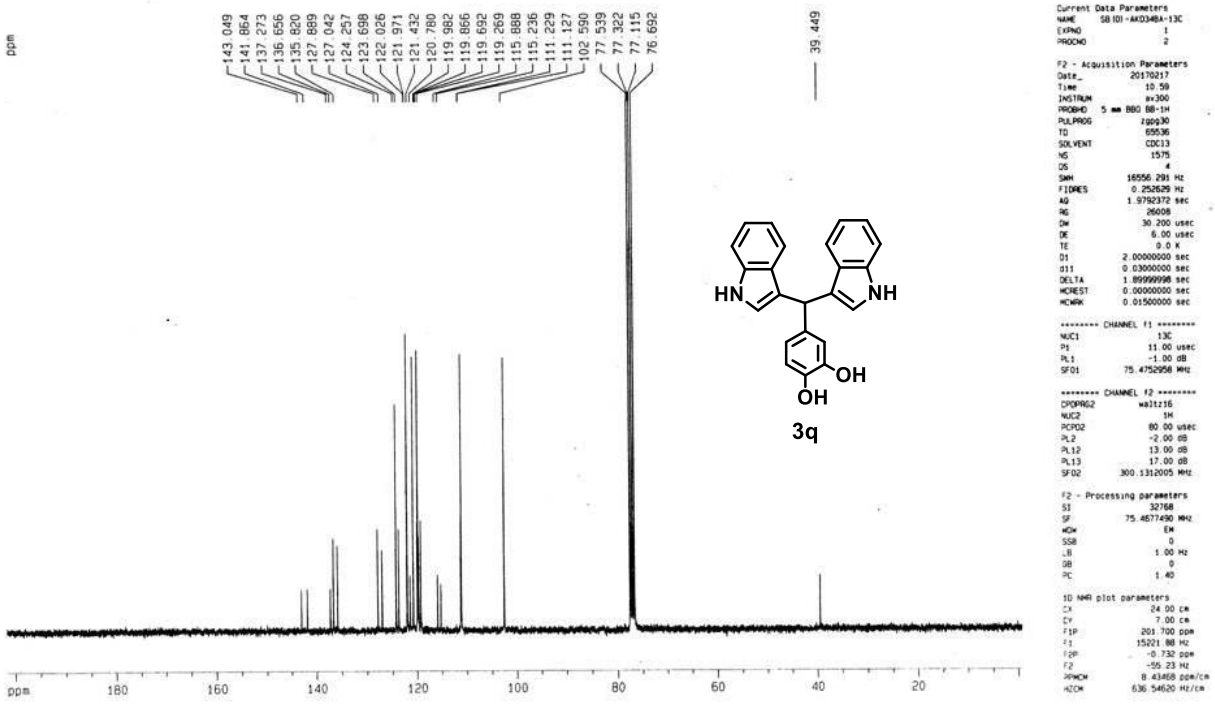

Figure 18: [1]H NMR of 4-(di(*1H*-indol-3-yl)methyl)benzene-1,2-diol (3q).

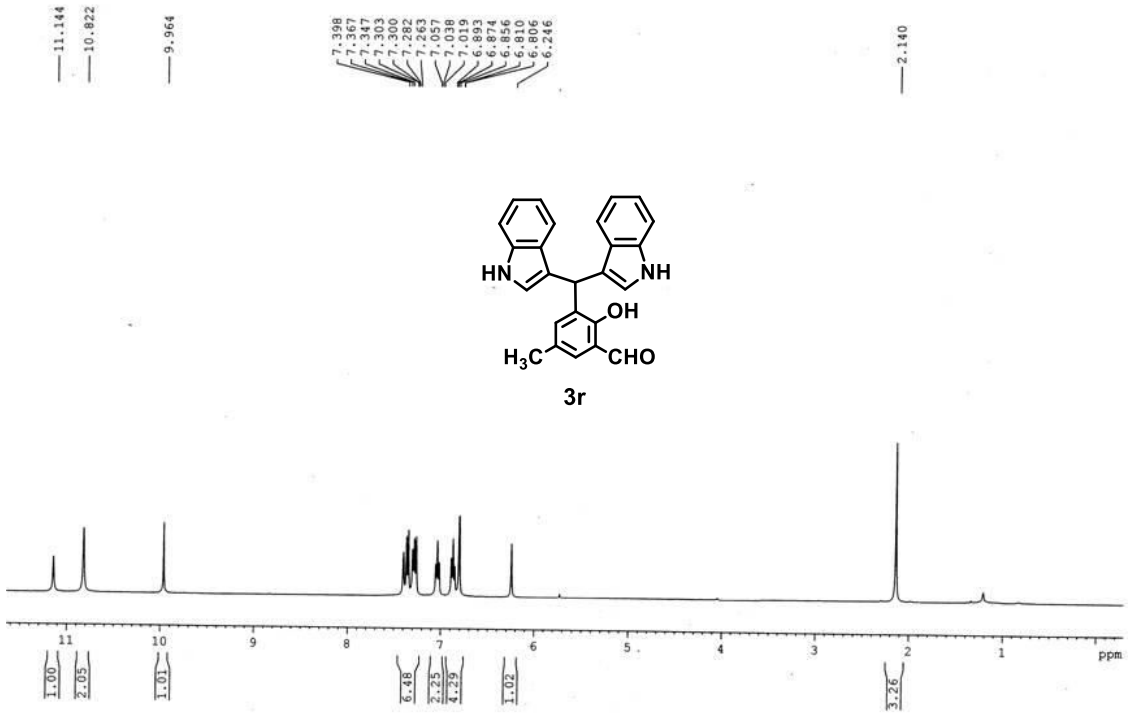

Figure 19: [1]H NMR of 3-(di(*1H*-indol-3-yl)methyl)-2-hydroxy-5-methylbenzaldehyde (3r).

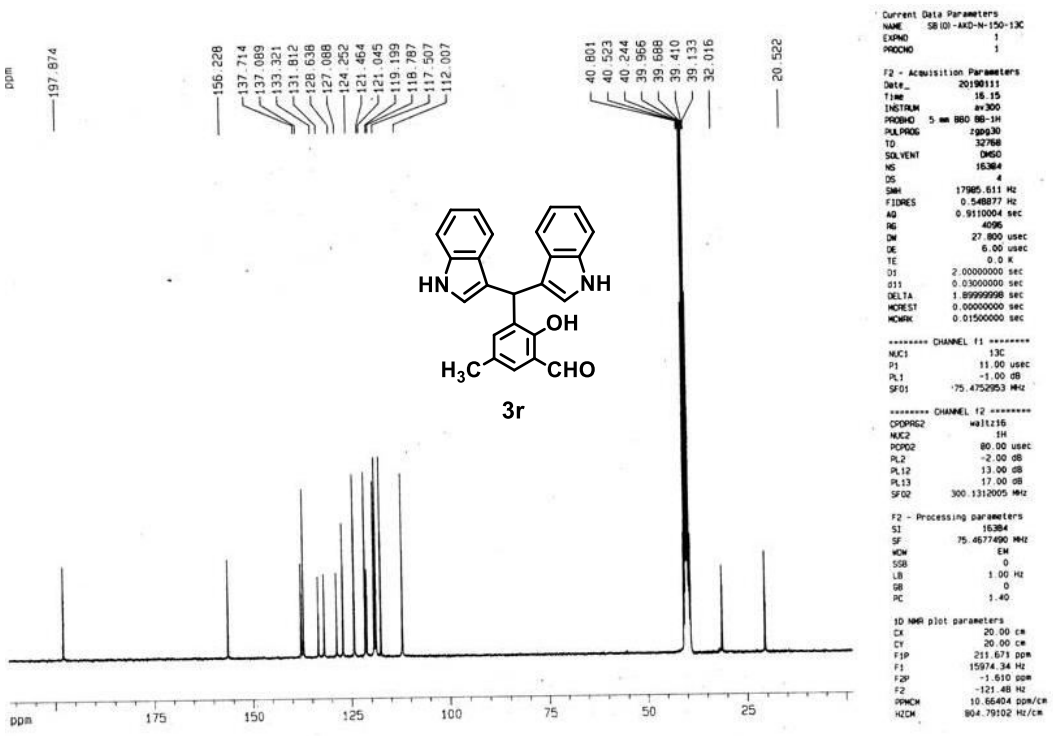

Figure 20: [13]C NMR of 3-(di(*1H*-indol-3-yl)methyl)-2-hydroxy-5-methylbenzaldehyde (3r).

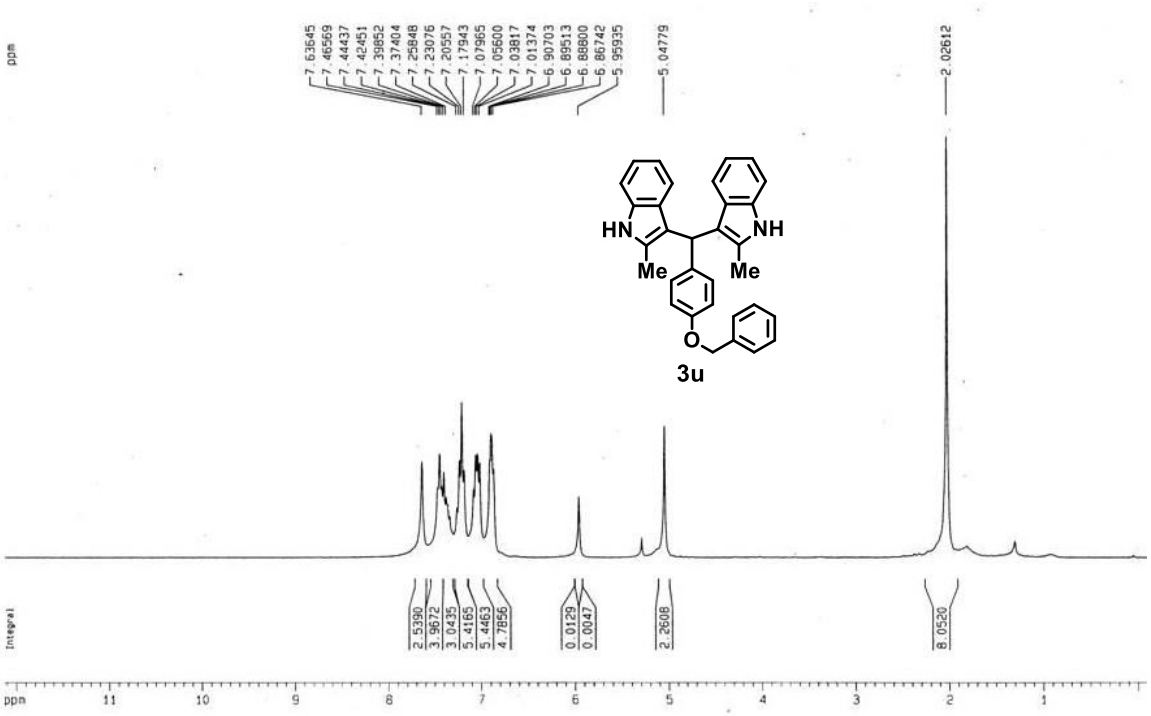

Figure 21: [1]H NMR of 3, 3'-((4-(benzyloxy)phenyl)methylene)bis(2-methyl-*1H*-indole) (3u).

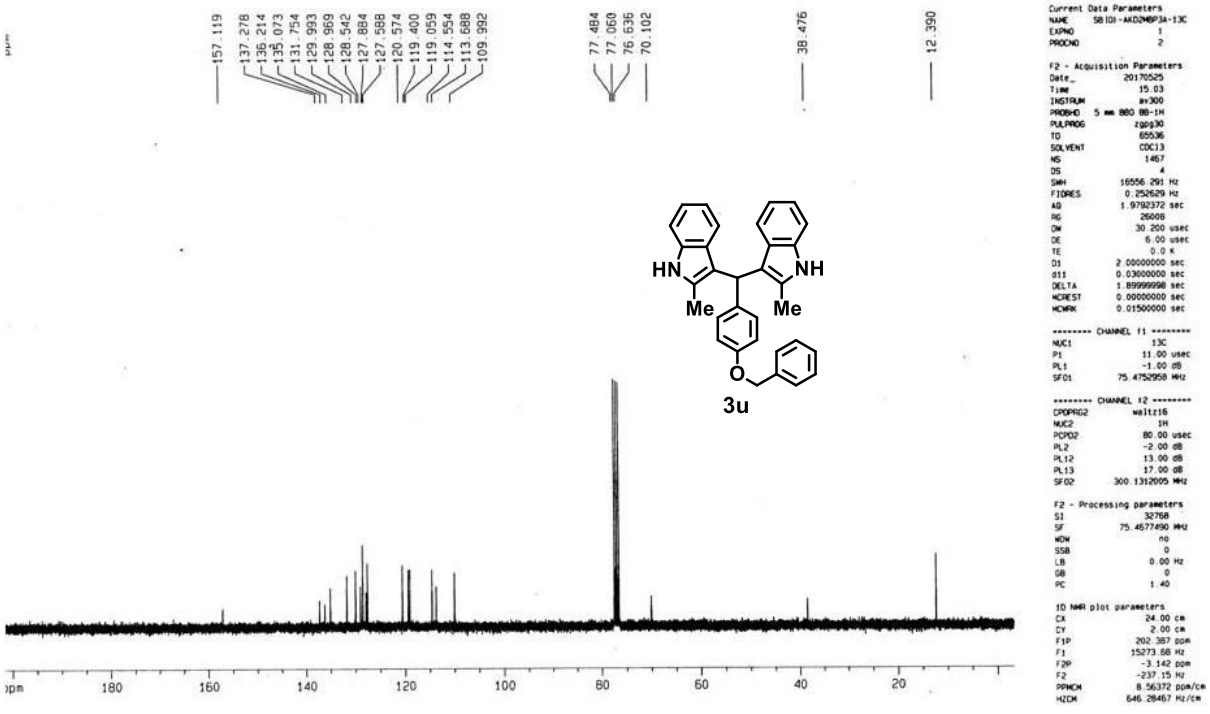

Figure 22: [1]H NMR of 3, 3'-((4-(benzyloxy)phenyl)methylene)bis(2-methyl-*1H*-indole) (3u).

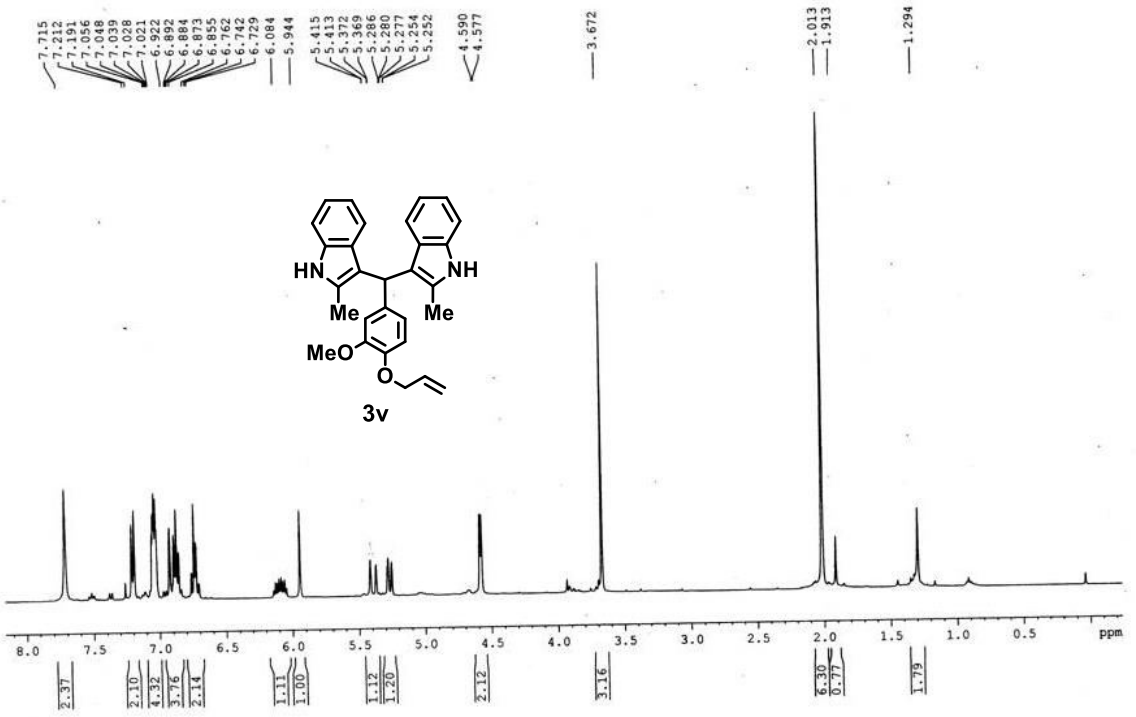

Figure 23: [1]H NMR of 3,3'-((4-(allyloxy)-3-methoxyphenyl)methylene)bis(2-methyl-*1H*-indole) (3v).

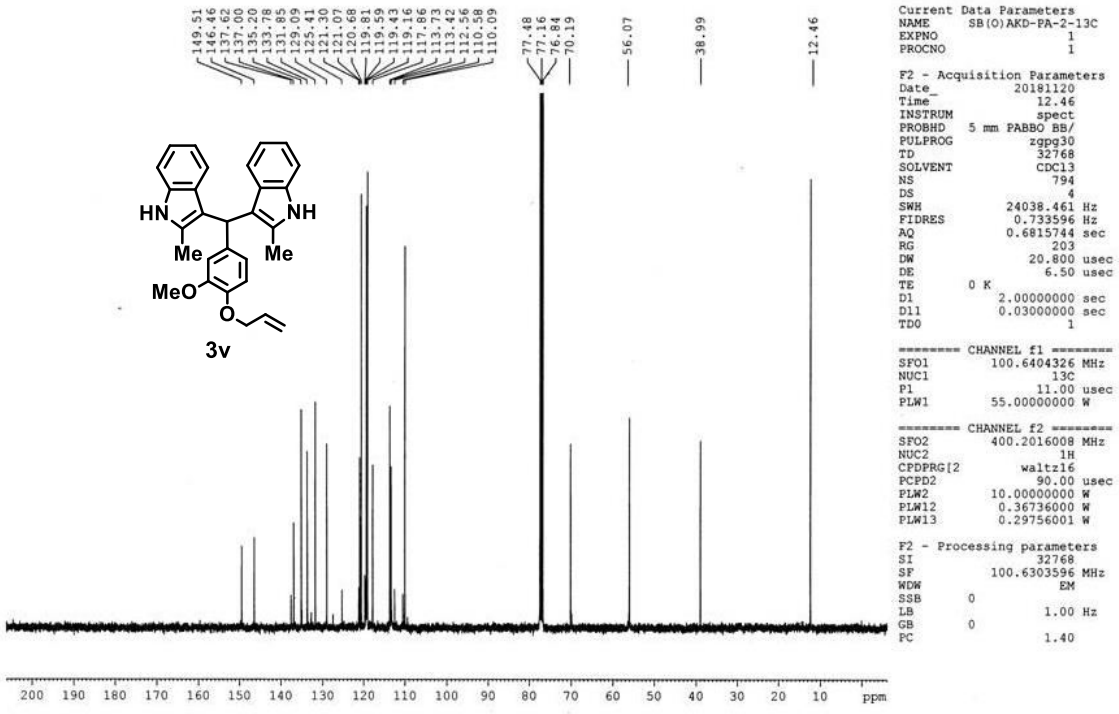

Figure 24: [13]C NMR of 3,3'-((4-(allyloxy)-3-methoxyphenyl)methylene)bis(2-methyl-*1H*-indole) (3v).

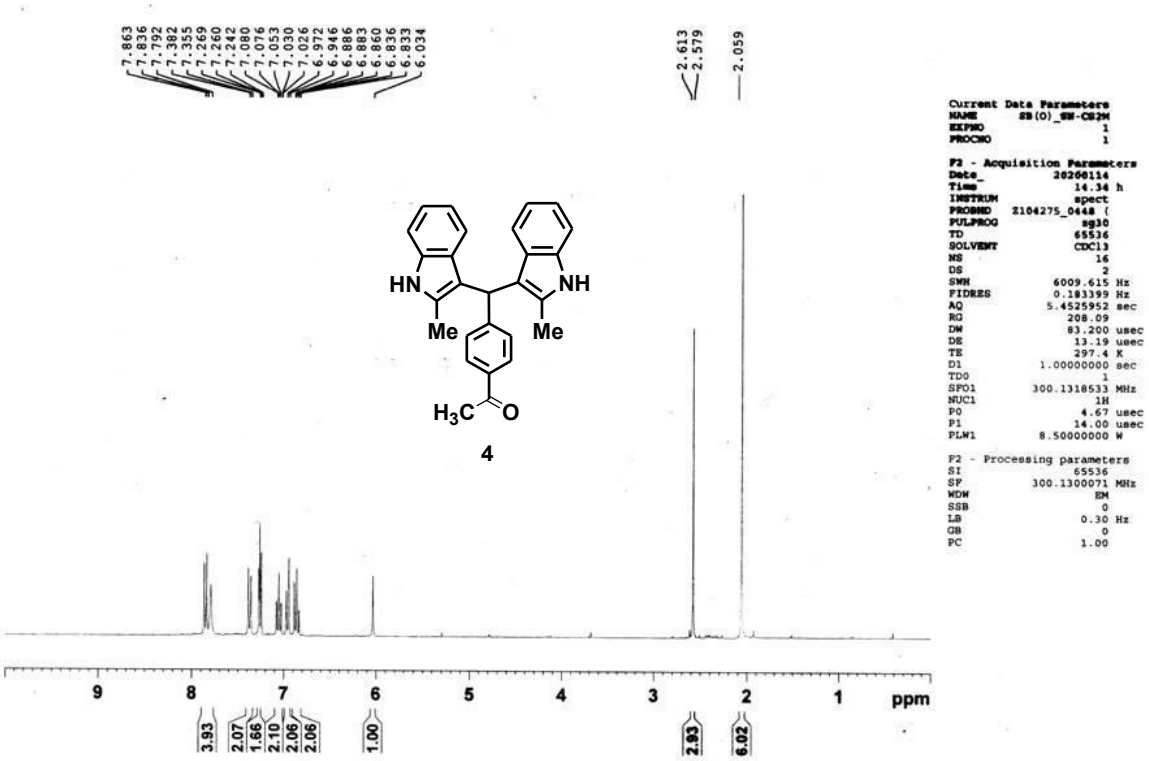

Figure 25: [1]H NMR of 1-(4-(bis(2-methyl-1H-indol-3-yl)methyl)phenyl)ethanone (4).

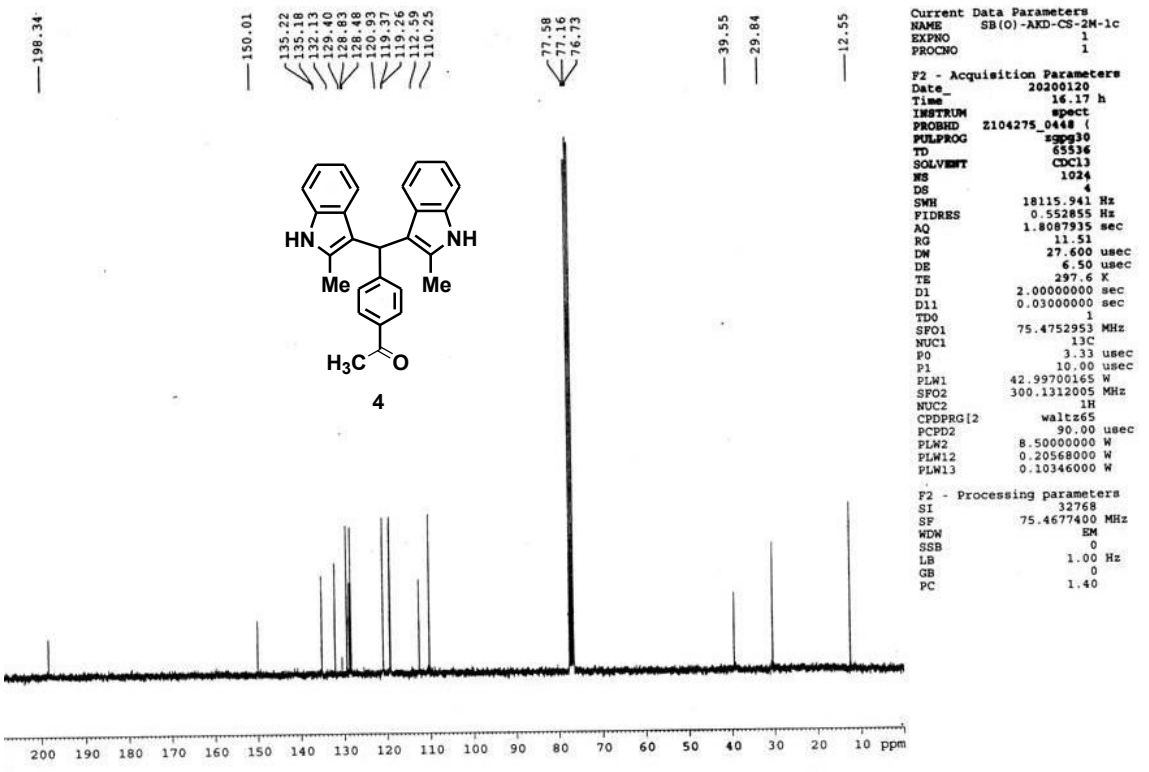

Figure 26: [13]C NMR of 1-(4-(bis(2-methyl-1H-indol-3-yl)methyl)phenyl)ethanone (4).

I. 6. References:

1. (a) C. Friedel, J. M. Crafts, *J. Chem. Soc.* **1877**, *32*, 725; (b) T. Okauchi, M. Itonaga, T. Minami, T. Owa, K. Kitoh, H. Yoshino, *Org. Lett.* **2000**, *2*, 1485; (c) O. Ottoni, A. D. V. F. Neder, A. K. B. Dias, R. P. A. C. Ruz, L. B. Aquino, *Org. Lett.* **2001**, *3*, 1005; (d) J. H. Wynne, W. M. Stalick, *J. Org. Chem.* **2002**, *67*, 5850; (e) K. Mertins, I. Iovel, J. Kischel, A. Zapf, M. Beller, *Angew. Chem. Int. Ed.* **2004**, *44*, 238; (f) Y. X. Jia, J. H. Xie, H. F. Duan, L. X. Wang, Q. Lin Zhou, *Org. Lett.* **2006**, *8*, 1621; (g) Y. Q. Wang, J. Song, R. Hong, L. Hongming, L. Deng, *J. Am. Chem. Soc.* **2006**, *128*, 8156; (h) Bandini, M.; Tragni, M. *Org. Biomol. Chem.* **2009**, *7*, 1501-1507; (i) C. W. Downey, C. D. Poff, A. N. Nizinski, *J. Org. Chem.* **2015***, 20,* 10364; (j) X. F. Deng, Y. W. Wang, S. Zhang, L. Li, G. X. Li, G. Zhao, Z. Tang, *Chem. Commun.* **2020**, *56*, 2499.
2. (a) T. R. Garbe, M. Kobayashi, N. Shimizu, *J. Nat. Prod.* **2000**, *63*, 596; (b) M. Shiri, M. A. Zolfigol, H. G. Kruger, Z. Tanbakouchian, *Chem. Rev.* **2010**, *110*, 2250; (c) N. Seyedi, H. Khabazzadeh, *Res. Chem. Intermed.* **2015**, *41*, 2603.
3. (a) C. Grosso, A. L. Cardoso, A. Lemos, J. Varela, M. J. Rodrigues, L. Custodio, L. Barreira, T. Melo, *Eur. J. Med. Chem.* **2015**, *93*, 9; (b) D. Li, T. Wu, K. Liang, C. Xia, *Org. Lett.* **2016**, *18*, 2228; (c) C. M. Bernt, G. Bottari, J. A. Barrett, S. L. Scott, K. Barta, P. C. Ford, *Catal. Sci. Technol.* **2016**, *6*, 2984; (d) A. Srivastava, A. Agarwal, S. K. Gupta, N. Jain, *RSC Adv.* **2016**, *6*, 23008.
4. (a) R. Pegu, R. Mandal, A. K. Guha, S. Pratihar, *New J. Chem.* **2015**, *39*, 5984; (b) D. Sain, C. Kumari, A. Kumar, S. Dey, *Supramol. Chem.* **2016**, *28*, 239.
5. (a) S. S. Mohapatra, P. Mukhi, A. Mohanty, S. Pal, A. O. Sahoo, D. Das, S. Roy, *Tetrahedron Lett.* **2015**, *56*, 5709; (b) K. Gopalaiah, S. N. Chandrudu, A. Devi, *Synthesis* **2015**, *47*, 1766; (c) S. R. Mendes, S. Thurow, F. Penteado, M. S. da. Silva, R. A. Gariani, G. Perin, E. J. Lenardao, *Green Chem.* **2015**, *17*, 4334; (d) D. Sun, G. Jiang, Z. Xie, Z. Le, *Chin. J. Chem.* **2015**, *33*, 409; (e) A. Swetha, B. M. Babu, H. M. Meshram, *Tetrahedron Lett.* **2015**, *56*, 1775.
6. (a) X. Wang, Z. Wang, G. Zhang, W. Zhang, Y. Wu, Z. Gao, *Eur. J. Org. Chem.* **2016**, 502; (b) A. Srivastava, A. Agarwal, S. K. Gupta, N. Jain, *RSC Adv.* **2016**, *6*, 23008; (c) N. X. Zhu, C. W. Zhao, J. C. Wang, Y. A. Li, Y. B. Dong, *Chem. Commun.* **2016**, *52*, 12702; (d) D. Z. Xu, J. Tong, C. Yang, *Synthesis*, **2016**, *48*, 3559; (e) K. Griffiths, P.

Kumar, G. R. Akien, N. F. Chilton, A. Abdul-Sada, G. J. Tizzard, S. J. Coles, G. E. Kostakis, *Chem. Commun.* **2016**, *52*, 7866.

7. (a) G. Gao, Y. Han, Z. H. Zhang, *ChemistrySelect* **2017**, *2*, 11561; (b) M. M. Zeydi, N. A. Mahmoodi, G. A. Terogeni, *Asian Journal of Green Chemistry,* **2017**, *1*, 78; (c) L. Ye, S. H. Cai, D. X. Wang, Y. Q. Wang, L. J. Lai, C. Feng, T. P. Loh, *Org. Lett.* **2017**, *22*, 6164; (d) A. Bahuguna, S. Kumar, V. Sharma, K. L. Reddy, K. Bhattacharyya, P. C. Ravikumar, V. Krishnan, *ACS Sustainable Chem. Eng.* **2017**, *5*, 8551; (e) D. Li, J. Wang, F. Chen, H. Jing, *RSC Adv.* **2017**, *7*, 4237; (f) K. Selvakumar, T. Shanmugaprabha, R. Annapoorani, P. Sami, *Synth. Commun.* **2017**, *47*, 913; (g) N. G. Boekell, D. J. Cerone, M. M. Boucher, P. K. Quach, W. N. Tentchou, C. G. Reavis, I. I. Okoh, J. A. Reid, H. E. Berg, B. A. Chang, C. S. Brindle, *SynOpen* **2017**, *1*, 97; (h) S. S. Mohapatra, Z. E. Wilson, S. Roy, S. V. Ley, *Tetrahedron*, **2017**, *73*, 1812.
8. (a) A. Bahuguna, S. Kumar, V. Krishnan, *ChemistrySelect.* **2018**, *3*, 314; (b) K. S. Du, J. M. Huang, *Org. Lett.* **2018**, *20*, 2911; (c) R. M. N. Kalla, S. C. Hong, I. Kim, *ACS Omega* **2018**, *3*, 2242; (d) C. Qiao, X. F. Liu, H. C. Fu, H. P. Yang, Z. B. Zhang, L. N. He, *Chem. Asian J.* **2018**, *13*, 2664; (e) A. Z. Halimehjani, V. Barati, *ChemistrySelect* **2018**, *3*, 3024; (f) X. Qi, H. J. Ai, N. Zhang, J. B. Peng, J. Ying, X. F. Wu, *Journal of Catalysis* **2018**, *362*, 74; (g) Y. Zhang, X. Yang, H. Zhou, S. Li, Y. Zhu, Y. Li, *Org. Chem. Front.* **2018**, *5*, 2120; (h) R. H. Khanmiri, Y. Kamel, Z. Keshvari, A. Mobaraki, G. H. Shahverdizadeh, E. Vessally, M. Babazadeh, *Applied Organometallic Chemistry*, **2018**, *32*, e4452.
9. (a) S. Guo, Z. Fang, B. Zhou, J. Hua, Z. Dai, Z. Yang, C. Liu, W. He, K. Guo, *Org. Chem. Front.* **2019**, *6*, 627; (b) W. Qiang, X. Liu, T. P. Loh, *ACS Sustainable Chem. Eng.* **2019**, *7*, 8429; (c) G. Basumatary, R. Mohanta, S. D. Baruah, R. C. Deka, G. Bez, *Catalysis Letters*, **2019**, *150*, 106; (d) R. Ali, M. Z. Ahamad, S. Singh, W. Haq, *Eur. J. Org. Chem.* **2019**, 1820; (e) B. R. Nemallapudi, G. V. Zyryanov, B. Avula, R. Reddy Guda, S. R. Cirandur, C. Venkataramaiah, W. Rajendra, S. Gundala, *Bioorganic chemistry* **2019**, *87,* 465; (f) X. Peng, Y. Zen, Q. Liu, L. Liu, H. Wang, *Org. Chem. Front.* **2019**, *6*, 3615; (g) Z. Wu, G. Wang, S. Yuan, D. Wu, W. Liu, B. Ma, S. Bi, H. Zhan, X. Chen, *Green Chem.* **2019**, *21*, 3542; (h) Y. Kim, J. Lee, J. Jung, S. G. Kim, *Tetrahedron Lett.* **2019**, *60*, 1625.

10. (a) L. Yuan, A. Palmieri, M. Petrini, *Adv. Synth. Catal.* **2020**, *362*, 1509; (b) N. Biswas, R. Sharma, D. Srimani, *Adv. Synth. Catal.* **2020**, *362*, 2902; (c) Y. Fu, Z. Lu, K. Fang, X. He, H. Xu, Y. Hu, *RSC Adv.* **2020**, *10*, 10848.
11. (a) Z. Shao, Y. Wang, Y. Liu, Q. Wang, X. Fu, Q. Liu, *Org. Chem. Front.* **2018**, *5*, 1248; (b) K. Jain, S. Chaudhuri, K. Pal, K. Das, *New J. Chem.* **2019**, *43*, 1299; (c) S. E. Hooshmand, B. Heidari, R. Sedghi, R. S. Verma, *Green Chem.* **2019**, *21*, 381; (d) R. A. Rather, Z. N. Siddiqui, *RSC Adv.* **2019**, *9*, 15749.
12. (a) M. Joharian, A. Morsali, A. A. Tehrani, L. Carlucci, D. M. Proserpio, *Green Chem.* **2018**, *20*, 5336; (b) S. Nandy, A. Ghatak, A. K. Das, S. Bhar, *Synlett*. **2018**, *29*, 2208; (c) H. Miao, K. Ma, H. Zhu, K. Yin, Y. Zhang, Y. Cui, *RSC Adv.* **2019**, *9*, 14580; (d) H. Zou, J. Dai, R. Wang, *Chem. Commun.* **2019**, *55*, 5898.
13. Q. Wang, Y. Chen, Y. Liu, *Polym, Chem-UK,* **2013**, *4*, 4192.
14. (a) M. E. Brewster, T. Loftsson, *Adv. Drug. Deliver. Rev.* **2007**, *59*, 645; (b) V. A. Marcolino, G. M. Zanin, L. R. Durrant, M. D. T. Benassi, G. Matioli, *J. Agric. Food Chem.* **2011**, *59*, 3348; (c) A. Ikeda, M. Ishikawa, R. Aono, J. Kikuchi, M. Akiyama, W. Shinoda, *J. Org. Chem.* **2013**, *78*, 2534.
15. (a) B. Madhav, S. N. Murthy, B. A. Kumar, K. Ramesh, Y. V. D. Nageswar, *Tetrahedron Lett.* **2012**, *53*, 3835; (b) S. Noel, B. Leger, A. Ponchel, K. Philippot, A. D. Nowicki, A. Roucoux, E. Monflier, *Catal. Today.* **2014**, *235*, 20; (c) F. Hapiot, H. Bricout, S. Menuel, S. Tilloy, E. Monflier, *Catal. Sci. Technol.* **2014**, *4*, 1899; (d) A. Kumar, R. D. Shukla, *Green Chem.* **2015**, *17,* 848.
16. A. Ghatak, S. Khan, S. Bhar, *Adv. Synth. Catal.* **2016**, *358*, 435.
17. (a) M. G. Usha, R. J. Wittebort, *J. Am. Chem. Soc.* **1992**, *114*, 1541; (b) E. Sabadini, T. Cosgrove, F. C. Egidio, *Carbohydr. Res.* **2006**, *341*, 270.
18. https://www.nwmissouri.edu/naturalsciences/sds/b/BetaCyclodextrin%20hydrate.pdf
19. (a) P. Ehrlich, *Med. Woche*. **1901**, 151; (b) F. H. Seyedeh, Z. Toktam, N. Zahra, *Bull. Korean Chem. Soc.* **2013**, *34*, 117.
20. C. Huo, C. Sun, C. Wang, X. Jia, W. Chang, *ACS Sustainable Chem. Eng.* **2013**, *1*, 549.
21. (a) F. He, P. Li, Y. Gu, G. Li, *Green Chem.* **2009**, *11*, 1767; (b) J. R. Satam, K. D. Parghi, R. V. Jayaram, *Catal. Commun.* **2008**, *9*, 1071; (c) S. M. Baghbanian, Y. Babajani, H. Tashakorian, S. Khaksar, M. Farhang, *C. R. Chimie.* **2013**, *16*, 129; (d) S. Handy, N. M. Westbrook, *Tetrahedron Lett.* **2014**, *55*, 4969; (e) M. A. Zolfigol, R. A.

Nasrabadi, S. Baghery, *Appl. Organometal. Chem.* **2016**, *30*, 273; (f) P. H. Tran, X. T. T. Nguyen, D. K. N. Chau, *Asian J. Org. Chem.* **2018**, *7*, 232.

CHAPTER II

Chemoselective and Ligand-free Aerobic Oxidation of Benzylic Alcohols to Carbonyl Compounds using Alumina-supported Mesoporous Nickel Nanoparticle as an Efficient Recyclable Heterogeneous Catalyst

II. Chemoselective and Ligand-free Aerobic Oxidation of Benzylic Alcohols to Carbonyl Compounds using Alumina-supported Mesoporous Nickel Nanoparticle as an Efficient Recyclable Heterogeneous Catalyst

II.1. Introduction

Design and development of efficient and sustainable strategies for important organic transformations by identifying alternative reaction conditions avoiding hazardous and expensive reagents represent a great challenge in both academic research and the chemical industry. Transition metal nanoparticles present fascinating aspects to the scientific community because of their quantum size, electron confining ability, high surface-to-volume ratio, unique catalytic activity, and good selectivity compared to their corresponding bulk material.[1] Owing to their intrinsic and well-established advantages, the development of a facile, economically viable, and environmentally feasible method for the synthesis of transition metal nanoparticles has gained substantial interest in the last decades. Notably, the advantages of transition metal nanocatalysts supported on chemically robust solid materials are due to mild reaction conditions applicable to wide range of substrates with good selectivity along with easy recovery and recyclability of the catalysts without detectable loss of their catalytic activity. A comprehensive account of the recent significant advances on the utilization of transition metal nanocatalysts during various important organic reactions followed by a concise account of different synthetic protocols for the oxidative transformation of benzylic alcohols to carbonyl compounds are going to be described in the following sections.

II.2. Organic reactions using transition metal nanocatalyst: A review

Acharyya *et al.*[2a] have synthesized cetyl alcohol mediated water-based Ag nanoparticles supported on Mn_3O_4 spinel in a one-pot method and the catalysts were characterized by FTIR, XRD, XPS, SEM, TEM, Raman, and ICP-AES. One dimensional whisker-like structure was observed through electron microscopy images. The catalyst was effectively oxidized styrene to styrene oxide in the presence of molecular O_2 as an oxidant (Scheme 1). Several reaction parameters like the pressure of oxygen gas, reaction temperature, and time were screened and styrene conversion of 67% with a styrene oxide selectivity of 100% was observed. This catalyst could not show any leaching up to five runs which exhibited the heterogeneity of the catalyst.

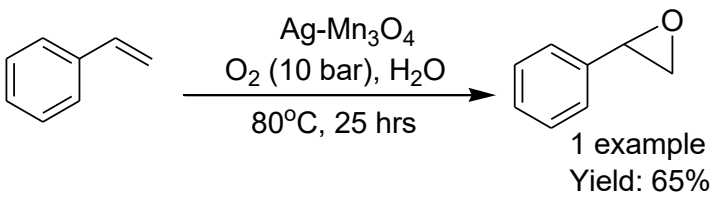

Scheme 1 Ag-Mn_3O_4 catalyzed aerobic oxidation of styrene

Heterogeneous Au nanoparticles supported on CeO_2 (Au/CeO_2) were prepared by Berrichi *et al.*[2b] and utilized as an efficient catalyst for the synthesis of structurally diverse propargyl amines via a three-component (A^3) coupling reaction of secondary amines, dichloromethane, and terminal alkynes (Scheme 2). The C-Cl bond of dichloromethane and the C-H bond of terminal alkyne were activated by CeO_2 supported Au nanoparticles. The nanocatalyst was characterized by TEM, XRD, and DR-UV visible spectroscopy. The supported nanocatalyst was recycled up to three times.

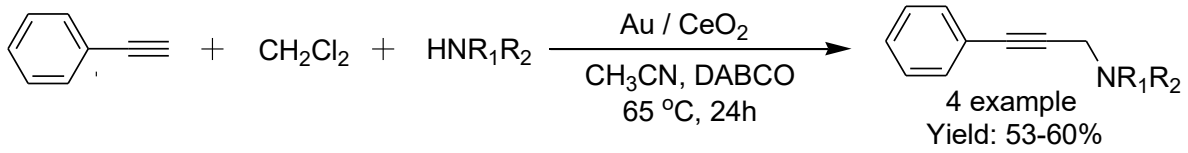

Scheme 2 Synthesis of propargyl amines catalyzed by Au/CeO_2

Borah *et al.*[2c] have developed a green and efficient protocol for the synthesis of Pd nanoparticles using poly(ethylene glycol) (PEG) as the stabilizer and *Colocasia esculenta* Linn. (locally known as 'kochu') leaf extract as a reducing agent. The bio-synthesized nanoparticles were thoroughly characterized by UV-visible, FTIR, XRD, and SEM analysis and exhibited excellent catalytic efficiency towards Suzuki-Miyaura cross-coupling reaction between aryl halides and phenylboronic acids under mild reaction conditions (Scheme 3). Various functional groups were also compatible in the reaction conditions and produced the desired cross-coupling products with high yields. The catalysts were recovered and recycled in subsequent runs without significant loss of their catalytic activity.

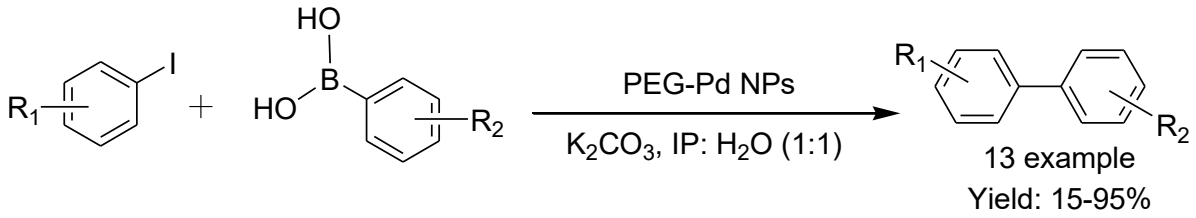

Scheme 3 Suzuki-Miyaura cross-coupling reaction catalyzed by PEG-Pd NPs

Martinez *et al.*[2d] prepared efficient, stable and solid palladium nanoparticles supported on synthetic clay (laponite) which was used as a heterogeneous catalyst in a Mizoroki-Heck reaction using iodobenzene and butyl acrylate under solvent-free conditions and with or without activated by microwave radiation (Scheme 4). Here, triethylamine (Et_3N) was used as a mild base in this cross-coupling reaction. The catalysts were recovered by extracting the reaction products with an auxiliary solvent and recycled up to thirteen times with good results.

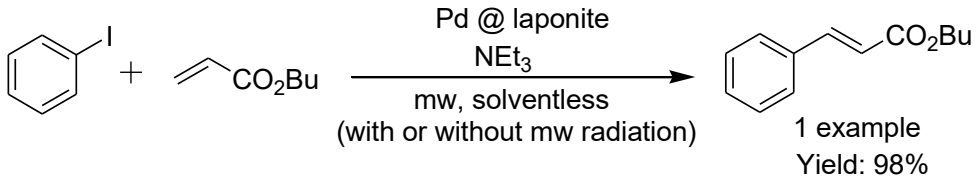

Scheme 4 Mizoroki-Heck reaction catalyzed by Pd@laponite

Bhar and his group developed an economical protocol[2e] for the chemoselective reductive homocoupling of benzylic halides in an aqueous medium using alumina-supported nickel nanoparticles as a stable recyclable heterogeneous catalyst at room temperature under ambient atmosphere (Scheme 5). Here hydrazine hydrate was used as the co-reductant and the reactions neither necessitate any other metal nor the requirement of high temperature. Chemically sensitive moieties like alkoxycarbonyl, methylenedioxy, benzyloxy, benzyl, methoxy, chloro, bromo, and nitro were well tolerated, and desired bibenzyl derivatives were obtained with excellent yields. Secondary and tertiary benzyl halides were also equally efficient and reacted to furnish the desired homocoupling products without any elimination. The catalyst was recovered and recycled without marginal loss of its efficiency.

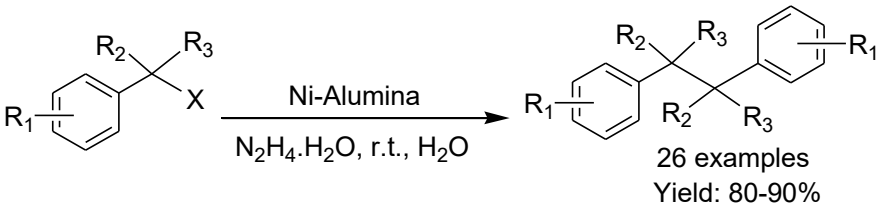

Scheme 5 Ni-Alumina catalyzed reductive homocoupling of benzylic halides

Copper-rhodanine derivative complex crafted onto Fe_3O_4@SiO_2 nanoparticle was synthesized by Rezaei *et al.*[3a] and employed their catalytic activity for the one-pot efficient synthesis of primary amides from differently substituted aldehydes and $NH_2OH.HCl$ in an aqueous medium (Scheme 6). The attractive features of the present protocol were the use of water as the green reaction medium rather than the employment of toxic, expensive, and harmful organic solvents, high yields of desired products, simple work-up procedure and

magnetic separation of the catalyst along with its reusability up to eight times without detectable loss of its catalytic efficiency.

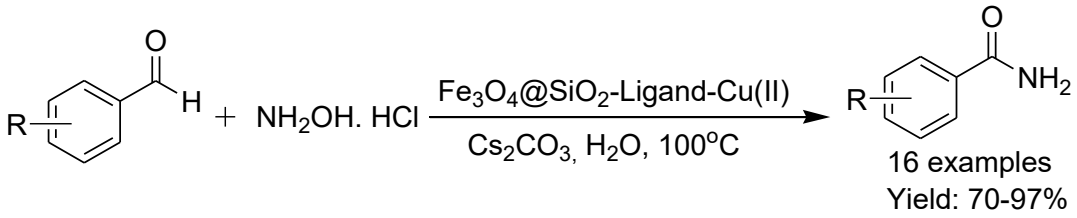

Scheme 6 Synthesis of primary amides from aldehydes catalyzed by Fe_3O_4 nanoparticle

A polystyrene-anchored cryptand 22-copper (I) iodide complex catalyst was developed by Rezaei *et al.*[3b] and this heterogeneous and recyclable catalyst was efficiently employed for the cross-coupling reaction of aryl halides and thiols in aqueous media under aerobic conditions (Scheme 7). The notable features of this methodology were the use of water as the eco-friendly reaction medium, low catalyst loading, easy separation, and reusability of the catalyst, high yield of cross products, and tolerance of a wide variety of substituted reactants.

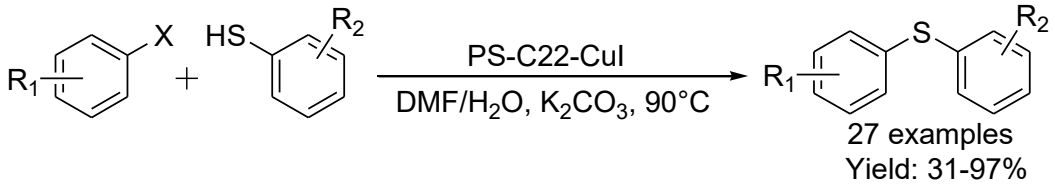

Scheme 7 Cu catalyzed cross-coupling reaction of aryl halides and thiols in an aqueous medium

Veisi and his co-workers[3c] demonstrated that the sulfonic acid groups loaded on the surface of polydopamine (PDA)-encapsulated Fe_3O_4 (Fe_3O_4@PDA-SO_3H) nanocatalyst could be efficiently utilized as a heterogeneous and recyclable nanocatalyst for the acetylation of alcohols, phenols, amines, and thiols with acetic anhydride at room temperature under solvent-free conditions (Scheme 8). The attractive features of the present method were simple preparation of the catalyst, solvent-free conditions, excellent yields, tolerance to various functional groups, easy separation of the catalyst by magnetic decantation, reusability of the catalyst up to 12 times without any noticeable loss in the activity.

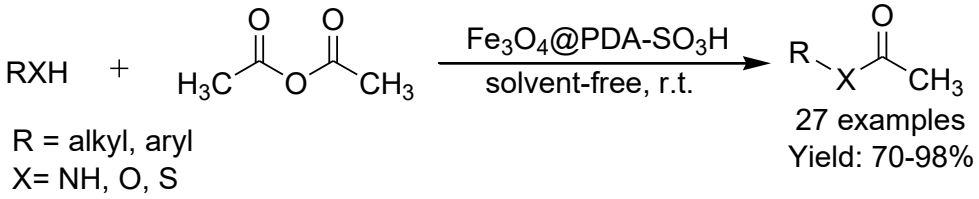

Scheme 8 Acetylation reaction using Fe_3O_4@PDA-SO_3H nanocatalyst

The leaf extract of *Euphorbia prolifera* was used as a reducing and stabilizing agent for the green synthesis of Ag/zeolite nanocomposite by Hatamifard *et al.*[3d] The phenolic acid and flavonoids present in the *Euphorbia prolifera* leaf extract was responsible for the reduction of the Ag(I) to Ag (0) as well as stabilization of Ag/zeolite nanocomposite (Scheme 9). The catalysts were characterized by FTIR, XRD, TEM, FESEM, and EDS analyses. The catalytic activity of the synthesized nanocatalyst was tested for the ligand and base-free hydroxylation of phenylboronic acid to phenol in presence of H_2O_2 and also reduction of 4-nitrophenol (4-NP), congo red (CR), methyl orange (MO), methylene blue (MB), and rhodamine B (RhB) at room temperature.

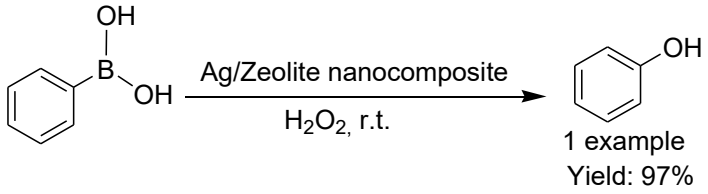

Scheme 9 Ag/Zeolite NPs catalyzed hydroxylation of phenylboronic acid to phenol

Borah *et al.*[4a] developed an environmentally benign protocol for the plant-mediated synthesis of Cu_2O nanoparticles using *Musa balbisiana colla* fruit extracts as the reducing agent within a very short reaction time. The synthesized nanoparticles were successfully characterized by SEM, TEM, and XRD methods. This heterogeneous catalytic system was employed for the *ipso*-hydroxylation of aryl and heteroaryl boronic acids to phenols using aqueous H_2O_2 as an oxidant (Scheme 10). The advantages of this methodology were the easy preparation of catalyst without using an external reducing agent, base-free reaction condition, recyclable up to five runs, short reaction time, and excellent yields of products.

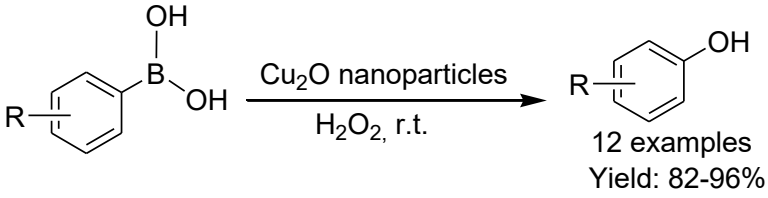

Scheme 10 Cu_2O NPs catalyzed hydroxylation of phenylboronic acid to phenol

Clave *et al.*[4b] developed a plant-derived eco-compatible synthesis of Pd nanoparticles (EcoPd) using the roots of *Eichhornia crassipes* (water hyacinth) as the reducing agent. The EcoPd NP was well characterized by FTIR, TEM, and XPS analysis and was found to be the highly efficient recyclable catalyst for ligands or additive-free Suzuki cross-coupling reaction in glycerol solvent by using K_2CO_3 as a weak base under Ar atmosphere at 120^oC (Scheme 11). Several heteroaryl bromides cross-coupled with phenylboronic acid under this eco-

compatible condition and produced the coupling products in good to high yields. The catalyst was reused for up to four runs without decreasing its catalytic activity.

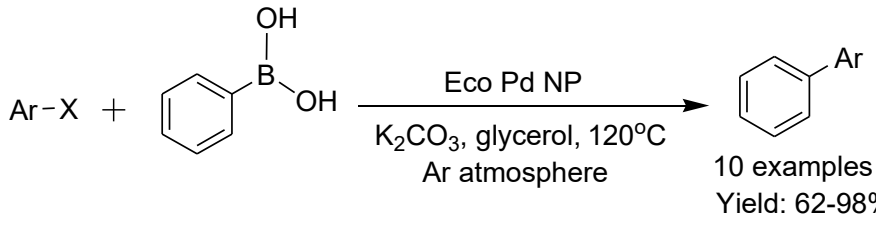

Scheme 11 Pd NPs catalyzed ligands or additives-free Suzuki cross-coupling reaction

Visible-light-driven Sonogashira cross-coupling reaction of aryl halides with phenylacetylene was developed using silicon carbide supported Pd NPs (Pd/SiC) as the heterogeneous catalyst under copper and ligand-free conditions (Scheme 12).[4c] In the presence of visible light, the photo-excited electrons in SiC were transferred to Pd NPs. The cleavage of the carbon-halogen bond in aryl halide was facilitated by these high-energy electrons. The final cross-coupled products were achieved by the substitution and reductive elimination processes.

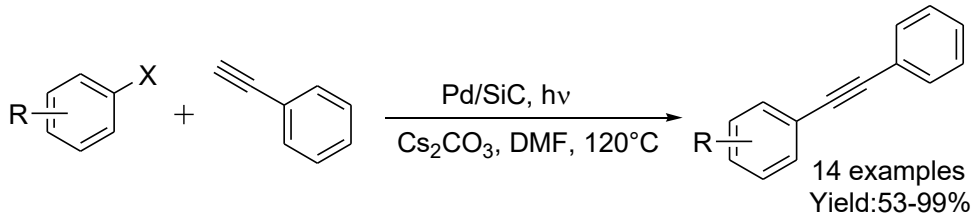

Scheme 12 Pd/SiC catalyzed Sonogashira cross-coupling reaction

The biological procedure was reported for the synthesis of CuO NPs[4d] using the aqueous leaves extract of *Thymbra spicata* as the reducing and capping agent and the synthesized nanoparticles were characterized by UV-vis, FTIR, XRD, TEM, FESEM, and EDX analyses. The CuO NPs were found to be an efficient catalyst for the ligand-free N-arylation of aniline and indole with aryl halides using K_2CO_3 as the week base (Scheme 13). Aryl halides bearing both electron-donating and withdrawing substituents were well tolerated and the N-arylated products were obtained in good yields. The heterogeneous catalyst was recycled in the seven consecutive cycles with almost consistent catalytic reactivity.

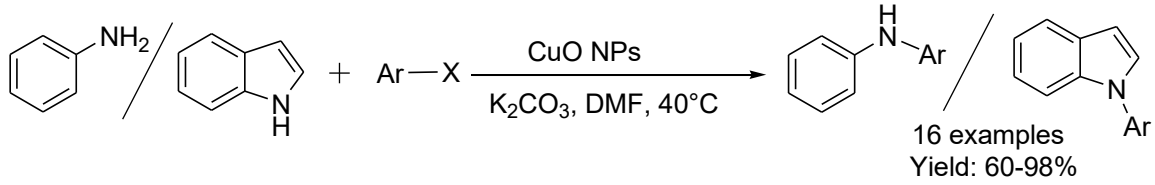

Scheme 13 CuO NPs catalyzed ligand-free N-arylation of aniline and indole with aryl halides

Aerobic oxidative cross-dehydrogenative coupling (CDC) of phenylglyoxals with secondary amines in an aqueous medium under ambient condition using water dispersed Au nanoparticles as an efficient and recyclable catalyst was reported by Thirukovela *et al.* (Scheme 14).[5a] The importance of aerial oxygen in this cross-dehydrogenative coupling (CDC) reaction was investigated by carrying out the reaction in an inert N_2 atmosphere and there was no formation of the desired product. A series of biologically important α-keto amides were obtained with high yields. The catalyst was recycled up to five catalytic runs without decreasing the product yields.

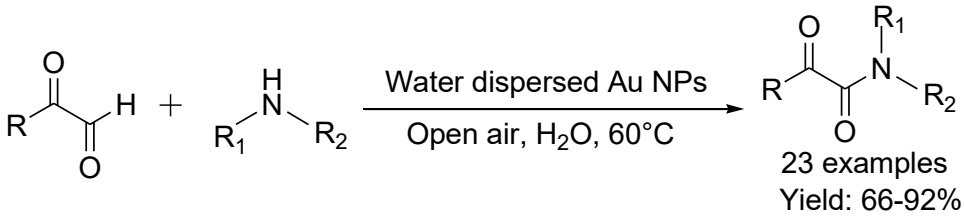

Scheme 14 Au NPs catalyzed Cross-dehydrogenative coupling (CDC) reaction

BINAP-Cu complex supported by hydrotalcite ([Cu(binap)I]$_2$@HT) has been prepared by Wang and his co-workers.[5b] This heterogeneous catalyst was proved to be an efficient recyclable catalyst for the borrowing hydrogen reaction of aniline with benzyl alcohol using KOH as the strong base under solvent-free conditions (Scheme 15). Various substituents like fluoro, chloro, bromo, methyl, methoxy, and ester were well tolerated and the desired N-benzylated amines were obtained with good yields. The catalyst was also effective for the synthesis of *1H*-benzo[d]imidazole using *ortho*-phenylenediamine and benzyl alcohol under the optimized reaction conditions. The catalyst was recycled and negligible leaching was observed through ICP experiment.

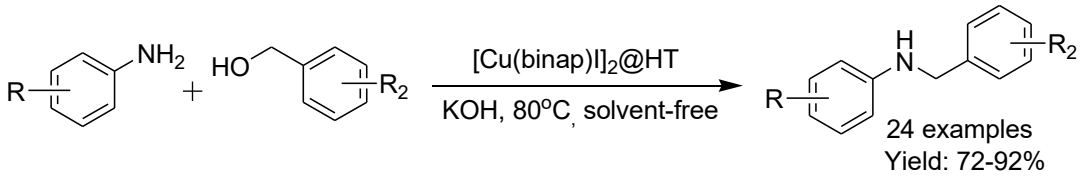

Scheme 15 Reaction of anilines with benzyl alcohols in the presence of Cu(binap)I]$_2$@HT

A microwave-assisted green protocol for the selective oxidative transformation of styrene to benzaldehyde under solvent-free conditions was reported by Martins *et al.*[5c] in the presence of a series of transition-metal (Mn to Zn) ferrite NPs and *t*-BuOOH as an external oxidant (Scheme 16). The $CoFe_2O_4$ nanoparticles were found to be an efficient catalyst for this oxidation. After the completion of the reaction, the catalyst was separated by using an external magnet. There was no significant loss of catalytic activity when the catalyst was

reused up to five consecutive runs. The low E-factor value indicated the sustainability of the present catalytic system.

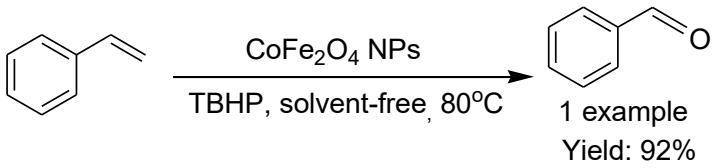

Scheme 16 $CoFe_2O_4$ NPs catalyzed the oxidative transformation of styrene to benzaldehyde

Biogenic route was developed for the synthesis of $CuFe_2O_4$ magnetic nanoparticles[5d] using plant extract of *Camellia sinensis* var. Assamica (Tea) as the source of eco-friendly reducing agent and the nanoparticles were characterized by XRD, TEM, SEM, EDX, and VSM analyses. This was used as an effective eco-friendly catalyst for the acetylation of various amines, phenols, and alcohols under solvent-free conditions at room temperature (Scheme 17). The reaction occurred within a very short reaction time and the desired acetylated products were obtained in good to excellent yields. The catalyst was recycled up to four times without decreasing the product yields.

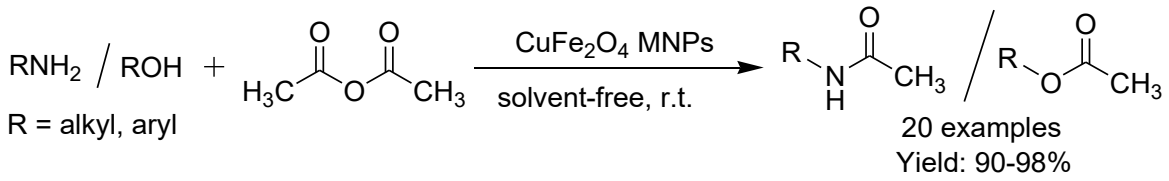

Scheme 17 $CuFe_2O_4$ NPs catalyzed acetylation reaction under solvent-free condition

Patel *et al.*[6a] developed a bi-functional heterogeneous catalyst consisting of nickel and supported 12-tungstophosphoric acid (Ni-TPA/ZrO_2) which was investigated for one-pot oxidative esterification of benzaldehyde and benzyl alcohol with methanol into their corresponding esters in the presence of H_2O_2 as the oxidant without using any base (Scheme 18). The bifunctionality of the catalyst was originated by combining their redox and acidic properties. The catalytic activity of Ni-TPA/ZrO_2 catalyst for the esterification of benzyl alcohol was lower than that of benzaldehyde because the former reaction involves the oxidation of benzyl alcohol to benzaldehyde. This catalyst was recovered and reused up to three runs without depleting its catalytic activity.

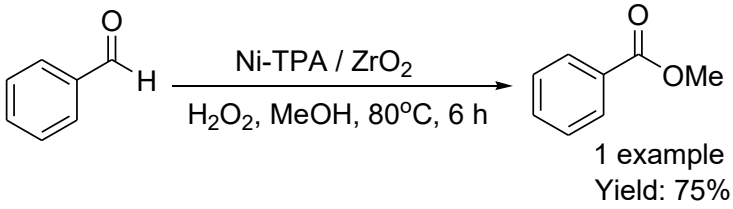

Scheme 18 Oxidative esterification of benzaldehyde catalyzed by Ni-TPA/ZrO_2

Pd nanoparticles supported on N, O-dual doped hierarchical porous carbon (Pd/N, O carbon) was prepared[6b] and employed as an efficient heterogeneous catalyst for the chemoselective transfer hydrogenation reaction of α,β-unsaturated carbonyl compounds using HCOOH as the hydrogen source (Scheme 19). This catalytic system exhibited excellent catalytic activity with exclusive selectivity to C=C bond reduction in the presence of C=O bond and tolerance of various functional groups with good to excellent yields. The synergistic effect of Pd NPs with incorporated heteroatoms on carbon played a critical role in promoting the transfer hydrogenation reaction. The catalyst was recycled six times without significant loss of its activity as well as selectivity.

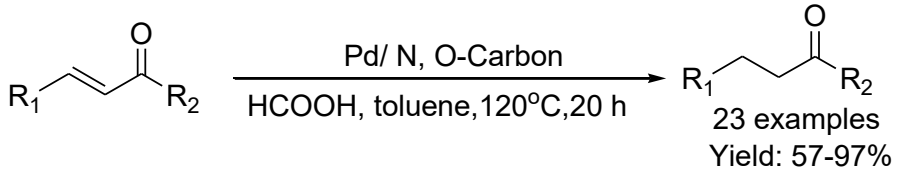

Scheme 19 Pd-catalyzed chemoselective reduction of α,β-unsaturated carbonyl compounds

Silver supported iron oxide nanoparticles (Ag/Fe_2O_3 NPs) were synthesized through surfactant-assisted hydrothermal process[6c] and were characterized by UV-vis, FTIR, SEM, TEM, XPS, BET, and ICP-AES analyses. The Ag/Fe_2O_3 NPs were found to be effective for catalytic one-pot oxidation of aniline to azoxybenzene in the presence of H_2O_2 as the oxidant (Scheme 20). The high catalytic activity of Ag/Fe_2O_3 NPs was observed through the synergistic effect between Fe_2O_3 nanospheres and surface Ag nanoparticles. The investigation results showed that the 1.8% Ag loading was effective for 92% aniline conversion and 94% azoxybenzene selectivity. ICP-AES analysis confirmed the heterogeneous nature of the catalyst and the amount of Ag and Fe remained nearly the same even after five catalytic runs with a negligible amount of silver leaching (concentration of Ag and Fe were < 2 ppb).

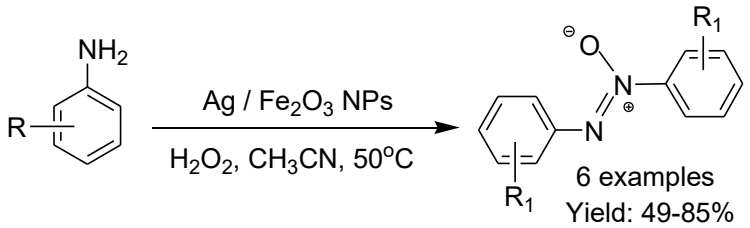

Scheme 20 Ag/Fe_2O_3 catalysed oxidation of aniline to azoxybenzene

Leng and his group[6d] have prepared Au nanoparticle-immobilized on L-cysteine-paired porous ionic copolymer and employed as a heterogeneous catalyst in the oxidative coupling of a wide variety of benzylic and secondary alcohols with aliphatic as well as aromatic

primary amines to synthesize differently functionalized imines in presence of TBHP as an external oxidant under additive-free conditions (Scheme 21). The Au NPs with small particle sizes of 2-3 nm were narrowly distributed and highly dispersed on DVB-[MimLcy]$_3$ (Au/DVB-[MimLcy]$_3$) which accounts for the excellent catalytic performance in these oxidative coupling reactions. The catalyst was recovered and reused several times without marginal loss of reactivity.

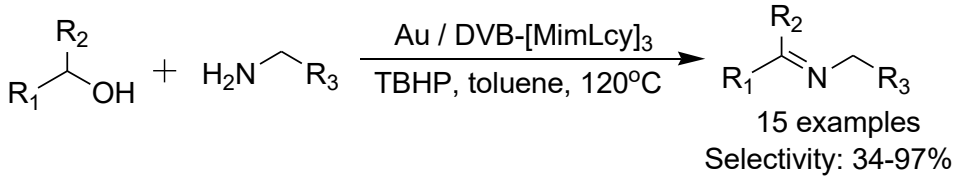

Scheme 21 Au NPs catalyzed oxidative coupling of alcohols with anilines

Nagaoka and his co-workers[6e] have prepared a series of noble metal nanoparticles (such as Ru, Rh, Ir, Pd, and Pt) by microwave-assisted alcohol reduction and used for the hydrogenation of benzoic acid to cyclohexane carboxylic acid in the presence of H_2 at atmospheric pressure (Scheme 22). Among the tested catalysts, polyvinylpyrrolidone stabilized Rh nanoparticles (Rh-PVP NPs) showed an excellent catalytic efficiency in the selective hydrogenation of aromatic ring in benzoic acid with the tolerance of different functional groups under solvent-free conditions and produced the desired hydrogenated products in good to excellent yields. This catalyst was found to be equally active for the hydrogenation of quinoline to 1,2,3,4-tetrahydroquinoline which made this methodology quite attractive. The catalyst can also be reused without a marginal decrease in its activity.

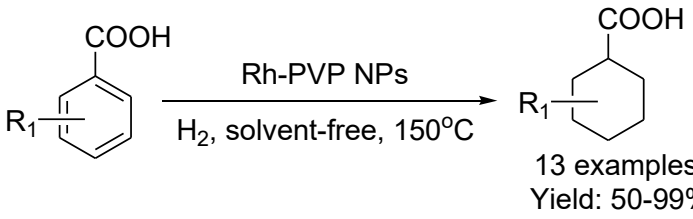

Scheme 22 Rh NPs catalyzed hydrogenation of benzoic acid to cyclohexane carboxylic acid

Chung and his group[7a] have prepared Rh-nanoparticles loaded on carbon fullerene-C60 (Rh(0)NPs/Fullerene-C60) and the catalytic activity was tested towards Suzuki cross-coupling reactions with the tolerance of a variety of functionalized substrates (Scheme 23). Occurrence of Rh-nanoparticles uniformly decorated on the surface of fullerene-C60 was confirmed by transmission electron microscopy (TEM) analysis. The crystalline properties of the synthesized Rh nanocatalyst were observed by X-ray diffraction (XRD) study. The oxidation state of Rh in the nanocatalyst was zero which was confirmed by X-ray

photoemission spectroscopy (XPS) analysis. The reusability of Rh(0)NPs/Fullerene-C60 was tested and found to be good without much deplement of its activity.

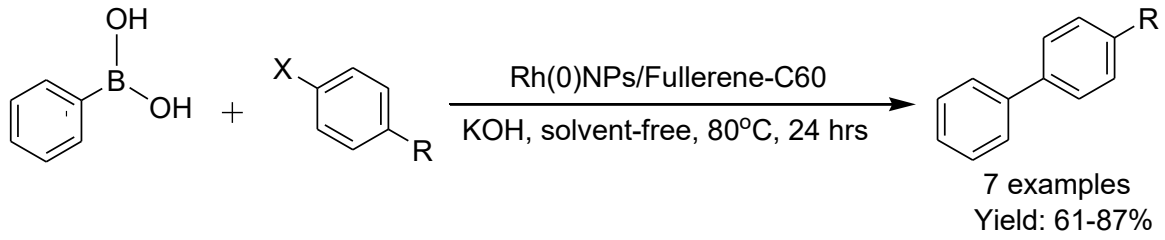

Scheme 23 Rh NPs catalyzed Suzuki cross-coupling reaction under solvent-free condition

Baran *et al.*[7b] have prepared Pd NPs using Fe_3O_4/chitosan/pumice hybrid beads as the stabilizing agent without adding any toxic reducing resource. These Pd NPs@Fe_3O_4/chitosan/pumice hybrid beads were used as the heterogeneous catalyst for the effective cyanation of aryl halides to the formation of aryl nitriles in the presence of $K_4[Fe(CN)_6]$ as the cyanating agent and Na_2CO_3 as the mild base (Scheme 24). The efficiency of the catalyst was obvious from the yields of the benzonitriles formed. A maximum yield of 98% was reported and the catalyst displayed good recyclability. A broad range of haloarenes with various functional moieties was well tolerated and produced the desired aryl nitriles with good to excellent yields. The nanoparticles were recovered and reused several times without significant palladium leaching.

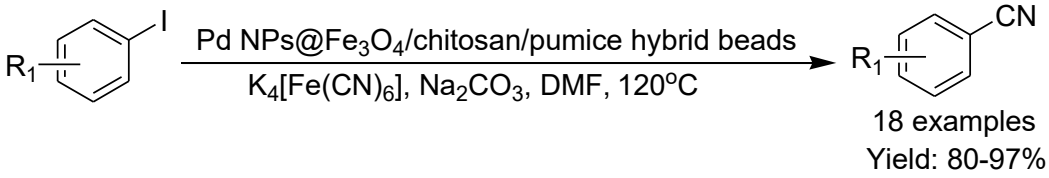

Scheme 24 Pd NPs catalyzed cyanation of aryl halides using $K_4[Fe(CN)_6]$ as cyanating agent

Gogoi and his group[7c] developed a green protocol for the synthesis of bimetallic Pd/Cu NPs supported on graphene oxide through the bio-reduction of $Pd(NO_3)_2$ and $CuSO_4.5H_2O$ using the leaf extract of Tulsi (Ocimum sanctum) as the reducing as well as stabilizing agent (Scheme 25). The synthesized nanoparticles were characterized by FTIR, HRTEM, XRD, XPS, ICP-AES, and BET analysis. This bimetallic Pd/Cu@GO nanocatalyst was investigated for the Sonogashira cross-coupling reaction of aryl iodides with aromatic as well as aliphatic alkynes using Et_3N as the base and resulted in moderate to the excellent yield of the desired coupling products. ICP-AES analysis of the filtrate was carried out and the result showed the Pd or Cu content below detection level (i.e. <0.01 ppm). This study further confirmed the heterogeneous nature and stability of the catalyst.

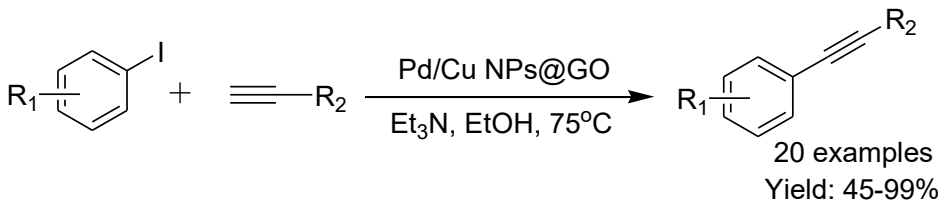

Scheme 25 Pd/Cu NPs catalyzed Sonogashira cross-coupling reaction

II. 2. 1. References:

1. a) D. L. Fedlheim, C. A. Foss, *Metal Nanoparticles: Synthesis, Characterization, and Applications*, CRC Press, **2001**; b) D. Astruc, F. Lu, J. R. Aranzaes, *Angew. Chem., Int. Ed*. **2005**, *44*, 7852; c) *Nanoparticles and Catalysis*, ed. Astruc, D. Wiley-VCH, Weinheim, **2008**; d) R. Hudson, Y. Feng, R. S. Varma, A. Moores, *Green Chem.* **2014**, *16*, 4493; e) T. Aditya, A. Pal, T. Pal, *Chem. Commun.* **2015**, *51*, 9410; f) C. Shan, K. Wu, H. J. Yen, C. N. Villarrubia, T. Nakotte, X. Bo, M. Zhou, G. Wu, H. L. Wang, *ACS Appl. Mater. Interfaces* **2018**, *10*, 15665.
2. a) S. S. Acharyya, S. Ghosh, S. K. Sharma, R. Bal, *RSC Adv.* **2015**, *5*, 89879; b) A. Berrichi, R. Bachir, M. Benabdallah, N. C. Braham, *Tetrahedron Lett*. **2015**, *56*, 1302; c) R. K. Borah, H. J. Saikia, A. Mahanta, V. K. Das, U. Bora, A. J. Thakur, *RSC Adv.* **2015**, *5*, 72453; d) A. V. Martinez, K. Invernizzi, A. Leal-Duaso, J. A. Mayoral, J. I. Garcia, *RSC Adv*. **2015**, *5*, 10102; e) S. Khan, A. Ghatak, S. Bhar, *Tetrahedron Lett*. **2015**, *56*, 2480.
3. a) M. Rezaei, K. Amani, K. Darvishi, *Catalysis Commun.* **2016**, *91*, 38; b) N. Rezaei, B. Movassagh, *Tetrahedron Lett*. **2016**, *57*, 1625; c) H. Veisi, S. Taheri, S. Hemmati, *Green Chem.* **2016**, *18*, 6337; d) A. Hatamifard, M. Nasrollahzadeh, S. M. Sajadi, *New J. Chem.* **2016***, 40,* 2501.
4. a) R. Borah, E. Saikia, S. J. Bora, B. Chetia, *Tetrahedron Lett*. **2017**, *58*, 1211; b) G. Clave, F. Pellissier, S. Campidelli, C. Grison, *Green Chem.* **2017**, *19*, 4093; c) B. Wang, X. Guo, G. Jin, X. Guo, *Catalysis Commun.* **2017**, *101*, 36; d) H. Veisi, S. Hemmati, H. Javaheri, *Tetrahedron Lett*. **2017**, *58*, 3155.
5. a) N. S. Thirukovela, R. Balaboina, R. Vadde, C. S. Vasam, *Tetrahedron Lett*. **2018**, *59*, 3749; b) Z. Xu, X. Yu, X. Sang, D. Wang, *Green Chem.* **2018**, *20*, 2571; c) N. M. R. Martins, A. J. L. Pombeiro, L. M. D. R. S. Martins, *Catalysis Commun.* **2018**, *125*, 15; d) R. Chutia, B. Chetia, *New J. Chem.* **2018***, 42,* 15200.
6. a) A. Patel, A. Patel, *RSC Adv.* **2019**, *9*, 1460; b) T. Song, Y. Duan, Y. Yang, *Catalysis Commun.* **2019**, *120*, 80; c) B. Paul, S. K. Sharma, S. Adak, R. Khatun, G.

Singh, D. Das, V. Joshi, S. Bhandari, S. S. Dhar, R. Bal, *New J. Chem.* **2019**, *43*, 8911; d) S. Du, C. Zhang, Y. Jiang, P. Jiang, Y. Leng, *Catalysis Commun.* **2019**, *129*, 105746; e) C. Chaudhari, H. Imatome, Y. Nishida, K. Sato, K. Nagaoka, *Catalysis Commun.* **2019**, *126*, 55.

7. a) M. Gopiraman, S. Saravanamoorthy, S. Ullah, A. Ilangovan, I. S. Kim, I. M. Chung, *RSC Adv.* **2020**, *10*, 2545; b) T. Baran, *Carbohydr. Polym.* **2020**, *237*, 116105; c) S. Sultana, S. D. Mech, F. L. Hussain, P. Pahari, G. Borah, P. K. Gogoi, *RSC Adv.* **2020**, *10*, 23108.

II. 3. Oxidation of alcohols using transition metal nanocatalyst: A review

Cobalt Schiff base complex functionalized starch-coated maghemite nanoparticles (CoL_2@SMNP) were synthesized by Jafarpour *et al.*[1a] and investigated as the heterogeneous catalyst for the oxidation of a variety of benzylic alcohols to the related carbonyl compounds using molecular oxygen as the oxidant and n-hydroxyphthalimide (NHPI) as the radical generator (Scheme 1). Electron-donating substituents on the phenyl rings accelerated the reaction, whereas electron-withdrawing retarded it. The oxidation of 4-nitro- and 4-methoxy benzyl alcohols produced 35% and 72% yields of the corresponding aldehydes respectively at the same reaction time (16 h). Besides, this catalytic protocol remained inactive towards aliphatic alcohols. The aforesaid nanocatalyst was successfully recovered by an external magnet and reused efficiently. The protocol was also effective for the oxidation of alkylbenzenes to carbonyl compounds.

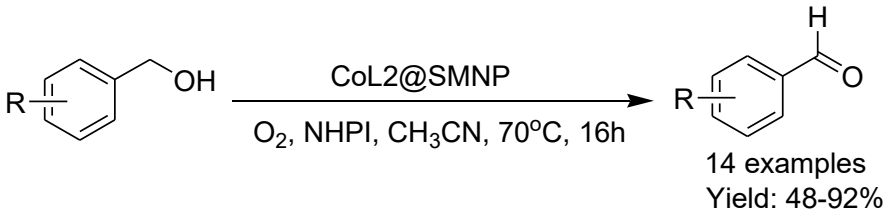

Scheme 1 CoL2@SMNP catalyzed oxidation of benzylic alcohols to aldehydes

Du *et al.*[1b] have utilized a one-step hydrothermal method for the preparation of flower-like hierarchical nickel aluminum-layered double hydroxide (NiAl-LDH) microstructures as the multifunctional support for the synthesis of Au nanocatalyst. The catalytic efficiency of the synthesized Au/NiAl-LDH nanoparticle was investigated through the oxidation of various alcohols in the presence of molecular O_2 as the oxidant and benzyl alcohol was chosen as the model substrate to evaluate the structure-activity relationships (Scheme 2). Besides, the catalytic activity of flower-like Au/NiAl-LDH nanocatalyst was dramatically increased by

60% due to the confinement nature of the hierarchical pores which promoted the effective collisions between substrates and active sites. By identifying the oxidation states and the redox process, the synergistic effect between Au and Ni was also investigated.

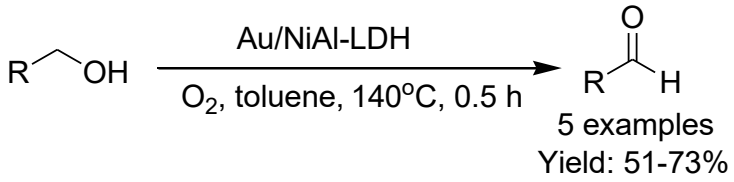

Scheme 2 Oxidation of alcohols using Au/NiAl-LDH nanocatalyst

Copper nanoparticles supported on cellulose template[1c] were utilized as an efficient reusable heterogeneous nanocatalyst for the aerobic oxidation of a wide range of primary benzylic alcohols in a mixture of water (3.5 mL) and acetonitrile (1.5 mL) as the solvent using aerial oxygen as the eco-compatible oxidant under microwave irradiation (Scheme 3). Several electron-donating as well as electron-withdrawing groups were well survived and produced the corresponding carbonyl compounds in good yields. This catalytic system was silent towards the oxidation of secondary benzylic alcohols even after longer reaction time as well as higher reaction temperature. Therefore, they studied the selectivity of this oxidative protocol using the equimolar mixture of benzyl alcohol and 1-phenylethanol and observed that only benzaldehyde was obtained as the only product keeping 1-phenylethanol intact.

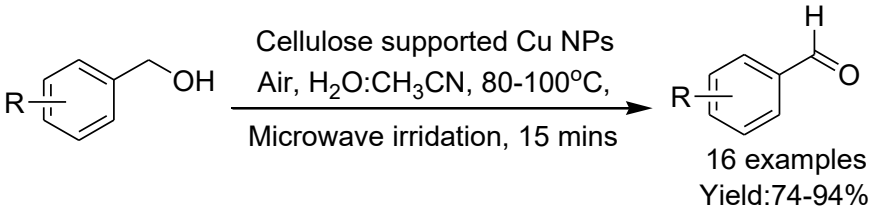

Scheme 3 Cu NPs catalyzed oxidation of alcohols under microwave irradiation

Yang *et al.*[2a] have prepared cobalt-oxide (Co_3O_4) nanoparticles supported on ordered mesoporous carbon CMK-3 (Co_3O_4/CMK-3) (CMK: carbon material from Korea) through the hydrothermal method. The synthesized nanoparticles were characterized by several spectroscopic techniques such as FESEM, TEM, XRD, XPS, FTIR, N_2 adsorption-desorption, Raman, and ICP-AES analysis. The particle size of cobalt oxide nanocatalyst was also characterized and found to be ~2 nm which were uniformly dispersed over the surface of CMK-3. The catalytic performance of Co_3O_4/CMK-3 was investigated towards the oxidation of benzyl alcohol to benzaldehyde using molecular oxygen as the oxidant and DMF as the solvent at 110°C (Scheme 4).

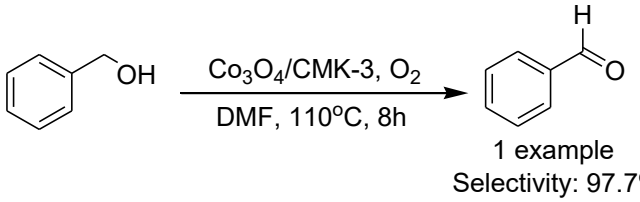

Scheme 4 Oxidation of benzyl alcohol to benzaldehyde catalyzed by Co_3O_4/CMK-3

Binuclear rhodium(II) complex[2b] was used as an efficient reusable catalyst for the aerobic oxidation of primary and secondary alcohols to produce carboxylic acids and ketones respectively in the presence of aerial oxygen as an oxidant and NaOH as the base in an aqueous medium (Scheme 5). It was observed that primary benzylic alcohols with electron-donating groups were more reactive compared to the electron-withdrawing substituents. Primary benzylic alcohols with oxygen-, sulfur- and nitrogen-containing heterocycles afforded the corresponding carboxylic acids in moderate to good yields. Secondary cyclic as well as benzylic alcohols responded efficiently under this protocol and produced the desired ketones with moderate to good yields. The catalyst could be recycled several times without much loss its catalytic activity.

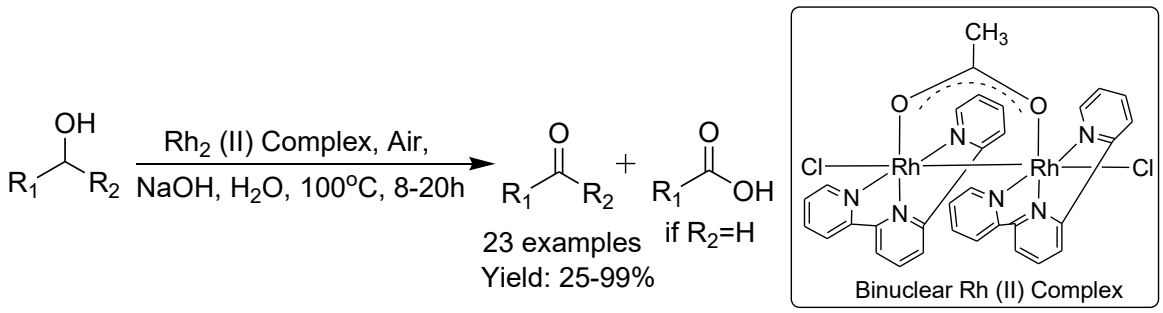

Scheme 5 Rh_2 (II) complex catalyzed aerobic oxidation of alcohols

Kadam *et al.*[2c] have used a low-temperature approach for the synthesis of manganese dioxide (MnO_2) nanoparticles using $MnSO_4$ as the metal precursor supported by the surface of graphene oxide (GO) through wet precipitation technique. The formation of γ-phase MnO_2 in MnO_2/GO nanocomposites was confirmed by Raman spectroscopy and XRD analysis. Transmission electron microscopy (TEM) analyses showed that γ-MnO_2 exists as needle and flower-like structures in graphene oxide (GO) with approximately 15 nm average particle size. The catalytic activity of γ-MnO_2/GO nanocomposites was demonstrated through the aerobic oxidation of primary benzyl alcohols bearing electron-releasing and electron-withdrawing groups to the corresponding carbonyl compounds under mild reaction conditions (Scheme 6).

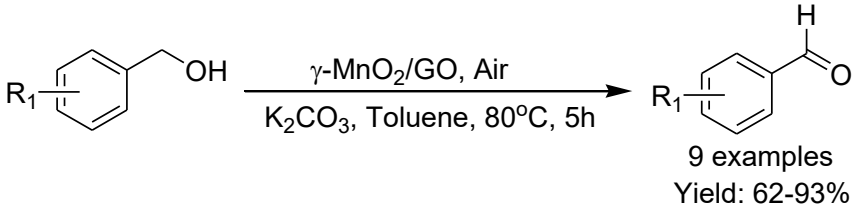

Scheme 6 γ-MnO_2/GO nanocomposites catalyzed aerobic oxidation of benzylic alcohols

An eco-friendly approach was reported for the synthesis of Pd nanoparticles using water extract of Oak fruit bark as a reducing, capping, and stabilizing agent.[3a] The synthesized Pd NPs were characterized by UV-Vis, FTIR, XRD, TEM, FESEM, and EDX techniques. This plant-mediated heterogeneous nanocatalyst was found to bear excellent catalytic efficiency in the aerobic oxidation of primary and secondary benzylic alcohols to the corresponding carbonyl compounds by using K_2CO_3 as a mild base under ambient conditions (Scheme 7). The catalyst was easily recoverable and recyclable up to six times maintaining its activity.

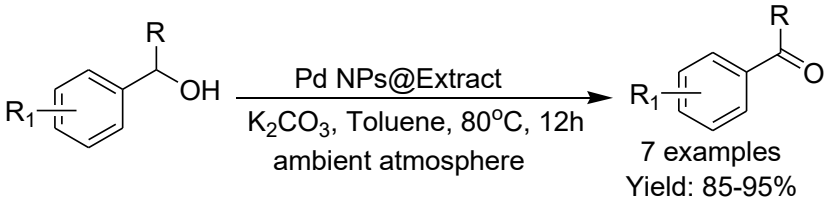

Scheme 7 Aerobic oxidation of benzylic alcohols catalyzed by Pd NPs@Extract

`

Shojaei *et al.*[3b] have synthesized $CuCr_2O_4$ and $CuCr_2O_4/TiO_2$ nanocomposites using the sol-gel method and the catalysts were characterized by transmission electron microscopy (TEM), scanning electron microscopy (SEM), and X-ray diffraction (XRD). The results displayed that Cu (+2) chromite has a cubic normal spinel structure with about 25-40 nm of particle sizes. The catalytic attributes of synthesized $CuCr_2O_4$ and $CuCr_2O_4/TiO_2$ nanocomposite were investigated for the oxidation of benzylic alcohols in moderate to good yields of the desired carbonyl compounds under reflux, photo-irradiation, and microwave irradiation using TBHP as the oxidant (Scheme 8). It was observed that the catalytic efficacy under reflux condition was much better than that of other conditions. Pure $CuCr_2O_4$ or TiO_2 showed poor catalytic activity, whereas $CuCr_2O_4/TiO_2$ displayed significant catalytic efficiency due to improved electron-hole separation.

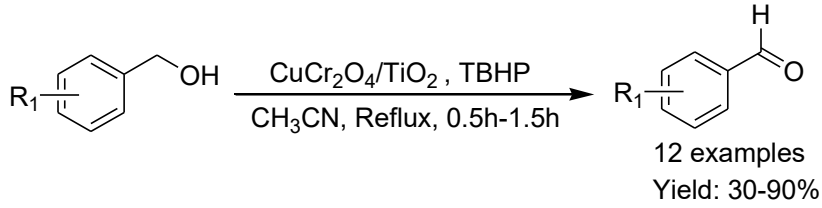

Scheme 8 Oxidation of benzylic alcohols catalyzed by $CuCr_2O_4/TiO_2$

Silica-supported bimetallic copper/silver nanoparticles (Cu/Ag@SiO_2 NPs) were synthesized under ultrasonic irradiation by Saha *et al.*[3c] and also characterized by FESEM, HRTEM, and XRD studies. The results demonstrated that Cu/Ag NPs were uniformly distributed on silica (SiO_2) surfaces with an average particle size of 79.47 nm. The catalytic application of the prepared nanoparticles was tested for the oxidation of primary as well as secondary benzylic alcohols to the related carbonyls using *tert*-butyl hydroperoxide (TBHP) as the oxidant (Scheme 9). The catalyst was heterogeneous, recovered simply by filtration and reused efficiently eight times without significant loss of its activity. Moreover, the catalyst was effective for the oxidation of benzoin to benzil without any by-product.

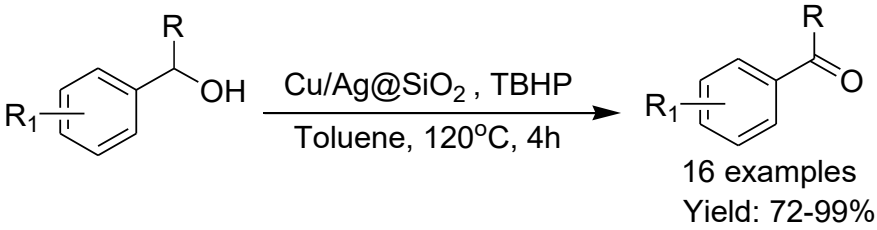

Scheme 9 Cu/Ag@SiO_2 catalyzed oxidation of benzylic alcohols using TBHP as an oxidant

Lee and his co-workers[3d] have disclosed magnetically recoverable and sustainable catalyst prepared by immobilization of an iron (III) amine bis(phenolate) complex on silica (SiO_2) coated magnetic nanoparticles (Fe_3O_4@SiO_2-APTES-FeL^{GDC}). The synthesized nanoparticles were utilized as an efficient heterogeneous catalyst in the oxidation of aromatic as well as aliphatic alcohols to the corresponding ketone (or acid) in the presence of TBHP as an external oxidant (Scheme 10). It has been observed that the alcohols bearing electron-withdrawing substituents (-Cl,-Br, and -NO_2) were oxidized better than the alcohols with electron-donating substituents (-Me, -MeO, and -iPr) under the optimized reaction conditions. Moreover, this catalyst was efficiently utilized for the oxidation of sulfides to sulfoxides in the presence of H_2O_2 as the oxidant.

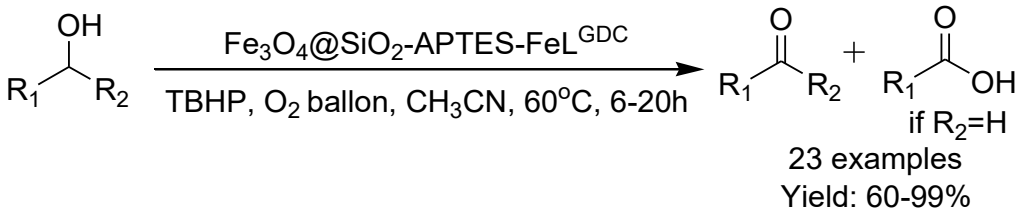

Scheme 10 Fe_3O_4@SiO_2-APTES-FeL^{GDC} catalyzed oxidation of alcohols

R. S. Varma and his group[3e] have synthesized palladium nanoparticles over titanium cluster surface (Pd@TiC) and demonstrated its application towards the aerobic oxidation of primary as well as secondary benzylic alcohols to the corresponding carbonyl compounds

under visible light (20W domestic bulb) irradiation (Scheme 11). The notable features of this catalytic reaction were the use of aerial oxygen as an eco-friendly oxidant and utilization of light energy to accomplish the efficient oxidative transformation of alcohols to carbonyls without the formation of undesired side products. The Pd@TiC nanocatalyst was found to be highly stable and could be efficiently recycled several times without marginal loss in its catalytic activity.

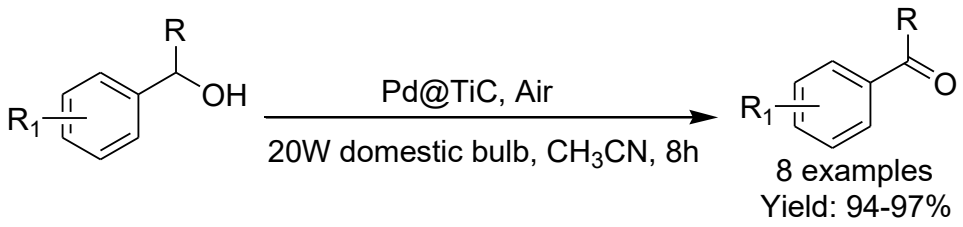

Scheme 11 Pd@TiC catalyzed visible light-mediated oxidation of benzylic alcohols

Hasanpour *et al.*[4a] have synthesized nickel-riboflavin nano complex (Ni(II)Rf_2) via the incorporation of $Ni(OAc)_2$ with riboflavin under ultrasound irradiation and the catalyst was thoroughly characterized by various spectroscopic methods such as UV-vis, FTIR, TEM, EDX, TGA, and ICP-AES analyses. The activity of the catalyst was tested in the aerobic oxidation of a wide range of benzylic alcohols to aldehydes in ethyl acetate as a safe solvent and NHPI (N-hydroxyphthalimide) as the additive (Scheme 12). Different primary and secondary benzyl alcohols showed good to excellent yields, except for those where the aromatic ring bearing nitro substituents. Moreover, oxidation of sulfides to the corresponding sulfoxides was successfully achieved in the presence of H_2O_2 as the oxidant under solvent-free conditions using this catalytic protocol. The catalyst was recovered and recycled efficiently without decreasing its reactivity.

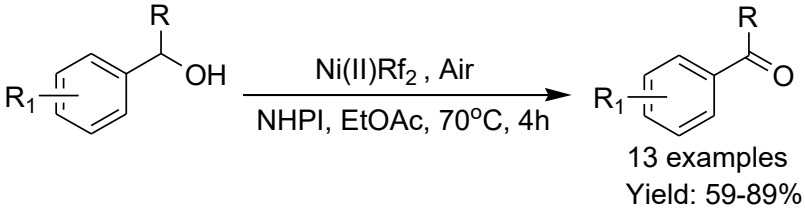

Scheme 12 Oxidation of benzylic alcohols catalyzed by Ni(II)Rf_2 complex

Srivastava and his group[4b] have prepared RuO_2-supported Mn_3O_4 nanocatalyst through the reaction of $RuCl_3$ with MnO_2 molecular sieves in aqueous formaldehyde solution. UV-vis, XRD, XPS, TEM, SEM, N_2 adsorption techniques were used to characterize the synthesized nanocatalyst and the results showed the dispersion of RuO_2 species on the highly crystalline surface of Mn_3O_4. The catalytic system was successfully applied for the oxidation of

aliphatic, aromatic, and hetero-aromatic benzylic alcohols using molecular oxygen or air (flow, 10 mL/min) as an oxidant (Scheme 13). Aliphatic alcohol, such as 1-octanol, was oxidized to 1-octanal as well as over-oxidized product 1-octanoic acid under the optimized reaction conditions. The catalyst was heterogeneous and recycled efficiently without appreciable loss in the catalytic activity even after five runs.

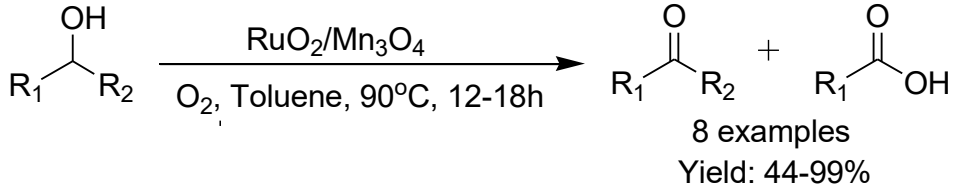

Scheme 13 RuO_2/Mn_3O_4 catalyzed oxidation of alcohols to carbonyls

Boruah *et al.*[4c] have developed Schiff base (SB) functionalized Merrifield resin (MR) supported molybdenum (VI) based heterogeneous catalyst (MR-SB-Mo) and characterized by different methods such as SEM, EDX, BET, elemental, thermal analysis. The synthesized MR-SB-Mo successfully served as an efficient catalyst for the oxidation of a wide range of alcohols such as primary and secondary benzylic as well as aliphatic alcohols to the corresponding aldehydes or ketones in the presence of 30% aqueous H_2O_2 as the green oxidant under solvent-free condition (Scheme 14). The catalyst was regenerated and reused efficiently for at least 5th cycles without loss in its catalytic efficiency and product selectivity.

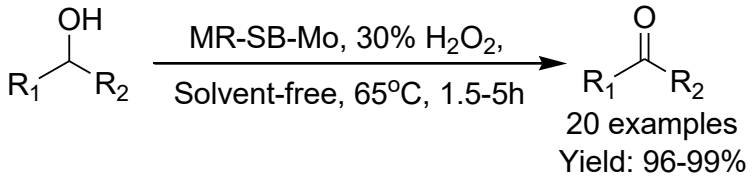

Scheme 14 MR-SB-Mo catalyzed oxidation of alcohols to carbonyls

V_2O_5 rods decorated on graphene oxide (V_2O_5@GO)[4d] have been synthesized using the sonication method and structural features of the prepared nanocomposites were characterized by FTIR, XRD, TEM, SEM, AFM, Raman, and UV-Visible spectroscopy techniques. The catalytic activity of V_2O_5@GO was examined in the oxidation of primary and secondary benzylic alcohols using molecular oxygen as an oxidant (Scheme 15). Although electron-rich and electron-deficient benzylic alcohols showed better results, hetero-aromatic alcohols exhibited poor conversion under the optimized reaction conditions. Aliphatic alcohols remained unaffected even longer reaction time. The catalyst was recycled and reused for two catalytic runs with some gradual decay in its reactivity.

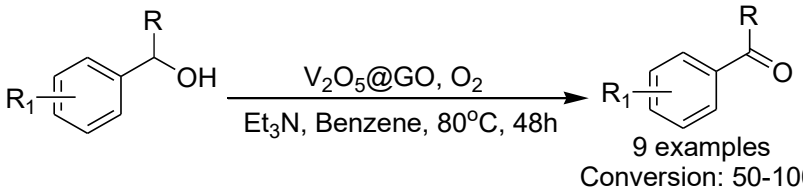

Scheme 15 Oxidation of benzylic alcohols to carbonyls catalyzed by V_2O_5@GO

Kashani *et al.*[4e] have prepared nano-silica thiol-based dendrimer polymer (nSTDP) supported Au nanoparticles (Au_{np}-nSTDP). The catalyst was easily synthesized by the reduction of $HAuCl_4$ with $NaBH_4$ as the reducing agent in the presence of nSTDP. The resulting Au_{np}-nSTDP nanocatalysts were characterized by UV-vis, FTIR, SEM, TEM, XPS, TGA, and ICP techniques. The characterization result showed that Au nanoparticles with an average size of 2-6 nm which was homogeneously distributed on the nano-silica functionalized thiolated dendritic polymer. The synthesized Au_{np}-nSTDP nanocatalyst was utilized in the oxidation of various alcohols in the presence of *tert*-butyl hydroperoxide (TBHP) as oxidant and K_2CO_3 as a mild base in acetonitrile-water solvent (Scheme 16). It was observed that aliphatic alcohols such as (1-hexanol and cyclohexanol) produced the corresponding carbonyl compounds with lower yields.

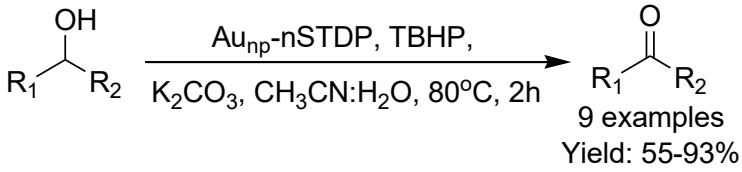

Scheme 16 Au_{np}-nSTDP catalyzed oxidation of alcohols to carbonyls

Copper nanoparticles immobilized on nano-cellulose (Cu@NC) were synthesized by Dutta *et al.*[5a] and applied as an efficient catalyst for the oxidative transformation of benzylic, allylic, and aliphatic alcohols to the corresponding aldehydes using air as the green oxidant and TEMPO (2,2,6,6-tetramethylpiperidinyl-1-oxyl) as stable nitroxyl radicals in water-ethylene glycol (EG) medium at room temperature (Scheme 17). The benzylic and allylic alcohols reacted efficiently and produced the desired carbonyl compounds with excellent yields, whereas aliphatic alcohols showed feeble response even after longer period of reaction time. Besides, this catalytic protocol was also applied for the oxidation of sulfides to sulfoxides using H_2O_2 as the oxidant at room temperature.

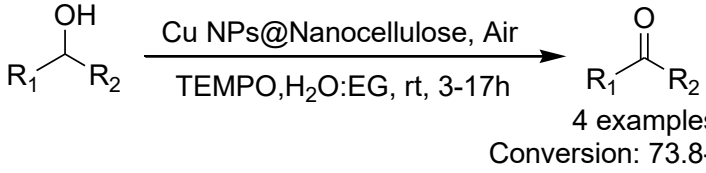

Scheme 17 Cu NPs@ Nanocellulose catalyzed oxidation of alcohols to carbonyls

Meher *et al.*[5b] demonstrated an aerobic oxidative protocol for the oxidation of both aliphatic as well as aromatic alcohols in the presence of Pd-PdO nanoparticles supported by reduced graphene oxide (Pd-PdO@rGO) as the heterogeneous catalyst using molecular oxygen as the primary oxidant in an aqueous medium (Scheme 18). It was observed that the co-existence of both metallic Pd and PdO immobilized on rGO was effective for this oxidation reaction. Aromatic alcohols with electron releasing substituents showed better catalytic performance compared to the electron-withdrawing substituents. Heterocyclic alcohols also participated under the optimized reaction conditions, but lower yields of the desired carbonyl compounds were observed. The Pd-PdO@rGO catalyst was recovered and recycled without detectable loss in its activity.

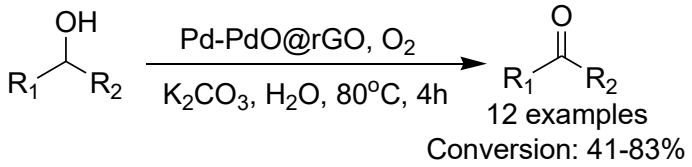

Scheme 18 Oxidation of alcohols to carbonyls using Pd-PdO@rGO nanocatalyst

Goksu *et al.*[6a] have synthesized bimetallic PtNi nanoparticles supported on Single-Walled Carbon Nanotube (PtNi@SWCNT) using a simple single-step reduction method. The characterization of the synthesized nanocatalyst was performed by X-ray diffraction (XRD) study, transmission electron microscopy (TEM), X-ray photoelectron spectroscopy (XPS), and elemental analysis through ICP-OES. This PtNi@SWCNT nanocatalyst was used as the promising material for the oxidation of a wide variety of benzylic alcohols to their corresponding carbonyl compounds using KOH as the base under a continuous stream of O_2 (Scheme 19). All the oxidation products were achieved with high selectivity up to 100% within 2 hours.

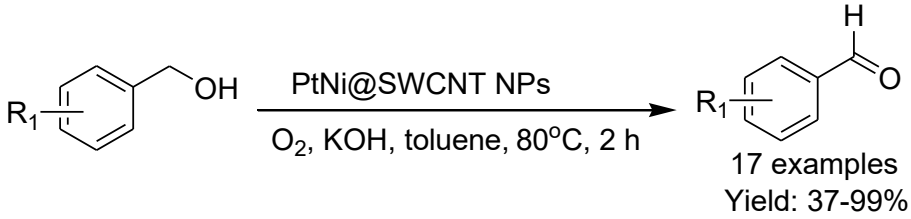

Scheme 19 Oxidation of benzylic alcohols to carbonyls using PtNi@SWCNT

$NiFe_2O_4$ nanoparticles[6b] have been synthesized by the combination of co-precipitation method with hydrothermal aging in the absence of any additive and utilized as an efficient, heterogeneous catalyst in the oxidation of benzylic alcohols to their corresponding carbonyl compounds in the presence of *t*-butyl hydroperoxide (TBHP) as the oxidant (Scheme 20).

Different spectroscopic techniques such as electron microscopy, photoelectron spectroscopy, diffractometry were used to characterize the synthesized nanocatalyst. Benzylic alcohols bearing electron-donating group at *p*-position of the benzene ring showed inferior conversion in comparison with the electron-withdrawing group. Benzylic alcohols with *para*-substituted electron-withdrawing groups exhibited a higher yield of the product, whereas *ortho*- and *meta*-substituted benzylic alcohols showed a lower yield of the product. The catalyst was magnetically recoverable and reusable up to the 5th cycles without losing their catalytic activity.

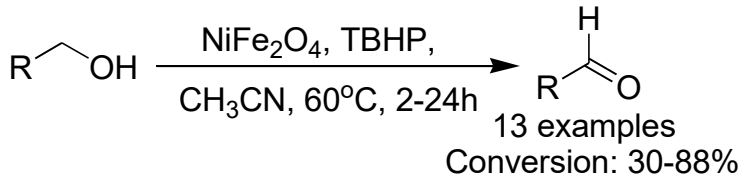

Scheme 20 $NiFe_2O_4$ catalyzed oxidation of alcohols to aldehydes

Oxidation of benzylic alcohols to their corresponding carbonyl derivatives have elaborated by Sen and his group[6c] using palladium nanoparticles supported by commercially available aluminum oxy-hydroxide (Pd/AlO(OH)) under ultrasonic irradiation and solvent-free conditions with a continuous stream of O_2 pressure in the presence of KOH as a strong base (Scheme 21). The synthesized nanoparticles were characterized by several analytical techniques including X-ray diffraction (XRD), transmission electron microscope (TEM), scanning electron microscope (SEM), and elemental analysis by ICP-OES. A series of electron-rich and electron-deficient aromatic alcohols were smoothly oxidized and produced the desired aldehydes with excellent yields within 3 hours.

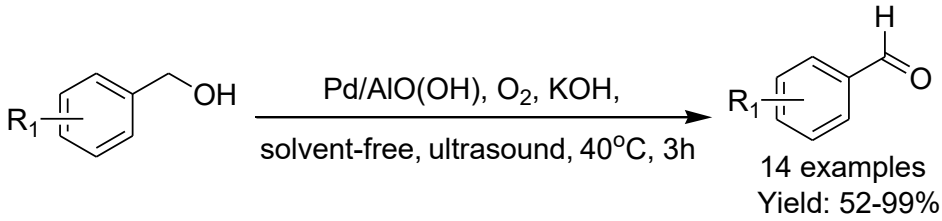

Scheme 21 Pd/AlO(OH) catalyzed oxidation of benzylic alcohols to carbonyls

Au nanoparticles supported on periodic mesoporous organosilica with an imidazolium framework (Au@PMO-IL)[6d] were synthesized and found to be a highly active catalyst for the aerobic oxidation of aliphatic as well as aromatic benzylic alcohols under mild reaction conditions. The prepared catalyst was characterized by transmission electron microscopy (TEM), X-ray photoelectron spectroscopy (XPS), nitrogen adsorption-desorption

measurement, elemental analysis (EA), thermogravimetric analysis (TGA), diffuse reflectance infrared Fourier transform spectroscopy (DRIFT) and inductively coupled plasma atomic emission spectroscopy (ICP-AES). The Au@PMO-IL nanocatalyst showed excellent catalytic activity in the oxidation of various types of alcohols in the presence of either K_2CO_3 (60 °C) or Cs_2CO_3 (35 °C) as the reaction bases in toluene solvent (Scheme 22). The catalyst was successfully recovered and reused for at least seven runs with good reactivity.

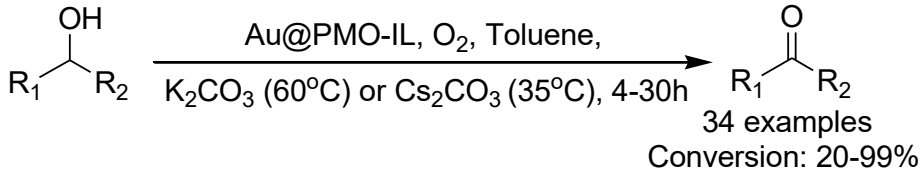

Scheme 22 Au@PMO-IL catalyzed oxidation of alcohols to carbonyl compounds

Fe_3O_4 nanoparticles anchored on graphene oxide (GO) sheet supported Cu(BDC) (BDC: benzene dicarboxylate) composite (Fe_3O_4/Cu-BDC/GO) were synthesized by Alamgholiloo *et al.*[6e] and its catalytic activity was tested for the oxidation of alcohols to their corresponding carbonyl compounds in the presence of molecular oxygen as the oxidant and TEMPO (2,2,6,6-tetramethylpiperidine-N-oxyl) as a stable nitroxide radical in acetonitrile solvent (Scheme 23). The characterization of the catalyst was investigated using FTIR, TEM, SEM, XPS, EDX, and AAS techniques. Primary benzylic alcohols with electron-donating or electron-withdrawing groups afforded good conversion and high yields, but, the oxidation of secondary aliphatic, aromatic, and hetero-aromatic alcohols gave moderate yields even with longer reaction time. The heterogeneity of Fe_3O_4/Cu-BDC/GO catalyst was well maintained even after seven catalytic cycles.

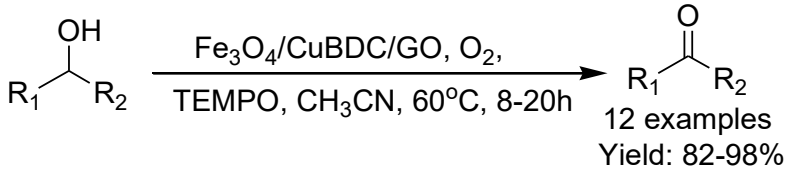

Scheme 23 Fe_3O_4/Cu-BDC/GO catalyzed oxidation of alcohols to carbonyl compounds

Thus the aforesaid comprehensive overview on the recent findings about the application of various transition metal nanocatalysts for important organic reactions including oxidation of alcohols with a plethora of catalysts, substrates, reagents as well as solvents has explored to substantiate the urgency, essentiality, and timeliness of the current investigation going to be elaborated in the next section.

II.4. Present Investigation

II.4.1. Background of the Present Investigation

Compounds containing carbonyl moiety represent an interesting group of molecules due to their versatility as substrates for vital transformations in synthetic organic chemistry as well as important structural sub-units present in several pharmaceuticals, agrochemicals, perfumes, dyes, and flavoring agents[7] along with their applicability towards the construction of a wide variety natural products and bioactive molecules.[8] Therefore, oxidation reactions of alcohols to the carbonyl compounds are specially important for synthetic organic chemists.

Chemoselective oxidation of alcohols to their corresponding carbonyl compounds with minimum over-oxidation and other side reactions is one of the most industrially significant reactions in fine and industrial organic chemistry. Recently, oxidative transformations using aerial oxygen have attracted immense attention[9] because it is the most abundant, inexpensive, safe, economically viable, and eco-friendly oxidant compared to other conventional analogues and produces water as the sole by-product. Organic transformations using heterogeneous catalysts have gained significant interest due to their operational simplicity, unique selectivity, cost-effectiveness as well as the easy recovery and efficient recyclability of the catalyst compared to the conventional homogeneous counterparts. Heterogeneous catalytic systems involving complexes of various transition metals[1-6] have been also reported in the last few years. Serious drawbacks of the reported protocols are associated with the utilization of harmful and expensive metal catalysts,[1b,2b,3a,3c,3e,4b,4c,4e,5b,6a,6c,6d] requirement of high concentration of oxidants,[3b,3c,3d,4e,6b] employing high oxygen pressure,[1a,1b,2a,3d,4b,4d,5b,6a,6c,6d,6e] multistep synthesis of catalysts,[1a,1b,2b,3d,4b,6d,6e] lack of chemoselectivity,[1b,2b,3d,4b,4c,5a,6d,6e] generation of over oxidised product,[2b,3d,4b] and relatively long reaction time.[1a,2b,3d,4b,4d,5a,6b,6d,6e] Therefore, the development of a cost-effective, operationally simple, economically viable, easily accessible, and efficient catalytic system for the chemoselective oxidation of alcohols using most abundant aerial oxygen as the source of an eco-friendly oxidant is of great demand in the present environmental scenario. In this connection, we enumerate our new findings on the excellent catalytic performance of alumina-supported nickel nanoparticles (Ni-Alumina)[10] for highly chemoselective and ligand-free oxidative transformation of benzylic alcohols to the corresponding carbonyl compounds in the presence of aerial oxygen as the source of an eco-friendly oxidant.

II.4.2. Results and Discussion

II.4.2.1. Preparation of alumina supported Ni nanoparticles

To a solution of nickel chloride hexahydrate (4.75g, 20mmol) in distilled water (15mL), neutral alumina (20.0g) was added under the stirring condition to get the slurry of nickel chloride on neutral alumina. It was dried thoroughly in the air when nickel chloride adsorbed on neutral alumina was obtained as a greenish-white easy flowing powder. To the magnetically stirred suspension of this material in methanol (20mL), sodium borohydride (1.512g, 40mmol) was added in small portions and stirring was continued for another 1 hour under ambient atmosphere. By this time, the greenish-white mass turned grey. Then it was filtered, washed successively with methanol (3×5mL), water (3×10mL), and methanol (2×5mL). The residue was dried at 130^{o}C for 2 hours to afford alumina-supported nickel nanoparticles (21.10g, referred to as Ni-Alumina) as a grey free-flowing powder. It can be stored under the ambient condition for months without appreciable deterioration of its catalytic activity.

II.4.2.2. Characterization of alumina supported Ni nanoparticles

Although a few organic reactions were reported in the literature using alumina supported Ni nanoparticles but still, the catalyst was not thoroughly characterized. So, we characterized the catalyst with the help of X-ray diffraction (XRD), transmission electron microscopy (TEM), high-resolution transmission electron microscopy (HRTEM), scanning electron microscopy (SEM), Energy-dispersive X-ray spectroscopy (EDX), elemental mapping analyses, X-ray photoelectron spectroscopy (XPS), Dynamic light scattering (DLS), Zeta potential analysis, and N_2 adsorption-desorption isotherm.

X-ray diffraction (XRD) analysis: To determine the crystalline nature of the synthesized nanocatalyst, powder X-ray diffraction of the sample was recorded (Figure 1). The result indicates that the sample is composed of both metallic Ni and NiO supported on alumina. The diffraction peaks observed at 45.4^{o} (111), 55.3^{o} (200), 77.5^{o} (220), and 95.6^{o} (222) attributed to the metallic Ni phase and other characteristic peaks observed at 37.3^{o} (111), 42.8^{o} (200), 60.9^{o} (220), 72.3^{o} (331), and 85.4^{o} (222) were assigned to the presence of NiO phase. The observed results are closely matched with the theoretical values from metallic Ni (cubic structure, JCPDS# 01-071-3740) and NiO (cubic structure, JCPDS# 01-089-3080).[11]

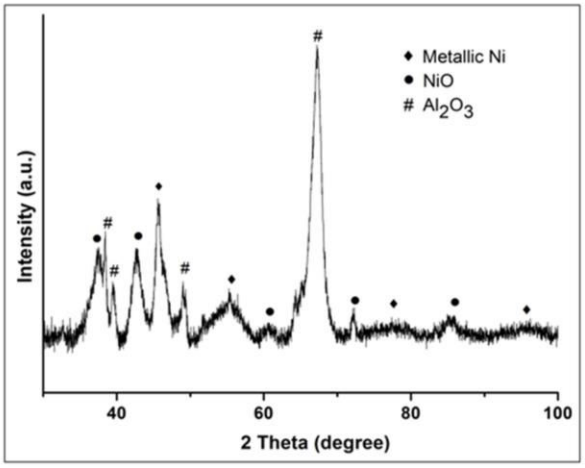

Figure 1 X-ray diffraction analysis of Ni nanoparticles supported on alumina.

Transmission Electron Microscopy (TEM) and high-resolution transmission electron microscopy (HRTEM) analysis: To investigate the structural details of Ni nanocatalyst, transmission electron microscopy (TEM) and high-resolution transmission electron microscopy (HRTEM) were utilized for characterization of the samples. The results are in presented Figure 2. From the images, the crystalline nature of the synthesized nanocatalyst was observed with lattice fringe spacing of 0.203 nm and 0.240 nm corresponding to the d value for cubic Ni (111) and cubic NiO (111) respectively. The corresponding SAED pattern (selected area electron diffraction) also revealed the polycrystalline nature of the nanocatalyst. The results are in good agreement with the XRD analysis.

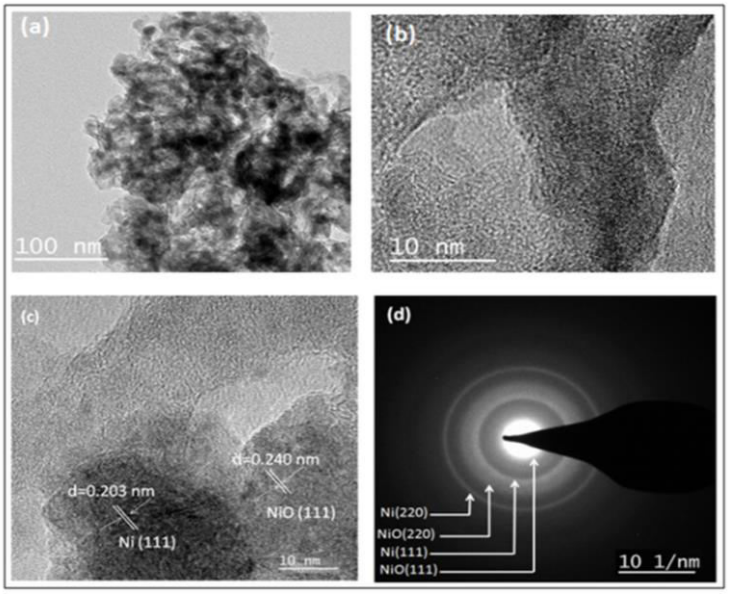

Figure 2 TEM images of Ni nanoparticles@Al_2O_3: a) distribution of Ni catalysts, b) and c) HRTEM, d) selected area electron diffraction (SAED).

Scanning Electron Microscopy (SEM), Energy Dispersive X-ray Spectroscopy (EDX), and elemental mapping analysis: Scanning electron microscopy (SEM) image is presented in Figure 3a. It has been observed that nickel nanoparticles have a nanocrystalline structure with an irregular spread on the supported alumina. EDX (Energy-dispersive X-ray spectroscopy) analysis was also performed to ensure the chemical composition of the synthesized nanocatalyst (Figure 3b). The result shows the strong elemental signal of Ni, Al, and O and their relative proportions in the nanoparticles. Additionally, the spatial distribution of each element was also investigated by a mapping experiment which demonstrated that the distributions of Ni, Al, and O elements are well arranged in the structure of nanocatalyst (Figure 3c).

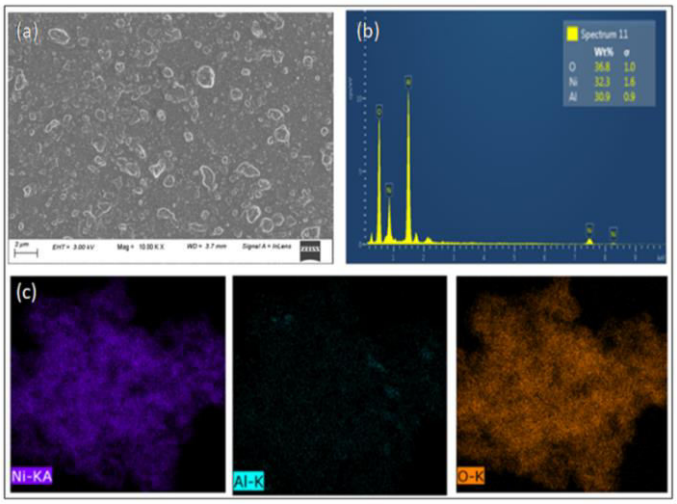

Figure 3 (a) SEM images, (b) EDX spectra, and (c) elemental mapping images of Ni nanoparticles supported on alumina.

X-ray photoelectron spectroscopy (XPS) analysis: XPS analysis has been carried out to investigate the oxidation state of the Ni species in the nanocatalyst (Figure 4). A high-resolution spectrum of the Ni 2p core level region was recorded to identify the presence of Ni species. The Ni $2p_{3/2,1/2}$ binding energy peaks observed at 853.8 and 871.6 eV along with associated satellite peaks at 859.7 and 877.7 eV correspond to Ni metal. The peaks observed at 855.8 and 873.7 eV with satellite peaks at 864.2 and 881.5 eV are attributed to Ni oxide species present on the nanocatalyst surface. Binding energy peak values of Ni metal are on the higher side because of the nanoparticle nature of the Ni metal species. The peak positions are closely matched with the reported literature.[12] However, the intensities of the core level peaks indicate the predominant presence of elemental Ni atoms over Ni oxide species on the surface of the nanocatalyst. The appearance of oxidized Ni is due to the probable chemical sorption of oxygen or it could be the surface oxidation during the preparation and storage of

nanocatalyst. According to the basic principle of XPS, the area ratio of $2p_{3/2}$ to $2p_{1/2}$ would be 2 which can be observed in the present study.

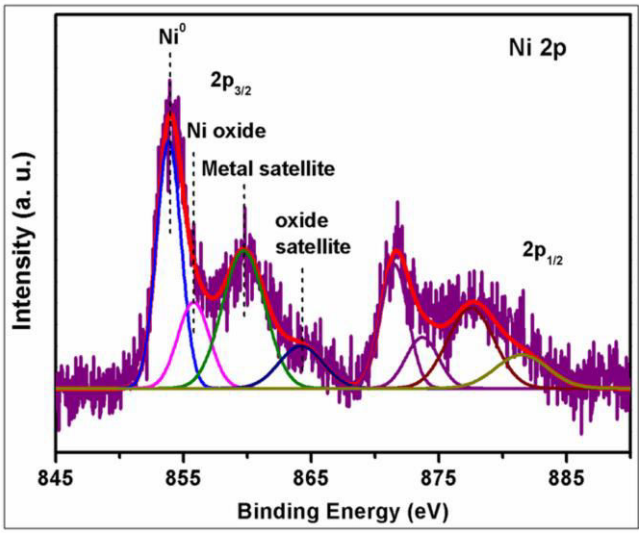

Figure 4 X-ray photoelectron spectroscopic analysis of alumina supported Ni nanoparticles.

Dynamic light scattering (DLS) and Zeta potential analysis: The particle size distribution (Figure 5a) and zeta potential analysis (Figure 5b) of the synthesized alumina-supported nickel nanoparticle were investigated by a dynamic light scattering (DLS) experiment in an aqueous dispersion. The average particle size of Ni-Alumina is 36.5 nm. The stability of Ni-Alumina was also evaluated via zeta potential analysis. Nanoparticles with zeta potential values greater than +30 mV or less than -30 mV are considered as high degrees of stability.[13] The synthesized Ni-Alumina revealed a zeta potential of -32.5 mV owing to their enhanced stability by preventing the agglomeration of the nanoparticles encapsulated in the pore of alumina.

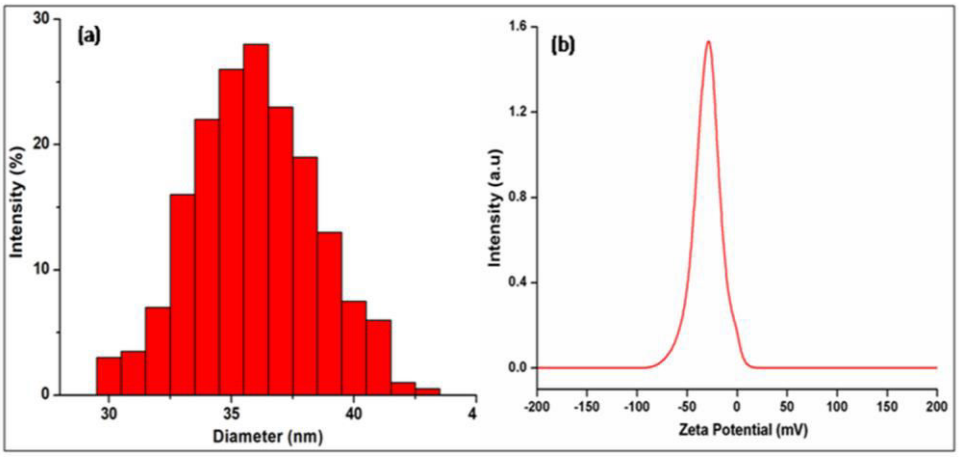

Figure 5 (a) DLS (dynamic light scattering) and (b) Zeta potential analysis of alumina supported Ni nanoparticles.

N_2 adsorption-desorption isotherm: The specific surface area and porosity of the synthesized Ni-Alumina were evaluated by the Brunauer-Emmett-Teller (BET) method with N_2 adsorption-desorption isotherms. The results were shown in Figure 6. The isotherm belonged to type III isotherm with a discrete hysteresis loop at a relative P/P_0 range 0.4 to 1.0, disclosed a mixed H3 and H1 type (according to the IUPAC classification) which signified the mesoporous nature of the synthesized nanocatalyst (Figure 6a). The BET surface area was found to be 108 m^2g^{-1}. The corresponding pore size distribution was calculated from the desorption part of the isotherm which centered around 2.8 nm (Figure 6b) indicating also the mesoporous behavior of the nanocatalyst.

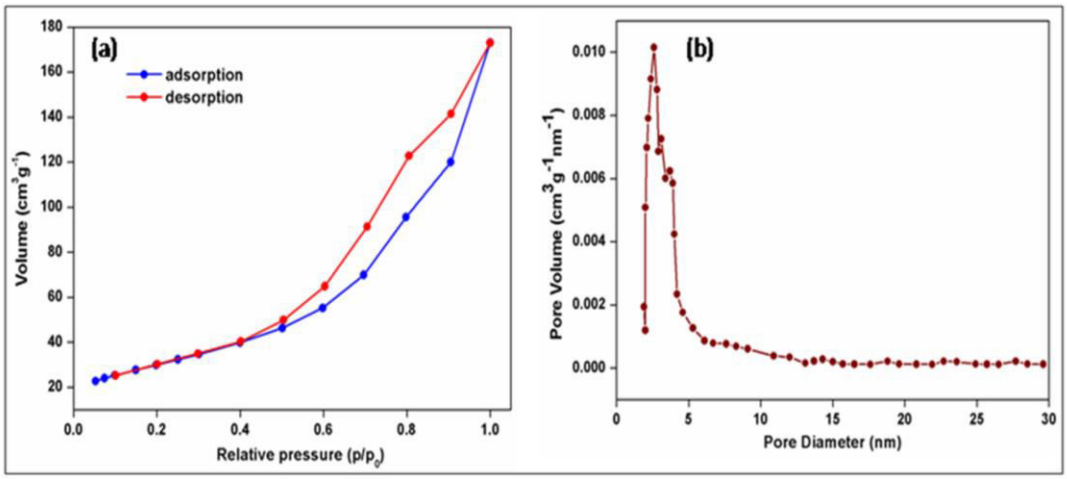

Figure 6 (a) Nitrogen adsorption-desorption isotherm and (b) corresponding pore size distribution plot for Ni-alumina.

The nanocatalyst had considerable stability towards heat and moisture. Thus the encapsulation of Ni nanoparticles inside the pores of the alumina support was quite evident. When freshly prepared powdered Ni nanoparticles (without alumina support) were kept to ambient atmosphere, black nanoparticles (Ni^0) turned to greenish powder (Ni^{II}) after one day. So the supported catalyst had greater stability towards heat and moisture compared to unsupported ones.

II.4.2.3. Catalytic efficiency of Ni-Alumina

To check the efficacy of Ni-Alumina we initially investigated the reaction conditions for the aerobic oxidation of 4-methoxybenzyl alcohol **1a** (1 mmol) in the presence of different bases in various solvents at different temperatures to obtain the corresponding aldehyde **2a**. The reaction was also carried out varying the amounts of catalyst to obtain the optimum conditions (Table 1).

Table 1 Ni-Alumina catalyzed optimization of reaction conditions

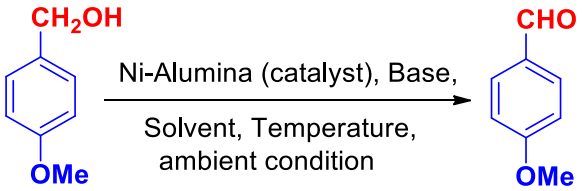

1a **2a**

Entry	Catalyst (mol%)	Base	Solvent (mL)	Temperature (^oC)	Time (h)	Yield[b] (%)
1	--	--	Toluene	Reflux	12h	--
2	--	KOH	Toluene	Reflux	12h	--
3	--	KO^{t}Bu	Toluene	Reflux	12h	--
4	2	--	Toluene	Reflux	12h	Trace
5	3	KO^{t}Bu	Toluene	80^{o}C	10h	76
6	4	KO^{t}Bu	Toluene	80^{o}C	10h	80
7	4	NaO^{t}Bu	Toluene	80^{o}C	10h	73
8	**5**	**KO^{t}Bu**	**Toluene**	**80^{o}C**	**7h**	**90[c]**
9	6	KO^{t}Bu	Toluene	80^{o}C	7h	90
10	7	KO^{t}Bu	Toluene	80^{o}C	7h	91
11	8	KO^{t}Bu	Toluene	80^{o}C	7h	91
12[d]	5	KO^{t}Bu	Toluene	80^{o}C	7h	--
13	5	K_2CO_3	Toluene	80^{o}C	9h	42
14	5	KOH	Toluene	80^{o}C	9h	63
15	5	NaOH	Toluene	80^{o}C	10h	60
16	5	KO^{t}Bu	xylene	80^{o}C	10h	78
17	5	Et_3N	Toluene	80^{o}C	12h	42
18	5	Pyridine	acetonitrile	80^{o}C	12h	35

[a]Reaction conditions: **1a** (1.0 mmol), base (1.2 mmol), catalyst and temperature (as indicated), solvent (3 mL) under ambient condition. [b]Isolated yield. [c]GC yield (>99%). [d]The reaction was carried out under an inert (argon) atmosphere.

The reaction did not occur in the absence of Ni-Alumina both in the absence (entry 1) as well as in the presence of a base (entries 2, 3); the unreacted substrate **1a** was isolated intact in all the cases. The trace amount of product was isolated after 12h when the reaction was carried out under reflux condition in toluene using 2 mol% of catalyst in the absence of base (entry 4). The extent of conversion was increased to 76% within 10h using 3 mol% of Ni-Alumina as a catalyst and potassium tert-butoxide (1.2 mmol) as a base (entry 5) when the reaction was carried out at 80^{o}C. Increasing the amount of catalyst to 4 mol%, the extent of conversion was slightly increased to 80% after 10h (entry 6). A less satisfactory result was obtained with NaO^{t}Bu instead of KO^{t}Bu (entry 7). Other bases such as K_2CO_3, KOH, NaOH, Et_3N, and pyridine resulted in moderate yields (entries 13, 14, 15, 17, and 18). Hence

potassium tert-butoxide was found to be the most effective base in this reaction. These observations demonstrated the very necessity of the co-existence of both Ni-Alumina and base for effective oxidative transformation. A better result was obtained within 7h when the reaction was performed with Ni-alumina (5 mol%) and potassium tert-butoxide (1.2 mmol) (entry 8). The efficient conversion of the substrate **1a** to the corresponding aldehyde **2a** was achieved without the formation of any over-oxidized by-products as monitored by GC analysis (GC Yield: >99%) (entry 8). Moreover, when the crude reaction mixture was treated with diazomethane, no trace of methyl 4-methoxybenzoate (expected to be obtained from 4-methoxybenzoic acid due to over-oxidation of **1a**) was observed in the ^{1}H NMR spectrum; occurrence of **2a** as the exclusive reaction product was thus clearly evident. This observation suggested the inherent selectivity of this protocol. Excess catalyst beyond this proportion (5 mol%) did not show further increase in the substrate conversion and the yield of the reaction remained more or less the same (entries 9-11). Therefore, the conditions, as delineated in entry 8, have been chosen as the optimized condition for further reactions to extend the substrate scope and establish the general applicability as well as the selectivity of the aforesaid protocol. The inferior performance was observed when the reaction was carried out in xylene and acetonitrile (entries 16 and 18). It is extremely important to note that no aldehyde was detected in the reaction mixture when the reaction was carried out under an inert (Ar) atmosphere in the absence of aerial oxygen (entry 12), the substrate **1a** was recovered unaffected. Therefore, the essentiality of aerial oxygen along with both Ni-Alumina and potassium *tert*-butoxide towards this oxidative transformation has been firmly substantiated. Interestingly, in contrast to most of the methods involving metal nanocatalysts, no inert atmosphere was required for the reaction described under Table 1, rather the inert atmosphere has been found detrimental (entry 12) for this reaction. The aforesaid oxidative protocol did neither occur with neutral alumina alone nor with nickel nanopowder without support nor with alumina-supported nickel chloride or with nickel oxide nanoparticles. The importance of alumina-supported nickel nanoparticles for this oxidative organic transformation in terms of its better stability and superior catalytic activity was thereby firmly established.

To demonstrate the generality and scope of this newly developed protocol, primary and secondary benzylic alcohols **1** bearing various electron-withdrawing and electron-donating substituents at different positions of the aromatic ring were reacted under the optimized condition where the corresponding carbonyl compounds **2** were obtained with good yield (Table 2).

Table 2 Ni-alumina catalyzed oxidative transformation of alcohols under ambient condition

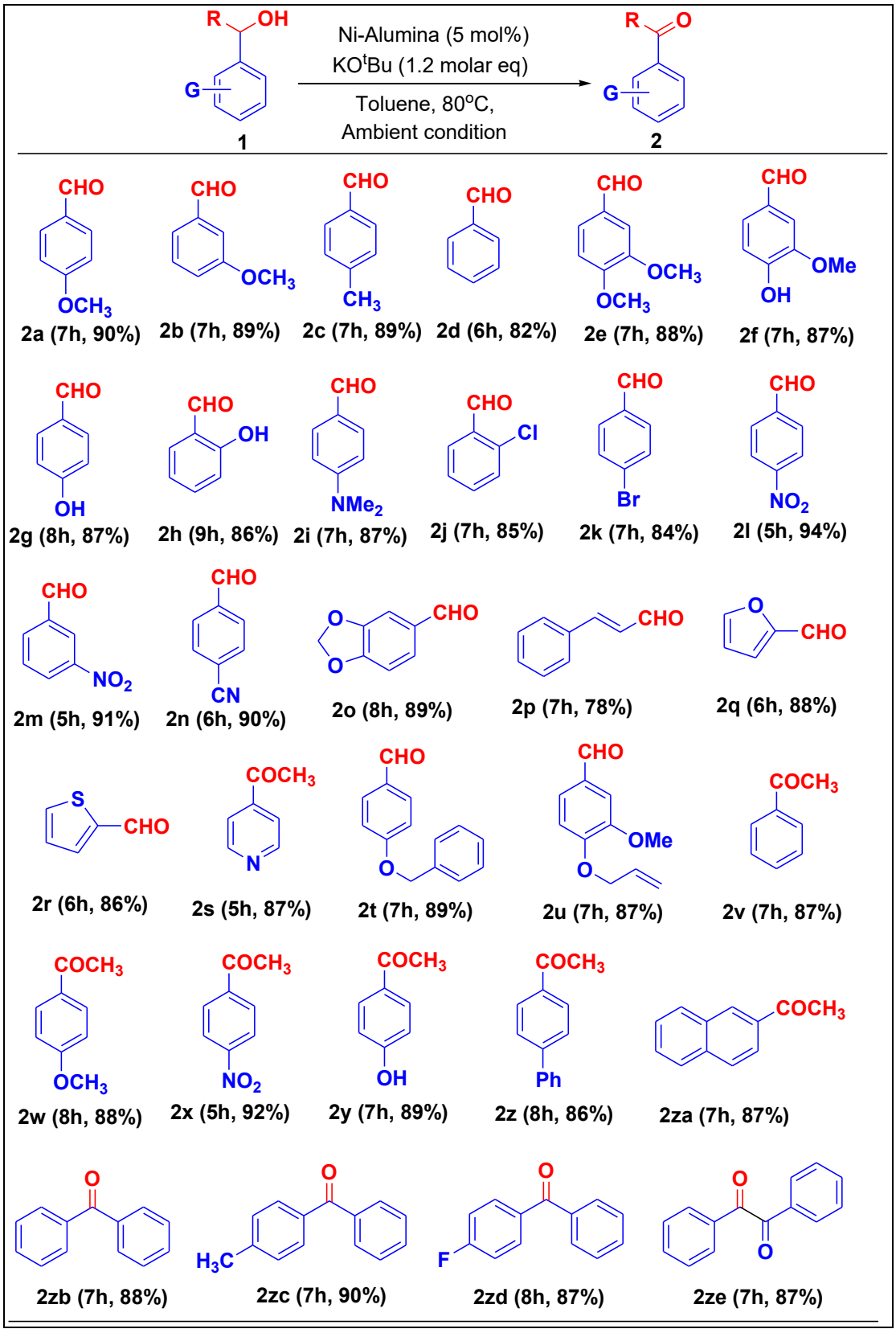

Reaction conditions: **1** (1.0 mmol), KO^{t}Bu (1.2 molar eq), catalyst (5 mol%), toluene (3 mL) at 80^{o}C for indicated time under ambient condition. Yield refers to that of the isolated pure product.

As evident from Table 2, primary benzylic alcohols bearing electron-donating substituents produced the corresponding aldehydes in good yield (**2a-2e**). Phenolic-OH groups did not interfere during this reaction (**2f-2h**). Highly deactivated benzyl alcohol, such as 4-N,N-dimethylaminobenzyl alcohol (**1i**), also responded efficiently under the optimized condition with a shorter reaction time to furnish **2i** in 87% yield. Halogenated alcohols were also compatible and desired products **2j** and **2k** were formed without any dehalogenation. Primary benzylic alcohols bearing electron-withdrawing substituents, which are generally less susceptible to oxidation, furnished the corresponding aldehydes under the present reaction condition in good yield. Nitro-substituted primary benzylic alcohols were oxidized smoothly to the corresponding aldehydes (**2l and 2m**) taking less time for completion and the yields (94% and 91% respectively) were comparable with the electron-rich analogues. The progress of the reaction of primary benzylic alcohols **1l** and **1a** (bearing 4-NO_2 and 4-OMe substituents respectively) was monitored separately at different time intervals under the optimized reaction condition (Figure 7). It was observed that the reaction was faster in the case of 4-nitrobenzyl alcohol (**1l**) compared to 4-methoxybenzyl alcohol (**1a**) and better conversion was achieved in the former case. Therefore, the electronic effect of the substituents towards this Ni-alumina catalyzed oxidative protocol was conclusively established.

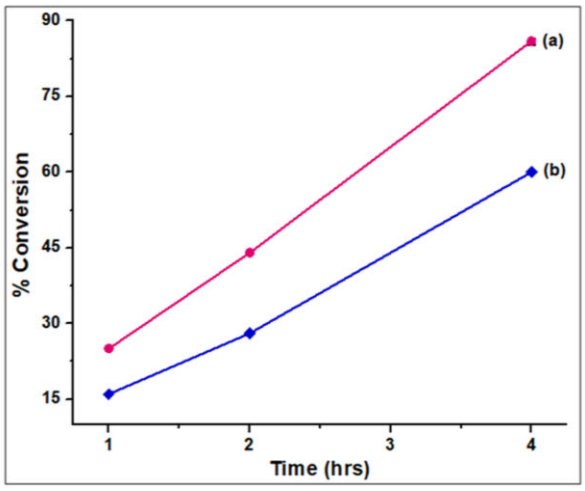

Figure 7 Plot of the percentage conversion of (a) 4-nitrobenzyl alcohol (**1l**) and (b) 4-methoxybenzyl alcohol (**1a**) using Ni Alumina (5 mol%), KO^{t}Bu (1.2 mmol), toluene (3mL) at 80^{o}C under ambient condition.

Hydrolyzable functional groups, like -CN and methylenedioxy also survived under the aforesaid protocol to produce the corresponding aldehydes **2n** (90%) and **2o** (89%) respectively. One signal at δ 117.6 in the ^{13}C NMR spectrum of **2n** confirmed the survival of

the –CN group. This is not commonly observed in some literature reports.[3a,4a,4c,5b] The oxidation of cinnamyl alcohol afforded the mixture of cinnamaldehyde (**2p**) and cinnamic acid in 82:18 ratio (determined by 400 MHz ^{1}H NMR spectroscopy) under optimized reaction condition, wherefrom **2p** was isolated with 78% yield. To extend the substrate scope, this study was further extended to more challenging substrates with vulnerable heterocyclic moieties. Acid-sensitive heteroaryl moieties along with the formyl group as well as ketomethyl group also survived during this reaction and the products were obtained in good yields (**2q-2s**). It is important to note that highly vulnerable groups like O-benzyl and O-allyl moieties were also tolerated under the optimized reaction condition to produce **2t** and **2u** with 89% and 87% yields respectively.

This procedure was also effective for secondary benzylic alcohols. 1-Phenylethanol (**1v**) behaved similarly to produce the corresponding ketone (**2v**) with 87% yield. Substrates with a wide variety of substituents, including methoxy, nitro, hydroxyl, and phenyl also responded smoothly to yield the corresponding ketones (**2w-2z**). 2-Acetylnaphthalene (**2za**) was obtained in 87% yield under the optimized protocol. Diarylcarbinols afforded the diaryl ketones (**2zb**-**2zd**) in good yield. α-Hydroxyketone (**1ze**) also reacted efficiently to produce 1,2-diketone (**2ze**) in 87% yield. Interestingly, aliphatic primary and secondary alcohols did not respond to the present protocol where the substrates were recovered unchanged.

Encouraged by the above observations, we ventured to investigate the chemoselectivity of this Ni-alumina catalyzed oxidative protocol. Therefore, an intermolecular competition reaction was carried out with an equimolecular mixture of 4-methoxybenzyl alcohol (**1a**) and 1-heptanol under the optimized condition which produced the 4-methoxybenzaldehyde (**2a**) exclusively, and 1-heptanol was recovered unaffected (Scheme **1**). This is an immensely important and additional attribute of the said protocol in contrast to many earlier reports where no such chemoselectivity was observed.[1b,2c,3d,4b,4c,5a,6d,6e]

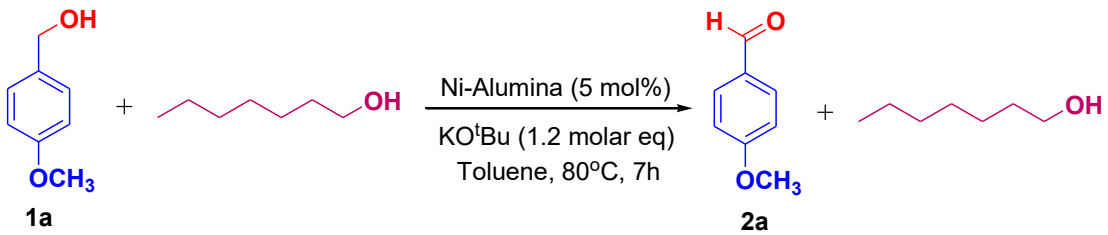

Scheme 1 Intermolecular competition experiment to demonstrate chemoselectivity

The aforesaid protocol was further applied to the intramolecular competition experiments where the substrates **3a** and **3b,** under the optimized condition, produced **4a** and **4b**

respectively (Scheme **2**). It was found that in both cases, benzylic alcohol was selectively oxidized to the corresponding carbonyl group and the primary aliphatic alcohol moiety remained intact. The occurrence of –CHO moiety in **4a** and $–COCH_3$ moiety in **4b** was confirmed by the singlet at δ = 9.85 ppm in **4a** and at δ = 2.52 ppm in **4b** (in the ^1H NMR spectrum) as well as a signal at δ = 191.1 ppm in **4a** and at δ = 197.4 ppm in **4b** (in the ^{13}C NMR spectrum). Survival of primary alcohol moiety in **4a** and **4b** was further substantiated through acetylation of **4a** and **4b** to the mono acetates **5a** and **5b** respectively which was further confirmed by a singlet at δ = 2.06 ppm in **5a** and at δ = 2.08 ppm in **5b** (in the ^1H NMR spectrum) as well as a signal at δ = 170.8 ppm in **5a** and at δ = 170.9 ppm in **5b** (in the ^{13}C NMR spectrum).

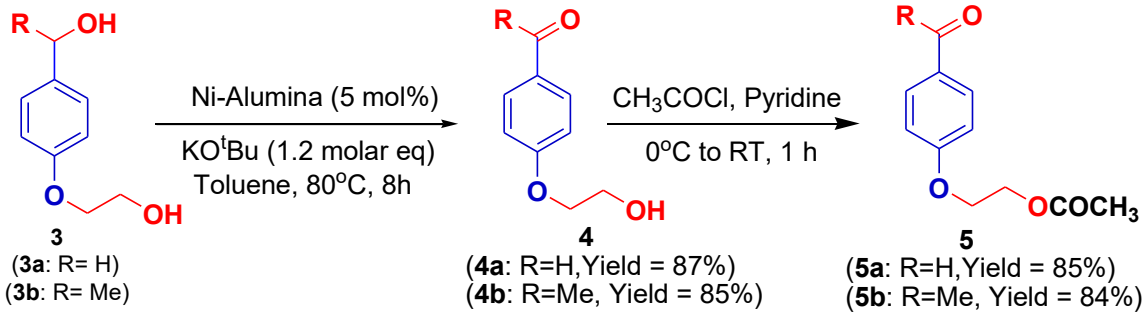

3 (**3a**: R= H) (**3b**: R= Me)

4 (**4a**: R=H,Yield = 87%) (**4b**: R=Me, Yield = 85%)

5 (**5a**: R=H,Yield = 85%) (**5b**: R=Me, Yield = 84%)

Scheme 2 Chemoselective oxidation of 1° and 2°-benzylic alcohol

To gain insight into the mechanistic aspect of the present oxidative protocol, some control experiments were performed (Scheme 3). The aforesaid oxidative protocol did not work with neutral alumina as well as alumina-supported nickel chloride, nickel nanopowder without any support, and with nickel oxide nanoparticle in the absence of any support (Scheme 3a). This observation suggested that alumina acted as a support to the metallic nanoparticles in this reaction. Notably, when the reaction was tested under a nitrogen atmosphere, the substrate 4-methoxybenzyl alcohol **1a** was recovered unaffected (Scheme 3b). Therefore, the essentiality of the oxygen atmosphere towards this oxidative transformation was conclusively proved. It was observed that when the reaction was carried out under O_2 atmosphere in the presence as well as in the absence of NaO^{t}Bu, the yields of the reaction were 87 % and 21 % respectively within 7h (Schemes 3c and 3d). The reaction was better when the oxidation of 4-methoxybenzyl alcohol **1a** was performed in the presence of KO^{t}Bu as the base under O_2 atmosphere (yield 98% after time 3h, Scheme 3e) than in the presence of NaO^{t}Bu as well as in the absence of KO^{t}Bu or NaO^{t}Bu. These experiments revealed that both KO^{t}Bu and O_2 atmosphere were required for the effective oxidative transformation.

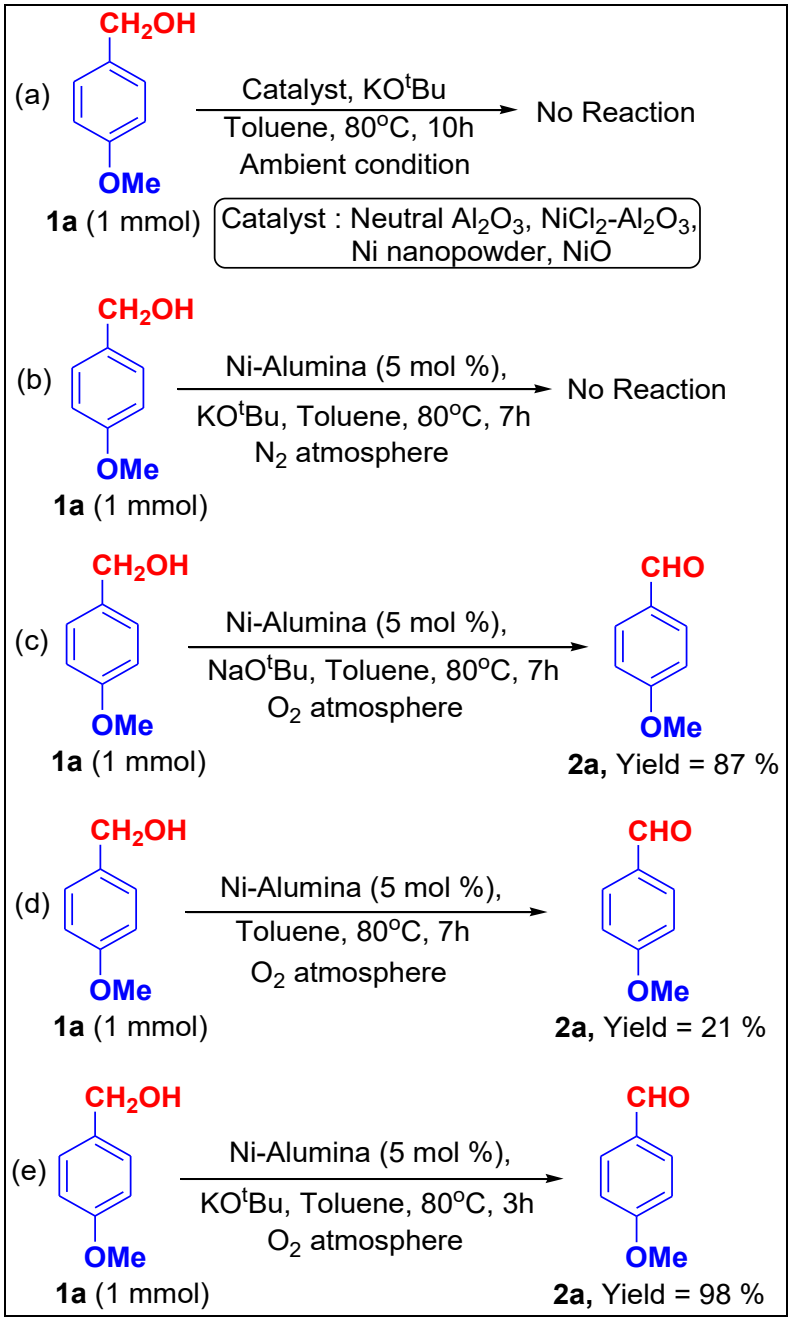

Scheme 3 Control experiments for the oxidative transformation of alcohols

Based on the aforesaid investigations and literature reports,[14,15] the plausible mechanism for this Ni-Alumina catalyzed oxidative transformation is depicted in Scheme 4. The coupling of alcoholic oxygen to the metallic nickel and coordination of the aromatic ring with the catalyst surface seems to be the initiation step of this catalytic reaction. The corresponding carbonyl compounds (aldehydes or ketones) were subsequently obtained by the removal of a hydrogen atom from the benzylic position in the presence of KO^{t}Bu. Aerial oxygen acts as an environmentally benign oxidant regenerating Ni (0) with the generation of hydrogen peroxide which is subsequently decomposed into water and oxygen as an

innocuous by-product. The presence of hydrogen peroxide was detected by the development of dark blue color when the reaction mixture was added to a mixture of KI, starch, and acetic acid. The reluctance of aliphatic alcohols towards this oxidative protocol might be due to the lack of proper coordination of the alkyl moiety to the catalyst surface. Thus, the high chemoselectivity of the present oxidative protocol towards the benzylic alcohols in the presence of aliphatic alcohols along with the efficient recyclability (*vide infra*) of the catalyst (Ni-Alumina) can be justified.

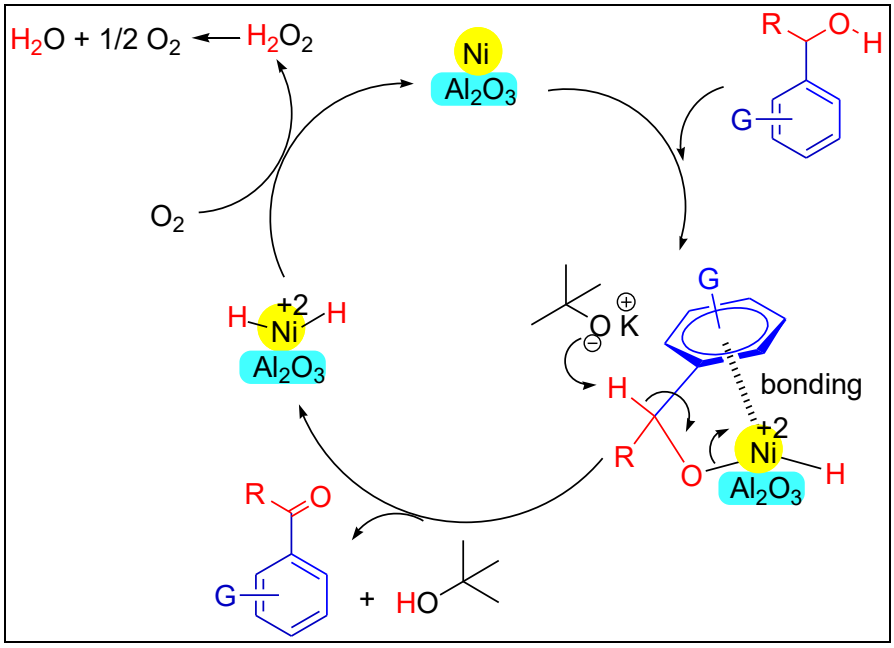

Scheme 4 Plausible mechanism for the Ni-alumina catalyzed oxidation of alcohols

Gram scale applicability:

To evaluate the practical applicability of this catalytic system, a gram scale reaction with **1a** (1.104g, 8 mmol) was performed under the optimized reaction conditions and the desired product **2a** was isolated in 88% yield (0.957g). An almost similar result was obtained as that of the small-scale reaction (Scheme **5**).

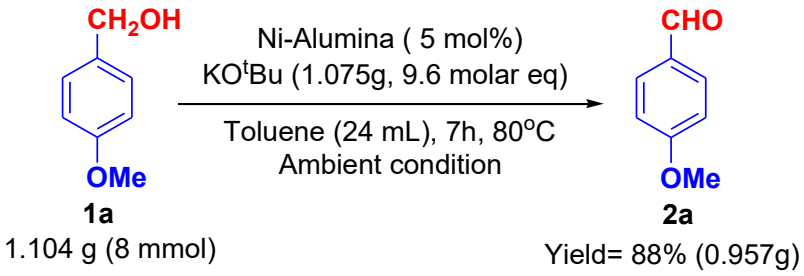

Scheme 5 Gram scale reaction of **1a** to demonstrate the practicability

Catalyst reusability:

The recovery and reusability of the catalytic system are extremely important in order to achieve a sustainable protocol. In this pursuit, the recyclability of the catalyst was investigated using 4-methoxybenzyl alcohol **1a** (1 mmol), KO^{t}Bu (1.2 mmol), Ni-Alumina (5 mol%), toluene (3 mL) at 80^{o}C under ambient condition. After the completion of the reaction, the catalyst was separated by filtration and the crude product was isolated from the filtrate through the extraction of ethyl acetate (an eco-compatible solvent). The residue was washed repeatedly with EtOAc followed by water, dried at 120^{o}C for one hour, and used directly for the next reaction. The isolated catalyst was used for successive reactions with a little variation of yield (Figure 8).

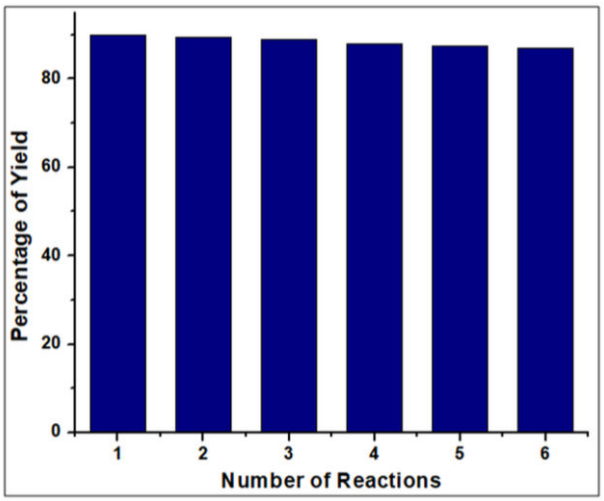

Figure 8 Recycling test of Ni-alumina catalyst using **1a** (1 mmol), KO^{t}Bu (1.2 mmol), Ni-Alumina (5 mol%), toluene (3mL) at 80^{o}C under ambient condition.

The recovered catalyst (after recycling for six times) was further analyzed by XRD, TEM, SEM, and EDX techniques (Figure 9) to confirm the recyclability and stability of the nanocatalyst. The XRD result showed the disappearance of the peak at about 55 degrees of the recovered nanocatalyst. It could be due to the oxidation of Ni(0) to Ni(II) as a result of atmospheric air exposure during the recycling process or sample analysis time. The TEM, SEM, and EDX results showed that the structural morphology of the recovered nanocatalyst did not change much during this investigation.

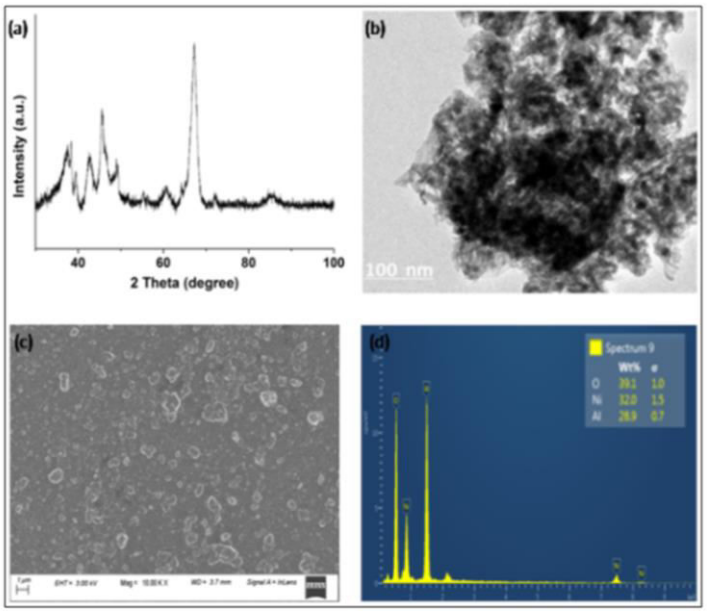

Figure 9 (a) XRD of Ni-alumina (after recycled six times), (b) TEM of Ni-alumina (after recycled six times), (c) SEM of Ni-alumina (after recycled six times), (d) EDX of Ni-alumina (after recycled six times).

"Hot filtration method (Sheldon's test)" of the catalyst:

Furthermore, to observe the heterogeneity of Ni-alumina "hot filtration method (Sheldon's test)"[16] was performed using **1a** as the substrate. When 27% conversion of the substrate was noted after 2h, the catalyst was separated by filtration under hot conditions. The "catalyst-free" filtrate was then kept under optimized reaction conditions. Further conversion of **1a** was not observed at all even after 11h (Figure 10). This study indicated that practically no soluble catalytically active species was present in the filtrate. Hence, the heterogeneity of Ni-alumina was conclusively proved.

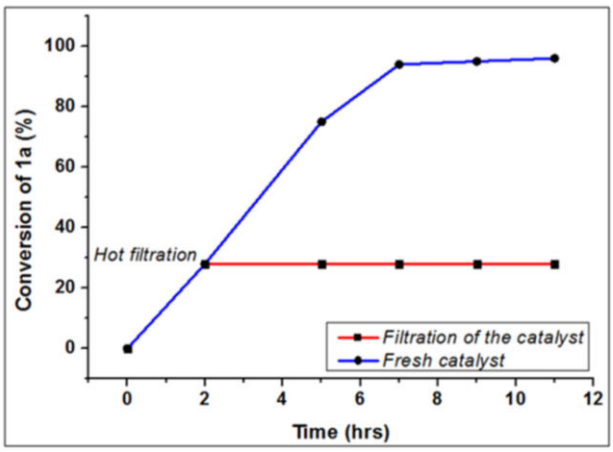

Figure 10 Heterogeneity test of Ni-alumina catalyst using **1a** (1 mmol), KO^{t}Bu (1.2 mmol), Ni-Alumina (5 mol%), toluene (3mL) at 80^{o}C under ambient condition.

Comparison of the catalytic efficiency of Ni-alumina with the literature reports:

To establish further the catalytic eligibility and capability of Ni-Alumina in this oxidative transformation, a comparative study was carried out with the previously reported heterogeneous catalyst (Table 3).

TABLE 3 Comparison of the efficiency of Ni-Alumina with reported heterogeneous catalyst[a]

Entry	Catalyst	Oxidant	Additive	Solvent	Time (h), Temp. (^oC)	Yield (%)
1	PtNi@SWCNT[15]	O_2	KOH	Toluene	2h, 80^oC	98[b]
2	Pd@TiC[17]	Air	Visible light	CH_3CN	8h, 20W bulb	96[c]
3	Au@PMO-IL[18]	O_2	Cs_2CO_3	Toluene	3h, 35^oC	99[b]
4	Au_{np}-nSTDP[19]	TBHP	K_2CO_3	CH_3CN:H_2O	2h, 80 °C	91[b]
5	CoL_2@SMNP[20]	O_2	NHPI	CH_3CN	16h, 70^oC	65[c]
6	Fe_3O_4/CuBDC/GO[21]	O_2	TEMPO	CH_3CN	14.5h, 60^oC	95[b]
7	Cu/Ag@SiO_2[22]	TBHP	--	Toluene	4h, 120^oC	98[c]
8	Cu NPs@NC[23]	Air	TEMPO	H_2O:EG[d]	5h, r.t.	95[c]
9	$NiFe_2O_4$ NPs[24]	TBHP	--	CH_3CN	3h, 60^oC	79[c]
10	Ni-Alumina (***This work***)	Air	KO^{t}Bu	Toluene	7h, 80^oC	90[c]

[a]The comparative studies were carried out using 4-methoxybenzylalcohol (**1a**) as the model substrate, [b]GC yield, [c]Isolated yield, [d]EG (Ethylene glycol).

Even though these reported oxidative protocols listed in Table 3 have their merits, but still the scope is limited due to the utilization of expensive and toxic metal catalysts, multistep synthesis of catalysts, involving the high concentration of oxidants as well as high oxygen pressure, lack of chemoselectivity, generation of over oxidized product and tedious product isolation procedure. Therefore, apart from being eco-compatible, the present Ni-Alumina catalyzed oxidative protocol from catalyst preparation to product isolation is operationally very simple, economically more attractive, and utilizes environmentally benign aerial oxygen as an eco-friendly oxidant. Thus the present study has developed a novel, utilitarian and sustainable method for chemoselective oxidation of benzylic alcohols to carbonyl compounds under an ambient atmosphere with the tolerance of various sensitive moieties using easily accessible and economically viable supported metal nanoparticles as a stable and recyclable heterogeneous catalyst with greater merits and wider applicability in comparison to many earlier reports.

II.4.3. Conclusion

In conclusion, we have developed an efficient protocol for the chemoselective oxidation of benzylic alcohols to carbonyl compounds using economically affordable alumina-supported mesoporous nickel nanoparticles as a stable recyclable heterogeneous catalyst in the presence of aerial oxygen as an eco-friendly oxidant. The aliphatic alcoholic moiety did not take part in this oxidative reaction. The present sustainable catalytic system shows excellent chemoselectivity which has been substantiated through intermolecular as well as intramolecular competition experiments. This oxidative protocol was also effective on a gram scale, which is of significant advantage in the light of large scale preparation with the prospects of industrial application. The attractive features of the present study are procedural simplicity, appreciable stability and efficiency of the catalyst, excellent chemoselectivity, easy recovery, good recyclability, and tolerance of various sensitive moieties during the reaction.

II.5. Experimental

Materials and Instrumentation

All reactants were purchased from SRL, AVRA Chemicals, Alfa-aesar, Spectrochem, and Sigma Aldrich and used as received without further purification. ^{1}H and ^{13}C NMR spectra were obtained on a Bruker-300 spectrometer (300 MHz) and JEOL Spectrometer (400 MHz) in $CDCl_3$ and DMSO-d_6 solutions with TMS as an internal reference. Field Emission Scanning Electron Microscopy (FE-SEM) images were recorded with a Zeiss (Zemini) scanning electron microscope. Energy-dispersive X-ray spectroscopy (EDX) experiment was carried out by using a Hitachi S3400N SEM-EDX instrument. Transmission electron microscopic images were collected on a JEOL 2010 TEM operated at 200 kV. XRD data of the powder sample were obtained in transmission mode using a Bruker D2 Phaser X-ray diffractometer (30 kV, 10 mA) using Cu-Kα (λ = 1.5406 Å) radiation. Chemical states of the heterogeneous material were determined by X-ray photoelectron spectroscopy (XPS) using a PHI 5000 (versa Probe II, FEI Inc). The particle size distribution and zeta potential were evaluated by the dynamic light scattering (DLS) system (Malvern Zetasizer Nano). The specific surface area and porosity of the catalyst were characterized by the Brunauer-Emmett-Teller (BET) method with N_2 adsorption-desorption isotherms, measured at 77 K using Quantachrome Autosorb® iQ-MP / iQ-XR. GC analysis was performed using Perkein Elmer Clarus 600 Gas Chromatograph. Column chromatography was performed on silica gel (60-

120 mesh) from SRL, India. Thin layer chromatographic separations were performed on pre-coated silica gel plates using silica gel G for TLC (E. Merck).

Purification of reagent:

Activated Alumina:-

Neutral alumina was taken in a 100mL round-bottomed flask. It was heated slowly and then strongly around 180-190^{o}C under reduced pressure through a $CaCl_2$ drying tube for 3 hours and cooled and stored in a desiccator.

General experimental procedure for the Ni-Alumina catalyzed oxidation of alcohols:

To a stirred suspension of appropriate alcohol **1** (1 mmol) in toluene (3 mL), Ni-Alumina (5 mol%) was added followed by K^{t}OBu (1.2 mmol). The reaction mixture was stirred at 80°C and the progress of the reaction was monitored by thin-layer chromatography (TLC). After completion of the reaction, the reaction mixture was cooled to room temperature, ethyl acetate (15 mL) was added to dissolve the product and the catalyst was separated simply by filtration. The residue (recovered catalyst) was thoroughly washed with EtOAc (3×5 mL) followed by water (3×5 mL). The aqueous washing was repeatedly extracted with ethyl acetate (4×5 mL). The combined organic extracts were washed with water (4×5 mL) and dried over anhydrous Na_2SO_4. The crude product **2** was obtained by removal of the solvent under reduced pressure which was further purified by column chromatography on a short column of silica gel using 5-15% ethyl acetate-hexane as eluent.

Procedure for the Ni-alumina catalyzed gram scale oxidation of 4-methoxybenzyl alcohol (1a):

To a stirred suspension of 4-methoxybenzyl alcohol (**1a**) (1.104g, 8 mmol) in toluene (24 mL), Ni-alumina (0.4g, 5 mol%) was added followed by K^{t}OBu (1.075g, 9.6 molar eq). The reaction mixture was stirred at 80°C and the progress of the reaction was monitored by thin-layer chromatography (TLC). After completion of the reaction, the reaction mixture was cooled to room temperature, ethyl acetate was added to dissolve the product and the catalyst was separated simply by filtration. The residue (recovered catalyst) was thoroughly washed with EtOAc followed by water. The aqueous reaction mixture was repeatedly extracted with ethyl acetate. The combined organic extracts were washed with water and dried over anhydrous Na_2SO_4. The crude product was obtained by removal of the solvent under reduced pressure which was further purified by column chromatography on a short column (Yield: 88%, 0.957 g).

Spectral and analytical data of the compounds:

4-methoxy-benzaldehyde (2a) [5b]: Yield: 90%; ^{1}H NMR ($CDCl_3$, 300 MHz); δ (ppm): 3.85 (3H, s); 6.96 (2H, d, *J* = 9.0 Hz); 7.79 (2H, d, *J* = 9.0 Hz); 9.84 (1H, s). ^{13}C NMR ($CDCl_3$, 75 MHz); δ (ppm): 56.1, 114.3, 129.4, 130.2, 166.8, 190.2.

3-methoxy-benzaldehyde (2b)[25a]: Yield: 89%; ^{1}H NMR ($CDCl_3$, 400 MHz); δ (ppm): 3.85 (3H, s); 7.15-7.17 (1H, m); 7.38-7.45 (3H, m); 9.96 (1H, s). ^{13}C NMR ($CDCl_3$, 100 MHz); δ (ppm): 55.5, 112.1, 121.1, 121.6, 123.6, 130.1, 137.8, 160.2, 192.2.

4-methyl-benzaldehyde (2c)[25b]: Yield: 89%; ^{1}H NMR ($CDCl_3$, 400 MHz); δ (ppm): 2.42 (3H, s); 7.31 (2H, d, *J* = 8.0 Hz); 7.76 (2H, d, *J* = 8.0 Hz); 9.94 (1H, s). ^{13}C NMR ($CDCl_3$, 100 MHz); δ (ppm): 21.9, 129.7, 129.9, 134.2, 145.6, 192.1.

Benzaldehyde (2d)[25a]: Yield: 82%; ^{1}H NMR ($CDCl_3$, 300 MHz); δ (ppm): 7.45-7.49 (2H, m); 7.57-7.62 (1H, m); 7.81-7.85 (2H, m); 9.92 (1H, s).

3,4-dimethoxy-benzaldehyde (2e)[25c]: Yield: 88%; ^{1}H NMR ($CDCl_3$, 400 MHz); δ (ppm): 3.92 (3H, s); 3.95 (3H, s); 6.96 (1H, d, *J* = 8.0 Hz); 7.39 (1H, s); 7.43-7.46 (1H, m); 9.84 (1H, s). ^{13}C NMR ($CDCl_3$, 100 MHz); δ (ppm): 56.0, 56.2, 108.9, 110.4, 126.9, 130.2, 149.7, 154.6, 190.9.

4-hydroxy-3-methoxy-benzaldehyde (2f)[25d]: Yield: 87%; ^{1}H NMR ($CDCl_3$, 300 MHz); δ (ppm): 3.94 (s, 3H); 6.45 (s, 1H); 7.01 (d, 1H, *J* = 9.0 Hz); 7.39 (t, 1H, 9.0 Hz); 9.80 (s, 1H). ^{13}C NMR ($CDCl_3$, 75 MHz); δ (ppm): 56.1, 108.9, 114.4, 127.5, 129.9, 147.2, 151.8, 190.9.

4-hydroxy-benzaldehyde (2g)[4c]: Yield: 87%; ^{1}H NMR ($CDCl_3$, 400 MHz); δ (ppm): 6.96-7.00 (2H, m); 7.79-7.83 (2H, m); 9.85 (1H, s). ^{13}C NMR ($CDCl_3$, 100 MHz); δ (ppm): 116.1, 129.5, 132.7, 162.2, 191.7.

2-hydroxy-benzaldehyde (2h)[25e]: Yield: 86%; ^{1}H NMR ($CDCl_3$, 400 MHz); δ (ppm): 6.96-7.02 (2H, m); 7.49-7.55 (2H, m); 9.89 (1H, s); 11.0 (1H, s). ^{13}C NMR ($CDCl_3$, 100 MHz); δ (ppm): 117.7, 119.9, 133.8, 137.1, 161.7, 196.7.

4-dimethylamino-benzaldehyde (2i)[25f]: Yield: 87%; ^{1}H NMR ($CDCl_3$, 400 MHz); δ (ppm): 3.06 (6H, s); 6.67 (2H, d, *J* = 9.0 Hz); 7.71 (2H, d, *J* = 8.0 Hz); 9.71 (1H, s). ^{13}C NMR ($CDCl_3$, 100 MHz); δ (ppm): 40.1, 111.0, 125.4, 132.0, 154.4, 190.3.

2-chloro-benzaldehyde (2j)[25g]: Yield: 85%; ^{1}H NMR ($CDCl_3$, 400 MHz); δ (ppm): 7.50 (2H, d, *J* = 8.0 Hz); 7.81 (2H, t, *J* = 8.0 Hz); 9.97 (1H, s). ^{13}C NMR ($CDCl_3$, 100 MHz); δ (ppm): 129.5, 130.9, 134.7, 141.0, 190.9.

4-bromo-benzaldehyde (2k)[4c]: Yield: 85%; ^{1}H NMR ($CDCl_3$, 400 MHz); δ (ppm): 7.66-7.68 (2H, m); 7.72-7.75 (2H, m); 9.67 (1H, s). ^{13}C NMR ($CDCl_3$, 100 MHz); δ (ppm): 129.9, 131.0, 132.5, 135.1, 191.1.

4-nitro-benzaldehyde (2l)[4c]: Yield: 94%; ^{1}H NMR ($CDCl_3$, 300 MHz); δ (ppm): 8.06 (2H, d, *J* = 6.0 Hz); 8.37 (2H, d, *J* = 6.0 Hz); 10.1 (1H, s). ^{13}C NMR ($CDCl_3$, 75 MHz); δ (ppm): 124.5, 130.4, 140.1, 151.1, 190.1.

3-nitro-benzaldehyde (2m)[25g]: Yield: 91%; ^{1}H NMR ($CDCl_3$, 300 MHz); δ (ppm): 7.76 (1H, s); 8.22 (1H, d, *J* = 6.0 Hz); 8.47 (1H, d, *J* = 6.0 Hz); 10.2 (1H, s). ^{13}C NMR ($CDCl_3$, 75 MHz); δ (ppm): 124.4, 128.6, 130.4, 134.6, 137.4, 148.8, 189.7.

4-cyano-benzaldehyde (2n)[25h]: Yield: 90%; ^{1}H NMR ($CDCl_3$, 400 MHz); δ (ppm): 7.80-7.82 (2H, m); 7.95-7.97 (2H, m); 10.1 (1H, s). ^{13}C NMR ($CDCl_3$, 100 MHz); δ (ppm): 117.6, 129.9, 132.3, 138.8, 190.5.

Benzo[1,3]dioxole-5-carbaldehyde (2o)[25h]: Yield: 89%; ^{1}H NMR ($CDCl_3$, 400 MHz); δ (ppm): 6.02 (2H, s); 6.88 (1H, d, *J* = 6.0 Hz); 7.24-7.27 (1H, m); 7.35-7.37 (1H, m); 9.76 (1H, s). ^{13}C NMR ($CDCl_3$, 100 MHz); δ (ppm): 102.2, 106.9, 108.4, 128.7, 131.9, 148.8, 153.2, 190.3.

3-phenyl-propenal (2p)[25b]: Yield: 82%; ^{1}H NMR ($CDCl_3$, 300 MHz); δ (ppm): 6.42 (1H, d, *J* = 6.0 Hz); 7.15-7.19 (3H, m); 7.31-7.35 (2H, m); 7.52 (1H, d, *J* = 6.0 Hz); 9.62 (1H, s).

Furan-2-carbaldehyde (2q)[5b]: Yield: 88%; ^{1}H NMR ($CDCl_3$, 400 MHz); δ (ppm): 6.55-6.57 (1H, m); 7.21-7.25 (1H, m); 7.66 (1H, s); 9.61 (1H, s).

Thiophene-2-carbaldehyde (2r)[25a]: Yield: 86%; ^{1}H NMR ($CDCl_3$, 400 MHz); δ (ppm): 7.16-7.19 (1H, m); 7.71-7.75 (2H, m); 9.90 (1H, s). ^{13}C NMR ($CDCl_3$, 100 MHz); δ (ppm): 128.4, 135.2, 136.4, 144.1, 183.0.

1-pyridin-4-yl-ethanone (2s)[25h]: Yield: 87%; ^{1}H NMR ($CDCl_3$, 400 MHz); δ (ppm): 2.61 (3H, s); 7.69-7.71 (2H, m); 8.78 (2H, d, *J* = 6.0 Hz). ^{13}C NMR ($CDCl_3$, 100 MHz); δ (ppm): 26.7, 121.3, 142.8, 151.0, 197.4.

4-benzyloxy-benzaldehyde (2t)[25h]: Yield: 89%; ^{1}H NMR ($CDCl_3$, 300 MHz); δ (ppm): 5.34 (2H, s); 6.88 (2H, d, *J* = 6.0 Hz); 7.72 (2H, d, *J* = 6.0 Hz); 7.19-7.25 (5H, m); 9.76 (1H, s).

4-(allyloxy)-3-methoxybenzaldehyde (2u)[25i]: Yield: 87%; ^{1}H NMR ($CDCl_3$, 300 MHz); δ (ppm): 3.91 (3H, s); 4.68 (2H, d, *J* = 3.0 Hz); 5.30-5.39 (2H, m); 6.02-6.13 (1H, m); 6.96 (1H, d, *J* = 9.0 Hz); 7.40 (2H, d, *J* = 6.0 Hz); 9.82 (1H, s). ^{13}C NMR ($CDCl_3$, 75 MHz); δ (ppm): 55.9, 69.7, 109.4, 110.2, 111.9, 112.9, 122.7, 126.5, 131.2, 132.3, 132.7, 149.9, 153.5, 190.8.

Acetophenone (2v)[5b]: Yield: 87%; ^{1}H NMR ($CDCl_3$, 300 MHz); δ (ppm): 2.57 (3H, s); 7.43 (2H, t, *J* = 6.0 Hz); 7.52 (1H, d, *J* = 6.0 Hz); 7.93 (2H, d, *J* = 6.0 Hz). ^{13}C NMR ($CDCl_3$, 100 MHz); δ (ppm): 26.5, 128.3, 128.5, 133.1, 137.2, 198.0.

4-methoxy-acetophenone (2w)[25c]: Yield: 88%; ^{1}H NMR ($CDCl_3$, 400 MHz); δ (ppm): 2.54 (3H, s); 3.85 (3H, s); 6.90-6.93 (2H, m); 7.90-7.93 (2H, m). ^{13}C NMR ($CDCl_3$, 100 MHz); δ (ppm): 26.4, 55.5, 113.7, 130.4, 130.7, 163.5, 196.9.

4-nitro-acetophenone (2x)[25j]: Yield: 92%; ^{1}H NMR ($CDCl_3$, 400 MHz); δ (ppm): 2.67 (3H, s); 8.09 (2H, d, *J* = 8.0 Hz); 8.30 (2H, d, *J* = 8.0 Hz). ^{13}C NMR ($CDCl_3$, 100 MHz); δ (ppm): 27.1, 123.9, 129.4, 141.4, 150.4, 196.4.

4-hydroxy-acetophenone (2y)[25h]: Yield: 89%; ^{1}H NMR ($CDCl_3$, 400 MHz); δ (ppm): 2.58 (3H, s); 6.93-6.96 (2H, m); 7.89-7.93 (2H, m). ^{13}C NMR ($CDCl_3$, 100 MHz); δ (ppm): 26.3, 115.5, 129.5, 131.2, 161.4, 198.7.

4-phenyl-acetophenone (2z)[25h]: Yield: 86%; ^{1}H NMR ($CDCl_3$, 400 MHz); δ (ppm): 2.41 (3H, s); 7.25 (2H, d, *J* = 8.0 Hz); 7.44 (2H, t, *J* = 8.0 Hz); 7.54 (1H, t, *J* = 8.0 Hz); 7.70 (2H, d, *J* = 8.0 Hz); 7.76 (2H, d, *J* = 8.0 Hz). ^{13}C NMR ($CDCl_3$, 100 MHz); δ (ppm): 21.7, 128.3, 128.5, 129.1, 129.7, 130.4, 131.9, 132.2, 134.9, 138.1, 143.2, 196.5.

1-(naphthalen-2-yl)ethanone (2za)[25c]: Yield: 87%; ^{1}H NMR ($CDCl_3$, 300 MHz); δ (ppm): 2.73 (3H, s); 7.55-7.63 (2H, m); 7.86-7.90 (2H, m); 7.97 (1H, d, *J* = 6.0 Hz); 8.02-8.05 (1H, m); 8.46 (1H, s).

Benzophenone (2zb)[25c]: Yield: 88%; ^{1}H NMR ($CDCl_3$, 300 MHz); δ (ppm): 7.45-7.50 (4H, m); 7.56-7.61 (2H, m); 7.80 (4H, m).

4-methyl-benzophenone (2zc)[25k]: Yield: 90%; ^{1}H NMR ($CDCl_3$, 300 MHz); δ (ppm): 2.38 (3H, s); 7.29 (2H, d, *J* = 8.0 Hz); 7.54 (2H, t, *J* = 8.0 Hz); 7.62 (1H, t, *J* = 8.0 Hz); 7.70 (2H, d, *J* = 8.0 Hz); 7.78 (2H, d, *J* = 8.0 Hz).

4-fluoro-benzophenone (2zd)[25k]: Yield: 87%; ^{1}H NMR ($CDCl_3$, 400 MHz); δ (ppm): 7.10-7.24 (2H, m); 7.42-7.58 (2H, m); 7.73-7.80 (2H, m); 7.82-7.85 (3H, m). ^{13}C NMR ($CDCl_3$, 100 MHz); δ (ppm): 115.4, 115.6, 128.4, 129.9, 132.5, 132.7, 133.5, 133.9, 137.6, 164.1, 166.7, 195.3.

Benzil (2ze)[25j]: Yield: 87%; ^{1}H NMR ($CDCl_3$, 400 MHz); δ (ppm): 7.46-7.50 (4H, m); 7.60-7.64 (4H, m); 7.95 (2H, d, *J* = 8.0 Hz). ^{13}C NMR ($CDCl_3$, 100 MHz); δ (ppm): 128.1, 129.1, 129.3, 129.4, 129.6, 129.7, 129.9, 130.2, 130.0, 134.7, 134.9, 135.5, 194.6.

4-(2-hydroxyethoxy)benzaldehyde (4a)[25l]: Yield: 87%; ^{1}H NMR ($CDCl_3$, 300 MHz); δ (ppm): 3.97 (2H, t, *J* = 4.5 Hz); 4.13 (2H, t, *J* = 4.5 Hz); 6.88 (2H, d, *J* = 6.0 Hz); 7.78 (2H, d, *J* = 6.0 Hz); 9.85 (1H, s). ^{13}C NMR ($CDCl_3$, 75 MHz); δ (ppm): 60.9, 69.6, 114.8, 129.9, 132.0, 163.8, 191.1.

1-(4-(2-hydroxyethoxy)phenyl)ethanone (4b)[25m]: Yield: 85%; ^{1}H NMR ($CDCl_3$, 300 MHz); δ (ppm): 2.52 (3H, s); 3.87 (2H, s); 4.11 (2H, s); 6.90 (2H, d, *J* = 6.0 Hz); 7.88 (2H, d, *J* = 6.0 Hz). ^{13}C NMR ($CDCl_3$, 75 MHz); δ (ppm): 26.3, 60.9, 69.5, 114.2, 130.3, 130.9, 162.8, 197.4.

2-(4-formylphenoxy)ethyl acetate (5a)[25n]: Yield: 85%; ^{1}H NMR ($CDCl_3$, 300 MHz); δ (ppm): 2.06 (3H, s); 4.25 (2H, t, *J* = 4.5 Hz); 4.44 (2H, t, *J* = 4.5 Hz); 7.01 (2H, d, *J* = 9.0 Hz); 7.83 (2H, d, *J* = 9.0 Hz); 9.89 (1H, s). ^{13}C NMR ($CDCl_3$, 75 MHz); δ (ppm): 29.7, 62.4, 66.1, 114.8, 130.4, 131.9, 163.4, 170.8, 190.7.

2-(4-acetyl-phenoxy)ethyl acetate (5b)[25m]: Yield: 84%; ^{1}H NMR ($CDCl_3$, 300 MHz); δ (ppm): 2.08 (3H, s); 2.53 (3H, s); 4.21 (2H, t, *J* = 4.3 Hz); 4.40 (2H, t, *J* = 4.3 Hz), 6.92 (2H, d, *J* = 9.0 Hz), 7.91 (2H, d, *J* = 9.0 Hz). ^{13}C NMR (75 MHz, $CDCl_3$); δ (ppm): 20.8, 26.3, 62.9, 66.0, 115.8, 129.9, 130.7, 162.3, 170.9, 196.8.

^{1}H NMR & ^{13}C NMR Spectra of Some Representative Compounds

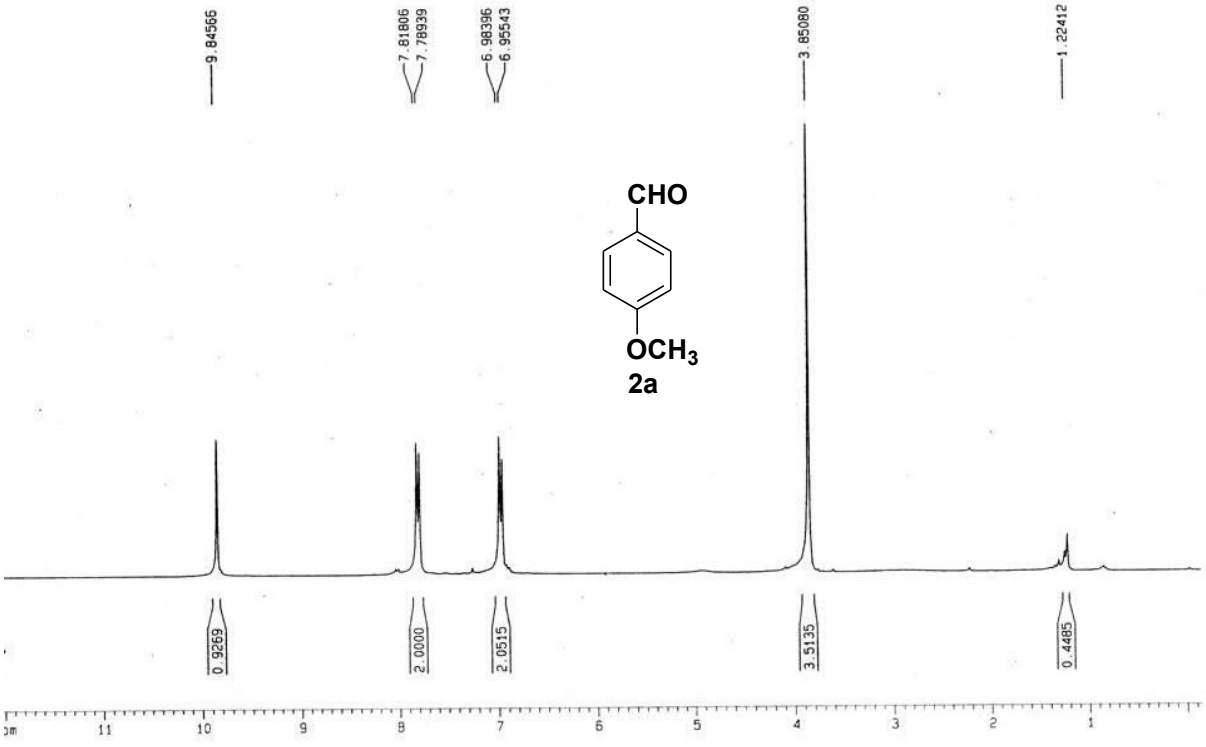

Figure 1 ^{1}H NMR of 4-methoxy-benzaldehyde (2a).

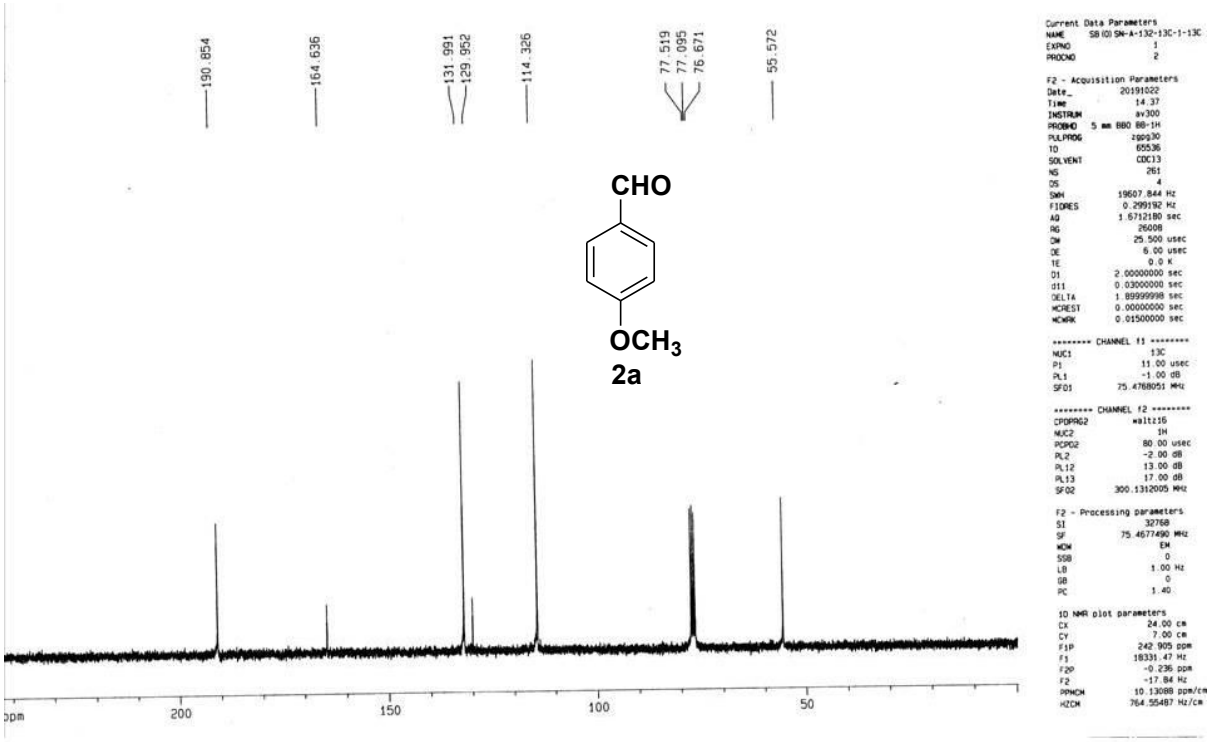

Figure 2 ^{13}C NMR of 4-methoxy-benzaldehyde (2a).

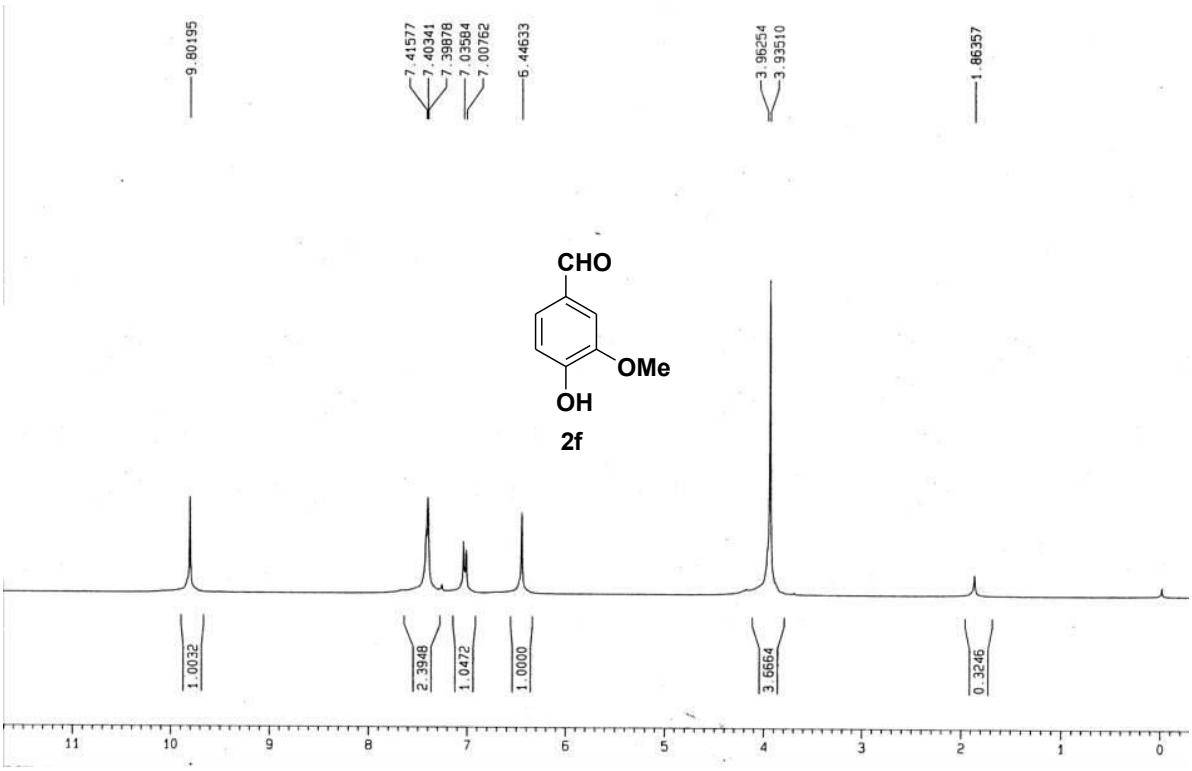

Figure 3 ^{1}H NMR of 4-hydroxy-3-methoxy-benzaldehyde (2f).

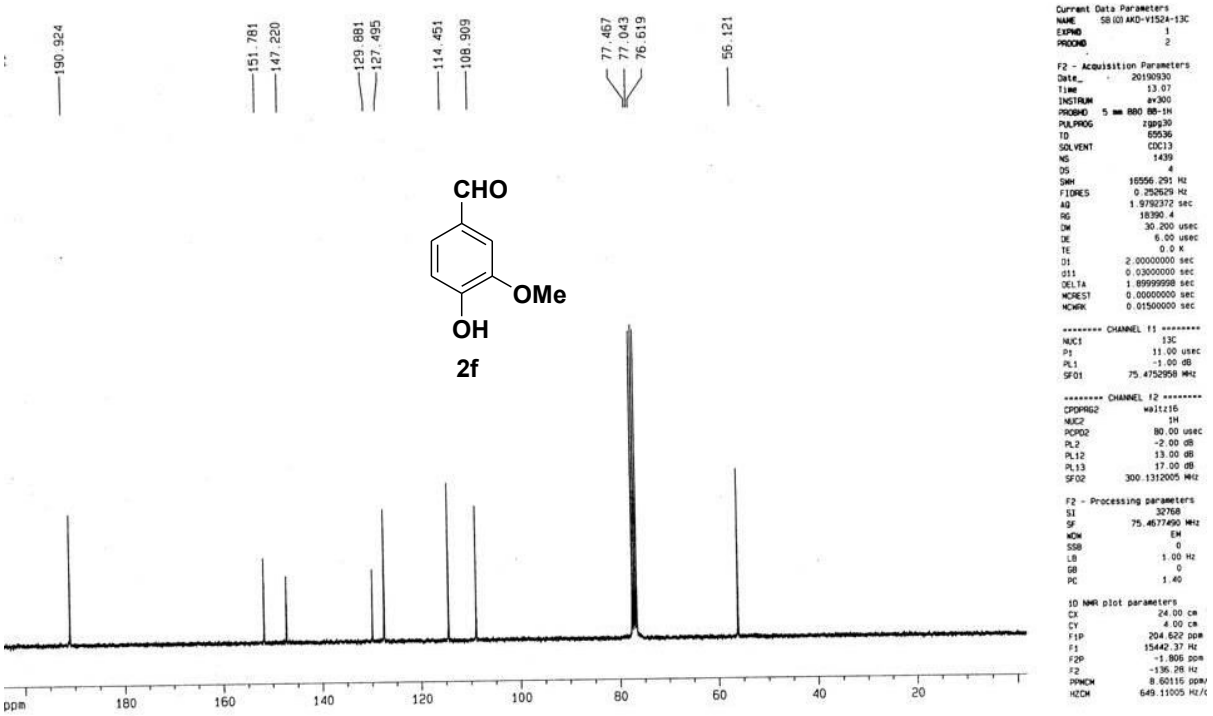

Figure 4 ^{13}C NMR of 4-hydroxy-3-methoxy-benzaldehyde (2f).

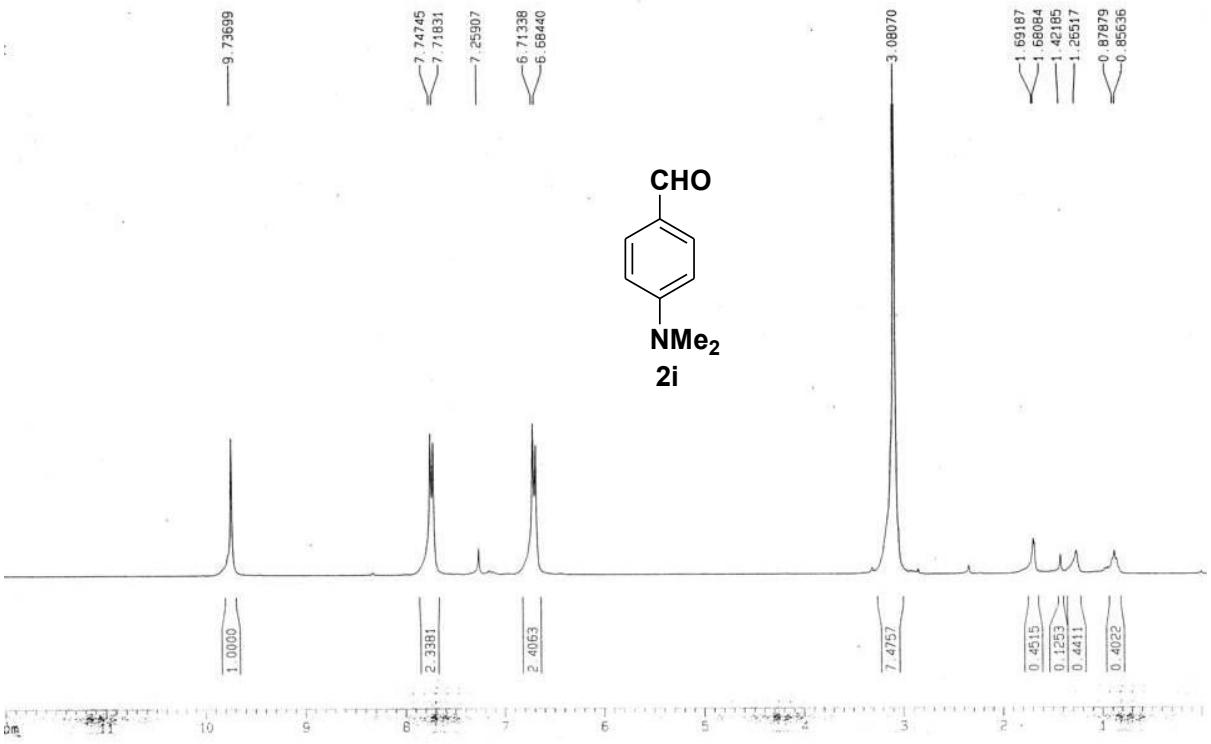

Figure 5 [1]H NMR of 4-dimethylamino-benzaldehyde (2i).

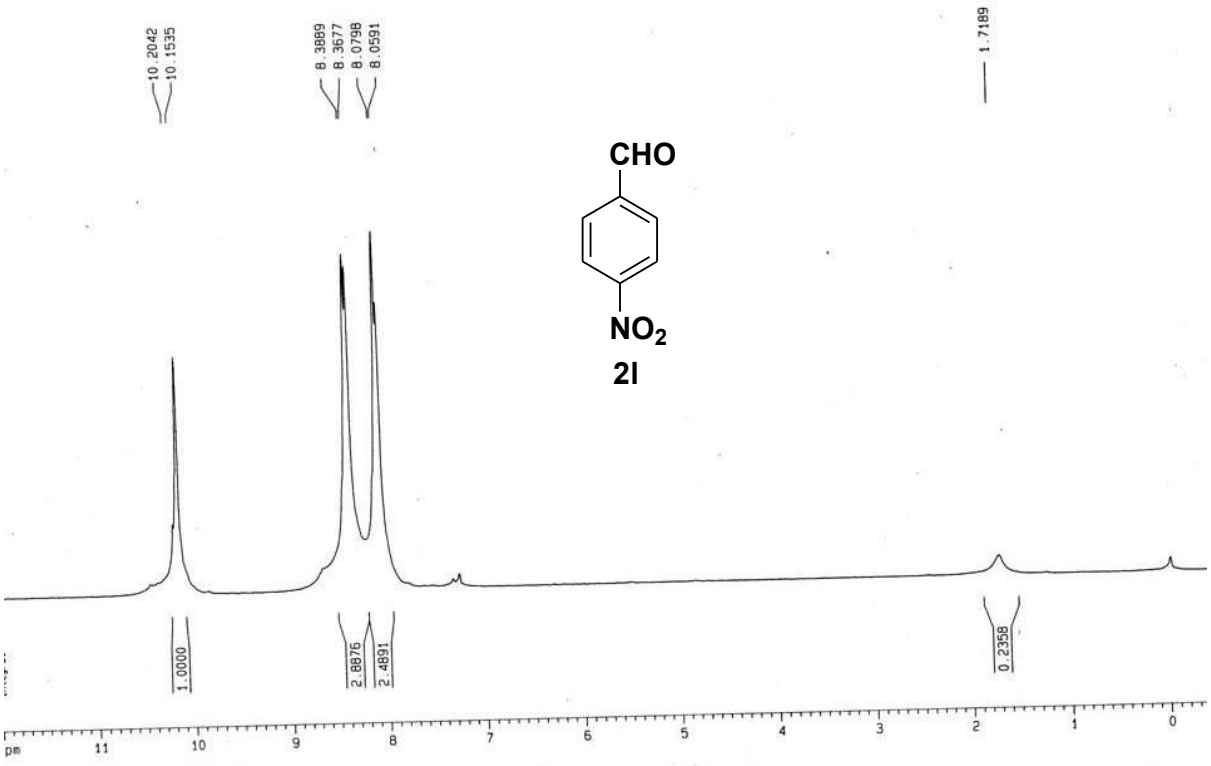

Figure 6 [1]H NMR of 4-nitro-benzaldehyde (2l).

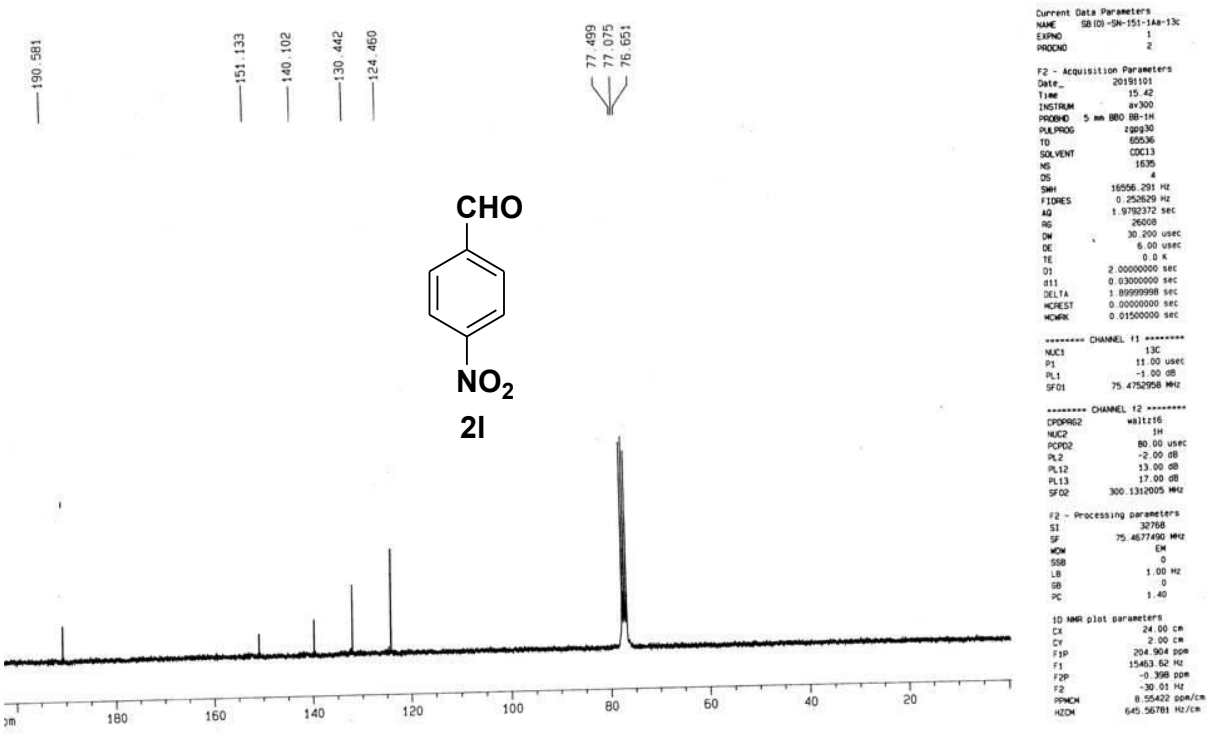

Figure 7 ^{13}C NMR of 4-nitro-benzaldehyde (2l).

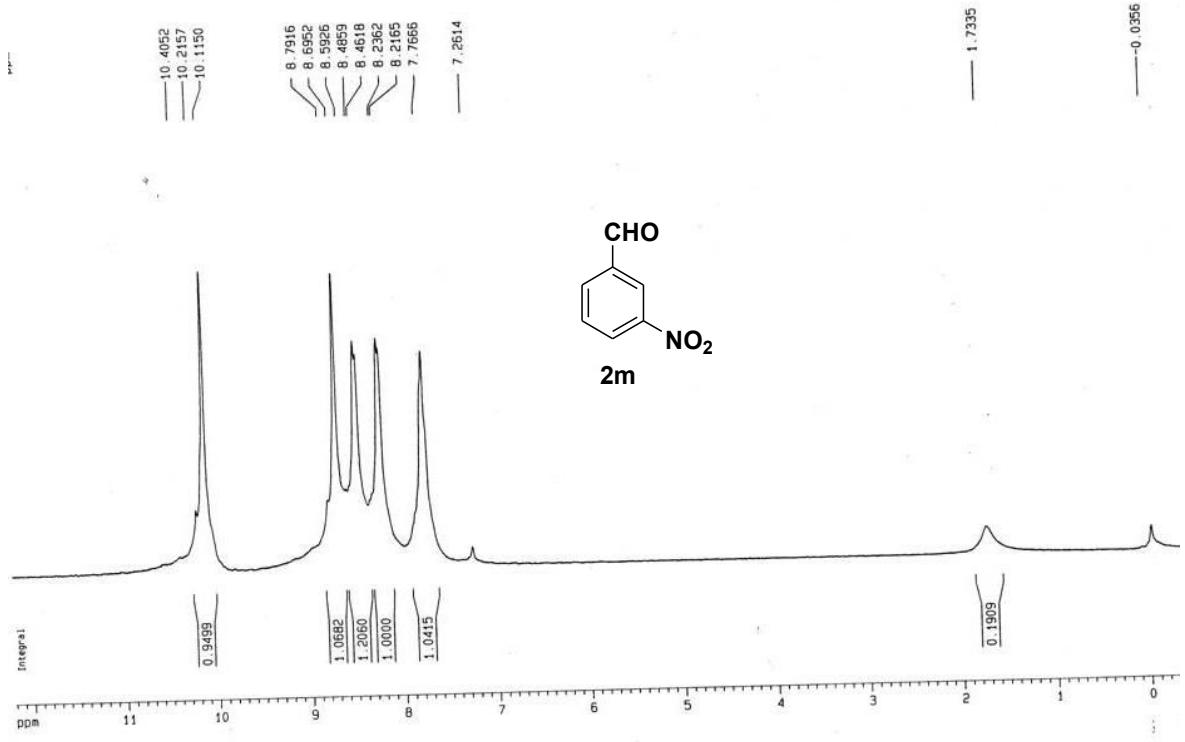

Figure 8 ^{1}H NMR of 3-nitro-benzaldehyde (2m).

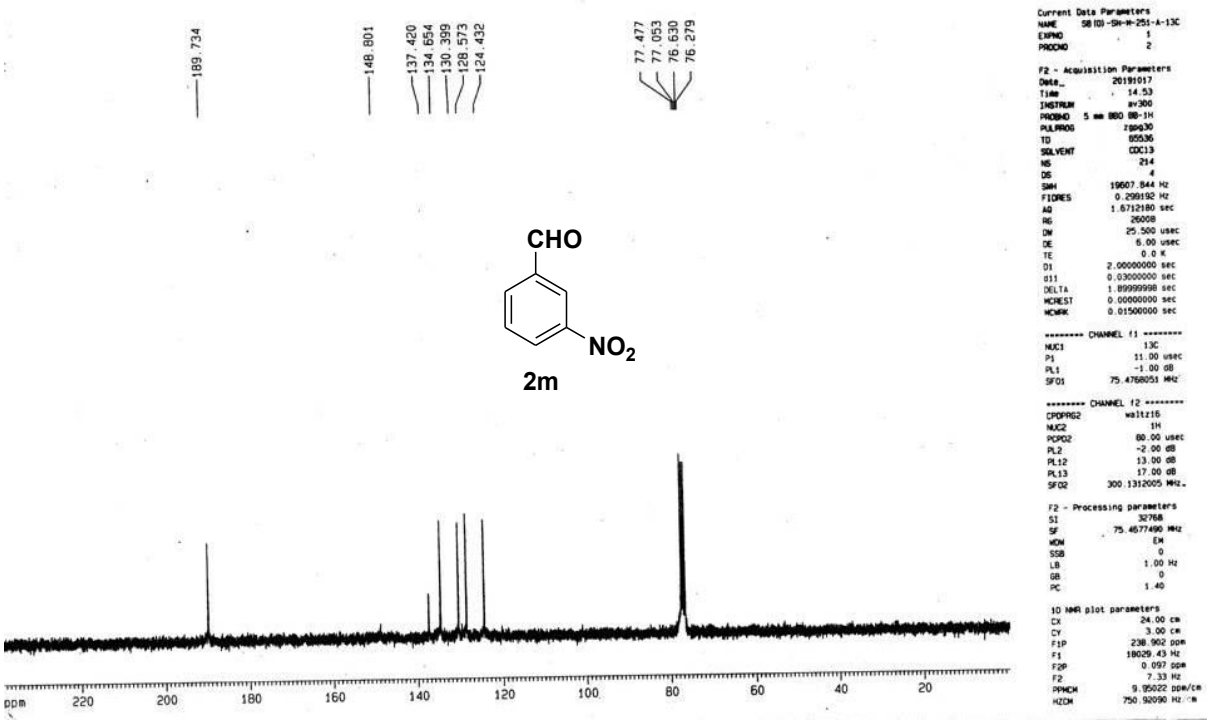

Figure 9 ^{13}C NMR of 3-nitro-benzaldehyde (2m).

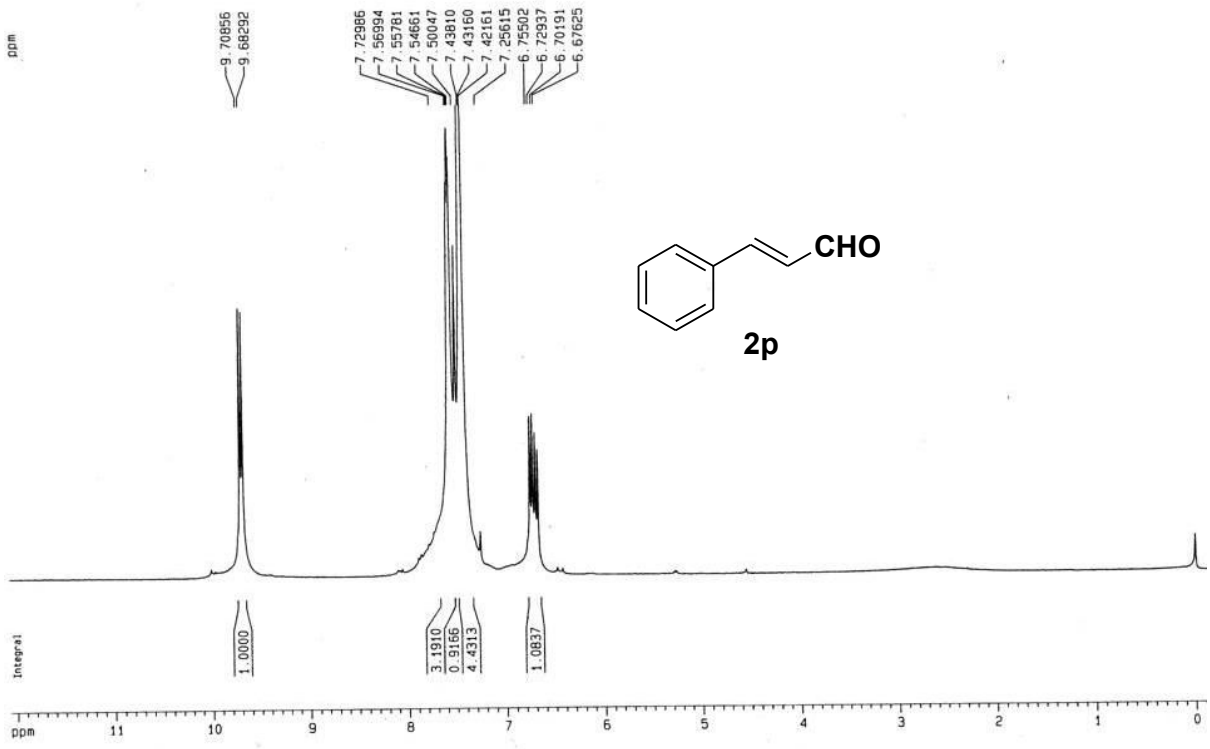

Figure 10 ^{1}H NMR of 3-phenyl-propenal (2p).

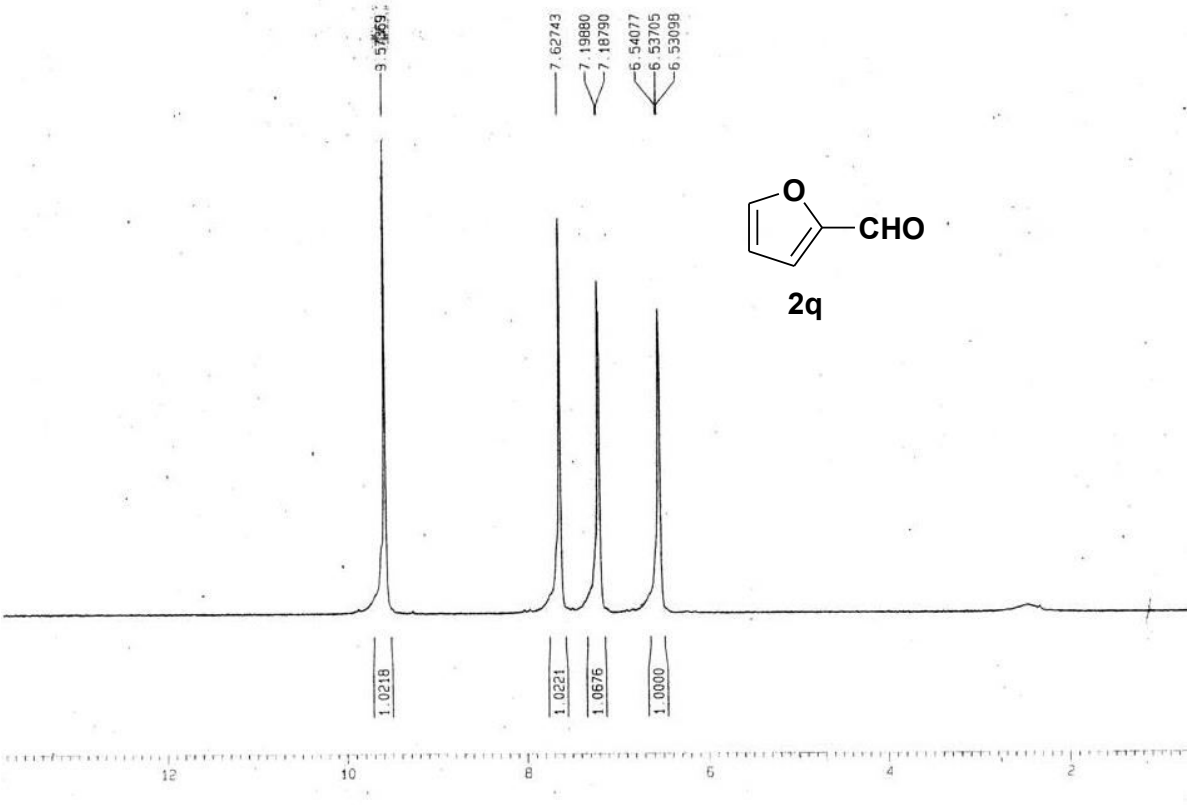

Figure 11 [1]H NMR of Furan-2-carbaldehyde (2q).

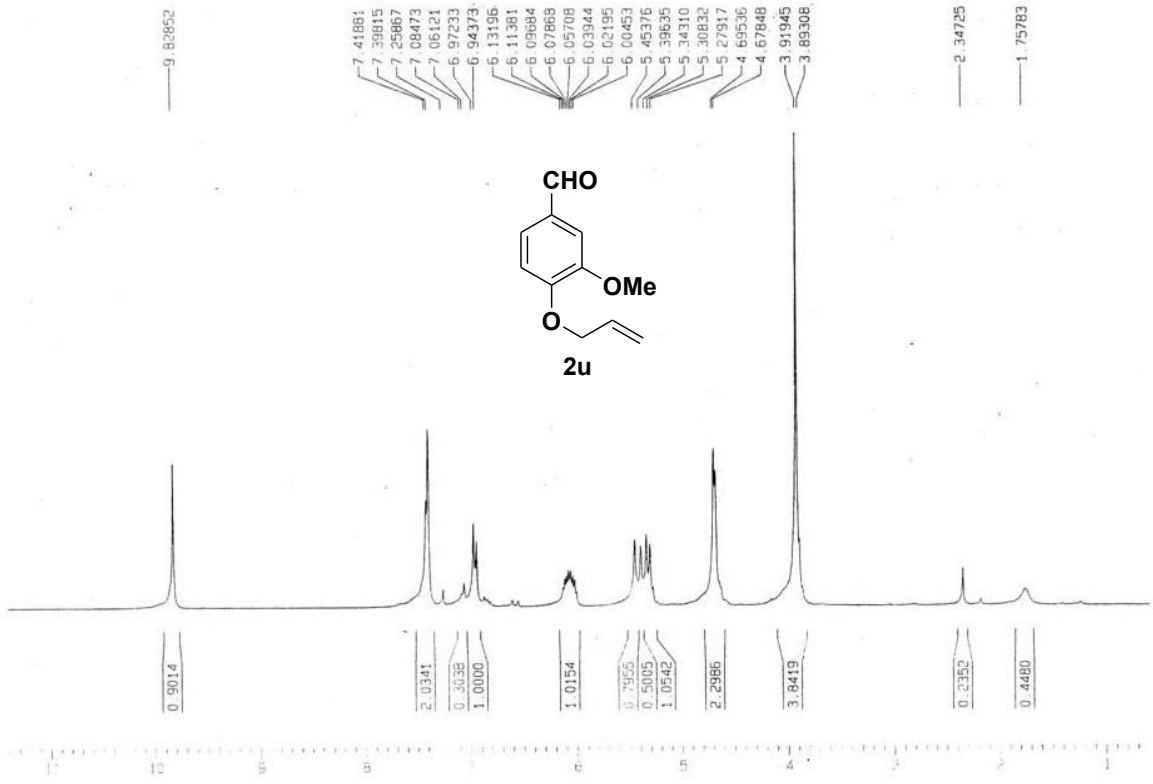

Figure 12 [1]H NMR of 4-(allyloxy)-3-methoxybenzaldehyde (2u).

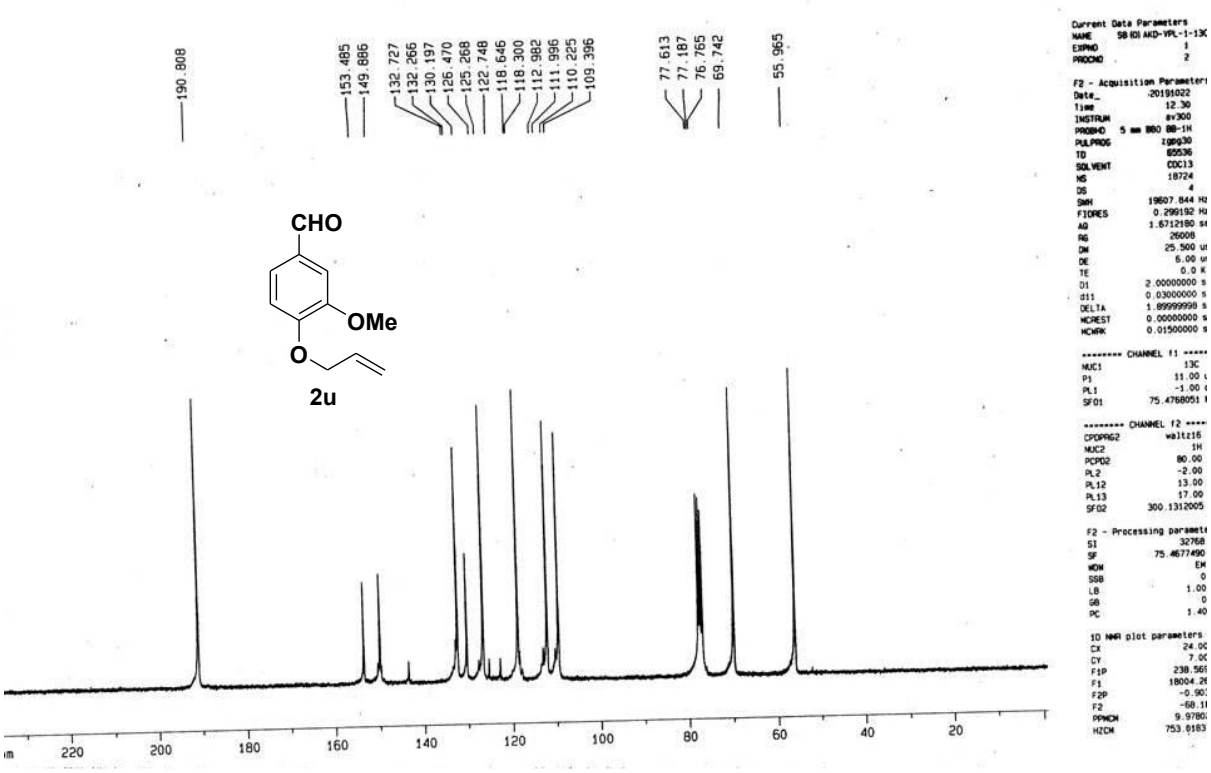

Figure 13 [1]H NMR of 4-(allyloxy)-3-methoxybenzaldehyde (2u).

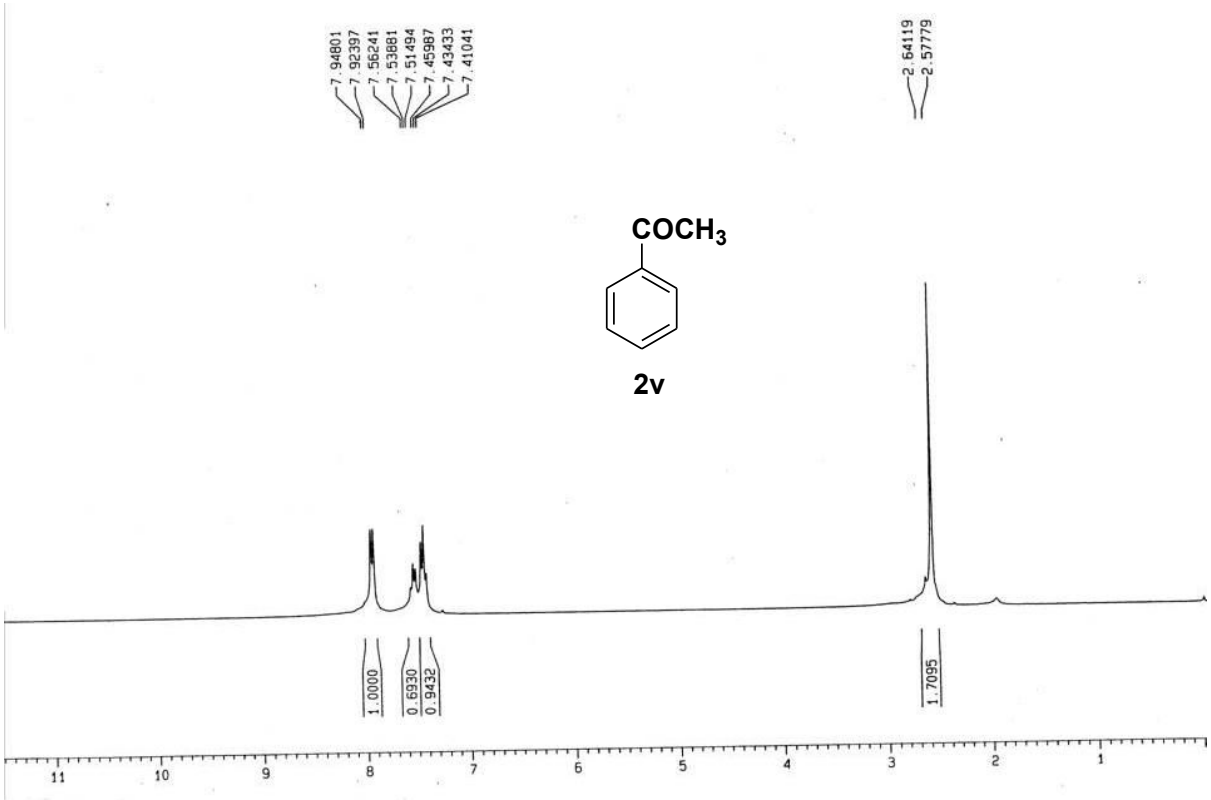

Figure 14 [1]H NMR of Acetophenone (2v).

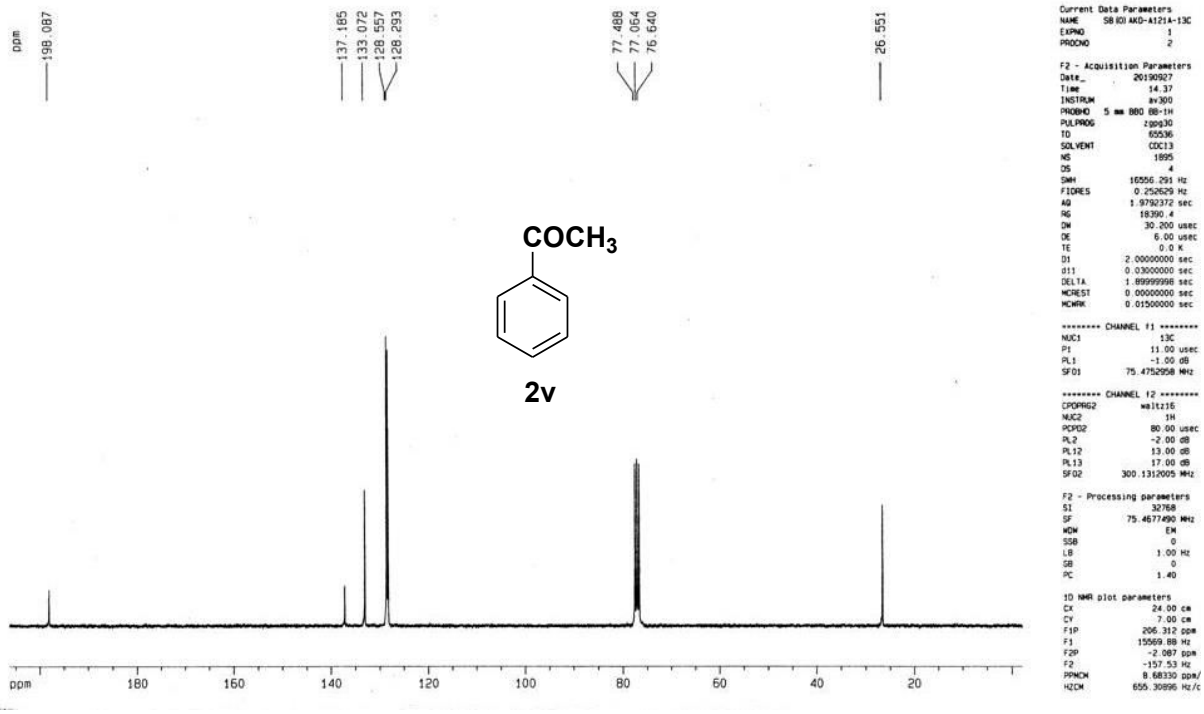

Figure 15 ^{13}C NMR of Acetophenone (2v).

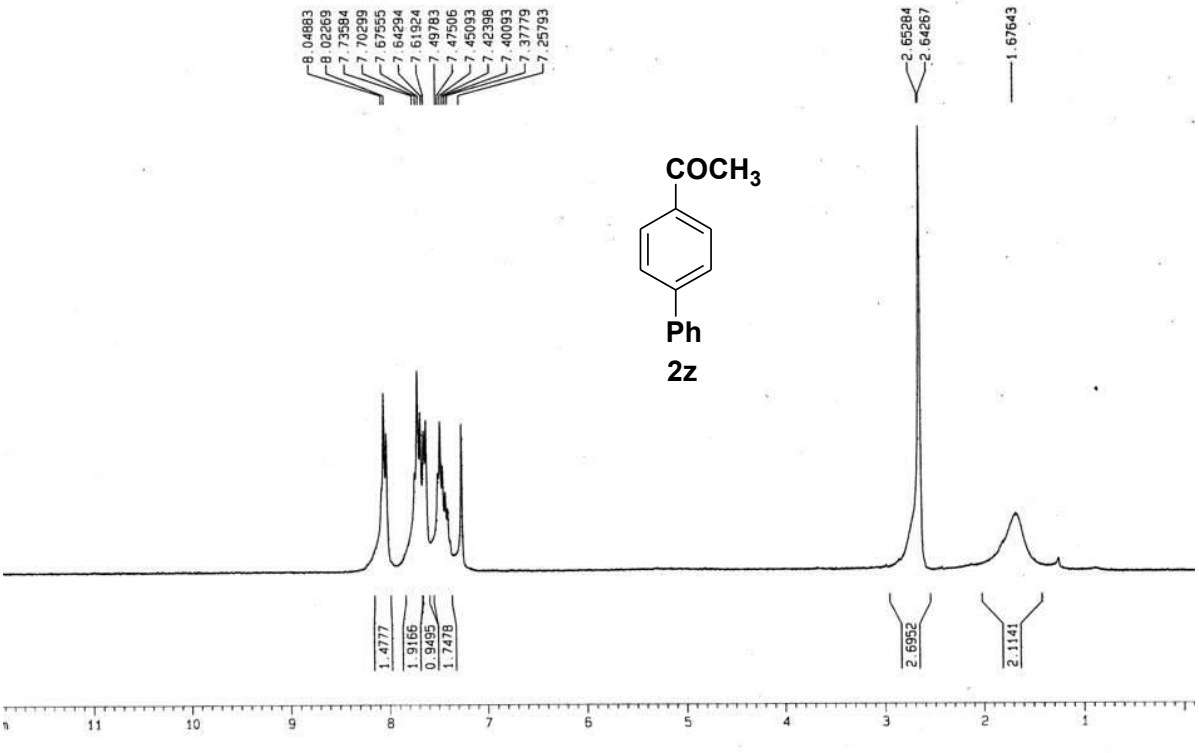

Figure 16 ^{1}H NMR of 4-phenyl-acetophenone (2z).

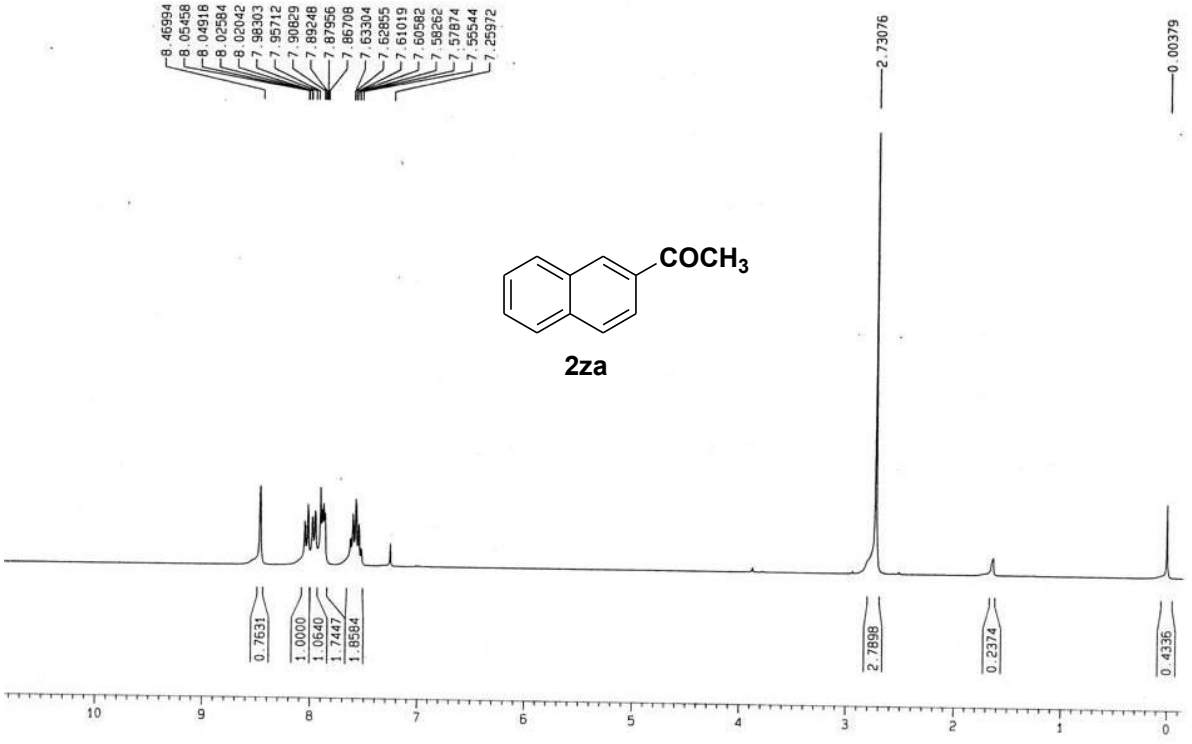

Figure 17 [1]H NMR of 1-(naphthalen-2-yl)ethanone (2za).

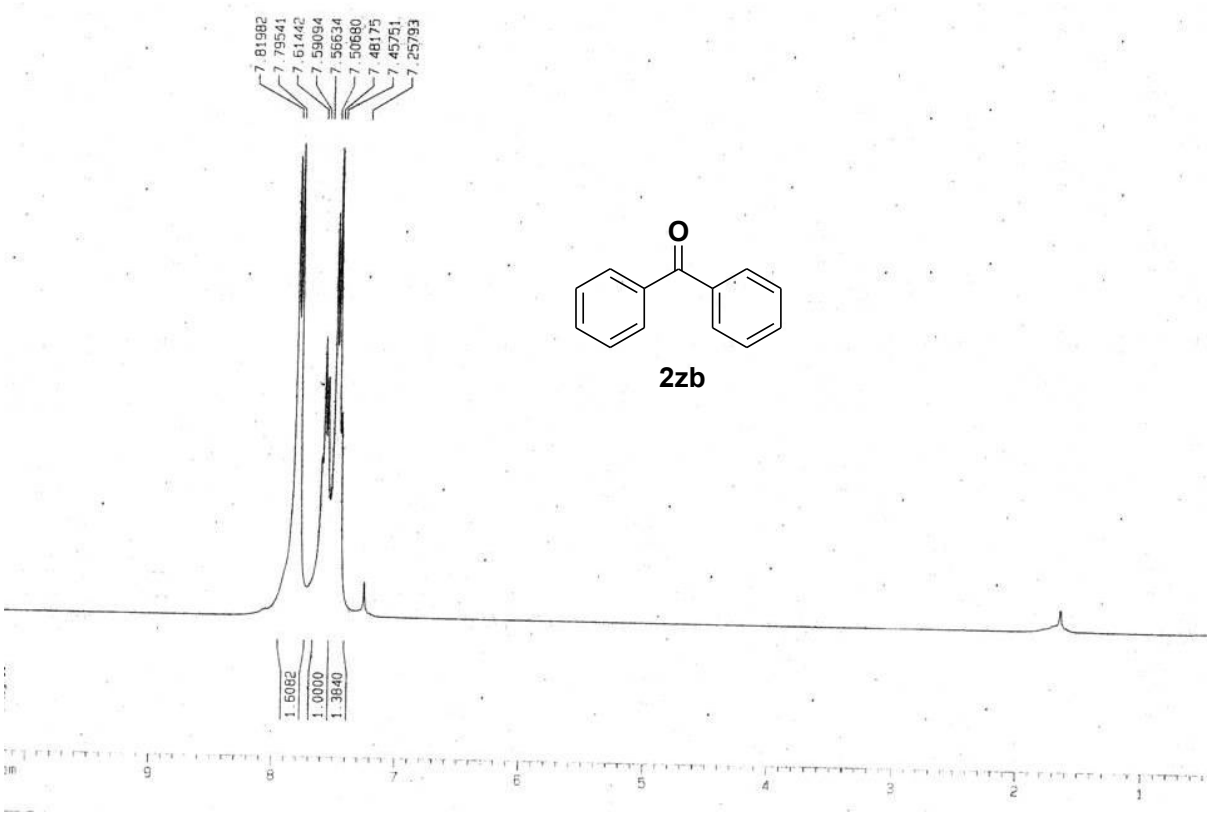

Figure 18 [1]H NMR of Benzophenone (2zb).

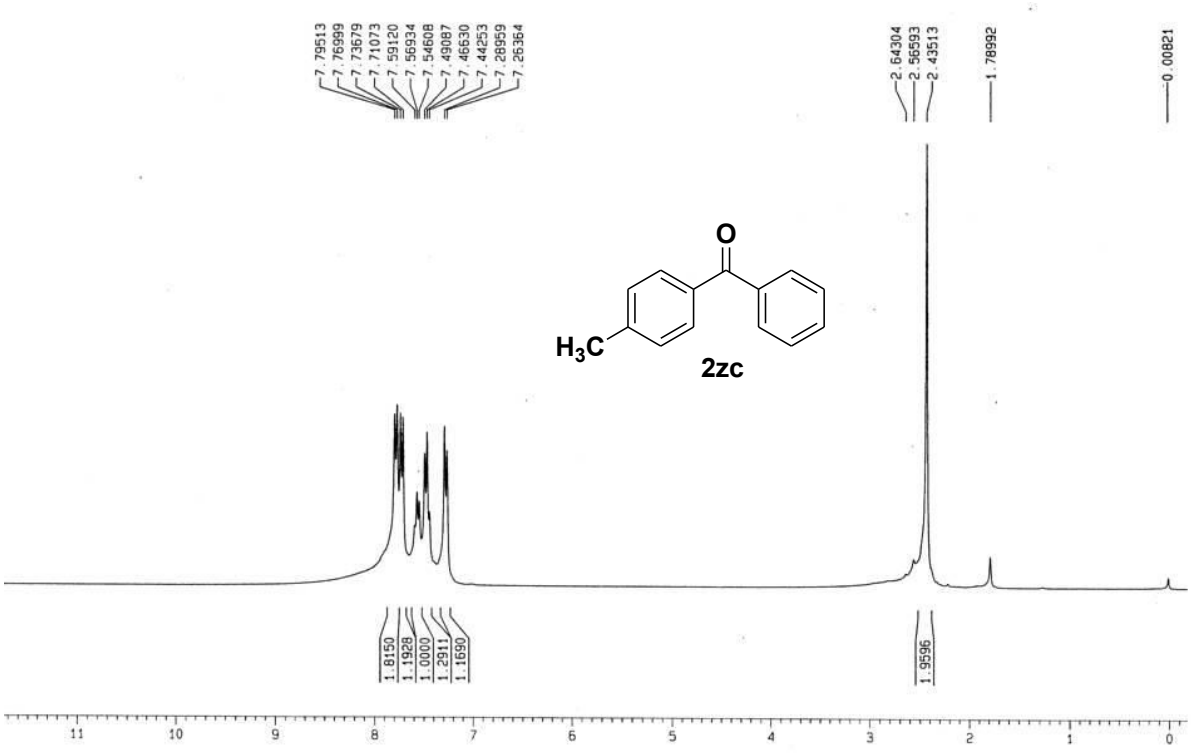

Figure 19 ^{1}H NMR of 4-methyl-benzophenone (2zc).

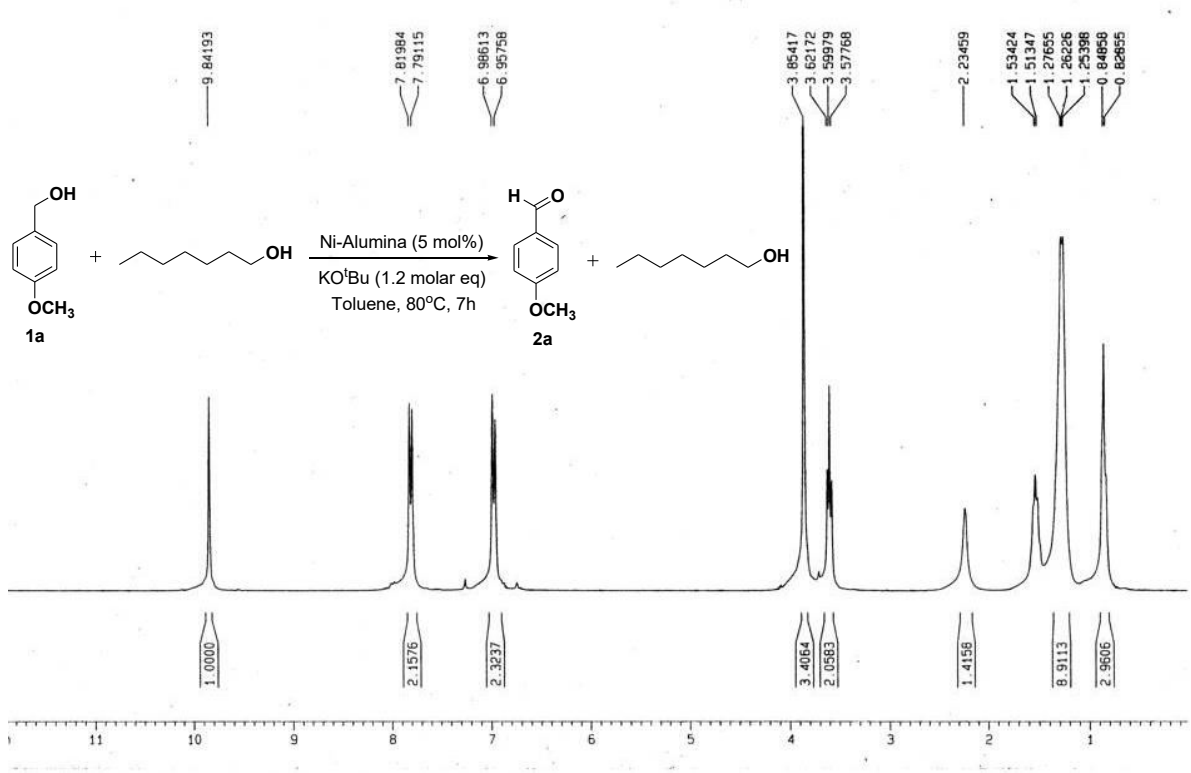

Figure 20 ^{1}H NMR of Intermolecular competition experiment.

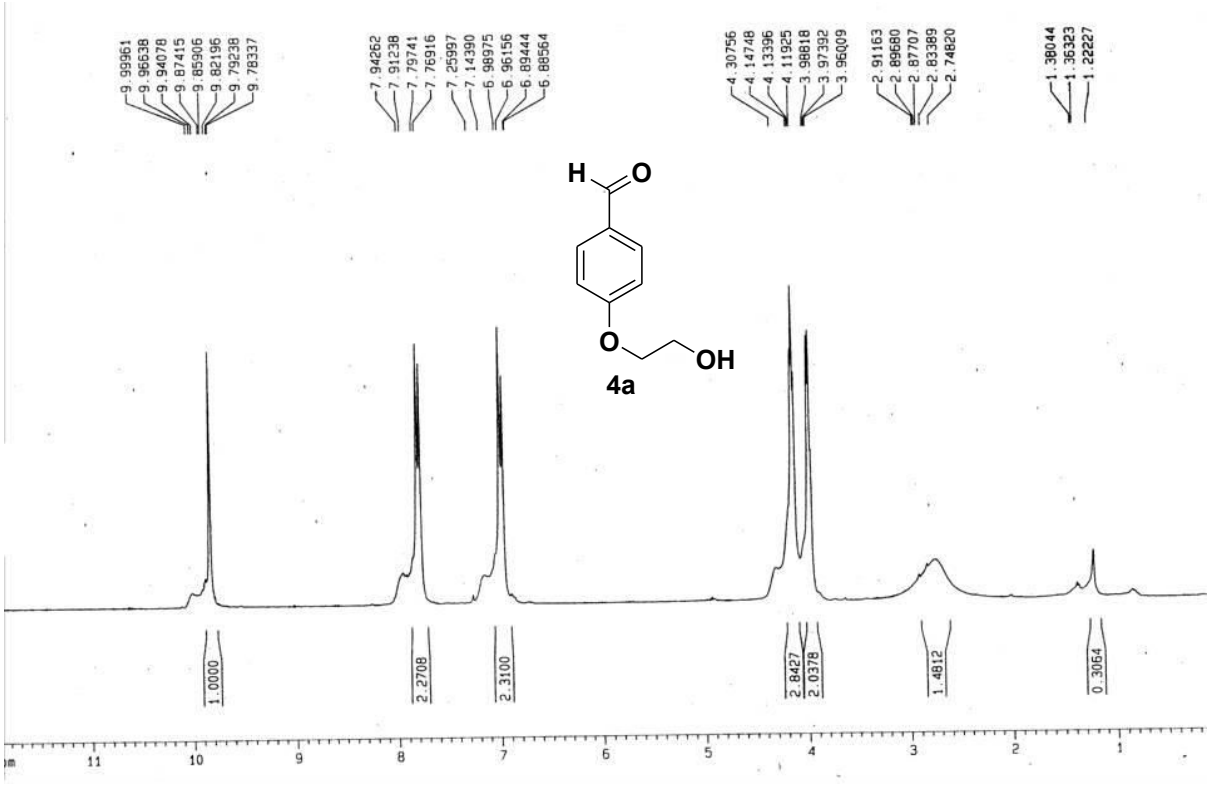

Figure 21 [1]H NMR of 4-(2-hydroxyethoxy)benzaldehyde (4a).

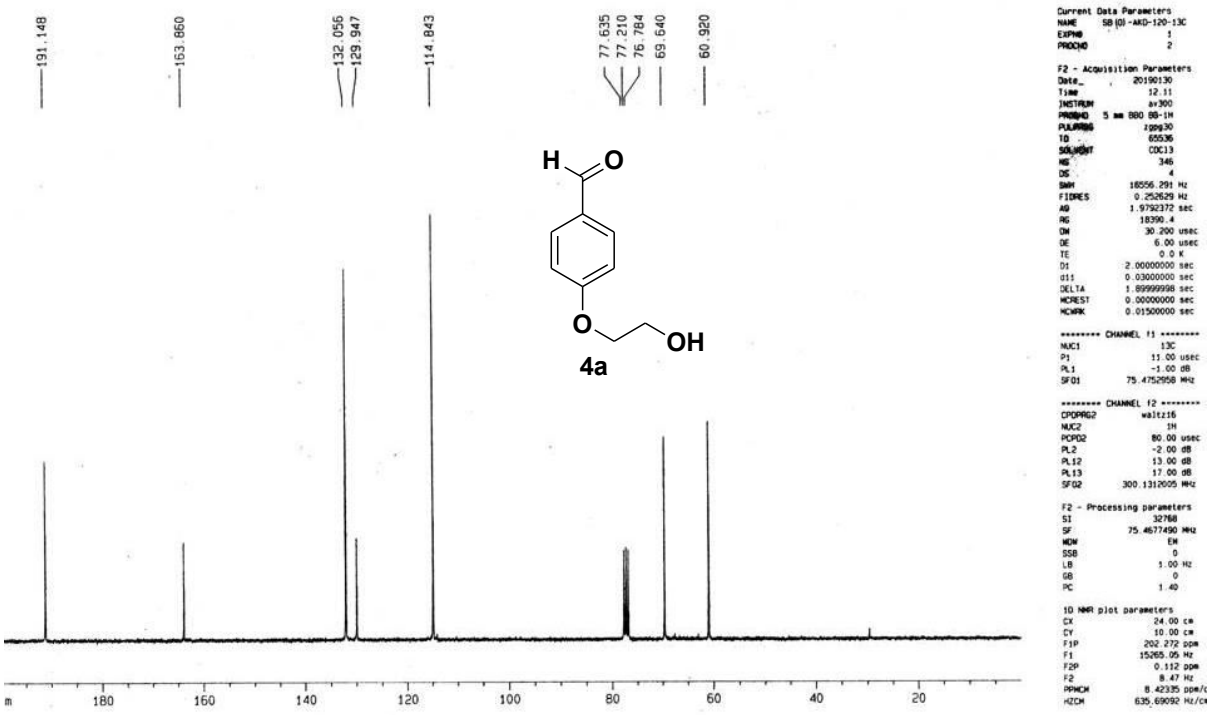

Figure 22 [13]C NMR of 4-(2-hydroxyethoxy)benzaldehyde (4a).

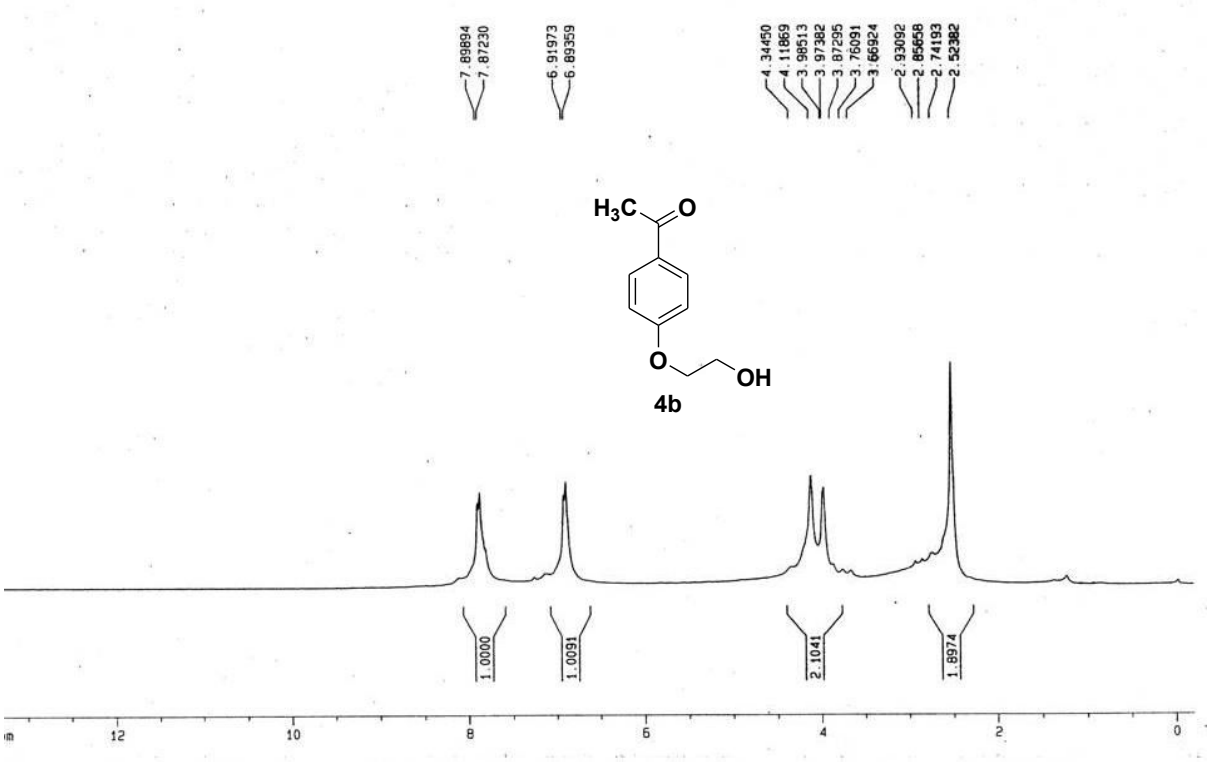

Figure 23 ^{1}H NMR of 1-(4-(2-hydroxyethoxy)phenyl)ethanone (4b).

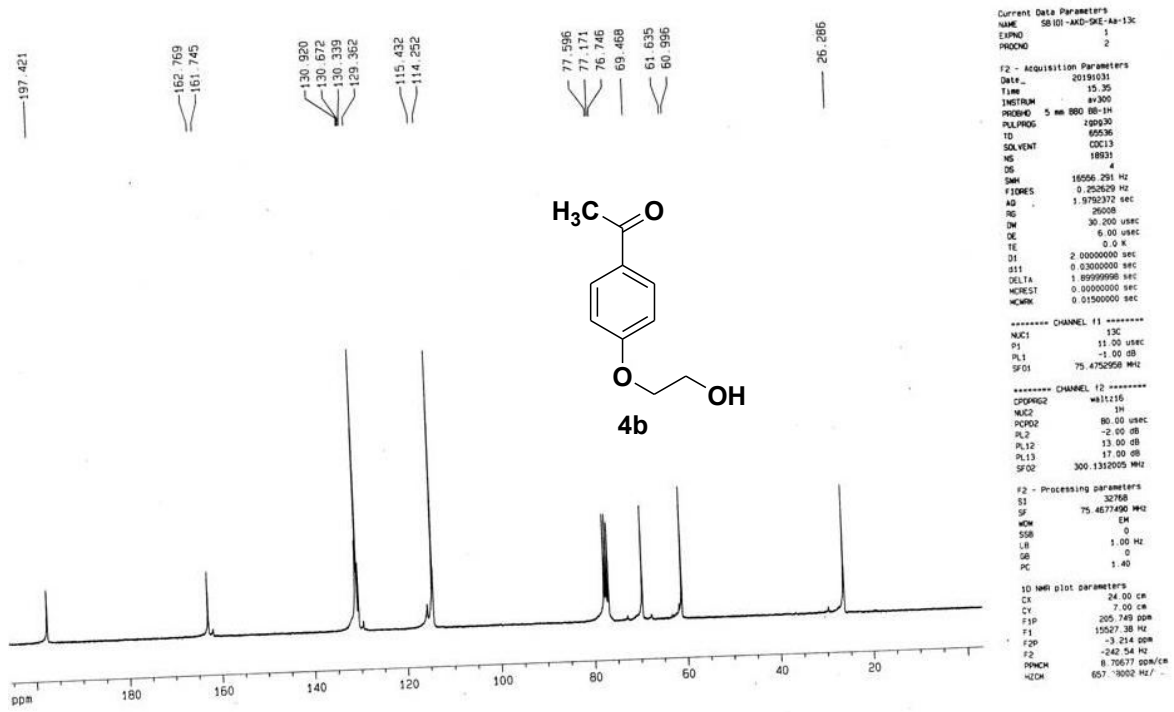

Figure 24 ^{13}C NMR of 1-(4-(2-hydroxyethoxy)phenyl)ethanone (4b).

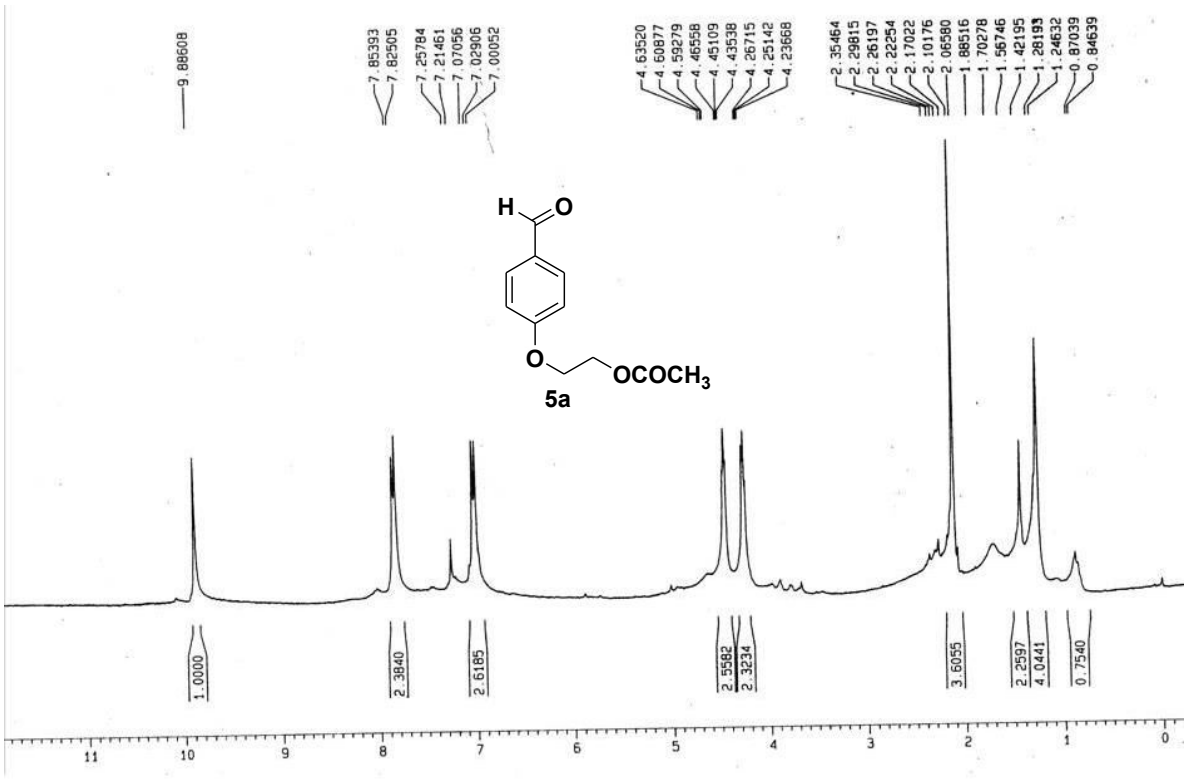

Figure 25 ^{1}H NMR of 2-(4-formylphenoxy)ethyl acetate (5a).

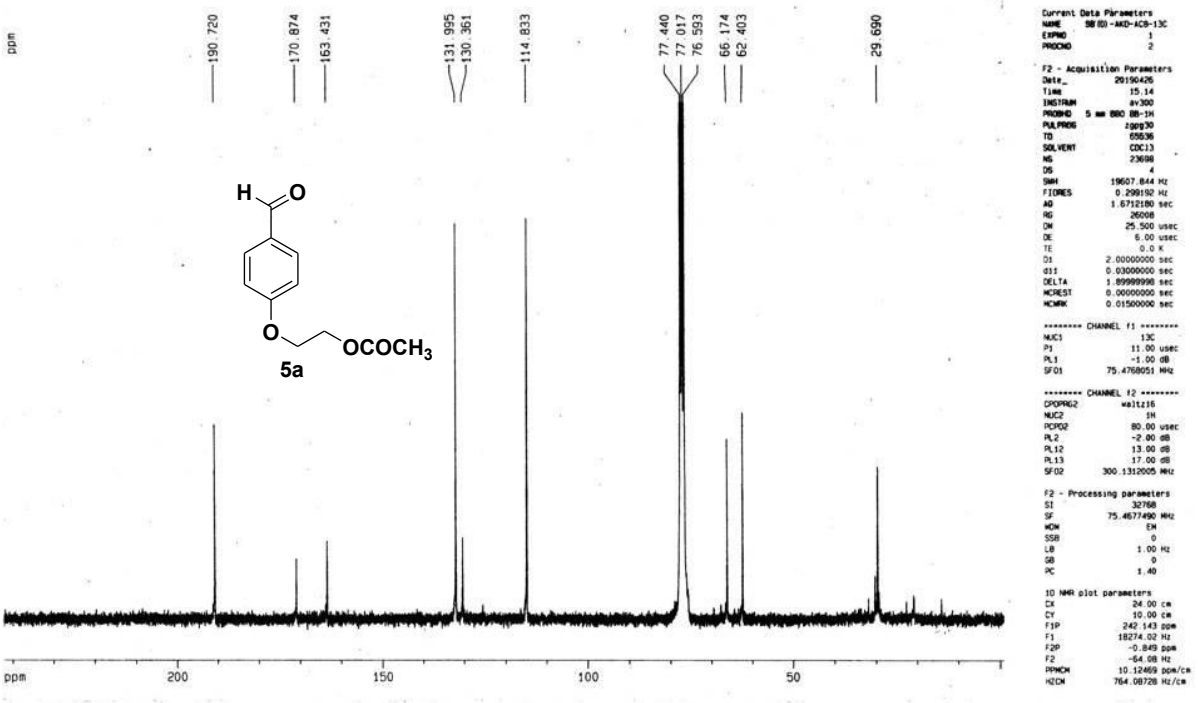

Figure 26 ^{13}C NMR of 2-(4-formylphenoxy)ethyl acetate (5a).

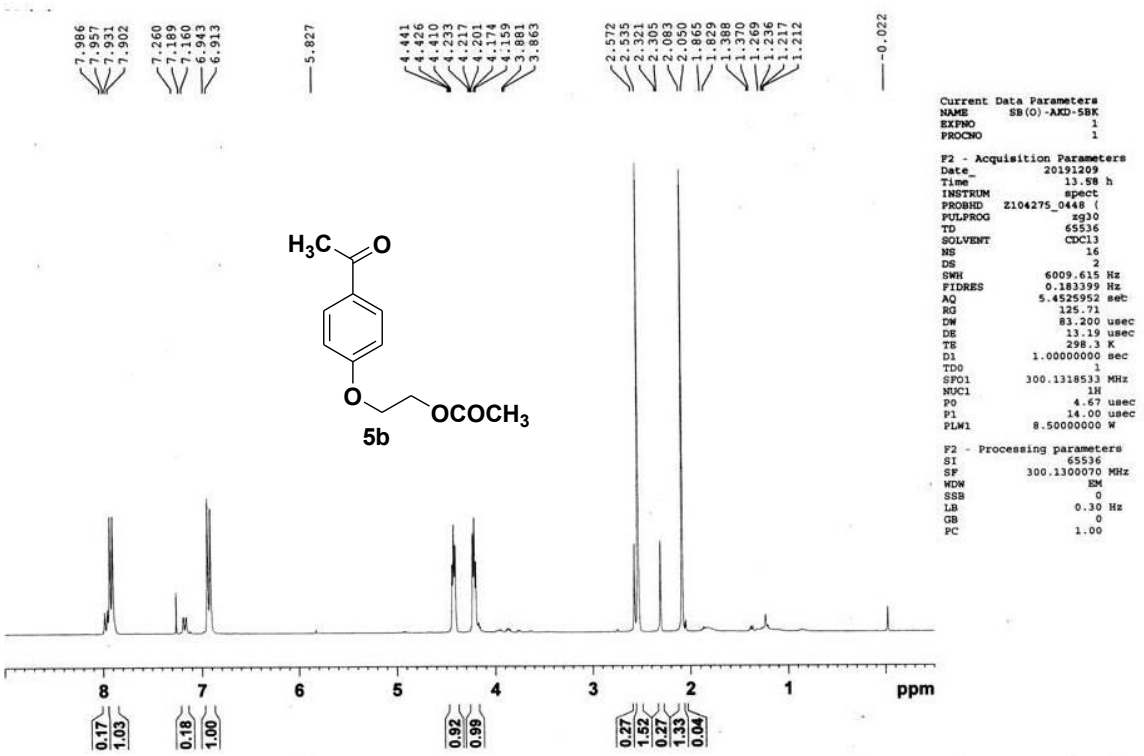

Figure 27 [1]H NMR of 2-(4-Acetyl-phenoxy) Ethyl Acetate (5b).

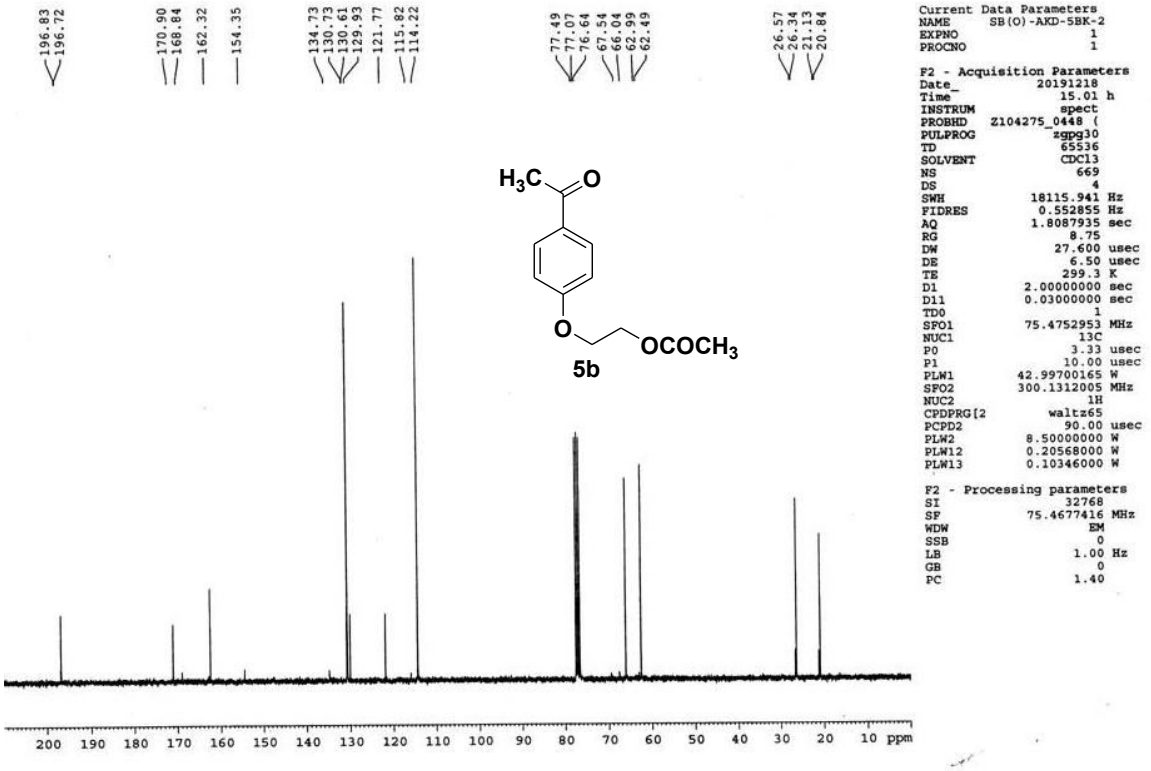

Figure 28 [13]H NMR of 2-(4-Acetyl-phenoxy) Ethyl Acetate (5b).

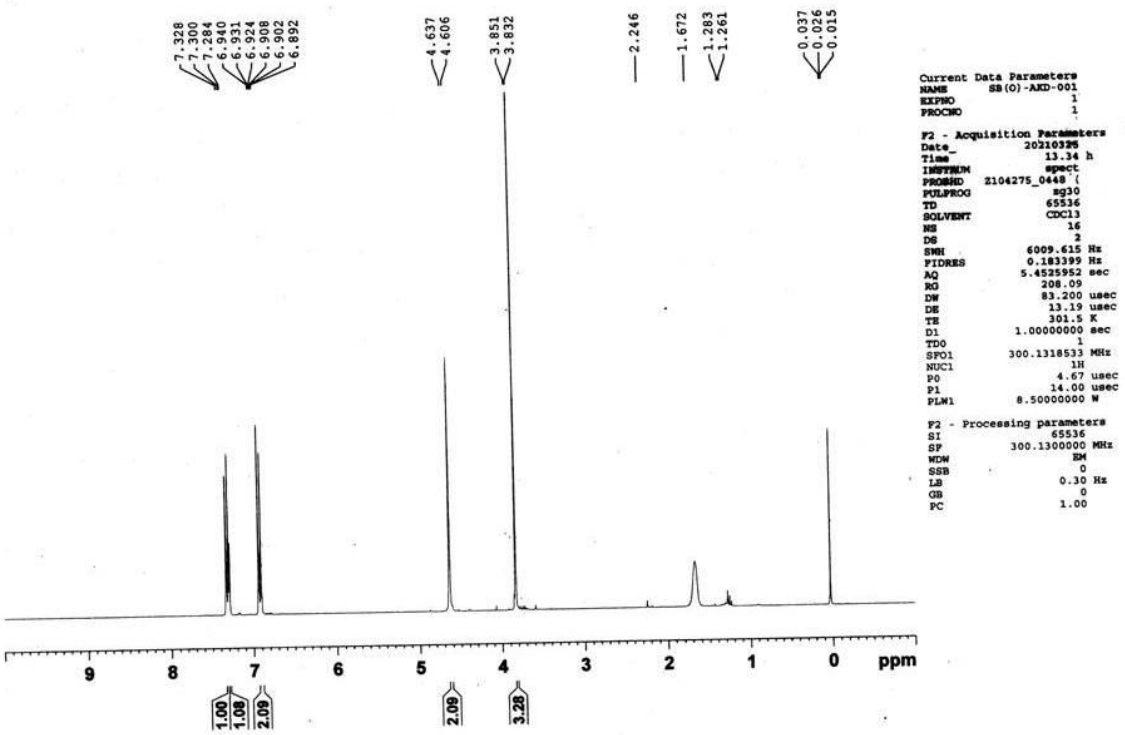

Figure 29 [1]H NMR of 4-methoxybenzyl alcohol.

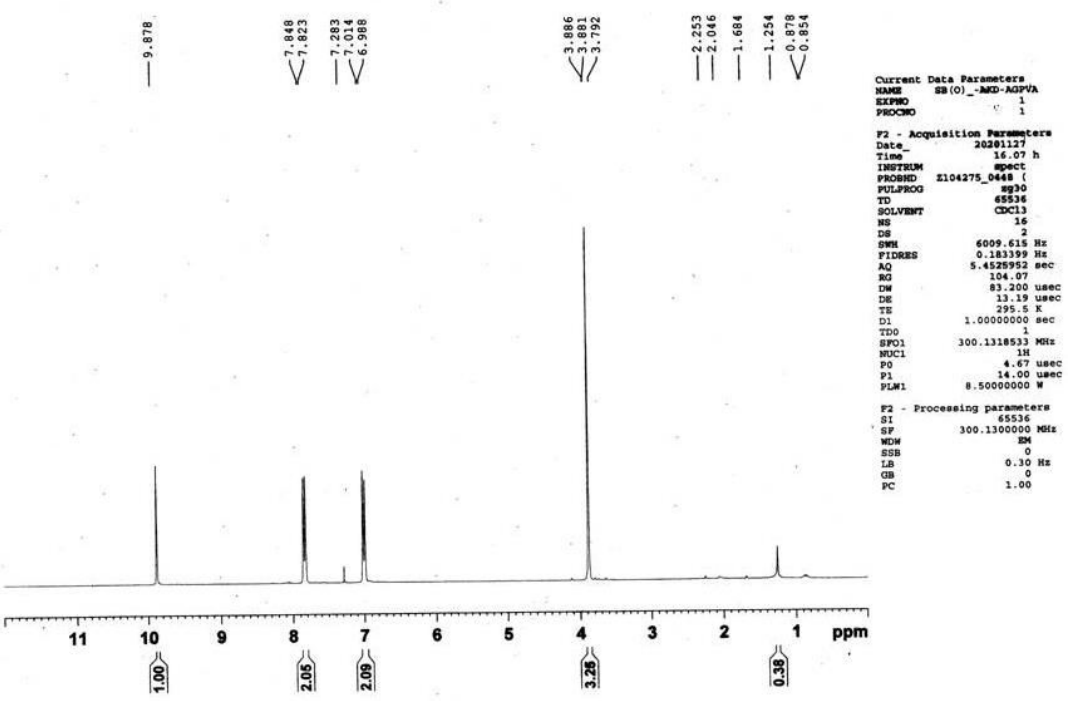

Figure 30 [1]H NMR of Reaction mixture.

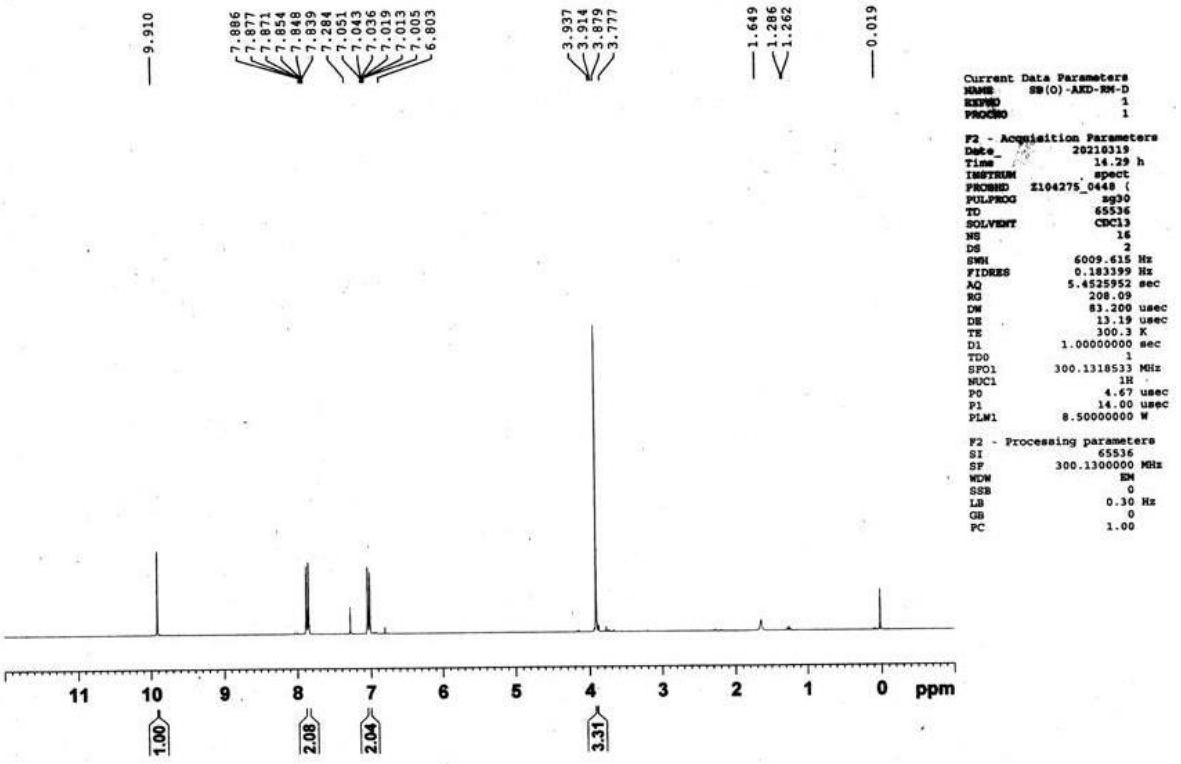

Figure 31 [1]H NMR of Reaction mixture with diazomethane treatment.

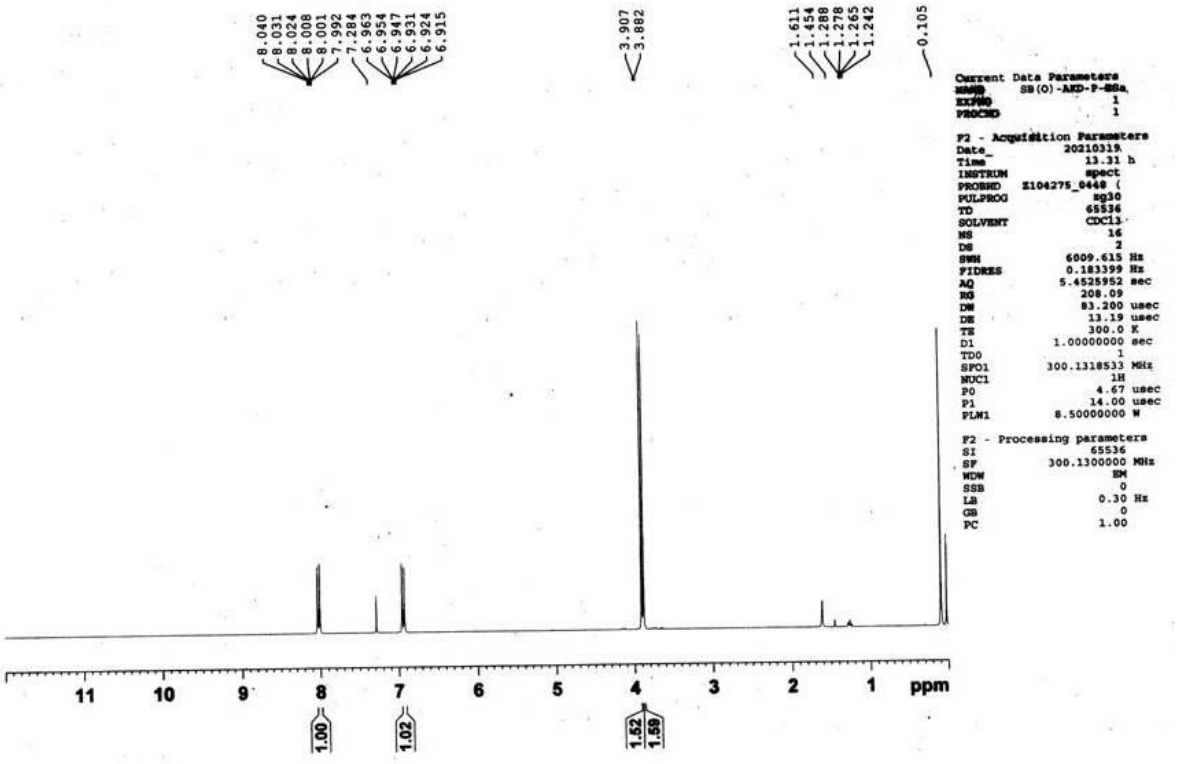

Figure 32 [1]H NMR of methyl-4-methoxy benzoate.

GC spectrum

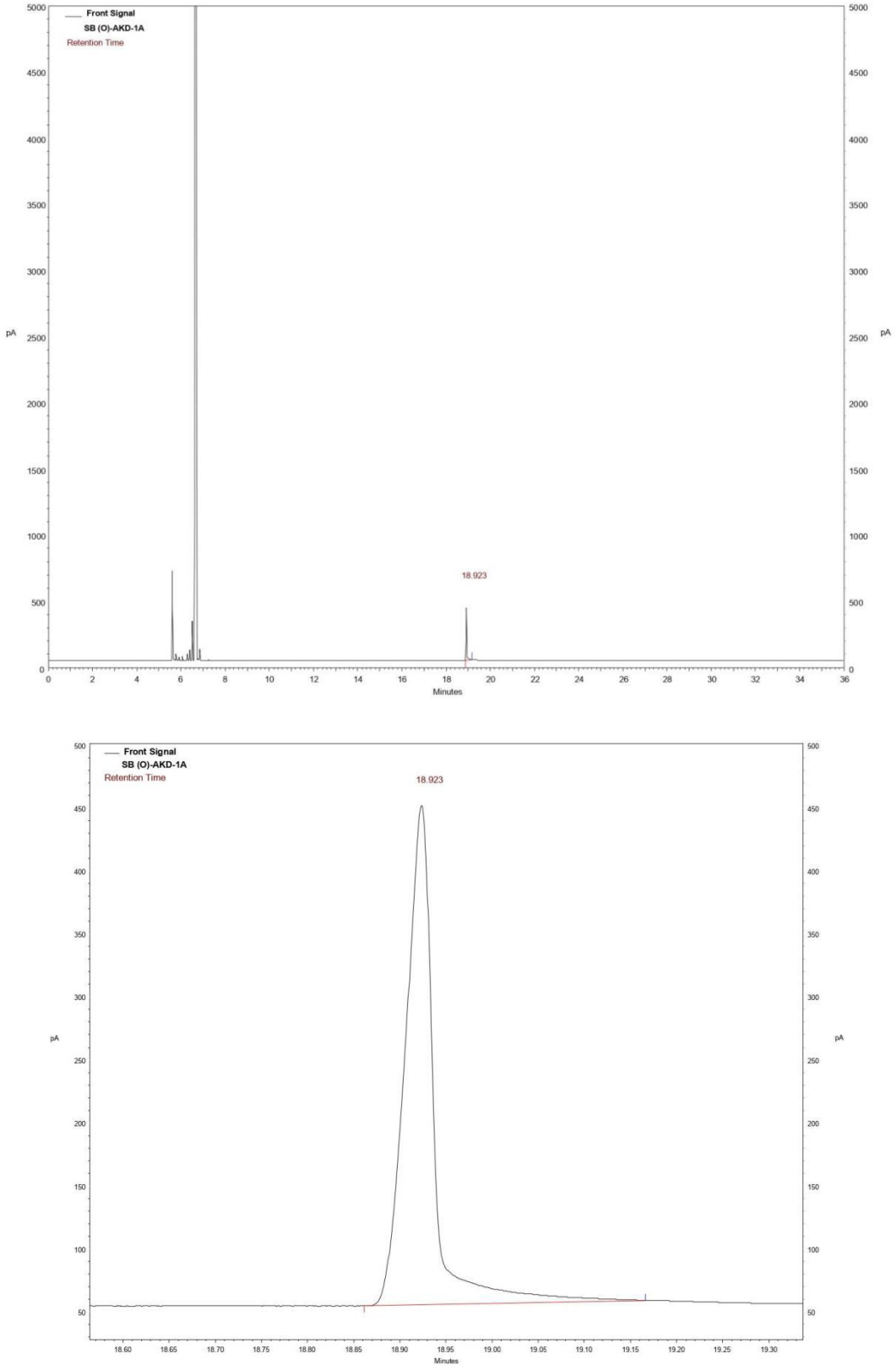

Figure 33 GC spectrum of 4-methoxybenzaldehyde

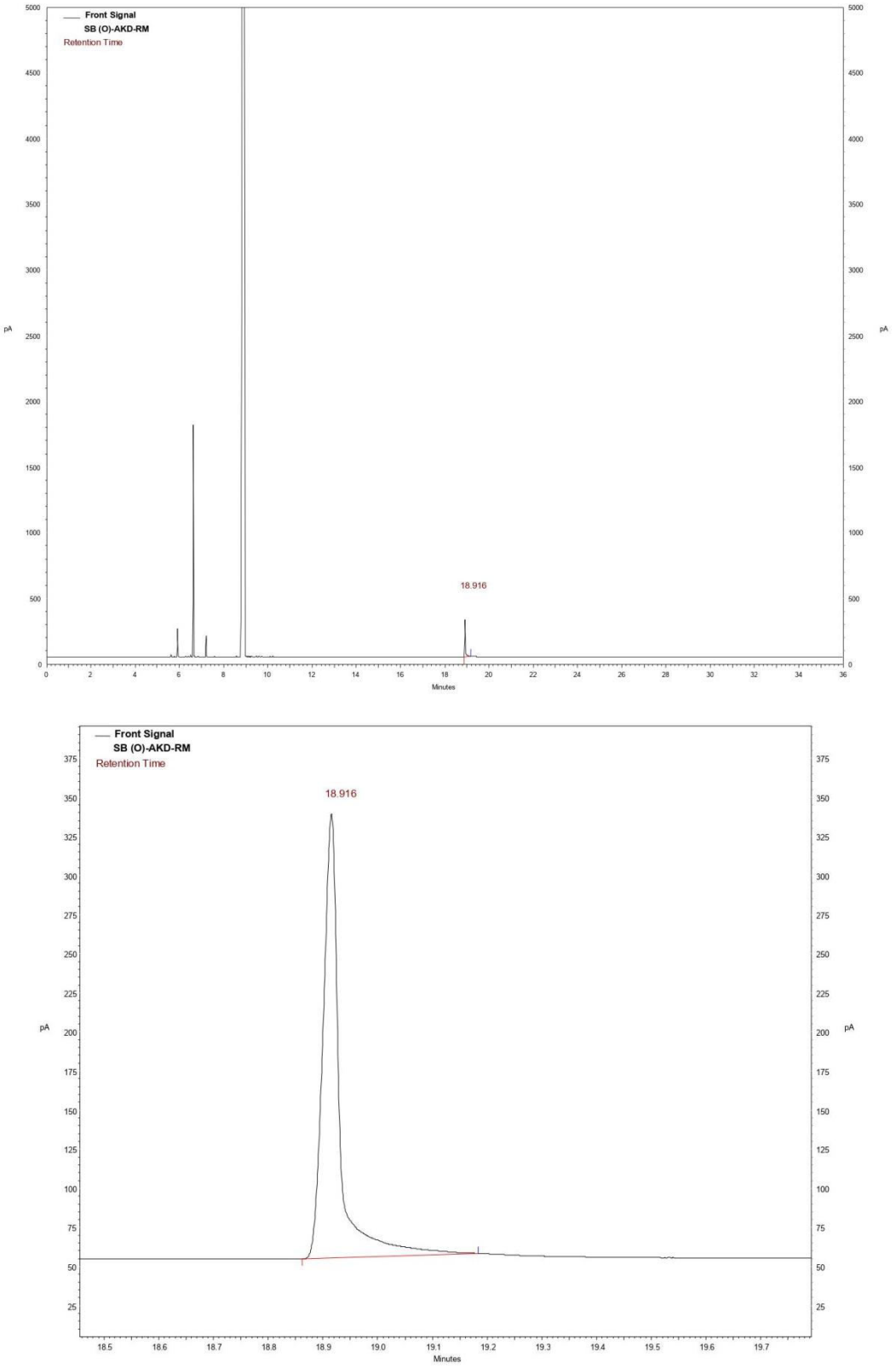

Figure 34 GC spectrum of reaction mixture

II.6. References:

1. (a) M. Jafarpour, A. Rezaeifard, V. Yasinzadeh, H. Kargar, *RSC Adv.* **2015**, *5*, 38460; (b) Y. Y. Du, Q. Jin, J. T. Feng, N. Zhang, Y. F. He, D. Q. Li, *Catal. Sci. Technol.*, **2015**, *5*, 3216; (c) D. Baruah, U. P. Saikia, P. Pahari, D. Konwar, *Tetrahedron Lett*. **2015**, *56*, 2543.
2. (a) X. Yang, S. Wu, L. Peng, J. Hu, X. Wang, X. Fu, Q. Huo, J. Guan, *RSC Adv.* **2016**,; (b) X. Wang, C. Wang, Y. Liu, J. Xiao, *Green Chem.* **2016**, *18*, 4605; (c) M. M. Kadam, K. B. Dhopte, N. Jha, V. G. Gaikar, P. R. Nemade, *New J. Chem.* **2016**, *40*, 1436.
3. (a) H. Veisi, S. Hemmati, M. Qomi, *Tetrahedron Lett.* **2017**, *58*, 4191; (b) A. F. Shojaei, F. Shirini, E. Hedayati, *Inorganic and Nano-Metal Chemistry,* **2017**, *47*, 1312; (c) A. Saha, S. Payra, S. Banerjee, *New J. Chem.* **2017**, *41,* 13377; (d) T. Karimpour, E. Safaei, B. Karimi, Y. Lee, *ChemCatChem.* **2017**, *9*, 1; (e) S. Verma, R. B. NasirBaig, M. N. Nadagouda, R. S. Varma, *Tetrahedron* **2017**, *73*, 5577.
4. (a) R. Hasanpour, F. Feizpour, M. Jafarpour, A. Rezaeifard, *New J. Chem.* **2018**, *42*, 7383; (b) B. Sarmah, B. Satpati, R. Srivastava, *ACS Omega* **2018**, *3*, 7944; (c) J. J. Boruah, S. P. Das, *RSC Adv.* **2018**, *8*, 34491; (d) N. Anbu, M. B. RubyKamalam, K. Sethuraman, A. Dhakshinamoorthy, *ChemistrySelect* **2018**, *3*, 12725; (e) S. H. Kashani, A. L. Isfahani, M. Moghadam, S. Tangestaninejad, V. Mirkhani, I. M. Baltork, *Appl Organometal Chem.* **2018**, *32*, e4440.
5. (a) A. Dutta, M. Chetia, A. A. Ali, A. Bordoloi, P. S. Gehlot, A. Kumar, D. Sarma, *Catalysis Lett.* **2019**, *149*, 141; (b) S. Meher, R. K. Rana, *Green Chem.* **2019**, *21*, 2494.
6. (a) H. Goksu, K. Cellat, F. Sen, *Sci. Rep.* **2020***, 10,* 9656; (b) S. Iraqui, S. S. Kashyap, H. Rashid, *Nanoscale Adv.* **2020**, *2*, 5790; (c) H. Goksu, F. Sen, *Sci. Rep.* **2020***, 10,* 5731; (d) B. Karimi, A. Bigdeli, A. A. Safari, M. Khorasani, H. Vali, S. K. Karimvand, *ACS Comb. Sci.* **2020**, *22*, 70; (e) H. Alamgholiloo, S. Rostamnia, K. Zhang, T. H. Lee, Y. S. Lee, R. S. Varma, H. W. Jang, M. Shokouhimehr, *ACS Omega* **2020**, *5*, 5182.
7. (a) S. Caron, R. W. Dugger, S. G. Ruggeri, J. A. Ragan, D. H. B. Ripin, *Chem. Rev.* **2006**, *106*, 2943; (b) Y. Uozumi, Y. M. A. Yamada, *Chem. Rec.* **2009**, *9*, 51.
8. (a) M. Passiniemi, A. M. Koskinen, *Beilstein J. Org. Chem.* **2013**, *9*, 2641; (b) Y. T. Ma, H. F. Fan, Y. Q. Gao, H. Li, A. L. Zhang, J. M. Gao, *Chem. Biol. Drug Des.* **2013**, *81*, 545.

9. (a) S. Biswas, B. Dutta, A. M. Kanakkithodi, R. Clarke, W. Song, R. Ramprasad, S. L. Suib, *Chem. Commun.,* **2017**, *53*, 11751; (b) M. Sdahl, J. Conrad, C. Braunberger, U. Beifuss, *RSC Adv.*, **2019**, *9*, 19549.
10. (a) A. Ghatak, S. Khan, R. Roy, S. Bhar, *Tetrahedron Lett.* **2014**, *55,* 7082; (b) S. Khan, A. Ghatak, S. Bhar, *Tetrahedron Lett.* **2015**, *56*, 2480.
11. A. Charvieux, L. L. Moigne, L. G. Borrego, N. Duguet, E. Metay, *Eur. J. Org. Chem.* **2019**, 6842.
12. I. D. Inaloo, S. Majnooni, H. Eslahi, M. Esmaeilpour, *New J. Chem.* **2020,** *44***,** 13266.
13. S. G. Hernandez-Leon, J. A. Sarabia-Sainz, G. R. Montfort, J. A. Huerta-Ocampo, A. M. Guzman-Partida, M. R. Robles-Burgueno, A. J. Burgara-Estrella, L. Vazquez-Moreno, *RSC Adv.* **2019**, *9*, 11038.
14. H. Goksu, F. Sen, *Sci. Rep.* **2020***, 10,* 5731.
15. H. Goksu, K. Cellat, F. Sen, *Sci. Rep.* **2020***, 10,* 965.
16. H.E.B. Lempers, R.A. Sheldon, *J. Catal.* **1998**, *175*, 62.
17. S. Verma, R. B. NasirBaig, M. N. Nadagouda, R. S. Varma, *Tetrahedron* **2017**, *73*, 5577.
18. B. Karimi, A. Bigdeli, A. A. Safari, M. Khorasani, H. Vali, S. K. Karimvand, *ACS Comb. Sci.* **2020**, *22*, 70.
19. S. H. Kashani, A. L. Isfahani, M. Moghadam, S. Tangestaninejad, V. Mirkhani, I. M. Baltork, *Appl Organometal Chem.* **2018**, *32*, e4440.
20. M. Jafarpour, A. Rezaeifard, V. Yasinzadeh, H. Kargar, *RSC Adv.* **2015**, *5*, 38460.
21. H. Alamgholiloo, S. Rostamnia, K. Zhang, T. H. Lee, Y. S. Lee, R. S. Varma, H. W. Jang, M. Shokouhimehr, *ACS Omega* **2020**, *5*, 5182.
22. A. Saha, S. Payra, S. Banerjee, *New J. Chem.* **2017**, *41, 13377*.
23. A. Dutta, M. Chetia, A. A. Ali, A. Bordoloi, P. S. Gehlot, A. Kumar, D. Sarma, *Catalysis Lett.* **2019**, *149*, 141.
24. S. Iraqui, S. S. Kashyap, H. Rashid, *Nanoscale Adv.* **2020**, https://doi.org/10.1039/D0NA00591F.
25. (a) L.W. Zhan, L. Han, P. Xing, B. Jiang, *Org. Lett.* **2014**, *16*, 5990; (b) L. Wang, S. S. Shang, G. S. Li, L. H. Ren, Y. Lv, S. Gao, *J. Org. Chem.* **2016**, *81*, 2189; (c) W. Dai, Y. Lv, L. Wang, S. Shang, B. Chen, G. Li, S. Gao, *Chem. Commun.* **2015**, *51*, 11268; (d) M. Guan, C. Wang, J. Zhang, Y. Zhao, *RSC Adv.* **2014**, *4*, 48777; (e) H. Cong, T. Yamato, Z. Tao, *New J. Chem.* **2013**, *37*, 3778; (f) D. Shen, C. Miao, D. Xu, C. Xia, W. Sun, *Org. Lett.* **2015**, *17*, 54; (g) Z. Hao, N. Li, X. Yan, Y. Li, S. Zong, H. Liu, Z.

Han, J. Lin, *New J. Chem.* **2018**, *42*, 6968; (h) G. F. Zha, W. Y. Fang, J. Leng, H. L. Qin, *Adv. Synth. Catal.* **2019**, *361*, 2262; (i) S. S. Sakate, S. B. Kamble, R. V. Chikate, C. V. Rode, *New J. Chem.* **2017**, *41*, 4943; (j) M. J. King, Y. E. Jung, C. Y. Lee, J. Kim, *Tetrahedron Lett.* **2018**, *59*, 2722; (k) T. Guo, Y. Gao, Z. Li, J. Liu, K. Guo, *Synlett*. **2019**, *30*, 329; (l) R. T. Mofrad, S. Tahmasebi, E. Payami, *Appl Organometal Chem.* **2019**, *33*, 4773; (m) S. Nandy, A. Ghatak, A. K. Das, S. Bhar, *Synlett.* **2018**, *29*, 2208; (n) X. Jiang, J. Zhou, Y. Zhou, H. Sun, J. Xu, F. Feng, W. Qu, *Molecules*, **2018**, *23*, 1715.

CHAPTER III

Synthesis of Magnetite (Fe_3O_4) Nanoparticles using Natural Resource: Recyclable Catalyst for Eco-friendly Chemoselective Reduction of Nitroarenes in Aqueous Medium

III. Synthesis of Magnetite (Fe_3O_4) Nanoparticles using Natural Resource: Recyclable Catalyst for Eco-friendly Chemoselective Reduction of Nitroarenes in Aqueous Medium

III.1. Introduction

Suitably designed amines are widely documented as recurrent pharmacophores such as antibiotic linezolid (Zyvox),[1] HIV protease inhibitor amprenavir (Agenerase),[2] and sildenafil (Viagra).[3] Besides, functionalized aromatic amines represent one of the most important feedstock's for the synthesis of pharmaceuticals, agrochemicals, dyes, pigments, polymers, pesticides, rubber materials, and chelating agents.[4] Aromatic amines are conventionally synthesized by the reduction of corresponding nitroaromatics employing the stoichiometric amount of reducing agents which generate a significant amount of waste into the environment.[5] From the standpoint of green and sustainable perspective, catalytic transfer hydrogenation using transition metal nano-catalysts for the reduction of nitroarenes has fascinated the scientific community because of its eco-friendliness. A concise survey of the current developments for the reduction of nitroarenes using transition metal nano-catalysts is being presented in the following review.

III.2. Reduction of nitroarenes using transition metal nano-catalysts: A review

M. Beller and his group[6a] have demonstrated the synthesis of Co_3O_4 nano-particles through the pyrolysis (at 800°C for 2h under an argon atmosphere) of cobalt(II)-phenanthroline complexes on carbon surface surrounded by a modified nitrogen-doped graphene layer (NGr) (Co_3O_4-NGr/C). The synthesized nano-catalysts were shown to exhibit high catalytic activity for the hydrogenation of nitroarenes to the corresponding anilines using formic acid as the hydrogen source in the presence of Et_3N as a base and THF as a solvent at 100°C (Scheme 1). Various functional groups were well tolerated with good to excellent yields of the desired products. The catalyst was readily recycled up to six catalytic runs without noticeable loss of its catalytic activity.

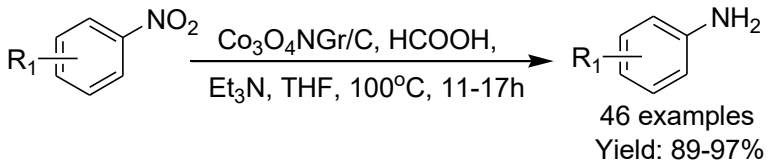

Scheme 1 Co_3O_4-NGr/C catalyzed hydrogenation of nitroarenes to anilines

Modified palladium magnetic nanoparticles (Fe@Pd NPs)[6b] were prepared by embedding in mesoporous carbon (MC) (Fe@Pd-MC) and exhibited good catalytic performance towards the hydrogenation of nitroarenes under an atmosphere of hydrogen as the hydrogen source at room temperature (Scheme 2). It has been observed that several reducible functional groups, such as -OH, -$COCH_3$, -CN, and -COOH remained intact under the optimized reaction conditions. The efficient catalytic activity of Fe@Pd-MC in the hydrogenation of nitroarenes was probably due to the larger pore size of Fe@Pd-MC which significantly enhanced the efficient contact between active sites (Fe@Pd NPs) and reactants for the rapid commencement and formation of desired products in excellent yields.

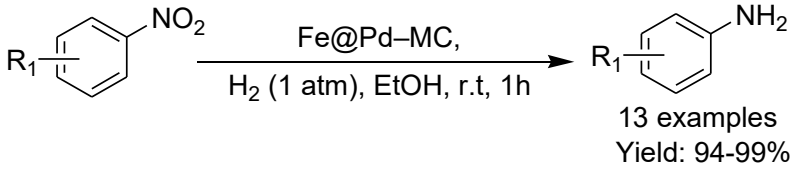

Scheme 2 Hydrogenation of nitroarenes catalyzed by Fe@Pd-MC

Aluminium oxy-hydroxide-supported Pd nanoparticles[6c] (Pd/AlO(OH)) was utilized as an efficient catalyst for the reduction of aromatic as well as aliphatic nitro compounds to their corresponding primary amines with good to high yields in the presence of $NaBH_4$ as the hydrogen donor using water/methanol (v/v = 7/3) as the solvent mixture at room temperature (Scheme 3). Various nitro compounds were successfully reduced by performing the Pd/AlO(OH) catalyzed reduction reaction and produced the desired amines in short reaction times with maximum yields up to 99%. The catalyst could be easily recovered and reused several times with negligible leaching of palladium.

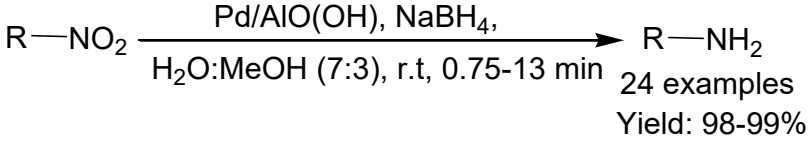

Scheme 3 Pd/AlO(OH) catalyzed reduction of nitro compounds

Patil *et al.*[6d] have developed Pd nanoparticles stabilized by PEG-6000 and well-characterized by using various spectroscopic techniques such as SEM, TEM, XRD, XPS, and EDAX. The developed catalytic system was tested for the hydrogenation of nitroarenes using dimethylamine borane (Me_2NHBH_3) as the hydrogen source at room temperature (Scheme 4). Various structurally varied amines were synthesized from the corresponding nitroarenes with good to excellent yields. The catalyst was successfully reused up to the 4th catalytic runs without detectable loss in its reactivity.

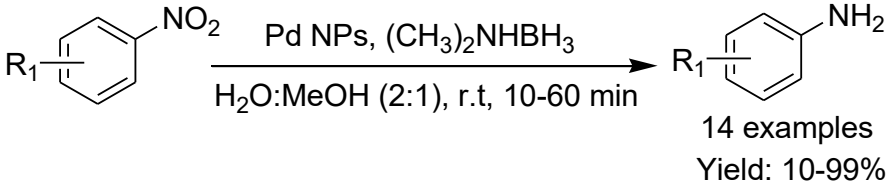

Scheme 4 Pd NPs catalyzed reduction of nitroarenes using Me_2NHBH_3

γ-Fe_2O_3@porous carbon nanocatalyst[7a] was synthesized via facile pyrolysis of a Fe-based MOF, $Fe_3O(FA)_3(H_2O)_2(NO_3)$ (called Fe-MIL-88A, FA=fumaric acid) at 500°C. The resultant nanocatalyst showed good catalytic activity for the hydrogenation of aliphatic as well as aromatic nitro compounds to their related amines in the presence of hydrazine hydrate ($N_2H_4.H_2O$) as the co-reductant in EtOH solvent under refluxing at 85^{o}C (Scheme 5). Several functionalized nitro compounds were successfully reduced to the corresponding substituted anilines with high conversion and good selectivity. The γ-Fe_2O_3 based nanocatalyst was easily recovered with an external magnet and reused efficiently several times without any detectable loss of catalytic activity.

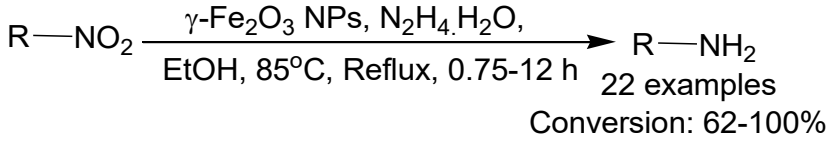

Scheme 5 Reduction of nitro compounds using γ-Fe_2O_3 nanoparticles

Huang *et al.*[7b] have prepared palladium nanoclusters supported on N-doped ordered mesoporous CMK-3 carbon (Pd/N-CMK-3) via a facile impregnation approach with aqueous solutions of H_2PdCl_4 and 1,10-phenanthroline in two steps. Various substituted nitroarenes were successfully hydrogenated to the corresponding aromatic amines with H_2 as the hydrogen donor under pressure using Pd/N-CMK-3 as the efficient heterogeneous catalyst under the solvent-free condition with good conversion and high selectivity (Scheme 6). It has been observed that

halogenated nitroaromatics produced small amounts of dechlorinated anilines with increasing reaction time. The Pd/N-CMK-3 catalyst was easily recovered for multiple recycling with no obvious loss of its catalytic performance.

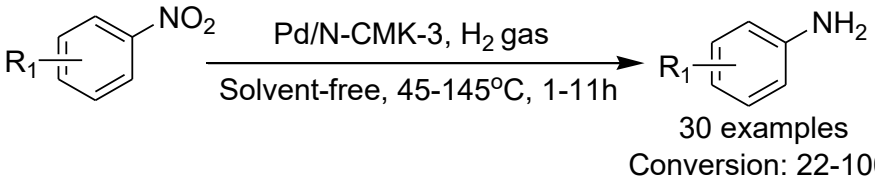

Scheme 6 Pd/N-CMK-3 catalyzed hydrogenation of nitroarenes to aromatic amines

Binaphthyl-stabilized Pt nanoparticles (Pt-BNP)[7c] were used as a heterogeneous catalytic system for the reduction of nitroaromatics under H_2 atmosphere in an aqueous medium at room temperature (Scheme 7). Various sensitive moieties like ketone, ester, amide, acid, nitrile, and halides were survived well in this protocol and produced the desired hydrogenated products in good yields. The Pt-BNP catalyst was quantitatively recovered and then efficiently recycled up to five times with good catalytic activity. TEM images of fresh and recovered nanocatalyst were compared and it was observed that there was no significant change in the particle size.

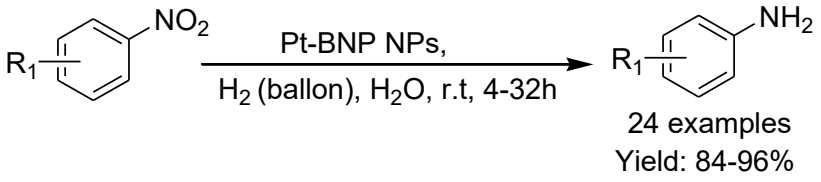

Scheme 7 Pt-BNP catalyzed hydrogenation of nitroarenes to aromatic amines

Palladium incorporated cyclohexane diamine (DACH) functionalized β-cyclodextrin catalytic system (DACH-Pd-β-CD) has been developed by Guo *et al.*[7d] The catalyst was characterized through NMR, TEM, XRD, and EDS analytical techniques. The catalytic efficiency was demonstrated by the reduction of nitroarenes using $NaBH_4$ as the reducing agent in an aqueous medium at room temperature (Scheme 8). Nitroaromatics bearing both electron-donating and electron-withdrawing substituents were well survived and yielded the desired amines with good to excellent yields. Furthermore, the catalyst could be easily recovered with maintenance of high catalytic activity even after five catalytic reactions, and no leaching of Pd was detected.

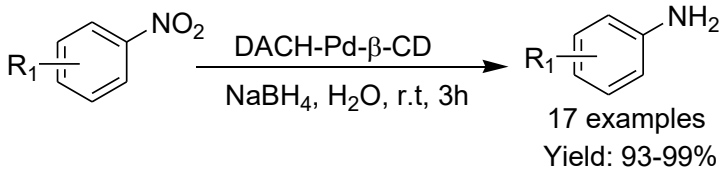

Scheme 8 DACH-Pd-β-CD catalyzed hydrogenation of nitroarenes to aromatic amines

Yang *et al.*[8a] reported a well-shaped magnetic metal-organic framework (MOF) composite namely Cu-BTC@Fe_3O_4 (BTC =1,3,5-benzenetricarboxylate) and exhibited high catalytic activity in the reduction of nitro substrates to the related primary amines. Here, $NaBH_4$ was used as the reducing agent and EtOH: H_2O (2:1) as the solvent mixture under mild reaction conditions (Scheme 9). The reaction proceeded smoothly to afford the corresponding reduced products in good to high yields. The reaction was also extended to aliphatic nitro compounds such as 1-nitrohexane and nitrocyclohexane which were successfully reduced to the corresponding amines with good yields. The catalyst was easily separated with an external magnet and reused without marginal loss in its reactivity for six consecutive cycles.

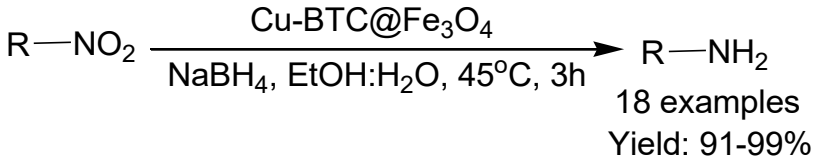

Scheme 9 Reduction of nitroarenes to aromatic amines catalyzed by Cu-BTC@Fe_3O_4

Tamura *et al.*[8b] have designed MoO_x-modified silica-supported ruthenium nanoparticles (Ru-MoO_x/SiO_2) as an efficient heterogeneous catalyst for the reduction of the nitro group in functionalized nitroarenes with H_2 gas under solvent-free condition (Scheme 10). Incorporation of MoO_x to the Ru/SiO_2 species provided the active site between MoO_x and Ru metal. Therefore, the substrates were strongly adsorbed on MoO_x, and hydride species were formed on Ru metal. Various structurally varied nitroarenes were smoothly reduced and provided the corresponding substituted aminoarenes with excellent conversion.

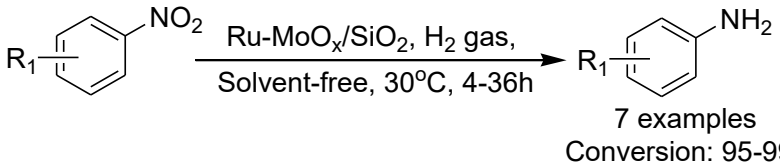

Scheme 10 Ru-MoO_x/SiO_2 catalyzed reduction of nitroarenes to aminoarenes

Metal-organic framework (MOF) derived nickel nanoparticles embedding within porous graphitic carbon layers composites (Ni@C)[8c] have been prepared via facile pyrolysis of Ni containing MOF and characterized by transmission electron microscopy (TEM), X-ray diffraction (XRD), X-ray photoelectron spectroscopy (XPS) and N_2 adsorption-desorption techniques. The resulting nanocomposites served as an effective catalyst for the hydrogenation of substituted aromatic and aliphatic nitro compounds to their corresponding amines under H_2 pressure (Scheme 11). The hot-filtration experiment and recycling test revealed the heterogeneity and catalytic stability of Ni@C catalysts during the liquid phase hydrogenation process.

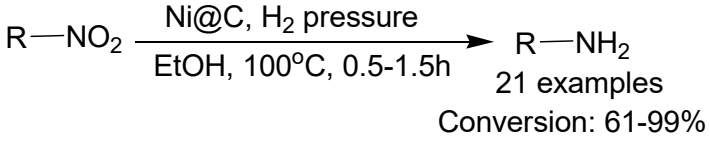

Scheme 11 Reduction of nitro compounds catalyzed by Ni@C under H_2 pressure

Gold nanoparticles[8d] (Au NPs) supported on magnetic polyionic liquid (PIL), namely MNP@PIL@Au have been synthesized by chemical reduction of $HAuCl_4$ with sodium borohydride ($NaBH_4$) and well-characterized using XRD, TEM, FTIR, TGA, EDS, and AAS analytic techniques. The catalytic application of MNP@PIL@Au was tested for the efficient reduction of various nitroarenes to aminoarenes using $NaBH_4$ as the reducing agent under green and mild conditions and provided the desired amines with good yields (Scheme 12). This catalytic protocol selectivity reduced the nitro group in the halonitroarenes as well as alkyne-substituted nitroarenes without affecting the halo and alkyne moieties. The catalyst was magnetically separated and readily reused (up to 8 runs) without much loss of its activity.

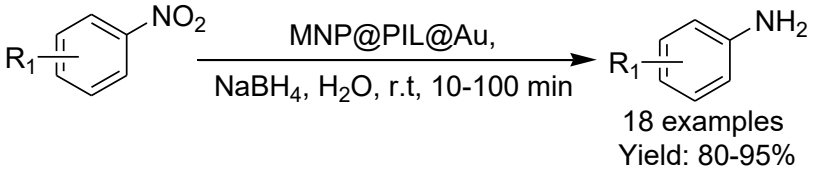

Scheme 12 MNP@PIL@Au catalyzed reduction of nitroarenes to aminoarenes

Zhou *et al.*[8e] have prepared carbon-wrapped magnetic nanosphere (Fe_3O_4@C) via simple hydrothermal conditions and then rhodium nanoparticles (Rh NPs) were successfully loaded onto it through a direct reduction of Rh(III). The synthesized Fe_3O_4@C-Rh nanocatalyst was characterized by using various spectroscopic techniques, including Fourier transform infrared spectrometer (FT-IR), transmission electron microscopy (TEM), X-Ray Diffraction (XRD), and

X-ray photoelectron spectroscopy (XPS). The Fe_3O_4@C-Rh nanocatalyst exhibited high catalytic efficiency for the catalytic transfer hydrogenation of a variety of nitroarenes to aminoarenes using hydrazine hydrate ($N_2H_4.H_2O$) as the hydrogen source in an aqueous medium (Scheme 13). The catalyst was easily recovered using an external magnet and reused efficiently in the next successive catalytic cycles without decreasing its efficiency.

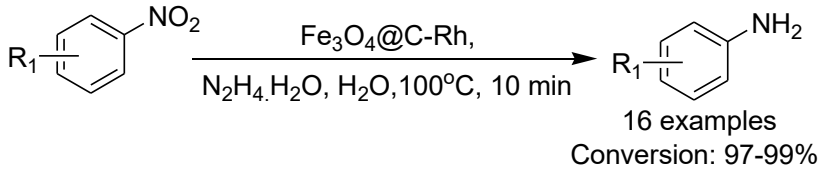

Scheme 13 Fe_3O_4@C-Rh catalyzed reduction of nitroarenes to aminoarenes

Hosseini *et al.*[9a] have synthesized Au nanoparticles decorated on SBA-15 functionalized symmetrical tridentate NNN-pincer ligand (SBA@Pincer@AuNPs) which was efficiently employed as the heterogeneous catalyst for selective reduction of various nitroaromatics to substituted aminoarenes in aqueous medium using $NaBH_4$ as a reducing agent at room temperature (Scheme 14). The SBA-15 functionalized symmetrical tridentate NNN-pincer ligand stabilized the Au nanoparticles effectively and prevented the agglomeration of nanoparticles due to strong ligation of the pincer ligand. The catalyst was successfully recovered and recycled with negligible leaching.

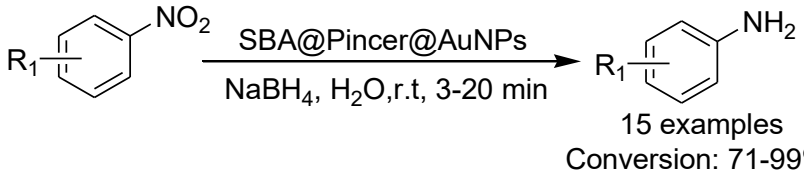

Scheme 14 SBA@Pincer@AuNPs catalyzed reduction of nitroarenes to aminoarenes

Covalent-triazine framework (CTF) supported Pd nanoparticles (Pd@CTF) was successfully prepared by Li *et al.*[9b] and employed as an effective catalyst for the catalytic transfer hydrogenation of various substituted aromatic and aliphatic nitro compounds to the corresponding amines at room temperature using formic acid (FA) and ammonium formate ($HCOONH_4$) as the hydrogen donor (Scheme 15). The synergistic effect between the covalent-triazine framework (CTF) and Pd NPs led to the outstanding catalytic efficiency of the catalyst. The Pd@CTF catalyst could be readily reused for 5th consecutive runs without significant loss of its catalytic reactivity.

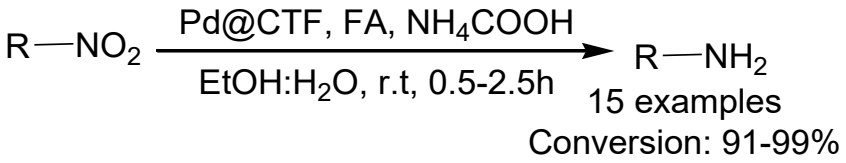

Scheme 15 Pd@CTF catalyzed reduction of nitro compounds

Palladium (Pd) nanoparticles immobilized on halloysite (Hal) composed cyclodextrin modified melamine-based polymer (Pd@HTMC)[9c] have been synthesized and applied as an efficient heterogeneous catalyst for the hydrogenation of various nitro-aromatics to the corresponding arylamines under H_2 pressure in an aqueous medium (Scheme 16). The addition of melamine-based polymer effectively anchored the Pd metal through electrostatic interactions. The presence of cyclodextrin (CD) in the structure of Pd@HTMC catalyst could provide the generation of inclusion complex with the hydrophobic substrate. Furthermore, CD acted as the capping agent as well as effectively stabilized the Pd nanoparticles. The recycling experiments revealed good recyclability (up to six reaction runs) of Pd@HTMC with a slight loss in its reactivity and leaching of Pd.

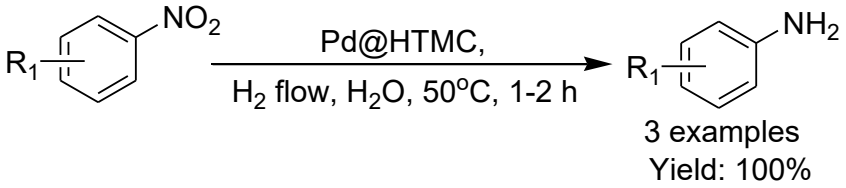

Scheme 16 Pd@HTMC catalyzed reduction of nitroarenes to aminoarenes

Kureshy and his group[9d] have synthesized nitrogen-rich graphitic-carbon stabilized cobalt nanoparticles (Co@g-C/N-800) by simple chelation of $Co(OAc)_2$ with cucurbit[6]uril (CB[6]) and calcination under controlled temperature (800°C) and argon (Ar) atmosphere. The synthesized Co@g-C/N-800 nano-catalyst was characterized by HR-TEM, PXRD, and other physicochemical techniques and the results showed high dispersion of Co NPs on the solid matrix. The applicability of Co@g-C/N-800 was tested for selective hydrogenation of nitro group in the substituted nitroarenes with molecular hydrogen using water-tetrahydrofuran (1:1) as the solvent mixture (Scheme 17). Under optimized reaction conditions, a broad range of functionalized nitroarenes was reduced with high selectivity at 50°C in good to excellent conversions without producing any dehalogenation products.

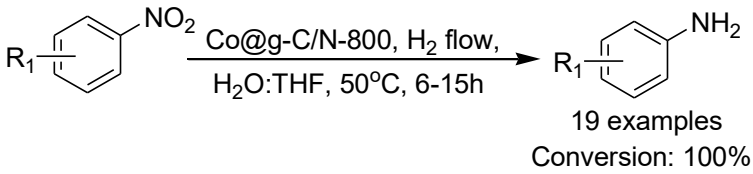

Scheme 17 Co@g-C/N-800 catalyzed reduction of nitroarenes to aminoarenes

AgPd nanoparticles supported on reduced graphene oxide (AgPd/RGO) has been synthesized by Liu *et al.*[9e] and applied as an effective recyclable catalyst for the reduction of nitro groups in aromatic as well as aliphatic nitro compounds in the presence of formic acid (FA) and ammonium formate ($HCOONH_4$) as the reducing agent under ambient reaction condition (Scheme 18). Variously substituted nitro compounds were smoothly converted to their corresponding primary amines with high conversion as well as good selectivity. The synergetic interaction between reduced grapheme oxide support and AgPd nanoparticles was highly responsible for the impressive catalytic attributes of AgPd/RGO catalyst.

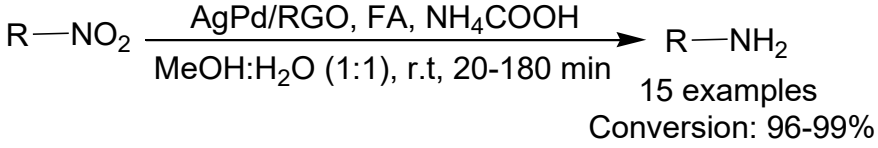

Scheme 18 AgPd/RGO catalyzed reduction of nitro compounds to primary amines

Nickel nanoparticle embedded on ordered mesoporous carbon surface modified by nitrogen-doped graphene (NGr) (Ni/NGr@OMC-800)[9f] has been synthesized and employed as the recyclable catalyst for the reduction of nitroarenes to the corresponding aminoarenes under H_2 atmosphere in an aqueous medium at 100°C (Scheme 19). The synthesized nanocatalyst exhibited good selectivity as well as higher conversion towards the reduction of diversely functionalized nitroaromatics with excellent yields of aromatic anilines. The Ni/NGr@OMC-800 nano-catalyst was easily recovered for several recycling reactions without a change in its catalytic reactivity.

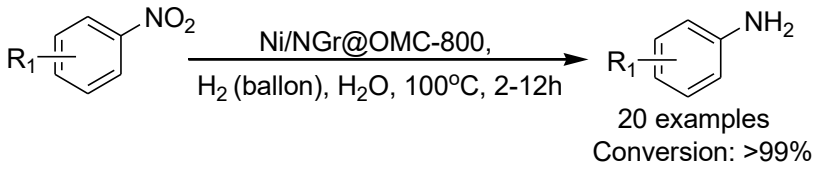

Scheme 19 Heterogeneous Ni catalysed hydrogenation of nitroarenes

Bimetallic nickel-cobalt porous material[10a] was developed through the pyrolysis of ZIF-67 anchored with Ni ions. Here, $Ni(NO_3)_2$ was introduced as an etching agent and zeolite imidazole (ZIF-67) skeletons were transformed into hollow nanospheres. The synthesized NiCo bimetallic catalysts exhibited high catalytic activity towards hydrogen production by the hydrolysis of ammonia borane (NH_3BH_3) and thereby differently substituted nitroaromatics with reducible functional groups was successfully reduced with good selectivity to the corresponding aminoarenes with good to excellent conversions within 2 hours (Scheme 20).

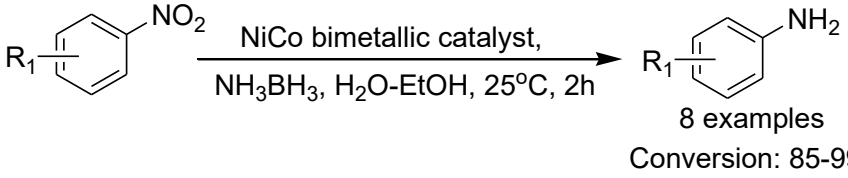

Scheme 20 Hydrogenation of functionalized nitrobenzene using NiCo bimetallic catalyst

Yuan *et al.*[10b] designed a non-noble metal-based nanoreactor by the high-temperature (700°C) carbonization of a resin polymer on the ZIF-67 surface. The resultant Co@ZDC@mC-700 nanocomposite comprised Co nanoparticles distributed on the ZIF-67-derived carbon framework (Co@ZDC) and shell comprised resin-derived mesoporous carbon (mc). The catalytic application of the synthesized material was tested to the reduction of nitroarenes in the presence of $N_2H_4 \cdot H_2O$ as the co-reductant (Scheme 21). Several functional groups were well tolerated with good to excellent conversions. In the case of *m*-nitroiodobenzene and *p*-nitroiodobenzene, slight dehalogenation was observed under the optimized reaction conditions. The Co@ZDC@mC-700 catalyst was successfully recovered and reused 6th cycles with a slight decrease in its catalytic efficiency.

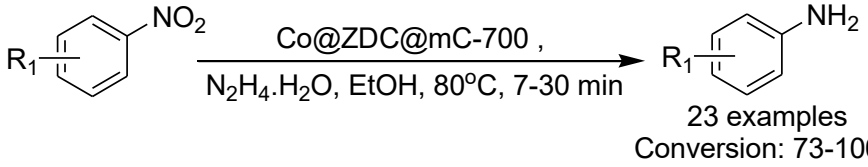

Scheme 21 Co@ZDC@mC-700 catalysed reduction of substituted nitrobenzenes

Plant mediated one-pot synthesis of Pd nanoparticles (Pd NPs) was developed using a plant extract from *Pulicaria odora* L. and $PdCl_2$ as the metal precursor under mild and green conditions by Enneiymy *et al.*[10c] The Pd NPs embedded by phytochemical resins obtained from the roots of *Pulicaria odora* L. and showed excellent catalytic activity for the chemoselective reduction of nitroarenes at room temperature in EtOH medium under H_2 pressure as the source of

hydrogen donor (Scheme 22). The catalyst was characterized by XRD, TEM, HRTEM, XPS, and BET techniques. The nanoparticles were easily recovered by filtration and reused seven times with marginal loss of its catalytic reactivity.

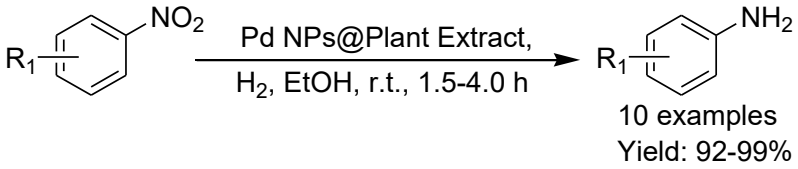

Scheme 22 Reduction of substituted nitrobenzenes using Pd NPs@Plant Extract

Mesoporous natural phosphate-supported palladium nanoparticles (Pd@NP)[10d] were synthesized by using the wetness impregnation method and characterized by various spectroscopic techniques. The crystalline size of the synthesized nanoparticles was 10.88 nm (based on the Scherrer equation). The prepared Pd@NP catalyst was successfully employed in the hydrogenation of 4-nitrophenol as a model substrate to the corresponding 4-aminophenol in the presence of $NaBH_4$ as a hydrogen source at room temperature (Scheme 23). Moreover, catalytic hydrogenation of various substituted nitroarenes was studied and monitored using gas chromatography as well as UV-visible spectroscopy. The synthesized catalyst exhibited a high catalytic activity upto the 4th runs with the extension of reaction time due to the agglomeration of Pd nanoparticles.

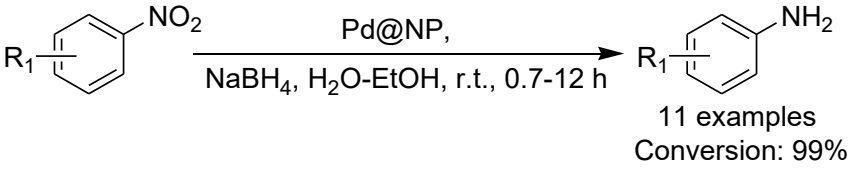

Scheme 23 Reduction of functionalized nitrobenzenes using Pd@NP

Wang *et al.*[10e] synthesized well-dispersed palladium nanoparticles (Pd NPs) stabilized on nanocrystalline Polyaniline (Pd@PANI) via a method that combined self-stabilized dispersion polymerization (SSDP) with camphor sulfonic acid ((+)-CSA) as a dopant. Fourier transform infrared (FTIR) spectroscopy, X-ray diffraction (XRD), Transmission electron microscopy (TEM), and X-ray photoelectron spectroscopy (XPS) techniques were used to characterize the nanoparticles. The catalytic activity of the Pd@PANI catalyst was evaluated through the reduction of various substituted nitroarenes to the related aminoarenes using $NaBH_4$ as a hydrogen source (Scheme 24). Polyaniline was not only a supporting reagent for palladium metal but also served as a nitrogen-containing ligand which synergistically enhanced the activity

of the catalyst. The catalyst was recycled and reused up to eight repeated cycles without deactivation.

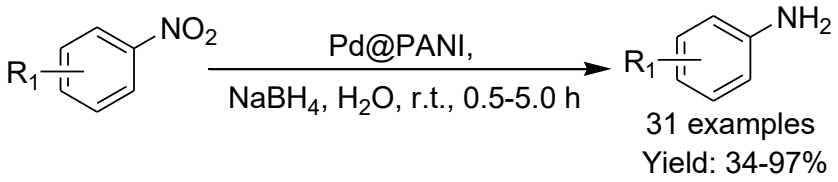

Scheme 24 Pd@PANI catalyzed reduction of functionalized nitrobenzenes

Sheng *et al.*[10f] developed highly dispersed Pt nanoparticles supported on ordered mesoporous carbon (CMK-3) modified with aqueous solutions of H_2PtCl_6 and 8-hydroxyquinoline (8-HQ) (Pt/CMK-3-HQ). The Pt/CMK-3-HQ was employed in the reduction of various substituted halogenated nitroarenes to the corresponding substituted haloanilines using hydrazine hydrate ($N_2H_4 \cdot H_2O$) as the co-reductant and exhibited high stability up to 20 catalytic cycles without loss in its catalytic efficiency (Scheme 25). The cooperation effect between Pt atoms and N species (from 8-HQ) in the structure of Pt/CMK-3-HQ promoted the heterolytic cleavage of $N_2H_4 \cdot H_2O$ to Pt-H^- / N-H^+ pairs and reduced the interaction between Pt atoms and halogen groups for activation of C-halogen bonds which attributed to the high catalytic activity as well as good chemoselectivity. Moreover, the Pt/CMK-3-HQ catalyst was readily recovered and reused without much loss in the catalytic efficiency.

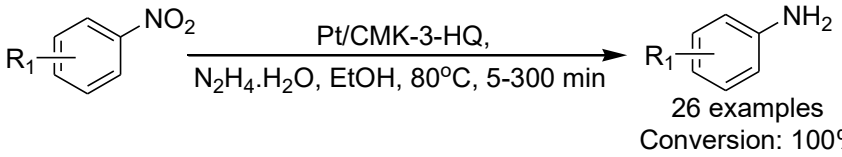

Scheme 25 Reduction of various halogenated nitroarenes using Pt/CMK-3-HQ catalyst

Graphitic carbon nitride nanosheets ($CNNS/rGO_{20}$) with nanostructured architectures were fabricated successfully by hydrothermal coassembly of carbon nitride nanosheets (CNNS) and graphene oxide (GO) followed by immobilization of Pd nanoparticles on CNNS/rGO hybrid by an impregnation method.[11a] The heterostructure ($CNNS/rGO_{20}$) provided higher dispersity of palladium as well as high surface area and thus providing much more active catalytic sites in the reduction of differently substituted aromatic as well as aliphatic nitro-compounds with high conversion and good selectivity in the presence of formic acid (FA) as the hydrogen donor

(Scheme 26). The excellent catalytic attribute of Pd-CNNS/rGO_{20} could be ascribed to the 3D architectures and synergetic interaction between CNNS and rGO.

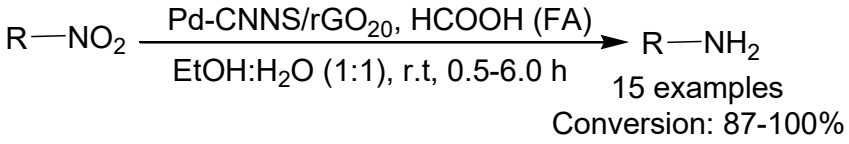

Scheme 26 Reduction of nitro-compounds using Pd-CNNS/rGO_{20} catalyst

Palladium nanoparticles (Pd NPs) supported by phosphine-functionalized hyper-cross-linked porous ionic copolymer (Pd@P(QP-TVP)) were developed through the free-radical copolymerization of quaternary phosphonium salt (QP) and tris(4-vinylphenyl) phosphine (TVP) followed by anion-exchange and chemical reduction method. The synthesized nanocatalyst featured a hierarchically porous structure, large surface area, amphiphilic surface wettability, high electron-donation effect of phosphine ligand, and strong interaction between Pd NPs and polymer scaffold. The catalytic applicability of Pd@P(QP-TVP) was demonstrated through the hydrogenation of various substituted nitroaromatics with H_2 as a hydrogen source in an aqueous medium (Scheme 27).[11b] The catalyst was highly stable and could be reused at least five runs without any loss of its efficiency.

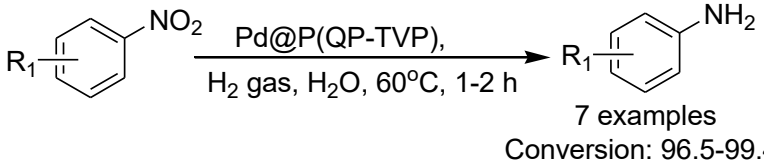

Scheme 27 Pd@P(QP-TVP) catalyzed hydrogenation of nitroaromatics using H_2 gas

Ruthenium-based nanocatalyst distributed on a carrier of glucose and melamine prepared by a simple in situ calcination method was successfully used for the hydrogenation of halogenated nitro-aromatics in the presence of H_2 gas as the hydrogen source in ethanolic medium (Scheme 28).[11c] Synthesized Ru nanoparticles were suitably dispersed on the nitrogen-doped carbon matrix (Ru/CN). Various halogenated functionalized nitroarenes were smoothly converted into the corresponding haloanilines with high conversion and good selectivity. The synergistic interaction between the active Ru metal and mixed N accelerated the dissociation of H_2 on Ru and enhanced the rate of the reaction. The catalyst was heterogeneous and successfully reused in the successive catalytic reactions without much depletion of its reactivity.

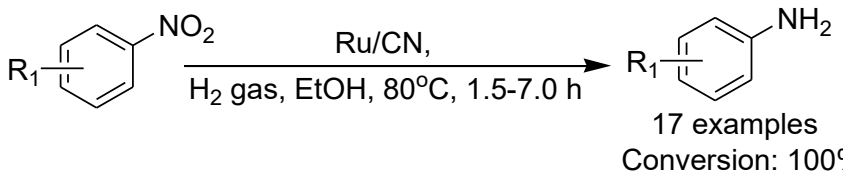

Scheme 28 Hydrogenation of nitroaromatics catalyzed by Ru/CN using H_2 gas

Thus the aforesaid concise account of the recent developments on the catalytic performance of various transition metal nanocatalysts for the reduction of nitroarenes with a plethora of catalysts, substrates, hydrogen sources as well as solvents has been presented to substantiate the urgency, necessity, and timeliness of the present investigation going to be described in the next section.

III. 3. Present investigation

III. 3.1. Background of the present investigation

Chemoselective reduction of nitroarenes bearing other reducible sensitive groups in the same molecule is one of the most challenging tasks to the researchers. To achieve this objective, several transition-metal based approaches including noble[6b,6c,6d,7b,7c,7d,8b,8d,8e,9a,9b,9c,9e,10c,10d,10e,10f,11a,11b,11c] and non-noble metals[6a,7a,8a,8c,9d,9f,10a,10b] employing H_2[6b,7b,7c,8b,9c,9d,9f,11b,11c] or other reducing agents[6a,6c,6d,7a,7d,8a,8e,9a,9b,9e,10a,10b,10e,10f,11a] were reported for the similar transformations during the last few years. Although the reported protocols have their merits but most of them also suffer from certain drawbacks such as use of expensive metal catalysts,[6b,6c,6d,7b,7c,7d,8b,8d,8e,9a,9b,9c,9e,10c,10d,10e,10f,11a,11b,11c] laborious methods for catalyst preparation,[6a,6b,7a,7b,7c,7d,8a,8c,8e,9a,9b,9c,9d,9e,9f,10a,10b,10f,11a,11b] pressurized hydrogen gas,[6b,7b,7c,8b,9c,9d,9f,11b,11c] poor selectivity,[6c,7a,8a,8c,9b,9e,11a] harsh reaction condition, [6b,7b,7c,8b,9c,9d,9f,11b,11c] high temperature,[6a,7b,8c,8e,9f] and prolonged reaction time.[6a,7a,7b,7c,8b,9d,9f,11a,11c] Therefore, to ensure the integrity for economic and environmental sustainability, organic transformations[12] using very simple and inexpensive catalytic system are extremely important to develop eco-friendly chemical processes due to cost-effectiveness, high atom efficiency, simplified isolation of product, easy recovery and recyclability of the catalysts.

Acacia Catechu (commonly known as "Khair") is an economically accessible as well as medicinally active plant that belongs to the Fabaceae family and is widely cultivated in Southern Asia, Malaysia, China, and India. *Acacia Catechu* consists of antioxidants such as catechin,

epicatechin, tannins, alkaloids, sugars, and other reducing molecules, which play a vital role due to its capping as well as stabilizing attributes for the production of NPs.[13] Therefore, water extract of the *Acacia Catechu* plant makes an alternative efficient platform for the synthesis of metallic nanoparticles from the viewpoint of eco-compatibility. Currently, iron-based catalysts have been attracted considerable interest because of their high abundance, cheapness, less toxicity, eco-friendliness and preferential alternative to the precious metal catalysts.[14] Inspired by these facts, we synthesized *Acacia Catechu*-assisted iron oxide nanoparticles (to be called as Fe_3O_4@Catechu hereafter) under the green condition without the involvement of any external reducing agents, pH treatment, toxic and hazardous reagents, organic solvents, high-temperature calcination, and rigorous experimental setup. The performance of the synthesized nanoparticles as an efficient and recyclable catalyst was explored towards the eco-friendly chemoselective reduction of nitroarenes under an ambient atmosphere in an aqueous medium in the presence of hydrazine hydrate as the source of hydrogen with the tolerance of various sensitive moieties.

III.3.2. Results and Discussion

III.3.2.1. Preparation of Fe_3O_4 NPs using natural resource:

The iron oxide NPs was synthesized via complete utilization of the natural resources, instead of chemical reagents to avoid wasteful dumping (Figure 1). *Acacia Catechu* (commonly known as "khair") was collected from the local market nearby Jadavpur University. The iron oxide nanoparticles were synthesized by direct mixing of $FeSO_4.7H_2O$ with the aqueous plant extract of *Acacia Catechu* at room temperature under ambient conditions. 2.0 g of *Acacia Catechu* was added into 100 mL of distilled water in a 250 ml Erlenmeyer flask and boiled for 30 minutes to obtain the aqueous extract. The color of the plant extract was red and filtered through a Whatman filter paper. In a 250 mL Erlenmeyer flask, 80 mL of the aqueous *Acacia Catechu* plant extract was mixed with 2.0g ferrous sulfate heptahydrate ($FeSO_4.7H_2O$) at room temperature under ambient atmosphere. The immediate appearance of the black color of the solution indicated the formation of iron oxide nanoparticles. The resulting iron oxide NPs were separated by centrifugation and the obtained black product was washed with MeOH and dried under vacuum.

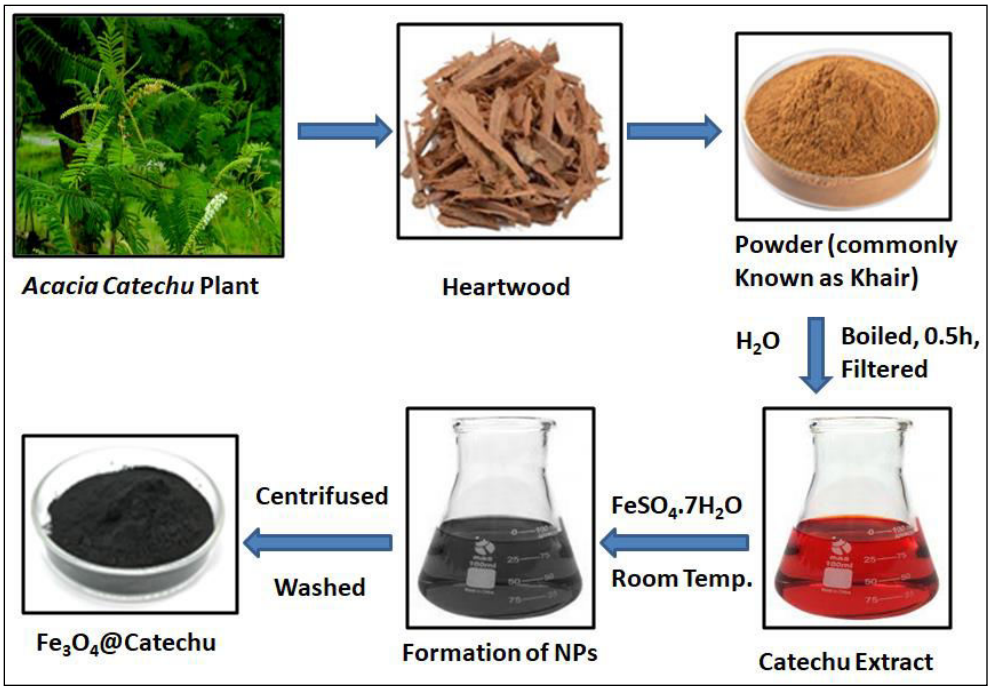

Figure 1 Schematic diagram for the biosynthesis of Fe_3O_4 NPs using plant extract of *Acacia Catechu*

III.3.2.2. Catalyst characterization:

Fourier transform infrared spectroscopy (FTIR) study: The active components of the plant extract responsible for the production of NPs were studied by the comparison of Fourier transform infrared spectroscopy (FTIR) of *Acacia Catechu* plant and Fe_3O_4@Catechu and presented in Figure 2. *Acacia catechu* showed the characteristic IR bands at 3321, 2929, 1634, 1435, and 1011 cm^{-1}. The intense broadband appeared at 3321 cm^{-1} due to the presence of phenolic –OH group and the absorption peak observed around 2929 cm^{-1} was related to the aliphatic –CH stretching. The peaks at 1634, 1435, and 1011 cm^{-1} in the FTIR spectrum of *Acacia Catechu* corresponded to vibrational stretching modes of carbonyl bond, C=C bond in the aromatic ring, and tensile vibration of the C-O-C bond respectively. It has been observed that the broadband at 3321 cm^{-1} in *Acacia Catechu* was found to be narrowed and appeared at a lower frequency around 3204 cm^{-1} in the FTIR spectrum of Fe_3O_4@Catechu. The appearance of a new signal at 615 cm^{-1} in Fe_3O_4@Catechu was assigned to the Fe-O bond which was absent in the IR spectrum of *Acacia Catechu*.[15] On the other hand, the IR bands at 3026, 1656, 1428, and 1069 in the Fe_3O_4@Catechu confirmed the presence of similar phytoconstituents in iron oxide nanoparticles. This observation suggested a good indication for the encapsulation as well as

stabilization of iron oxide nanoparticles by the biomolecules present in plant extract of *Acacia Catechu*.

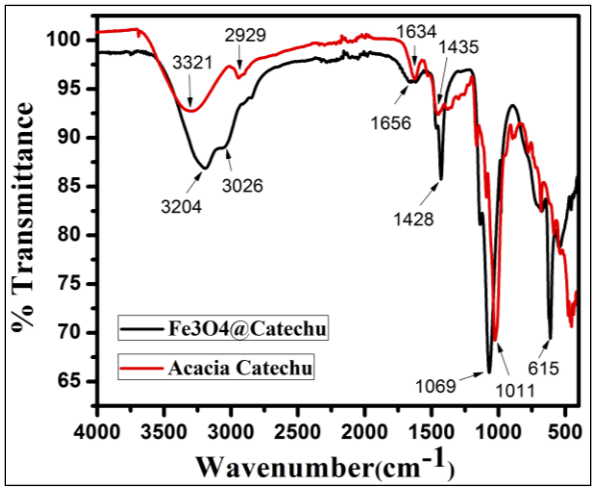

Figure 2 FTIR spectrum of *Acacia Catechu* and Fe_3O_4@Catechu

X-ray diffraction (XRD) analysis: XRD analysis of the biosynthesized Fe_3O_4 nanoparticles were recorded and presented in Figure 3. The XRD diffraction peaks of the *Acacia Catechu* assisted Fe_3O_4 nanoparticles observed at $2\theta = 30.2^o$ (2 2 0), 35.3^o (3 1 1), 42.8^o (4 0 0), 56.8^o (5 1 1), and 62.1^o (4 4 0) attributed to the crystalline nature of Fe_3O_4 NPs and the diffraction patterns were well matched with reported literature[16] as well as consistent with JCPDS Card No. 19-0629. The occurrence of extra peaks in the XRD spectra might be due to the crystallization of other phyto-constituents on the surfaces of the Fe_3O_4 NPs which concurred with the earlier literature reports for the synthesis of Fe_3O_4 NPs@*Tridax procumbens* leaf extract,[17] Ag NPs@*Areca catechu* leaf extract,[18] and Zn NPs@*Ziziphora clinopodioides* leaf extract.[19]

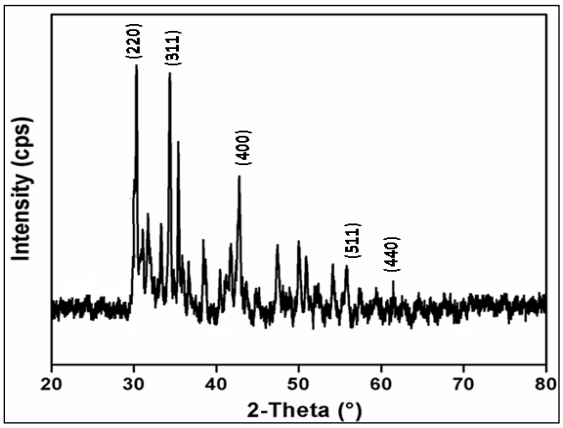

Figure 3 XRD analysis of Fe_3O_4@Catechu

Scanning Electron Microscopy (SEM), Energy Dispersive X-ray Spectroscopy (EDX), and elemental mapping analysis: To establish the shape and morphological features of Fe_3O_4@Catechu nanocatalyst, scanning electron microscopic images were recorded and presented in Figure 4a. It has been observed that the morphology of the nanocatalyst is near to be spherical. EDX (Energy Dispersive X-ray Spectroscopy) analysis provides additional information on the elementary composition of the synthesized Fe_3O_4@Catechu nanocatalyst (Figure 4b). The synthesized nanocatalyst contains elements of carbon (45.5%), oxygen (36.9%), sulfur (5.0%), and iron (12.7%). The EDX spectra also disclosed signals at around 0.8, 6.4, and 7.1 keV, which were attributed to the binding energies of the iron[20] and confirmed the formation of Fe_3O_4@Catechu nanocatalyst. The presence of other elements (C, O, and S) further supported the effective formation of the Fe_3O_4 NPs through the capping by the phyto-constituents present in the *Acacia Catechu* plant extract. Moreover, the elemental mapping experiment showed the spatial distribution of each element which demonstrated that the distributions of C, O, S, and Fe elements are well arranged in the structure of synthesized nanocatalyst (Figure 4c).

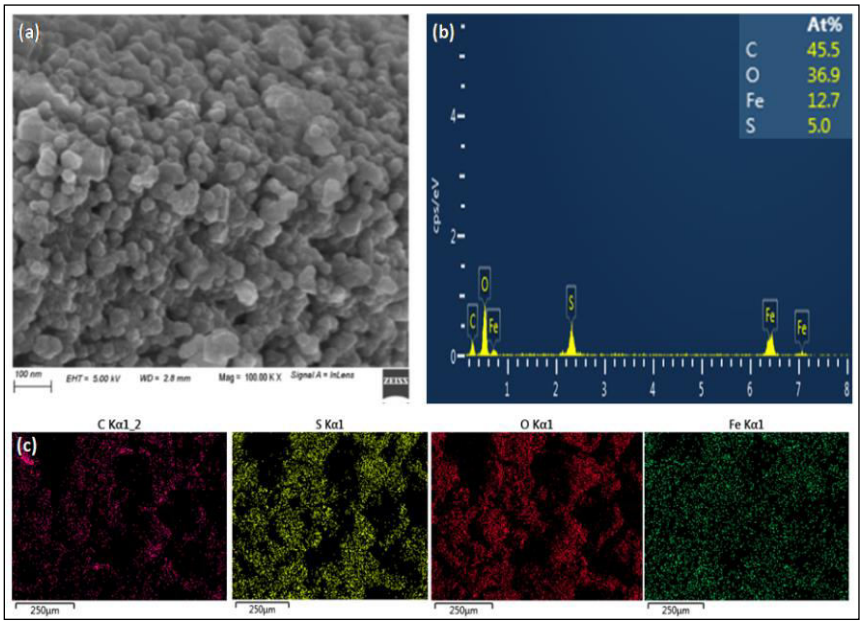

Figure 4 (a) SEM images, (b) EDX spectra, and (c) elemental mapping images of Fe_3O_4@Catechu.

Transmission Electron Microscopy (TEM) analysis: The morphology (Figure 5a) and particle size distribution histogram (Figure 5b) of the synthesized Fe_3O_4@Catechu was further evaluated

by Transmission Electron Microscopic (TEM) images. The TEM micrographs confirmed that the average particle size of the catechu-assisted iron oxide nanoparticles was 16.4 nm with a spherical shape inside the plant extract and they exhibited good catalytic efficiency as well as remarkable stability without further aggregation.

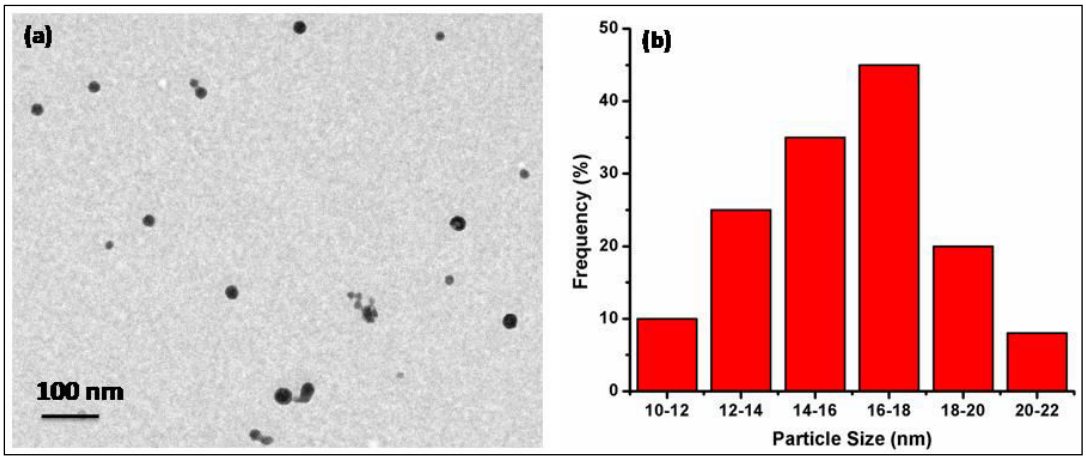

Figure 5 (a) TEM images and (b) particle size distribution histogram of Fe_3O_4@Catechu.

X-ray photoelectron spectroscopy (XPS) analysis: Fe_3O_4@Catechu nanocatalyst was further characterized by XPS analysis to ensure the oxidation state of iron (Figure 6). It is well known that iron in Fe_3O_4 comprises two oxidation states, namely Fe^{2+} which is octahedrally coordinated, and Fe^{3+} which is also distributed over both tetrahedral, as well as octahedral sites, and the ideal ratio of Fe^{2+}/Fe^{3+} is 1:2. It is also well known that with increasing the valence state, the binding energy of the metallic species increases. The wide scan spectra of Fe 2p level showed the binding energy at 708.6 eV and 721.9 eV is attributed for Fe(II)$2p_{3/2}$ and Fe(II)$2p_{1/2}$ for octahedral species respectively, whereas Fe(III)$2p_{3/2}$ and Fe(III)$2p_{1/2}$ for tetrahedral species is also found with a binding energy of 711.4 eV and 726.8 eV respectively. The absorption peak with the binding energy of 711.7 eV and 727.1 eV is assigned for Fe(III)$2p_{3/2}$ and Fe(III)$2p_{1/2}$ with octahedral coordination respectively. These results are comparable with the reported literature.[21] It has been observed that the ratio of Fe^{2+}, Oh/(Fe^{3+}, Td + Fe^{3+}, Oh) was 0.497 and 0.496 for $2p_{3/2}$ and $2p_{1/2}$ transition respectively, which is very close to the ideal value of 0.5 expected from the stoichiometry of Fe_3O_4.[22]

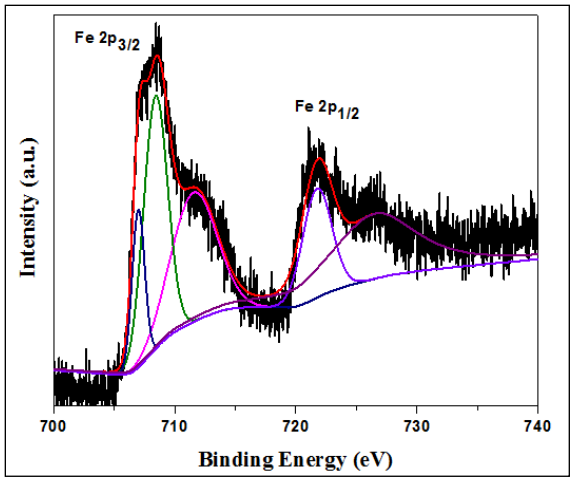

Figure 6 XPS analysis of Fe_3O_4@Catechu

N_2 adsorption-desorption isotherm: To get an idea about the specific surface area and porosity of the synthesized Fe_3O_4@Catechu nanocatalyst, Brunauer-Emmett-Teller (BET) method with N_2 adsorption-desorption isotherms studies were carried out. The results were presented in Figure 7. The isotherm displayed type IV characteristics (according to the IUPAC classification) with a small hysteresis loop starting from at a relative P/P_0 0.5 to 1.0, which demonstrated the synthesized nanocatalyst was mesoporous in nature (Figure 7a). The specific surface area was calculated using the BET equation and it was found to be 55 m^2g^{-1}. The corresponding pore size distribution (Figure 7b) was centered around 15.2 nm (calculated from the desorption part) which also confirmed the mesoporous behavior of the nanocatalyst.

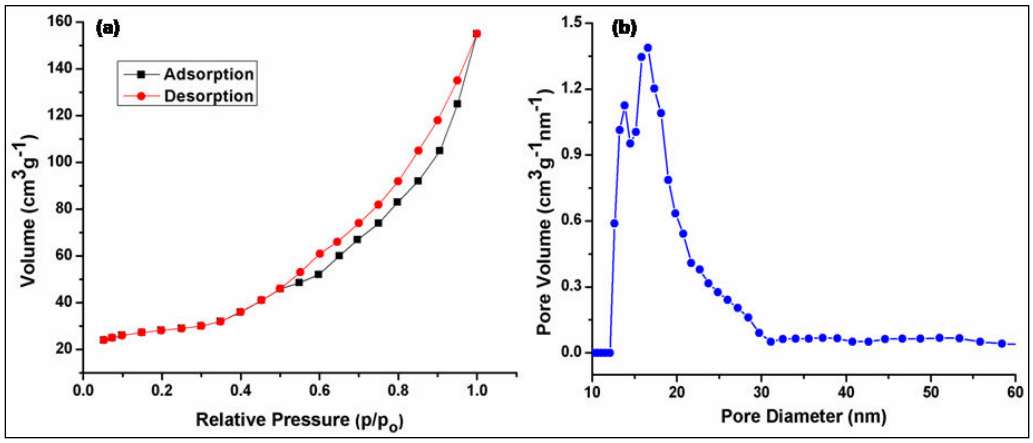

Figure 7 (a) N_2 adsorption-desorption isotherm and (b) pore size distribution of Fe_3O_4@Catechu.

III.3.2.3. Catalytic activity of Fe_3O_4@Catechu:

The catalytic efficiency of Fe_3O_4@Catechu was examined using *p*-nitrotoluene **1a** as a model substrate in the presence of $N_2H_4.H_2O$ as the source of hydrogen at different temperatures as well as solvents under ambient atmosphere to obtain the optimum condition. The results are presented in Table 1.

Table 1 Optimization of Fe_3O_4@Catechu catalyzed reductive organic transformation[a]

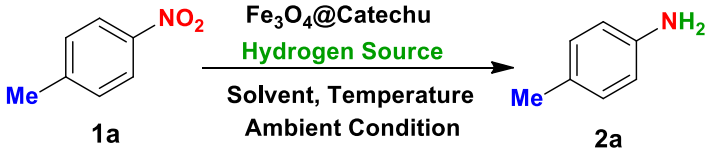

Entry	Solvent (mL)	Catalyst (mol %)	Hydrogen Source (mmol)	Temperature (^oC)	Time (hrs)	Yield[b] (%)
1	H_2O	-	-	60^oC	5.0	-
2	H_2O	-	$N_2H_4.H_2O$	60^oC	5.0	-
3	H_2O	2	-	60^oC	5.0	-
4	H_2O	4	$N_2H_4.H_2O$	RT	4.0	69
5	H_2O	4	$N_2H_4.H_2O$	60^oC	1.5	92
6	H_2O	6	$N_2H_4.H_2O$	60^oC	1.5	93
7	EtOH	4	$N_2H_4.H_2O$	60^oC	2.0	80
8	CH_3CN	4	$N_2H_4.H_2O$	60^oC	4.0	67
9	DMSO	4	$N_2H_4.H_2O$	60^oC	4.0	64
10	DMF	4	$N_2H_4.H_2O$	60^oC	4.0	58
11	DCM	4	$N_2H_4.H_2O$	Reflux	4.0	37
12	Toluene	4	$N_2H_4.H_2O$	80^oC	4.0	42

[a]Reaction conditions: **1a** (1 mmol), hydrogen source (3 mmol), catalyst and temperature (as indicated), solvent (2 mL) under ambient condition. [b]Isolated yield.

Before the process of optimization, the efficacy of Fe_3O_4@Catechu was compared in the presence of different types of solvents. Organic transformations in aqueous medium using nonhazardous and inexpensive catalysts have drawn considerable interest because water is the most abundant, non-toxic, environmentally acceptable, and economically affordable reaction

medium compared to other organic solvents.[23] Therefore, the reduction reaction was initially carried out in an aqueous medium in the absence of both Fe_3O_4@Catechu and hydrogen source, the unreacted substrate was isolated intact (entry 1). Similarly, the reaction neither took place in the presence of $N_2H_4.H_2O$ alone (entry 2) nor with Fe_3O_4@Catechu alone (entry 3). Interestingly, a moderate amount of *p*-toluidine **2a** was obtained when the reaction was carried out in presence of both Fe_3O_4@Catechu (2 mol%) as a catalyst and $N_2H_4.H_2O$ as the hydrogen source at room temperature (entry 4). Surprisingly, when Fe_3O_4@Catechu (4 mol%) as a catalyst and $N_2H_4.H_2O$ as the co-reductant were used in an aqueous medium, the yield of the reaction was significantly increased to 92% within 1.5h at 60^oC (entry 5). Excess catalyst beyond this proportion did not show further increase in the substrate conversion and the yield of the reaction remained more or less the same (entry 6). The aforesaid reductive transformation did neither occur with catechu extract alone nor with iron salt without support. Thus the importance of the co-existence of both catalyst and co-reductant for this reductive organic transformation was conclusively established. Next, the investigations for the performance of different solvents such as EtOH, CH_3CN, DMSO, DMF, DCM, and toluene were also tested. Among them, EtOH (entry 7), CH_3CN (entry 8), and DMSO (entry 9) afforded moderate yield of the desired product, but the reaction was less responsive in DMF, DCM, and toluene solvent even under reflux and a longer period of reaction time (entries 10-12). It is noteworthy that the universally green, environmentally benign, economically affordable solvent, namely, water, has come out as the best choice as a reaction medium for this reaction.

Next, different kinds of hydrogen sources such as $NaBH_4$, HCOOH, $HCOONH_4$, $C_6H_{12}O_6$ (glucose), and CH_4N_2S (thiourea) were also examined to further improving the catalytic performance of Fe_3O_4@Catechu (Figure 8). In this comparative study, $N_2H_4.H_2O$ was found to be the most potent hydrogen source in this reductive transformation. It is important to note that $N_2H_4.H_2O$ acts as a hydrogen donor which produces only N_2 as a by-product and is easily available, inexpensive, and easy to handle.[24] Therefore, the condition, as delineated in entry 5, has been chosen as the optimized condition for further studies. Importantly, no inert atmosphere was required for the reaction described in Table 1 in contrast to most of the methods involving metal nanocatalysts.

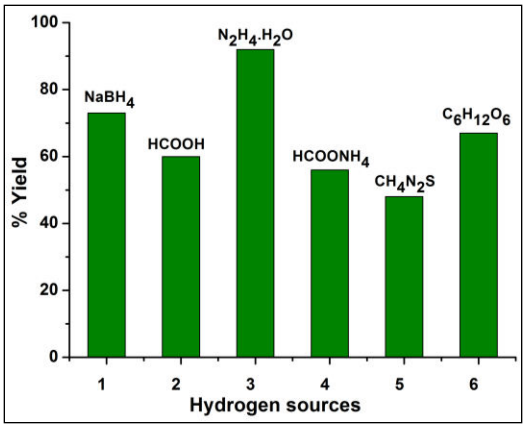

Figure 8 Effect of hydrogen sources using **1a** (1 mmol), Fe_3O_4@Catechu (4 mol%), hydrogen source (3 mmol), water (2 mL) at 60°C under ambient condition; % of yield was the isolated yield of **2a.**

To investigate the scope of the reduction process, various structurally functionalized nitroaromatics were subjected to the reduction in the presence of $N_2H_4.H_2O$ as a hydrogen source and Fe_3O_4@Catechu as the eco-friendly catalyst (Scheme 1). The outcomes are presented in Table 2.

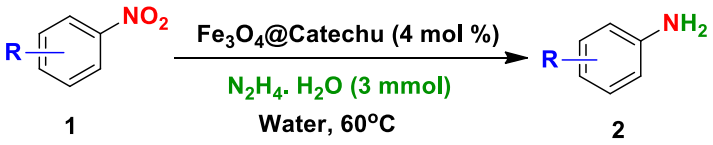

Scheme 1 Reduction of nitroarenes (**1**) in aqueous medium using Fe_3O_4@Catechu as an eco-friendly catalyst

As noted in Table 2, a variety of diverse nitroarenes with different electronic and steric features were smoothly converted into the corresponding amines in good to excellent yield. Nitrobenzene as well as nitroarenes bearing electron-donating substituents was successfully converted to the amines (**2a-2d)** in excellent yield (**entries 1-4**). Interestingly, halogenated nitroaromatics **(1e-1h)** were also efficiently reduced to halogenated anilines (**entries 5-8**), which are commonly used as precursors for agrochemicals, with no discernible dehalogenation and formation of biphenyl compounds through the sp^2-sp^2 coupling, which was previously reported in several hydrogenation procedures. Importantly, the reduction of amino-functionalized nitroarenes **(1i-1k)** smoothly produced the corresponding phenylenediamines **(2i-2k)** in excellent yield without the occurrence of any side product (**entries 9-11**).

Table 2 Fe_3O_4@Catechu catalyzed reduction of diversely functionalized nitroarenes[a]

Entry	Substrate	Product	Time (hrs)	Yield (%)[a]
Reduction of nitroarenes bearing electron-donating substituents				
1	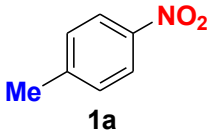 1a	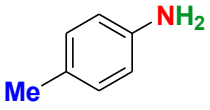 2a	1.5	92
2	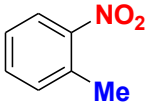 1b	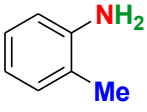 2b	1.5	90
3	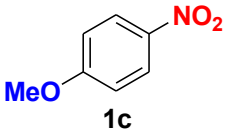 1c	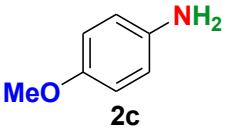 2c	1.5	91
4	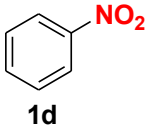 1d	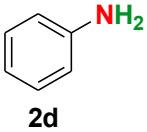 2d	1.5	90
Reduction of halogenated nitroarenes				
5	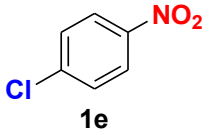 1e	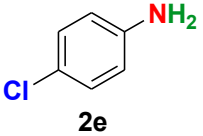 2e	1.0	88
6	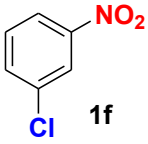 1f	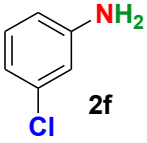 2f	1.5	86
7	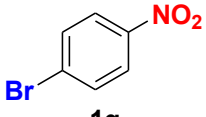 1g	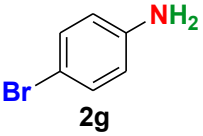 2g	1.0	89
8	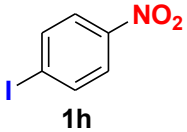 1h	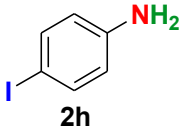 2h	1.0	87

Synthesis of multi-aminoarenes				
9	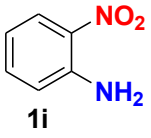 1i	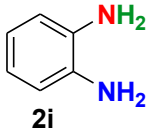 2i	1.0	92
10	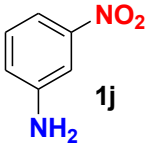 1j	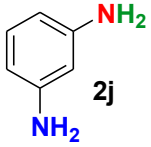 2j	1.0	90
11	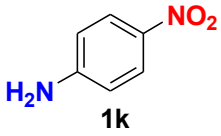 1k	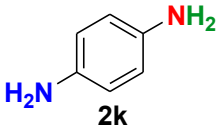 2k	1.0	91
12	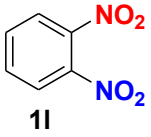 1l	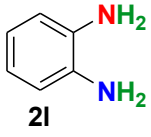 2l	1.0	94
13	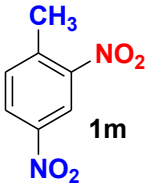 1m	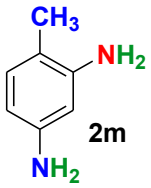 2m	1.5	93
14	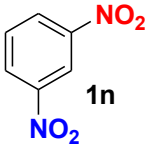 1n	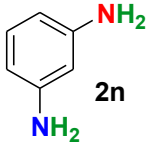 2n	1.0	93
Reduction of nitrophenols				
15	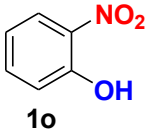 1o	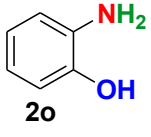 2o	1.5	86
16	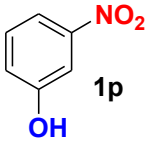 1p	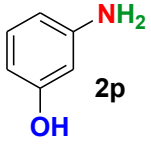 2p	1.5	88

17	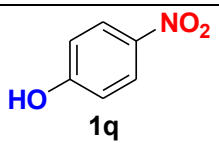 1q	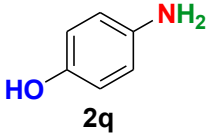 2q	1.5	89
Reduction of nitroarenes with non-reducible groups				
18	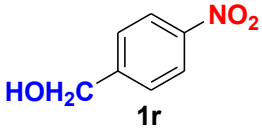 1r	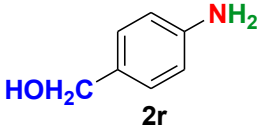 2r	2.0	87
19	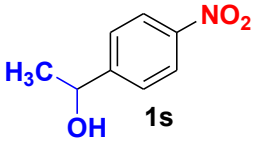 1s	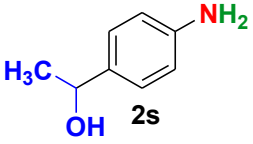 2s	2.0	88
Chemoselective nitro reductions with reducible and hydrolysable groups				
20	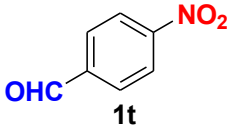 1t	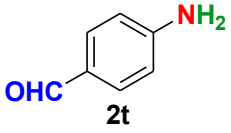 2t	1.5	90
21	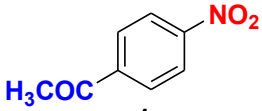 1u	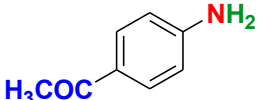 2u	1.5	89
22	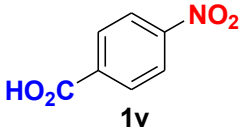 1v	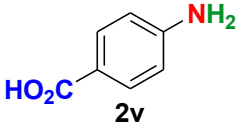 2v	2.0	87
23	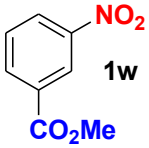 1w	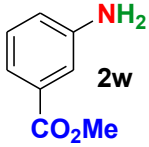 2w	1.0	87
24	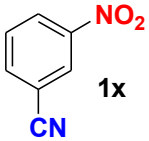 1x	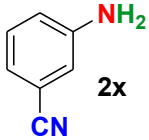 2x	1.0	89

Reductions of nitroarenes with highly vulnerable moieties				
25	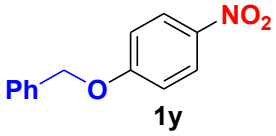 1y	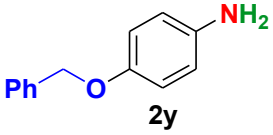 2y	2.0	87
26	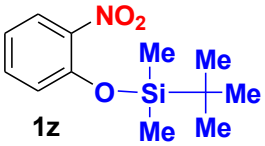 1z	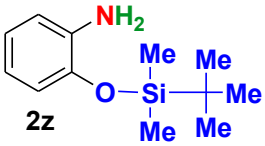 2z	2.0	85
Reduction of polynuclear aromatic and heterocyclic nitroarenes				
27	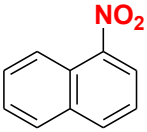 1za	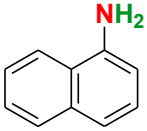 2za	1.5	88
28	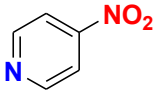 1zb	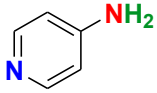 2zb	1.0	90
29	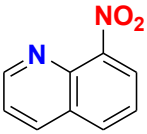 1zc	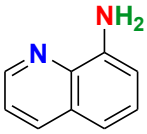 2zc	1.0	92

[a]Reaction conditions: **1a** (1.0 mmol), Fe_3O_4@Catechu (4 mol%), $N_2H_4.H_2O$ (3.0 mmol), water (2 mL) at 60°C for indicated time under ambient condition. The yield of the isolated pure product is fully characterized spectroscopically.

Similar multi-amino arenes **(2l-2n)** were obtained by the reduction of corresponding nitroaromatics in excellent yield (**entries 12-14**), which are important intermediates in the dyes industries. Notably, phenolic –OH group present at *ortho*-/*meta*-/*para*-position of the aromatic ring was not affected and produced the corresponding aminophenol **(2o-2q)** with high yield without much aerial oxidation of the reduced product (**entries 15-17**). Nitrophenols belong to the

group of major organic pollutants found in wastewater from industrial and agricultural origins. Hence, the present sustainable protocol bears the promise of being a potential method for wastewater treatment. Nitroaromatics with non-reducible groups such as benzylic primary **1r** as well as secondary alcohols **1s** were also compatible and desired products were formed in 87% and 88% yield respectively (**entries 18, 19**).

Next, we investigated the chemoselectivity of the present protocol for the reduction of nitroarenes in the presence of other reducible functional groups. Remarkable survival of the formyl group, which is highly susceptible to aerial oxidation as well as highly responsive towards reductive transformations, was noted in this aqueous protocol (entry **20**). The ketomethyl moiety in nitroarene **1u** was also unaffected during the present reaction where the aminoketone **2u** was obtained as the product in good yield without any self-condensation leading to Schiff's base (entry **21**). *p*-Nitrobenzoic acid **1v** was reduced to *p*-aminobenzoic acid **2v** in 87% yield (entry **22**) without affecting the carboxylic acid group. Notably, methoxycarbonyl moiety also remained intact during the present reductive transformation where the corresponding aminoester **2w** was obtained in excellent yield (entry **23**). The remarkable survival of acid-sensitive hydrolyzable as well as reducible functional group –CN was noted in this aqueous protocol, where the corresponding product **2x** was obtained with 89% yield (entry **24**). The survival of -CN was confirmed by the signal at δ 119.2 (specific for –CN) in the ^{13}C-NMR spectrum of the reduced product **2x**. This is an immensely important and additional attribute of the said protocol in contrast to several earlier literature reports[8a,8c,9a,9b,9e,10c,10d] where no such chemoselectivity was observed. Interestingly, highly vulnerable moieties like O-benzyl and O-silyl were also remained unaffected under the aforesaid optimized reaction condition and produced the reduction products **2y** and **2z** with 87% and 85% yield respectively (**entries 25, 26**). It is extremely surprising to note that this is not commonly observed in the recent literatures.[6a-6c, 7a-7c,8a-8d,9a,9b,9d,10a-10c,11a]

The nitro groups in the polynuclear aromatic, such as 1-nitronaphthalene (**1za**) as well as heterocyclic systems, such as 4-nitropyridine (**1zb**) and 8-nitroquinoline (**1zc**), were also efficiently reduced to their corresponding amines in good yields (entries **27**-**29**). Notably, heterocyclic moiety remained unaffected in this protocol, hence **2zb** and **2zc** was obtained in higher yield which is not observed in many of the reported protocols.[6b,6d,7d,8a,8b,8d,9a,9b,9d,9e,10d]

Gram Scale Applicability:

To further explore the synthetic scalability as well as the practical utility of our newly developed biogenic-approach based eco-friendly catalytic system, a gram scale reaction of nitroaromatics decorated with the most challenging reducible and hydrolyzable functional groups was performed (Scheme 2). The outcomes were almost similar to those of the small scale reactions.

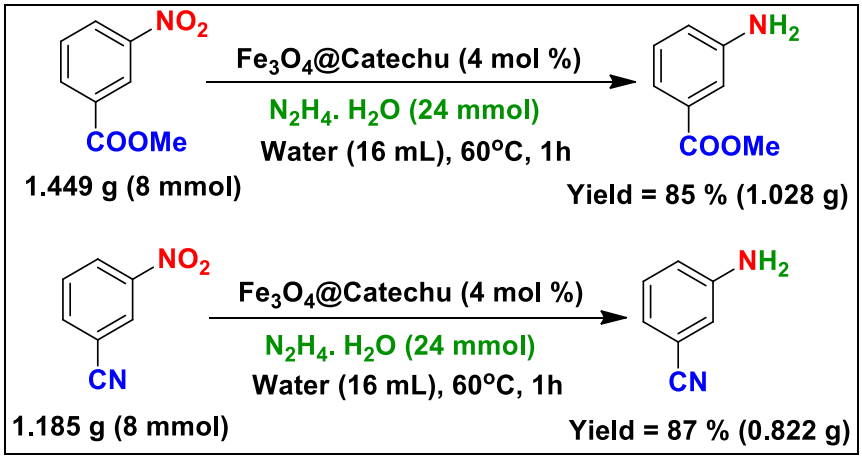

Scheme 2 Gram scale reaction of sensitive nitroarenes to demonstrate the practicability as well as chemoselectivity

Reusability of Fe_3O_4@Catechu:

The recovery, as well as recyclability of the catalyst, is very essential to meet the criteria of "Green and Sustainable Chemistry". Therefore, the recycling experiment was performed using *p*-nitrotoluene **1a** (1 mmol), $N_2H_4.H_2O$ (3 mmol), Fe_3O_4@Catechu (4 mol%), water (2 mL) at 60°C under ambient condition. After the completion of the reaction, the crude product was simply extracted with ethyl acetate (an eco-compatible solvent) and the catalyst was separated by centrifugation and it was washed repeatedly with MeOH and dried before reuse. The study revealed that the catalytic activity of Fe_3O_4@Catechu remained mostly unaltered throughout five successive reactions and a little variation of yield was observed (Figure 9a). Moreover, the stability of the recycled catalyst was also established by using FTIR (Figure 9b), SEM (Figure 9c) and TEM (Figure 9d) analysis, and no significant changes were observed.

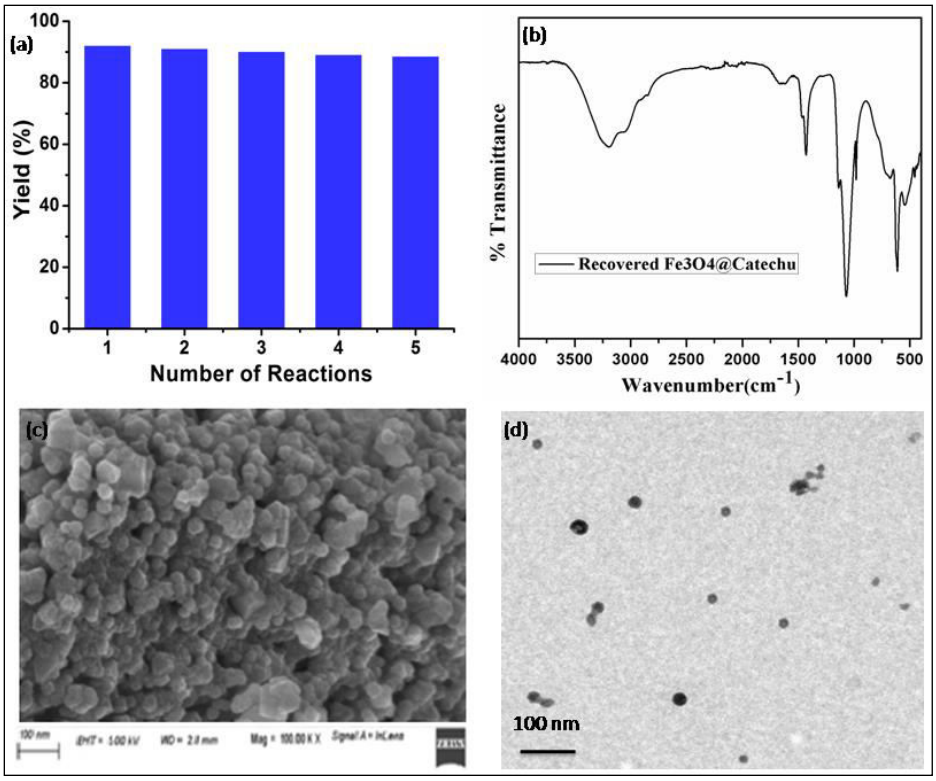

Figure 9 (a) Recycling study of Fe_3O_4@Catechu, (b) FTIR of Fe_3O_4@Catechu (after recycled five times), (c) SEM image of Fe_3O_4@Catechu (after recycled five times), (d) TEM image of Fe_3O_4@Catechu (after recycled five times).

"Heterogeneity (Sheldon's test)"of Fe_3O_4@Catechu:

Furthermore, Sheldon's test[25] of Fe_3O_4@Catechu was carried out to evaluate the heterogeneity of the catalyst in this reductive transformation using *p*-nitrotoluene (**1a)** as the substrate (Figure 10). After 45 minutes of the reaction when 58% conversion of the substrate was noted, the catalyst was separated by centrifugation and the "catalyst-free" filtrate was then kept under identical reaction conditions. It was observed that there was no further formation of **2a** and the extent of conversion of **1a** remained constant throughout the process. This study indicated that practically no soluble catalytically active species was present in the filtrate and the leaching of the catalyst during the reaction was extremely minimized. Hence, the heterogeneity of Fe_3O_4@Catechu was conclusively proved.

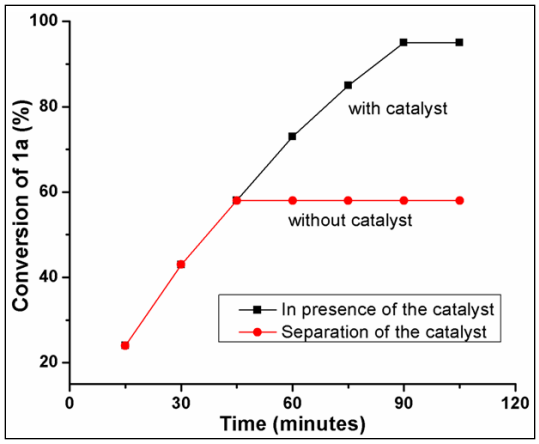

Figure 10 Heterogeneity test of Fe_3O_4@Catechu nanocatalyst using **1a** (1 mmol), Fe_3O_4@Catechu (4 mol%), $N_2H_4.H_2O$ (3 mmol), water (2 mL) at 60°C under ambient condition**.**

III. 4. Conclusion:

An eco-friendly method for the synthesis of highly stable non-noble magnetite (Fe_3O_4) nanoparticles under ambient conditions using natural feedstock as a capping as well as a stabilizing agent without conventional treatments fulfilling the special requirement of pH, high-temperature calcination, and rigorous experimental setup has been developed. This newly developed sustainable catalytic system was suitable for the chemoselective reduction of nitroaromatics under an ambient atmosphere in an aqueous medium. Chemically susceptible motifs like benzyloxy, t-butyldimethylsilyloxy, alkoxycarbonyl, formyl, oxo, keto, carboxylic acid, chloro, bromo, iodo and cyano were well tolerated during the reaction. Therefore, the present study has come out with greater merits and wider applicability compared to many earlier reports. Thus, a sustainable catalytic system has been developed with specific features including low preparation cost, high stability, unique reactivity, efficient recovery, and good recyclability and tolerance of various sensitive moieties during the reaction.

III.5. Experimental Section:

Materials and Instrumentation:

All reactants were purchased from Sigma Aldrich, SRL, AVRA Chemicals, Alfa-aesar, Spectrochem, and SDFCL and used as received without further purification. Melting points were determined in open capillary on electrical bath which is uncorrected. ^1H and ^{13}C NMR spectra

were obtained on a Bruker-300 spectrometer (300 MHz) and JEOL Spectrometer (400 MHz) in $CDCl_3$ and DMSO-d_6 solutions with TMS as an internal reference. FTIR spectrums were done in Perkin-Elmer Spectrum Version 10.4.1. XRD data of the powder sample were obtained in transmission mode using a Bruker D2 Phaser X-ray diffractometer (30 kV, 10 mA) using Cu-Kα (λ = 1.5406 Å) radiation. Field Emission Scanning Electron Microscopy (FE-SEM) images were recorded with a Zeiss (Zemini) scanning electron microscope. Transmission electron microscopic images were collected on a JEOL 2010 TEM operated at 200 kV. Chemical states of the heterogeneous material were determined by X-ray photoelectron spectroscopy (XPS) using a PHI 5000 (versa Probe II, FEI Inc). The specific surface area and porosity of the catalyst were characterized by the Brunauer-Emmett-Teller (BET) method with N_2 adsorption-desorption isotherms, measured at 77 K using Quantachrome Autosorb® iQ-MP / iQ-XR. Column chromatography was performed on silica gel (60–120 mesh) from SRL, India. Thin layer chromatographic separations were performed on pre-coated silica gel plates using silica gel G for TLC (E. Merck).

General procedure for the reduction of nitroaromatics in aqueous medium using Fe_3O_4@Catechu as an eco-friendly catalyst:

To a stirred suspension of appropriate nitroaromatics **1** (1.0 mmol) in 2 mL water, Fe_3O_4@Catechu (4 mol%) was added followed by hydrazine hydrate (3.0 mmol). The reaction mixture was stirred for the required period at 60^{o}C. The progress of the reaction was monitored by thin-layer chromatography (TLC). After completion of the reaction, the reaction mixture was cooled to room temperature, ethyl acetate (15 mL) was added to dissolve the product and the catalyst was separated simply by centrifugation. The catalyst was washed with MeOH (3×5 mL) and dried for reuse. The aqueous reaction mixture was repeatedly extracted with ethyl acetate (3×5 mL). The combined organic extracts were washed with water (3× 10 mL) and dried over anhydrous Na_2SO_4. The crude product **2** was obtained by removal of the solvent under reduced pressure which was further purified by column chromatography on a short column of silica gel (60-120 mesh) using 2-10% ethyl acetate-hexane as eluent.

Spectral and analytical data of the compounds:

4-toluidine (2a)[6c]: Yield: 92%; Brown solid; Mp 44-45°C (Lit.[26] 44-46°C); ^{1}H NMR ($CDCl_3$, 300MHz); δ (ppm): 7.01 (2H, d, *J* = 9.0 Hz); 6.64 (2H, d, *J* = 9.0 Hz); 3.53 (2H, br.s); 2.29 (3H, s); ^{13}C NMR ($CDCl_3$, 75 MHz); δ (ppm): 143.9, 129.8, 127.8, 115.4, 20.5.

2-toluidine (2b)[7b]: Yield: 90%; Yellow liquid; ^{1}H NMR ($CDCl_3$, 300MHz); δ (ppm): 7.15-7.19 (2H, m); 6.85 (1H, t, *J* = 6.0 Hz); 6.76 (1H, d, *J* = 9.0 Hz); 3.65 (2H, br.s); 2.27 (3H, s); ^{13}C NMR ($CDCl_3$, 75 MHz); δ (ppm): 144.7, 130.6, 127.1, 122.4, 118.7, 115.1, 17.4.

4-aminoanisole (2c)[7a]: Yield: 91%; White solid; Mp 55-57°C (Lit.[26] 57-58°C); ^{1}H NMR ($CDCl_3$, 300MHz); δ (ppm): 7.18 (2H, d, *J* = 8.3 Hz); 6.60 (2H, d, *J* = 8.3 Hz); 3.79 (3H, s); 3.34 (2H, br.s); 3.75 (3H, s); ^{13}C NMR ($CDCl_3$, 75 MHz); δ (ppm): 150.3, 141.3, 116.9, 114.2, 55.3.

Aniline (2d)[6c]: Yield: 90%; Yellow liquid; ^{1}H NMR ($CDCl_3$, 300MHz); δ (ppm): 7.15 (2H, t, *J* = 7.8 Hz); 6.75 (1H, t, *J* = 7.3 Hz); 6.67 (2H, d, *J* = 7.6 Hz); 3.79 (2H, br.s); ^{13}C NMR ($CDCl_3$, 75 MHz); δ (ppm): 146.4, 129.4, 118.6, 115.2.

4-chloroaniline (2e)[7a]: Yield: 88%; Grey solid; Mp 72-73°C (Lit.[26] 70-71°C); ^{1}H NMR ($CDCl_3$, 300MHz); δ (ppm): 7.03 (2H, d, *J* = 8.6 Hz); 6.48 (2H, d, *J* = 8.6 Hz); 4.37 (2H, br.s); ^{13}C NMR ($CDCl_3$, 75 MHz); δ (ppm): 144.7, 128.8, 122.9, 115.2.

3-chloroaniline (2f)[7a]: Yield: 86%; colourless liquid; ^{1}H NMR ($CDCl_3$, 300MHz); δ (ppm): 7.05 (1H, t, *J* = 7.5 Hz); 6.80 (1H, s); 6.71 (1H, d, *J* = 8.1 Hz); 6.51-6.65 (1H, m); 3.79 (2H, br.s); ^{13}C NMR ($CDCl_3$, 75 MHz); δ (ppm): 147.7, 134.8, 130.4, 118.5, 114.9, 113.3.

4-bromoaniline (2g)[7a]: Yield: 89%; Off-white solid; Mp 65-67°C (Lit.[26] 66-67°C); ^{1}H NMR ($CDCl_3$, 300MHz); δ (ppm): 7.21 (2H, d, *J* = 8.5 Hz); 6.49 (2H, d, *J* = 8.5 Hz); 3.41 (2H, br.s); ^{13}C NMR ($CDCl_3$, 75 MHz); δ (ppm): 146.1, 131.5, 115.9, 119.1.

4-iodoaniline (2h)[7c]: Yield: 87%; White solid; Mp 60-63°C; ^{1}H NMR ($CDCl_3$, 300MHz); δ (ppm): 7.40 (2H, d, *J* = 8.7 Hz); 6.47 (2H, d, *J* = 8.7 Hz); ^{13}C NMR ($CDCl_3$, 75 MHz); δ (ppm): 146.0, 137.9, 117.2, 79.4.

Benzene-1,2-diamine (2i)[6c]: Yield: 92%; Brown solid; Mp 101-103°C (Lit.[26] 103-104°C); ^{1}H NMR ($CDCl_3$, 300MHz); δ (ppm): 6.75 (2H, d, *J* = 8.4 Hz); 6.70 (2H, d, *J* = 8.4 Hz); 3.31 (4H, br.s); ^{13}C NMR ($CDCl_3$, 75 MHz); δ (ppm): 135.3, 118.0, 115.3.

Benzene-1,3-diamine (2j)[6c]: Yield: 90%; Brown solid; Mp 65-66°C (Lit.[26] 63-65°C); ^{1}H NMR ($CDCl_3$, 300MHz); δ (ppm): 6.94 (1H, t, *J* = 7.8 Hz); 6.11-6.14 (2H, m); 6.03 (1H, s); 3.50 (4H, br.s); ^{13}C NMR ($CDCl_3$, 75 MHz); δ (ppm): 147.5, 130.2, 106.0, 101.9.

Benzene-1,4-diamine (2k)[6c]: Yield: 91%; Brown solid; Mp 142-144°C (Lit.[26] 143-144°C); ^{1}H NMR ($CDCl_3$, 300MHz); δ (ppm): 6.72 (4H, s); 2.77 (4H, br.s); ^{13}C NMR ($CDCl_3$, 75 MHz); δ (ppm): 138.7, 115.0.

Benzene-1,2-diamine (2l)[6c]: Yield: 94%; Brown solid; Mp 101-103°C (Lit.[26] 103-104°C); ^{1}H NMR ($CDCl_3$, 300MHz); δ (ppm): 6.73 (2H, d, *J* = 8.3 Hz); 6.68 (2H, d, *J* = 8.3 Hz); 3.30 (4H, br.s); ^{13}C NMR ($CDCl_3$, 75 MHz); δ (ppm): 135.1, 118.3, 115.1.

4-methylbenzene-1,3-diamine (2m)[8d]: Yield: 93%; Yellow solid; Mp 103-105°C; ^{1}H NMR ($CDCl_3$, 300MHz); δ (ppm): 6.82 (2H, d, *J* = 8.1 Hz); 6.00 (2H, d, *J* = 8.1 Hz); 3.25 (4H, br.s); 2.07 (3H, s); ^{13}C NMR ($CDCl_3$, 75 MHz); δ (ppm): 145.5, 145.3, 131.1, 112.9, 106.0, 102.2, 16.4.

Benzene-1,3-diamine (2n)[6c]: Yield: 93%; Brown solid; Mp 65-66°C (Lit.[26] 63-65°C); ^{1}H NMR ($CDCl_3$, 300MHz); δ (ppm): 6.91 (1H, t, *J* = 7.8 Hz); 6.10-6.15 (2H, m); 6.01 (1H, s); 3.52 (4H, br.s); ^{13}C NMR ($CDCl_3$, 75 MHz); δ (ppm): 147.7, 130.4, 106.1, 101.6.

2-aminophenol (2o)[7c]: Yield: 86%; Yellow solid; Mp 173-175°C (Lit.[26] 173-174°C); ^{1}H NMR ($CDCl_3$, 300MHz); δ (ppm): 6.54 (1H, d, *J* = 7.2 Hz); 6.45 (2H, s); 6.35 (1H, d, *J* = 7.2 Hz); 3.12 (2H, br.s); ^{13}C NMR ($CDCl_3$, 75 MHz); δ (ppm): 144.5, 135.2, 119.8, 118.2, 115.4, 114.9.

3-aminophenol (2p)[6c]: Yield: 88%; Yellow solid; Mp 119-121°C (Lit.[26] 120-123°C); ^{1}H NMR (DMSO-d_6, 300MHz); δ (ppm): 6.84 (1H, s); 6.01-6.09 (3H, m), 4.79 (2H, br.s); ^{13}C NMR (DMSO-d_6, 75 MHz); δ (ppm): 147.3, 136.4, 118.7, 117.1, 115.1, 110.5.

4-aminophenol (2q)[6c]: Yield: 89%; Yellow solid; Mp 282-284°C (Lit.[26] 281-283°C); ^{1}H NMR ($CDCl_3$, 300MHz); δ (ppm): 6.68 (2H, d, *J* = 8.4 Hz); 6.47 (2H, d, *J* = 8.4 Hz); 2.49 (2H, br.s); ^{13}C NMR ($CDCl_3$, 75 MHz); δ (ppm): 149.8, 138.8, 116.5, 116.0.

4-aminobenzyl alcohol (2r)[6b]: Yield: 87%; Brown solid; Mp 60-65°C; ^{1}H NMR ($CDCl_3$, 300MHz); δ (ppm): 7.14 (2H, d, *J* = 8.1 Hz); 6.65 (2H, d, *J* = 8.1 Hz); 4.53 (2H, s); 2.88 (2H, br.s); ^{13}C NMR ($CDCl_3$, 75 MHz); δ (ppm): 146.0, 131.1, 128.7, 115.1, 65.2.

1-(4-aminophenyl)ethanol (2s)[9b]: Yield: 88%; Brown solid; Mp 60-65°C; ^{1}H NMR ($CDCl_3$, 300MHz); δ (ppm): 7.06 (2H, d, *J* = 8.1 Hz); 6.55 (2H, d, *J* = 8.1 Hz); 4.64-4.71 (1H, q); 3.52 (2H, br.s); 1.38 (3H, d, *J* = 6.3 Hz); ^{13}C NMR ($CDCl_3$, 75 MHz); δ (ppm): 145.6, 136.2, 126.6, 115.3, 69.8, 24.9.

4-aminobenzaldehyde (2t)[7a]: Yield: 85%; Yellow solid; Mp 70-72°C (Lit.[26] 72-73°C); ^{1}H NMR ($CDCl_3$, 300MHz); δ (ppm): 9.69 (1H, s); 7.83 (2H, d, *J* = 8.7 Hz); 6.71 (2H, d, *J* = 8.7 Hz); 3.13 (2H, br.s); ^{13}C NMR ($CDCl_3$, 75 MHz); δ (ppm): 190.4, 153.8, 130.8, 126.5, 110.7.

1-(4-aminophenyl)ethanone (2u)[6b]: Yield: 84%; Orange solid; Mp 104-105°C; ^{1}H NMR ($CDCl_3$, 300MHz); δ (ppm): 7.81 (2H, d, *J* = 8.1 Hz); 6.66 (2H, d, *J* = 8.1 Hz); 4.20 (2H, br.s); 2.51 (3H, s); ^{13}C NMR ($CDCl_3$, 75 MHz); δ (ppm): 196.5, 151.2, 130.8, 127.8, 113.7, 26.0.

4-aminobenzoic acid (2v)[7c]: Yield: 82%; Yellow solid; Mp 186-187°C (Lit.[26] 186-189°C); ^{1}H NMR (DMSO-d_6, 300MHz); δ (ppm): 7.61 (2H, d, *J* = 8.4 Hz); 6.55 (2H, d, *J* = 8.4 Hz); 5.81 (2H, br.s); ^{13}C NMR (DMSO-d_6, 75 MHz); δ (ppm): 168.1, 153.5, 131.7, 117.4, 113.1.

Methyl-3-aminobenzoate (2w)[10e]: Yield: 87%; White solid; Mp 51-53°C; ^{1}H NMR ($CDCl_3$, 300MHz); δ (ppm): 7.40 (1H, d, *J* = 7.6 Hz); 7.31 (1H, s); 7.14 (1H, t, *J* = 7.6 Hz); 6.78-6.83 (1H, m); 3.83 (3H, s); 3.55 (2H, br.s); ^{13}C NMR ($CDCl_3$, 75 MHz); δ (ppm): 166.8, 146.5, 131.2, 128.9, 119.2, 114.5, 53.1.

3-aminobenzonitrile (2x)[9d]: Yield: 89%; Yellow solid; Mp 52-54°C; ^{1}H NMR ($CDCl_3$, 300MHz); δ (ppm): 7.18-7.25 (1H, m); 7.00 (1H, d, *J* = 7.5 Hz); 6.87 (2H, t, *J* = 6.7 Hz); 3.89 (2H, br.s); ^{13}C NMR ($CDCl_3$, 75 MHz); δ (ppm): 147.0, 130.1, 121.9, 119.2, 117.4, 112.8.

4-benzyloxyaniline (2y)[8b]: Yield: 87%; Brown solid; Mp 44-46°C; ^{1}H NMR ($CDCl_3$, 300MHz); δ (ppm): 7.30-7.43 (5H, m); 6.82 (2H, d, *J* = 8.7 Hz); 6.64 (2H, d, *J* = 8.7 Hz); 4.99 (2H, s); ^{13}C NMR ($CDCl_3$, 75 MHz); δ (ppm): 152.0, 140.3, 137.6, 128.8, 128.5, 127.8, 127.5, 125.9, 116.4, 116.1, 114.9, 70.8.

(2-aminophenoxy)(tert-butyl)dimethylsilane (2z)[9b]: Yield: 85%; Yellow liquid; ^{1}H NMR ($CDCl_3$, 300MHz); δ (ppm): 6.70-6.76 (4H, m); 2.39 (2H, br.s); 0.86 (9H, s); 0.02 (6H, s); ^{13}C NMR ($CDCl_3$, 75 MHz); δ (ppm): 144.2, 134.4, 121.5, 119.6, 117.2, 115.3, 29.3, 14.1, -0.01.

Naphthalen-1-amine (2za)[6c]: Yield: 88%; Yellow solid; Mp 46-47°C; ^{1}H NMR ($CDCl_3$, 300 MHz); δ (ppm): 7.81-7.89 (2H, m); 7.47-7.56 (2H, m); 7.33-7.39 (2H, m); 6.80 (1H, d, *J* = 6.8

Hz), 3.99 (2H, br.s); ^{13}C NMR ($CDCl_3$, 75 MHz); δ (ppm): 147.7, 144.5, 138.1, 135.8, 128.4, 127.2, 121.0, 115.8, 111.2.

4-aminopyridine (2zb)[7c]: Yield: 90%; White solid; Mp 153-155^{o}C; ^{1}H NMR (DMSO-d_6, 300MHz); δ (ppm): 7.61 (2H, d, *J* = 8.4 Hz); 6.55 (2H, d, *J* = 8.4 Hz); 5.81 (2H, br.s); ^{13}C NMR (DMSO-d_6, 75 MHz); δ (ppm): 154.7, 149.9, 109.3.

Quinolin-8-amine (2zc)[7b]: Yield: 92%; Yellow solid; Mp 66-67^{o}C; ^{1}H NMR ($CDCl_3$, 300 MHz); δ (ppm): 8.73 (1H, d, *J* = 7.8 Hz); 8.01 (1H, d, *J* = 8.1 Hz), 7.31-7.36 (2H, m), 7.11 (1H, d, *J* = 7.6 Hz), 6.91 (1H, d, *J* = 7.6 Hz), 4.71 (2H, br.s); ^{13}C NMR ($CDCl_3$, 75 MHz); δ (ppm): 147.3, 144.5, 138.7, 135.9, 130.1, 127.4, 121.5, 116.0, 110.3.

^{1}H NMR & ^{13}C NMR Spectra of Some Representative Compounds

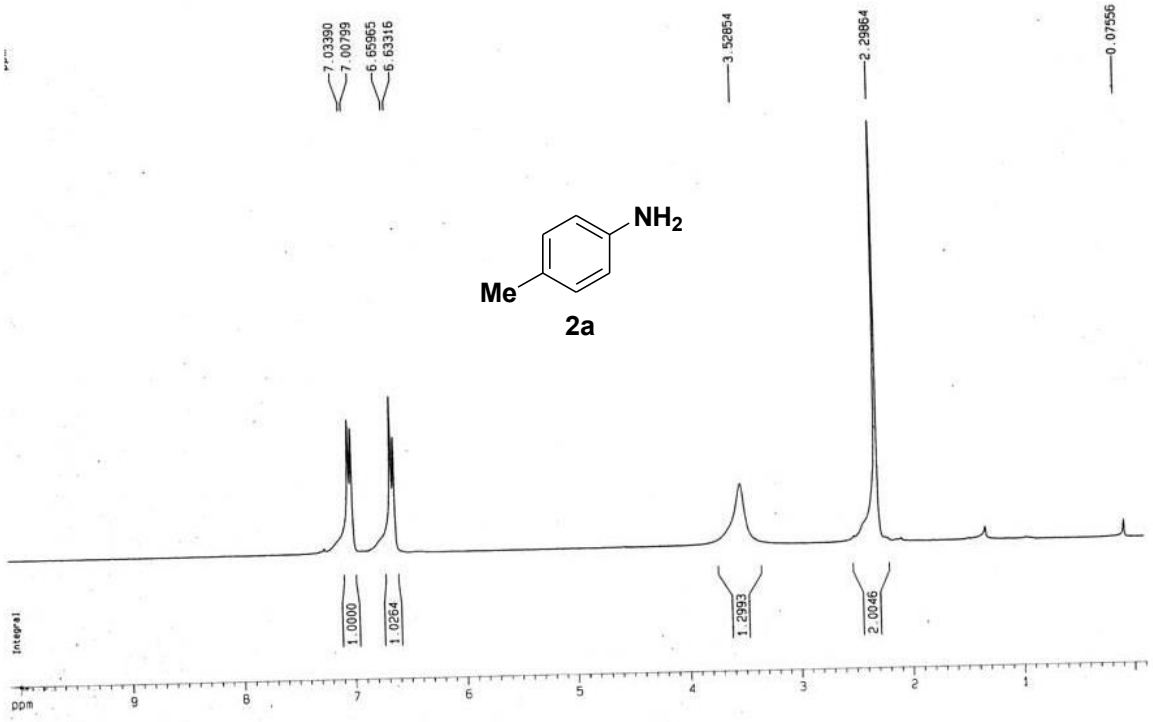

Figure 1 ^{1}H NMR of 4-toluidine (2a)

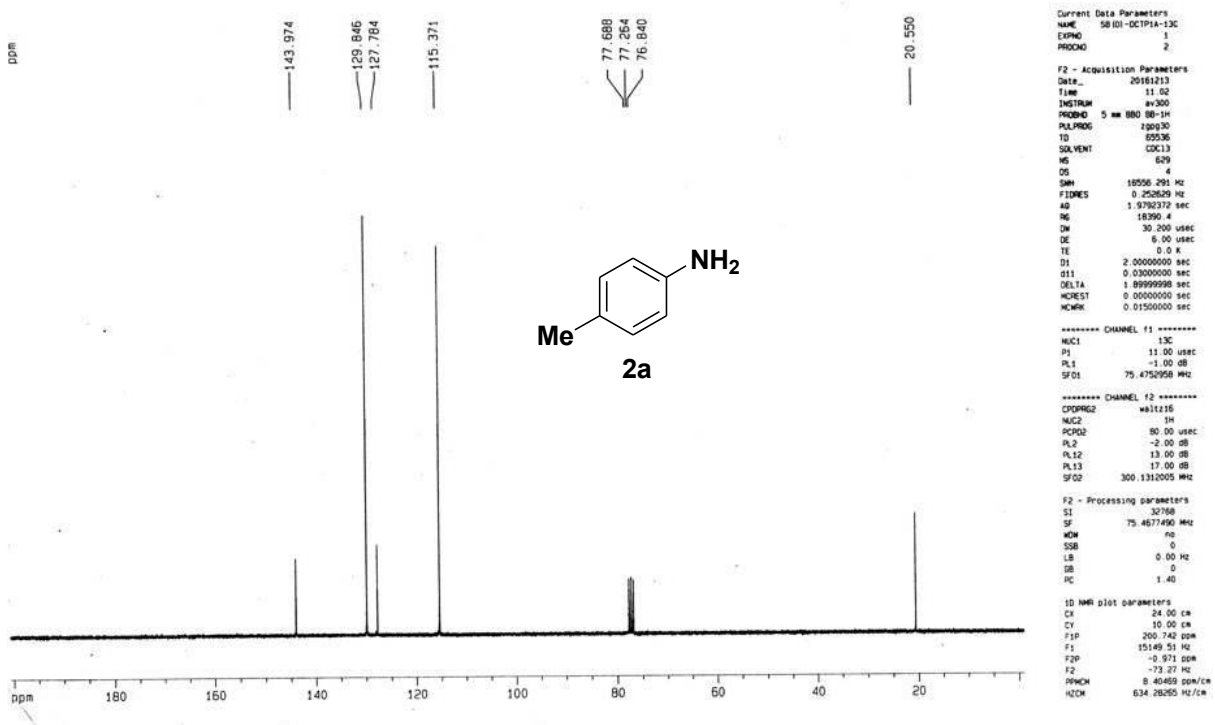

Figure 2 ^{13}C NMR of 4-toluidine (2a)

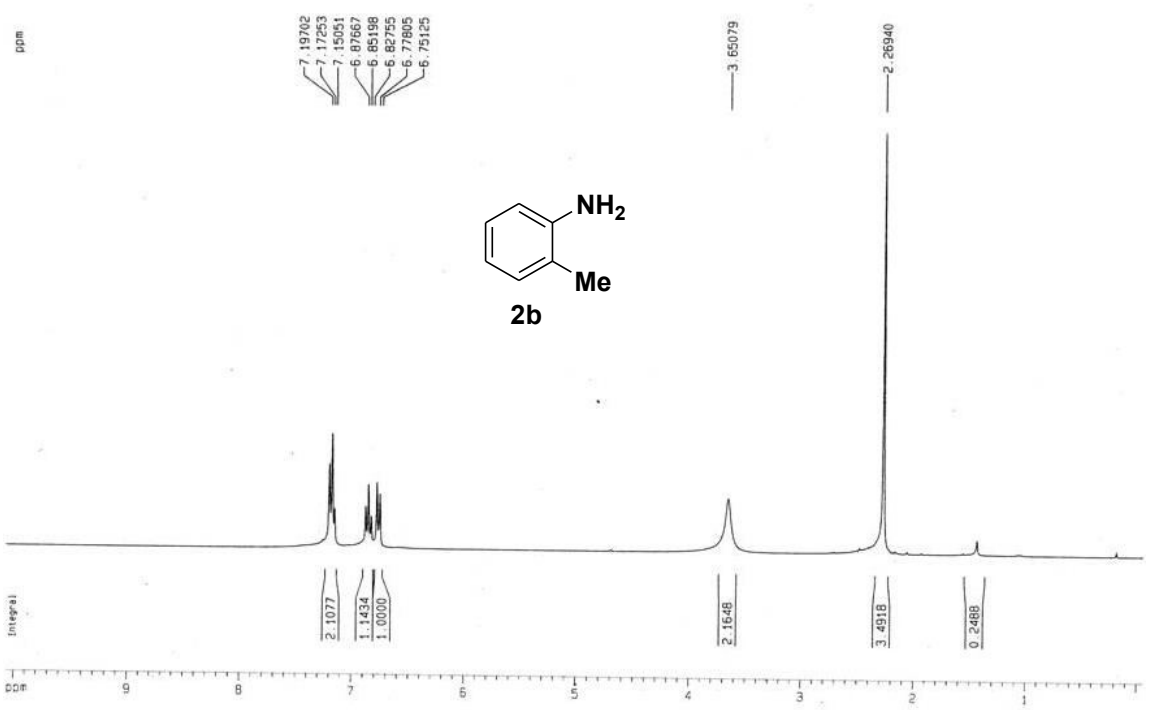

Figure 3 ^{1}H NMR of 2-toluidine (2b)

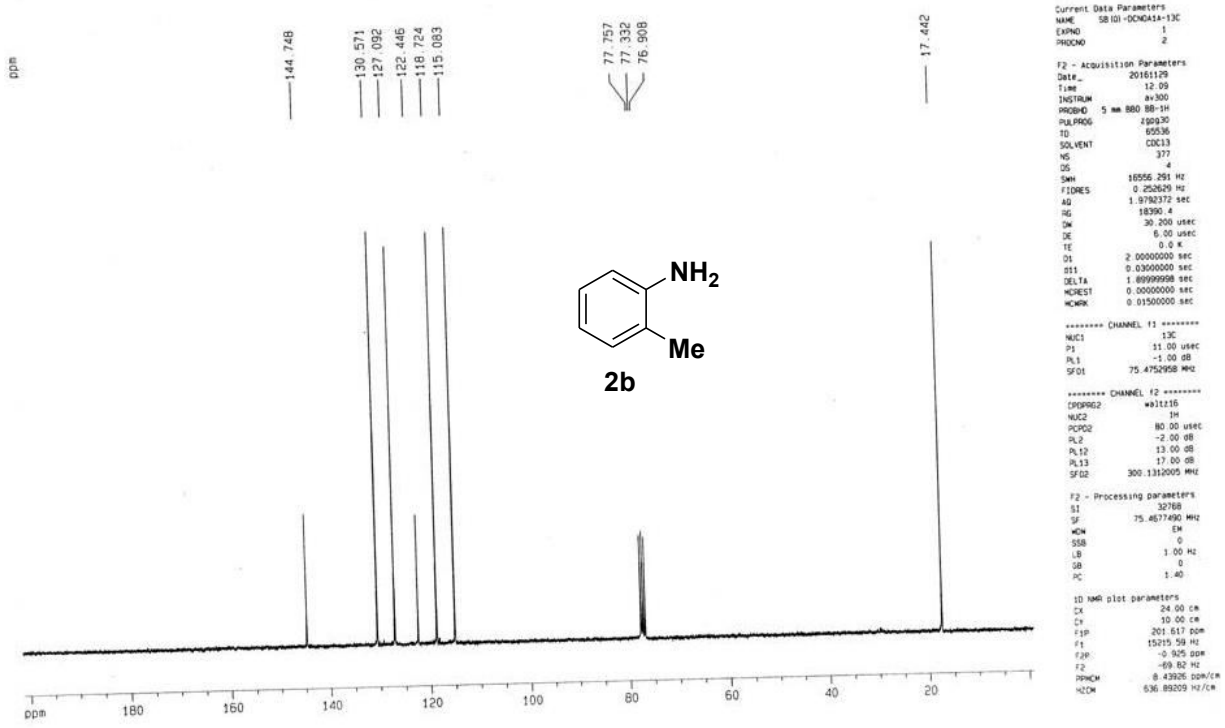

Figure 4 ^{13}C NMR of 2-toluidine (2b)

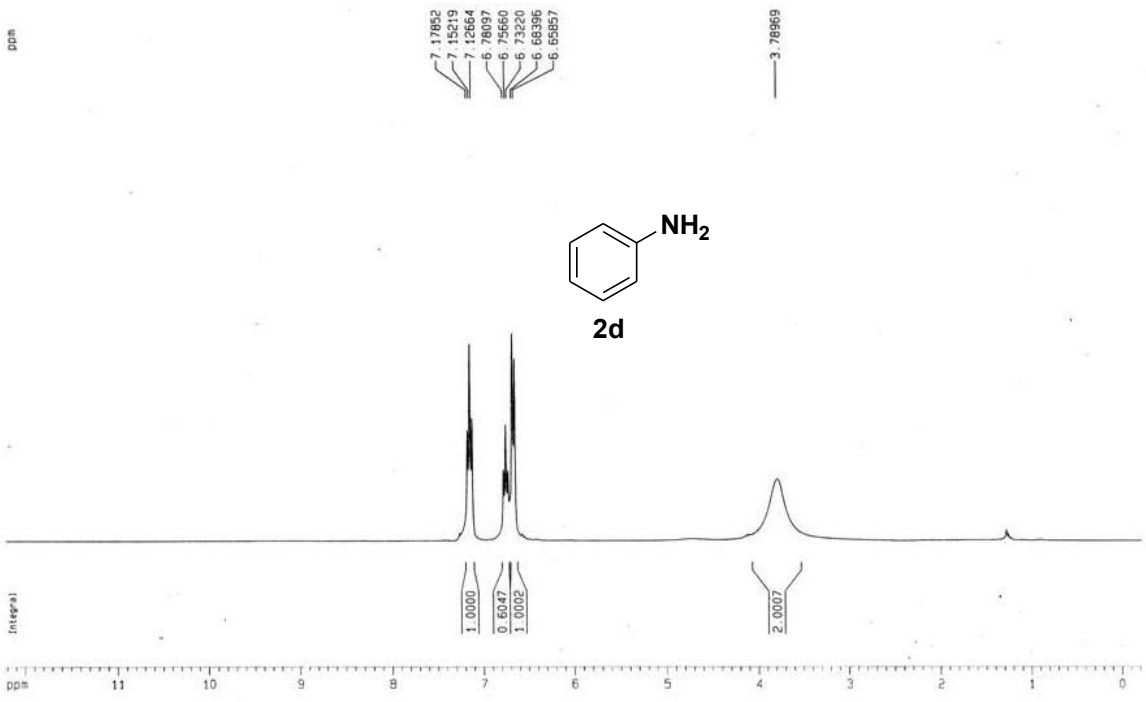

Figure 5 ^{1}H NMR of aniline (2d)

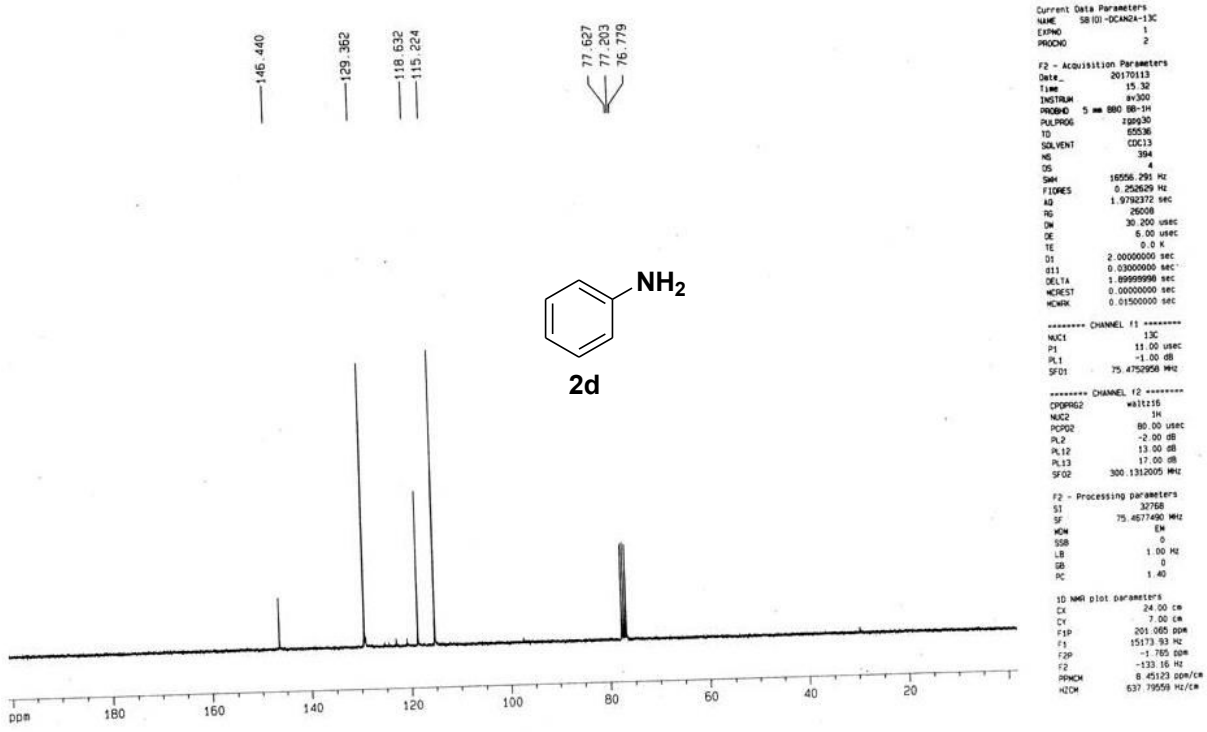

Figure 6 ^{13}C NMR of aniline (2d)

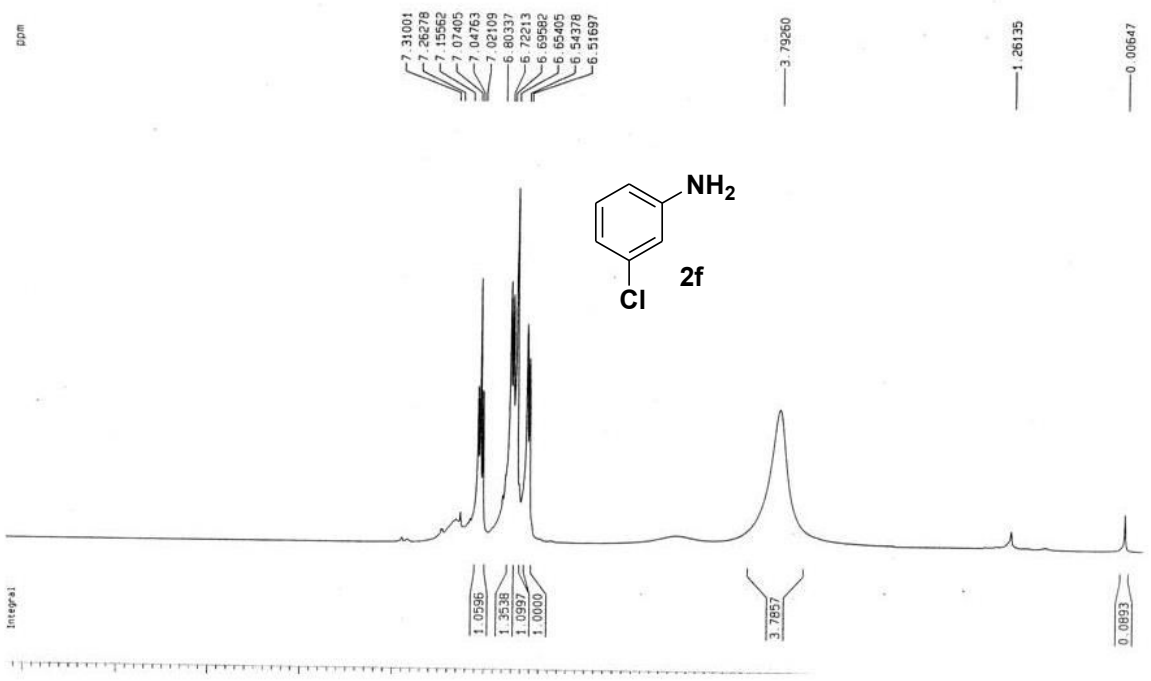

Figure 7 ^{1}H NMR of 3-chloroaniline (2f)

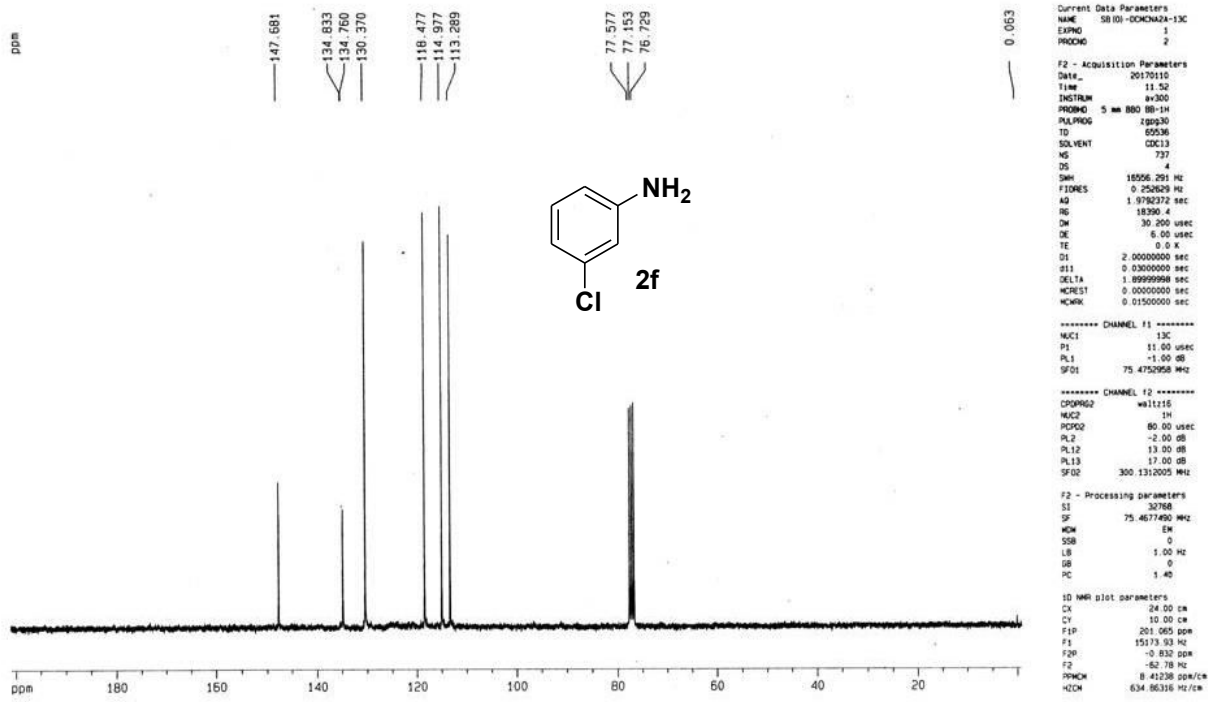

Figure 8 ^{13}C NMR of 3-chloroaniline (2f)

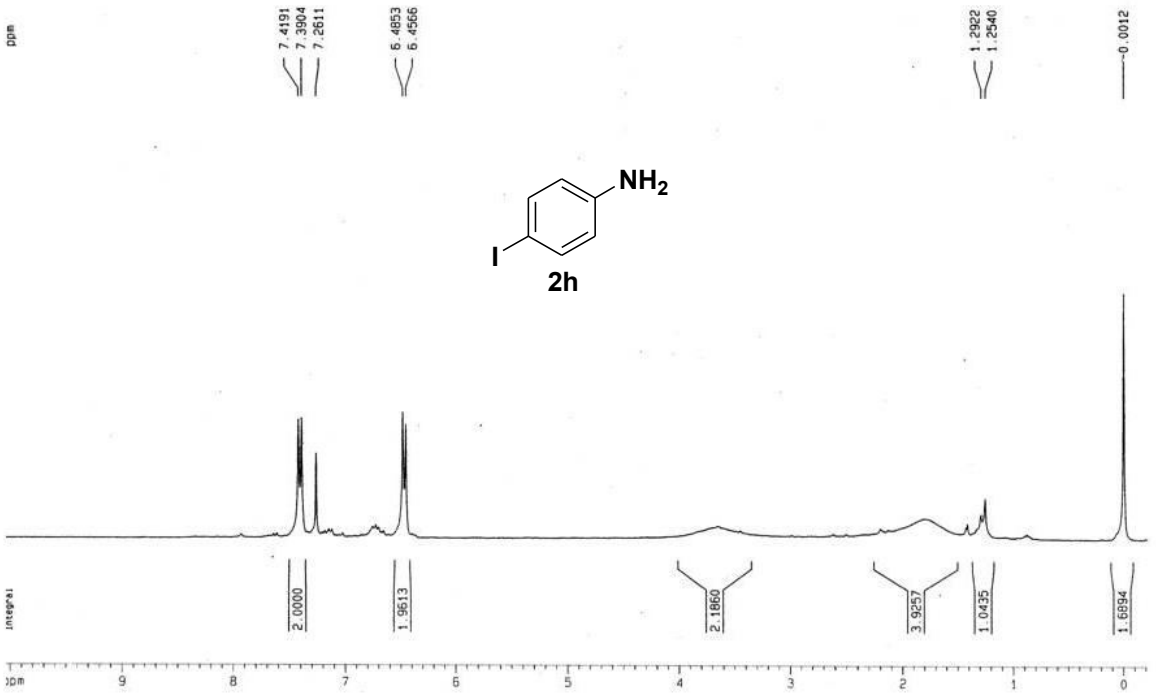

Figure 9 ^{1}H NMR of 4-iodoaniline (2h)

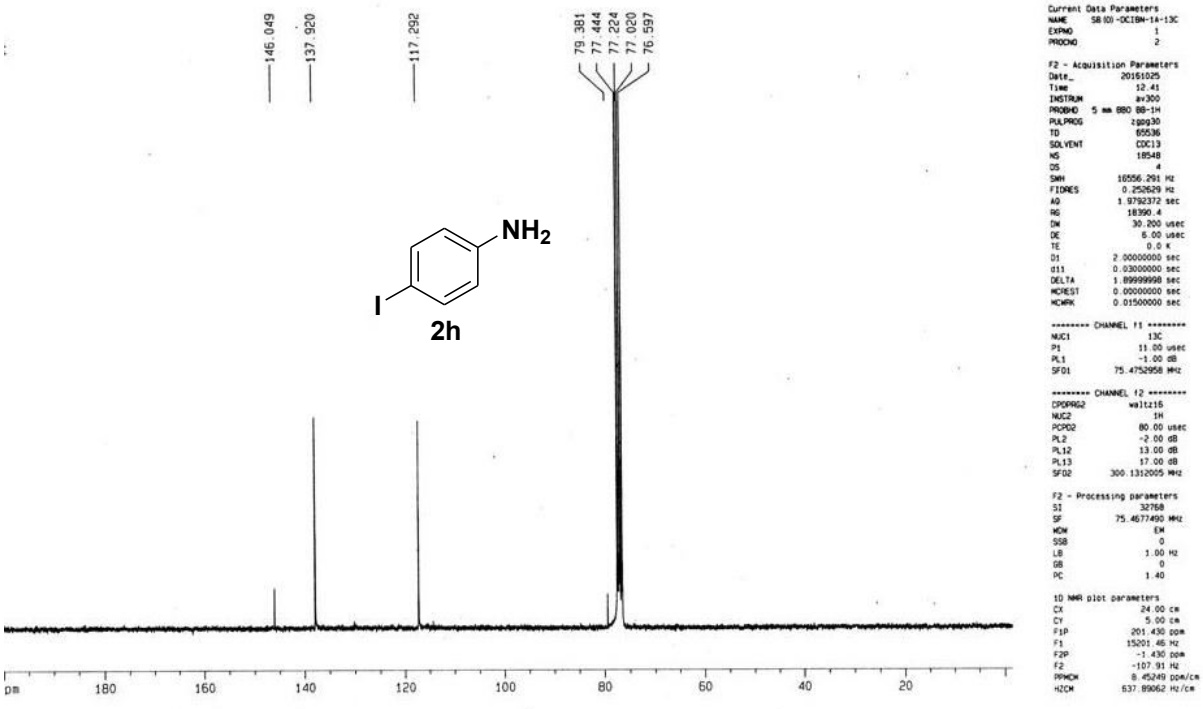

Figure 10 ^{13}C NMR of 4-iodoaniline (2h)

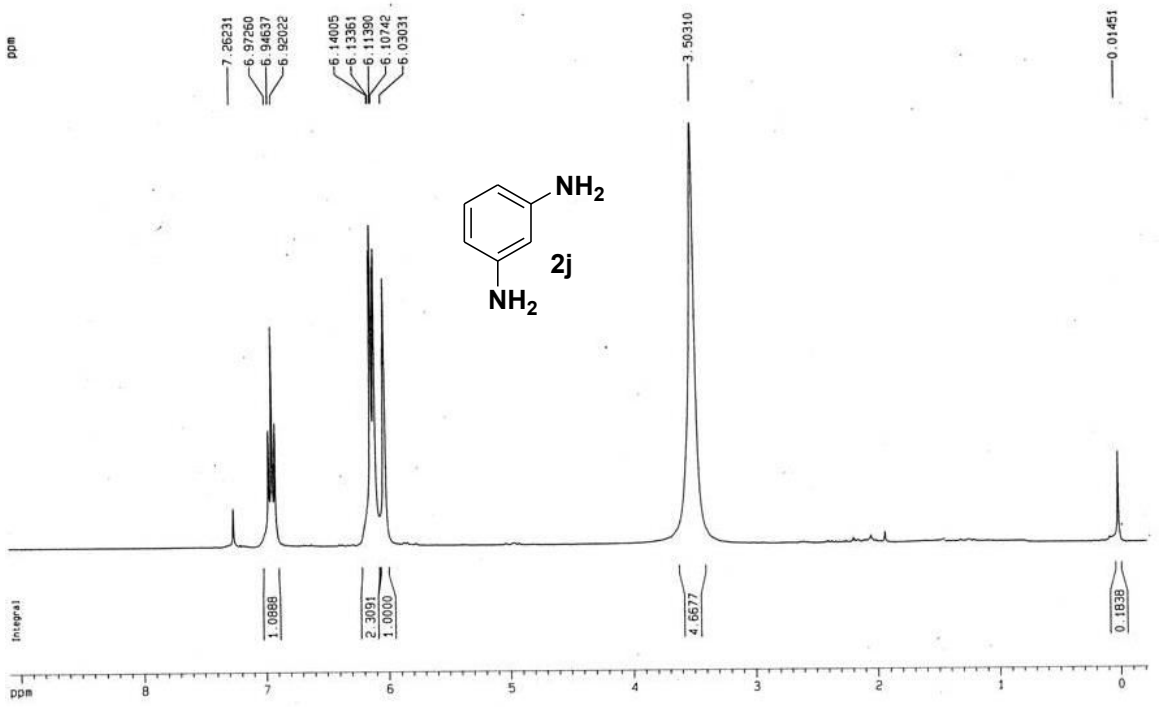

Figure 11 ^{1}H NMR of Benzene-1, 3-diamine (2j)

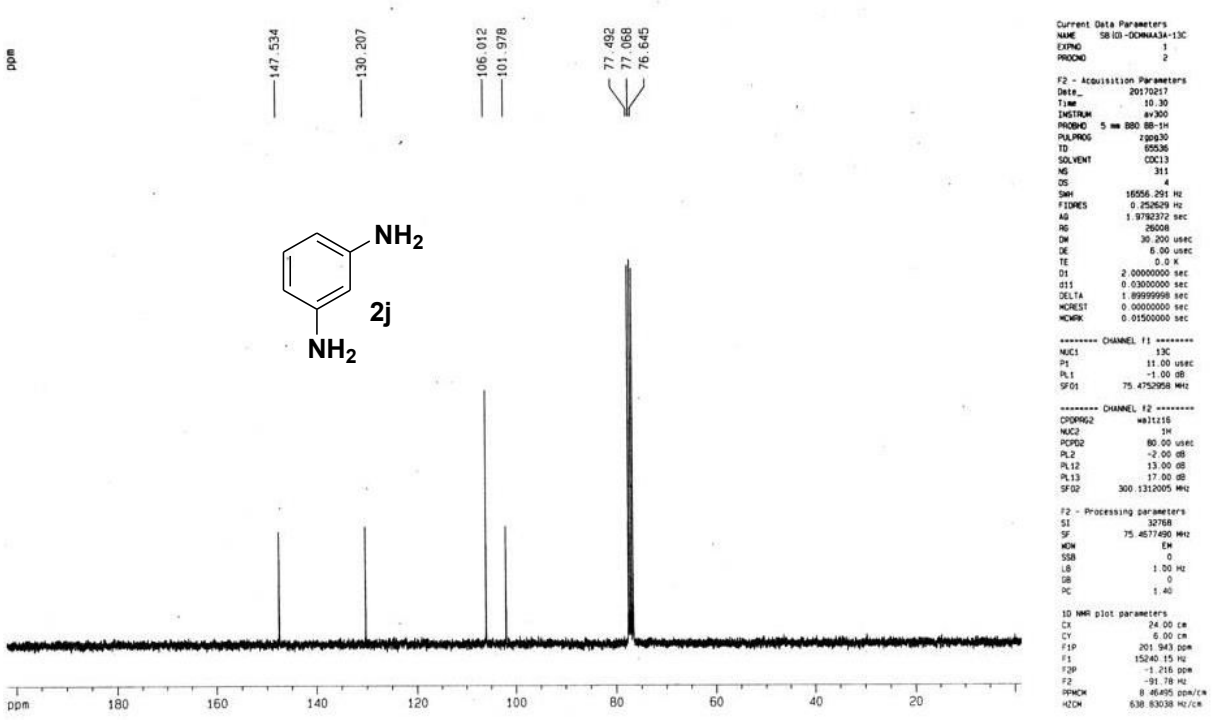

Figure 12 ^{13}C NMR of Benzene-1, 3-diamine (2j)

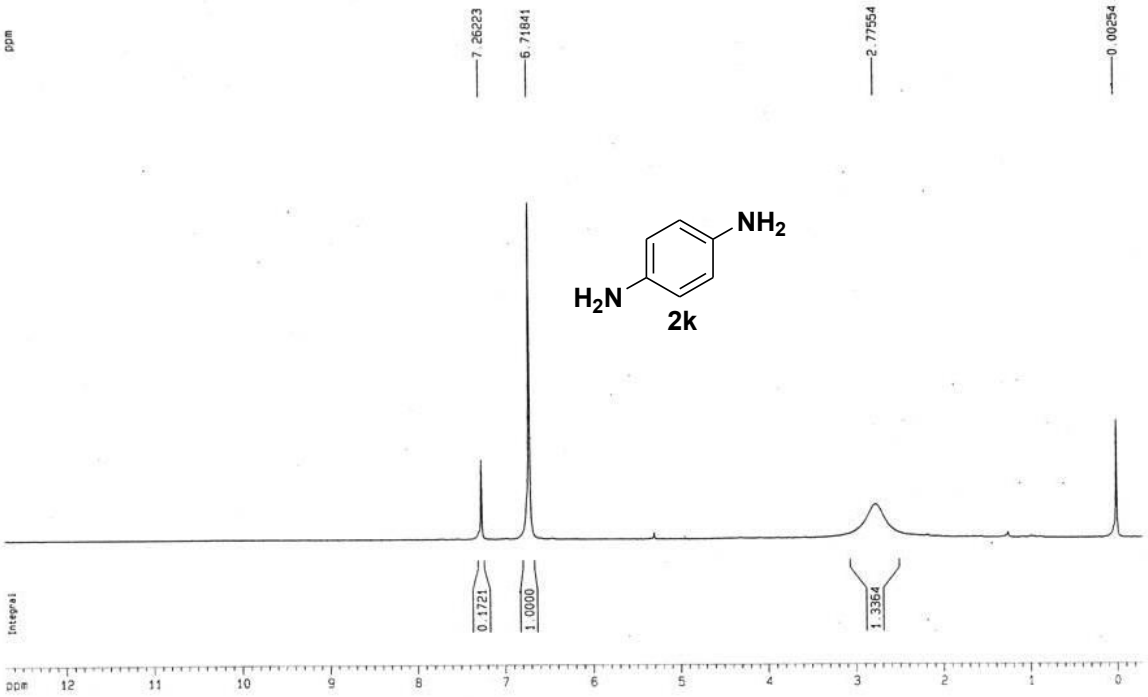

Figure 13 ^{1}H NMR of Benzene-1, 4-diamine (2k)

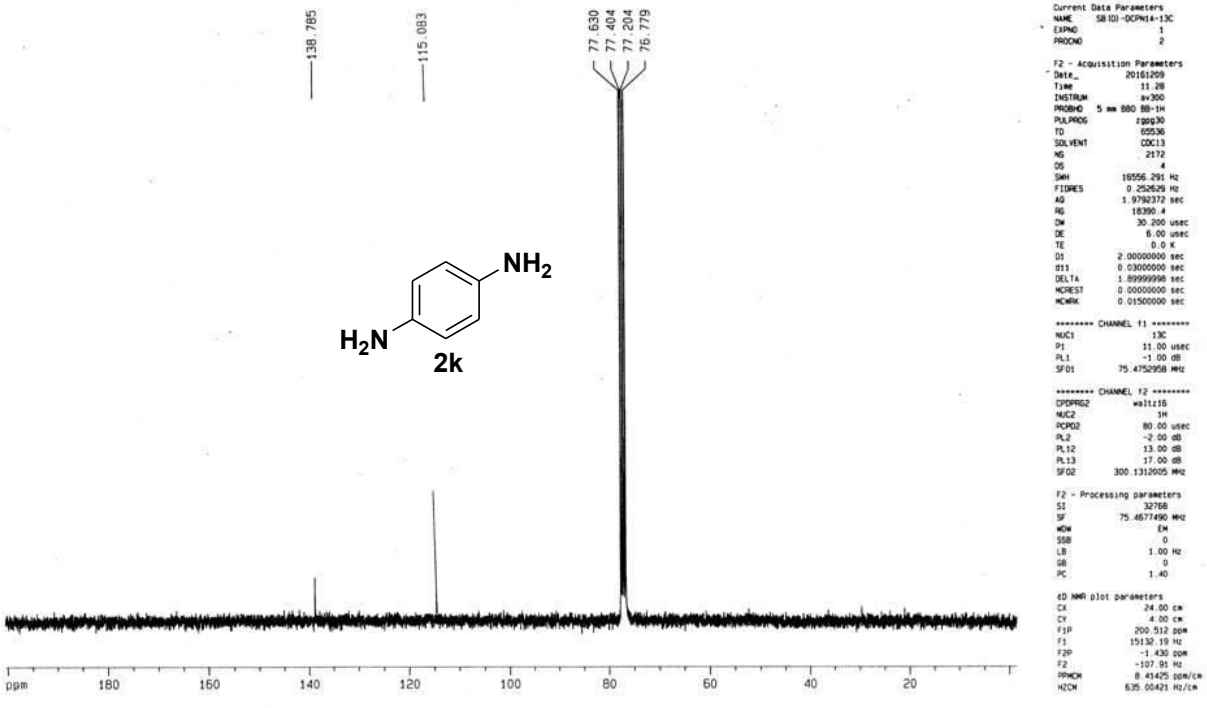

Figure 14 ^{13}C NMR of Benzene-1, 4-diamine (2k)

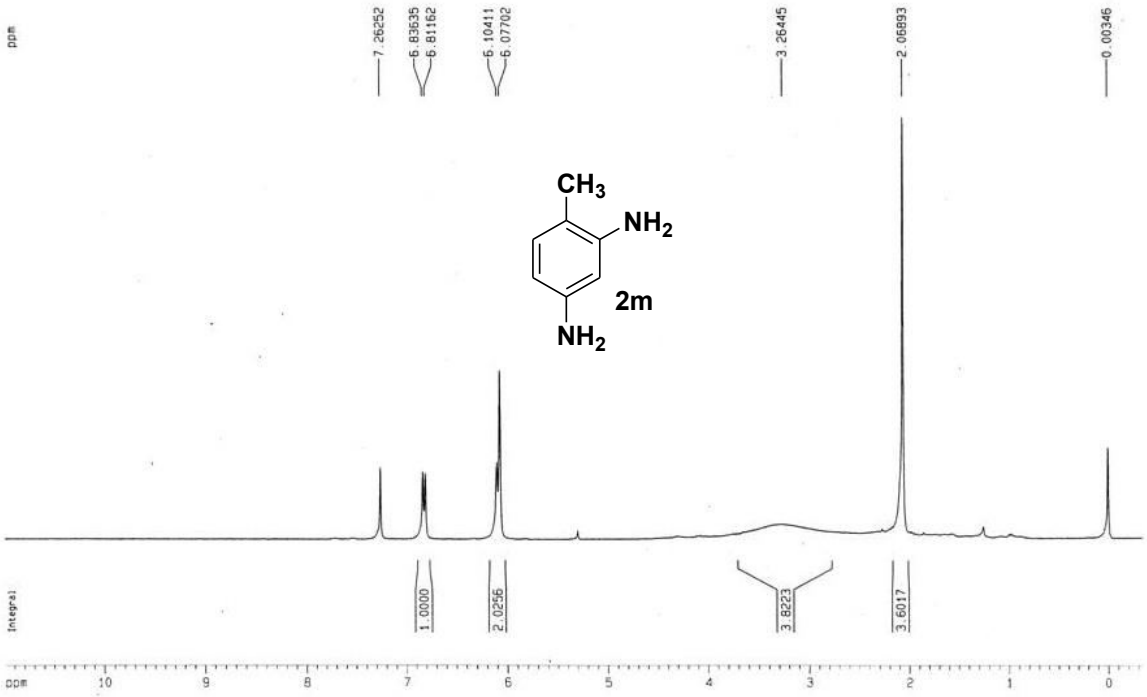

Figure 15 ^{1}H NMR of 4-methylbenzene-1, 3-diamine (2m)

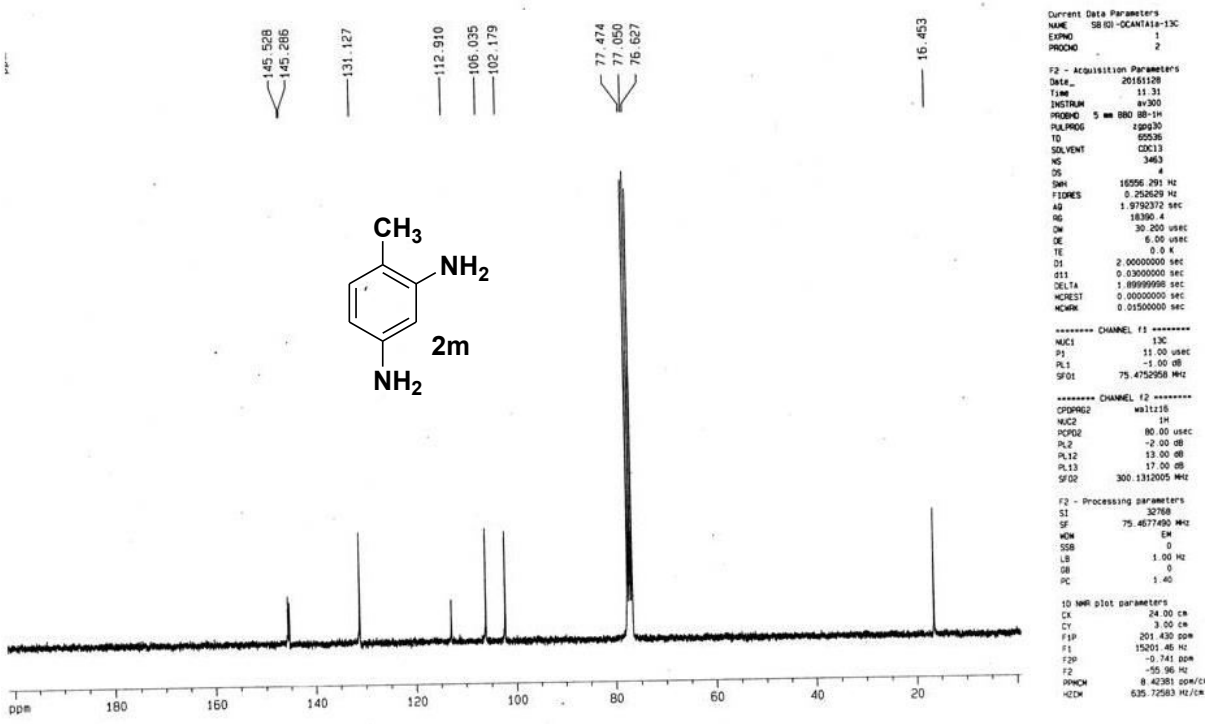

Figure 16 ^{13}C NMR of 4-methylbenzene-1, 3-diamine (2m)

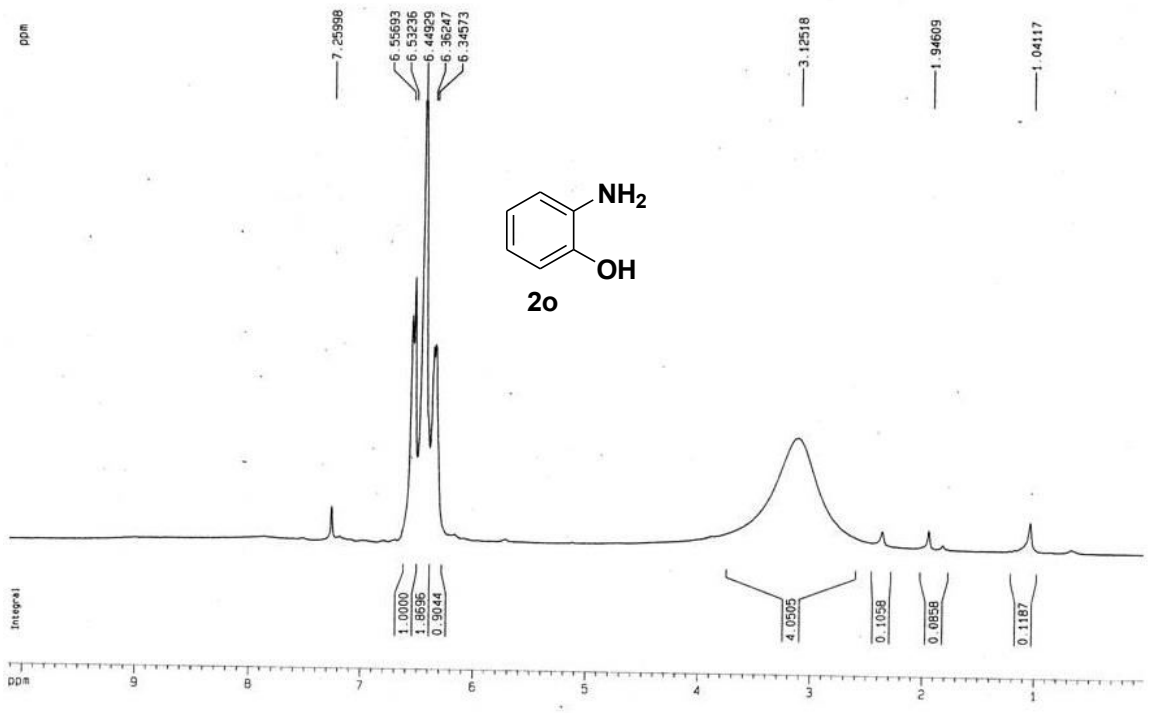

Figure 17 ^{1}H NMR of 2-aminophenol (2o)

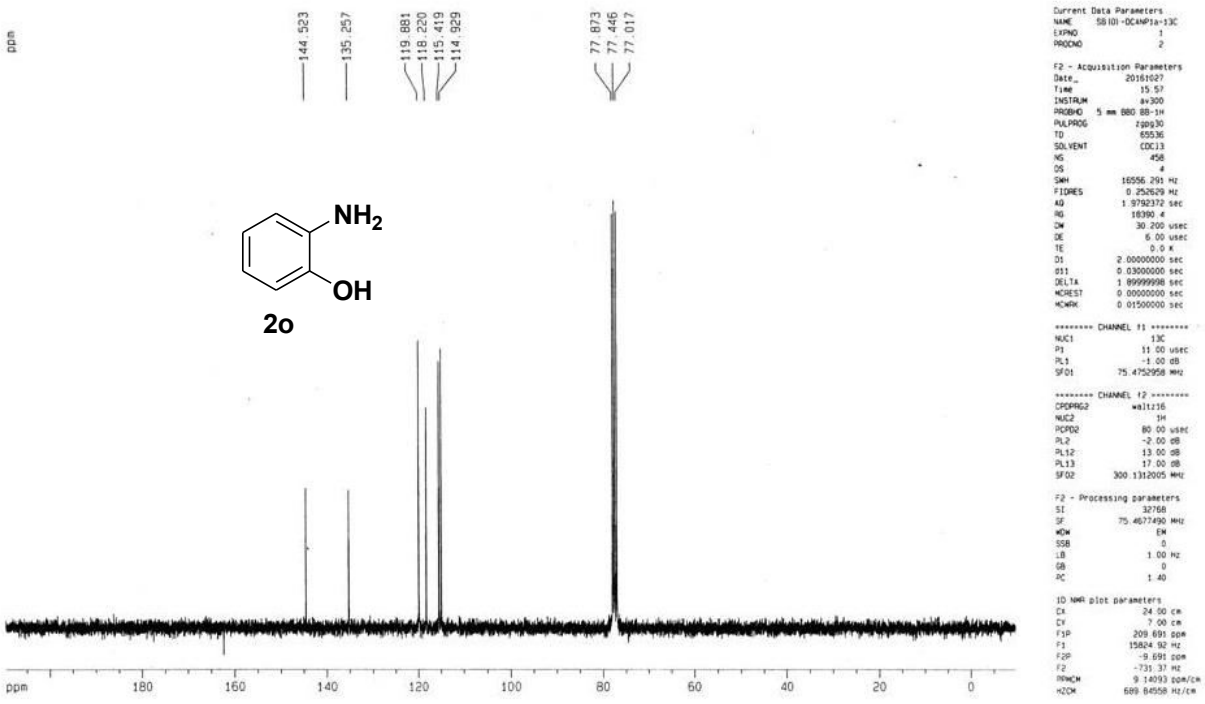

Figure 18 ^{13}C NMR of 2-aminophenol (2o)

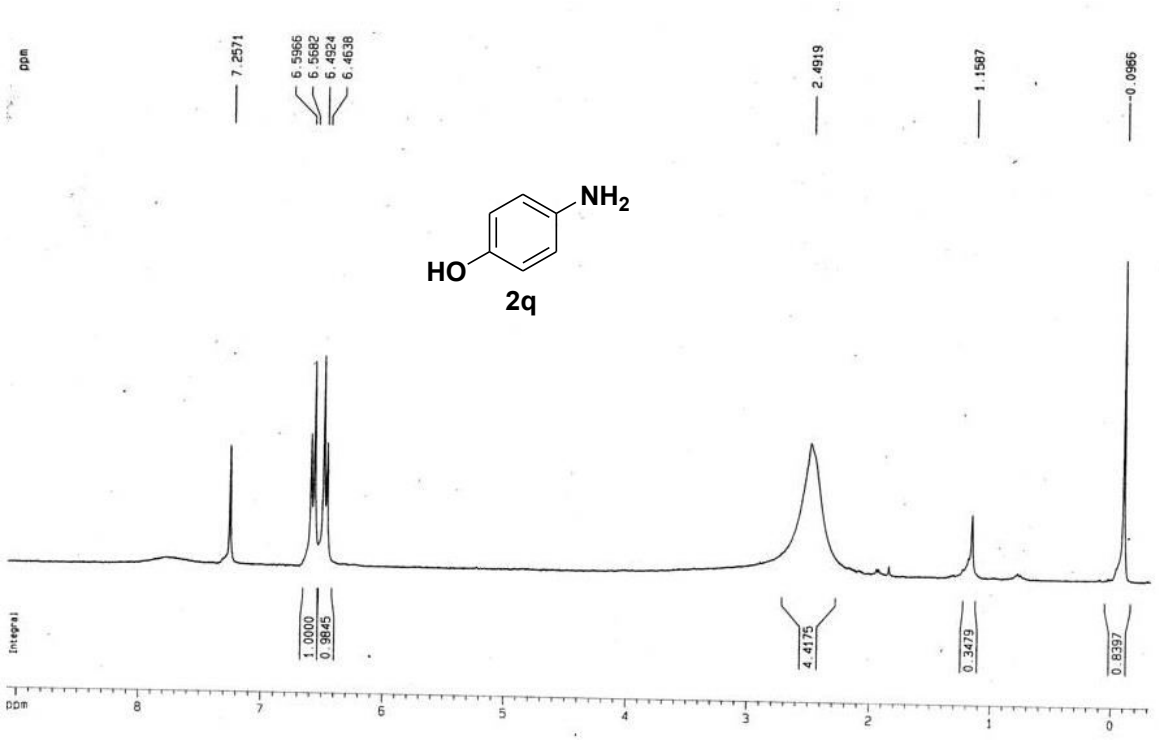

Figure 19 ^{1}H NMR of 4-aminophenol (2q)

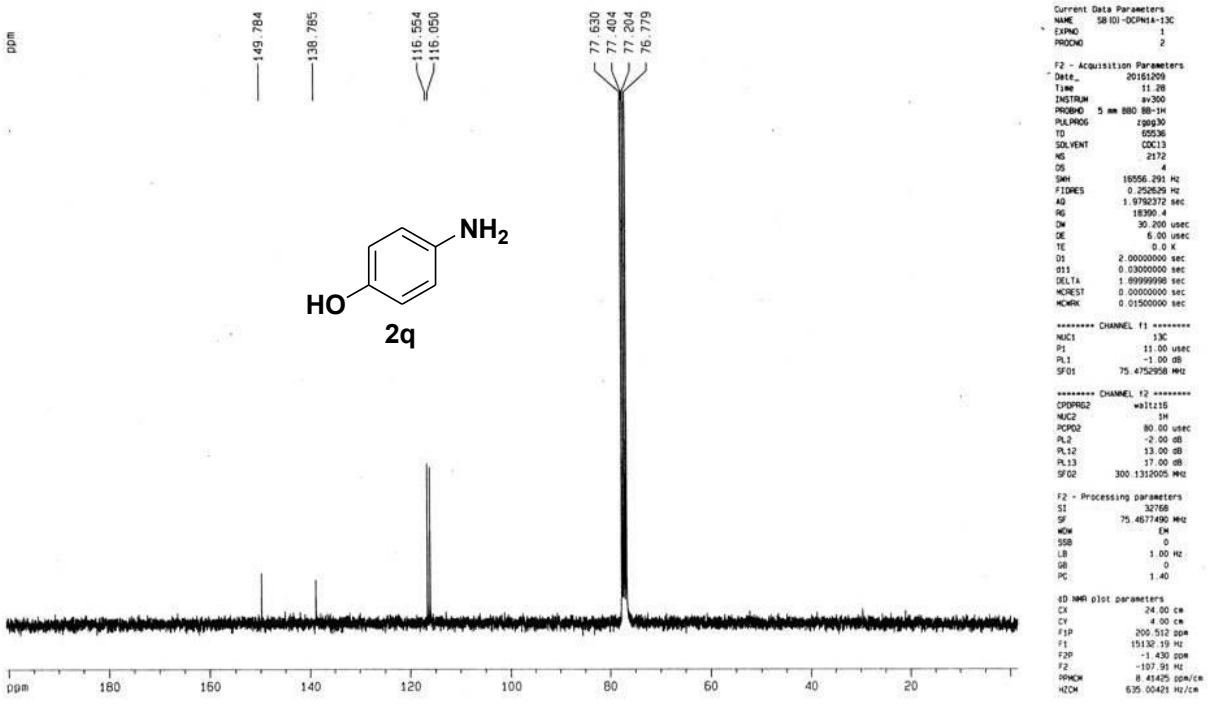

Figure 20 ^{13}C NMR of 4-aminophenol (2q)

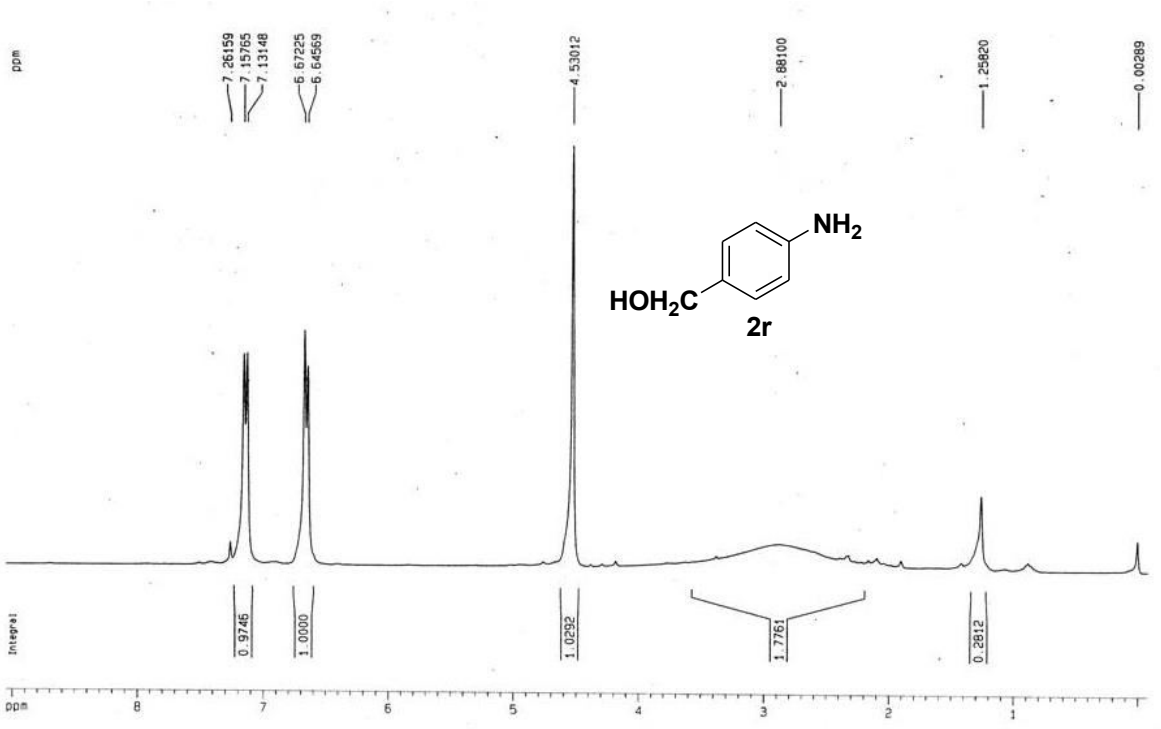

Figure 21 ^{1}H NMR of 4-aminobenzyl alcohol (2r)

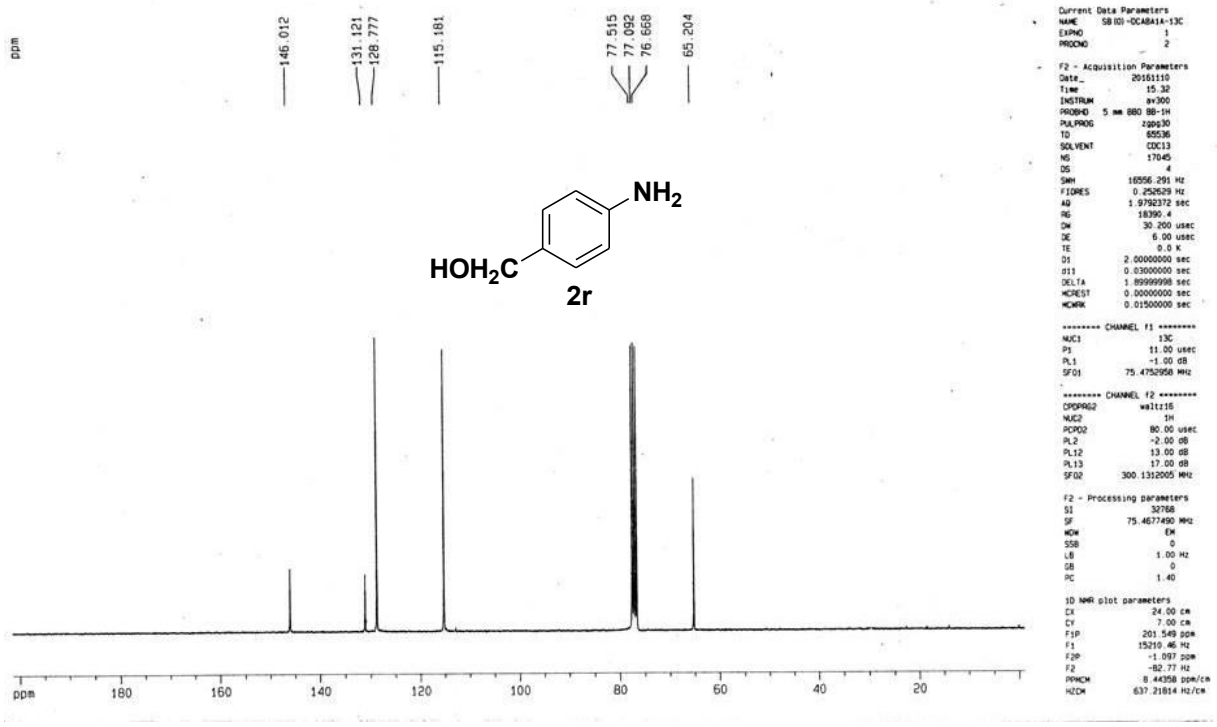

Figure 22 ^{13}C NMR of 4-aminobenzyl alcohol (2r)

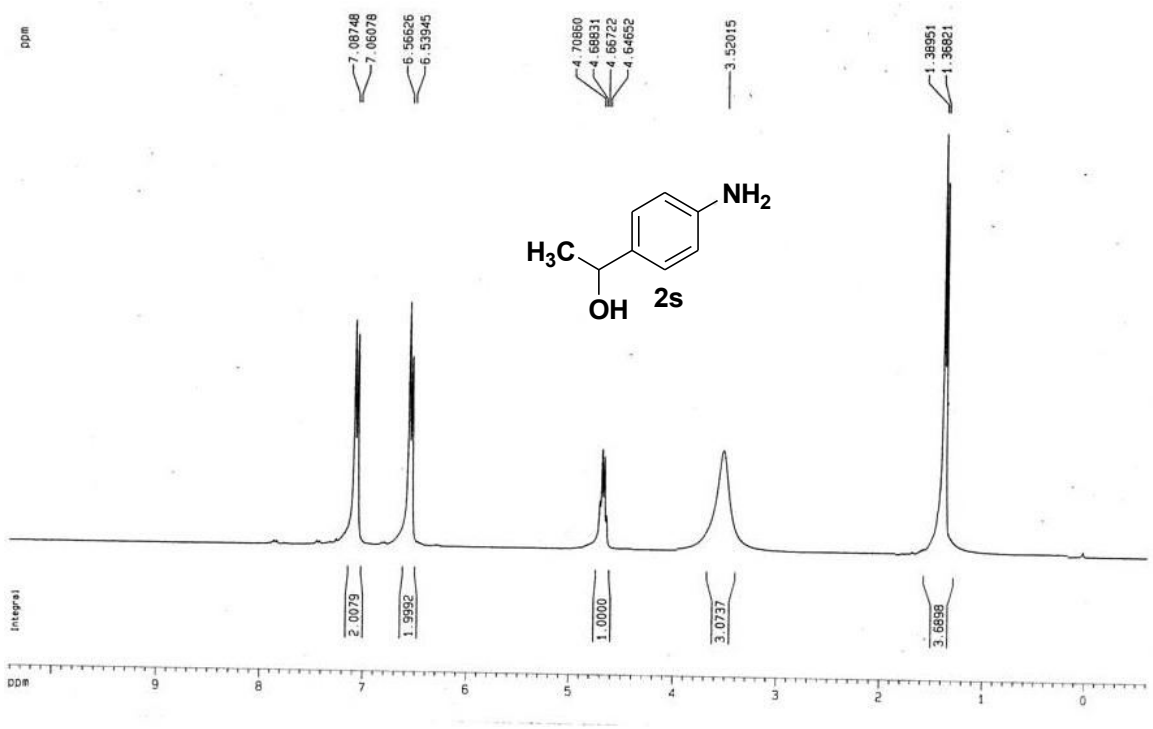

Figure 23 ^{1}H NMR of 1-(4-aminophenyl)ethanol (2s)

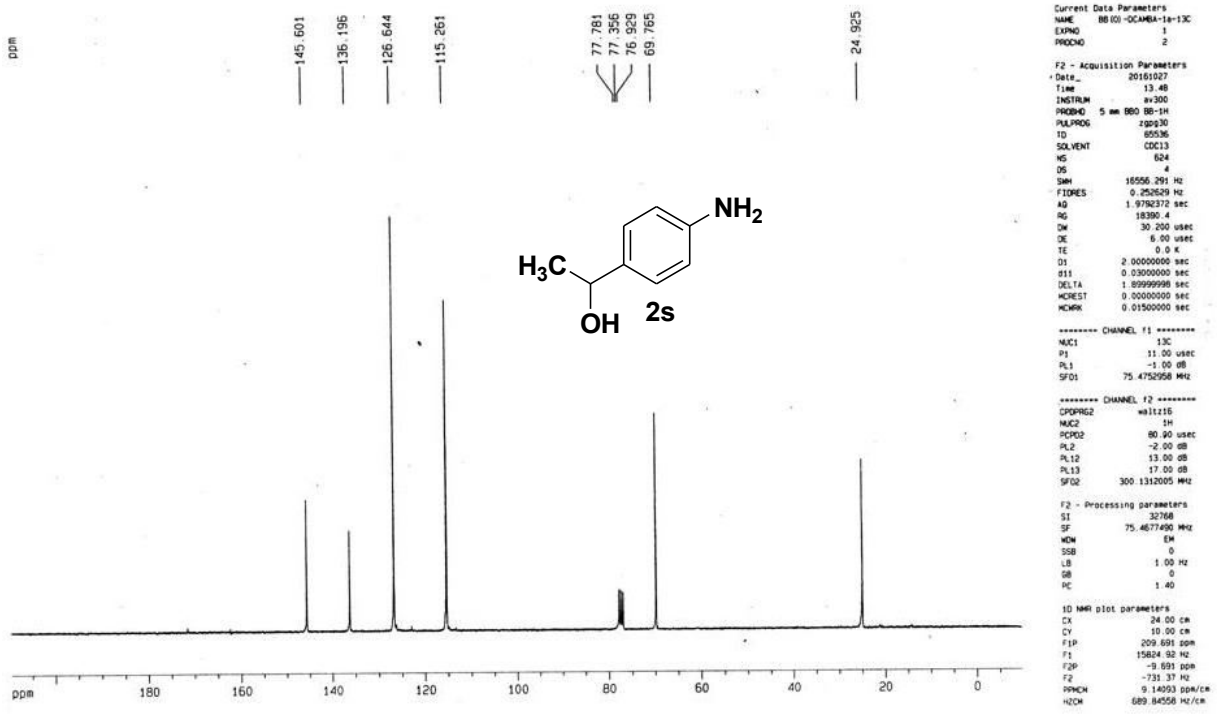

Figure 24 ^{13}C NMR of 1-(4-aminophenyl)ethanol (2s)

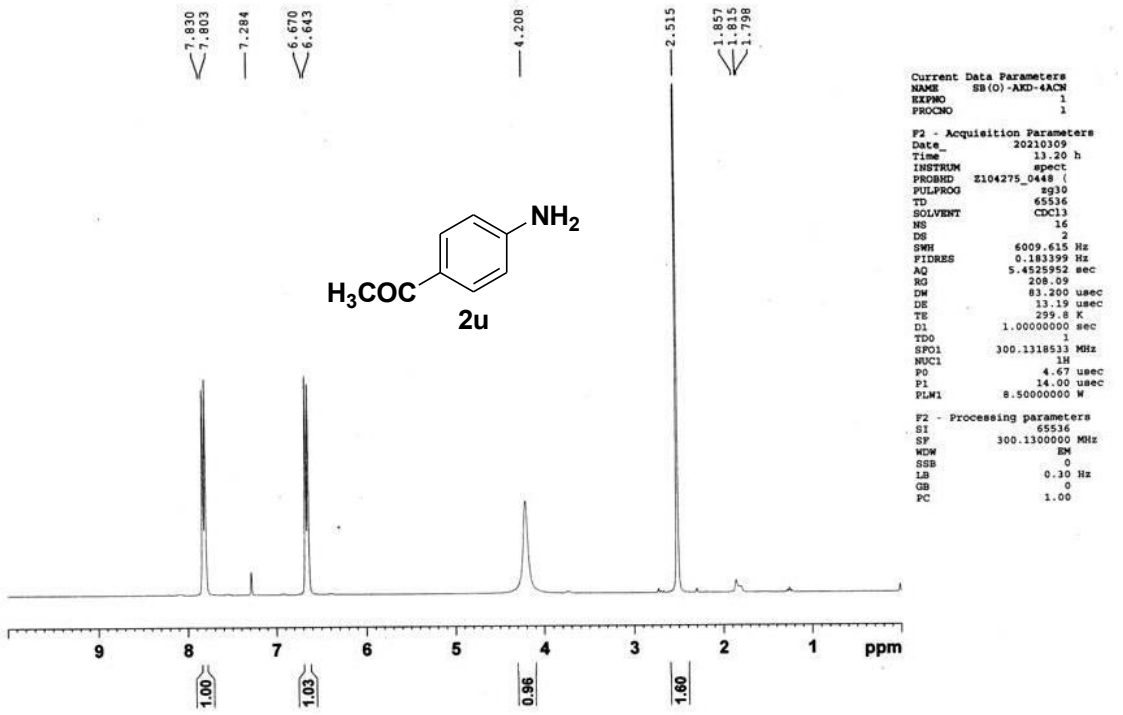

Figure 25 ^{1}H NMR of 1-(4-aminophenyl)ethanone (2u)

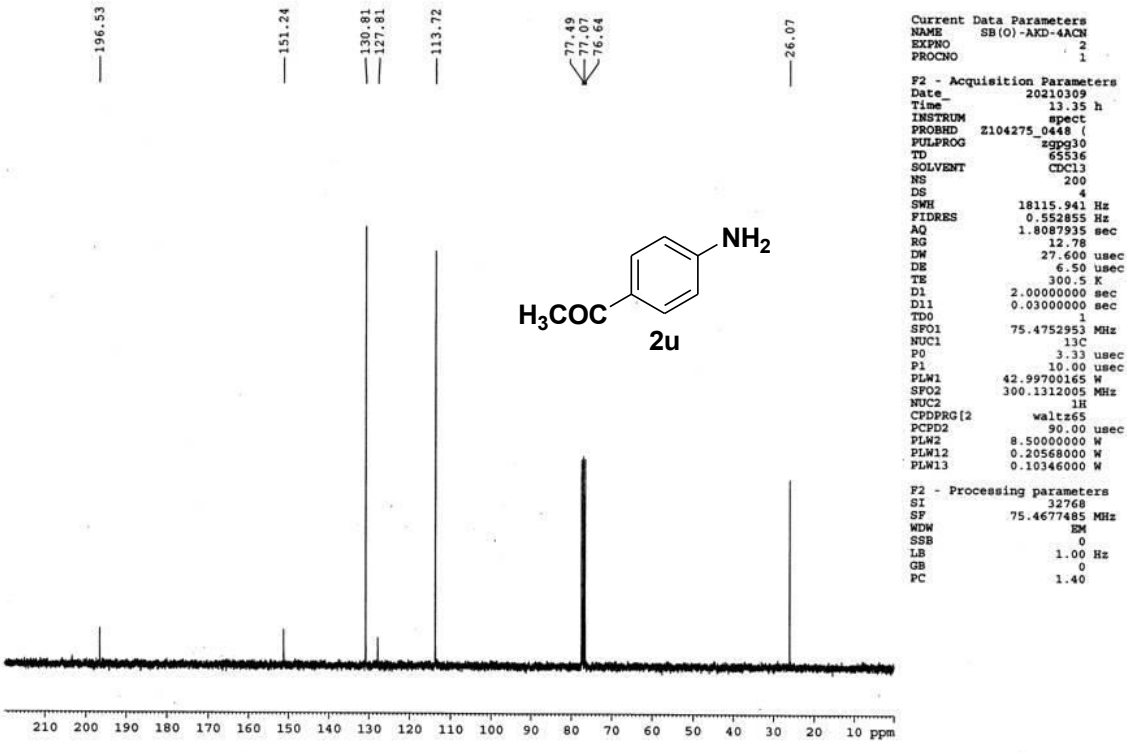

Figure 26 ^{13}C NMR of 1-(4-aminophenyl)ethanone (2u)

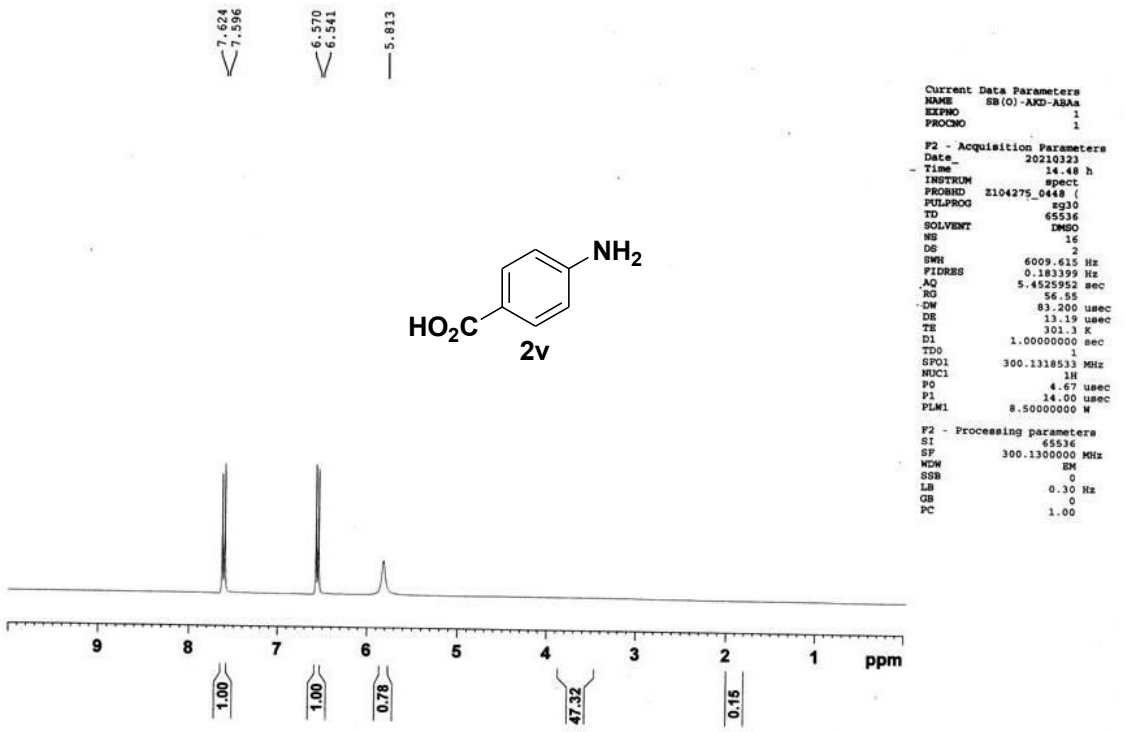

Figure 27 ^{1}H NMR of 4-aminobenzoic acid (2v)

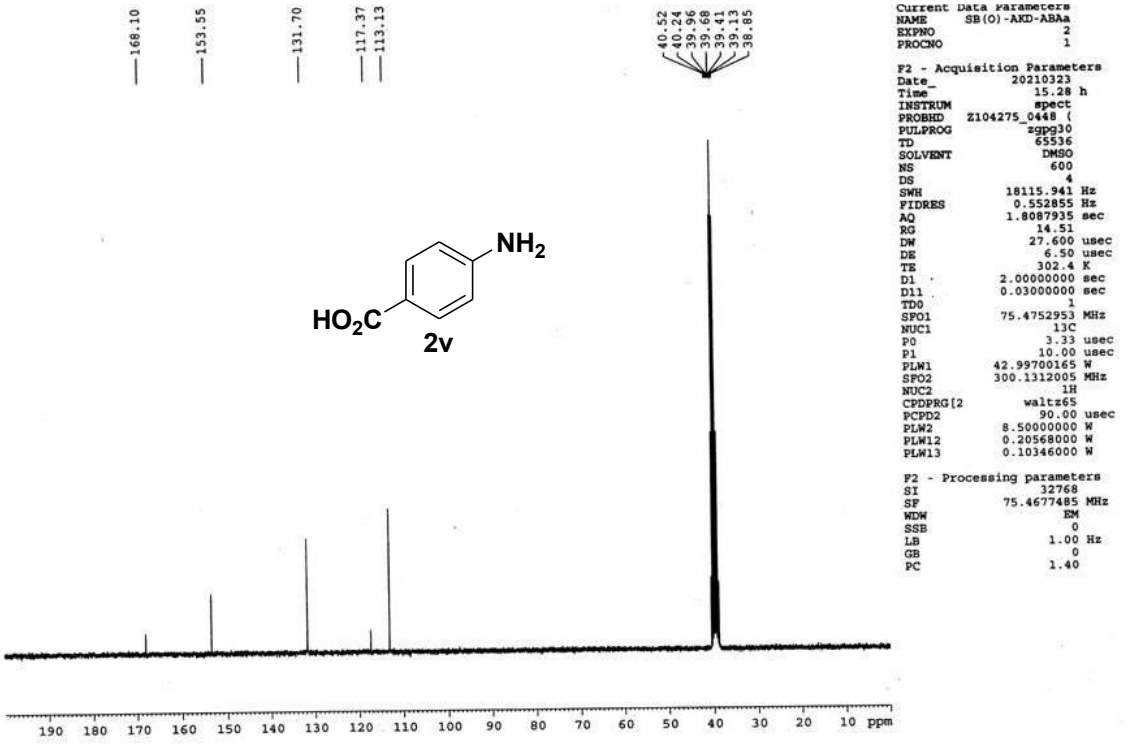

Figure 28 ^{13}C NMR of 4-aminobenzoic acid (2v)

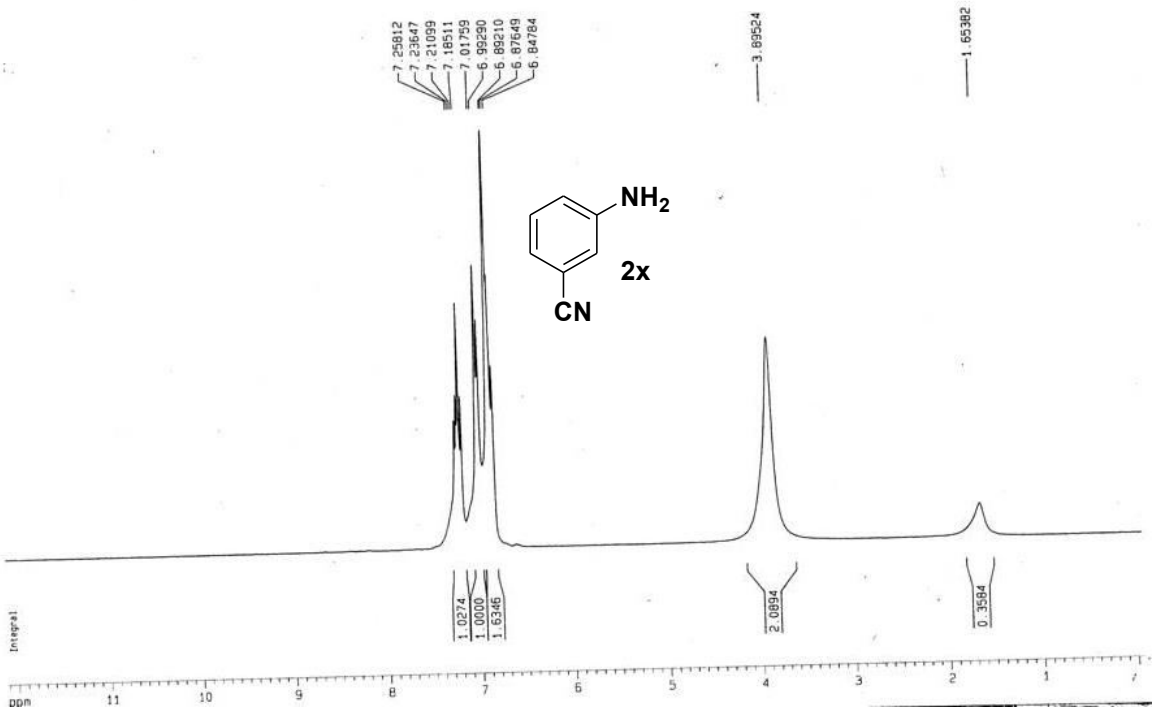

Figure 29 ^{1}H NMR of 3-aminobenzonitrile (2x)

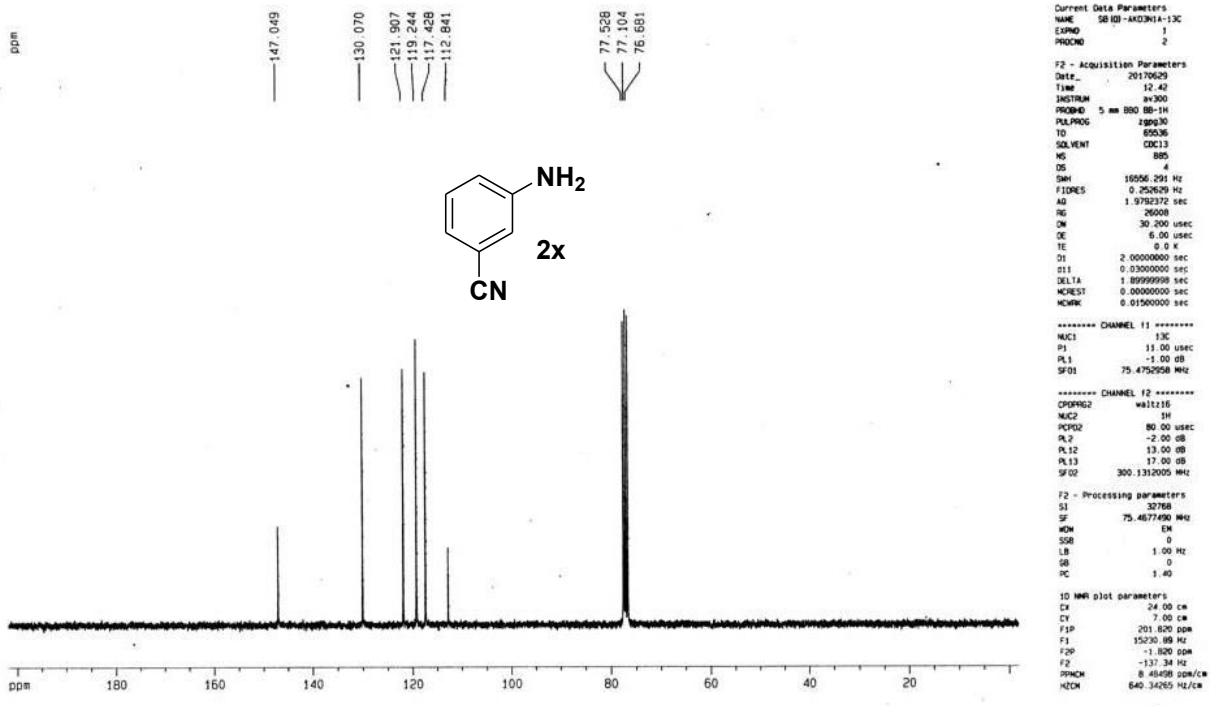

Figure 30 ^{13}C NMR of 3-aminobenzonitrile (2x)

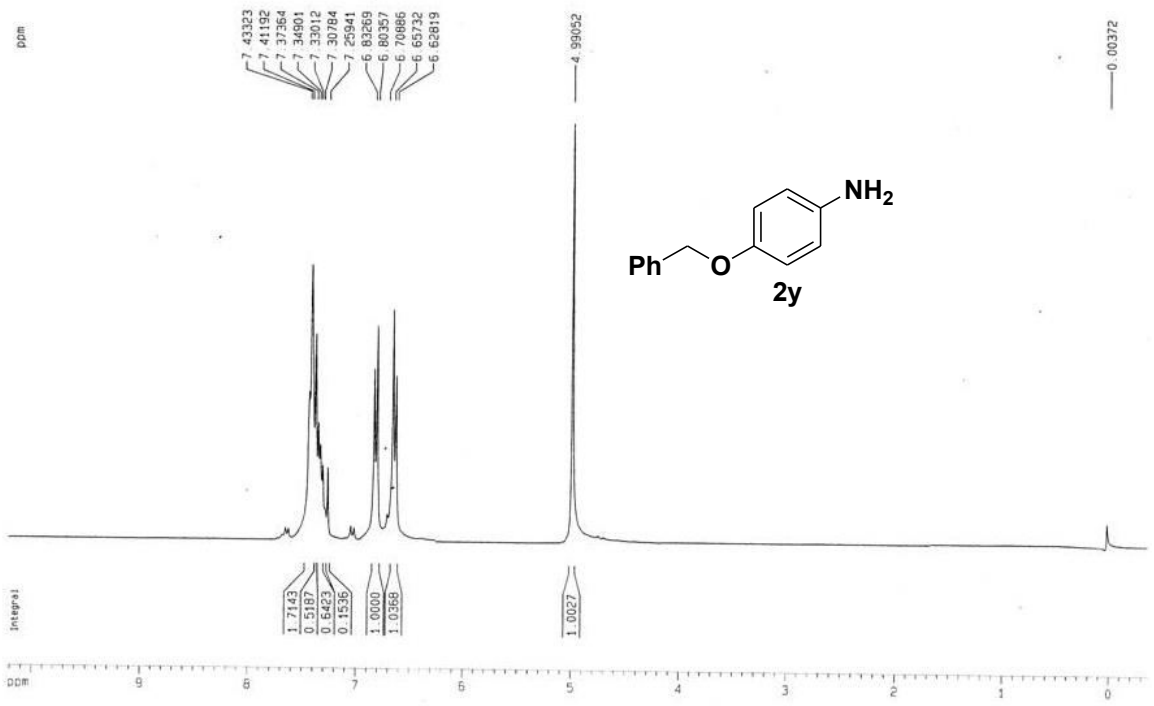

Figure 31 ^{1}H NMR of 4-benzyloxyaniline (2y)

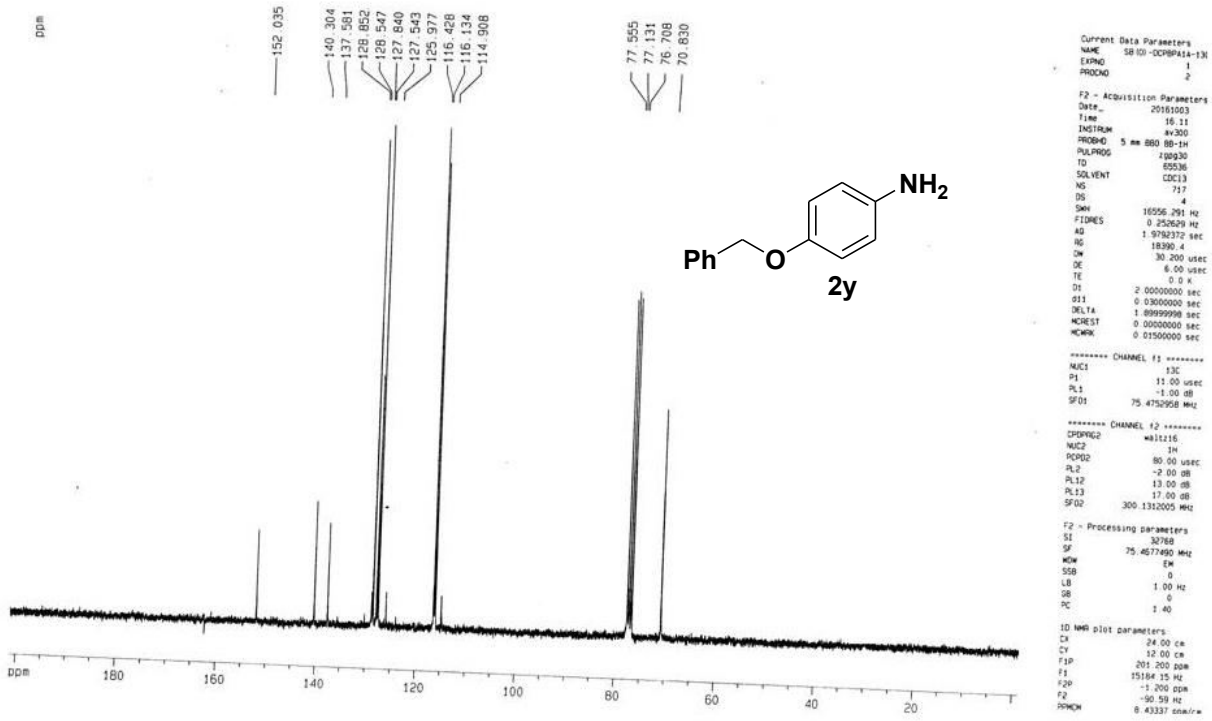

Figure 32 ^{13}C NMR of 4-benzyloxyaniline (2y)

III.6. References:

1. S. J. Brickner, D. K. Hutchinson, M. R. Barbachyn, P. R. Manninen, D. A. Ulanowicz, S. A. K. Garmon, C. Grega, S. K. Hendges, D. Toops, S. C. W. Ford, G. E. Zurenko, *J. Med. Chem.* **1996**, *39*, 673.
2. E. Farhan, D. Deininger, S. McGhie, J. Callaghan, M. S. Robertson, K. Rodgers, S. Rout, H. Singh, R. Tung, *PCT Int. Appl.* WO99/48885, **1999**.
3. D. J. Dale, P. J. Dunn, C. Golight, M. L. Hughes, P. C. Levett, A. K. Pearce, P. M. Searle, G. A. Ward, S. Wood, *Org. Process Res. Dev.* **2000**, *4*, 17.
4. (a) Z. Rappoport, *The chemistry of anilines*, John Wiley & Sons, **2007**; (b) S. Chandrasekhar, S. Prakash, C. L. Rao, *J. Org. Chem.* **2006**, *71*, 2196; (c) Q. Shi, R. Lu, L. Lu, X. Fu, D. Zhao, *Adv. Synth. Catal.* **2007**, *349*, 1877; (d) P. K. Mandal, J. S. McMurray, *J. Org. Chem.* **2007**, *72*, 6599; (e) S. Doherty, J. G. Knight, T. Backhouse, A. Bradford, R. A. B. Saunders, T. W. Chamberlain, R. Stones, A. Clayton, K. Lovelock, *Catal. Sci. Technol.* **2018**, *8*, 1454; (f) A. Celebioglu, F. Topuz, T. Uyarand, *New J. Chem.* **2019**, *43*, 3146.
5. (a) S. G. Ouellet, A. M. Walji, D. W. C. Macmillan, *Acc. Chem. Res.* **2007**, *40*, 1327; (b) M. Rueping, J. Dufour, F. R. Schoepke, *Green Chem.* **2011**, *13*, 1084; (c) S. M. Kelly, B. H. Lipshutz, *Org. Lett.* **2013**, *16*, 98; (d) D. Chusov, B. List, *Angew. Chem. Int. Ed.* **2014**, *5*3, 5199.
6. (a) R. V. Jagadeesh, D. Banerjee, P. B. Arockiam, H. Junge, K. Junge, M. M. Pohl, J. Radnik, A. Brückner, M. Beller, *Green Chem.* **2015**, *17*, 898; (b) Z. Dong, K. Liang, C. Dong, X. Li, X. Le, J. Ma, *RSC Adv.* **2015**, *5*, 20987; (c) H. Goksu, *New J. Chem.* **2015**, *39*, 8498; (d) N. M. Patil, M. A. Bhosale, B. M. Bhanage, *RSC Adv.* **2015**, *5*, 86529.
7. (a) Y. Li, Y. Zhou, X. Ma, H. Jiang, *Chem. Commun.* **2016**, *52*, 4199; (b) H. Huang, X. Wang, M. Tan, C. Chen, X. Zou, W. Ding, X. Lu, *ChemCatChem* **2016**, *8*, 1485; (c) S. S. Kotha, N. Sharma, G. Sekar, *Tetrahedron Lett.* **2016**, *57*, 1410; (d) Y. Guo, J. Li, F. Zhao, G. Lan, L. Li, Y. Liu, Y. Si, Y. Jiang, B. Yang, R. Yang, *RSC Adv.* **2016**, *6*, 7950.
8. (a) S. Yang, Z. Zhang, Q. Chen, M. He, L. Wang, *Appl Organometal Chem.* **2017**, e4132; (b) M. Tamura, N. Yuasa, Y. Nakagawa, K. Tomishige, *Chem. Commun.* **2017**, *53*, 3377; (c) B. Tang, W. Song, E. Yang, X. Zhao, *RSC Adv.* **2017**, *7*, 1531; (d) F. M. Moghaddam, S. E. Ayati, H. M. Firouzi, S. H. Hosseini, A. Pourjavadi, *Appl Organometal Chem.* **2017**,

e3825; (e) J. Zhou, Z. Chen, Z. Hu, K. Li, Y. Ai, S. Li, L. Qi, Z. Tang, L. Liu, H. Sun, *ChemistrySelect* **2017**, *2*, 6762.

9. (a) S. H. Hosseini, N. Zohreh, S. Alipour, C. Busuioc, R. Negrea, *Catalysis Commun.* **2018**, *108*, 93; (b) J. Li, L. Zhang, X. Liu, N. Shang, S. Gao, C. Feng, C. Wang, Z. Wang, *New J. Chem.* **2018**, *42*, 9684; (c) S. Sadjadi, M. Akbari, E. Monflier, M. Heravi, B. Leger, *New J. Chem.* **2018**, *42*, 15733; (d) S. Nandi, P. Patel, N. Khan, A. V. Biradar, R. I. Kureshy, *Inorg. Chem. Front.* **2018**, *5*, 806; (e) X. Liu, C. Wang, S. Cheng, N. Shang, S. Gao, C. Feng, C. Wang, Y. Qiao, Z. Wang, *Catalysis Commun.* **2018**, *108*, 103; (f) H. Huang, X. Wang, Y. Sheng, C. Chen, X. Zou, X. Shang, X. Lu, *RSC Adv.* **2018**, *8*, 8898.
10. (a) H. Miao, K. Ma, H. Zhu, K. Yin, Y. Zhang, Y. Cui, *RSC Adv.* **2019**, *9*, 14580; (b) M. Yuan, H. Zhang, C. Yang, F. Wang, Z. Dong, *ChemCatChem* **2019**, *11*, 3327; (c) M. Enneiymy, C. L. Drian, J. M. Becht, *New J. Chem.* **2019**, *43*, 17383; (d) A. A. Mekkaoui, S. Jennane, A. Aberkouks, B. Boualy, A. Mehdi, M. A. Ali, L. Firdoussi, S. Houssame, *Appl Organometal Chem*. **2019**, e5117; (e) G. Wang, S. Yuan, Z. Wu, W. Liu, H. Zhan, Y. Liang, X. Chen, B. Ma, S. Bi, *Appl Organometal Chem*. **2019**, *33*, e5159; (f) Y. Sheng, X. Wang, Z. Xing, X. Chen, X. Zou, X. Lu, *ACS Sustainable Chem. Eng.* **2019**, *7*, 8908.
11. (a) L, Zhang, L. Zhang, S. Cheng, X. Zhou, N. Shang, S. Gao, C. Wang, *Appl Organomet Chem.* **2020**, e5684; (b) Y. Lei, Z. Chen, G. Lan, R. Wang, X. Zhou, *New J. Chem.* **2020**, *44*, 3681; (c) S. Yue, X. Wang, S. Li, Y. Sheng, X. Zou, X. Lu, C. Zhang, *New J. Chem.* **2020**, *44*, 11861.
12. (a) A. K. Das, N. Sepay, S. Nandy, A. Ghatak, S. Bhar, *Tetrahedron Lett.* **2020***, 61,* 152231; (b) S. Nandy, A. K. Das, S. Bhar, *Synth. Commun.* **2020**, *50*, 3326.
13. (a) D. Shen, Q. Wu, M. Wang, Y. Yang, E. J. Lavoie, J. E. Simon, *J. Agric Food Chem.* **2006**, *54*, 3219; (b) X. C. Li, C. Liu, L. X. Yang, R. Y. Chen, *J Asian Nat Prod Res.* **2011**, *13*, 826; (c) B. D. Hiraganahalli, V. C. Chinampurdur, S. Dethe, *Pharmacogn Mag.* **2012**, *8*, 116; (d) S. J. Stohs, D. Bagchi, *Phytother. Res.* **2015**, *29*, 818; (e) C. Crestini, H, Lange, G. Bianchetti, *J. Nat. Prod.* **2016**, *79*, 2287.
14. (a) K. Murugesan, T. Senthamarai, M. Sohail, M. Sharif, N. V. Kalevaru, R. V. Jagadeesh, *Green Chem.* **2018**, *20*, 266; (b) Y. Liu, M. Su, D. Li, S. Li, X. Li, J. Zhao, F. Liu, *RSC Adv.* **2020**, *10*, 6763.

15. M. Yamaura, R. L. Camilo, L. C. Sampaio, M. A. Macedo, M. Nakamurad, H. E. Toma, *J. Magn. Magn. Mater.* **2004**, *279*, 210.
16. M. Qi, K. Zhang, S. Li, J. Wu, C. Pham-Huy, X. Diao, H. He, *New J. Chem.* **2016**, *40*, 4480.
17. M. Senthil, C. Ramesh, *Digest Journal of Nanomaterials and Biostructures*, **2012**, *7*, 1655.
18. G. Shruthi, K. Shiva Prasad, T. P. Vinod, V. Balamurugan, C. Shivamallu, *ChemistrySelect* **2017**, *2*, 10354.
19. B. Mahdavi, S. Saneei, M. Qorbani, M. Zhaleh, A. Zangeneh, M. M. Zangeneh, E. Pirabbasi, N. Abbasi, H. Ghaneialvar, *Appl Organometal Chem*. **2019**, e5164.
20. P. Veerakumar, I. P. Muthuselvam, C. T. Hung, K. C. Lin, S. B. Liu, F. C. Chou, *ACS Sustainable Chem. Eng.* **2016**, *4*, 6772.
21. (a) T. Yamashita, P. Hayes, *Appl. Surf. Sci.* **2008**, *254*, 2441; (b) S. Poulin, R. Franca, L. M. Belanger, E. Sacher, *J. Phys. Chem. C.* **2010**, *114*, 10711; (c) N. Eltouny, P. Ariya, *Ind. Eng. Chem. Res.* **2012**, *51*, 12787.
22. D. Wilson, M. A. Langell, *Appl. Surf. Sci.* **2014**, *303*, 6.
23. (a) M. Joharian, A. Morsail, A. A. Tehrani, L. Carlucci, D. M. Proserpio, *Green Chem.* **2018**, *20*, 5336; (b) S. Nandy, A. Ghatak, A. K. Das, S. Bhar, *Synlett* **2018**, *29*, 2208; (c) H. Zou, J. Dai, R. Wang, *Chem. Commun.* **2019**, *55*, 5898.
24. A. Furst, R. C. Berlo, S. Hooton, *Chem. Rev*. **1965**, *65*, 51.
25. H. E. B. Lempers, R. A. Sheldon, *J. Catal.* **1998**, *175*, 62.
26. D. C. Gowda, B. Mahesh, *Synth. Commun.* **2000**, *30*, 3639.

CHAPTER IV

$Cu(OAc)_2$ Catalysed Aerobic Oxidative Transformation of Aldehydes to Nitriles under Ligand-Free Condition

IV. $Cu(OAc)_2$ Catalysed Aerobic Oxidative Transformation of Aldehydes to Nitriles under Ligand-Free Condition

IV.1. Introduction

Nitrile is an important functional group that has been used for various organic transformations towards the synthesis of dyes, pigments, materials, polymers, natural products, agrochemicals, and pharmaceuticals.[1] Moreover, nitriles also serve as a recurrent pharmacophore in many commercially available drugs, such as Bicalutamide® (prostate cancer and breast cancer therapies), Citalopram® (antidepressant drug), Etravirine® (anti-HIV), Fadrozole® (oncolytic drug), Letrozole® (breast cancer therapy), Periciazine® (anti-psychotic drug) and 5-lipoxygenase inhibitors have been recognized (Figure 1).[2] In view of their multifarious applications in a multitude of fields, development of new and improved synthetic strategies towards the construction of substituted nitrile derivatives remains attractive attention to the synthetic chemists of all times. This review summarizes the recent findings on the oxidative transformation of aldehydes to nitriles using different catalysts as well as various nitrogen sources in the field of synthetically useful organic transformations.

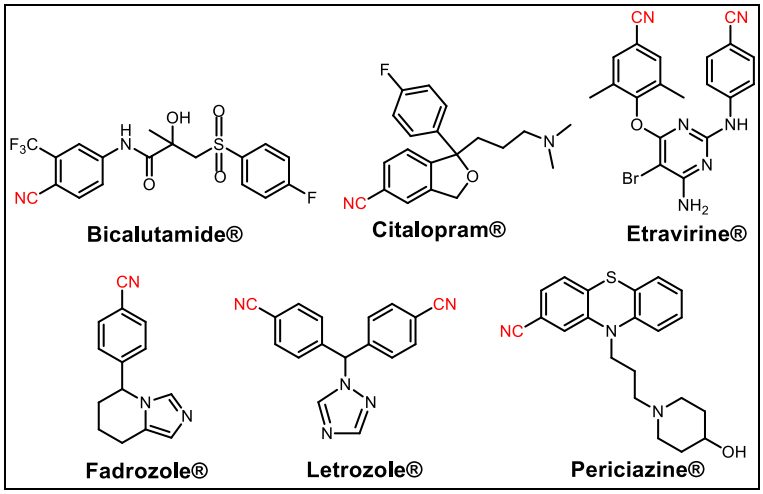

Figure 1 Some potent biologically active organonitrile drugs

IV.2. Oxidative transformation of aldehydes to nitriles: A review

J. Kim and his group[3a] have developed a transition-metal-free protocol for the oxidative transformation of aldehydes to nitriles in the presence of the catalytic amount of 4-acetamido-2,2,6,6-tetramethylpiperidine-N-oxyl (4-AcNH-TEMPO), $NaNO_2$, and HNO_3 under O_2 atmosphere using a balloon (Scheme 1). Aromatic aldehydes bearing several functional groups smoothly condensed with NH_4OAc as the nitrogen source and produced nitriles

selectively with moderate to good yields. Moreover, this protocol also effective for the aerobic oxidative conversion of primary alcohol instead of aldehyde by a one-pot sequential strategy.

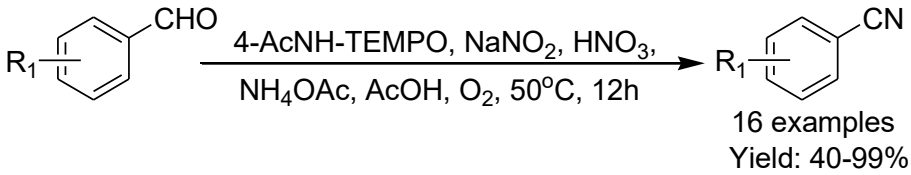

Scheme 1 4-AcNH-TEMPO catalyzed oxidative conversion of aldehydes to nitriles

Oxoammonium salt mediated another transition-metal-free protocol for the synthesis of nitriles directly from aldehydes was reported by Leadbeater and his group.[3b] They used 4-acetylamino-2,2,6,6-tetramethylpiperidine-1-oxoammonium tetrafluoroborate as an oxoammonium salt and hexamethyldisilazane (HMDS) as an ammonia surrogate in the presence of pyridine as the base in dichloromethane solvent (Scheme 2). Various structurally varied nitriles were synthesized from the corresponding aldehydes with good to excellent yields.

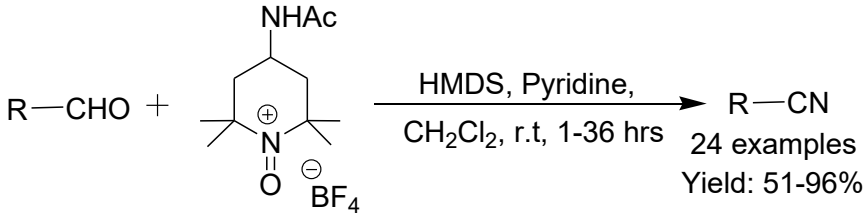

Scheme 2 Oxoammonium salt mediated synthesis of nitriles from aldehydes

Nimnual *et al.*[3c] described the synthesis of diversely functionalized nitriles starting from aldehydes in the presence of $ZrCl_4$ as the catalyst and $TMSN_3$ as the nitrogen source (Scheme 3). Aromatic aldehydes bearing both electron-donating and electron-withdrawing substituents were successfully participated and yielded the desired nitriles with moderate to good yields. It was observed that the reaction of salicylaldehyde provided the *o*-hydroxybenzonitrile with 43% yield and benzisoxazole with 29% yield in an almost 1.5:1 ratio.

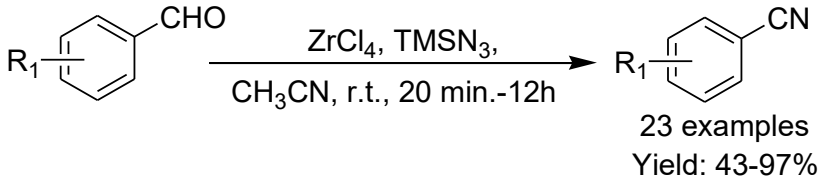

Scheme 3 $ZrCl_4$ catalyzed synthesis of nitriles from aldehydes using $TMSN_3$

Copper nanoparticles supported on sulfonic acid functionalized silica/carbon composites (Cu(0)-SilC_{cell}-SO_3H)[4a] were successfully synthesized and utilized as an efficient

heterogeneous catalyst for the direct conversion of aldehydes to nitriles using aqueous NH_3 as the nitrogen source and H_2O_2 as the oxidant (Scheme 4). Various oxidants such as molecular oxygen O_2, TBHP, and hydrogen peroxide (H_2O_2) were examined in the presence of aqueous ammonia at temperatures ranging from room temperature to 120°C. Hydrogen peroxide (H_2O_2) was found to be the best oxidant in this process. This protocol accommodated a broad range of various electron releasing as well as electron withdrawing substituents with good to excellent yields.

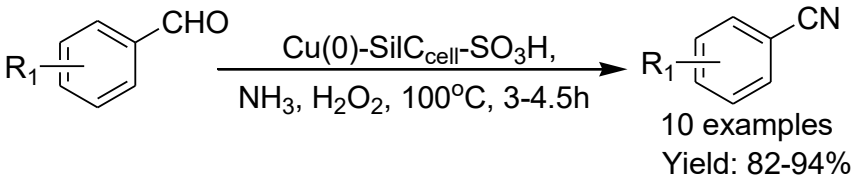

Scheme 4 Synthesis of nitriles from aldehydes using Cu(0)-$SilC_{cell}$-SO_3H nanocatalyst

Fang *et al.*[4b] described an efficient one-pot oxidative methodology for the preparation of nitriles from aldehydes using TEMPO (2,2,6,6-tetramethylpiperidine l-oxyl) as the catalyst, KPF_6/$NaNO_2$ or TBN (tert-butyl nitrite) as the co-catalyst, HMDS (hexamethyldisilazane) as the nitrogen source, molecular O_2 as the terminal oxidant under mild reaction conditions (Scheme 5). Various kinds of aldehydes including aromatic, aliphatic, and allylic aldehydes were well tolerated and converted into their corresponding nitriles with moderate to excellent yields.

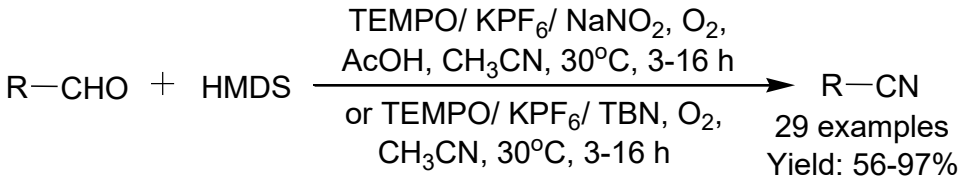

Scheme 5 Oxidative conversion of aldehydes to nitriles using HMDS

Aloe vera mediated silver nanoparticles (AgNPs-Av)[4c] using $AgNO_3$ as the metal precursor have been synthesized and well-characterized by Das *et al*. The catalytic efficacy of the prepared AgNPs-Av was tested for the one-pot conversion of aldehydes into nitriles using $K_4[Fe(CN)_6]$ as a cyanation agent under ambient conditions in an aqueous medium (Scheme 6). The oxidative conversion of benzaldehyde derivatives carrying different electron releasing and withdrawing moieties into their corresponding nitriles proceeded smoothly with good to excellent yields. The AgNPs-Av catalyst recycled up to the 3rd consecutive catalytic runs without significant loss in its reactivity.

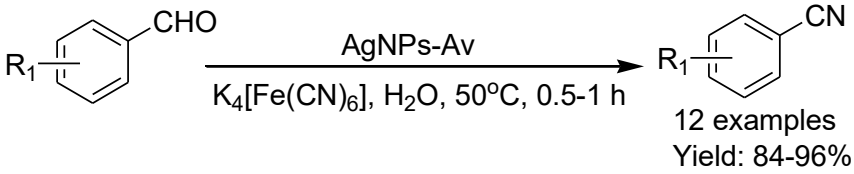

Scheme 6 Ag NPs catalyzed oxidative conversion of aldehydes to nitriles

CTAB stabilized Fe_3O_4 nanoparticles (Fe_3O_4-CTAB NPs)[4d] have been synthesized and characterized by SEM, TEM, and XRD analysis. The synthesized Fe_3O_4-CTAB NPs have been utilized as a competent catalyst for the direct synthesis of nitriles from aldehydes using hydroxylamine hydrochloride ($NH_2OH.HCl$) as the nitrogen source in DMF medium under reflux condition (Scheme 7). The reaction furnished only oxime and nitrile derivatives when the reaction was investigated at the temperature range between 50-70°C and reflux condition in DMF medium respectively. This methodology described the one-pot conversion of aromatic, heterocyclic, and aliphatic aldehydes to a variety of nitriles with moderate to good yields. The advantages of this protocol include the utilization of inexpensive and relatively less toxic nanocatalyst, good yields of the products, easy reaction setup as well as work-up process.

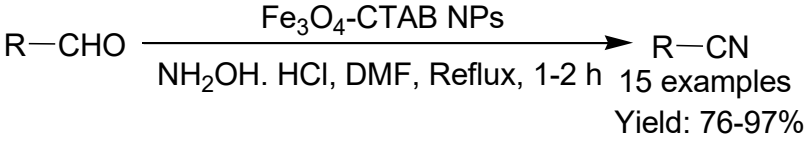

Scheme 7 Fe_3O_4-CTAB NPs catalyzed synthesis nitriles of aldehydes

Aerobic oxidative one-pot transformation of aromatic aldehydes into their corresponding aromatic nitriles was achieved by using a copper catalyst (Cu@C), which was produced by the pyrolysis of HKUST-1 ($Cu_3(BTC)_2$, BTC=1,3,5-benzenetricarboxylate).[4e] A series of aromatic aldehydes bearing various substituents underwent a smooth condensation with aqueous NH_3 and the subsequent oxidation to furnish the desired nitriles with moderate to good yields in the presence of Cu@C and TEMPO (2,2,6,6-tetramethyl-1-piperidinyloxy) in DMF medium (Scheme 8). The synthesized Cu@C catalyst was heterogeneous and reusable without the much loss of its reactivity.

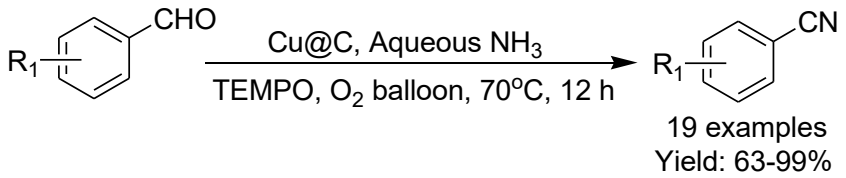

Scheme 8 Heterogeneous Cu catalyzed direct synthesis nitriles of aldehydes

An electrochemical approach[5a] was developed for the synthesis of nitriles from the corresponding aldehydes in an undivided cell using 4-acetamido- 2,2,6,6-tetramethylpiperidinyl-l-oxy (4-AcNH-TEMPO) as the catalyst and ammonium acetate as the nitrogen source in acetonitrile medium (Scheme 9). The electrocatalytic activity of 4-AcNH-TEMPO for the one-pot conversion of aryl aldehydes to aryl nitriles was investigated by cyclic voltammetry measurements. This electrochemical methodology was applicable for a variety of aromatic aldehydes and afforded moderate to good yields of nitriles at room temperature. The present transition metal-free protocol showed significant advantages as it was performed without stoichiometric amounts of reactive oxidants.

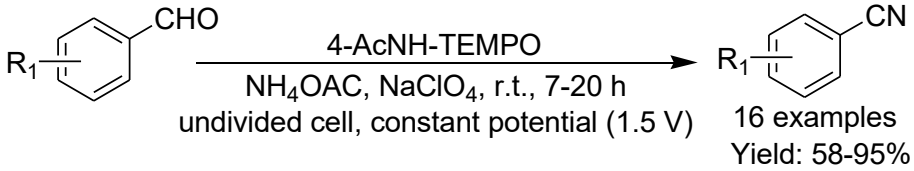

Scheme 9 Electrochemical synthesis of nitriles from aldehydes

Kim *et al.*[5b] have developed a 4-acetamido-2,2,6,6-tetramethylpiperidine-1-oxoammonium tetrafluoroborate (4-AcNH-TEMPO$^+$BF$_4^-$) mediated oxidative protocol for the one-pot conversion of aldehydes to nitriles using readily accessible NH_4OAc as the nitrogen source in an acetic acid medium under N_2 atmosphere (Scheme 10). A variety of aliphatic as well as aromatic aldehydes was successfully converted into the corresponding nitriles in good yields. Moreover, the present metal-free protocol was also effective on large scale. The oxoammonium salt (4-AcNH-TEMPO$^+$BF$_4^-$) was recovered by simple acid-base extraction and followed by oxidation with NaOCl, HBF_4, and $NaBF_4$.

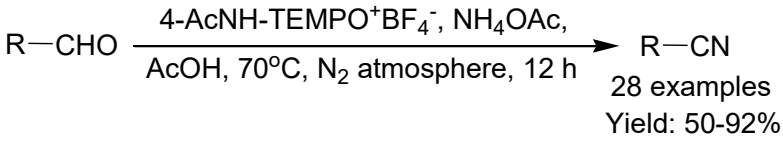

Scheme 10 4-AcNH-TEMPO$^+$BF$_4^-$ mediated one-pot conversion of aldehydes to nitriles

Shen and his group[5c] have described an efficient methodology for the oxidative synthesis of nitriles directly from aldehydes using iodine (I_2) as the catalyst, *tert*-butyl hydroperoxide (TBHP) as an external oxidant, ammonium acetate (NH_4OAc) as the nitrogen source, and sodium carbonate (Na_2CO_3) as the weak base under mild reaction conditions (Scheme 11). The present I_2/TBHP catalytic system was highly effective to convert a wide range of aromatic, heteroaromatic, allylic, and aliphatic aldehydes into their corresponding nitriles with good to excellent yields. Aromatic aldehydes carrying electron-withdrawing

substituents were smoothly converted into the desired nitriles within 5 h, whereas aromatic aldehydes carrying electron-donating substituents required prolonged time to complete their transformation.

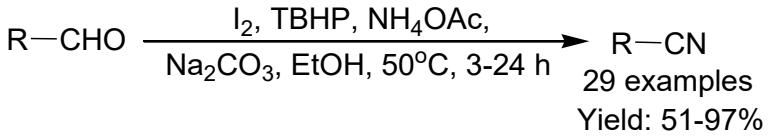

Scheme 11 I_2-TBHP catalyzed direct synthesis of nitriles from aldehydes

Visible light-mediated dual catalytic system for the oxidation of aromatic aldehydes to aromatic nitriles was described by Leadbeater and his co-workers[6a] using $Ru(bpy)_3(PF_6)_2$ as the photoredox catalyst and 4-acetamido-TEMPO as the pro-oxidants (Scheme 12). Here, $(NH_4)_2S_2O_8$ (ammonium perdisulfate) was employed as an efficient and inexpensive nitrogen source as well as acted as the terminal oxidant for this oxidative transformation. This protocol was employed for the generation of a wide range of aryl nitrile products with moderate to good yields.

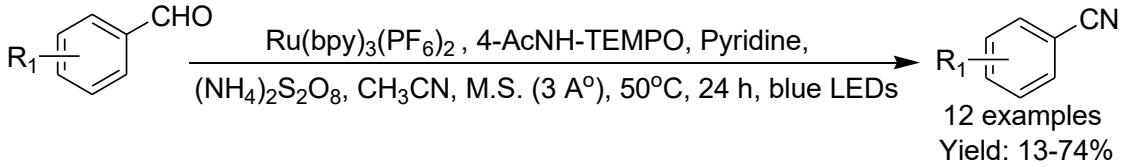

Scheme 12 Visible light-mediated photooxidation of aldehydes to nitriles

Nanoscale Fe_2O_3-based catalyst has been prepared by Murugesan *et al.*[6b] using the impregnation method of an in situ generated $Fe(II)(1,10\text{-phen})_3(OAc)_2$ complex on commercial carbon and subsequent pyrolysis at 800°C for 2h under an argon atmosphere (Fe-phen/C-800; phen=1,10-phenanthroline). The catalytic activity of Fe-phen/C-800 has been tested during the oxidative synthesis of nitriles starting from aldehydes in the presence of aqueous ammonia as the nitrogen source under the O_2 atmosphere (Scheme 13). Various functionalized and structurally diverse aldehydes bearing aromatic, heterocyclic, and aliphatic moieties well responded and produced the nitrile derivatives with moderate to good yields. This methodology was also applicable for the synthesis of amide derivatives from aldehydes in an aqueous medium.

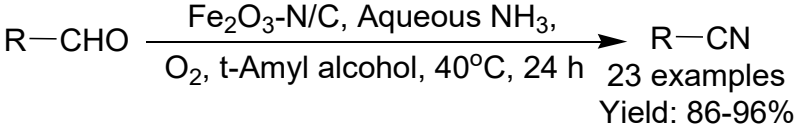

Scheme 13 Fe_2O_3-N/C-catalyzed synthesis of nitriles from aldehydes

The continuous-flow methodology was applied for the direct synthesis of nitriles from aldehydes via the classical Schmidt reaction in the presence of triflic acid (TfOH) as the catalyst and trimethylsilyl azide ($TMSN_3$) as the nitrogen source in acetonitrile medium using micro-reactor technology (Scheme 14).[7a] Substituted benzaldehydes bearing electron-donating and electron-withdrawing substituents reacted well in this protocol and the desired nitriles were achieved with good to excellent yields.

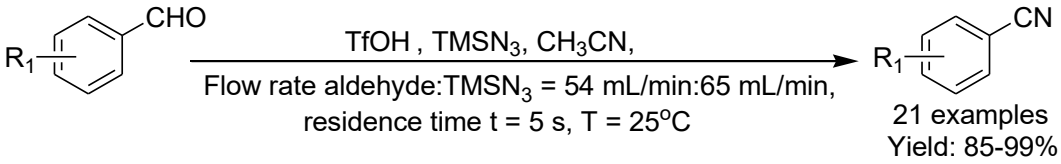

Scheme 14 Continuous-flow synthesis of nitriles from aldehydes

Chen *et al.*[7b] disclosed the direct oxidative conversion of aldehydes to nitriles mediated by $FeCl_2$ as an efficient catalyst in the presence of aqueous NH_3 as the nitrogen source, NaI as the iodine source, and $Na_2S_2O_8$ as the oxidant (Scheme 15). Both alkyl and aryl aldehydes successfully participated and produced the corresponding nitriles in good to excellent yields. Several electron-donating and electron-withdrawing groups, such as methyl, methoxy, dimethylamino, fluoro, chloro, bromo, nitro, cyano and alkoxycarbonyl were well tolerated. Moreover, the present catalytic system was also effective for the preparation of febuxostat and its intermediate (ethyl 2-[3-cyano-4-(2-methylpropoxy)phenyl]-4-methyl-5-thiazolecarboxylate).

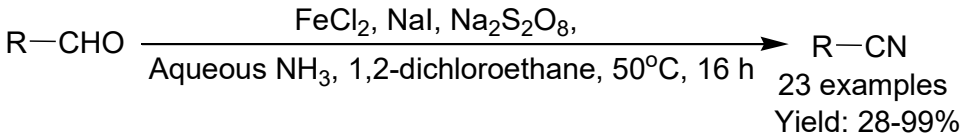

Scheme 15 Direct conversion of aldehydes to nitriles using $FeCl_2$/NaI/$Na_2S_2O_8$/Aq. NH_3

Visible light-driven oxidative transformation of aldehydes to nitriles was reported by Verma *et al.*[7c] using Co@g-C_3N_4 (g-C_3N_4 = graphitic carbon nitride) as the photocatalyst and $NH_2OH.HCl$ as the nitrogen source in an aqueous methanolic medium at room temperature (Scheme 16). Aromatic aldehydes bearing both electron-donating substituents (such as Me, OMe, OH, NHAc, ^{t}Bu) and electron-withdrawing substituents (such as F, Cl, Br, CF_3, CN, NO_2, Ac) at various positions of the phenyl ring were smoothly converted to the corresponding nitriles with good to excellent yield. Moreover, the reusability of Co@g-C_3N_4 was investigated up to five catalytic runs and it was found that the catalytic efficiency of the catalyst remained more or less the same.

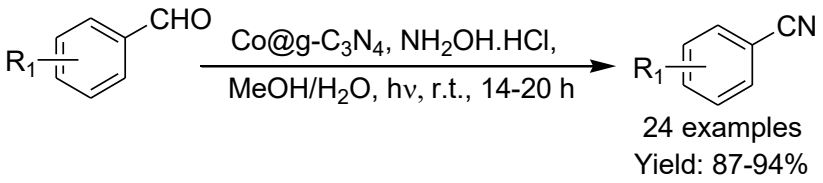

Scheme 16 Visible light-driven oxidative conversion of aldehydes to nitriles

Nandi *et al.*[7d] reported an oxidative catalytic strategy for the direct conversion of aldehydes to nitriles by the combination of photoredox catalysis with oxoammonium cations under visible light irradiation. The reaction was investigated using $Ru(bpy)_3(PF_6)_2$ as the photocatalyst, $NH_4CO_2NH_2$ (ammonium carbamate) as the nitrogen source, 4-acetamido-TEMPO (ACT) as the primary oxidant, and $(NH_4)_2S_2O_8$ (ammonium persulfate) as the secondary oxidant (Scheme 17). Several aromatic aldehydes bearing both electron releasing and electron-withdrawing groups successfully produced the corresponding nitriles with moderate to good yields.

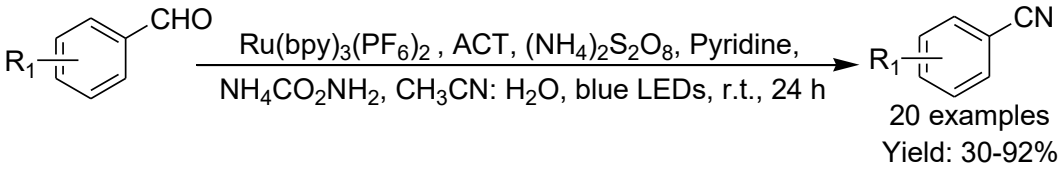

Scheme 17 Photooxidation of aldehydes to nitriles catalyzed by $Ru(bpy)_3(PF_6)_2$

Thus in the aforementioned brief account, the metal-free as well as metal-mediated oxidative transformation of aldehydes to nitriles with a plethora of substrates, catalysts, nitrogen sources and solvents has been explored to validate the necessity, inevitability, and suitability of the present exploration going to be described in the next section.

IV.3. Present investigation

IV.3.1. Background of the present investigation

The classical methods for preparing aryl nitriles involve Sandmeyer reaction[8a-8d] of aromatic diazonium salts and Rosenmund-von Braun reaction[8e] of aryl halides, which require the stoichiometric amount of highly toxic CuCN and harsh reaction conditions. Other alternative approaches for nitrile synthesis such as hydrocyanation of alkenes,[9] Kolbe nitrile synthesis,[10] methyl arenes,[11] oxidative rearrangement of alkene,[12a] benzyl or allyl halides,[12b,] and cyanation of aryl halides[13] were reported in the last few years, but many of these methods suffer limitations such as high temperature (>100^{o}C), use of toxic and corrosive reagents, the requirement of capricious ligands, inert atmosphere, lower atom economy and poor functional group tolerance. Recently, the direct oxidative transformation of aldehyde to nitrile

has received substantial interest due to their operational simplicity, better atom efficiency, cost-effectiveness as well as obviation of the isolation of intermediates compare to traditional ones. Therefore, several synthetic strategies using different nitrogen sources viz., NH_4OAc,[3a,5a,5b,5c] $TMSN_3$,[3c,7a] $NH_4CO_2NH_2$,[7d] $NH_2OH.HCl$,[4d,7c] NH_3,[4a,4e,6b,7b] hexamethyldisilazane (HMDS)[3b,4b] in the presence of various catalysts has been developed in the last few years. However, despite the potential utility of the reported protocols, the use of hazardous reagents, expensive ligands, toxic solvents as well as additives, and laborious catalyst preparation along with the production of large amounts of waste into the environment and tedious work-up procedures limits their application from the green and sustainable perspective.

Therefore, development of highly efficient protocol by avoiding the use of toxic and expensive metal catalysts and utilizing the less hazardous and inexpensive reagents for the synthesis of nitriles is of great demand in the perspective of the present environmental scenario. In continuation of our efforts toward the development of novel eco-compatible methodologies, we report herein a mild and efficient oxidative protocol for the direct transformation of aldehydes to nitriles using non-toxic copper acetate as an inexpensive catalyst and ammonium acetate as the source of nitrogen in the presence of environmentally benign aerial oxygen as an eco-friendly oxidant under ligand and base free condition with a broad substrate scope and tolerance of various sensitive moieties during the reaction.

IV.3.2. Results and Discussion

IV.3.2.1. Catalytic efficiency of $Cu(OAc)_2$

Firstly, we conducted a series of experiments to optimize the reaction conditions for the oxidative transformation of 4-methoxybenzaldehyde **1a** to the corresponding nitrile **2a** in the presence of different copper salts as well as various nitrogen sources, and the results are presented in Table 1. The reaction did neither occur at all in the absence of any copper salt (Entry 1) as well as $CuSO_4$ with $(NH_4)_2SO_4$ in EtOH solvent (Entry 5), the unreacted substrates were isolated intact. Moreover, the reaction could not proceed well to improve the yield when the reaction was performed in presence of $CuSO_4$ with aqueous NH_3 in DMSO medium (Entry 2), $CuSO_4$ with $(NH_4)_2SO_4$ in DMSO and CH_3CN medium (Entries 3, 4), $CuCl_2$ with NH_4Cl in DMSO and DMF solvent (Entries 6, 7) and $Cu(NO_3)_2$ with NH_4NO_3 in DMSO and CH_3CN medium (Entries 8, 9).

Table 1 Optimization of reaction conditions[a]

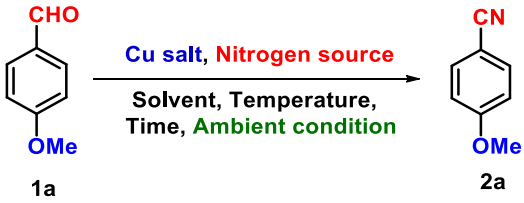

1a 2a

Entry	Cu salt (mol %)	Nitrogen source (mmol)	Solvent (mL)	Temp. (^oC)	Time (hrs)	Yield[b] (%)
1	--	NH_4OAc	DMSO	60°C	12h	--
2	$CuSO_4$	Aq. NH_3	DMSO	60°C	12h	28
3	$CuSO_4$	$(NH_4)_2SO_4$	DMSO	60°C	12h	47
4	$CuSO_4$	$(NH_4)_2SO_4$	CH_3CN	60°C	12h	35
5	$CuSO_4$	$(NH_4)_2SO_4$	EtOH	60°C	12h	--
6	$CuCl_2$	NH_4Cl	DMSO	60°C	12h	45
7	$CuCl_2$	NH_4Cl	DMF	60°C	12h	49
8	$Cu(NO_3)_2$	NH_4NO_3	DMSO	60°C	12h	53
9	$Cu(NO_3)_2$	NH_4NO_3	CH_3CN	60°C	12h	42
10	$Cu(OAc)_2$	NH_4OAc	CH_3CN	60°C	12h	73
11	***$Cu(OAc)_2$***	***NH_4OAc***	***DMSO***	***60°C***	***10h***	***90***
12[c]	$Cu(OAc)_2$	NH_4OAc	DMSO	60°C	10h	--
13	$Cu(OAc)_2$	NH_4OAc	H_2O	60°C	10h	36
14	$Cu(OAc)_2$	NH_4OAc	EtOH	Reflux	14h	54
15	$Cu(OAc)_2$	NH_4OAc	DCM	Reflux	14h	49
16	$Cu(OAc)_2$	$HCOONH_4$	DMSO	60°C	8h	--
17	$Cu(OAc)_2$	Aq. NH_3	DMSO	60°C	10h	23
18	CuO	NH_4OAc	DMSO	60°C	8h	--
19	CuCl	NH_4OAc	DMSO	60°C	8h	--

[a]Reaction conditions: **1a** (1.0 mmol), Cu salt (10 mol%), nitrogen source (1.5 mmol), solvent (3 mL), temperature (as indicated), under ambient condition. [b]Isolated yield. [c]The reaction was carried out under an inert (argon) atmosphere.

Interestingly the extent of conversion was increased to 73% when the reaction was studied in the presence of $Cu(OAc)_2$ along with NH_4OAc at 60°C in CH_3CN medium (Entry 10). Surprisingly when the reaction was performed using $Cu(OAc)_2$ along with NH_4OAc in DMSO medium under ambient atmosphere, the extent of conversion was increased to 90% within a shorter reaction time (Entry 11). But, when the reaction was performed under an

inert (Ar) atmosphere in the absence of aerial oxygen, no trace of nitrile **2a** was detected in the reaction mixture, the substrate **1a** remained intact. This observation indicated the importance of atmospheric oxygen as the eco-friendly oxidant during the aforementioned transformation (Entry 12). No significant improvement of yield was found in the presence of $Cu(OAc)_2$ with NH_4OAc in H_2O medium (Entry 13). This reaction was less responsive in ethanol (EtOH) and dichloromethane (DCM) as the solvent even under reflux and a longer period of reaction time (entries 14, 15). Interestingly, no reaction took place when ammonium formate ($HCOONH_4$) was used as the nitrogen source instead of ammonium acetate (CH_3COONH_4) in the presence of copper acetate (Entry 16). However, a lower yield was obtained in the presence of aqueous NH_3 (Entry 17). The inferior performance was observed in the case of CuO and CuCl (entries 18, 19). Among the screened copper salts and nitrogen sources, $Cu(OAc)_2$ was the most effective catalyst and NH_4OAc was the best option as the nitrogen source. Less toxicity, good stability and cheaper price of ammonium acetate (NH_4OAc) were found to be good attributes to be a better alternative nitrogen source of NH_3. Therefore, the conditions, as delineated in entry 11, have been chosen as the optimized reaction condition for further studies.

To explore the substrate scope and limitation of this oxidative protocol, a systematic investigation on all kinds of aromatic, heterocyclic, naphthyl, and aliphatic aldehydes **1** was carried out under the optimized reaction conditions to obtain the corresponding nitriles **2** (Scheme 1). The results are summarized in Table 2.

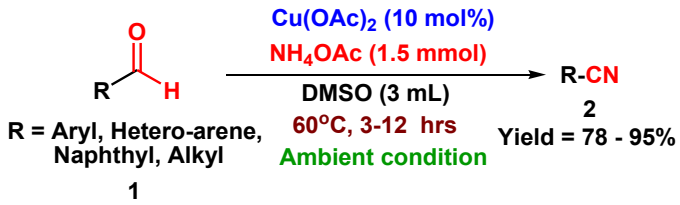

Scheme 1 $Cu(OAc)_2$ catalyzed direct oxidative transformations of aldehydes to nitriles

As evident from Table 2, benzaldehyde as well as other aryl aldehydes bearing electron-donating substituents showed an excellent reactivity and furnished the products (**2a-2e**) in high yields. Aryl aldehydes bearing phenolic -OH group were also equally efficient under the optimized reaction condition to produce the products **2f**-**2i** in good yield. Deactivated aromatic aldehydes such as N, N-dimethylaminobenzaldehyde, and 2-aminobenzaldehyde afforded the corresponding nitriles **2j** and **2k** under the present reaction condition in excellent yield. This protocol was also effective for the substrates bearing halogen which produced the nitriles **2l** and **2m** in good yield within a shorter reaction time without any dehalogenated product.

Table 2 $Cu(OAc)_2$ catalyzed direct oxidative transformations of aldehydes to nitriles

Entry	Substrate	Product	Time (hrs)	Yield (%)[a]
Synthesis of benzonitriles bearing electron-donating substituents				
1	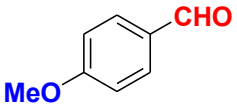 1a	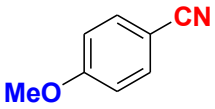 2a	10	90
2	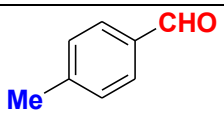 1b	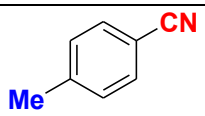 2b	10	91
3	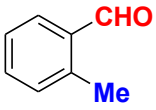 1c	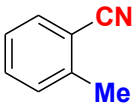 2c	10	89
4	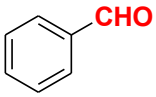 1d	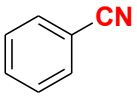 2d	7.5	90
5	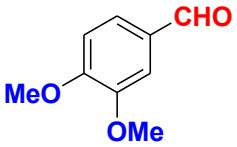 1e	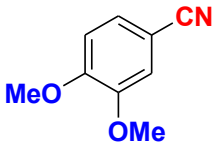 2e	10	90
Synthesis of hydroxy functionalized benzonitriles				
6	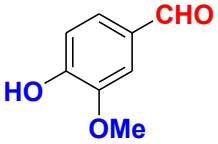 1f	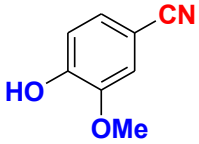 2f	10	89
7	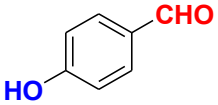 1g	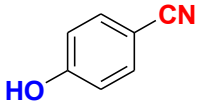 2g	10	87
8	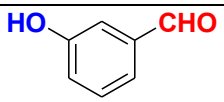 1h	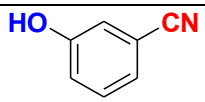 2h	10	89
9	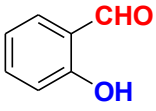 1i	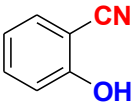 2i	10	88

Synthesis of amino functionalized benzonitriles				
10	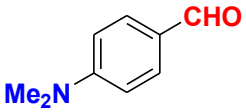 1j	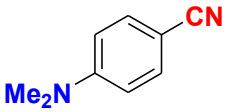 2j	9.0	88
11	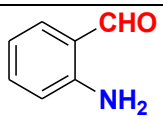 1k	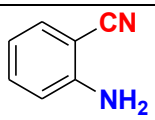 2k	9.0	89
Synthesis of halogenated benzonitriles				
12	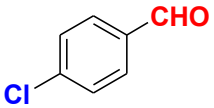 1l	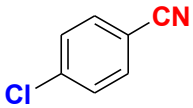 2l	6.0	93
13	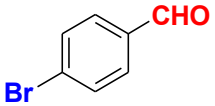 1m	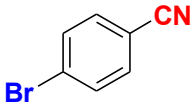 2m	6.0	91
Synthesis of nitro functionalized benzonitriles				
14	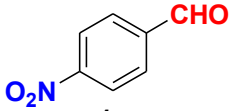 1n	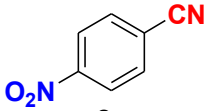 2n	3.0	95
15	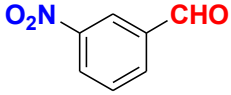 1o	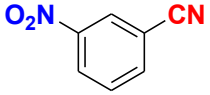 2o	3.0	94
Selectivity towards the synthesis of nitriles				
16[a]	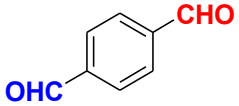 1p	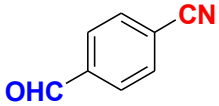 2p	6.0	88
17[b]	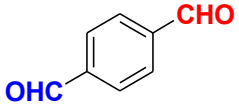 1q	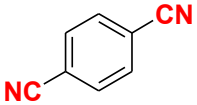 2q	6.0	87
18	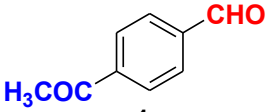 1r	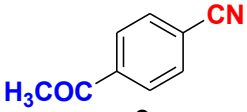 2r	6.0	88

Synthesis of nitriles bearing naphthyl, methylenedioxy and alkenyl moiety				
19	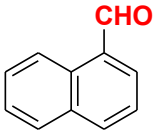 1s	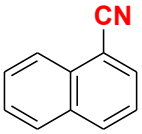 2s	11	86
20	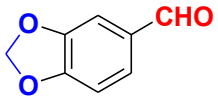 1t	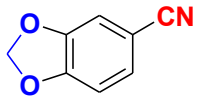 2t	10	88
21	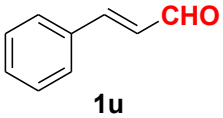 1u	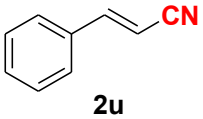 2u	10	83
Synthesis of acid sensitive heterocyclic nitriles				
22	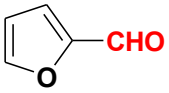 1v	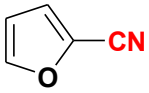 2v	10	79
23	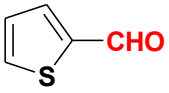 1w	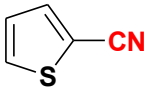 2w	10	81
24	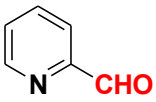 1x	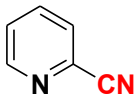 2x	10	83
25	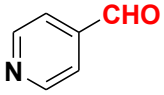 1y	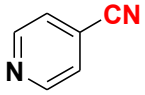 2y	10	80
Synthesis of highly vulnerable nitriles				
26	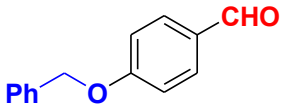 1z	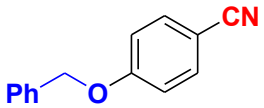 2z	10	86
27	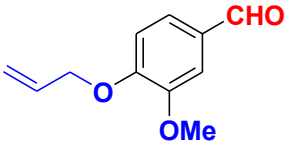 1za	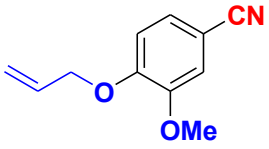 2za	10	84

28	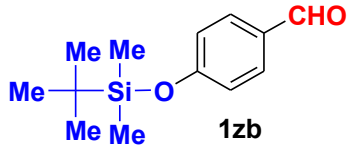 1zb	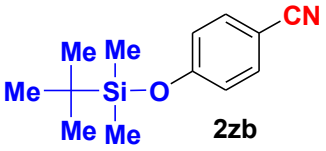 2zb	10	85
Synthesis of aliphatic nitrile				
29	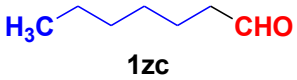 1zc	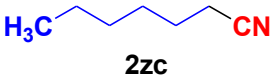 2zc	12	78

Reaction conditions: **1a** (1.0 mmol), $Cu(OAc)_2$ (10 mol%), NH_4OAc (1.5 mmol), DMSO (3 mL), 60°C, under ambient condition. [a]NH_4OAc (1.5 mmol) and [b]NH_4OAc (3.0 mmol) were used for 1 mmol of substrate.

Aldehydes carrying with electron-withdrawing groups (-NO_2) at *m*- and *p*- positions underwent efficient transformation to the corresponding nitriles **2n** and **2o** with excellent yields within 3 hours. Quite interestingly, terephthaldehyde was converted to the 4-formylbenzonitrile **(2p)** and terephthalonitrile (**2q)** in excellent yield with 1.5 mmol and 3.0 mmol of ammonium acetate respectively as the source of nitrogen with respect to 1 mmol of substrate. The structure of **2p** was substantiated by the singlet at δ 10.10 (due to –C<u>H</u>O) along with two doublets at δ 7.98 (due to aromatic protons *ortho* to –CHO) and at δ 7.84 (due to aromatic protons *ortho* to –CN). In the ^{13}C NMR spectrum of **2p**, simultaneous occurrence of two signals at δ 190.6 and δ 117.6 proves the co-existence of –<u>C</u>HO and –<u>C</u>N groups respectively. 4-Formylbenzonitrile (**2p)** furnished terephthalonitrile **2q** in good yield using 1.5 mmol of ammonium acetate. The formation of **2q** was confirmed by the presence of only one singlet due to chemically equivalent aromatic hydrogens at δ 7.52 in its ^1H NMR spectrum as well as from the signal (at δ 118.2) specific for <u>C</u>N in the ^{13}C NMR spectrum. This regioselectivity is an extremely important attribute of the present protocol in contrast to many reported methods where no such selectivity was observed.[3b,3c,7a,7d] 4-Acetylbenzaldehyde reacted smoothly to furnished 4-acetylbenzonitrile **2r** with 88% yield within 6 hours. Therefore, it can be concluded that the reaction was highly selective for aldehyde. The method was also successful for **2s** containing naphthyl moiety with satisfactory yield within 11 hours. Hydrolyzable groups like methylenedioxy *in* **2t** also survived under the aforesaid protocol. This is not commonly observed in some literature reports.[3c,4d,7a,7c] The present method was extended to the synthesis of cinnaminonitrile **2u**.

Acid-sensitive electron-rich as well as electron-deficient heteroaromatic moieties also survived during this reaction (**2v-2y**) which paved the way towards the construction of

important molecular skeletons densely loaded with heterocycles in good yields. It is extremely surprising to note the fact that highly vulnerable groups like O-benzyl, O-allyl, and O-t-butylsilyl were also tolerated under the optimized reaction condition to furnish to **2z, 2za,** and **2zb** respectively with satisfactory yields. This is not commonly observed in some literature reports.[3a,3c,4d,5a,5b,5c,7a,7c,7d] Furthermore, aliphatic nitrile **2zc** was also produced quite efficiently during a longer period under the aforesaid protocol.

IV.3.2.2. Kinetic Investigations

We next performed the kinetic experiments of the aforesaid protocol in order to determine the order of the reaction. Therefore, two identical experiments were carried out following the general procedure varying only the concentration of 4-methoxybenzaldehyde **1a** (Table 3).

Table 3 Experimental details to determine the reaction order

Run	**1a**	NH_4OAc	$Cu(OAc)_2$	DMSO
Run 1	1 mmol	1.5 mmol	10 mol%	3 mL
Run 2	2 mmol	1.5 mmol	10 mol%	3 mL

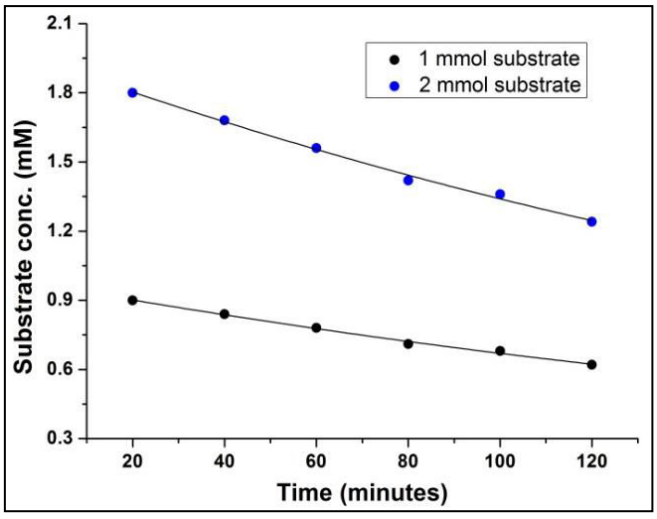

Figure 2 Dependence of the initial rate of the reaction on [4-methoxybenzaldehyde] using $Cu(OAc)_2$ (10 mol%), NH_4OAc (1.5 mmol), DMSO (3 mL), 60°C, under ambient condition.

The initial rate of the reaction for the different runs was calculated to determine the order with respect to aldehyde **1a**. The kinetic studies showed that the reaction rate was dependent on the concentration of 4-methoxybenzaldehyde **1a** only (Figure 2). Therefore, the aforesaid atom-economical oxidative protocol follows first-order kinetics.

Initial slope for Run 1 at 60 minutes = 0.0135 = 13.5×10^{-3} (mM)/min

Initial slope for Run 2 at 60 minutes = 0.0269 = 26.9×10^{-3} (mM)/min

Simplified rate equation for this system

(r) = k [4-methoxybenzaldehyde]^{a} [NH_4OAc]^{b} [$Cu(OAc)_2$]^{c} [DMSO]^{d}

(all terms have their usual significance)

Now for Run 1, $r_1=13.5\times10^{-3}$(mM)/min= k[1]^{a} [NH_4OAc]^{b} [$Cu(OAc)_2$]^{c} [DMSO]^{d} .....(1)

Now for Run 2, $r_2=26.9\times10^{-3}$(mM)/min=k [2]^{a} [NH_4OAc]^{b} [$Cu(OAc)_2$]^{c} [DMSO]^{d} .....(2)

Comparing the initial rate,

$r_1/r_2 = (13.5/26.9) = (1/2)^{a}$

or, $0.502 = 0.5^{a}$

or, log 0.502 = a log 0.5

or, a = log 0.502 / log 0.5

or, a = -0.299 / -0.301

or, a = 0.99 ~ 1

So, Rate = k [4-methoxybenzaldehyde]^{1}

Table 2 demonstrated that both electron-donating as well as electron-withdrawing substituents showed an excellent reactivity and produced the desired products in excellent yield with different time intervals and an electronic effect was observed in this direct oxidative transformation of aldehydes to nitriles. Therefore, kinetic experiments were carried out using several electronically disparate benzaldehydes following the general procedure (Figure 3).

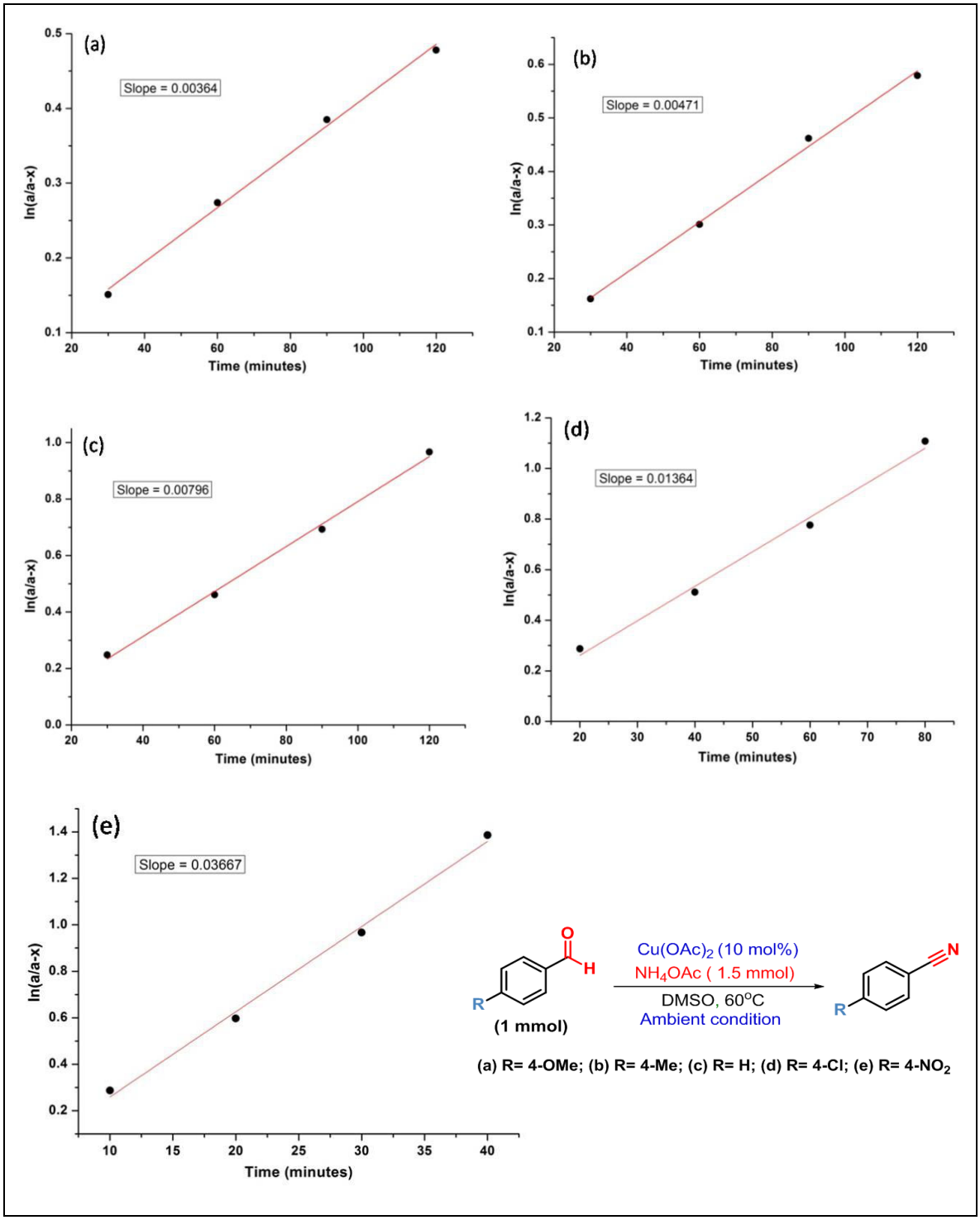

Figure 3 Determination of rate constant for the electronically disparate aldehydes during the synthesis of nitriles (a-e).

It was evident from Figure 3 that the reactions with electron-withdrawing substituent were faster than with electron-donating substituent and better conversion was achieved within a shorter reaction time in the former case. It was also evident that the reaction with 4-nitrobenzaldehyde was nine times faster than with 4-methoxybenzaldehyde. Therefore,

Hammett analysis (Table 4) was carried out using various substituted benzaldehydes under the optimized reaction conditions. A very good linear relationship was observed when relative rates [$\log(k_X/k_H)$] with these substituted benzaldehydes were plotted against the substituent constant (σ) (Figure 4). It was also observed that a positive ρ value of +0.95 and the reactivity sequence: *p*-NO_2 >*p*-Cl >*p*-H >*p*-Me >*p*-OMe for this oxidative protocol. This observation further suggested that the electron-withdrawing substituent should enhance the reaction and the results were consistent with the reactivity of the substrates reported in Table 2.

Table 4 Hammett Analysis with the para-substitution Constant (σ_P)

Substrate	$k\times10^{-4}$ (min^{-1})	k_X/k_H	$\log (k_X/k_H)$	σ_P	ρ
4-methoxybenzaldehyde	36.4	0.457	-0.340	-0.268	
4-methylbenzaldehyde	47.1	0.591	-0.228	-0.170	
benzaldehyde	79.6	1	0	0	+ 0.95
4-chlorobenzaldehyde	136.4	1.713	0.234	0.230	
4-nitrobenzaldehyde	366.7	4.606	0.663	0.780	

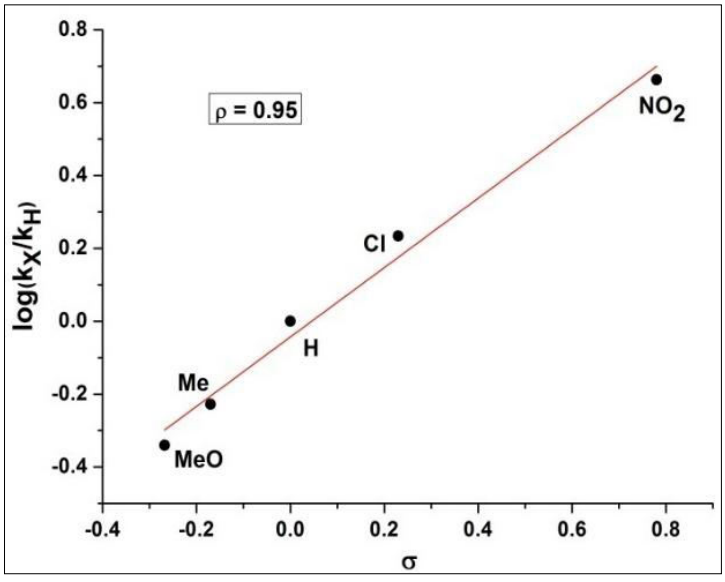

Figure 4 Hammett analysis of electronically disparate aldehydes for the direct synthesis of nitriles from aldehydes using standard reaction conditions.

IV.3.2.3. Mechanistic pathway

Based on the aforesaid investigations and literature precedence,[3a,14a,14b,14c] a plausible mechanistic pathway for this oxidative transformation is depicted in Scheme 1. First of all, $Cu(OAc)_2$ activates the carbonyl carbon to react with NH_4OAc to form aldimine intermediate (A). Then the unstable aldimine intermediate (A) reacts with $Cu(OAc)_2$ to form the iminylcuprate intermediate (B), which on subsequent oxidation forms the corresponding nitrile **2** with the liberation of CuOAc which further oxidized to $Cu(OAc)_2$ in the presence of aerial oxygen. Here, $Cu(OAc)_2$ serving as a Lewis acid and aerial oxygen acts as an eco-friendly oxidant towards this oxidative transformation.

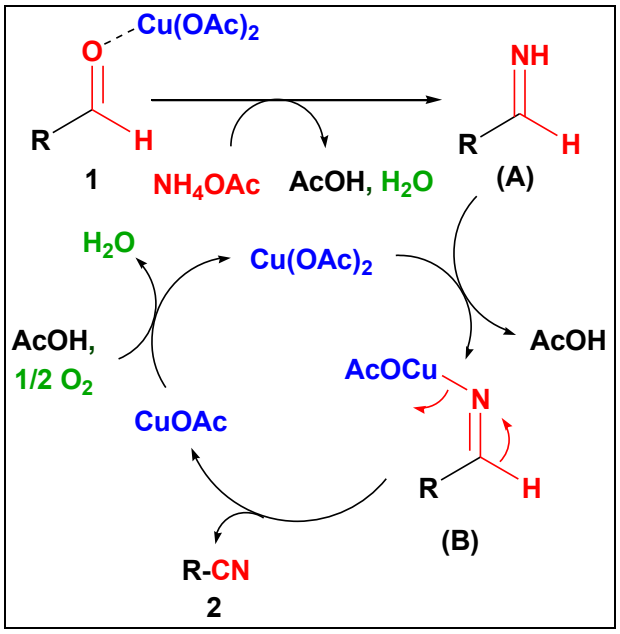

Scheme 2 Plausible mechanism for the oxidative transformation of aldehydes to nitriles.

IV.3.2.4. Scale-up Experiment

To ensure the synthetic scalability and practical applicability of our newly developed oxidative protocol, a gram scale reaction of 4-methoxybenzaldehyde **1a** was performed (Scheme 3) which was almost the same as that in the small scale reaction. The reaction mixture was extracted with EtOAc and the crude was further purified by column chromatography on a short column of silica gel using 1-5% ethyl acetate-hexane as eluent to obtain **2a**. Therefore, $Cu(OAc)_2$ / NH_4OAc catalyzed oxidative protocol can be readily scaled up to gram-scale, which bears a significant prospect for industrial production.

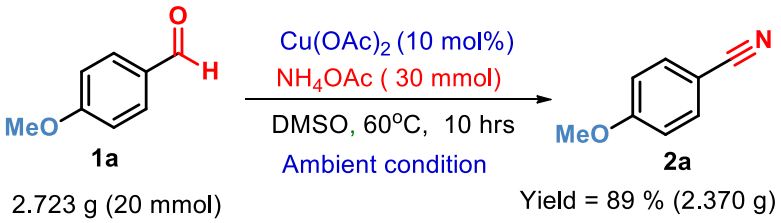

Scheme 3 Gram scale applicability of $Cu(OAc)_2/NH_4OAc$ catalyzed oxidative protocol.

IV.4. Conclusion

We have developed an oxidative protocol for the direct conversion of aldehydes to nitriles using commercially available non-toxic copper acetate as an inexpensive catalyst and ammonium acetate as the source of nitrogen in the presence of environmentally benign aerial oxygen as an eco-friendly oxidant under ligand-free and base-free condition. The kinetic experiments showed the first-order dependency on the aldehyde substrate in the reaction rate. Moreover, Hammett's analysis confirmed that the reaction was faster with the electron-deficient aldehydes. Notably, the synthetic utility and practical applicability of this newly developed protocol were demonstrated through a scale-up experiment. The salient features of the present protocol are procedural simplicity, ready accessibility and lower toxicity of the copper catalyst as well as the nitrogen source, sustainability in terms of using aerial oxygen as an eco-friendly oxidant, and tolerance of various sensitive moieties during the reaction.

IV.5. Experimental

Materials and methods

All reactants were purchased from SRL, AVRA Chemicals, Alfa-aesar, Spectrochem, and Sigma Aldrich and used as received without further purification. ^{1}H and ^{13}C NMR spectra were obtained on a Bruker spectrometer (300 MHz and 400 MHz) in $CDCl_3$ and DMSO-d_6 solutions with TMS as an internal reference. Melting points were determined in open capillary on electrical bath which is uncorrected. Column chromatography was performed on silica gel (60-120 mesh) from SRL, India. Thin layer chromatographic separations were performed on pre-coated silica gel plates using silica gel G for TLC (E. Merck).

General experimental procedure for the $Cu(OAc)_2$ catalyzed oxidative transformation of aldehydes to nitriles:

To a stirred suspension of aldehyde **1** (1.0 mmol) and ammonium acetate (1.5 mmol) in DMSO (3 mL), $Cu(OAc)_2$ (10 mol %) was added. The reaction mixture was stirred for an appropriate time at 60°C under ambient atmosphere. The progress of the reaction was monitored with TLC. Then the reaction mixture was cooled to room temperature, ethyl acetate (15 mL) was added to dissolve the product. The reaction mixture was repeatedly extracted with ethyl acetate (3×5 mL). The combined organic extracts were washed with water (3× 5 mL) and dried over anhydrous Na_2SO_4. The crude product **2** was obtained by removal of the solvent under reduced pressure which was further purified by column chromatography on a short column of silica gel using 1-10% ethyl acetate-hexane as eluent.

Procedure for the $Cu(OAc)_2$ catalyzed gram-scale synthesis of nitrile (2a):

To a stirred suspension of 4-methoxybenzaldehyde **1a** (20.0 mmol, 2.723 g) and ammonium acetate (30.0 mmol, 2.310 g) in DMSO (60 mL), $Cu(OAc)_2$ (0.336 g, 10 mol %) was added and the reaction mixture was stirred for the appropriate time at 60°C under ambient atmosphere. The progress of the reaction was monitored with TLC. Then the reaction mixture was cooled to room temperature, ethyl acetate (300 mL) was added to dissolve the product. The reaction mixture was repeatedly extracted with ethyl acetate (3×100 mL). The combined organic extracts were washed with water (3× 100 mL). After drying with anhydrous sodium sulfate, the solvent was removed under reduced pressure to furnish the crude product **2a**, which was further purified by column chromatography on a short column of silica gel using ethyl acetate-hexane as eluent. (Yield: 89%, 2.370 g).

(iv) Spectral and analytical data of the compounds:

4-methoxybenzonitrile (2a)[3a]: Yield: 90%; White solid; Mp 57-59 ^{0}C (Lit.[17b] 58-60 ^{0}C); ^{1}H NMR ($CDCl_3$, 300 MHz); δ (ppm): 7.57 (2H, d, *J* = 8.4 Hz); 6.93 (2H, d, *J* = 8.4 Hz); 3.84 (3H, s). ^{13}C NMR ($CDCl_3$, 75 MHz); δ (ppm): 159.3, 131.5, 119.6, 117.1, 114.0, 56.1.

4-tolunitrile (2b)[3a]: Yield: 91%; Colorless liquid; ^{1}H NMR ($CDCl_3$, 300 MHz); δ (ppm): 7.50 (2H, d, *J* = 7.8 Hz); 7.24 (2H, d, *J* = 7.8 Hz); 2.38 (3H, s). ^{13}C NMR ($CDCl_3$, 75 MHz); δ (ppm): 145.1, 132.6, 128.9, 119.8, 111.6, 22.5.

2-tolunitrile (2c)[3a]: Yield: 89%; Colorless liquid; ^{1}H NMR ($CDCl_3$, 300 MHz); δ (ppm): 7.44-7.59 (2H, m); 7.23-7.31 (2H, m); 2.53 (3H, s). ^{13}C NMR ($CDCl_3$, 75 MHz); δ (ppm): 141.9, 132.6, 132.4, 130.2, 126.2, 118.1, 112.7, 20.4.

Benzonitrile (2d)[3c]: Yield: 90%; Colorless liquid; ^{1}H NMR ($CDCl_3$, 300 MHz); δ (ppm): 7.57-7.64 (3H, m); 7.43-7.48 (2H, m). ^{13}C NMR ($CDCl_3$, 75 MHz); δ (ppm): 133.9, 133.1, 129.6, 119.5, 113.4.

3, 4-dimethoxybenzonitrile (2e)[3c]: Yield: 90%; White solid; Mp 70-72 ^{0}C (Lit.[17b] 69-71 ^{0}C); ^{1}H NMR ($CDCl_3$, 300 MHz); δ (ppm): 7.24 (1H, d, *J* = 1.5 Hz); 7.04 (1H, s); 6.87 (1H, d, *J* = 8.1 Hz); 3.94 (3H, s); 3.90 (3H, s). ^{13}C NMR ($CDCl_3$, 75 MHz); δ (ppm): 152.8, 149.4, 126.5, 119.1, 113.8, 111.2, 103.6, 56.0, 55.8.

4-hydroxy-3-methoxybenzonitrile (2f)[16a]: Yield: 89%; White solid; Mp 88-90 ^{0}C (Lit.[17b] 87-89 ^{0}C); ^{1}H NMR ($CDCl_3$, 300 MHz); δ (ppm): 7.19 (1H, d, *J* = 7.5 Hz); 7.06 (1H, s); 6.92 (1H, d, *J* = 7.8 Hz); 3.89 (3H, s). ^{13}C NMR ($CDCl_3$, 75 MHz); δ (ppm): 150.1, 146.8, 127.5, 119.3, 113.9, 109.0, 103.1, 56.2.

4-hydroxybenzonitrile (2g)[16a]: Yield: 87%; White solid; Mp 110-112 ^{0}C (Lit.[17b] 111-112 ^{0}C); ^{1}H NMR ($CDCl_3$, 300 MHz); δ (ppm): 7.54 (2H, d, *J* = 8.4 Hz); 6.94 (2H, d, *J* = 8.4 Hz). ^{13}C NMR ($CDCl_3$, 75 MHz); δ (ppm): 160.5, 134.3, 119.3, 116.5, 102.7.

3-hydroxybenzonitrile (2h)[16b]: Yield: 89%; White solid; Mp 79-81 ^{0}C; ^{1}H NMR (DMSO-d_6, 300 MHz); δ (ppm): 7.28-7.33 (2H, m); 7.19 (1H, s); 7.09-7.17 (1H, m). ^{13}C NMR (DMSO-d_6, 75 MHz); δ (ppm): 156.5, 131.2, 124.7, 121.2, 119.5, 117.8, 110.4.

2-hydroxybenzonitrile (2i)[16a]: Yield: 88%; White solid; Mp 97-99 ^{0}C (Lit.[4c] 96-98 ^{0}C); ^{1}H NMR ($CDCl_3$, 300 MHz); δ (ppm): 7.48-7.51 (2H, m); 6.95-6.98 (2H, m); 4.89 (1H, br s). ^{13}C NMR ($CDCl_3$, 75 MHz); δ (ppm): 158.8, 134.7, 132.9, 120.7, 119.1, 116.7, 102.8.

4-(dimethylamino)benzonitrile (2j)[16a]: Yield: 88%; White solid; Mp 70-72 ^{0}C (Lit.[17a] 71-73 ^{0}C); ^{1}H NMR ($CDCl_3$, 300 MHz); δ (ppm): 7.45 (2H, d, *J* = 8.7 Hz); 6.63 (2H, d, *J* = 8.7 Hz). ^{13}C NMR ($CDCl_3$, 75 MHz); δ (ppm): 152.5, 133.6, 120.6, 111.8, 97.4, 39.8.

2-aminobenzonitrile (2k)[16c]: Yield: 89%; Yellow solid; Mp 48-50 ^{0}C (Lit.[17a] 49-51 ^{0}C); ^{1}H NMR ($CDCl_3$, 300 MHz); δ (ppm): 7.29-7.38 (2H, m); 6.70-6.75 (2H, m); 4.41 (2H, br s). ^{13}C NMR ($CDCl_3$, 75 MHz); δ (ppm): 149.7, 134.0, 132.4, 117.9, 117.6, 115.2, 95.9.

4-chlorobenzonitrile (2l)[3a]: Yield: 93%; White solid; Mp 92-94 ^{0}C (Lit.[17a] 91-93 ^{0}C); ^{1}H NMR ($CDCl_3$, 300 MHz); δ (ppm): 7.60 (2H, d, *J* = 8.4 Hz); 7.46 (2H, d, *J* = 8.4 Hz). ^{13}C NMR ($CDCl_3$, 75 MHz); δ (ppm): 139.3, 132.8, 129.2, 118.8, 110.3.

4-bromobenzonitrile (2m)[3a]: Yield: 91%; White solid; Mp 108-110 ^{0}C (Lit.[17a] 109-111 ^{0}C); ^{1}H NMR ($CDCl_3$, 300 MHz); δ (ppm): 7.62 (2H, d, *J* = 8.4 Hz); 7.51 (2H, d, *J* = 8.4 Hz). ^{13}C NMR ($CDCl_3$, 75 MHz); δ (ppm): 133.4, 132.6, 127.9, 118.0, 111.3.

4-nitrobenzonitrile (2n)[3a]: Yield: 95%; Yellow solid; Mp 147-150 ^{0}C (Lit.[17a] 146-148 ^{0}C); ^{1}H NMR ($CDCl_3$, 300 MHz); δ (ppm): 8.36 (2H, d, *J* = 8.7 Hz); 7.88 (2H, d, *J* = 8.7 Hz). ^{13}C NMR ($CDCl_3$, 75 MHz); δ (ppm): 150.1, 133.5, 124.2, 118.3, 116.8.

3-nitrobenzonitrile (2o)[16a]: Yield: 94%; White solid; Mp 114-116 ^{0}C (Lit.[4c] 115-116 ^{0}C); ^{1}H NMR ($CDCl_3$, 300 MHz); δ (ppm): 7.18-7.25 (1H, m); 7.00 (1H, d, *J* = 7.5 Hz); 6.84-6.89 (2H, m). ^{13}C NMR ($CDCl_3$, 75 MHz); δ (ppm): 147.0, 130.1, 121.9, 119.2, 117.4, 112.8.

4-formylbenzonitrile (2p)[16c]: Yield: 88%; White solid; Mp 98-100 ^{0}C (Lit.[17a] 100-101 ^{0}C); ^{1}H NMR ($CDCl_3$, 300 MHz); δ (ppm): 10.1 (1H, s); 7.98 (2H, d, *J* = 8.1 Hz); 7.84 (2H, d, *J* = 8.1 Hz). ^{13}C NMR ($CDCl_3$, 75 MHz); δ (ppm): 190.6, 138.7, 132.9, 130.6, 129.9, 117.6.

Terephthalonitrile (2q)[16c]: Yield: 87%; White solid; Mp 225-227 ^{0}C (Lit.[17a] 224-226 ^{0}C); ^{1}H NMR ($CDCl_3$, 300 MHz); δ (ppm): 7.52 (s, 4H). ^{13}C NMR ($CDCl_3$, 75 MHz); δ (ppm): 132.7, 118.2, 116.6.

4-acetylbenzonitrile (2r)[16c]: Yield: 88%; Light yellow solid; Mp 56-58 ^{0}C (Lit.[17a] 55-57 ^{0}C); ^{1}H NMR ($CDCl_3$, 300 MHz); δ (ppm): 8.03 (2H, d, *J* = 8.1 Hz); 7.77 (2H, d, *J* = 8.1 Hz); 2.64 (3H, s). ^{13}C NMR ($CDCl_3$, 75 MHz); δ (ppm): 196.6, 139.9, 132.5, 128.7, 117.9, 116.3, 26.7.

1-naphthonitrile (2s)[15]: Yield: 86%; White solid; Mp 33-35 ^{0}C (Lit.[17a] 35-37 ^{0}C); ^{1}H NMR ($CDCl_3$, 300 MHz); δ (ppm): 8.21 (1H, d, *J* = 8.4 Hz,), 8.02 (1H, d, *J* = 8.6 Hz), 7.76–7.83 (4H, m), 7.48 (1H, t, *J* = 7.8 Hz). ^{13}C NMR (75 MHz, $CDCl_3$); δ (ppm): 133.5, 132.9, 132.1, 131.8, 128.7, 128.1, 127.0, 125.6, 124.7, 118.1, 110.2.

Benzo[d][1,3]dioxole-5-carbonitrile (2t)[3a]: Yield: 88%; White solid; Mp 92-94 ^{0}C; ^{1}H NMR ($CDCl_3$, 300 MHz); δ (ppm): 7.41 (1H, s); 7.14-7.20 (1H, m), 6.98 (1H, d, *J* = 8.2 Hz), 6.01 (2H, s). ^{13}C NMR (75 MHz, $CDCl_3$); δ (ppm): 150.6, 148.2, 127.9, 119.0, 111.1, 108.8, 105.7, 101.3.

Cinnamonitrile (2u)[3c]: Yield: 83%; Colorless oil; ^{1}H NMR ($CDCl_3$, 400 MHz); δ (ppm): 7.37-7.49 (6H, m), 5.83 (1H, d, *J* = 16.3 Hz). ^{13}C NMR (100 MHz, $CDCl_3$); δ (ppm): 150.1, 132.9, 131.4, 129.3, 127.5, 118.8, 95.8.

Furan-2-carbonitrile (2v)[3a]: Yield: 79%; Viscous oil; ^{1}H NMR ($CDCl_3$, 400 MHz); δ (ppm): 7.58 (1H, d, *J* = 1.5 Hz), 6.96-7.02 (2H, m). ^{13}C NMR (100 MHz, $CDCl_3$); δ (ppm): 147.5, 132.2, 125.3, 119.8, 111.6.

Thiophene-2-carbonitrile (2w)[3a]: Yield: 81%; Colorless liquid; ^{1}H NMR ($CDCl_3$, 400 MHz); δ (ppm): 7.60 (2H, d, *J* = 4.3 Hz), 7.01-7.06 (1H, m). ^{13}C NMR (100 MHz, $CDCl_3$); δ (ppm): 138.2, 131.4, 126.5, 118.1, 109.2.

Picolinonitrile (2x)[15]: Yield: 83%; Colorless liquid; ^{1}H NMR ($CDCl_3$, 300 MHz); δ (ppm): 8.72 (1H, d, *J* = 4.5Hz), 7.62-7.71 (3H, m). ^{13}C NMR (75 MHz, $CDCl_3$); δ (ppm): 151.3, 135.7, 133.3, 127.6, 124.9, 117.6.

Isonicotinonitrile (2y)[16d]: Yield: 80%; White solid; Mp 78-79 ^{0}C (Lit.[17b] 77-78 ^{0}C); ^{1}H NMR ($CDCl_3$, 300 MHz); δ (ppm): 8.82 (2H, d, *J* = 13.5 Hz); 7.55 (2H, d, *J* = 13.5 Hz). ^{13}C NMR ($CDCl_3$, 75 MHz); δ (ppm): 152.3, 126.8, 120.7, 117.3.

4-(benzyloxy)benzonitrile (2z)[15]: Yield: 86%; White solid; Mp 95-98 ^{0}C; ^{1}H NMR ($CDCl_3$, 300 MHz); δ (ppm): 7.58 (2H, d, *J* = 8.4 Hz); 7.25-7.40 (5H, m); 7.01 (2H, d, *J* = 8.4 Hz); 5.11 (2H, s). ^{13}C NMR ($CDCl_3$, 75 MHz); δ (ppm): 161.9, 134.0, 131.7, 128.5, 128.2, 127.4, 119.1, 115.6, 14.5, 104.2, 70.3.

4-(allyloxy)-3-methoxybenzonitrile (2za)[16e]: Yield: 84%; Light yellow liquid; ^{1}H NMR ($CDCl_3$, 300 MHz); δ (ppm): 7.24 (1H, d, *J* = 9.0 Hz); 7.08 (1H, s); 6.88 (1H, d, *J* = 8.4 Hz); 6.00-6.11 (1H, m); 5.31-5.45 (2H, m); 4.65 (2H, d, *J* = 4.8 Hz); 3.88 (3H, s). ^{13}C NMR ($CDCl_3$, 75 MHz); δ (ppm): 151.9, 149.5, 132.1, 126.2, 119.2, 118.8, 114.3, 112.9, 104.0, 69.7, 56.2.

4-((tert-butyldimethylsilyl)oxy)-3-methoxybenzonitrile (2zb)[16f]: Yield: 85%; Colorless liquid; ^{1}H NMR ($CDCl_3$, 300 MHz); δ (ppm): 7.05 (1H, s); 6.94 (2H, m); 3.89 (3H, s); 0.88 (9H, s); 0.06 (6H, s). ^{13}C NMR ($CDCl_3$, 75 MHz); δ (ppm): 150.2, 146.9, 126.9, 119.2, 115.4, 113.9, 103.1, 56.2, 25.6, 17.9, -3.64.

Heptanenitrile (2zc)[16a]: Yield: 78%; Colorless liquid; ^{1}H NMR ($CDCl_3$, 300 MHz); δ (ppm): 1.56 (3H, t); 1.24-1.30 (7H, m); 0.88 (3H, t). ^{13}C NMR ($CDCl_3$, 75 MHz); δ (ppm): 119.2, 31.9, 30.5, 29.3, 28.8, 22.6, 14.0.

^{1}H NMR & ^{13}C NMR Spectra of Some Representative Compounds

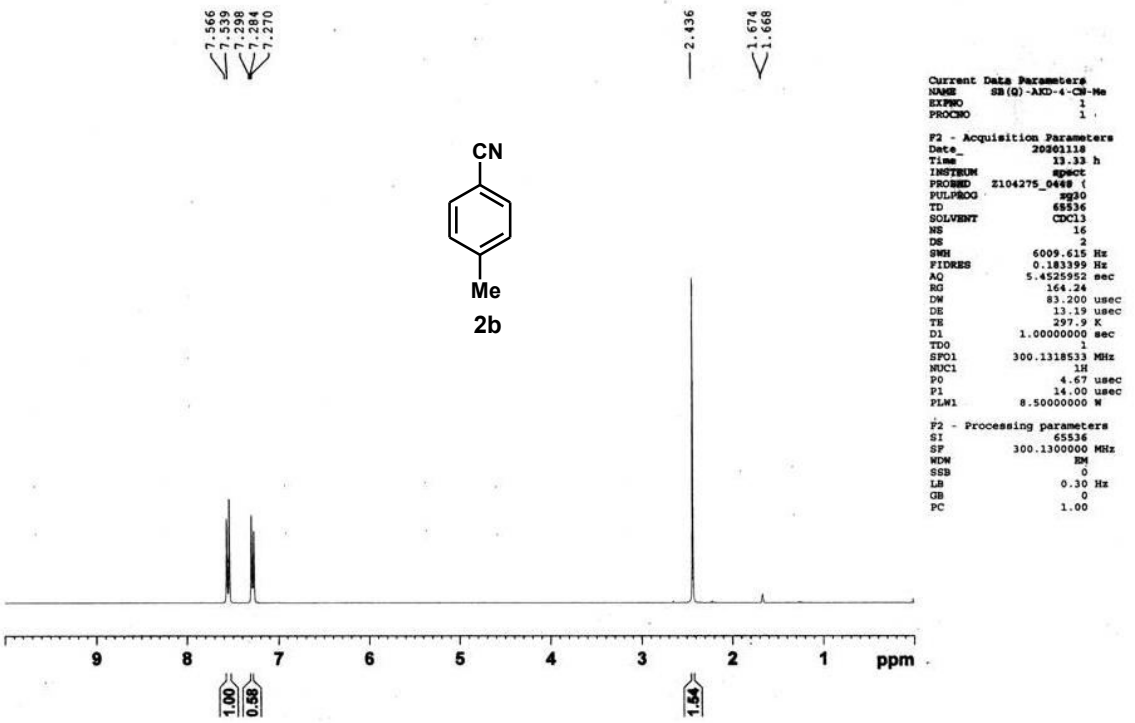

Figure 1 ^{1}H NMR of 4-tolunitrile (2b)

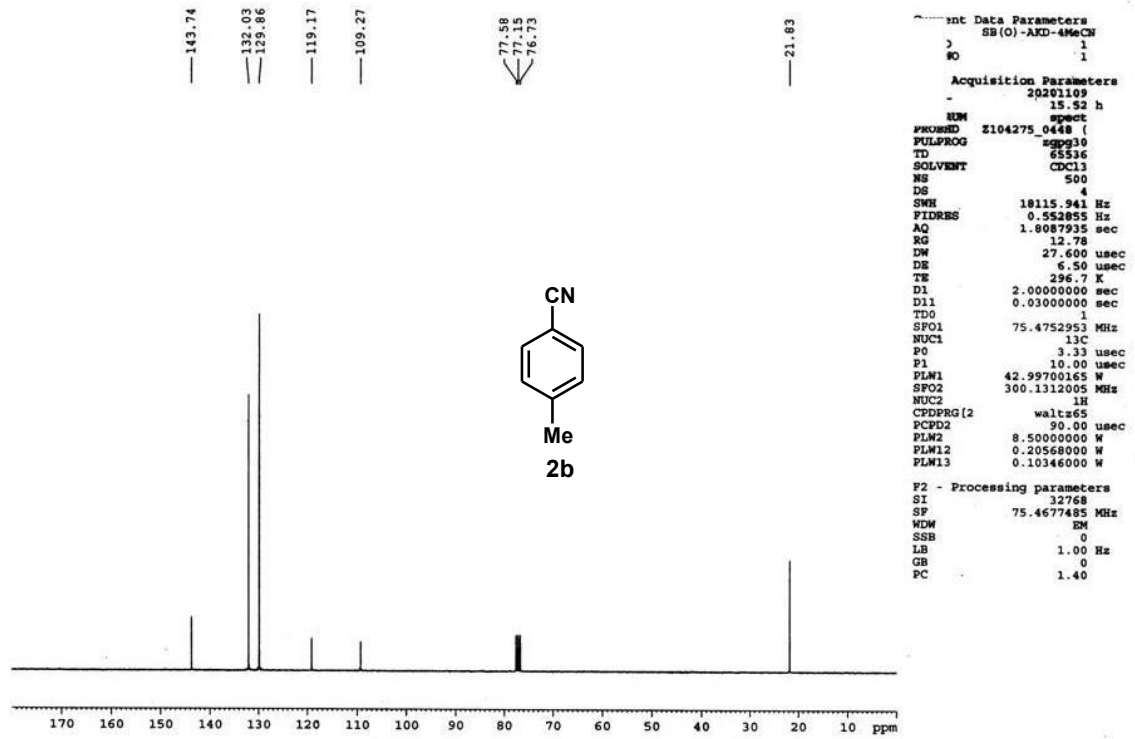

Figure 2 ^{13}C NMR of 4-tolunitrile (2b)

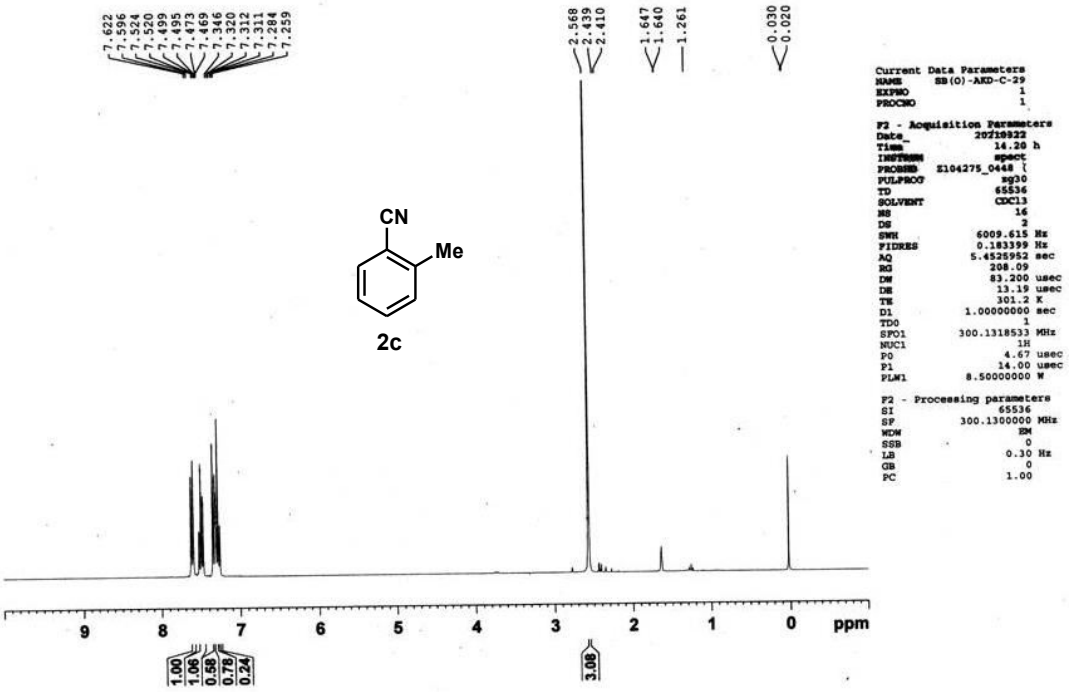

Figure 3 ^{1}H NMR of 2-tolunitrile (2c)

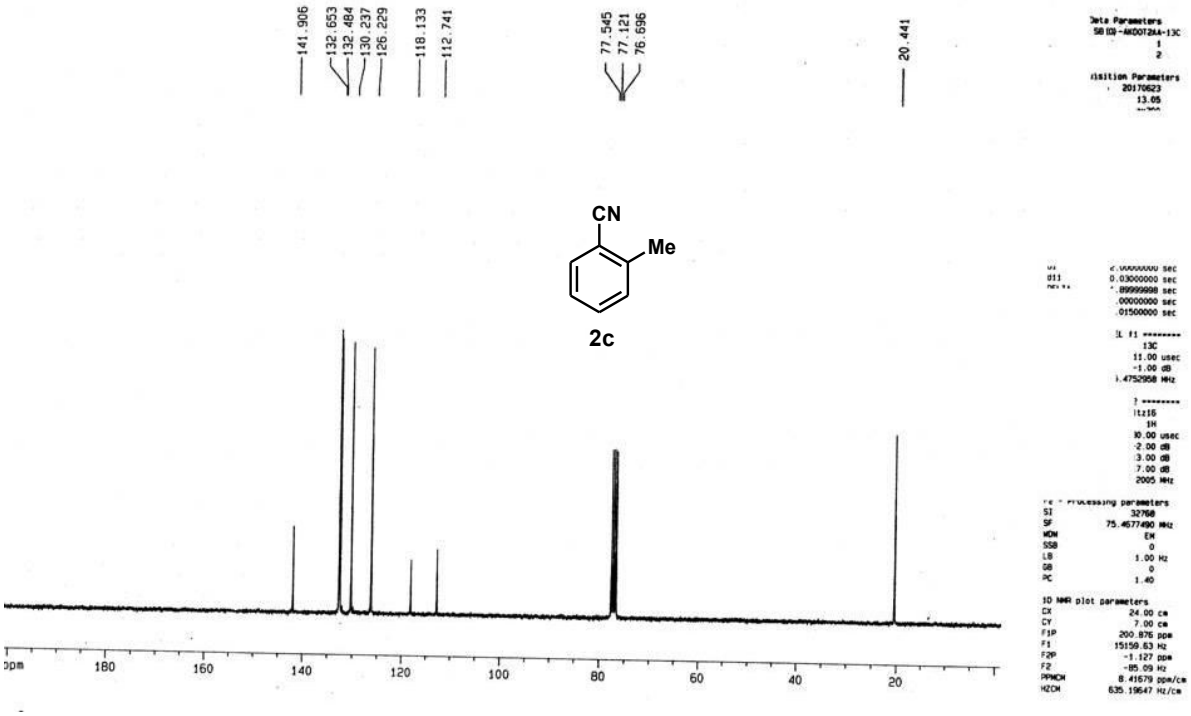

Figure 4 ^{13}C NMR of 2-tolunitrile (2c)

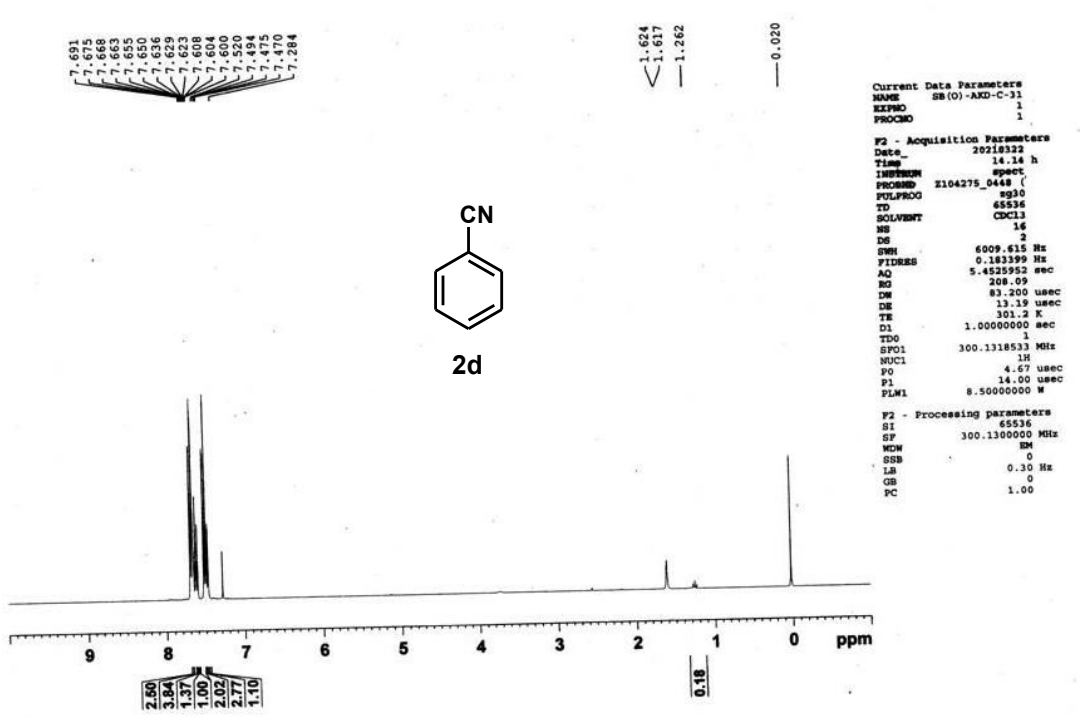

Figure 5 ^{1}H NMR of Benzonitrile (2d)

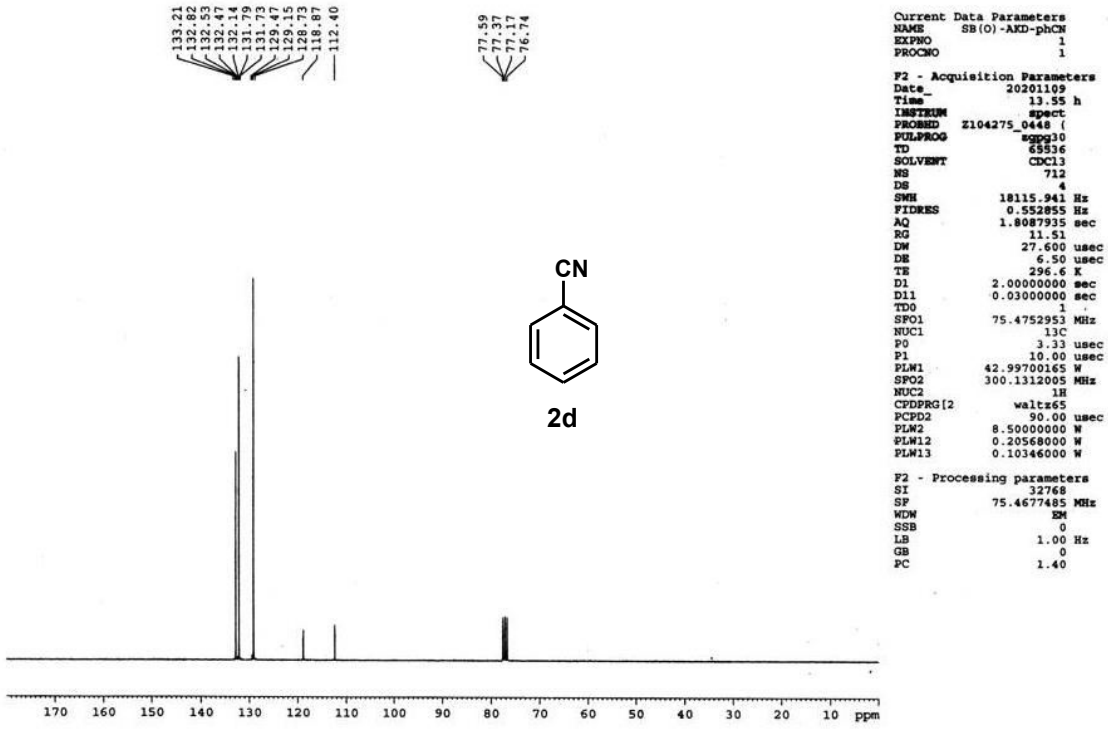

Figure 6 ^{13}C NMR of Benzonitrile (2d)

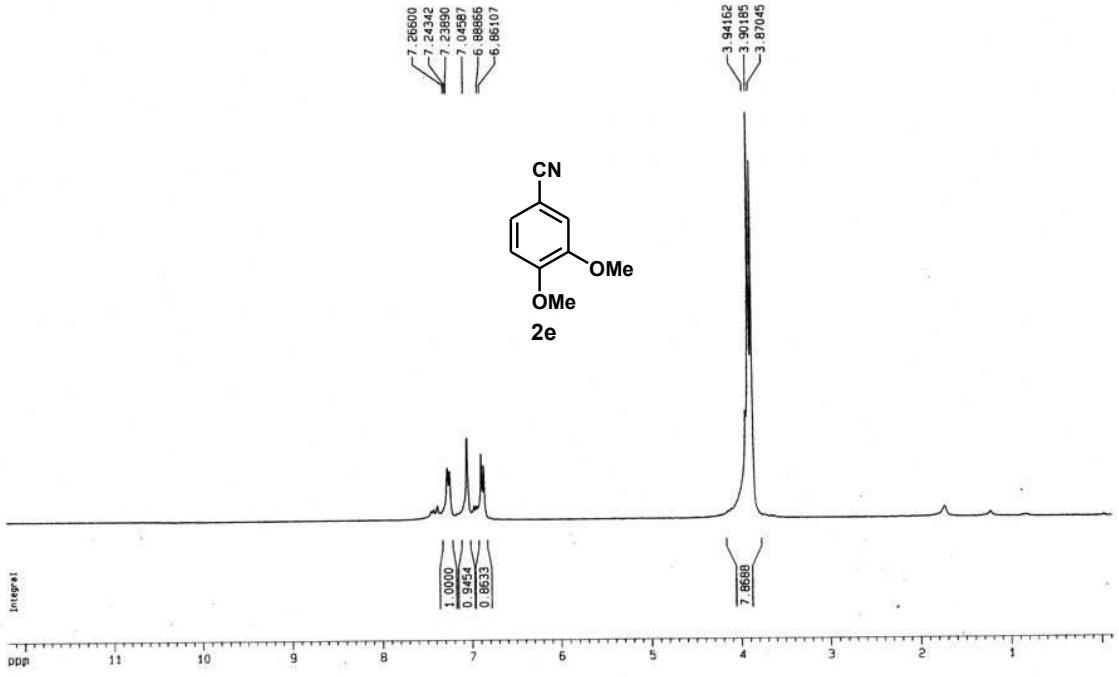

Figure 7 [1]H NMR of 3, 4-dimethoxybenzonitrile (2e)

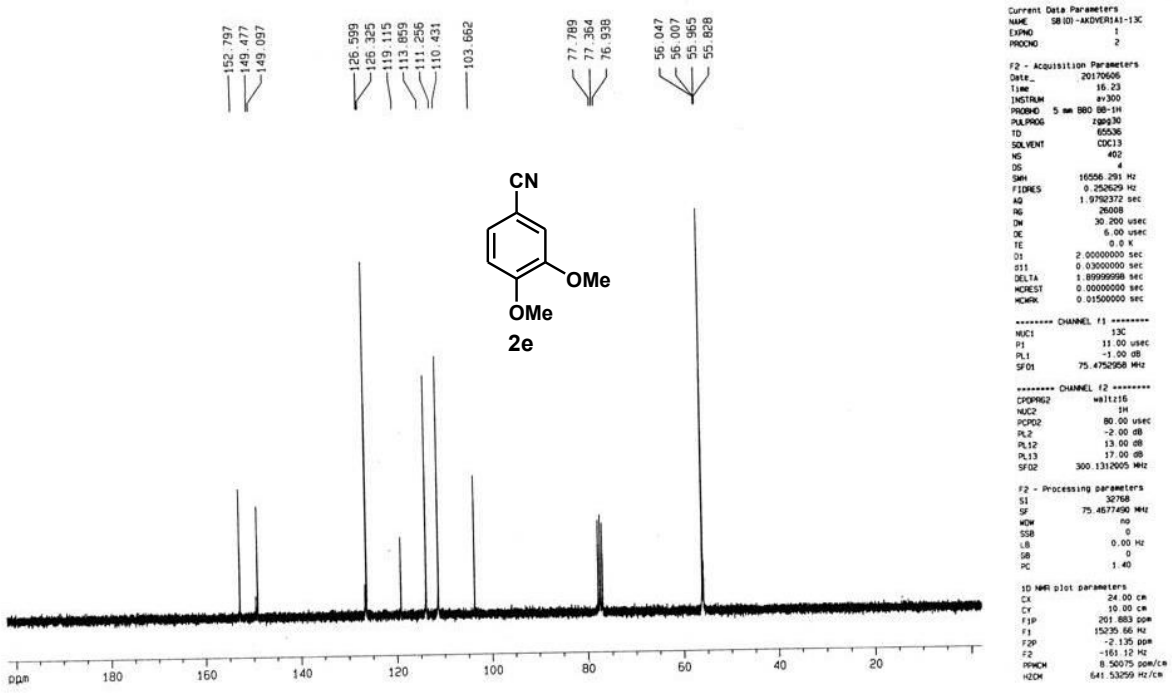

Figure 8 [13]C NMR of 3, 4-dimethoxybenzonitrile (2e)

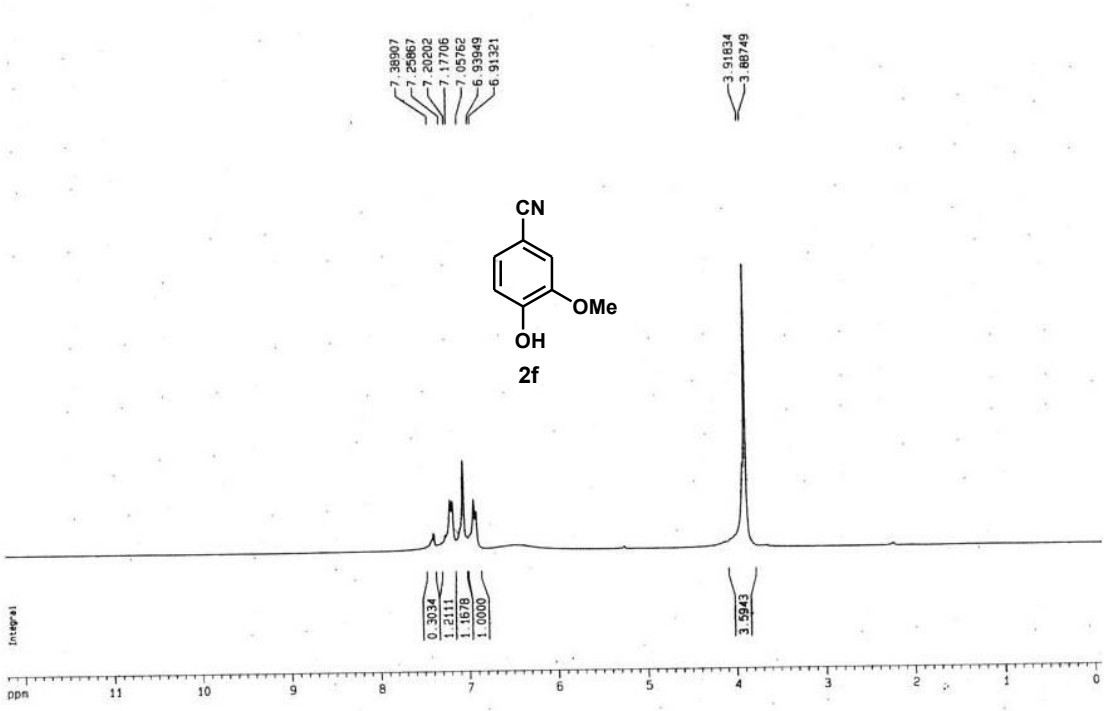

Figure 9 ^{1}H NMR of 4-hydroxy-3-methoxybenzonitrile (2f)

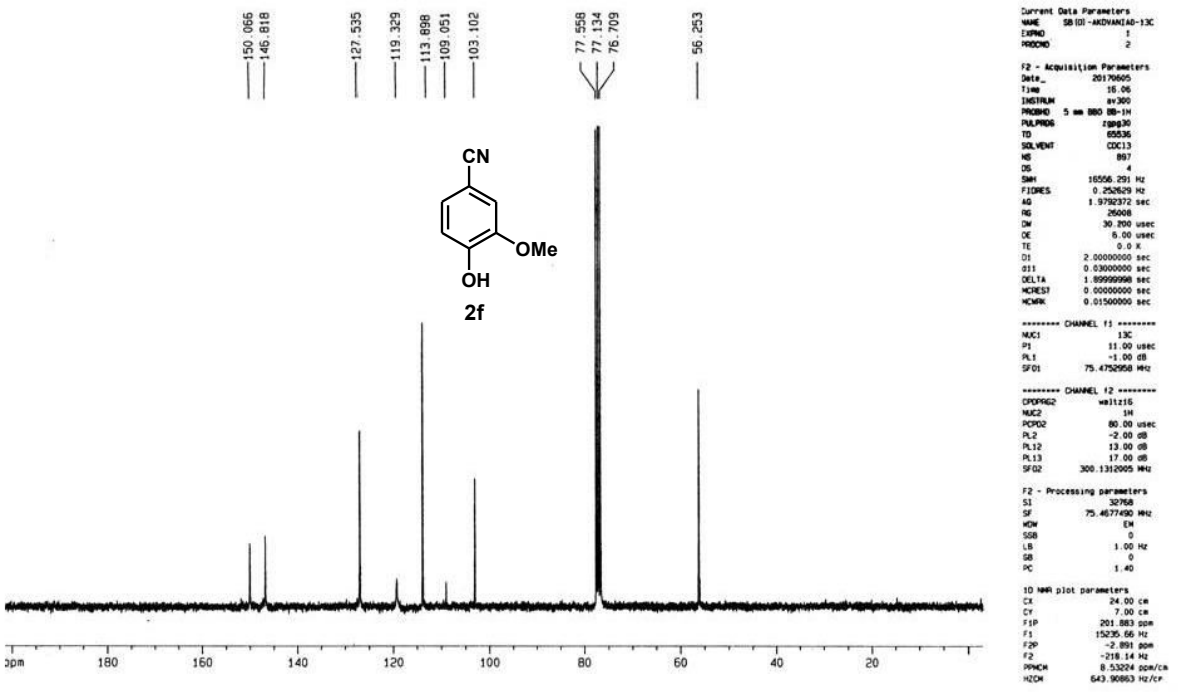

Figure 10 ^{13}C NMR of 4-hydroxy-3-methoxybenzonitrile (2f)

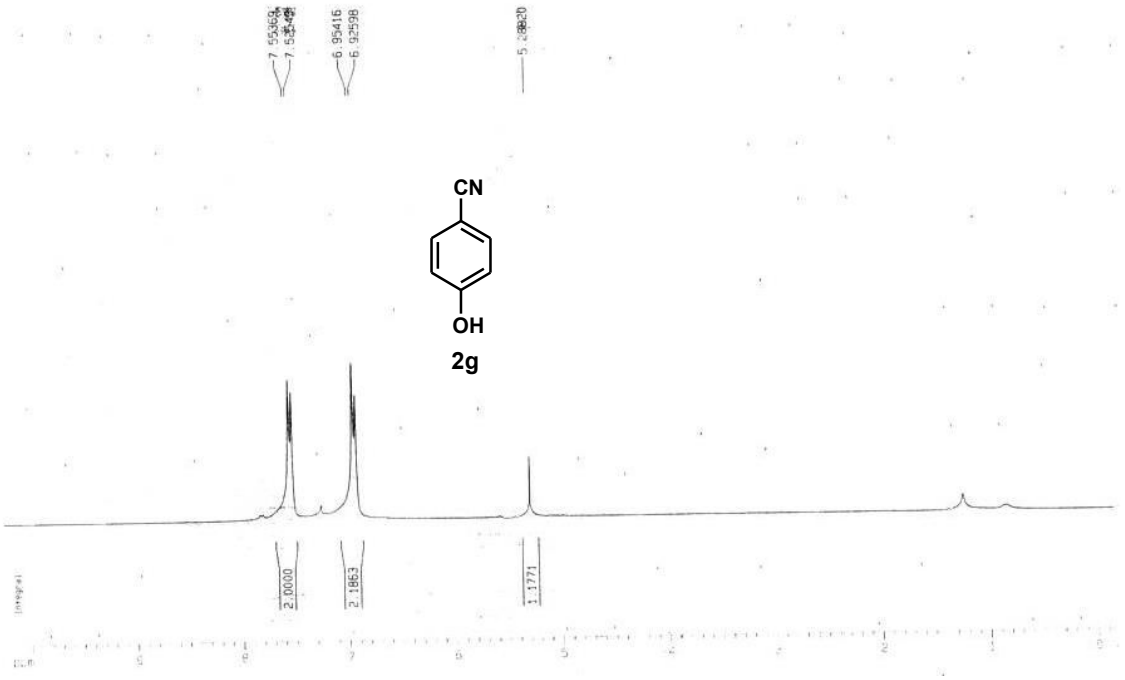

Figure 11 ^{1}H NMR of 4-hydroxybenzonitrile (2g)

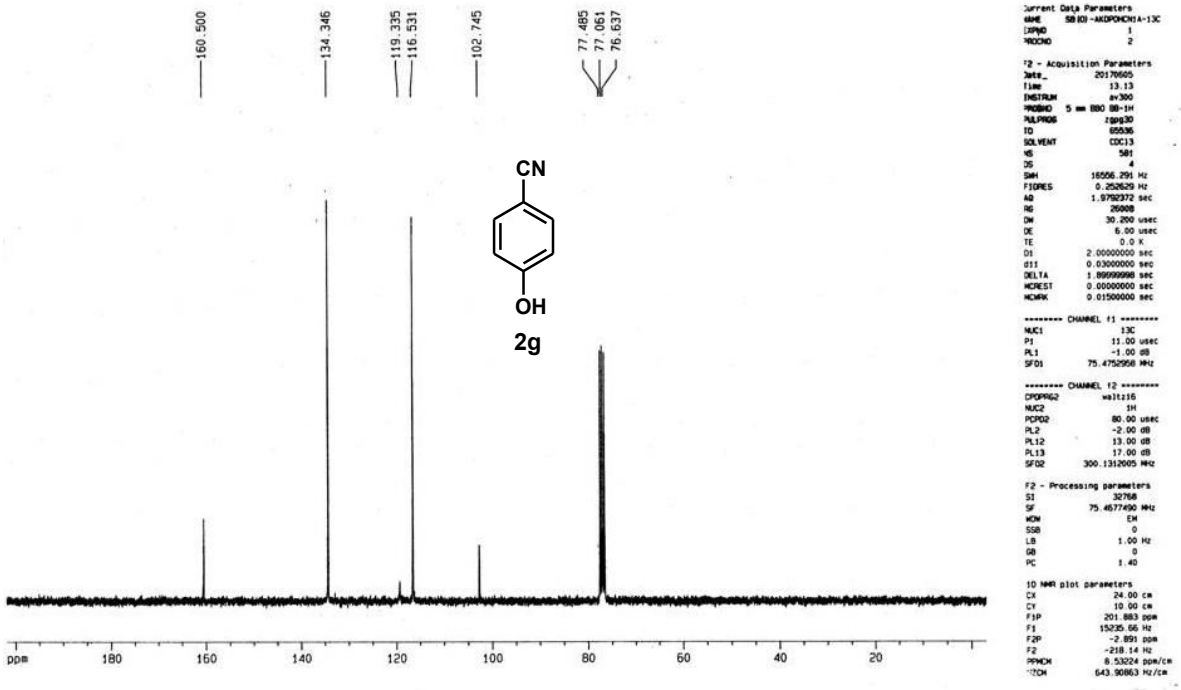

Figure 12 ^{13}C NMR of 4-hydroxybenzonitrile (2g)

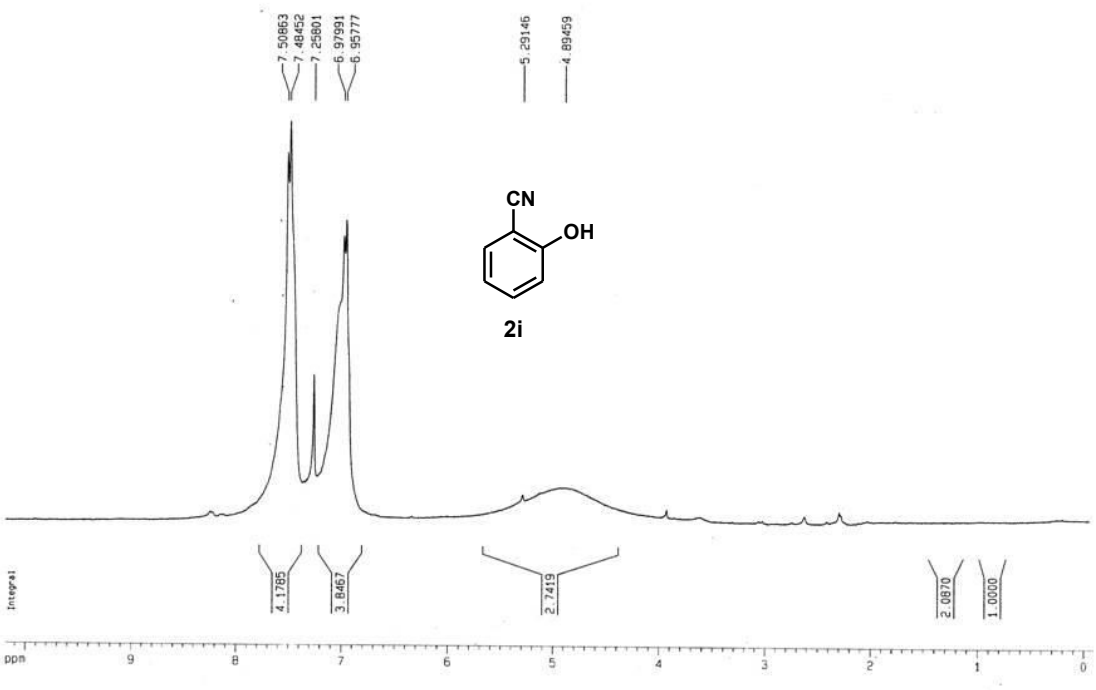

Figure 13 [1]H NMR of 2-hydroxybenzonitrile (2i)

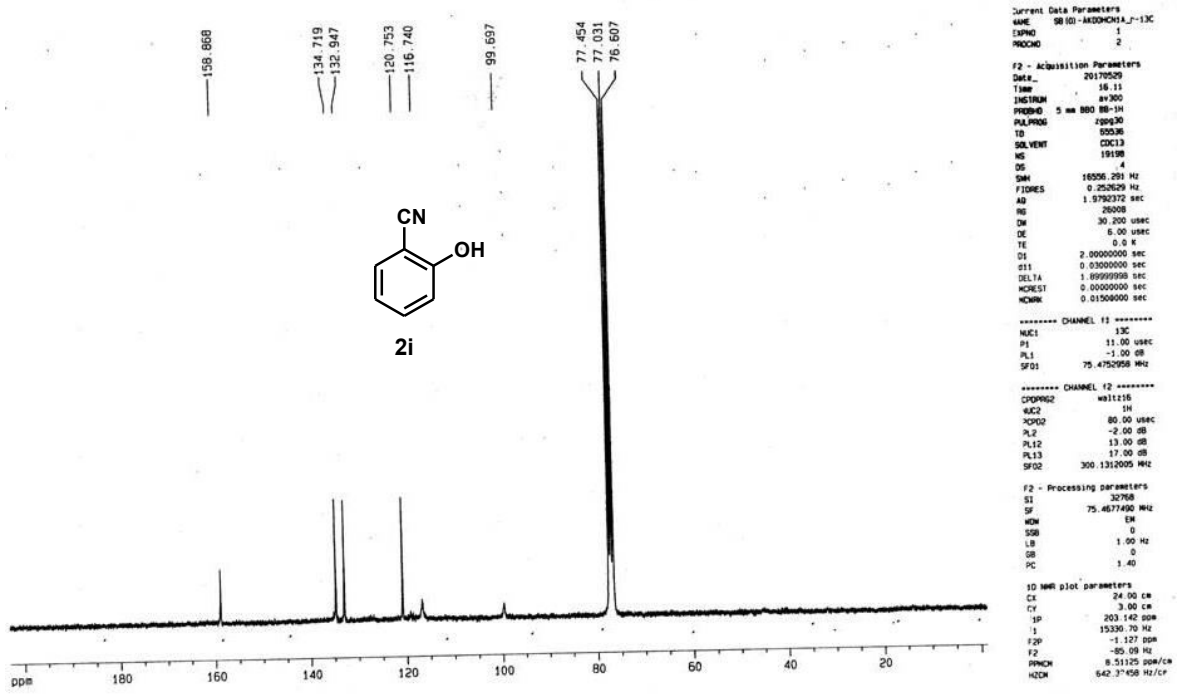

Figure 14 [13]C NMR of 2-hydroxybenzonitrile (2i)

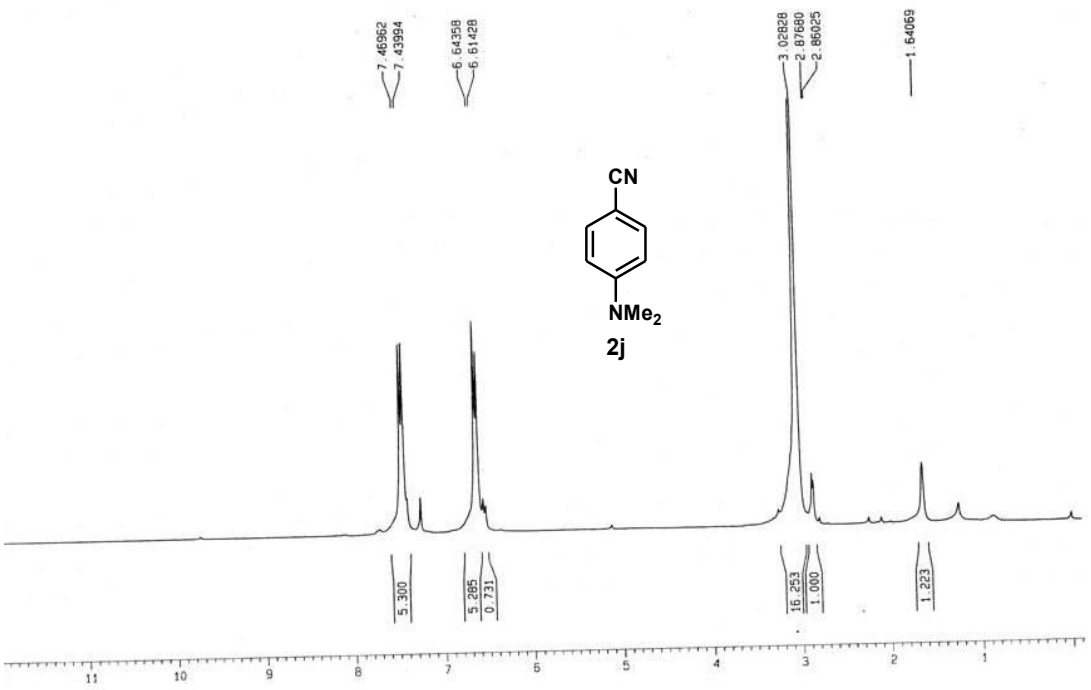

Figure 15 ^{1}H NMR of 4-(dimethylamino)benzonitrile (2j)

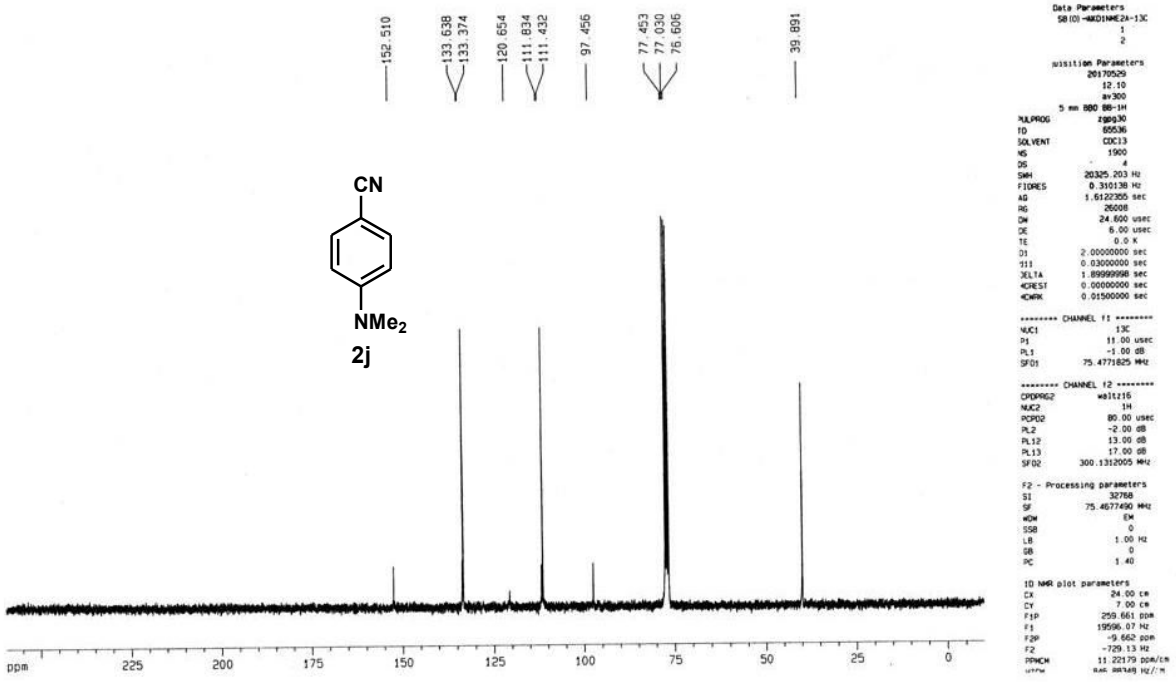

Figure 16 ^{13}C NMR of 4-(dimethylamino)benzonitrile (2j)

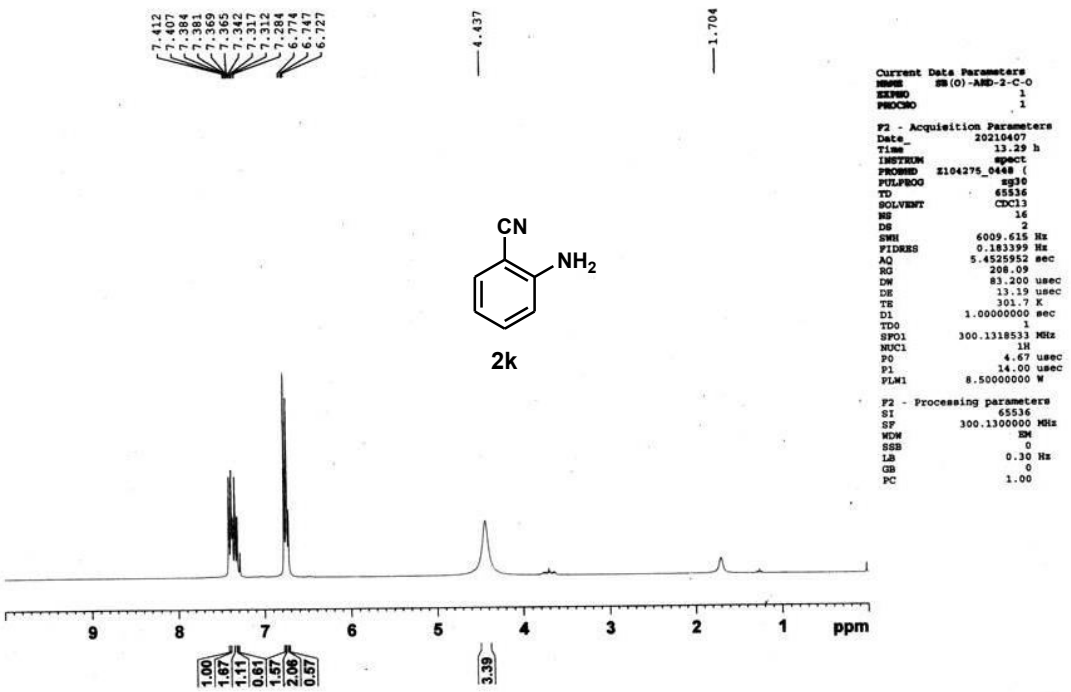

Figure 17 ^{1}H NMR of 2-aminobenzonitrile (2k)

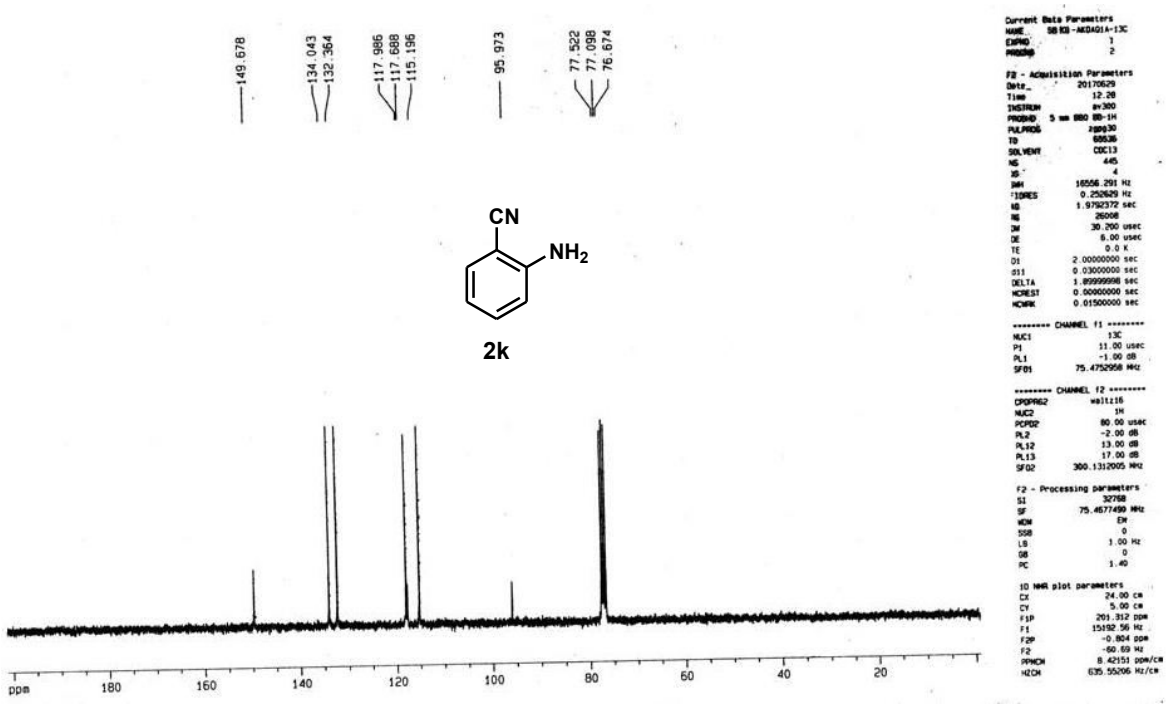

Figure 18 ^{13}C NMR of 2-aminobenzonitrile (2k)

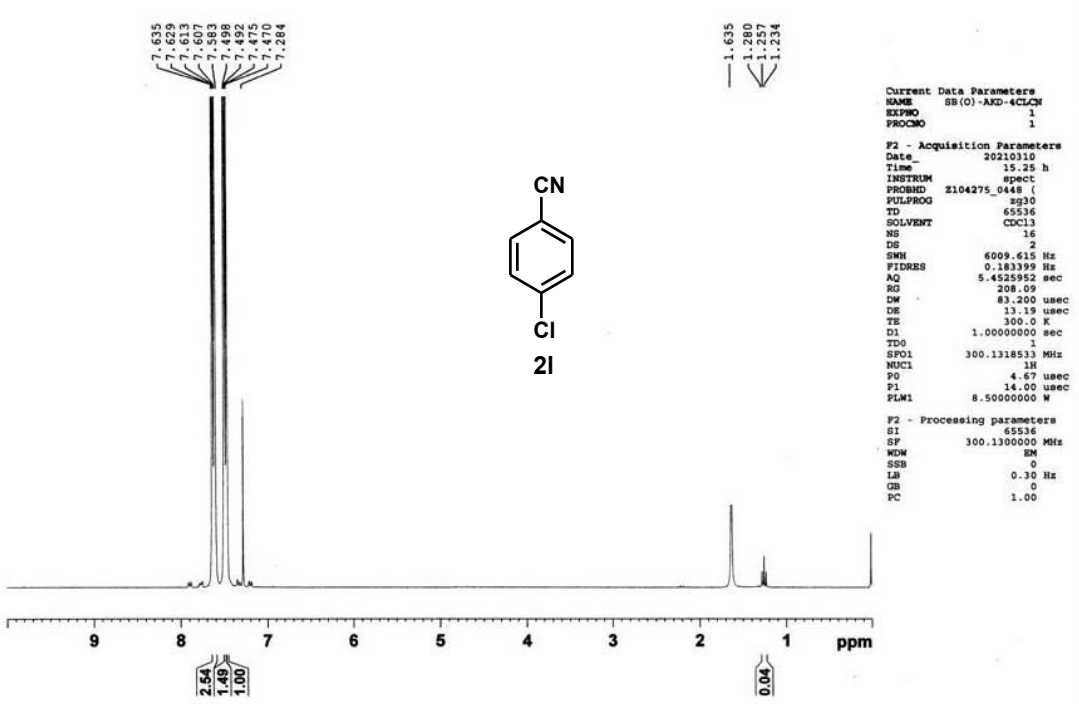

Figure 19 ^{1}H NMR of 4-chlorobenzonitrile (2l)

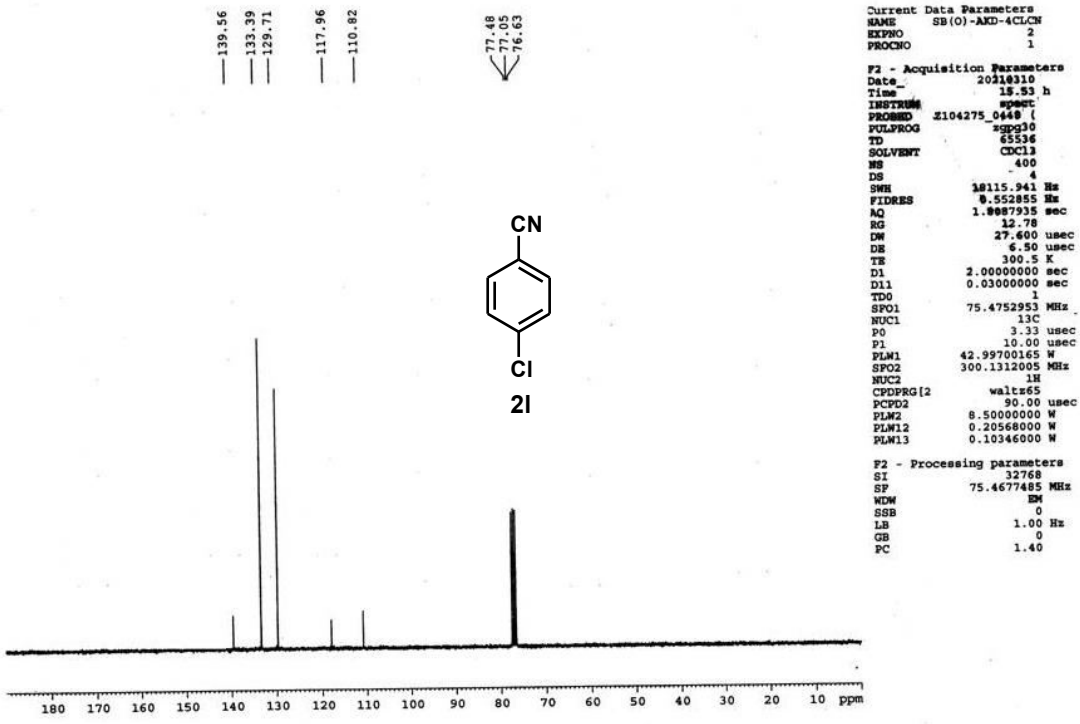

Figure 20 ^{13}C NMR of 4-chlorobenzonitrile (2l)

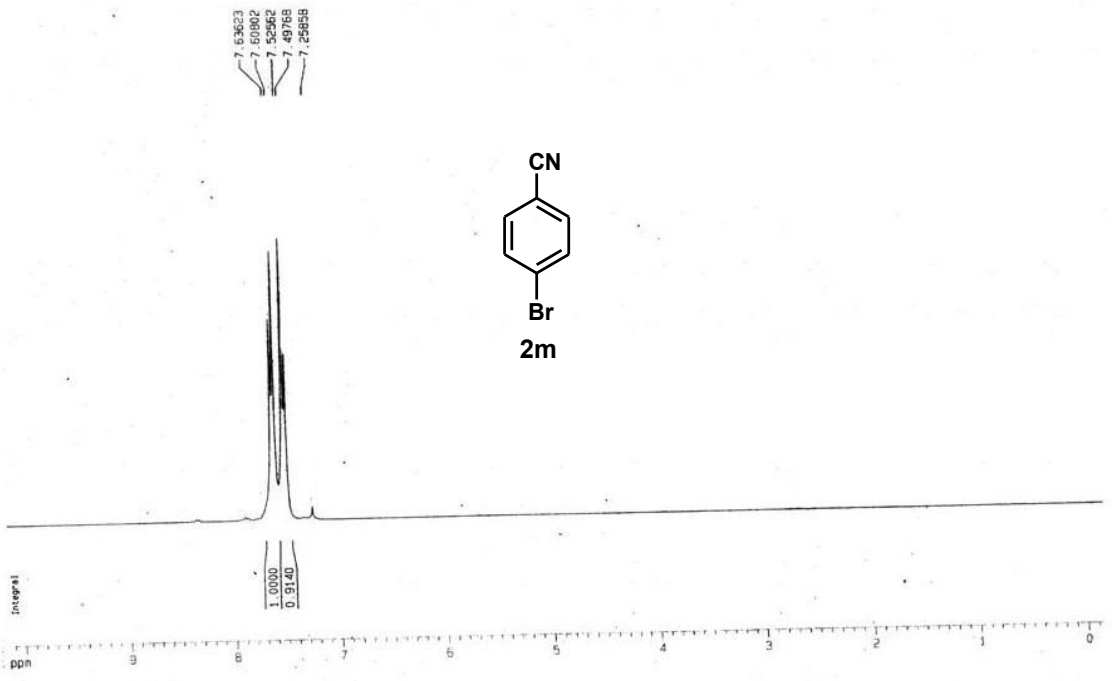

Figure 21 ^{1}H NMR of 4-bromobenzonitrile (2m)

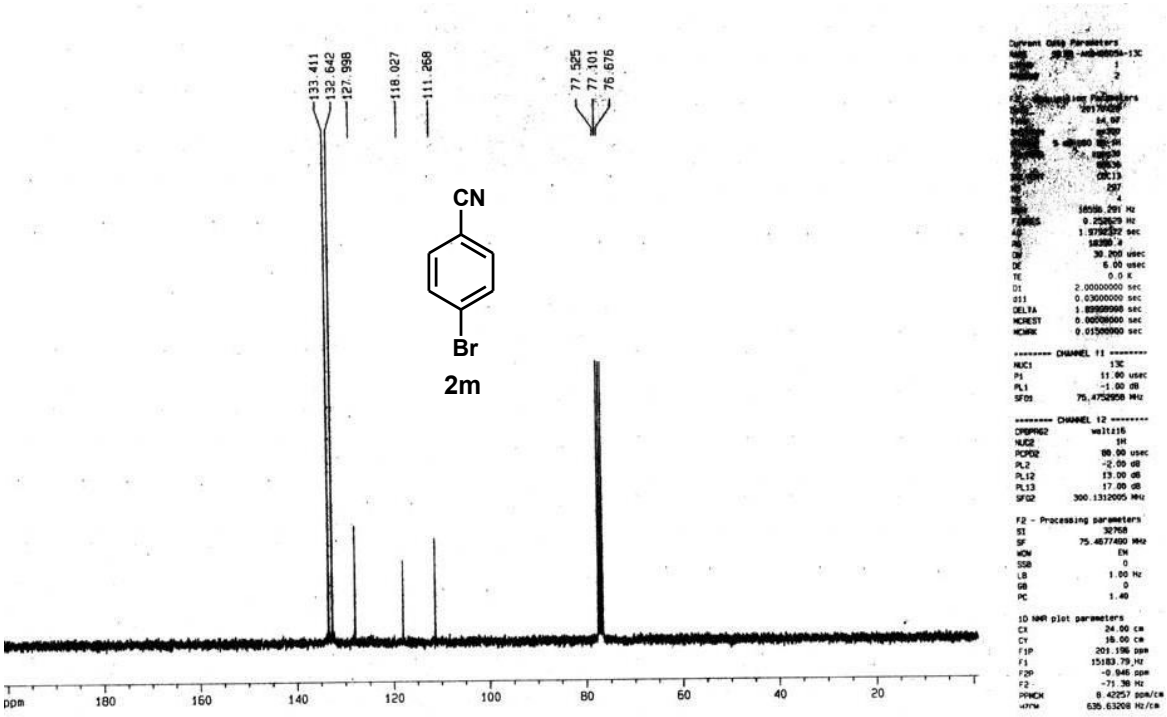

Figure 22 ^{13}C NMR of 4-bromobenzonitrile (2m)

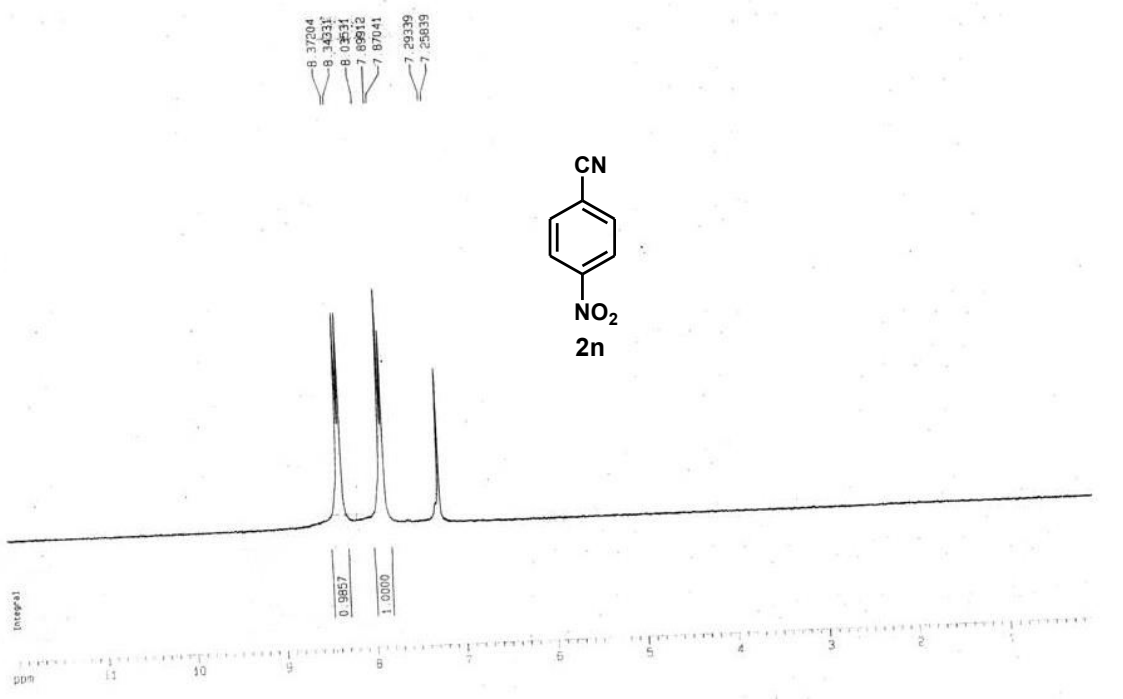

Figure 23 ^{1}H NMR of 4-nitrobenzonitrile (2n)

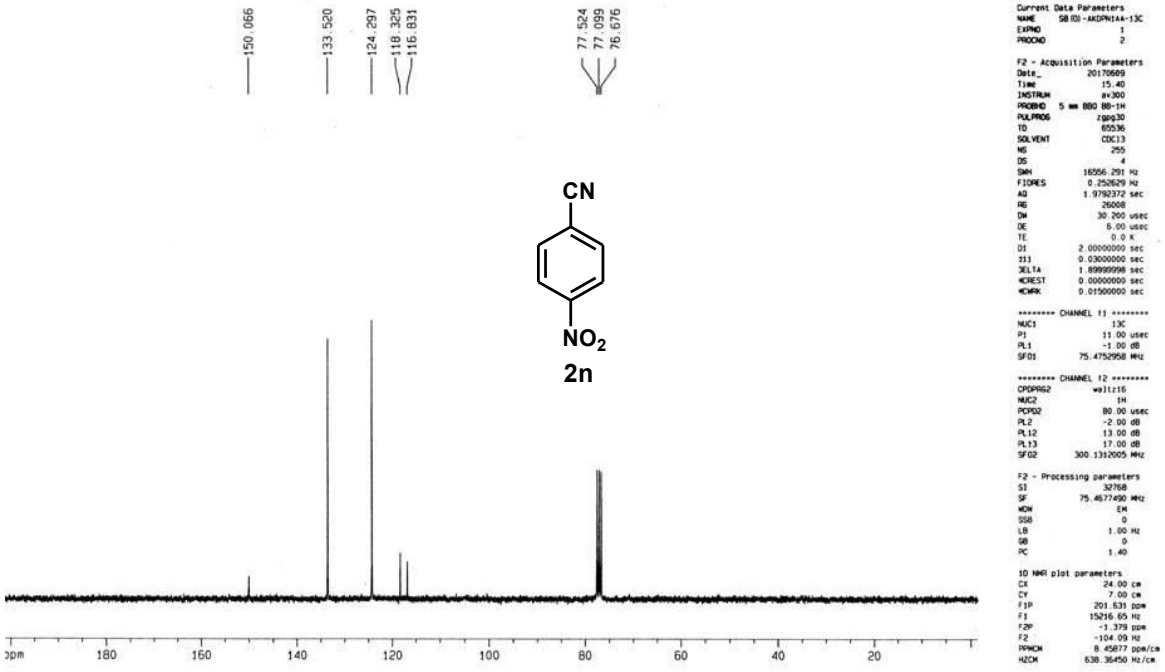

Figure 24 ^{13}C NMR of 4-nitrobenzonitrile (2n)

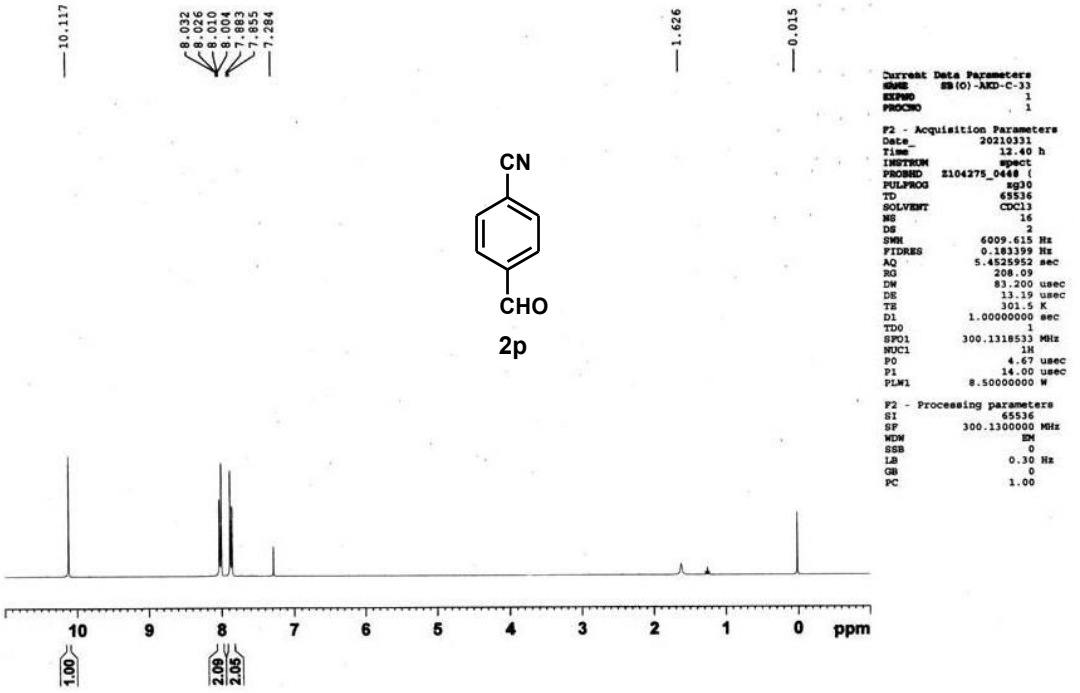

Figure 25 ^{1}H NMR of 4-formylbenzonitrile (2p)

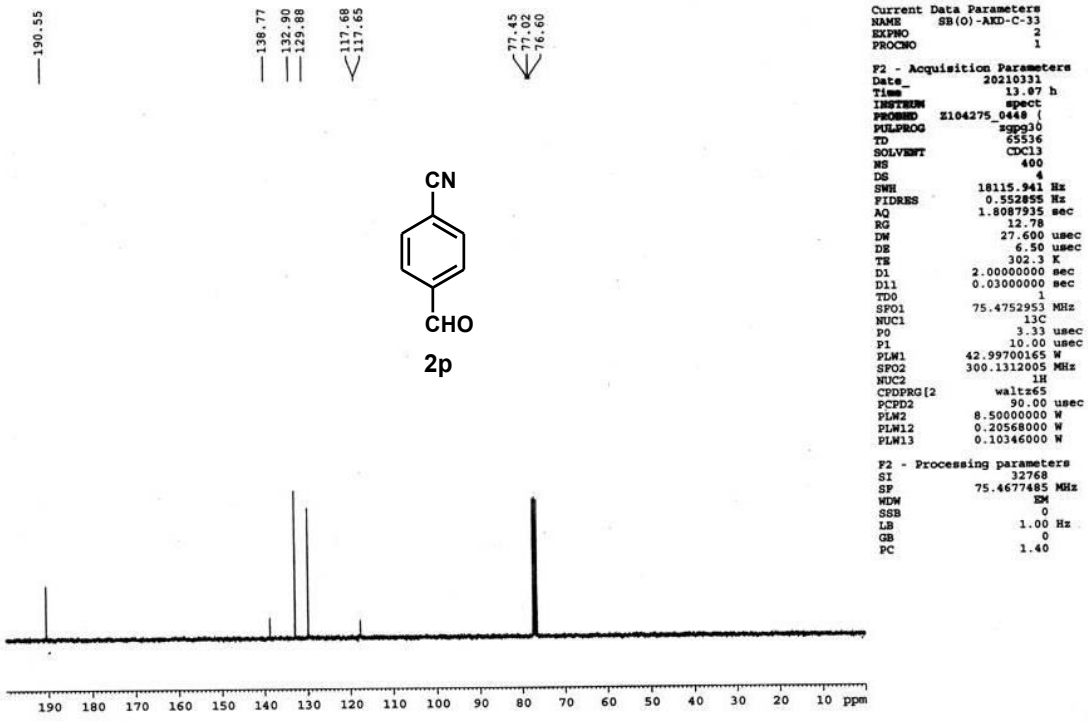

Figure 26 ^{13}C NMR of 4-formylbenzonitrile (2p)

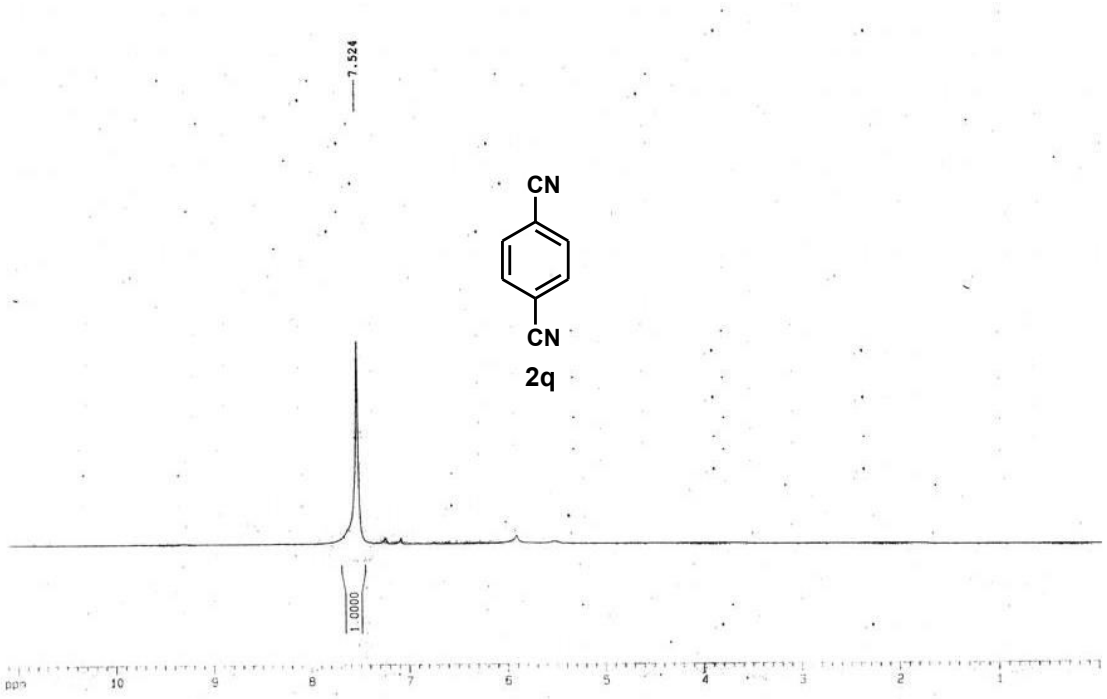

Figure 27 ^{1}H NMR of Terephthalonitrile (2q)

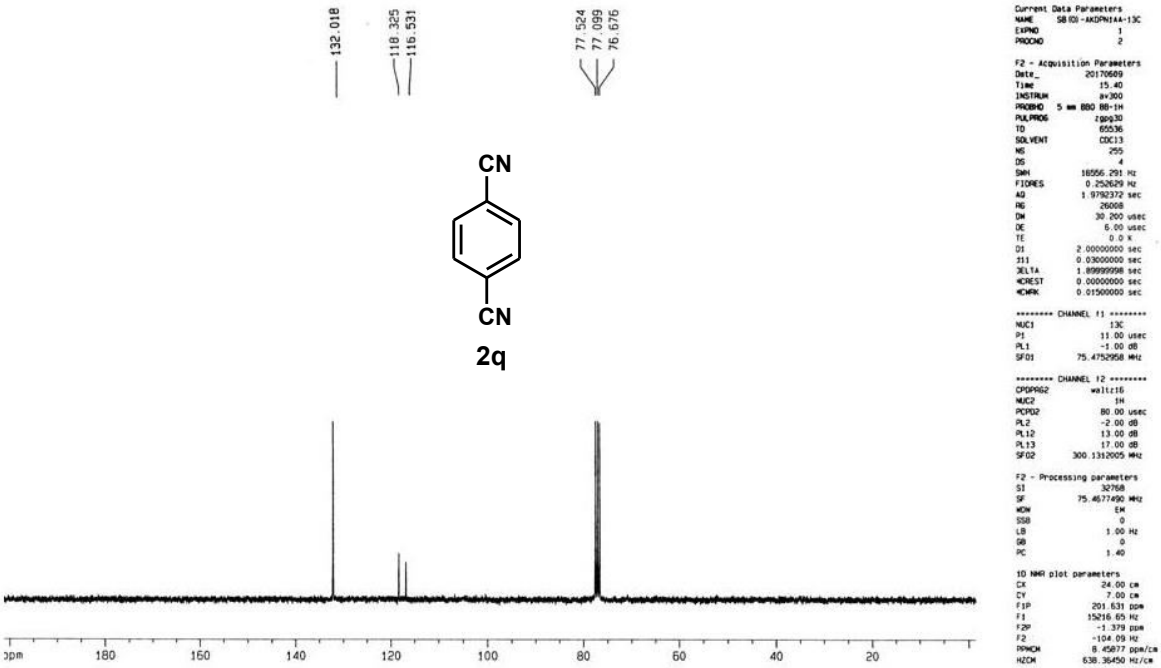

Figure 28 ^{13}C NMR of Terephthalonitrile (2q)

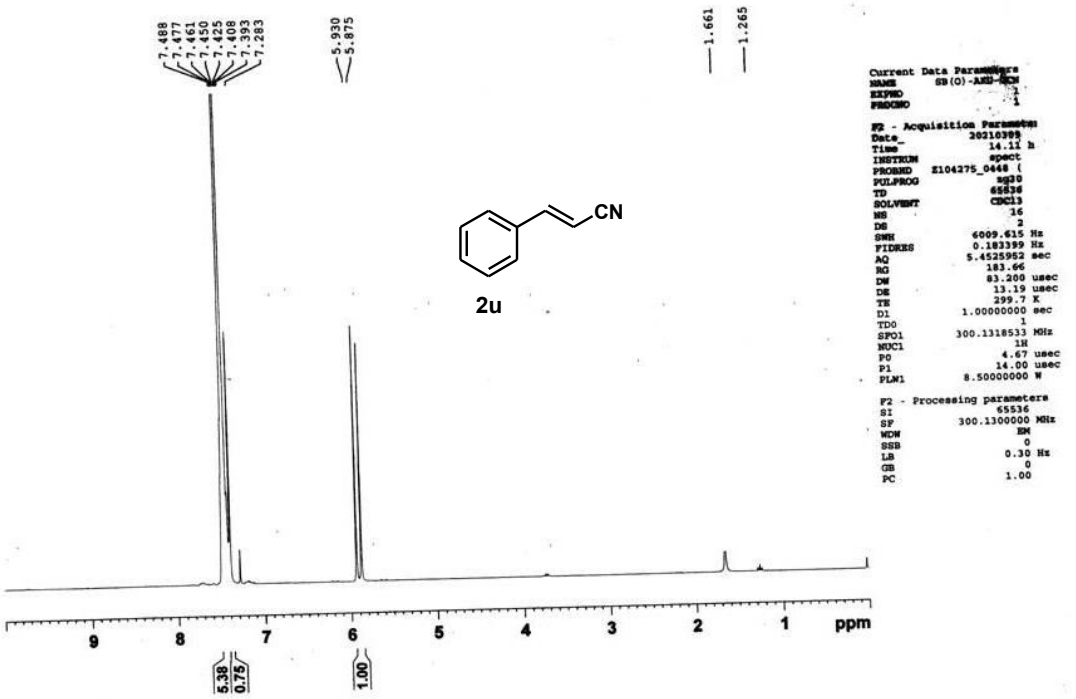

Figure 29 ^{1}H NMR of Cinnamonitrile (2u)

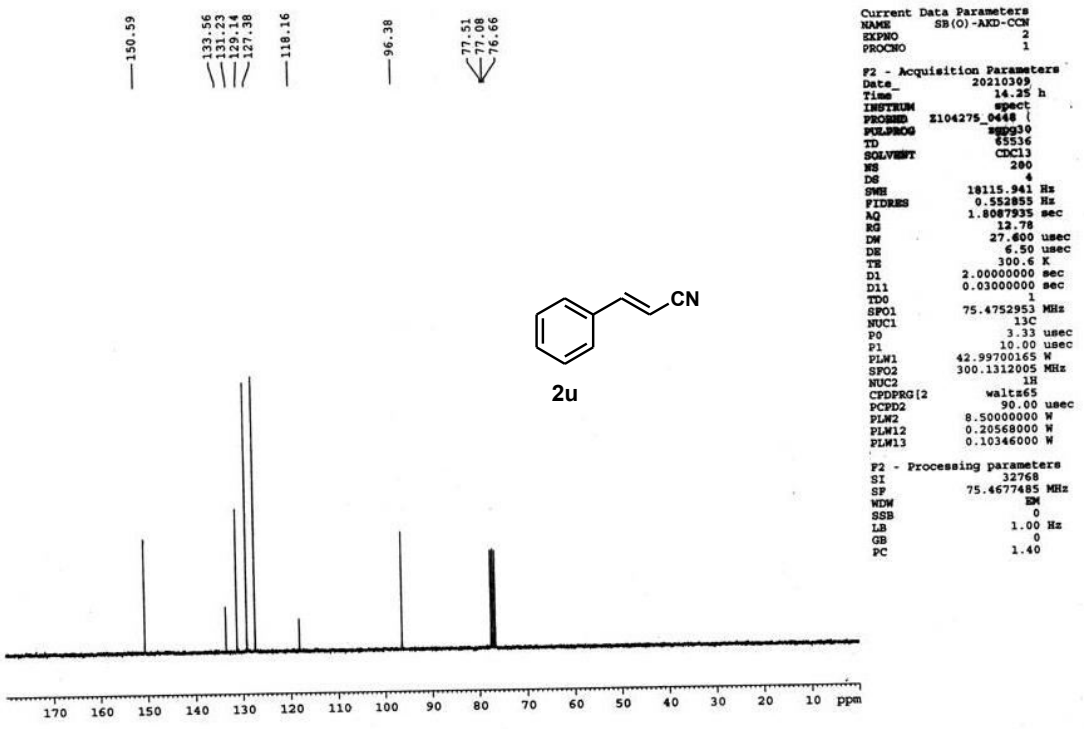

Figure 30 ^{13}C NMR of Cinnamonitrile (2u)

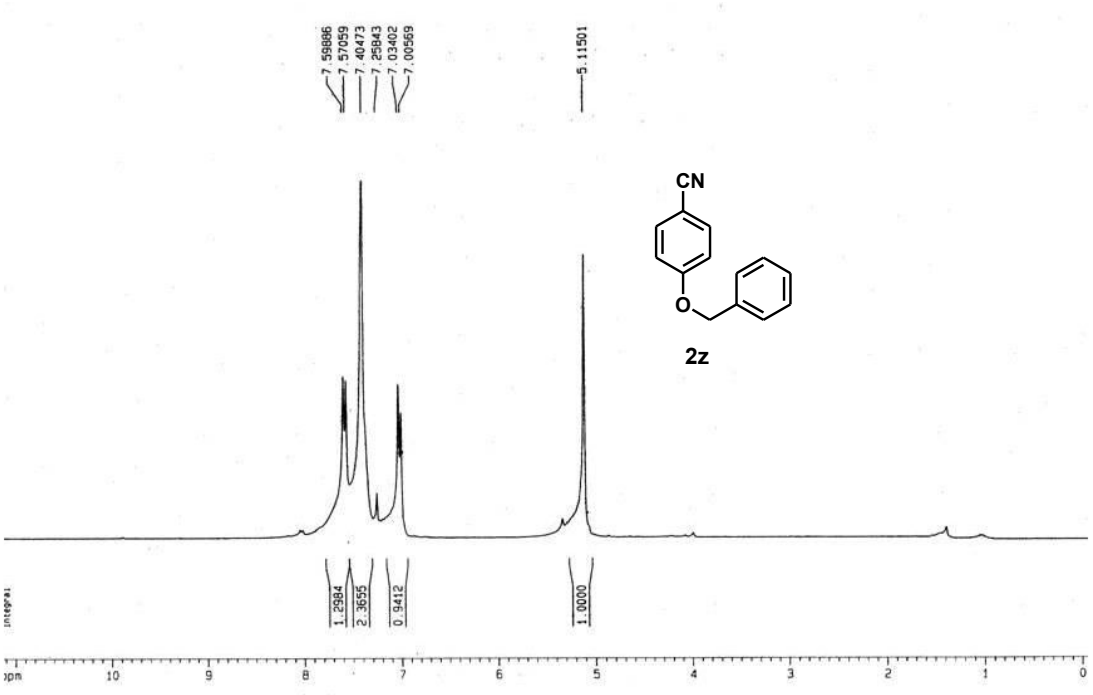

Figure 31 ^{1}H NMR of 4-(benzyloxy)benzonitrile (2z)

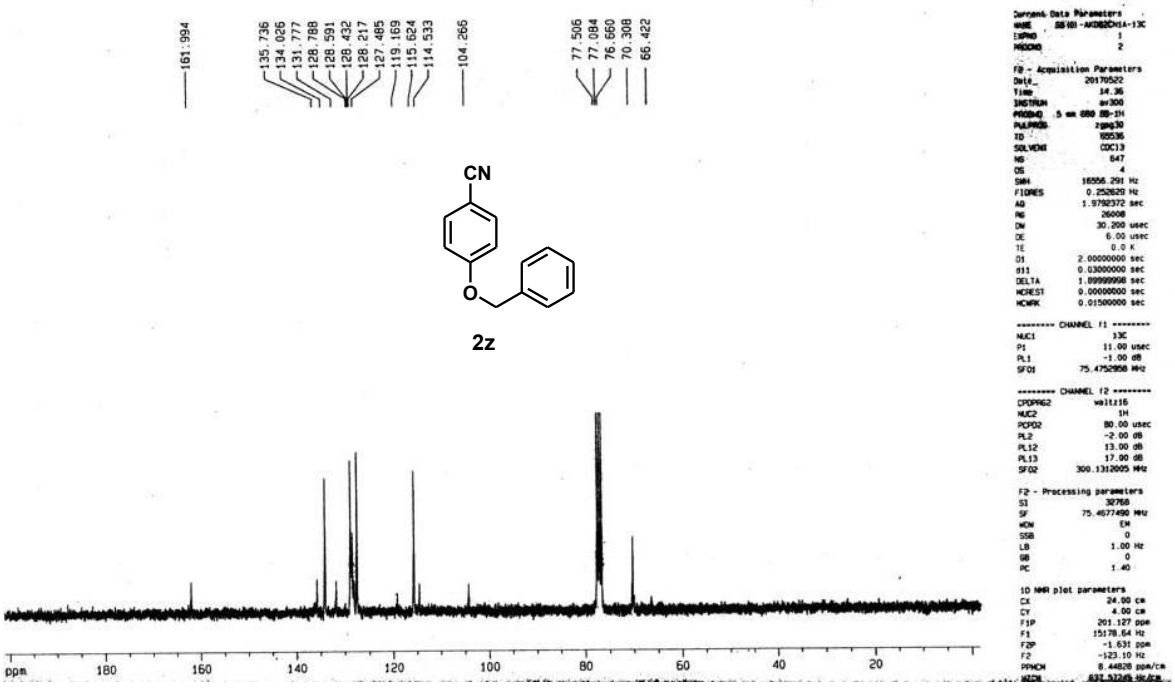

Figure 32 ^{13}C NMR of 4-(benzyloxy)benzonitrile (2z)

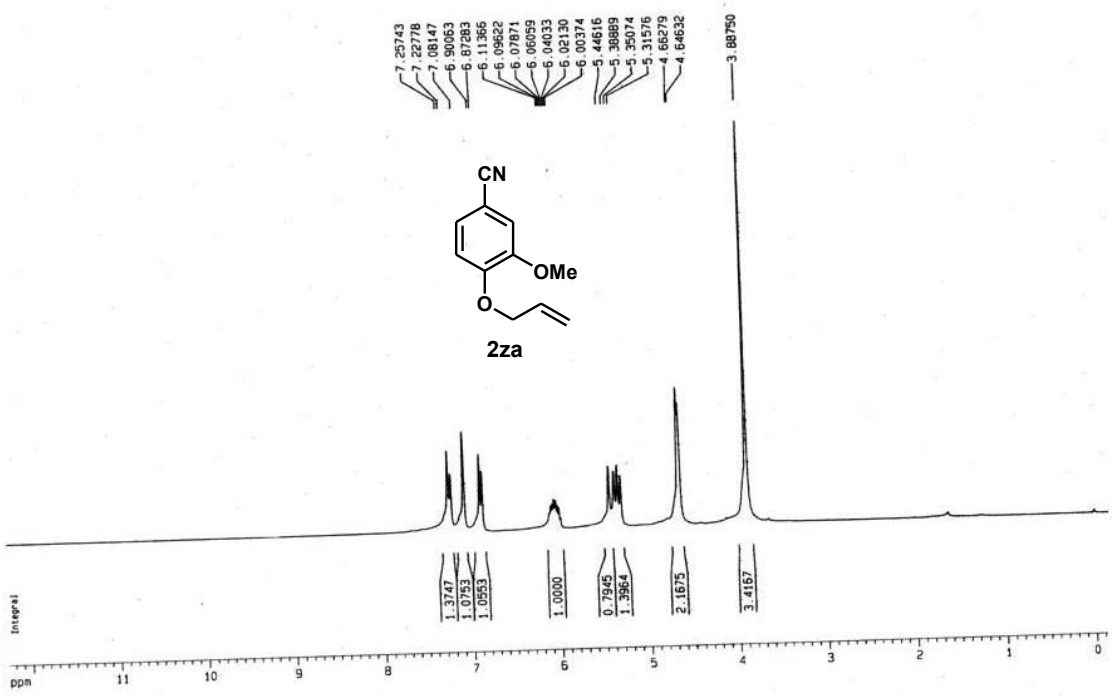

Figure 33 [1]H NMR of 4-(allyloxy)-3-methoxybenzonitrile (2za)

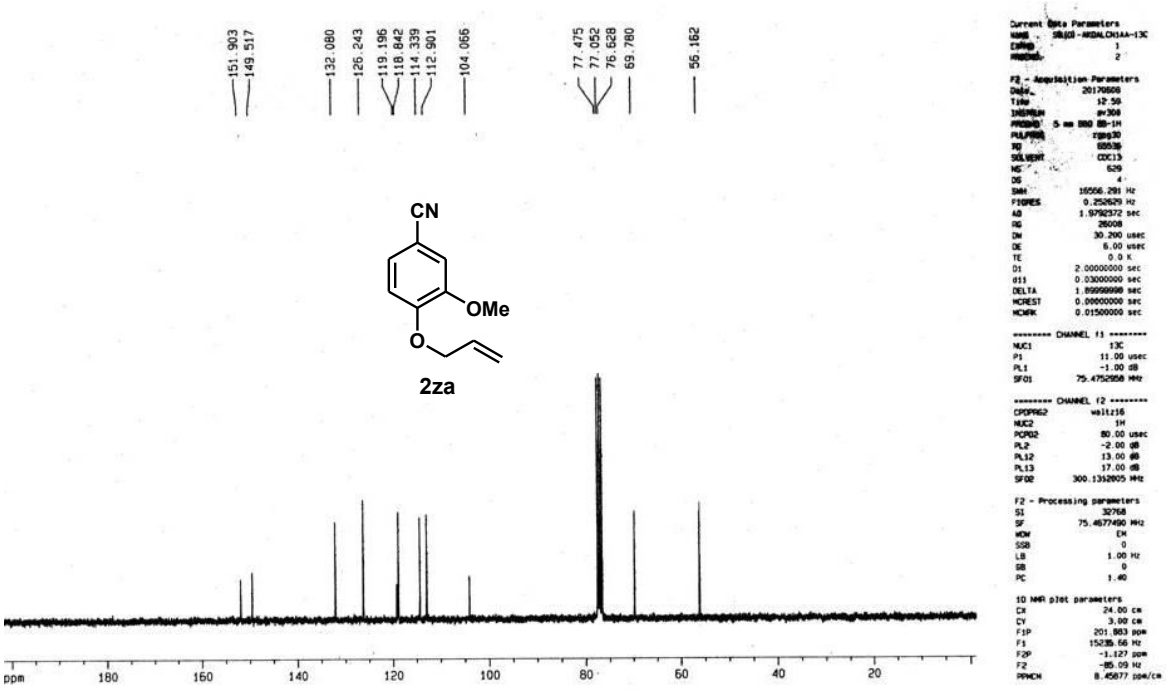

Figure 34 [13]C NMR of 4-(allyloxy)-3-methoxybenzonitrile (2za)

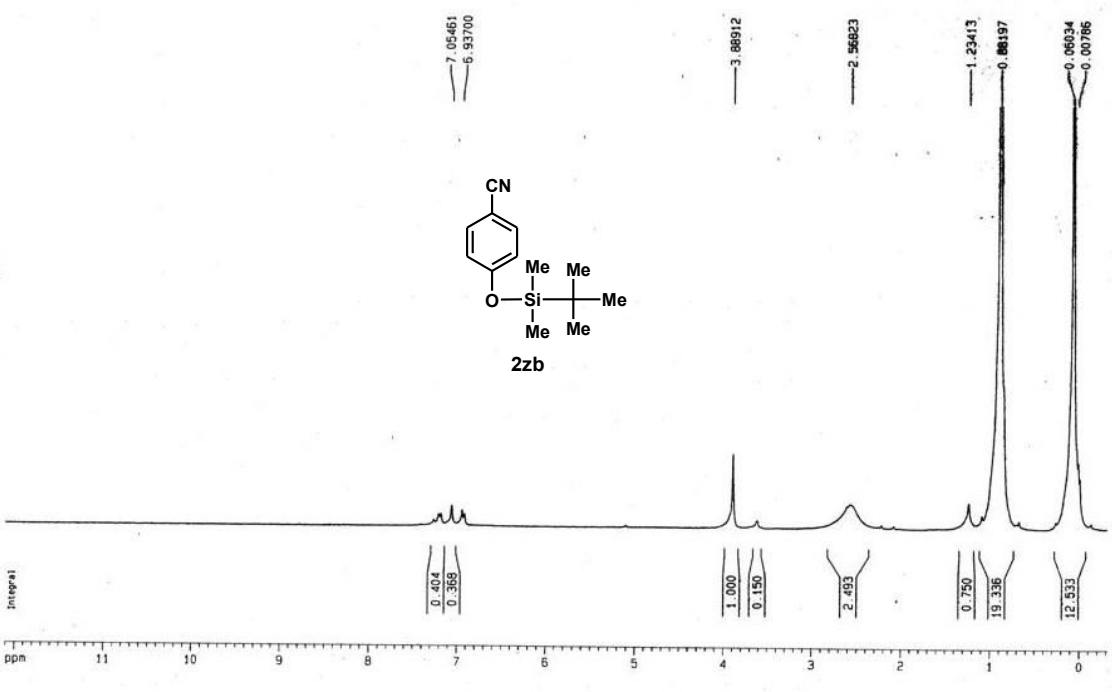

Figure 35 ^{1}H NMR of 4-((tert-butyldimethylsilyl)oxy)-3-methoxybenzonitrile (2zb)

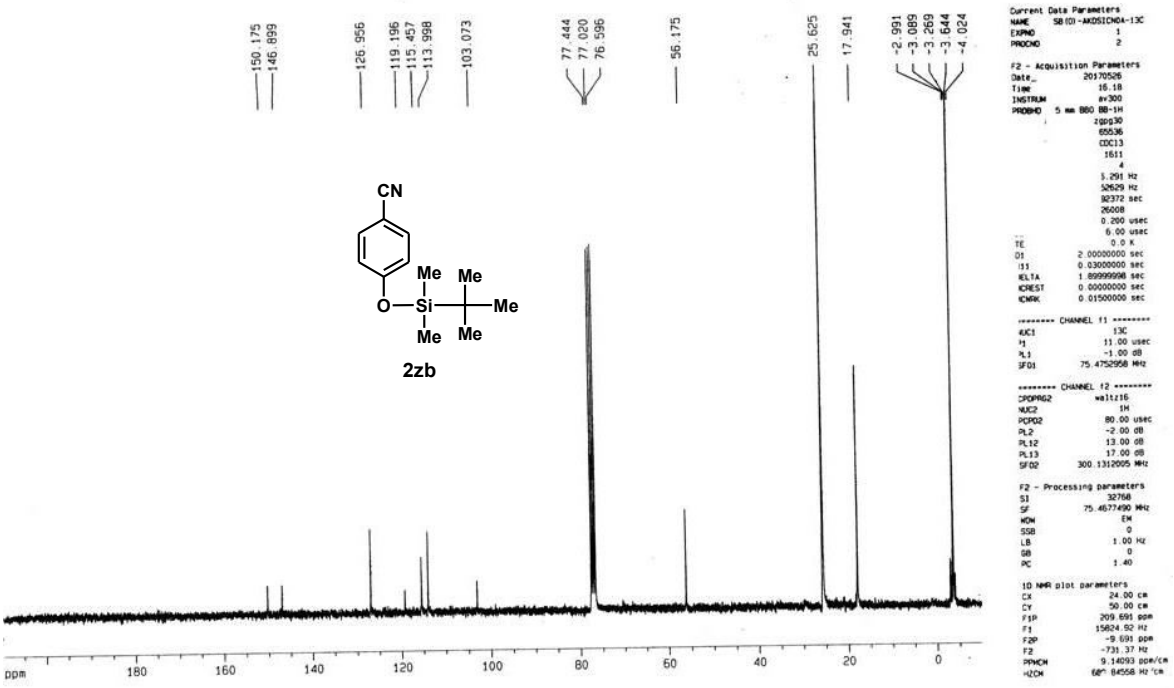

Figure 36 ^{13}C NMR of 4-((tert-butyldimethylsilyl)oxy)-3-methoxybenzonitrile (2zb)

IV.6. References:

1. (a) Houben-Wiley Grundnann C. In: Falbe J, ed. Methodender Organischen Chemie, E5. Stuttgart: Georg Thieme Verlag; **1985**, 1313; (b) R. C. Larock, In Comprehensive Organic Transformations: a Guide to Functional Group Preparations; Wiley-VCH: Weinheim, Germany, **1989**, 819; (c) A. Kleemann, J. Engel, B. Kutscher, D. Reichert, Pharmaceutical Substances: Syntheses, Patents, Applications, 4th ed.; Georg Thieme: Stuttgart, **2001**.
2. (a) M. N. Janakirman, K. D. Watenpaugh, K. T. Chong, *Bioorg Med Chem Lett.* **1998**, *8,* 1237; (b) D. Dube, M. Blouin, C. Brideau, *Bioorg Med Chem Lett.* **1998**; *8*, 1255; (c) S. I. Murahashi, *Sci. Synth.* **2004**, *19*, 345. Georg Thieme; (d) S. J. Collier, P. Langer, *Sci. Synth*. **2004**, *19*, 403. Georg Thieme; (e) L. H. Jones, N. W. Summerhill, N. A. Swain, J. E. Mills, *Med Chem Commun.* **2010**, *1*, 309; (f) A. M. Sweeney, P. Grosche, D. Ellis, K. Combrink, P. Erbel, N. Hughes, F. Sirockin, S. Melkko, A. Bernardi, P. Ramage, N. Jarousse, E. Altmann, *ACS Med. Chem. Lett.* **2014**, *5*, 937.
3. (a) J. Noh, J. Kim, *J. Org. Chem.* **2015**, *80*, 11624; (b) C. B. Kelly, K. M. Lambert, M. A. Mercadante, J. M. Ovian, W. F. Bailey, N. E. Leadbeater, *Angew. Chem. Int. Ed.* **2015**, *54*, 4241; (c) P. Nimnual, J. Tummatorn, C. Thongsornkleeb, S. Ruchirawat, *J. Org. Chem.* **2015**, *80*, 8657.
4. (a) M. Bhardwaj, M. Kour, S. Paul, *RSC Adv.* **2016**, *6*, 99604; (b) C. Fang, M. Li, X. Hu, W. Mo, B. Hu, N. Sun, L. Jin, Z. Shen, *Adv Synth Catal.* **2016**, *358*, 1157; (c) V. K. Das, S. N. Harsh, N. Karak, *Tetrahedron Lett.* **2016**, *57*, 549; (d) P. Ghosh, B. Saha, G. C. Pariyar, A. Tamang, R. Subba, *Tetrahedron Lett.* **2016**, *57*, 3618; (e) Y. Yoon, B. R. Kim, C. Y. Lee, J. Kim, *Asian J. Org. Chem.* **2016**, *5*, 746.
5. (a) X. Yang, Z. Fan, Z. Shen, M. Li, *Electrochimica Acta* **2017**, *226*, 53; (b) M. J. Kim, J. Mun, J. Kim, *Tetrahedron Lett.* **2017**, *58*, 4695; (c) C. Fang, M. Li, X. Hu, W. Mo, B. Hu, N. Sun, L. Jin, Z. Shen, *RSC Adv.* **2017**, *7*, 1484.
6. (a) J. Nandi, M. L. Witko, N. E. Leadbeater, *Synlett* **2018**, *29*, 2185; (b) K. Murugesan, T. Senthamarai, M. Sohail, M. Sharif, N. V. Kalevaru, R. V. Jagadeesh, *Green Chem.* **2018**, *20*, 266.
7. (a) W. Zhan, M. Tong, L. Ji, H. Zhang, Z. Ge, X. Wang, R. Li, *Chinese Chemical Letters*, **2019**, *30*, 973; (b) H. Chen, S. Sun, H. Xi, K. Hu, N. Zhang, J. Qu, Y. Zhou, *Tetrahedron Lett.* **2019**, *60*, 1434; (c) F. Verma, P. Shukla, S. R. Bhardiya, M. Singh, A. Rai, V. K. Rai, *Catal. Commun.* **2019**, *119*, 76; (d) J. Nandi, N. E. Leadbeater, *Org. Biomol. Chem.* **2019**, *17*, 9182.

8. (a) T. Sandmeyer, *Ber. Dtsch. Chem. Ges.* **1884**, *17*, 1633; (b) T. Sandmeyer, *Chem. Ber.* **1884**, *17*, 2650; (c) T. Sandmeyer, *Chem. Ber.* **1885**, *18*, 1492; (d) T. Sandmeyer, *Chem. Ber.* **1885**, *18*, 1946; (e) K.W. Rosenmund, E. Struck, *Chem. Ber.* **1919**, *2*, 1749.
9. (a) L. Friedman, H. Shechter, *J Org Chem.* **1960**; *25*, 877; (b) W. Wilting, M. Janssen, C. Muller, M. Lutz, A. L. Spek, D. Vogt, *Adv. Synth. Catal.* **2007**, *349*, 350; (c) G. Wang, X. Xie, W. Xu, Y. Liu, *Org. Chem. Front.* **2019**, *6*, 2037.
10. (a) G. P. Ellis, T. M. Romney-Alexander, *Chem Rev.* **1987**, *87*, 779; (b) D. W. Kim, C. E. Song, D. Y. Chi, *J Org Chem.* **2003**, *68*, 4281.
11. (a) W. Zhou, L. Zhang, N. Jiao, *Angew. Chem. Int. Ed.* **2009**, *48*, 7094; (b) D. Tsuchisya, Y. Kawagoe, K. Moriyama, H. Togo, *Org. Lett.* **2013**, *15*, 4194; (c) Y. Kawagoe, K. Moriyama, H. Togo, *Eur. J. Org. Chem.* **2014**, 4115; (d) S. Guo, G. Wan, S. Sun, Y. Jiang, J. T. Yu, *Chem. Comm.* **2015**, *51*, 5085.
12. (a) C. Qin, N. Jiao, *J. Am. Chem. Soc.* **2010**, *132*, 15893; (b) W. Zhou, J. Xu, L. Zhang, N. Jiao, *Org. Lett.* **2010**, *12*, 2888.
13. (a) M. Shevlin, *Tetrahedron Lett.* **2010**, *51*, 4833; (b) P. Y. Yeung, C. M. So, C. P. Lau, F. Y. Kwong, *Org. Lett.* **2011**, *13*, 648; (c) D. T. Cohen, S. L. Buchwald, *Org. Lett.* **2015**, *17*, 202; (d) D. Ganapathy, S. S. Kotha, G. Sekar, *Tetrahedron Lett.* **2015**, *56*, 175; (e) S. Xu, T. Cai, Z. Yun, *Synlett* **2016**, 221; (f) D. D. Beattie, T. Schareina, M. Beller, *Org. Biomol. Chem.* **2017**, *15,* 4291.
14. (a) G. Brasche, S. L. Buchwald, *Angew. Chem. Int. Ed.* **2008**, *47*, 1932; (b) L. Zhang, G. Y. Ang, S. Chiba, *Org. Lett.* **2010**, *12*, 3682; (c) B. B. Feng, J. Q. Liu, X. S. Wang, *J. Org. Chem.* **2017**, *82,* 1817.
15. Y. Zhao, G. Mei, H. Wang, G. Zhang, C. Ding, *Synlett.* **2019**, *30*, 1484.
16. (a) P. Ghosh, B. Saha, G. C. Pariyar, A. Tamang, R. Subba, *Tetrahedron Lett.* **2016**, *57*, 3618; (b) D. J. Quinn, G. J. Haun, G. Moura-Letts, *Tetrahedron Lett.* **2016**, *57*, 3844; (c) E. Niknam, F. Panahi, A. K. Nezhad, *Eur. J. Org. Chem.* **2020**, *18,* 2699; (d) R. J. Song, J. C. Wu, Y. Liu, G. B. Deng, C. Y. Wu, W. T. Wei, J. H. Li, *Synlett.* **2012**, *23*, 2491; (e) P. Maity, D. Kundu, T. Ghosh, B. C. Ranu, *Org. Chem. Front.* **2018**, *5*, 1586; (f) Y. Kim, Y. H. Rhee, J. Park, *Org. Biomol. Chem.* **2017**, *15*, 1636.
17. (a) E. Niknam, F. Panahi, A. K. Nezhad, *Eur. J. Org. Chem.* **2020**, *18,* 2699; (b) M. Sridhar, M. K. K. Reddy, V. V. Sairam, J. Raveendra, K. R. Godala, C. Narsaiah, C. Ramanaiah, C. S. Reddy, *Tetrahedron Lett.* **2012**, *53*, 3421.

LIST OF PUBLICATIONS

(A) PUBLISHED PAPERS INCLUDED IN THESIS (Reprints enclosed):

1. Catalytic efficiency of β-cyclodextrin hydrate-chemoselective reaction of indoles with aldehydes in aqueous medium, A. K. Das, N. Sepay, S. Nandy, A. Ghatak, S. Bhar, *Tetrahedron Lett.* **2020**, *61*, 152231.

2. Chemoselective and ligand-free aerobic oxidation of benzylic alcohols to carbonyl compounds using alumina supported mesoporous nickel nanoparticle as an efficient recyclable heterogeneous catalyst, A. K. Das, S. Nandy, S. Bhar, *Appl Organomet Chem.* **2021**, *35*, e6282.

(B) PUBLISHED PAPERS NOT INCLUDED IN THESIS

1. Chemoselective and Metal-Free Synthesis of Aryl Esters from the Corresponding Benzylic Alcohols in Aqueous Medium Using TBHP/TBAI as an Efficient Catalytic System, S. Nandy, A. K. Das, A. Ghatak, S. Bhar, *Synlett.* **2018,** *29*, 2208.

2. Chemoselective formation of C-N bond in wet acetonitrile using Amberlyst®-15(H) as a recyclable catalyst, S. Nandy, A. K. Das, S. Bhar, *Syn Commun.* **2020**, *50*, 3326.

(C) MANUSCRIPTS UNDER PREPARATION:

1. Synthesis of Magnetite (Fe_3O_4) Nanoparticles using Natural Resource: Recyclable Catalyst for Eco-friendly Chemoselective Reduction of Nitroarenes in Aqueous Medium, A. K. Das, S. Bhar.

2. $Cu(OAc)_2$ Catalysed Aerobic Oxidative Transformation of Aldehydes to Nitriles under Ligand-Free Condition, A. K. Das, S. Bhar.

Tetrahedron Letters 61 (2020) 152231

Contents lists available at ScienceDirect

Tetrahedron Letters

journal homepage: www.elsevier.com/locate/tetlet

Catalytic efficiency of β-cyclodextrin hydrate-chemoselective reaction of indoles with aldehydes in aqueous medium

Asit Kumar Das [a], Nayim Sepay [b], Sneha Nandy [b], Avishek Ghatak [c], Sanjay Bhar [b,*]

[a] Department of Chemistry, Krishnath College, Berhampore, Murshidabad 742101, India
[b] Department of Chemistry, Jadavpur University, Kolkata 700032, India
[c] Department of Chemistry, Dr. A. P. J. Abdul Kalam Govt. College, New Town, Kolkata 700156, India

ARTICLE INFO

Article history:
Received 6 May 2020
Revised 3 July 2020
Accepted 8 July 2020
Available online 20 July 2020

Keywords:
Aldehydes
Catalysis
Chemoselectivity
Water

ABSTRACT

The catalytic efficiency of β-cyclodextrin hydrate has been investigated towards the eco-compatible synthesis of bis-(indolyl)methanes in aqueous medium by the chemoselective reaction of indoles with differently substituted aryl and alkyl aldehydes under mild reaction conditions. The catalytic attributes of β-cyclodextrin hydrate were also demonstrated through molecular docking and DFT studies. Reactions were slower in D_2O than in H_2O. Aryl and alkyl ketones remained unaffected under the present condition. Excellent chemoselectivity has been established through intermolecular as well as intramolecular competition experiments. Calculation of Green Chemistry Metrices showed high atom economy and small E-factor for the reaction.

© 2020 Elsevier Ltd. All rights reserved.

Introduction

Cyclodextrins (CDs) are a family of macrocyclic oligosaccharides linked together by α-1,4 glucopyranose subunits and produced enzymatically from starch. β-Cyclodextrin (β-CD) consists of seven D-glucopyranose units forming a cyclic, hollow cone-shaped cavity and possessing hydrophilic exterior due to upper and lower rims decorated with hydroxyl groups as well as hydrophobic internal pocket that embrace substrates selectively [1] through inclusion complexes. But, β-Cyclodextrin hydrate (β-CDH) contains exchangeable hydrogen atoms [2] associated with protonic conductivity which is similar to that of hydrated proteins. The water molecules are present inside and outside of β-CD hydrate (β-CDH) provides an efficient path for the extended movement of protons which is also responsible for the protonic conductivity via a concerted and co-operative translocation of protons through the so-called flip-flop hydrogen bond [3]. The catalytic applications [4] of CDs for the synthesis of biologically important compounds have been reported. But surprisingly the catalytic attributes of β-cyclodextrin hydrate, which behaves differently from β-cyclodextrin, have not been explored much after the maiden report from our group [5].

Friedel-Crafts reaction is one of the cornerstone reactions for fundamental carbon–carbon (C—C) bond formation and construction of important classes of building blocks [6]. Bis-(indolyl) methanes (BIMs) are prominent and privileged structural motif in bioactive metabolites as well as compounds of both terrestrial and marine origin [7]. A broad range of biologically and pharmacologically active compounds, such as anticancer [8a], antitumor [8b], antifungal [8c], and HIV-1 integrase inhibitor [8d] also carry this structural unit. Therefore, various synthetic strategies such as solid acids [9a,9b], Lewis acids [9c–9f], hetero-polyacids [9g], ionic liquids [9h,9i], and many other transition metal-free protocols [9j–9q] have been developed during the last few years. Several homogeneous and heterogeneous systems, such as Fe [10a], Cu [10b], Zn [10c], Ag [10d], Sc [10e], Mo [10f], Pd [10g], Nb [10h], Ni-Dy complex [10i], and $Dy(OTf)_3$-ILs [10j], were also reported for the similar transformations. Even though these reported protocols are satisfactory, but they also suffer from certain disadvantages such as high temperature [9a,10g], long reaction time [9p,9q,10c,10g,10i,10j], harsh reaction condition [10g], use of expensive metal catalysts [10e–10j], limitation in gram scale production [9a,10a,10d,10h,10i,10j], insufficient recovery of catalyst [10b,10d,10e,10g,10i], lack of chemoselectivity [9a,9h,9m,9n,10a,10d,10f,10j,10k], and involvement of organic solvents [9e,9g,10b,10d,10e,10g,10k] having poor scope to recover and recycle. Therefore, an operationally simple, catalytically efficient, and eco-compatible protocol for the chemoselective synthesis of bis-(indolyl)methanes through the three component reaction [11] involving indoles [12] is of great demand from the standpoint of sustainability. The use of

* Corresponding author.
E-mail address: sanjay.bhar@jadavpuruniversity.in (S. Bhar).

https://doi.org/10.1016/j.tetlet.2020.152231
0040-4039/© 2020 Elsevier Ltd. All rights reserved.

Table 1
Optimization of reaction conditions[a].

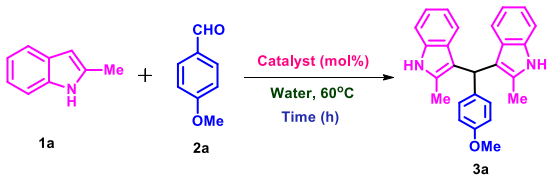

Entry	Catalyst	Mole (%)	Time (h)	Yield of **3a** (%)[b]
1	–	–	10	–
2	β-CD	2	3	52
3	β-CD	6	6	61
4	β-CD	8	6	68
5	β-CD hydrate	2[c]	6	80
6	β-CD hydrate	4[c]	3	92
7	β-CD hydrate	6[c]	5	92
8	β-CD hydrate	8[c]	3	93
9	α- CD	10	10	25
10	γ-CD	10	10	20
11	18-crown-6	6	8	Trace
12	Starch	6	8	–

[a] Reaction conditions: **1a** (1.0 mmol), **2a** (0.5 mmol), catalyst (as indicated), water (3 mL) at 60 °C. [b]Isolated yield. [c]Based on the molecular formula $C_{42}H_{70}O_{35}\cdot 11H_2O$. [13]

Table 2
Comparative study between β-CD and β-CD hydrate.[a]

Entry	Catalyst	Solvent (3 mL)	Mole (%)	Time (h)	Conversion(%)[b]
1	β-CD	H_2O	4	3	67
2	β-CD	D_2O	4	3	28
3	β-CD hydrate	H_2O	4	3	100
4	β-CD hydrate	D_2O	4	3	62

[a] Reaction conditions: **1a** (1.0 mmol), **2a** (0.5 mmol), temperature 60 °C. [b]Measured by ^{1}H NMR.

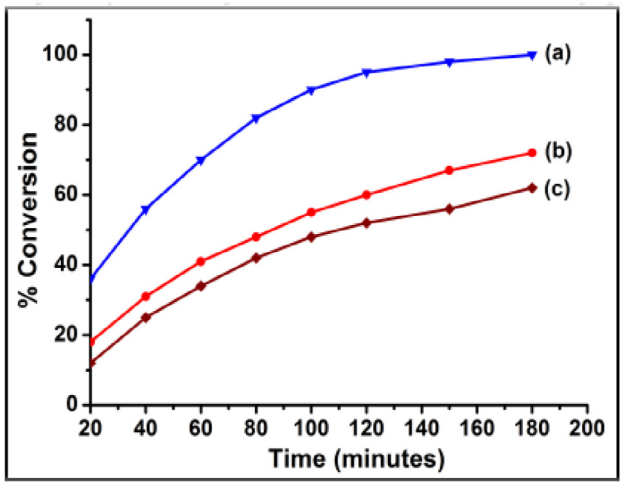

Fig. 1. Plot of the percentage conversion of **3a** with time using **1a** (1.0 mmol), **2a** (0.5 mmol) and catalyst (4 mol %) at 60 °C in solvent (3 mL); (a) β-CD hydrate in H_2O; (b) β-CD in H_2O; (c) β-CD hydrate in D_2O.

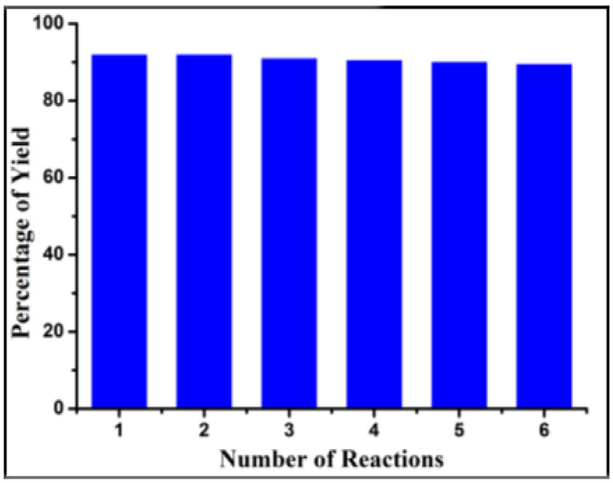

Fig. 2. Recycling of β-CD hydrate using **1a** (1.0 mmol), **2a** (0.5 mmol) and β–CD hydrate (4 mol %) as catalyst at 60 °C for 3 h in water (3 mL); % of yield was the isolated yield of **3a**.

β-cyclodextrin hydrate (β- CD hydrate) as a mildly acidic, efficient and recyclable catalyst during an organic reaction in aqueous medium has been reported [5] for the first time from our group. In continuation of our investigations in this direction we report herein the synthesis of bis-(indolyl)methanes using β-CD hydrate as an eco-friendly catalyst through chemoselective Friedel-Crafts alkylation of substituted indoles with differently substituted aromatic and aliphatic aldehydes in aqueous medium where the assistive role of water molecules present inside the cavity of β-CD hydrate was established.

Results and discussion

We initiated our experiments by investigating the Friedel-Crafts alkylation reaction between 2-methylindole **1a** (1 mmol) with 4-methoxybenzaldehyde **2a** (0.5 mmol) in water at 60 °C in the presence of different catalysts with the variation of reaction time and catalyst loading to obtain the corresponding bis-(indolyl)methanes **3a** (Table 1).

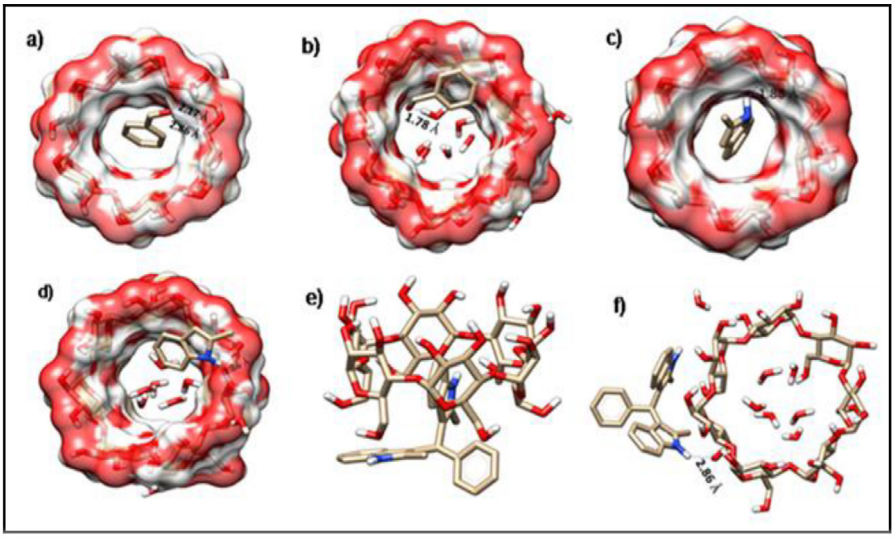

Fig. 3. Docking poses showing the interaction sites of a) benzaldehyde with β-CD, b) benzaldehyde with β-CD hydrate, c) 2-methylindole with β-CD, d) 2-methylindole with β-CD hydrate, e) bis-(indolyl)methane with β-CD, f) bis-(indolyl)methane with β-CD hydrate.

As shown in Table 1, the reaction did not occur at all in the absence of any catalyst (Entry 1), the unreacted substrates were isolated intact. The reaction was less responsive in presence α-CD (Entry 9), γ-CD (Entry 10) and 18-crown-6 (Entry 11). With β-CD, **3a** was obtained with moderate yield (entries 2–4). Surprisingly, when β-CD hydrate was used as a catalyst in lesser amount (2 mol %) the yield of the reaction was significantly increased to 80% (entry 5) but no reaction took place in the absence of β-CD hydrate even at higher temperature (80 °C). Therefore, the necessity, efficacy and applicability of β-CD hydrate for this organic transformation were firmly established. Looking for an improvement in yield, the amount of catalyst was increased. Best result was obtained using 4 mol % of β-CD hydrate where the yield was increased to 92% in lesser time (entry 6). Excess catalyst beyond this proportion (4 mol %) did not afford to better substrate conversion and increment of the yield (entries 7, 8). Hence the optimized condition for further studies has been chosen according to entry 6. Using starch as the catalyst in place of β-cyclodextrin hydrate, the reaction did not occur at all and the unreacted substrates were isolated intact (entry 12). The greater catalytic efficacy of β-CD hydrate in the present metal-free reaction in aqueous medium (entries 5–8) compared to β-CD (entries 2–4) is at par with our previous experience [5]. To further establish the efficacy of β-CD hydrate, we next carried out a comparative study between β-CD and β-CD hydrate using **1a** (1 mmol) and **2a** (0.5 mmol) in presence of H_2O and D_2O at 60 °C (Table 2).

It was observed that the reactions were faster in the presence of β-CD hydrate in H_2O as well as in D_2O compared to β-CD. Furthermore, the progress of the reaction was monitored at different time intervals using β-CD and β-CD hydrate separately as catalyst under the optimized reaction condition using H_2O as well as D_2O as the reaction medium (Fig. 1). It was evident from Fig. 1 that the reactions in H_2O were faster than in D_2O and better conversion was achieved in the former case. Hence, the isotope effect rendered by the reaction medium has been observed. The extent of conversion using β-CD as catalyst in H_2O was moderate. Hence the essentiality of water molecules inside the cavity of β-CD hydrate was conclusively proved.

β- CD hydrate bears negligible toxicity as evident from its MSDS [14]. This is sparingly soluble in water under ambient condition but becomes completely miscible in aqueous reaction medium at the reaction temperature (60 °C). Thus it offers the advantages of homogeneous catalysts during the reaction as well as the benefits of heterogeneous catalysts during isolation of the products and separation of the catalyst. After the completion of the reaction, the reaction mixture was cooled in ice-water and crude product was dissolved in ethyl acetate. The precipitated catalyst was separated by filtration, washed with ethyl acetate, dried and reused directly in a fresh reaction with a little variation of yield (Fig. 2). The reactions took place in aqueous condition and did not require inert environment and any organic co-solvent as the reaction medium. It utilizes ethyl acetate as an eco-friendly solvent for the isolation of the product. Moreover, the reactions are highly atom-efficient and generate water as the sole and innocuous side-product. Therefore, this novel β-CD hydrate catalyzed metal-free Friedel-Crafts alkylation reaction in aqueous medium

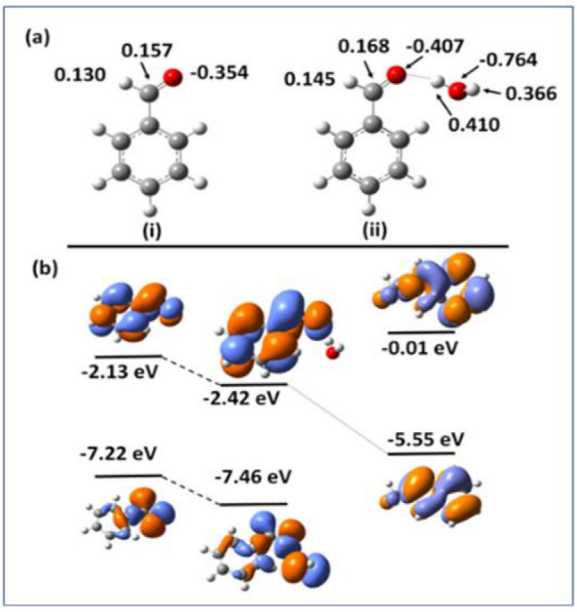

Fig. 4. (a) Optimized structures of benzaldehyde with and without hydrogen bonded water and (b) The frontier orbital energy level of HOMO and LUMO of 2-methylindole and benzaldehyde with as well as without hydrogen bonded water.

Table 3
β-CD hydrate catalysed reactions of indoles with aldehydes.

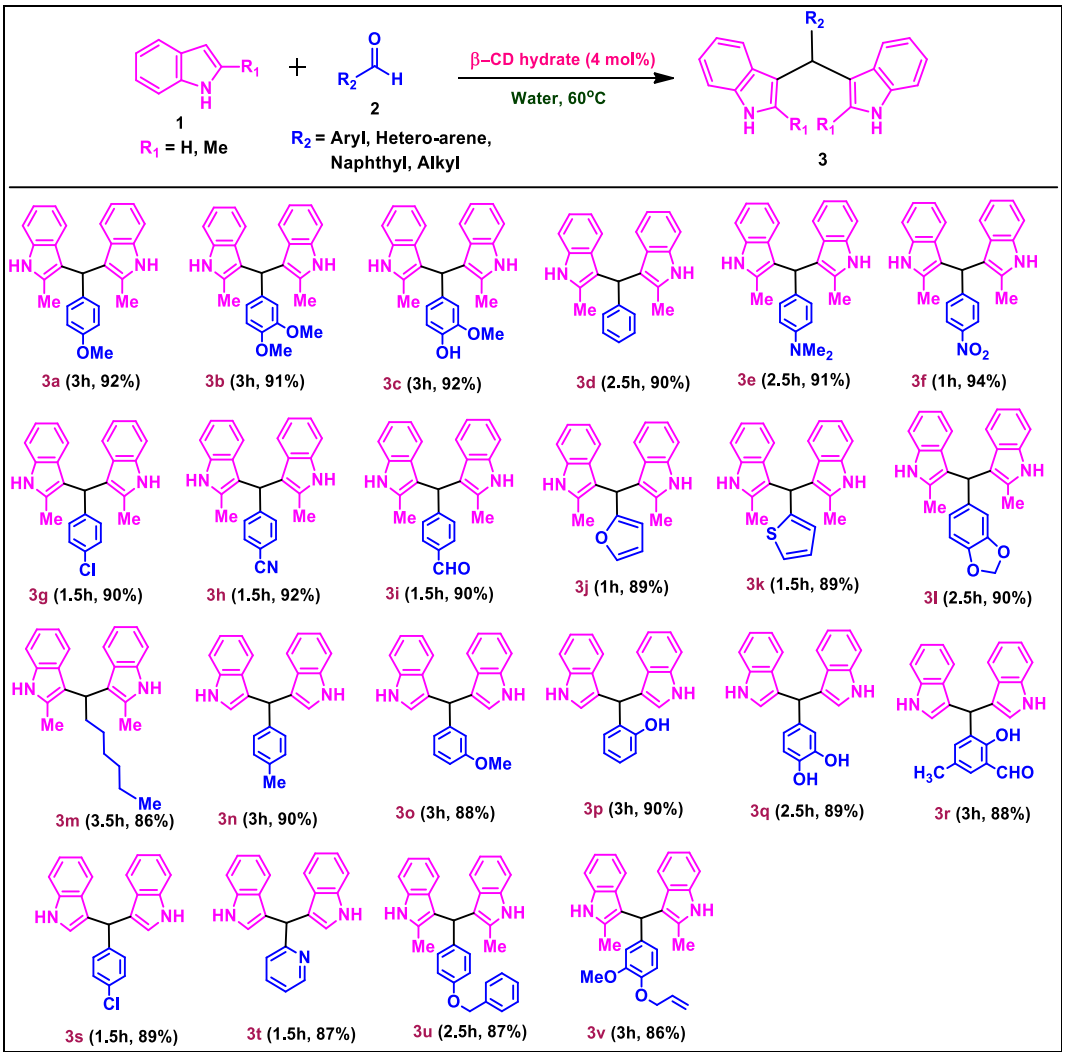

Reaction conditions: **1** (1.0 mmol), **2** (0.5 mmol), β CD hydrate (4 mol%), water (3 mL) at 60 °C for indicated time.

seems to be eco-compatible in terms of reaction medium, operational simplicity, and recyclability of catalysts and solvents of insignificant toxicity. The green metrics calculated for the optimized reaction (between **1a** and **2a**) show high atom economy and small E-factor (See the Supplementary Materials). So this metal-free catalytic protocol in aqueous medium is proved to be highly sustainable from the standpoints of efficacy, less toxicity, economical viability, recyclability of the catalyst as well as minimized waste formation.

The molecular docking study (Fig. 3) revealed that the presence of water molecules inside the cavity of β-CD hydrate (β-CDH) might facilitate the inclusion of the benzaldehyde more effectively through hydrogen bonding than simple β-CD due to different interaction of benzaldehyde with β-CDH and β-CD with a preferred orientation of the ligands inside the cavity. The docked pose of benzaldehyde was more included within the cavity of β-CDH than β-CD. The –CHO group of benzaldehyde formed one hydrogen bond (1.78 Å) with the water molecules present within the cavity of β-CDH (Fig. 3b) whereas the same formed two hydrogen bonds (2.17 Å and 2.86 Å) with the $-CH_2OH$ group of β-CD located near the wider side (secondary hydroxy rim) (Fig. 3a). However, the binding modes of 2-methylindole with β-CD and β-CDH seem to be nearly similar (Fig. 3c and 3d). The hydrogen bonding interaction of benzaldehyde with the water molecules inside the β-CDH cavity (which are also believed to possess more protic behavior due to flip-flop movement) might increase the electrophilicity of the formyl carbon; therefore the nucleophilic attack of 2-methylindole on benzaldehyde seems to be facilitated. The docked pose of corresponding bis-(indolyl)methane was more excluded through one hydrogen bonding interaction (2.86 Å) in the β-CDH whereas it was slightly included inside the cavity of β-CD (Fig. 3e and 3f).

We tried to get a deeper insight about the beneficiary effect of water molecules present inside the cavity of β-CD hydrate towards this aqueous reaction using density functional theory (DFT). The structures of 2-methylindole as well as benzaldehyde with hydrogen bonded water at a distance of 1.78 Å (Fig. 3b) and without hydrogen bonding (Fig. 3a) were optimized (Fig. 4). The result shows that the hydrogen bonding between carbonyl oxygen and water increases the positive Mulliken charge on the carbonyl carbon (Fig. 4a, ii). Thus, due to hydrogen bonding with the water molecule inside the cavity of β-CD hydrate, the electrophilicity of carbonyl carbon of benzaldehyde is increased accompanied with the greater stabilization of its HOMO and LUMO (Fig. 4b). Under hydrogen bonded condition, HOMO and LUMO of benzaldehyde

are stabilized by 0.24 eV and 0.29 eV respectively (Fig. 4b). Therefore, the nucleophilic attack by 2-methylindole through its high energy HOMO to the low energy LUMO of hydrogen bonded benzaldehyde is more facilitated with respect to benzaldehyde devoid of hydrogen bonding (Fig. 4b**,** shown with the dotted line). Calculations also indicate that the orbital coefficients of frontier molecular orbitals are enhanced due to hydrogen bonding on the carbonyl carbon atom of (ii) over (i) and its LUMO of same symmetry with the HOMO of C_2-C_3 bond in 2-methylindole (Fig. 4b). These observed results provide a supportive rationale towards the better catalytic attributes of β-CD hydrate compared to β-CD for the present reaction.

In order to explore the scope and limitations of this meal-free eco-friendly protocol, indoles **1** were reacted with structurally varied aldehydes **2** in aqueous medium in the presence of β-CD hydrate as a catalyst (Table 3). As evident from Table 3, 2-methylindole (**1a**) reacted efficiently with benzaldehyde as well as other aryl aldehydes bearing electron donating substituents (**2a**-**2e**) and electron withdrawing substituents (**2f**-**2i**) to give the corresponding bis-indolylmethanes with excellent yield (**3a-3i**). Reaction between **1a** and less electrophilic aromatic aldehyde (**2e**) under the optimized condition is known as the Ehrlich test [15].

Similarly, unsubstituted indole (**1b**) was found equally efficient to participate in the same protocol to yield the corresponding products (**3n**-**3s**). Phenolic-OH groups remained unaffected during this reaction and the reaction was very facile even with the –OH group at the *ortho*-position (**3p**,**3r**). Acid-sensitive heteroaryl moieties also survived during this reaction which paved the way towards the efficient construction of important molecular skeletons densely loaded with heterocycles (**3j**, **3k** and **3t**) in good yields. Hydrolysable group like methylenedioxy also remained unaffected in the aqueous reaction medium to produce **3l** in good yield. It is extremely important to note the remarkable survival of another acid-sensitive hydrolysable functional group –CN in this aqueous protocol, where the corresponding product **3h** was obtained with 92% yield. The survival of –CN was confirmed by the signal at δ119.4 (specific for –CN) in the ^{13}C-NMR spectrum of **3h**. With terephthaldehyde (**2i**), the bis-(indolyl)methane (**3i**) was obtained in high yield (90%) where one –CHO participated in the reaction and the other –CHO remained unaffected in spite of using higher concentration of **1a**. A sharp singlet at δ9.96 in ^{1}H NMR spectrum as well as a signal at δ197.0 in ^{13}C NMR spectrum confirmed the presence of one formyl group in **3i**. Such a regioselectivity was also observed in **3r.** This is an extremely important attribute of the present protocol in contrast to many reported methods where no such regioselectivity was observed [10d,e]. Aliphatic aldehyde (**2m**) also reacted quite efficiently in the present protocol with **1a** to produce **3m** in 86% yield. Highly vulnerable groups like O-benzyl and O-allyl were also tolerated under the optimized reaction condition to furnish the products **3u** and **3v** in 87% and 86% yields respectively. The bis-(indolyl) methane (**3q**), obtained in 89% yield through the reaction between 3,4-dihydroxybenzaldehyde and **1b**, has been reported to exhibit excellent biological activity such as HIV-1 integrase inhibition [9e].

Interestingly, aryl alkyl ketone, diaryl ketone and dialkyl ketone (acetophenone, benzophenone and 2-butanone respectively) as well as ester (methyl benzoate) did not react with indole under this β-CD hydrate catalyzed aqueous protocol where the substrates were recovered totally unaffected. Encouraged by the above observations, we ventured to investigate the chemoselectivity of our newly developed aqueous protocol. Intermolecular competition reaction was carried out with a mixture of 2-methylindole (**1a**), benzaldehyde (**2d**) and acetophenone (**2w**) under the optimised reaction condition which produced **3d** (derived from benzaldehyde) exclusively and acetophenone (**2w**) was recovered totally unaffected (Scheme 1).

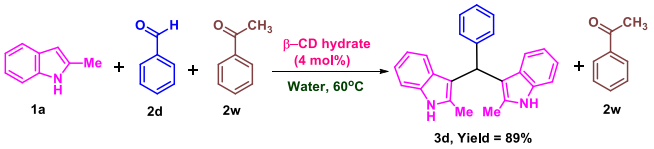

Scheme 1. Intermolecular competition experiment to demonstrate chemoselectivity.

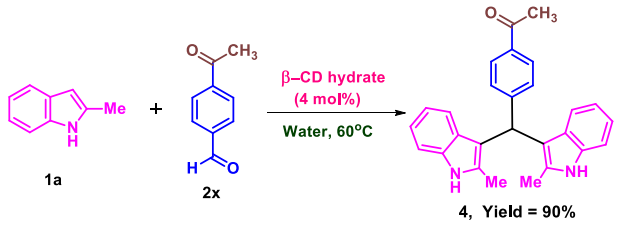

Scheme 2. Intramolecular competition experiment to demonstrate chemoselectivity.

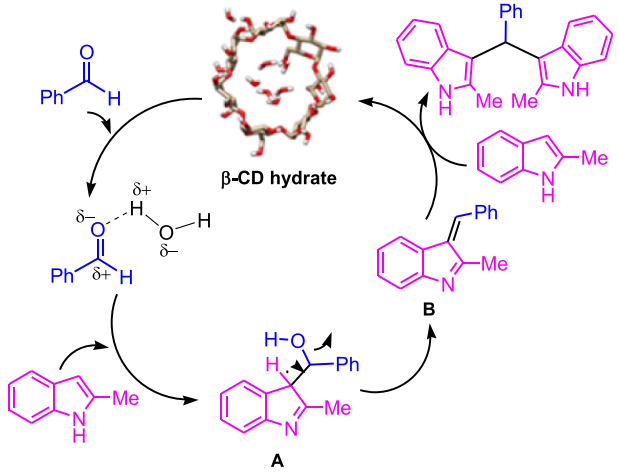

Scheme 3. Plausible mechanism for the synthesis of bis-(indol-3-yl)-methane catalysed by β-CD hydrate.

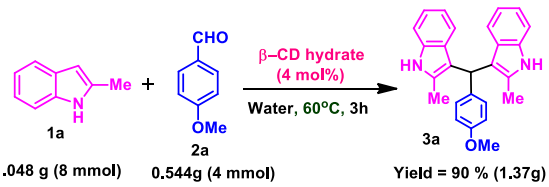

Scheme 4. Gram-scale applicability of β-CD hydrate catalysed protocol.

The aforesaid protocol was further applied to the intramolecular competition experiment with 4-acetylbenzaldehyde (**2x**) where only the formyl group reacted selectively with **1a** leading to the product **4** exclusively with 90% yield leaving the ketomethyl moiety totally intact (Scheme 2). This is a vital and additional attribute of the said protocol in contrast to many of the earlier reports [9a,9h,9m,9n,10a,10d,10f,10j,10k] where no such chemoselectivity was observed.

Table 4
Comparison of the catalytic efficiency of various catalysts reported in the literature for the synthesis of 3,3′-(p-tolylmethylene)bis(1H-indole).

Entry	Catalyst	Solvent	Time (h), Temp(°C)	Yield (%)	Ref.
1	–	Ethyl lactate: H_2O	0.5 h, U.S., RT	91	9n
2	[DABCO-H][HSO_4]	–	2 h, 90 °C	79	9o
3	α-chymotrypsin	H_2O	24 h, 70 °C	90	9p
4	Lipase enzyme	H_2O	36 h, 55 °C	95	9q
5	ZnO-RGO	EtOH:H_2O	12 h, RT	86	10c
6	TPPMS/CBr_4	CH_3CN	4 h, RT	72	10k
7	β-CD hydrate	H_2O	3 h, 60 °C	89	**This work**

A plausible mechanism for this β-CD hydrate catalyzed aqueous reaction is depicted in Scheme 3. Based on the aforsaid investigations (Figs. 3b and 4a, ii), it is presumed that nucleophilic attack from higher energy HOMO of 2-methylindole to lower energy LUMO of benzaldehyde (due to its hydrogen bonding with the water molecules inside the cavity of β-CD hydrate) is enhanced and the intermediate (A) was rapidly formed in the first step. Subsequent dehydration of the intermediate (A) forms the corresponding 3-arylidene-3*H*-indole (B), which on further nucleophilic attack by another 2-methylindole affords the product.

To demonstrate the practical utility and scalability of our newly developed protocol, a gram scale reaction between **1a** and **2a** was carried out (Scheme 4). The reaction mixture was extracted with EtOAc and the crude product **3a** was further purified by filtration chromatography on a short column of silica gel using ethyl acetate-hexane as eluent.

The comparison of our present metal-free protocol with some of the earlier reports is summarized in Table 4.

Some of the studies listed in Table 4 (entries 1–6) involved the use of costly catalyst [9p,9q,10c,10k], multistep synthesis of catalyst [9o,10c,10k], long reaction time [9p,9q,10c], lack of chemoselectivity [9n,10k], and the tedious product isolation procedure [9o] for the synthesis of BIMs. The present β-cyclodextrin hydrate-catalyzed metal-free protocol in aqueous medium mostly does away with these shortcomings (entry 7). Therefore, the present protocol seems to have enough potential to be a better, economically viable, eco-compatible and sustainable alternative with greater merits and wider applicability compared to many of the earlier methods reported for the construction of bis-(indolyl)methane framework.

Conclusion

Catalytic efficiency of β-cyclodextrin hydrate has been investigated towards the synthesis of bis-(indol-3-yl)-methanes through the Friedel-Crafts alkylation reaction of indoles with aryl, heteroaryl as well as alkyl aldehydes under mild reaction condition. This newly developed atom-economical protocol shows good chemoselectivity which has been substantiated through intermolecular as well as intramolecular competition experiments. Practical synthetic utility was also demonstrated by gram scale applicability. The salient features of the present method are procedural simplicity, excellent chemoselectivity, tolerance of various sensitive moieties during the reaction, wide substrate scope as well as eco-compatibility in terms of using water as the most innocuous reaction medium, the ready accessibility and recyclability of the catalyst of lower toxicity compared to most of the existing ones and minimization of waste formation owing to high atom economy and small E-factor.

Declaration of Competing Interest

The authors declare that they have no known competing financial interests or personal relationships that could have appeared to influence the work reported in this paper.

Acknowledgements

Financial assistance from RUSA 2-Programme and UGC-CAS-II programme in Chemistry at Jadavpur University are gratefully acknowledged. S. N. thanks DST, INSPIRE, New Delhi for senior research fellowship. Thanks to Mr. N. Dutta of IACS and Mr. R. Biswas of JU for necessary assistance.

Appendix A. Supplementary data

Supplementary data to this article can be found online at https://doi.org/10.1016/j.tetlet.2020.152231.

References

[1] Q. Wang, Y. Chen, Y. Liu, Polym. Chem.-UK 4 (2013) 4192.
[2] M.G. Usha, R.J. Wittebort, J. Mol. Biol. 208 (1989) 669–678.
[3] A. Anagnostopoulou, L. Apekis, G. Tsoukaris, IEEE Trans. Electr. Insul. 27 (1992) 801.
[4] (a) B. Madhav, S.N. Murthy, B.A. Kumar, K. Ramesh, Y.V.D. Nageswar, Tetrahedron Lett. 53 (2012) 3835–3838;
(b) S. Noel, B. Leger, A. Ponchel, K. Philippot, A.D. Nowicki, A. Roucoux, E. Monflier, Catal. Today. 235 (2014) 20–32;
[c] F. Hapiot, H. Bricout, S. Menuel, S. Tilloy, E. Monflier, Catal, Sci. Technol. 4 (2014) 1899–1908;
(d) A. Kumar, R.D. Shukla, Green Chem. 17 (2015) 848–851;
(e) V.V. Shinde, D. Jeong, S.W. Joo, E. Cho, S. Jung, Catal. Commun. 103 (2018) 83–87.
[5] A. Ghatak, S. Khan, S. Bhar, Adv. Synth. Catal. 358 (2016) 435–443.
[6] (a) C. Friedel, J.M. Crafts, J. Chem. Soc. 32 (1877) 725–791;
(b) T. Okauchi, M. Itonaga, T. Minami, T. Owa, K. Kitoh, H. Yoshino, Org. Lett. 2 (2000) 1485–1487;
(c) O. Ottoni, A.D.V.F. Neder, A.K.B. Dias, R.P.A.C. Ruz, L.B. Aquino, Org. Lett. 3 (2001) 1005–1007;
(d) J.H. Wynne, W.M. Stalick, J. Org. Chem. 67 (2002) 5850–5853;
(e) K. Mertins, I. Iovel, J. Kischel, A. Zapf, M. Beller, Angew. Chem., Int. Ed. 44 (2004) 238–242;
(f) Y.X. Jia, J.H. Xie, H.F. Duan, L.X. Wang, Q. Lin Zhou, Org. Lett. 8 (2006) 1621–1624;
(g) Y.Q. Wang, J. Song, R. Hong, Hongming, Li, Li Deng. J. Am. Chem. Soc. 128 (2006) 8156–8157;
(h) M. Bandini, M. Tragni, Org. Biomol. Chem. 7 (2009) 1501–1507;
(i) C.W. Downey, C.D. Poff, A.N. Nizinski, J. Org. Chem. 20 (2015) 10364–10369;
(j) X.F. Deng, Y.W. Wang, S. Zhang, L. Li, G.X. Li, G. Zhao, Z. Tang, Chem. Commun. 56 (2020) 2499–2502.
[7] T.R. Garbe, M. Kobayashi, N. Shimizu, J. Nat. Prod. 63 (2000) 596–598.
[8] (a) C. Grosso, A.L. Cardoso, A. Lemos, J. Varela, M.J. Rodrigues, L. Custodio, L. Barreira, T. Melo, Eur. J. Med. Chem. 93 (2015) 9–15;
(b) D. Li, T. Wu, K. Liang, C. Xia, Org. Lett. 18 (2016) 2228–2231;
(c) C.M. Bernt, G. Bottari, J.A. Barrett, S.L. Scott, K. Barta, P.C. Ford, Catal, Sci. Technol. 6 (2016) 2984–2994;
(d) A. Srivastava, A. Agarwal, S.K. Gupta, N. Jain, RSC Adv. 6 (2016) 23008–23011.
[9] (a) S.R. Mendes, S. Thurow, M.P. Fortes, F. Penteado, E.J. Lenardao, D. Alves, G. Perin, R.G. Jacob, Tetrahedron Lett. 53 (2012) 5402–5406;
(b) M. Esmaielpour, B. Akhlaghinia, R. Jahanshahi, J. Chem. Sci. 129 (2017) 313–328;
(c) K.A. Shaikh, Z.A. Mohammed, N.T. Patel, S.A. Syed, V.A. Patil, Res. J. Pharm. Biol. Chem. Sci. 1 (2010) 730–736;
(d) S.A. Sadaphal, K.F. Shelke, S.S. Sonar, B.R. Madje, M.S. Shingare, Bulletin of the Catalysis Scoeity of India 7 (2008) 111–114;
(e) A. Swetha, B.M. Babu, H.M. Meshram, Tetrahedron Lett. 56 (2015) 1775–1779;
(f) Z. Wu, G. Wang, S. Yuan, D. Wu, W. Liu, B. Ma, S. Bi, H. Zhan, X. Chen, Green Chem. 21 (2019) 3542–3546;

(g) K. Selvakumar, T. Shanmugaprabha, R. Annapoorani, Synth. Commun. 47 (2017) 913–927;
(h) P.H. Tran, X.T.T. Nguyen, D.K.N. Chau, Asian, J. Org. Chem. 7 (2018) 232–239;
(i) M. Dabiri, P. Salehi, M. Baghbanzadeh, M. Shakouri, S. Otokesh, T. Ekrami, R. Doosti, J. Iran. Chem. Soc. 4 (2007) 393–401;
(j) R.G. Vaghei, H. Veisi, J. Braz. Chem. Soc. 21 (2010) 193–201;
(k) K. Sujatha, P.T. Perumal, D. Muralidharan, M. Rajendaran, Indian. J. Chem. 48 (B) (2009) 267–272;
(l) A. Hasaninejad, M.R. Mohammadizadeh, S.F. Babamiri, in: International IUPAC Conference on, 2nd., Green Chemistry, Russia, 2008, pp. 14–19;
(m) V.D. Patil, G.B. Dere, P.A. Rege, J.J. Patil, Syn. Commun. 41 (2011) 736–747;
(n) G. Gao, Y. Han, Z.H. Zhang, ChemistrySelect. 2 (2017) 11561–11564;
(o) D.Z. Xu, J. Tong, C. Yang, Synthesis 48 (2016) 3559–3566;
(p) D. Sun, G. Jiang, Z. Xie, Z. Le, Chin. J. Chem. 33 (2015) 409–412;
(q) Y. Fu, Z. Lu, K. Fang, X. He, H. Xu, Y. Hu, RSC Adv. 10 (2020) 10848–10853.

[10] (a) D. Li, J. Wang, F. Chen, H. Jing, RSC Adv. 7 (2017) 4237–4242;
(b) J. Kothandapani, A. Ganesan, P. Vairaprakash, S.S. Ganesan, Tetrahedron Lett. 56 (2015) 2238–2242;
(c) A. Bahuguna, S. Kumar, V. Krishnan, ChemistrySelect. 3 (2018) 314–320;
(d) J. Beltra, M.C. Gimeno, R.P. Herrera, Beilstein J. Org. Chem. 10 (2014) 2206–2214;
(e) S.S. Mohapatra, Z.E. Wilson, S. Roy, S.V. Ley, Tetrahedron 73 (2017) 1812–1819;
(f) A. Bahuguna, S. Kumar, V. Sharma, K.L. Reddy, K. Bhattacharyya, P.C. Ravikumar, V. Krishnan, ACS Sustainable Chem. Eng. 5 (2017) 8551–8567;
(g) S. Guo, Z. Fang, B. Zhou, J. Hua, Z. Dai, Z. Yang, C. Liu, W. He, K. Guo, Org. Chem. Front. 6 (2019) 627–631;
(h) S.R. Mendes, S. Thurow, F. Penteado, M.S. da Silva, R.A. Gariani, G. Perin, E.J. Lenardao, Green Chem. 17 (2015) 4334–4339;
(i) N.S. Gorantla, P.G. Reddy, S.M. Abdul Shakoor, R. Mandal, S. Roy, K.C. Mondal, ChemistrySelect. 4 (2019) 7722–7727;
(j) M. Xueling, L. Sanzhong, H. Jiaqi, J.P. Cheng, Tetrahedron Lett. 45 (2004) 4567–4570;
(k) C. Huo, C. Sun, C. Wang, X. Jia, W. Chang, ACS Sustainable Chem. Eng. 1 (2013) 549–553.

[11] (a) W.G. Rajeswaran, R.B. Labroo, L.A. Cohen, J. Org. Chem. 64 (1999) 1369–1371;
(b) J.S. Yadav, B.V. Subba Reddy, N.N. Yadav, M.K. Gupta, Tetrahedron Lett. 49 (2008) 2815–2819;
(c) P. Srihari, V.K. Singh, D.C. Bhunia, J.S. Yadav, Tetrahedron Lett. 50 (2009) 3763–3766.

[12] T. Fukuyama, X. Chen, Ge Peng. *J. Am. Chem. Soc.* 116 (1994) 3127–3128.

[13] (a) M.G. Usha, R.J. Wittebort, J. Am. Chem. Soc. 114 (1992) 1541–1548;
(b) E. Sabadini, T. Cosgrove, F.C. Egidio, Carbohydr. Res. 341 (2006) 270–274.

[14] https://www.nwmissouri.edu/naturalsciences/sds/b/Beta-Cyclodextrin%20hydrate.pdf.

[15] (a) P Ehrlich, Med. Woche. (1901) 151; (b) F H Seyedeh, Z Toktam, N Zahra, Bull. Korean Chem. Soc. 34 (2013) 117.

Check for updates

Received: 10 December 2020 | Revised: 31 March 2021 | Accepted: 12 April 2021

DOI: 10.1002/aoc.6282

FULL PAPER

Applied Organometallic Chemistry WILEY

Chemoselective and ligand-free aerobic oxidation of benzylic alcohols to carbonyl compounds using alumina-supported mesoporous nickel nanoparticle as an efficient recyclable heterogeneous catalyst

Asit Kumar Das[1] | **Sneha Nandy**[2] | **Sanjay Bhar**[2]

[1]Department of Chemistry, Krishnath College, Berhampore, India

[2]Department of Chemistry, Jadavpur University, Kolkata, India

Correspondence
Sanjay Bhar, Department of Chemistry, Jadavpur University, Kolkata 700032, India.
Email: sanjay.bhar@jadavpuruniversity.in; sanjaybharin@yahoo.com

An economically efficient and operationally simple ligand-free protocol for the chemoselective oxidation of benzylic alcohols to carbonyl compounds has been developed using alumina-supported nickel nanoparticles as a stable recyclable heterogeneous catalyst along with potassium *tert*-butoxide in the presence of aerial oxygen as an eco-friendly oxidant. The aliphatic alcohols remained unaffected under the present condition. Excellent chemoselectivity has also been demonstrated through intermolecular and intramolecular competition experiments. This protocol accommodates a diverse range of substituents with the tolerance of various sensitive moieties during the reaction. The catalyst could be recovered by filtration and reused consecutively without any significant loss in the catalytic activity. Moreover, the heterogeneity of the catalyst has also been established by the "hot filtration method (Sheldon's test)".

KEYWORDS

aerial oxygen, chemoselectivity, oxidation, recyclable catalyst, sustainable chemistry

1 | INTRODUCTION

Compounds containing carbonyl moiety represent an interesting group of molecules due to their versatility as substrates for various fundamental synthetic transformations as well as important structural subunits present in several pharmaceuticals, agrochemicals, perfumes, dyes, and flavoring agents[1] as well as their applicability towards the construction of a wide variety natural products and bioactive molecules.[2] The development of efficient methods for selective oxidation of alcohols to corresponding carbonyl compounds without over-oxidation and other side reactions is a great challenge[3] in academic research and the chemical industry. Therefore, numerous methods including Corey oxidation with pyridinium chlorochromate (PCC),[4] Dess–Martin oxidation with periodinane (DMP),[5] Ley's oxidation with perruthenate,[6] Swern oxidation with activated DMSO,[7] and many others have been developed for this purpose. However, these reactions involve stoichiometric quantities of oxidants, most of which are relatively expensive, highly toxic, and cause serious environmental problems.

From the standpoint of sustainable chemistry, organic transformations using aerial oxygen as the source of an eco-friendly oxidant has attracted considerable attention[8] because it is most abundant, inexpensive, safe, economically viable, and environmentally benign compared with other conventional oxidants. To achieve this objective, several methods were developed during the last few years for the oxidation of alcohols involving transition-metal based homogeneous catalysis such as Mn(*S*-PMB)$(CF_3SO_3)_2/H_2O_2$,[9] Fe $(NO_3)_3$/DDQ/aerial oxygen,[10] $[Ni(PtBu_2NBn_2)(CH_3CN)_2]^{2+}$,[11] Schiff-Base Cu (II) Complexes/TEMPO/air,[12] Pd $(OAc)_2$/bis-triazole/

 © 2021 John Wiley & Sons, Ltd.

O_2,[13] $VOSO_4$/t-BuBpy/O_2,[14] Ru (II)-NNN complex/KO^{t}Bu,[15] and $K_2OsO_4.2H_2O/K_3[Fe(CN)_6]$[16] with good catalytic activity and selectivity. Major disadvantages associated with homogeneous catalysts were their poor recyclability, stability, and difficulty in handling, especially, during industrial operations. Moreover, these processes usually employed a large amount of environmentally ill-disposed heavy-metal waste that is undesirable from the standpoint of green and sustainable chemistry. Therefore, organic reactions using heterogeneous catalysts[17,18] have received substantial interest due to their operational simplicity, better selectivity, cost-effectiveness as well as recyclability compared with the traditional homogeneous counterparts. Heterogeneous systems involving complexes of various transition metals, like Fe_3O_4@SiO_2-APTES-FeL/TBHP/O_2,[19] Ni (II)riboflavin complex/H_2O_2,[20] Pd-PdO@rGO/O_2,[21] Pt@Ca-ZSM-5/aerial oxygen,[22] RuO_2-Supported Mn_3O_4/air,[23] binuclear Rh (II)complex/O_2,[24] Au@CeO_2/O_2,[25] V_2O_5@GO/O_2,[26] and Mo (VI)@Merrifield resin/H_2O_2,[27] have been also documented in recent years. Recently, Mahmoudi et al[28] developed an aerobic oxidative protocol for the oxidation of benzylic alcohols and alkylbenzenes to carbonyls using Fe_3O_4@SiO_2@(TEMPO)-co-(Chlorophyll-Co^{III}) as an efficient magnetically recyclable nanocatalyst in an aqueous medium under ambient conditions. Moreover, recent developments[29] on the application of supported metal nanoparticles for the oxidation of alcohols have been reported. Serious shortcomings of the existing oxidative protocols are associated with the involvement of harmful and expensive metal catalysts, employing high oxygen pressure, high concentration of oxidants, use of expensive ligands, generation of over oxidized product, lack of chemoselectivity, and relatively long reaction time. Therefore, the development of a cost-effective, operationally simple, easily accessible, and efficient catalytic system for the oxidation of alcohols using environmentally benign aerial oxygen as an eco-friendly oxidant is of great demand in the present environmental perspective. We report herein our new findings on the excellent catalytic attributes of alumina-supported Ni nanoparticles[30,31] for oxidative transformation during the highly chemoselective and ligand-free conversion of benzylic alcohols to the corresponding carbonyl compounds in the presence of aerial oxygen as an eco-friendly oxidant.

2 | EXPERIMENTAL

2.1 | Materials and instrumentation

All reactants were purchased from SRL, AVRA Chemicals, Alfa-aesar, Spectrochem, and Sigma Aldrich and used as received without further purification. ^{1}H and ^{13}C NMR spectra were obtained on a Bruker-300 spectrometer (300 MHz) and JEOL Spectrometer (400 MHz) in $CDCl_3$ and DMSO-d_6 solutions with TMS as an internal reference. Field emission scanning electron microscopy (FE-SEM) images were recorded with a Zeiss (Zemini) scanning electron microscope. Energy-dispersive X-ray spectroscopy (EDX) experiment was carried out by using a Hitachi S3400N SEM–EDX instrument. Transmission electron microscopic images were collected on a JEOL 2010 transmission electron microscopy (TEM) operated at 200 kV. XRD data of the powder sample were obtained in transmission mode using a Bruker D2 Phaser X-ray diffractometer (30 kV, 10 mA) using Cu-Kα ($\lambda = 1.5406$ Å) radiation. Chemical states of the heterogeneous material were determined by X-ray photoelectron spectroscopy (XPS) using a PHI 5000 (versa Probe II, FEI Inc). The particle size distribution and zeta potential were evaluated by the dynamic light scattering (DLS) system (Malvern Zetasizer Nano). The specific surface area and porosity of the catalyst were characterized by the Brunauer–Emmett–Teller (BET) method with N_2 adsorption–desorption isotherms, measured at 77 K using Quantachrome Autosorb® iQ-MP/iQ-XR. GC analysis was performed using Perkein Elmer Clarus 600 Gas Chromatograph. Column chromatography was performed on silica gel (60–120 mesh) from SRL, India. Thin layer chromatographic separations were performed on precoated silica gel plates using silica gel G for TLC (E. Merck).

2.2 | Preparation of alumina supported Ni nanoparticles

To a solution of nickel chloride hexahydrate (4.75 g, 20 mmol) in distilled water (15 ml), neutral alumina (20.0 g) was added under the stirring condition to get the slurry of nickel chloride on neutral alumina. It was dried thoroughly in the air when nickel chloride adsorbed on neutral alumina was obtained as a greenish-white easy flowing powder. To the magnetically stirred suspension of this material in methanol (20 ml), sodium borohydride (1.512 g, 40 mmol) was added in small portions, and stirring was continued for another 1 h under ambient atmosphere. By this time, the greenish-white mass turned grey. Then, it was filtered and washed successively with methanol (3 × 5 ml), water (3 × 10 ml), and methanol (2 × 5 ml). The residue was dried at 130°C for 2 h to afford alumina-supported nickel nanoparticles (21.10 g, referred to as Ni-Alumina) as a grey free-flowing powder. It can be stored under the ambient condition for months without appreciable deterioration of its catalytic activity.

2.3 | General experimental procedure for the Ni-Alumina catalyzed oxidation of alcohols

To a stirred suspension of appropriate alcohol **1** (1 mmol) in toluene (3 ml), Ni-Alumina (5 mol%) was added followed by K^{t}OBu (1.2 mmol). The reaction mixture was stirred at 80°C, and the progress of the reaction was monitored by thin-layer chromatography (TLC). After completion of the reaction, the reaction mixture was cooled to room temperature, ethyl acetate (15 ml) was added to dissolve the product, and the catalyst was separated simply by filtration. The residue (recovered catalyst) was thoroughly washed with EtOAc (3 × 5 ml) followed by water (3 × 5 ml). The aqueous washing was repeatedly extracted with ethyl acetate (4 × 5 ml). The combined organic extracts were washed with water (4 × 5 ml) and dried over anhydrous Na_2SO_4. The crude product **2** was obtained by removal of the solvent under reduced pressure, which was further purified by column chromatography on a short column of silica gel using 5%–15% ethyl acetate-hexane as eluent.

2.4 | Procedure for the Ni-Alumina catalyzed gram scale oxidation of 4-methoxybenzyl alcohol (1a)

To a stirred suspension of 4-methoxybenzyl alcohol (**1a**) (1.104 g, 8 mmol) in toluene (24 ml), Ni-Alumina (0.4 g, 5 mol%) was added followed by K^{t}OBu (1.075 g, 9.6 molar eq). The reaction mixture was stirred at 80°C, and the progress of the reaction was monitored by TLC. After completion of the reaction, the reaction mixture was cooled to room temperature, ethyl acetate (120 ml) was added to dissolve the product, and the catalyst was separated simply by filtration. The residue (recovered catalyst) was thoroughly washed with EtOAc (3 × 40 ml) followed by water (3 × 40 ml). The aqueous reaction mixture was repeatedly extracted with ethyl acetate (4 × 40 ml). The combined organic extracts were washed with water (4 × 40 ml) and dried over anhydrous Na_2SO_4. The crude product was obtained by removal of the solvent under reduced pressure, which was further purified by column chromatography on a short column (Yield: 88%, 0.957 g).

3 | RESULTS AND DISCUSSION

3.1 | Catalyst characterization

To determine the crystalline nature of the synthesized nanocatalyst, powder X-ray diffraction of the sample was recorded (Figure 1). The result indicates that the sample is composed of both metallic Ni and NiO supported on alumina. The diffraction peaks observed at 45.4°(111), 55.3°(200), 77.5°(220), and 95.6°(222) attributed to the metallic Ni phase, and other characteristic peaks observed at 37.3°(111), 42.8°(200), 60.9°(220), 72.3°(331), and 85.4°(222) were assigned to the presence of NiO phase.[32] The observed results are closely matched with the theoretical values from metallic Ni (cubic structure, JCPDS# 01-071-3740) and NiO (cubic structure, JCPDS# 01-089-3080).

To investigate the structural details of Ni nanocatalyst, TEM and high-resolution transmission electron microscopy (HRTEM) characterization were carried out on the samples (Figure 2). From the images, the crystalline nature of the synthesized nanocatalyst was observed with lattice fringe spacing of 0.203 and 0.240 nm corresponding to the *d* value for cubic Ni (111) and cubic NiO (111) respectively. The corresponding SAED pattern (selected area electron diffraction) also revealed the crystalline nature of the nanocatalyst.

Scanning electron microscopy (SEM) image is presented in Figure 3a. It has been observed that nickel nanoparticles have a nanocrystalline structure with an irregular spread on the supported alumina. EDX spectroscopy analysis was also performed to ensure the chemical composition of the synthesized nanocatalyst (Figure 3b). The result shows the strong elemental signal of Ni, Al, and O and their relative proportions in the nanoparticles. Additionally, the spatial distribution of each element was also investigated by a mapping experiment which demonstrated that the distributions of Ni, Al, and O elements are well arranged in the structure of nanocatalyst (Figure 3c).

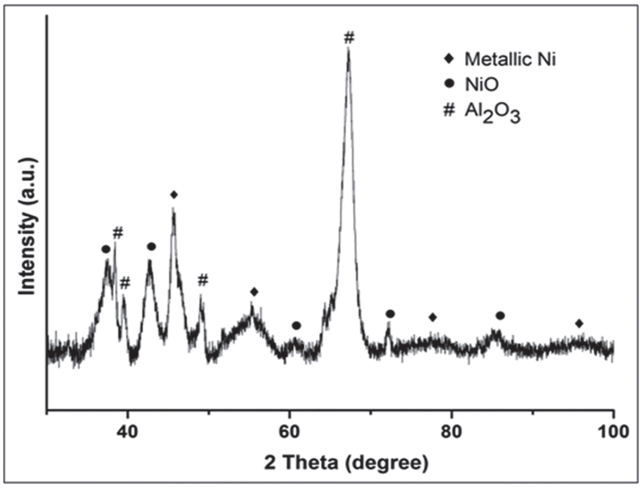

FIGURE 1 X-ray diffraction analysis of Ni nanoparticles supported on alumina

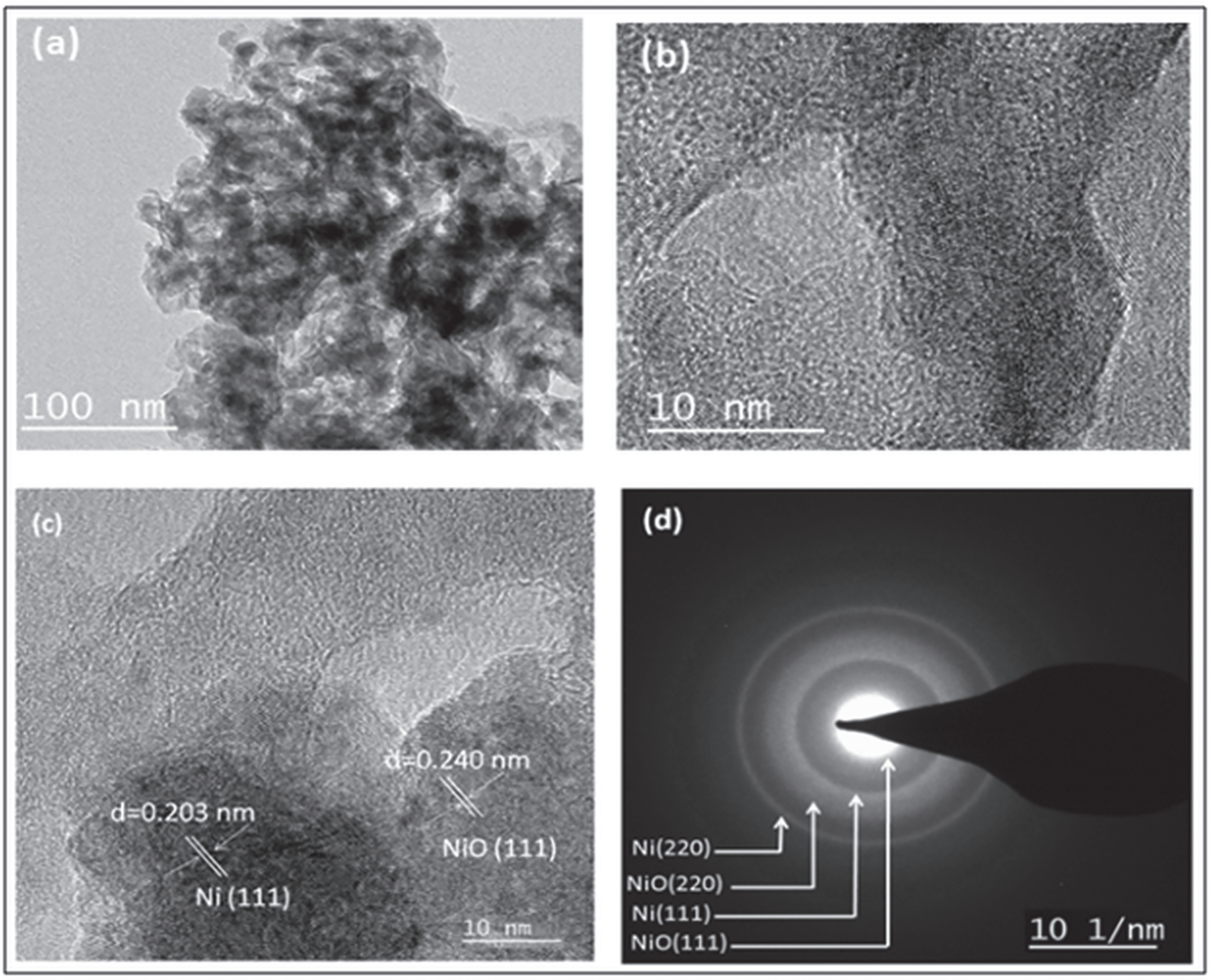

FIGURE 2 Transmission electron microscopy (TEM) images of Ni nanoparticles@Al_2O_3: distribution of Ni catalysts (a), transmission electron microscopy (HRTEM) (b and c), selected area electron diffraction (SAED) (d)

XPS analysis has been carried out to investigate the oxidation state of the Ni species in the nanocatalyst (Figure 4). A high-resolution spectrum of the Ni 2p core level region was recorded to identify the presence of Ni species. The Ni $2p_{3/2,1/2}$ binding energy peaks observed at 853.8 and 871.6 eV along with associated satellite peaks at 859.7 and 877.7 eV correspond to Ni metal. The peaks observed at 855.8 and 873.7 eV with satellite peaks at 864.2 and 881.5 eV are attributed to Ni oxide species present on the nanocatalyst surface. Binding energy peak values of Ni metal are on the higher side because of the nanoparticle nature of the Ni metal species. The peak positions are closely matched with the reported literature.[33] However, the intensities of the core level peaks indicate the predominant presence of elemental Ni atoms over Ni oxide species on the surface of the nanocatalyst. The appearance of oxidized Ni is due to the probable chemical sorption of oxygen or it could be the surface oxidation during the preparation and storage of nanocatalyst. According to the basic principle of XPS, the area ratio of $2p_{3/2}$ to $2p_{1/2}$ would be 2, which can be observed in the present study.

The particle size distribution (Figure 5a) and zeta potential analysis (Figure 5b) of the synthesized alumina-supported nickel nanoparticle were investigated by a DLS experiment in an aqueous dispersion. The average particle size of Ni-Alumina is 36.5 nm. The stability of Ni-Alumina was also evaluated via zeta potential analysis. Nanoparticles with zeta potential values greater than +30 mV or less than −30 mV are considered as high degrees of stability.[34] The synthesized Ni-Alumina revealed a zeta potential of −32.5 mV owing to their enhanced stability by preventing the agglomeration of the nanoparticles encapsulated in the pore of alumina.

The specific surface area and porosity of the synthesized Ni-Alumina were evaluated by the BET method

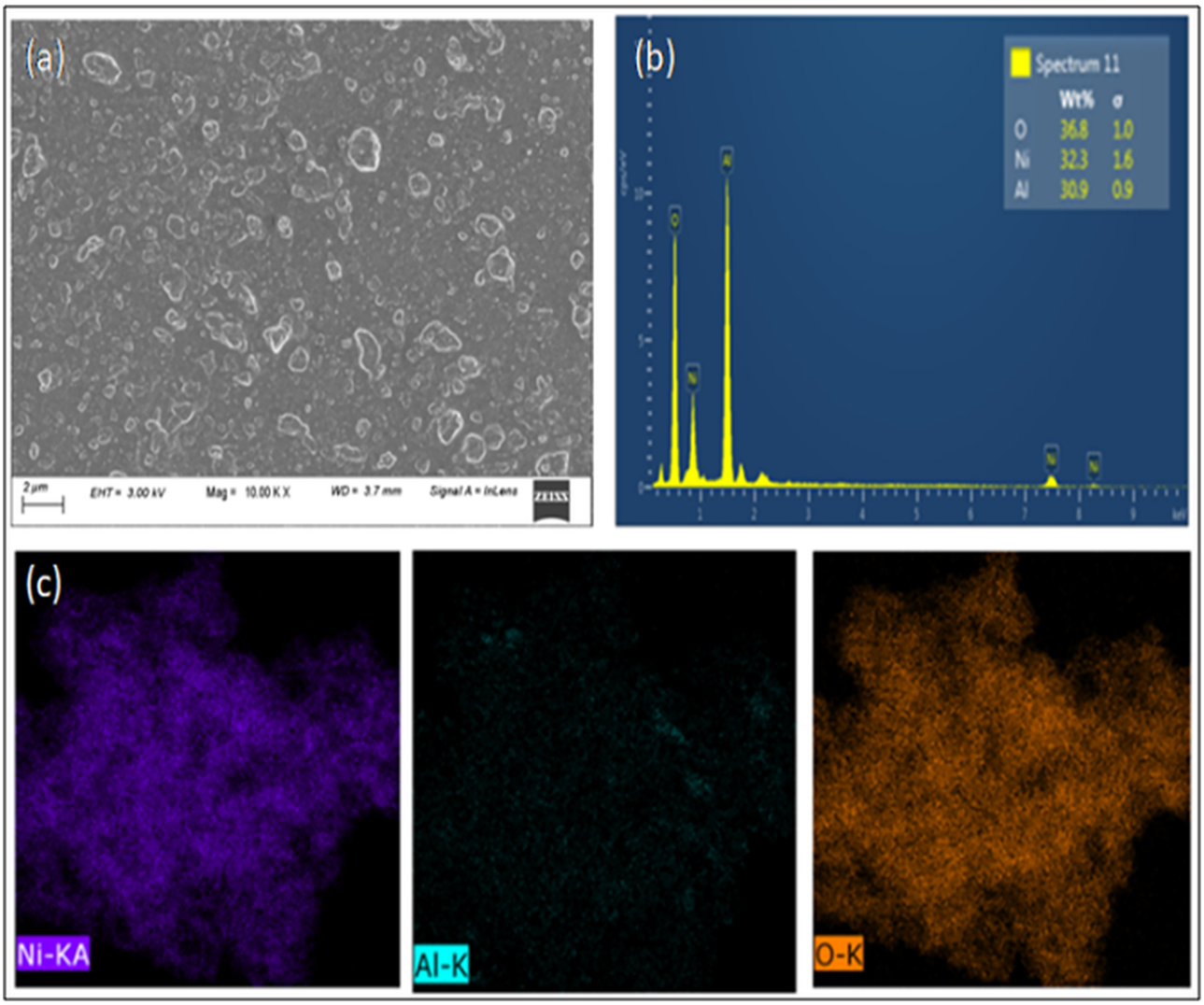

FIGURE 3 (a) Scanning electron microscopy (SEM) images, (b) energy-dispersive X-ray (EDX) spectra, and (c) elemental mapping images of Ni nanoparticles supported on alumina

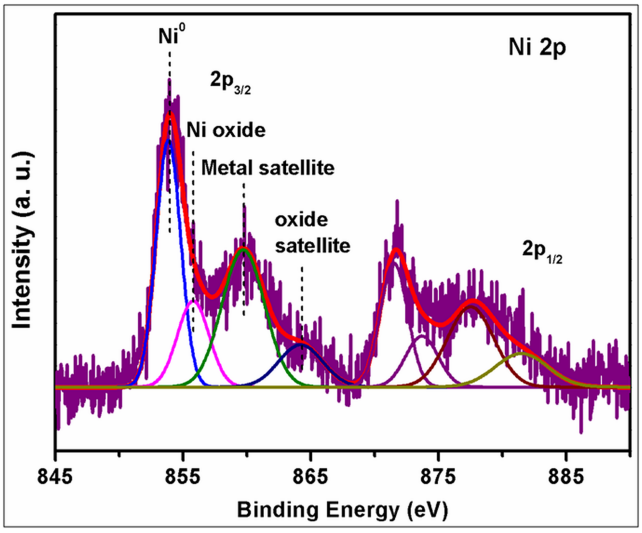

FIGURE 4 X-ray photoelectron spectroscopy (XPS) analysis of alumina supported Ni nanoparticles

with N_2 adsorption–desorption isotherms. The results were shown in Figure 6. The isotherm belonged to type III isotherm with a discrete hysteresis loop at a relative P/P_0 range 0.4 to 1.0, disclosed a mixed H3 and H1 type (according to the IUPAC classification), which signified the mesoporous nature of the synthesized nanocatalyst (Figure 6a). The BET surface area was found to be 108 $m^2\ g^{-1}$. The corresponding pore size distribution was calculated from the desorption part of the isotherm which centered around 2.8 nm (Figure 6b) indicating also the mesoporous behavior of the nanocatalyst.

3.2 | Catalytic efficiency

To check the efficacy of Ni-Alumina, we initially investigated the reaction conditions for the aerobic oxidation of 4-methoxybenzyl alcohol **1a** (1 mmol) in the presence

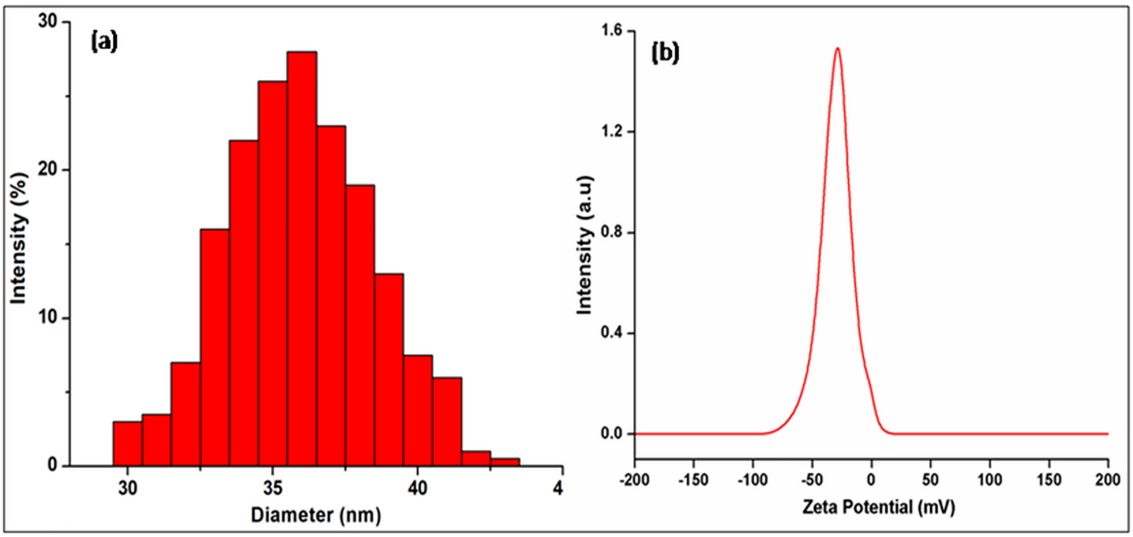

FIGURE 5 (a) Dynamic light scattering (DLS) and (b) zeta potential analysis of alumina supported Ni nanoparticles

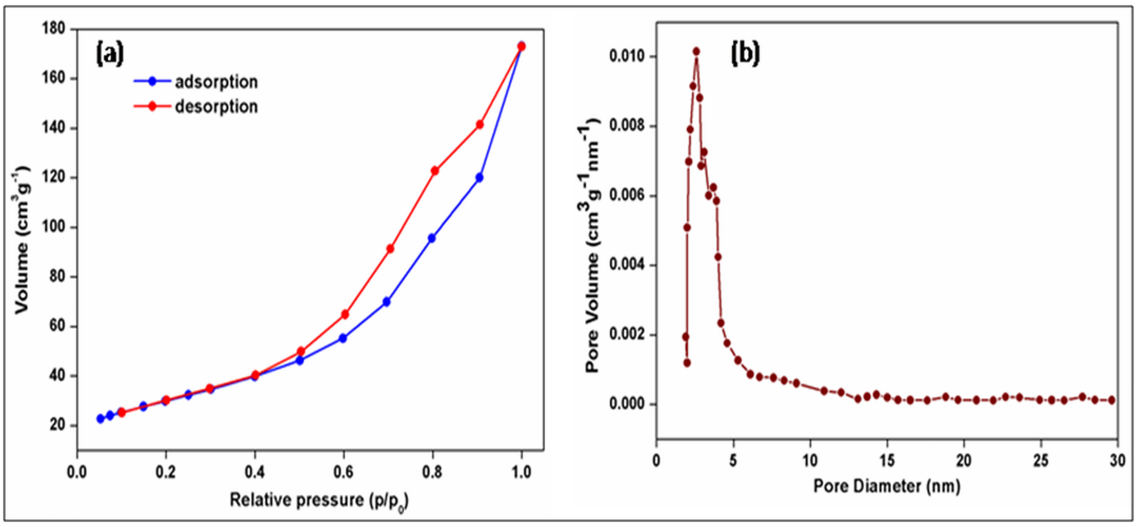

FIGURE 6 (a) Nitrogen adsorption–desorption isotherm and (b) corresponding pore size distribution plot for Ni–alumina

of different bases in various solvents at different temperatures to obtain the corresponding aldehyde **2a**. The reaction was also carried out varying the amounts of catalyst to obtain the optimum conditions (Table 1).

The reaction did not occur in the absence of Ni-Alumina both in the absence (Entry 1) as well as in the presence of a base (Entries 2 and 3); the unreacted substrate **1a** was isolated intact in all the cases. The trace amount of product was isolated after 12 h when the reaction was carried out under reflux condition in toluene using 2 mol% of catalyst in absence of base (Entry 4). The extent of conversion was increased to 76% within 10 h using 3 mol% of Ni-Alumina as a catalyst and potassium tert-butoxide (1.2 mmol) as a base (Entry 5) when the reaction was carried out at 80°C. Increasing the amount of catalyst to 4 mol%, the extent of conversion was slightly increased to 80% after 10 h (entry 6). A less satisfactory result was obtained with NaO^tBu instead of KO^tBu (Entry 7). Other bases such as K_2CO_3, KOH, NaOH, Et_3N, and pyridine resulted in moderate yields (Entries 13, 14, 15, 17, and 18). Hence, potassium *tert*-butoxide was found to be the most effective base in this reaction. These observations demonstrated the very necessity of the co-existence of both Ni-Alumina and base for effective oxidative transformation. A better result was obtained within 7 h when the reaction was performed with Ni-Alumina (5 mol%) and potassium *tert*-butoxide (1.2 mmol) (Entry 8). The efficient conversion of the

TABLE 1 Ni-Alumina catalyzed optimization of reaction conditions[a]

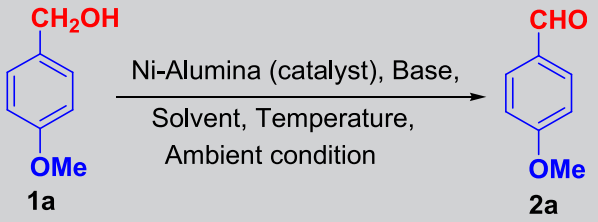

Entry	Catalyst (mol%)	Base	Solvent (mL)	Temperature (°C)	Time (h)	Yield[b] (%)
1	—	—	Toluene	Reflux	12	—
2	—	KOH	Toluene	Reflux	12	—
3	—	KO^{t}Bu	Toluene	Reflux	12	—
4	2	—	Toluene	Reflux	12	Trace
5	3	KO^{t}Bu	Toluene	80°C	10	76
6	4	KO^{t}Bu	Toluene	80°C	10	80
7	4	NaO^{t}Bu	Toluene	80°C	10	73
8	**5**	**KO^{t}Bu**	**Toluene**	**80°C**	**7**	**90**[c]
9	6	KO^{t}Bu	Toluene	80°C	7	90
10	7	KO^{t}Bu	Toluene	80°C	7	91
11	8	KO^{t}Bu	Toluene	80°C	7	91
12[d]	5	KO^{t}Bu	Toluene	80°C	7	—
13	5	K_2CO_3	Toluene	80°C	9	42
14	5	KOH	Toluene	80°C	9	63
15	5	NaOH	Toluene	80°C	10	60
16	5	KO^{t}Bu	Xylene	80°C	10	78
17	5	Et_3N	Toluene	80°C	12	42
18	5	Pyridine	acetonitrile	80°C	12	35

[a]Reaction conditions: 1a (1.0 mmol), base (1.2 mmol), catalyst and temperature (as indicated), solvent (3 ml) under ambient condition.
[b]Isolated yield.
[c]GC yield (>99%).
[d]The reaction was carried out under an inert (argon) atmosphere.

substrate **1a** to the corresponding aldehyde **2a** was achieved without the formation of any over-oxidized by-products as monitored by GC analysis (GC Yield: >99%) (entry 8). Moreover, when the crude reaction mixture was treated with diazomethane, no trace of methyl 4-methoxybenzoate (expected to be obtained from 4-methoxybenzoic acid due to over-oxidation of **1a**) was observed in the ^{1}H NMR spectrum; occurrence of **2a** as the exclusive reaction product was thus clearly evident. This observation suggested the inherent selectivity of this protocol. Excess catalyst beyond this proportion (5 mol%) did not show further increase in the substrate conversion, and the yield of the reaction remained more or less the same (Entries 9–11). Therefore, the conditions, as delineated in Entry 8, have been chosen as the optimized condition for further reactions in order to extend the substrate scope and establish the general applicability as well as the selectivity of the aforesaid protocol. The inferior performance was observed when the reaction was carried out in xylene and acetonitrile (Entries 16 and 18). It is extremely important to note that no aldehyde was detected in the reaction mixture when the reaction was carried out under an inert (Ar) atmosphere in the absence of aerial oxygen (Entry 12), and the substrate **1a** was recovered unaffected. Therefore, the essentiality of aerial oxygen along with both Ni-Alumina and potassium *tert*-butoxide towards this oxidative transformation has been firmly substantiated. Interestingly, in contrast to most of the methods involving metal nanocatalysts, no inert atmosphere is required for the reaction described

TABLE 2 Ni-Alumina catalyzed oxidative transformation of alcohols under ambient condition

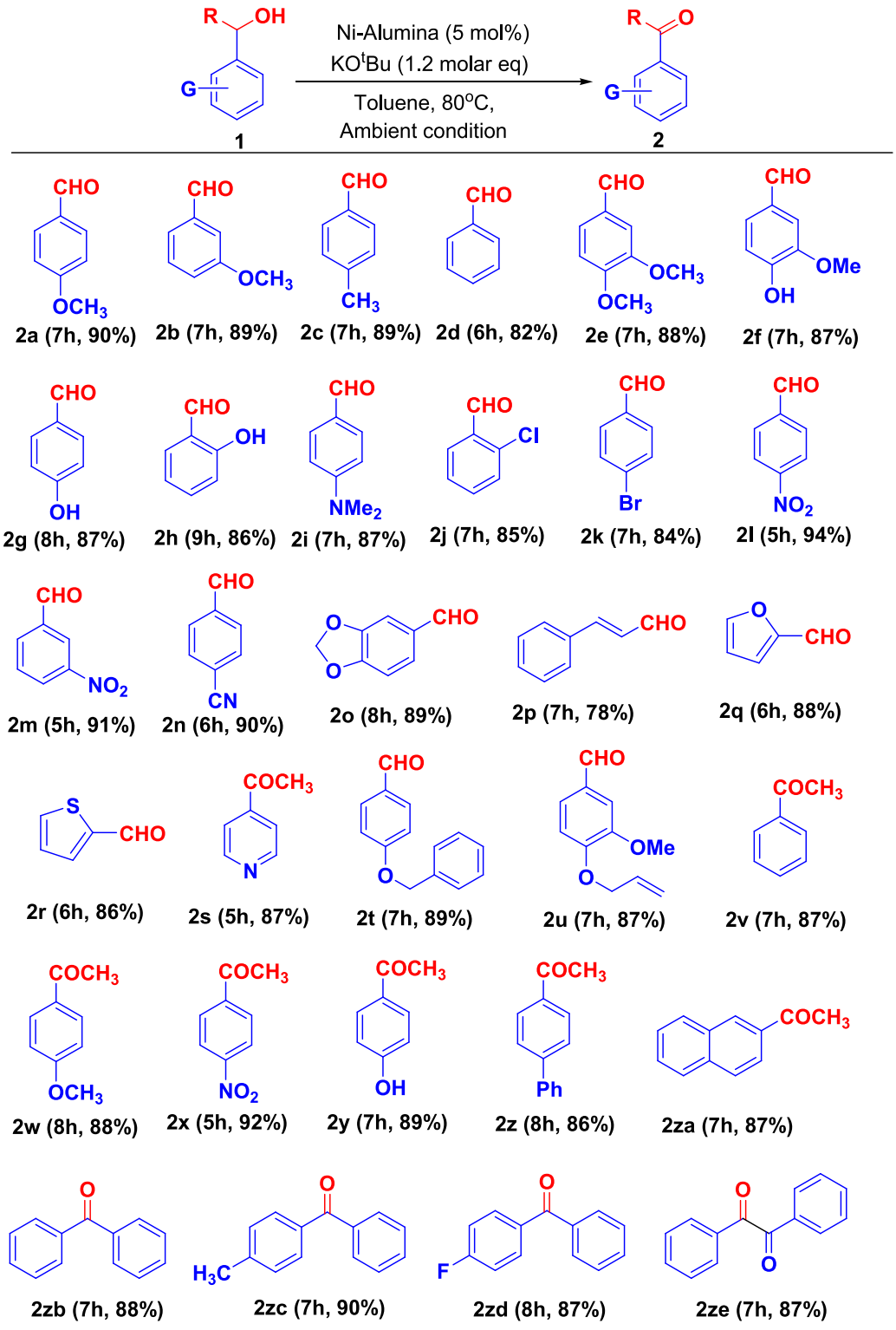

Note: Reaction conditions: **1a** (1.0 mmol), KO^{t}Bu (1.2 molar eq), catalyst (5 mol%), toluene (3 ml) at 80°C for indicated time under ambient condition. Yield refers to that of the isolated pure product.

under Table 1, rather the inert atmosphere has been found detrimental (Entry 12) for this reaction. The aforesaid oxidative protocol did neither occur with neutral alumina alone nor with nickel nanopowder without support nor with alumina-supported nickel chloride or with nickel oxide nanoparticle. The importance of alumina-supported nickel nanoparticles for this oxidative organic transformation in terms of its better stability and superior catalytic activity was thereby firmly established.

To demonstrate the generality and scope of this protocol, primary and secondary benzylic alcohols **1** bearing various electron-withdrawing and electron-donating substituents at different positions of the aromatic ring were reacted under the optimized condition where the corresponding carbonyl compounds **2** were obtained with good to excellent yields (Table 2).

As evident from Table 2, primary benzylic alcohols bearing electron-donating substituents produced the corresponding aldehydes in good yield (**2a–2e**). Phenolic-OH groups did not interfere during this reaction (**2f–2h**). Highly deactivated benzyl alcohol, such as 4-*N*,*N*-dimethylaminobenzyl alcohol (**1i**), also responded efficiently under the optimized condition with a shorter reaction time to furnish **2i** in 87% yield. Halogenated alcohols were also compatible and desired products **2j** and **2k** were formed without any dehalogenation. Primary benzylic alcohols bearing electron-withdrawing substituents, which are generally less susceptible to oxidation, furnished the corresponding aldehydes under the present reaction condition in good yield. Nitro-substituted primary benzylic alcohols were oxidized smoothly to the corresponding aldehydes (**2l** and **2m**) taking less time for completion, and the yields were comparable with the electron-rich analogues. The progress of the reaction of primary benzylic alcohols **1l** and **1a** (bearing 4-NO_2 and 4-OMe substituents, respectively) was monitored separately at different time intervals under the optimized reaction condition (Figure 7). It was observed that the reaction was faster in the case of 4-nitrobenzyl alcohol (**1l**) compared with 4-methoxybenzyl alcohol (**1a**) and better conversion was achieved in the former case. Therefore, the electronic effect of the substituents towards this Ni-Alumina catalyzed oxidative protocol was conclusively established.

Hydrolyzable functional groups, like –CN and methylenedioxy also survived under the aforesaid protocol to produce the corresponding aldehydes **2n** (90%) and **2o** (89%), respectively. This is not commonly observed in some literature reports.[21,23,24,27] The oxidation of cinnamyl alcohol afforded the mixture of cinnamaldehyde (**2p**) and cinnamic acid in 82:18 ratio (determined by 400 MHz ^{1}H NMR spectroscopy) under optimized reaction condition, wherefrom **2p** was isolated

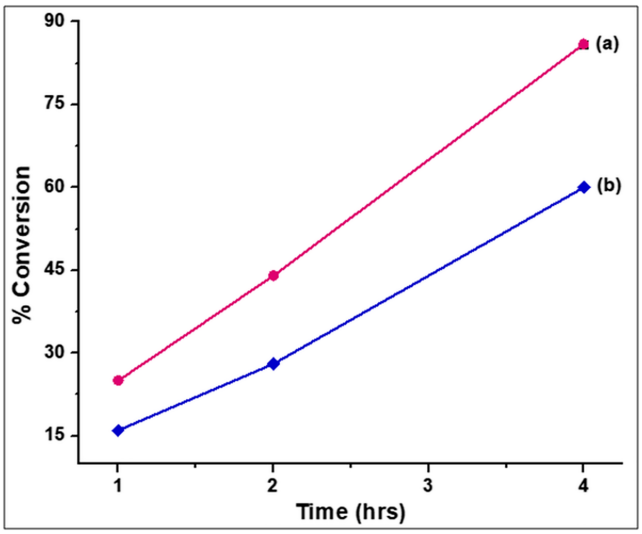

FIGURE 7 Plot of the percentage conversion of (a) 4-nitrobenzyl alcohol (**1l**) and (b) 4-methoxybenzyl alcohol (**1a**) using Ni Alumina (5 mol%), KO^{t}Bu (1.2 mmol), toluene (3 ml) at 80°C under ambient condition

with 78% yield. To extend the substrate scope, this study was further extended to more challenging heterocyclic moieties. Acid-sensitive heteroaryl moieties along with the formyl group as well as ketomethyl group also survived during this reaction and the products were obtained in good yields (**2q–2s**). It is important to note that highly vulnerable groups like *O*-benzyl and *O*-allyl moieties were also tolerated under the optimized reaction condition to produce **2t** and **2u** with 89% and 87% yields, respectively.

This procedure was also effective for secondary benzylic alcohols. 1-phenylethanol (**1v**) behaved similarly to produce the corresponding ketone (**2v**) with 87% yield. Substrates with a wide variety of substituents, including methoxy, nitro, hydroxyl, and phenyl also responded smoothly to yield the corresponding ketones (**2w–2z)**. 2-Acetylnaphthalene (**2za**) was obtained in 87% yield under the optimized protocol. Diarylcarbinols afforded the diaryl ketones (**2zb**–**2zd**) in good yield. α-Hydroxyketone (**1ze**) also reacted efficiently to produce 1,2-diketone (**2ze**) in 87% yield. Interestingly, aliphatic primary and secondary alcohols did not respond to the present protocol where the substrates were recovered unchanged.

Encouraged by the above observations, we ventured to investigate the chemoselectivity of this Ni-Alumina catalyzed oxidative protocol. Therefore, an intermolecular competition reaction was carried out with an equimolecular mixture of 4-methoxybenzyl alcohol (**1a**) and 1-heptanol under the optimized condition which produced the 4-methoxybenzaldehyde (**2a**) exclusively, and

1-heptanol was recovered unaffected (Scheme 1). This is an immensely important and additional attribute of the said protocol in contrast to many earlier reports where no such chemoselectivity was observed.[9,11,16,21,27,35,36]

The aforesaid protocol was further applied to the intramolecular competition experiments where the substrates **3a** and **3b**, under the optimized condition, produced **4a** and **4b**, respectively (Scheme 2). It was found that in both cases, benzylic alcohol was selectively oxidized to the corresponding carbonyl group and the primary aliphatic alcohol moiety remained intact. Survival of primary alcohol moiety in **4a** and **4b** was further substantiated through acetylation of **4a** and **4b** to the mono acetates **5a** and **5b** respectively.

To gain insight into the mechanistic aspect of the present oxidative protocol, some control experiments were performed (Scheme 3). The aforesaid oxidative protocol did not work with neutral alumina as well as alumina-supported nickel chloride, nickel nanopowder without any support, and with nickel oxide nanoparticle in the absence of any support (Scheme 3a). This observation suggested that alumina acted as a support to the metallic nanoparticles in this reaction. Notably, when the reaction was tested under a nitrogen atmosphere, the substrate 4-methoxybenzyl alcohol **1a** was recovered unaffected (Scheme 3b). Therefore, the essentiality of the oxygen atmosphere towards this oxidative transformation was conclusively proved. It was observed that when the reaction was carried out under O_2 atmosphere in the presence as well as in the absence of NaO^tBu, the yields of the reaction were 87% and 21% respectively within 7 h (Schemes 3c,d). The reaction was better when the oxidation of 4-methoxybenzyl alcohol **1a** was performed in the presence of KO^tBu as the base under O_2 atmosphere (yield 98% after time 3 h, Scheme 3e) than in the presence of NaO^tBu as well as in the absence of KO^tBu or NaO^tBu. These experiments revealed that both KO^tBu and O_2 atmosphere were required for the effective oxidative transformation.

Based on the aforesaid investigations and literature reports,[37,38] the plausible mechanism for this Ni-Alumina catalyzed oxidative transformation is depicted in Scheme 4. The coupling of alcoholic oxygen to the metallic nickel and coordination of the aromatic ring with the catalyst surface seems to be the initiation step of this catalytic reaction. The corresponding carbonyl compounds (aldehydes or ketones) were subsequently obtained by the removal of a hydrogen atom from the benzylic position in the presence of KO^tBu. Aerial oxygen acts as an environmentally benign oxidant regenerating Ni (0) with the generation of hydrogen peroxide that is subsequently decomposed into water and oxygen as an innocuous by-product. The presence of hydrogen peroxide was detected by the development of dark blue color when the reaction

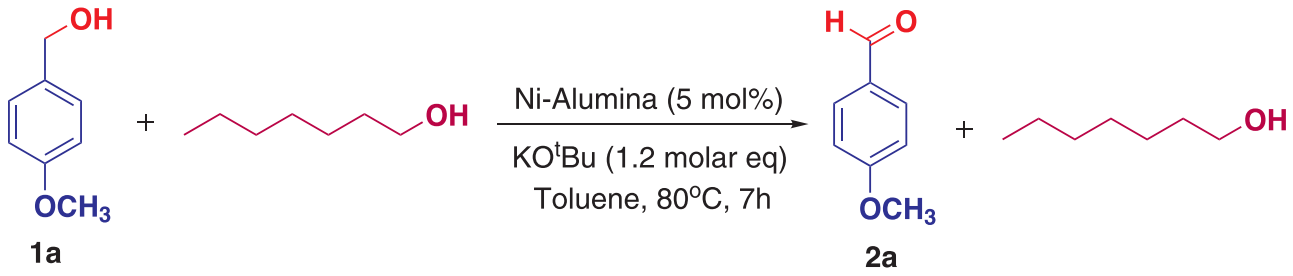

SCHEME 1 Intermolecular competition experiment to demonstrate chemoselectivity

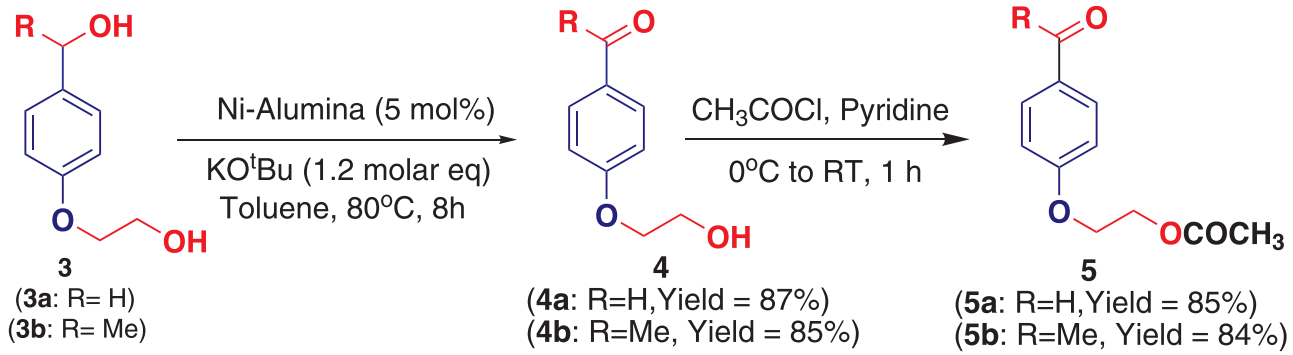

SCHEME 2 Chemoselective oxidation of 1° and 2°-benzylic alcohol

SCHEME 3 Control experiments for the oxidative transformation of alcohols

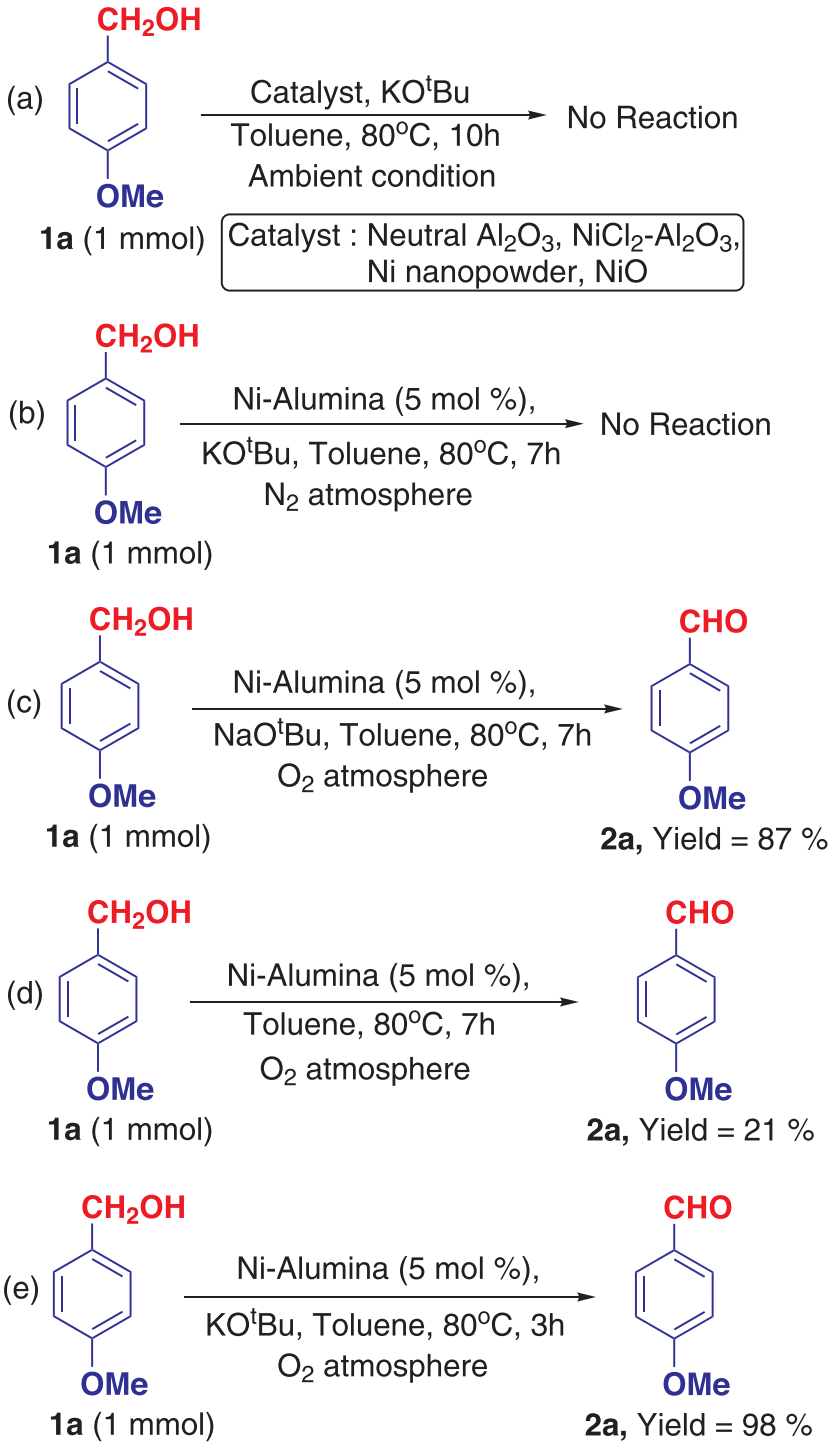

mixture was added to a mixture of KI, starch, and acetic acid. The reluctance of aliphatic alcohols towards this oxidative protocol might be due to the lack of proper coordination of the alkyl moiety to the catalyst surface. Thus, the high chemoselectivity of the present oxidative protocol towards the benzylic alcohols in the presence of aliphatic alcohols along with the efficient recyclability (vide infra) of the catalyst (Ni-Alumina) can be justified.

3.3 | Gram-scale applicability

To evaluate the practical applicability of this catalytic system, a gram-scale reaction with **1a** (1.104 g, 8 mmol) was performed under the optimized reaction conditions, and the desired product **2a** was isolated in 88% yield (0.957 g). An almost similar result was obtained as that of the small-scale reaction (Scheme 5).

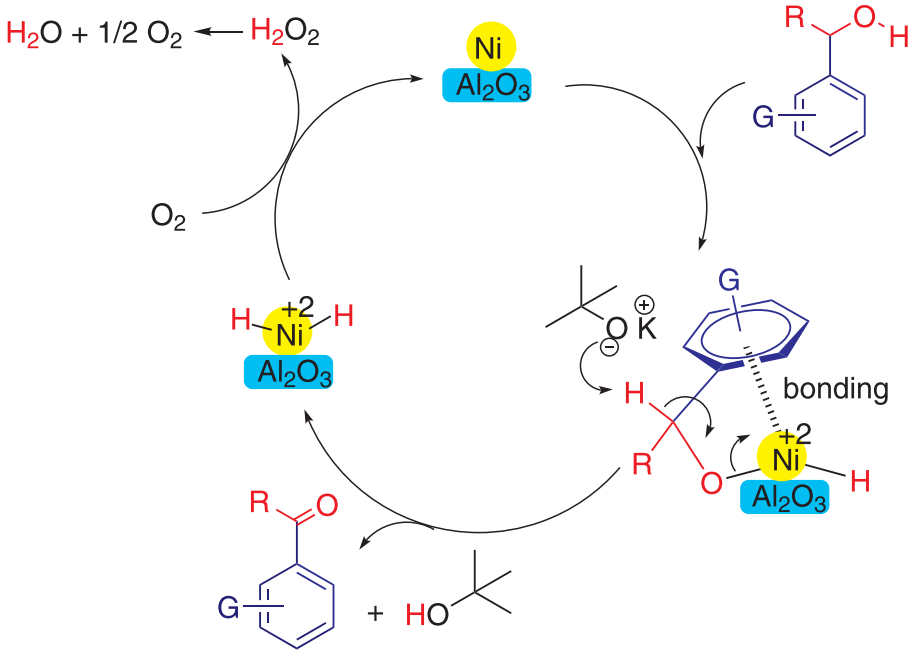

SCHEME 4 Plausible mechanism for the Ni-Alumina catalyzed oxidation of alcohols

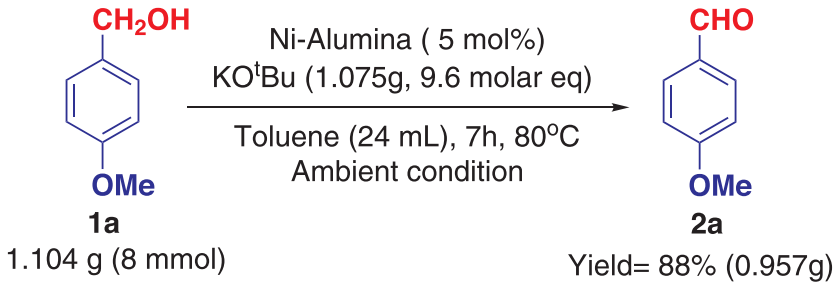

SCHEME 5 Gram scale reaction of **1a** to demonstrate the practicability

3.4 | Catalyst reusability

The recovery and reusability of the catalytic system are extremely important in order to achieve a sustainable protocol. In this pursuit, the recyclability of the catalyst was investigated using 4-methoxybenzyl alcohol **1a** (1 mmol), KO^{t}Bu (1.2 mmol), Ni-Alumina (5 mol%), and toluene (3 ml) at 80°C under ambient condition. After the completion of the reaction, the catalyst was separated by filtration, and the crude product was isolated from the filtrate through the extraction of ethyl acetate (an eco-compatible solvent). The residue was washed repeatedly with EtOAc followed by water, dried at 120°C for 1 h, and used directly for the next reaction. The isolated catalyst was used for successive reactions with a little variation of yield (Figure 8).

The recovered catalyst was further analyzed by XRD, TEM, SEM, and EDX techniques (Figure 9) to confirm

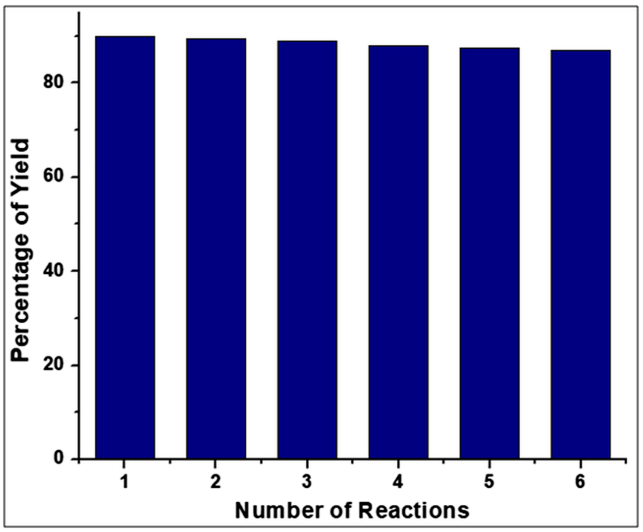

FIGURE 8 Recycling test of Ni-Alumina catalyst using **1a** (1 mmol), KO^{t}Bu (1.2 mmol), Ni-Alumina (5 mol%), toluene (3 ml) at 80°C under ambient condition

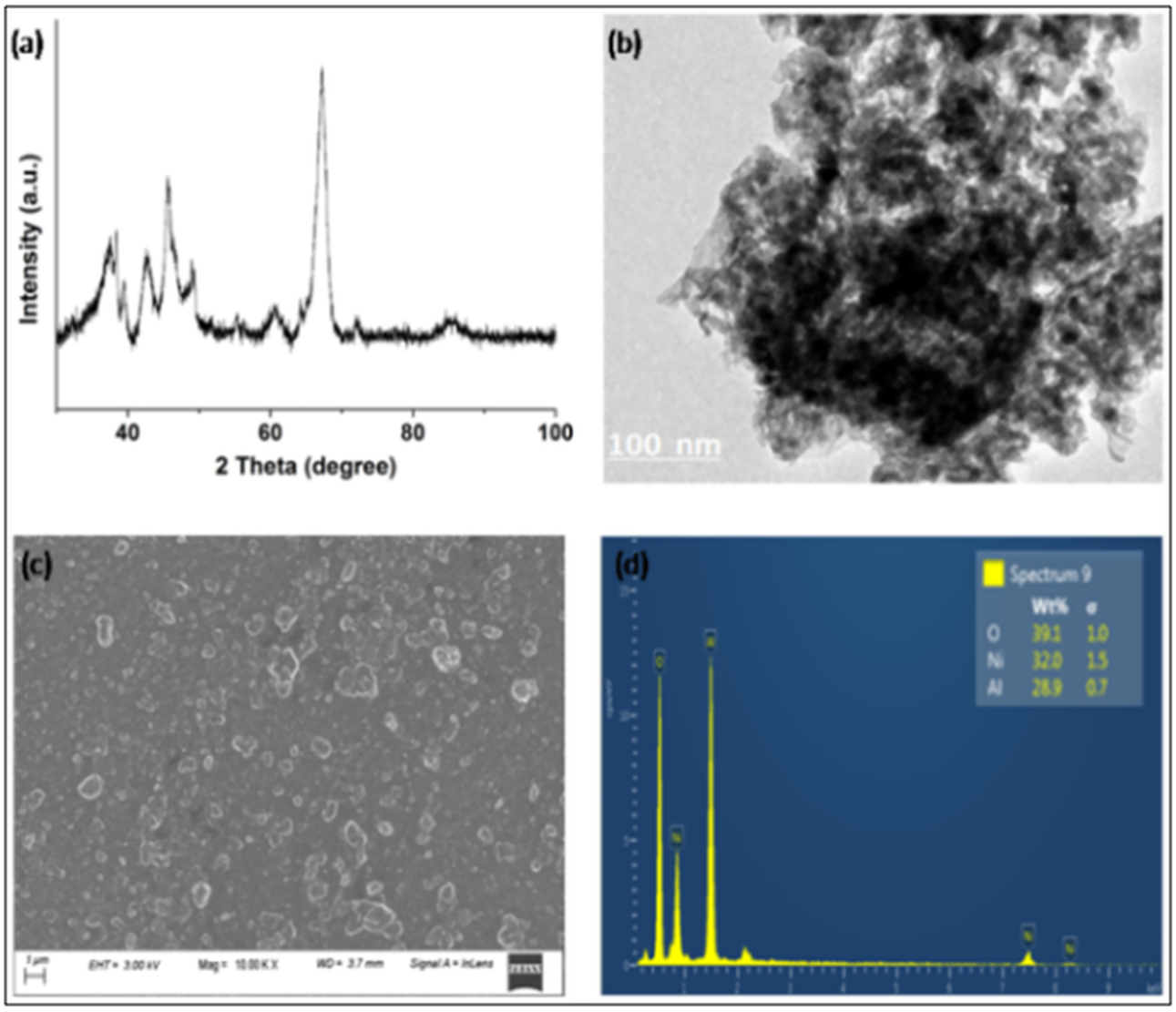

FIGURE 9 (a) XRD of Ni-Alumina (after recycled six times), (b) TEM of Ni-Alumina (after recycled six times), (c) SEM of Ni-Alumina (after recycled six times), (d) EDX of Ni-Alumina (after recycled six times)

the recyclability and stability of the nanocatalyst. The XRD result showed the disappearance of the peak at about 55° of the recovered nanocatalyst. It could be due to the oxidation of Ni (0) to Ni (II) as a result of atmospheric air exposure during the recycling process or sample analysis time. The TEM, SEM, and EDX results showed that the structural morphology of the recovered nanocatalyst did not change much during this investigation.

3.5 | "Hot filtration method (Sheldon's test)" of the catalyst

Furthermore, to observe the heterogeneity of Ni-Alumina "hot filtration method (Sheldon's test)"[39] was performed using **1a** as the substrate. When 27%

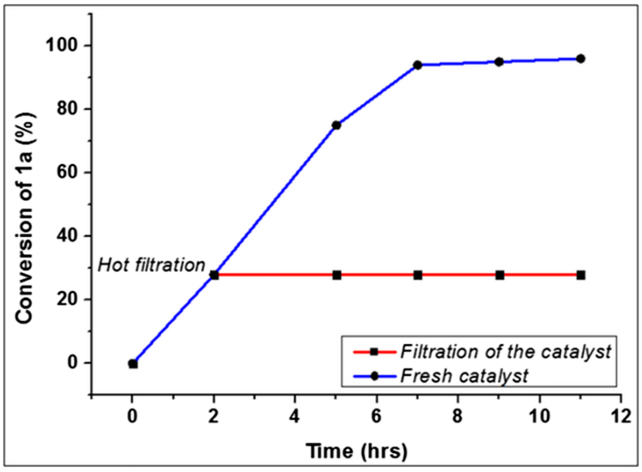

FIGURE 10 Heterogeneity test of Ni-Alumina catalyst using **1a** (1 mmol), KO^{t}Bu (1.2 mmol), Ni-Alumina (5 mol%), and toluene (3 ml) at 80°C under ambient condition

TABLE 3 Comparison of the efficiency of Ni-Alumina with reported heterogeneous catalyst[a]

Entry	Catalyst	Oxidant	Additive	Solvent	Time (h), Temp. (°C)	Yield (%)
1	PtNi@SWCNT[38]	O_2	KOH	Toluene	2 h, 80°C	98[b]
2	Pd@TiC[40]	Air	Visible light	CH_3CN	8 h, 20 W bulb	96[c]
3	Au@PMO-IL[41]	O_2	Cs_2CO_3	Toluene	3 h, 35°C	99[b]
4	Au_{np}-nSTDP[42]	TBHP	K_2CO_3	$CH_3CN:H_2O$	2 h, 80°C	91[b]
5	CoL_2@SMNP[43]	O_2	NHPI	CH_3CN	16 h, 70°C	65[c]
6	Fe_3O_4/CuBDC/GO[44]	O_2	TEMPO	CH_3CN	14.5 h, 60°C	95[b]
7	Cu/Ag@SiO_2[45]	TBHP	—	Toluene	4 h, 120°C	98[c]
8	Cu NPs@NC[46]	Air	TEMPO	H_2O:EG[d]	5 h, r.t.	95[c]
9	$NiFe_2O_4$ NPs[47]	TBHP	—	CH_3CN	3 h, 60°C	79[c]
10	Ni-Alumina (*This work*)	Air	KO^{t}Bu	Toluene	7 h, 80°C	90[c]

[a]The comparative studies were carried out using 4-methoxybenzylalcohol (**1a**) as the model substrate.
[b]GC yield.
[c]Isolated yield.
[d]EG (Ethylene glycol).

conversion of the substrate was noted after 2 h, the catalyst was separated by filtration under hot conditions. The "catalyst-free" filtrate was then kept under optimized reaction conditions. Further conversion of **1a** was not observed at all even after 11 h (Figure 10). This study indicated that practically no soluble catalytically active species was present in the filtrate. Hence, the heterogeneity of Ni-Alumina was conclusively proved.

3.6 | Comparison of the catalytic efficiency of Ni-Alumina with the literature reports

To further establish the catalytic eligibility and capability of Ni-Alumina as an efficient catalyst in this oxidative transformation, a comparative study was carried out with the previously reported heterogeneous catalyst (Table 3).

Even though these reported oxidative protocols listed in Table 3 have their merits, but still, the scope is limited due to the utilization of expensive and toxic metal catalysts, multistep synthesis of catalysts, involving the high concentration of oxidants as well as high oxygen pressure, lack of chemoselectivity, generation of over oxidized product, and tedious product isolation procedure. Therefore, apart from being eco-compatible, the present Ni-Alumina catalyzed oxidative protocol from catalyst preparation to product isolation is operationally very simple, economically more attractive, and utilizes environmentally benign aerial oxygen as an eco-friendly oxidant. Thus, the present study has developed a novel, utilitarian, and sustainable method for chemoselective oxidation of benzylic alcohols to carbonyl compounds under an ambient atmosphere with the tolerance of various sensitive moieties using easily accessible and economically viable supported metal nanoparticles as a stable and recyclable heterogeneous catalyst with greater merits and wider applicability in comparison to many earlier reports.

4 | CONCLUSION

We have developed an efficient protocol for the chemoselective oxidation of benzylic alcohols to carbonyl compounds using economically affordable alumina-supported mesoporous nickel nanoparticles as a stable recyclable heterogeneous catalyst in the presence of aerial oxygen as an eco-friendly oxidant. The aliphatic alcoholic moiety did not take part in this oxidative reaction. The present sustainable catalytic system shows excellent chemoselectivity that has been substantiated through intermolecular as well as intramolecular competition experiments. This oxidative protocol was also effective on a gram scale, which is of significant advantage in the light of large-scale preparation with the prospects of industrial application. The attractive features of the present study are procedural simplicity, appreciable stability and efficiency of the catalyst, excellent chemoselectivity, easy recovery, good recyclability, and tolerance of various sensitive moieties during the reaction.

ACKNOWLEDGMENTS

Financial assistance from RUSA-2-Programme and UGC-CAS-II program in Chemistry at Jadavpur University is gratefully acknowledged. S. N. thanks DST, INSPIRE, New Delhi for the senior research fellowship. The authors express sincere gratitude to Prof. A. Gayen of JU and Prof P. Bera of NAL, Bengaluru for helpful discussions. Special thanks are offered to Mr M. Maji, and Mr D. Panja of IIT Kanpur, Dr A. Das of IIT Guwahati, and Mr K. Mondal of IIT Madras for necessary assistance.

CONFLICT OF INTEREST

This is to declare that there is no conflict of interest in this article.

AUTHOR CONTRIBUTIONS

Asit Kumar Das: Conceptualization; investigation. **Sneha Nandy:** Investigation. **Sanjay Bhar:** Supervision.

DATA AVAILABILITY STATEMENT

The data that support the findings of this study are available in the supporting information of this article.

ORCID

Asit Kumar Das https://orcid.org/0000-0002-1722-7602
Sneha Nandy https://orcid.org/0000-0002-0742-5584
Sanjay Bhar https://orcid.org/0000-0001-8888-4143

REFERENCES

[1] Y. Uozumi, Y. M. A. Yamada, *Chem. Rec.* **2009**, *9*, 51.
[2] M. Passiniemi, A. M. Koskinen, *Beilstein J. Org. Chem.* **2013**, *9*, 2641.
[3] B. L. Ryland, S. S. Stahl, *Angew. Chem. Int. Ed.* **2014**, *53*, 8824.
[4] E. J. Corey, J. W. Suggs, *Tetrahedron Lett.* **1975**, *16*, 2647.
[5] D. B. Dess, J. C. Martin, *J. Org. Chem.* **1983**, *48*, 4155.
[6] P. W. Moore, T. J. Zerk, J. M. Burns, P. V. Bernhardt, C. M. Williams, *Eur. J. Org. Chem.* **2017**, 448.
[7] A. J. Mancuso, S. L. Huang, D. Swern, *J. Org. Chem.* **1978**, *43*, 2480.
[8] M. Sdahl, J. Conrad, C. Braunberger, U. Beifuss, *RSC Adv.* **2019**, *9*, 19549.
[9] D. Shen, C. Miao, D. Xu, C. Xia, W. Sun, *Org. Lett.* **2015**, *17*, 54.
[10] Y. Hu, L. Chen, B. Li, *Cat. Com.* **2018**, *103*, 42.
[11] C. J. Weiss, P. Das, D. L. Miller, M. L. Helm, A. M. Appel, *ACS Catal.* **2014**, *4*, 2951.
[12] W. Czepa, M. A. Fik, S. Witomska, M. Kubicki, G. Consiglio, P. Pawluc, V. Patroniak, *ChemistrySelect* **2018**, *3*, 9504.
[13] G. Urgoitia, A. Maiztegi, R. SanMartin, M. T. Herrero, E. Domınguez, *RSC Adv.* **2015**, *5*, 103210.
[14] K. Marui, Y. Higashiura, S. Kodama, S. Hashidate, A. Nomoto, S. Yano, M. Ueshima, A. Ogawa, *Tetrahedron* **2014**, *70*, 2431.
[15] Q. Wang, W. Du, T. Liu, H. Chai, Z. Yu, *Tetrahedron Lett.* **2014**, *55*, 1585.
[16] R. A. Farnandes, V. Bethi, *RSC Adv.* **2014**, *4*, 40561.
[17] A. K. Das, N. Sepay, S. Nandy, A. Ghatak, S. Bhar, *Tetrahedron Lett.* **2020**, *61*, 152231. https://doi.org/10.1016/j.tetlet.2020.152231
[18] S. Nandy, A. K. Das, S. Bhar, *SynCommun.* **2020**, *50*, 3326.
[19] T. Karimpour, E. Safaei, B. Karimi, Y. Lee, *ChemCatChem* **2017**, *9*, 1.
[20] R. Hasanpour, F. Feizpour, M. Jafarpour, A. Rezaeifard, *New J. Chem.* **2018**, *42*, 7383.
[21] S. Meher, R. K. Rana, *Green Chem.* **2019**, *21*, 2494.
[22] Y. Hong, X. Yan, X. Liao, R. Li, S. Xu, L. Xiao, J. Fan, *Chem. Commun.* **2014**, *50*, 9679.
[23] B. Sarmah, B. Satpati, R. Srivastava, *ACS Omega* **2018**, *3*, 7944.
[24] X. Wang, C. Wang, Y. Liu, J. Xiao, *Green Chem.* **2016**, *18*, 4605.
[25] M. Alhumaimess, Z. Lin, W. Weng, N. Dimitratos, N. F. Dummer, S. H. Taylor, J. K. Bartley, C. J. Kiely, G. J. Hutchings, *ChemSusChem* **2012**, *5*, 125.
[26] N. Anbu, M. B. RubyKamalam, K. Sethuraman, A. Dhakshinamoorthy, *ChemistrySelect* **2018**, *3*, 12725.
[27] J. J. Boruah, S. P. Das, *RSC Adv.* **2018**, *8*, 34491.
[28] B. Mahmoudi, A. Rostami, M. Kazemnejadi, B. A. Hamah-Ameen, *Green Chem.* **2020**, *22*, 6600.
[29] M. J. Ndolomingo, N. Bingwa, R. Meijboom, *J. Mater. Sci.* **2020**, *55*, 6195.
[30] A. Ghatak, S. Khan, R. Roy, S. Bhar, *Tetrahedron Lett.* **2014**, *55*, 7082.
[31] S. Khan, A. Ghatak, S. Bhar, *Tetrahedron Lett.* **2015**, *56*, 2480.
[32] A. Charvieux, L. L. Moigne, L. G. Borrego, N. Duguet, E. Metay, *Eur. J. Org. Chem.* **2019**, *2019*, 6842.
[33] I. D. Inaloo, S. Majnooni, H. Eslahi, M. Esmaeilpour, *New J. Chem.* **2020**, *44*, 13266.
[34] S. G. Hernandez-Leon, J. A. Sarabia-Sainz, G. R. Montfort, J. A. Huerta-Ocampo, A. M. Guzman-Partida, M. R. Robles-Burgueno, A. J. Burgara-Estrella, L. Vazquez-Moreno, *RSC Adv.* **2019**, *9*, 11038.
[35] L. Wang, S. S. Shang, G. S. Li, L. H. Ren, Y. Lv, S. Gao, *J. Org. Chem.* **2016**, *81*, 2189.
[36] X. Liu, Q. Xia, Y. Zhang, C. Chen, W. Chen, *J. Org. Chem.* **2013**, *78*, 8531.
[37] H. Goksu, F. Sen, *Sci. Rep.* **2020**, *10*, 5731. https://doi.org/10.1038/s41598-020-62695-4
[38] H. Goksu, K. Cellat, F. Sen, *Sci. Rep.* **2020**, *10*, 9656. https://doi.org/10.1038/s41598-020-66492-x
[39] H. E. Lempers, R. A. Sheldon, *J. Catal.* **1998**, *175*, 62.
[40] S. Verma, R. B. NasirBaig, M. N. Nadagouda, R. S. Varma, *Tetrahedron* **2017**, *73*, 5577.
[41] B. Karimi, A. Bigdeli, A. A. Safari, M. Khorasani, H. Vali, S. K. Karimvand, *ACS Comb. Sci.* **2020**, *22*, 70.
[42] S. H. Kashani, A. L. Isfahani, M. Moghadam, S. Tangestaninejad, V. Mirkhani, I. M. Baltork, *Appl. Organomet. Chem.* **2018**, *32*, e4440.
[43] M. Jafarpour, A. Rezaeifard, V. Yasinzadeh, H. Kargar, *RSC Adv.* **2015**, *5*, 38460.
[44] H. Alamgholiloo, S. Rostamnia, K. Zhang, T. H. Lee, Y. S. Lee, R. S. Varma, H. W. Jang, M. Shokouhimehr, *ACS Omega* **2020**, *5*, 5182.
[45] A. Saha, S. Payra, S. Banerjee, *New J. Chem.* **2017**, *41*, 13377.
[46] A. Dutta, M. Chetia, A. A. Ali, A. Bordoloi, P. S. Gehlot, A. Kumar, D. Sarma, *Catal. Lett.* **2019**, *149*, 141.
[47] S. Iraqui, S. S. Kashyap, H. Rashid, *Nanoscale Adv.* **2020**. https://doi.org/10.1039/D0NA00591F

SUPPORTING INFORMATION

Additional supporting information may be found online in the Supporting Information section at the end of this article.

How to cite this article: Das AK, Nandy S, Bhar S. Chemoselective and ligand-free aerobic oxidation of benzylic alcohols to carbonyl compounds using alumina-supported mesoporous nickel nanoparticle as an efficient recyclable heterogeneous catalyst. *Appl Organomet Chem*. 2021;35:e6282. https://doi.org/10.1002/aoc.6282

National Seminar on

EMERGING TRENDS IN CHEMISTRY (ETC-2017)

(Wednesday, February 15, 2017)

under

Centre for Advanced Studies II Program

Organized by

Department of Chemistry, Jadavpur University, Kolkata 700 032

This is to certify that ASIT KUMAR DAS *of* JADAVPUR UNIVERSITY *has ~~participated~~/presented a poster in the seminar organized by the Department of Chemistry, Jadavpur University, Kolkata 700 032 on Wednesday, February 15, 2017.*

Date: 15-02-2017
Place: Kolkata

KAUSIKISANKAR PRAMANIK
Convener

SUMAN DAS
Co-Conveners

A. Saha
AMRITA SAHA

ONE DAY NATIONAL LEVEL SEMINAR

on

Modern Trends in Chemistry for Sustainable Development

This is to certify that Prof./ Dr./Mr./Ms. ASIT KUMAR DAS

of JADAVPUR UNIVERSITY has participated/presented/~~delivered~~

(✓Poster/Oral/Paper presentation/Invited Lecture) entitled Synthesis of Fe_3O_4 Nanoparticles in the National Seminar on "*Modern Trends in Chemistry for Sustainable Development*" organized by the Department of Chemistry, Vijaygarh Jyotish Ray College, Kolkata and the Indian Chemical Society, Kolkata on March 03, 2020.

Prof. Chittaranjan Sinha	*Dr. Rajyasri Neogi*	*Dr. Dasarath Mal*
Honorary Secretary	Principal	Convener
Indian Chemical Society	Vijaygarh Jyotish Ray College	Vijaygarh Jyotish Ray College